

GEM Baseline 1

July 9, 1992

Abstract:

This document details parameters of the current GEM detector baseline design. This design will be used for an in-depth analysis of cost, schedule and physics performance.

GEM BASELINE 1

TABLE OF CONTENTS

- 1.0 OVERVIEW
- 2.0 SCHEDULE/MILESTONES
- 3.0 FACILITIES
- 4.0 DETECTOR INSTALLATION
- 5.0 DETECTOR ACCESS
- 6.0 BEAM LINE
- 7.0 MAGNET, FIELD SHAPER & CENTRAL DETECTOR
SUPPORT
- 8.0 MAGNETIC FIELD
- 9.0 TRACKER
- 10.0 CALORIMETER
- 11.0 MUONS
- 12.0 ALIGNMENT
- 13.0 ELECTRONICS
- 14.0 COMPUTING
- 15.0 TEST BEAMS
- 16.0 RADIATION ENVIRONMENT

OVERVIEW

TABLE OF CONTENTS

INTRODUCTION

Overview of GEM Detector and Systems
Purpose

FIGURES:

GEM Detector (3-D drawing)
GEM Detector Elevation
GEM Detector Layout
GEM Detector Layout (with section identifiers)
GEM Detector Sections (A-A, B-B)
Typical Azimuthal Cut in Barrel Region
GEM Coordinate System and Field Direction
GEM Central Tracker
GEM Central Tracker Cross Sections
Liquid Argon Calorimeter
Liquid Argon Calorimeter Barrel Cross Section
Scintillating Fiber Calorimeter
GEM Muon System Chamber Layout
GEM Barrel Region Chamber End View

OVERVIEW

OVERVIEW

1.0 INTRODUCTION

1.1 OVERVIEW OF GEM DETECTOR AND SYSTEMS

The GEM (Gammas, Electrons, Muons) experiment stresses the precise measurement of gammas, electrons and muons, and, to a lesser extent, neutrinos and hadron jets. The goal is also to produce a robust detector capable of running at luminosities beyond the design luminosity of 10^{33} . This philosophy is based on the belief that these are the fundamental signatures for most of the standard list of physics opportunities which might be opened up by the SSC energy and luminosity: electroweak symmetry breaking; supersymmetry and other extensions of the standard model; and top and other new quarks or leptons. GEM will have moderate capabilities in tracking and hadronic calorimetry which will round out the physics program through QCD and compositeness studies. The current baseline detector is shown in Figures 1.1 through 1.6.

The GEM detector consists essentially of five active systems and three passive structures. Moving concentrically outwards, the active systems consist of inner tracking, electromagnetic (EM) calorimetry, hadronic calorimetry, muon chambers, and a magnet. The passive devices consist of two forward field shapers and a central membrane support structure.

The inner tracking consists of an inner silicon tracking system surrounded by layers of wire chambers utilizing interpolating pads (IPC) for precision measurement of coordinates. The tracking detector serves to identify the primary event vertex; provide identification of photons by the absence of tracks; provide track information to aid in isolating electron, muon or photon candidates; and measure momenta of electrons and muons to aid in background rejection, identification, and sign selection. Tracker secondary goals are full reconstruction of charged tracks in an event, secondary vertex finding, and good momentum measurement of low momentum particles. Critical factors in the design of the system include high expected occupancy which limit the performance at high luminosity, and the amount of material in the tracking volume (including chambers themselves) which will contribute to secondary interactions of particles and photon conversions, adding to confusion in an event, adding background, and causing loss of signal. Since the precision of the silicon is $10\ \mu\text{m}$ and the IPC is $50\ \mu\text{m}$, a critical concern is alignment and stability of the system to take advantage of this resolution.

Source: M Marx
Update: 6/29/92

OVERVIEW

The electromagnetic calorimetry comprises the next layer of GEM. There are currently two options under consideration - a liquid argon/krypton sampling calorimeter, and a BaF crystal total absorption calorimeter. Both of these devices are intended to provide precise measurement of the energy of electrons and photons. It is also used to provide directional information for photons, and for rejection of hadronic backgrounds by shower shape or size. Signals in the EM are used to form a trigger for either electrons or photons. For BaF the challenge is to reduce systematic effects to a level commensurate with the intrinsic resolution of the calorimeter. For liquid argon/krypton, the challenge is to improve the resolution beyond the state of the art for the accordion plate structure, and to reduce instrumental effects produced by gaps between modules and walls. There is a premium to reduce the level of material in front of either calorimeter. The choice between barium fluoride and liquid/sampling EM calorimetry will be made in August, 1992.

Hadronic calorimetry in GEM is accomplished after the EM and also closes the forward regions. The options under study include liquid argon and scintillating fiber calorimeters. The function of these calorimeters is to measure hadronic energy and the tails of electromagnetic showers. It is used to help in identification of electrons and photons, to measure the energies of hadronic "jets", and by energy/momentum balance to deduce the passage of energetic non-interacting particles - neutrinos or new particles. Signals in the hadron calorimeter provide trigger information for electrons and photons, high energy jets, and missing energy. There are minimal requirements on depth which are needed for energy measurements, but more stringent requirements are necessary to reduce the background particles penetrating through the calorimetry to the muon system. The calorimeter must also provide energy measurements for muons traversing the calorimetry. In the forward regions there is a premium on angular coverage very close to the beam direction to avoid losing energy which could mimic a neutrino signal.

The muon chambers outside the central hadron calorimetry cover down to almost 9 degrees from either beam. Their primary function is to provide a precise measurement of a muon trajectory and also to provide a trigger signal for single and multiple muons, and to provide the correlation of a muon with the correct bunch crossing. Multiple layers of chambers form 3 superlayers, which are placed at the beginning, middle, and end of the magnetic volume to permit sagitta measurements. Options under consideration are cathode strip readout

Source: M Marx
Update: 6/29/92

OVERVIEW

chambers for the forward regions which provide spatial and trigger information; limited streamer tubes or pressurized drift tubes in the central region, used in conjunction with Resistive Plate Chambers which provide timing, trigger, and z coordinate. The choice of technology will be made after comparative performance tests to be done at the SSC in the summer of 1992.

Critical areas in the muon system include achieving needed precision of the chambers, alignment and stability at the level of 25 μm , and minimization of gaps in the coverage while minimizing the impact of support structure and material in the chambers themselves. This system should be sufficiently robust to operate at the highest SSC luminosities and at the highest muon energies likely to be encountered. This puts requirements on pattern recognition of muon tracks, and double hit resolution, so as to find muons near hadronic debris or debris from electromagnetic showers induced by high energy muons themselves. The position of the muon detectors must be precisely known within the layers of each module, and also with respect to the inner tracker and beam line.

The final active GEM system is the superconducting solenoid magnet within which all other detectors sit. This magnet provides an axially symmetric field, which bends the tracks of charged particles to facilitate measurement of their momentum. Measurement of momentum occurs in the inner tracking volume and muon system volume. The field produced by this system must be well understood and known to high precision, both in magnitude and direction. The magnetic field is returned through air, resulting in a large volume over which its effects can be felt - in the hall and on the surface. Care must be exercised to account for this return field in other experimental components. The magnet is in two halves which are independently mobile to allow access to the interior and to facilitate detector installation.

The forward field shapers are large cones of permeable steel, which provide a field component normal to the trajectories of forward-going muons. The large mass must be supported outside of the magnet, and the magnetic forces induced must be supported by the magnet itself. Uniformity of the shaper steel is important to have good understanding of the field in the muon volume, as is the placement of permeable support structures outside the coil.

The final system is the central membrane and support tube which supports the calorimetry and inner tracking. This device must be self

Source: M Marx
Update: 6/29/92

OVERVIEW

supporting and permit loading and access to the supported components, with the assistance of external structures. It is designed to occupy minimal space both radially and along the beam line, so as to minimize loss of measurement of muon tracks.

In addition to the detectors and structures GEM has an electronics system which shapes and digitizes the detector outputs, then, and forms three levels of triggers which reduce the data flow from 60 MHz to 10 Hz. The output from the electronics system is recorded by the data acquisition system.

GEM also includes surface facilities for major fabrication, final assembly and staging of installation into the underground hall.

1.2 PURPOSE

This document, GEM Baseline 1, specifies the parameters of the GEM detector as it is now known. It is intended as a resource document for many critical activities: designs of the various subsystems and their integration into the overall detector; costing of the detector; and the evaluation of the detector performance in key physics processes. In order that these activities can proceed it is necessary to freeze the detector parameters as given in this document. It is clearly recognized, at this early stage of the development of GEM, that there will be evolution of the parameters. However, this evolution must now proceed through a well defined process, which is initiated with the issuance of this Baseline 1. It is expected that revisions to the baseline will be issued periodically as required. After the document is issued no subsystem may change any of its parameters without following a controlled procedure.

Control and management of documents at the SSCL is governed by configuration management requirements laid down in the Configuration Management Plan prepared by SSCL Project Management Office and ratified by DOE. Until a separate book consisting entirely of technical and physics parameters exists this document will temporarily comply with SSCL Configuration Management directives. This implies signature control by GEM Management and the GEM Configuration Office. One signed copy will be kept at the SSCL for future reference.

For changes which do not affect the performance, cost or schedule of the subsystem itself, and do not affect the performance, cost or schedule of any other subsystem, a change may be effected by a memo to the Chief

Source: M Marx
Update: 6/29/92

OVERVIEW

Engineer and Integration Coordinator which describes the change. With their concurrence the change may be effected, and will be circulated to all members of the collaboration. In this way, all members will continue to work to the same baseline.

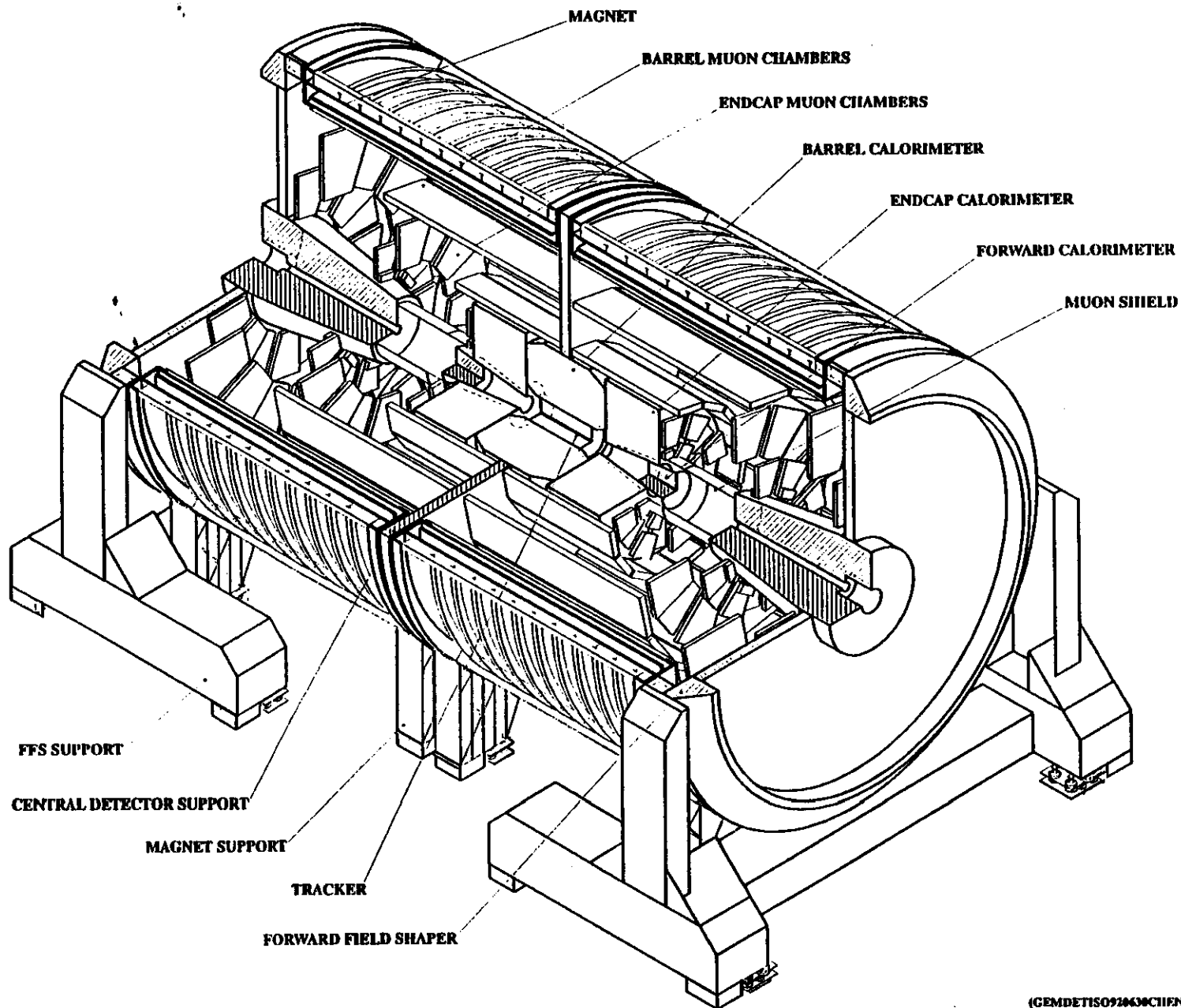
If any change affects the performance, cost or schedule of the system or any other system, or requires another system to accommodate the change within its design, the request for change will be forwarded to the Project Manager, Spokesmen, and Executive Committee for concurrence. The request should support the reason for such a change, and include an evaluation of its impact in terms of cost, schedule or performance.

All systems are expected to be studying the design as specified in the baseline: engineering; cost; and physics simulation. It is expected that when these studies are mature, a global iteration of the baseline will be required and a new Baseline issued. The expected time frame for the next iteration is early in June. It is expected that each subsequent iteration will involve fewer and smaller changes to the detector parameters, culminating in a Final Baseline concurrent with the Technical Design Report.

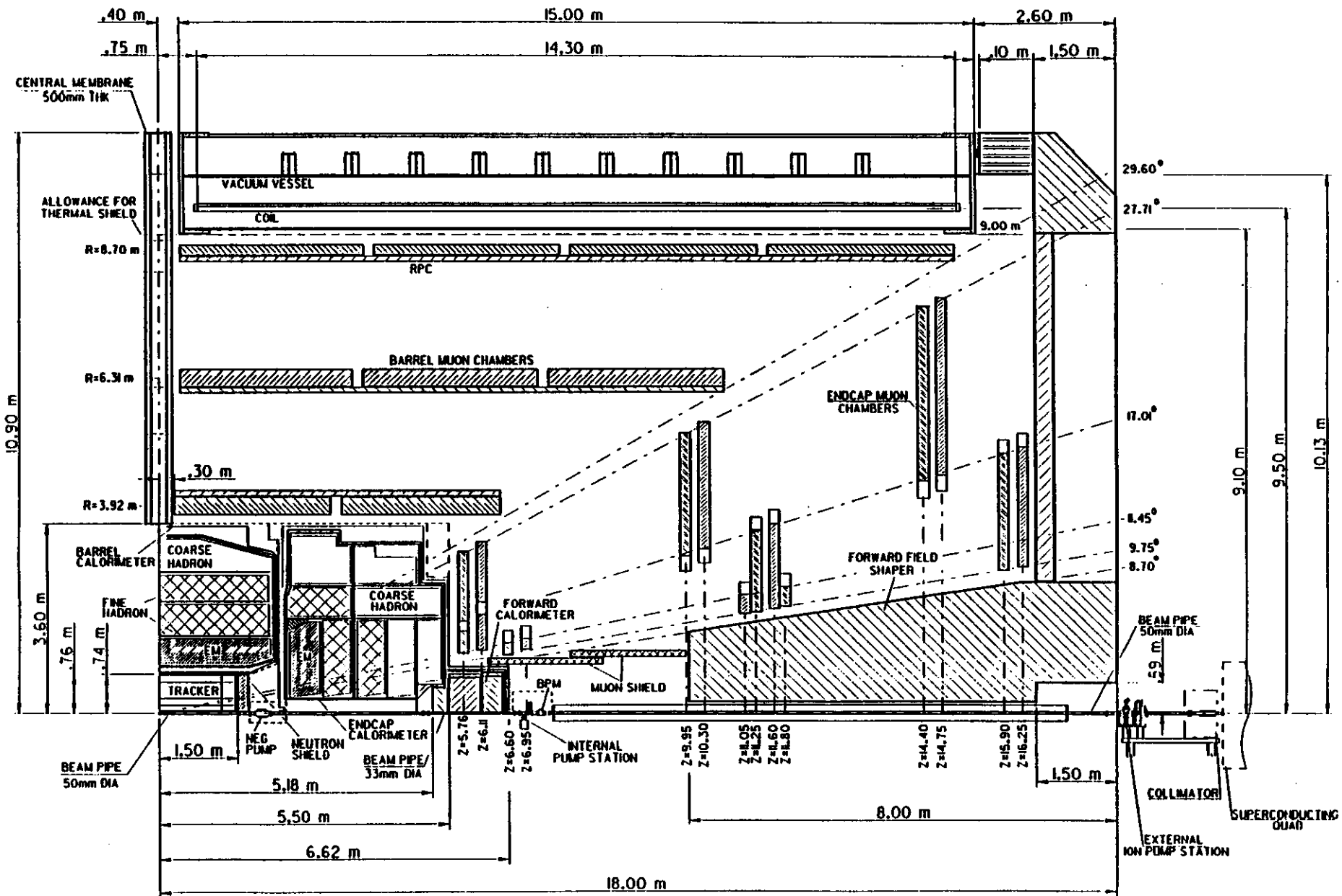
The format of this Baseline 1 is somewhat free form at the moment, with few guidelines having been issued to the systems. The document is intended to be comprehensive and informative, but not a replacement for a design report. In order to improve the format, suggestions for changes are solicited, and requests for additional information (or less!) should be directed to the Chief Engineer and Integration Coordinator. Thus the Baseline document itself will evolve into a concise and useful reference document for all collaborators working on GEM, and also for those interested in finding out about GEM.

Source: M Marx
Update: 6/29/92

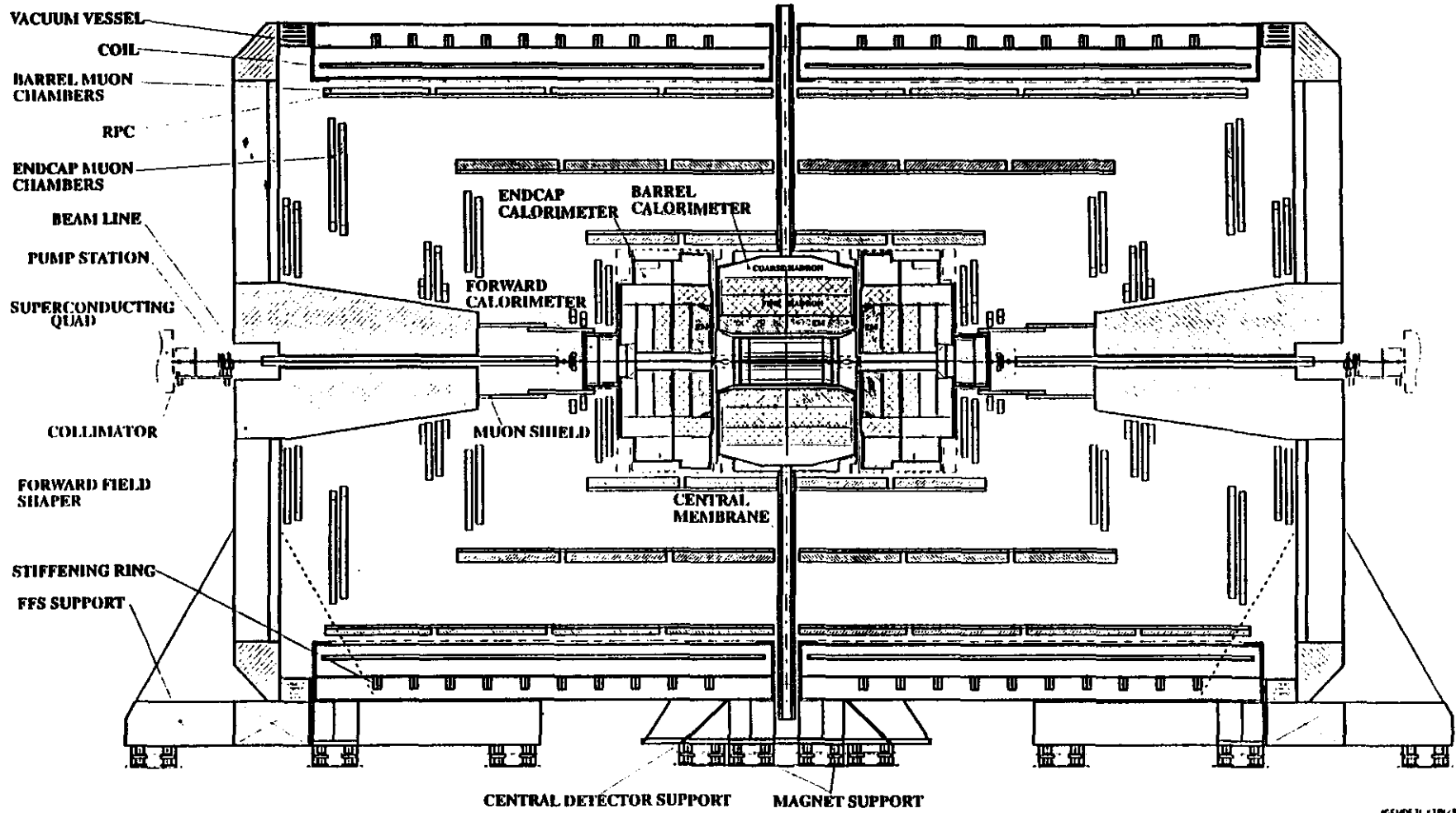
GEM DETECTOR



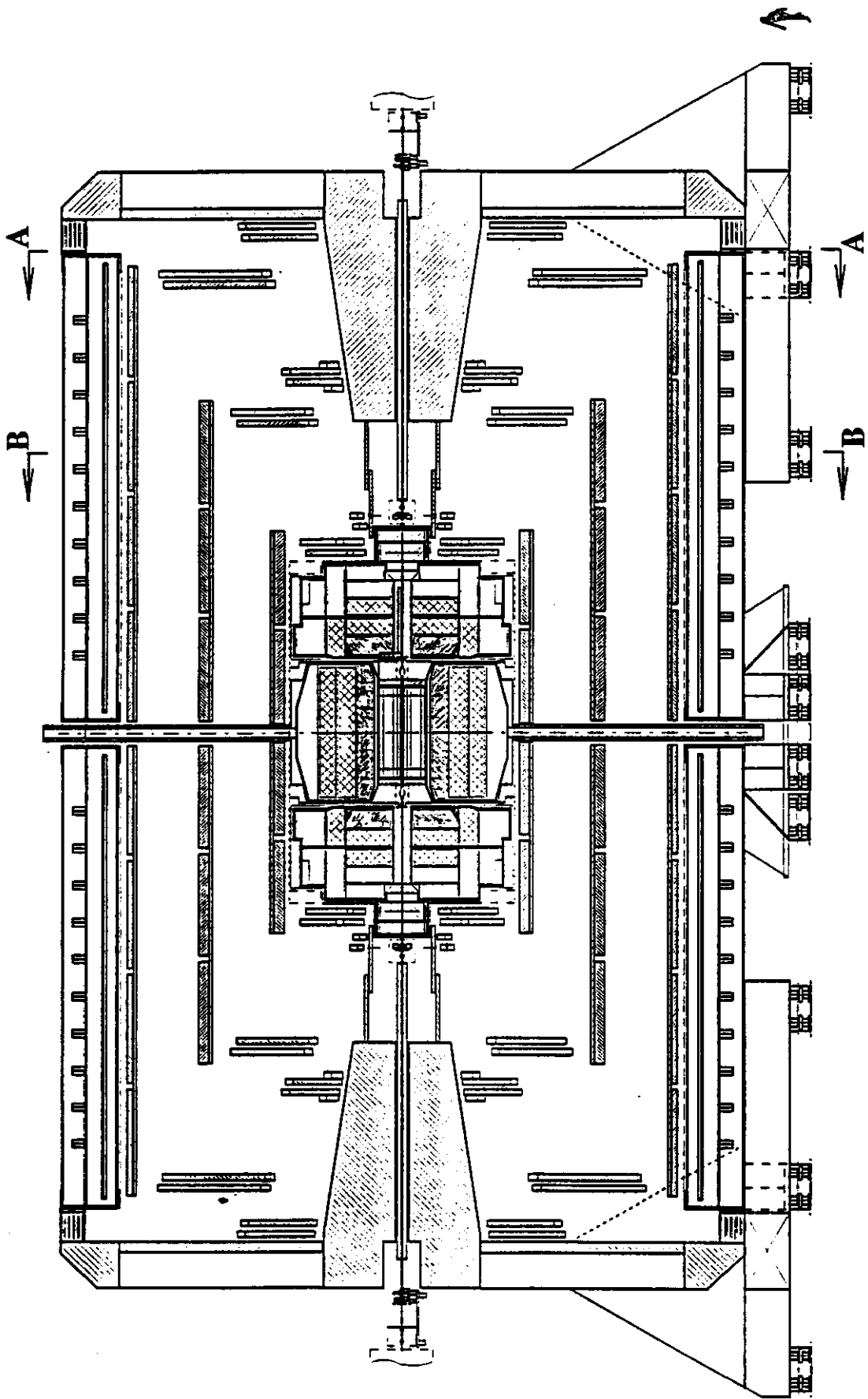
GEM DETECTOR ELEVATION

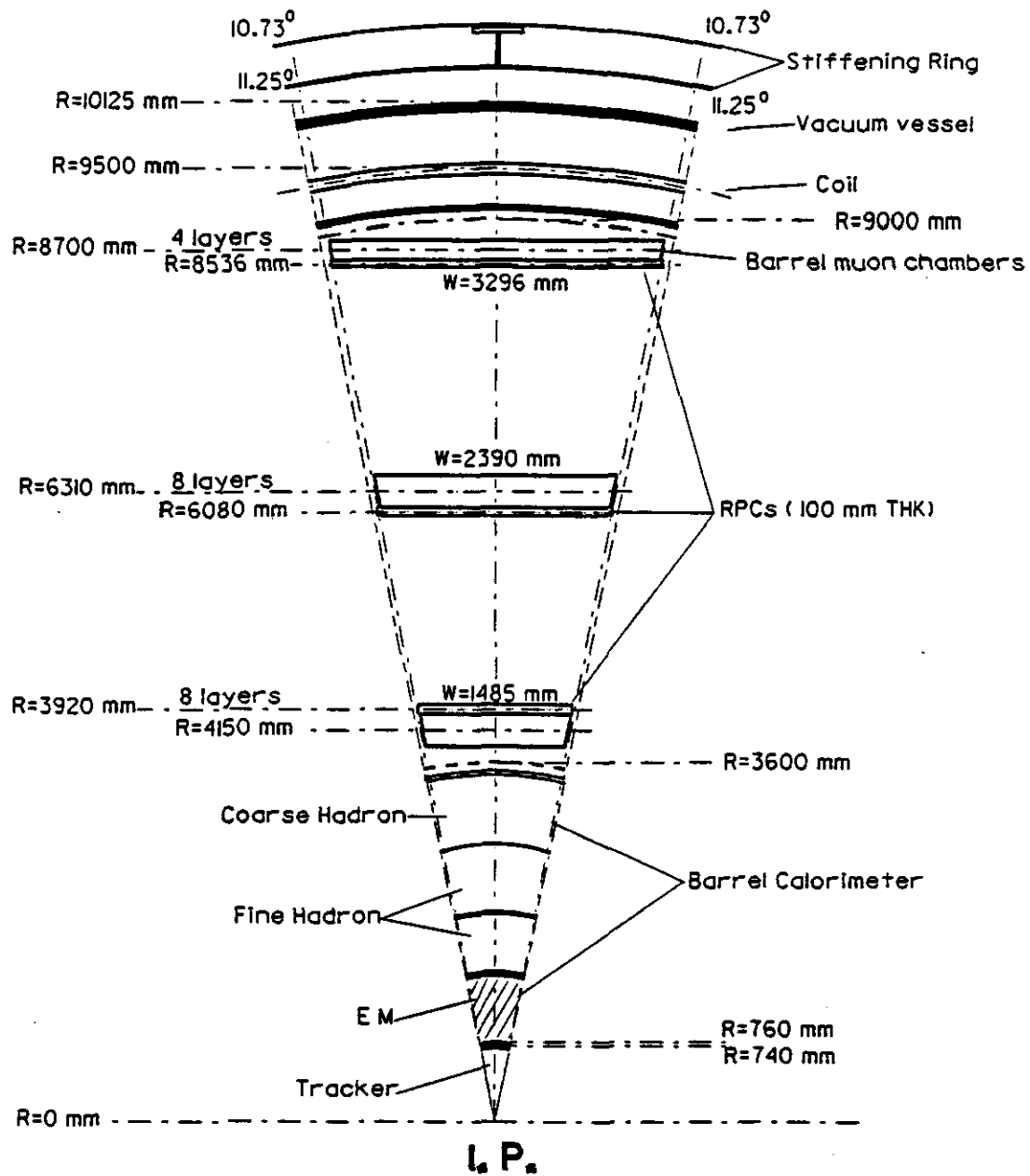


GEM DETECTOR LAYOUT



GEM DETECTOR LAYOUT

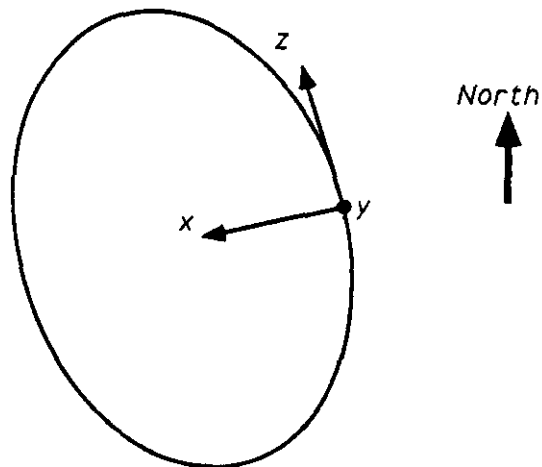
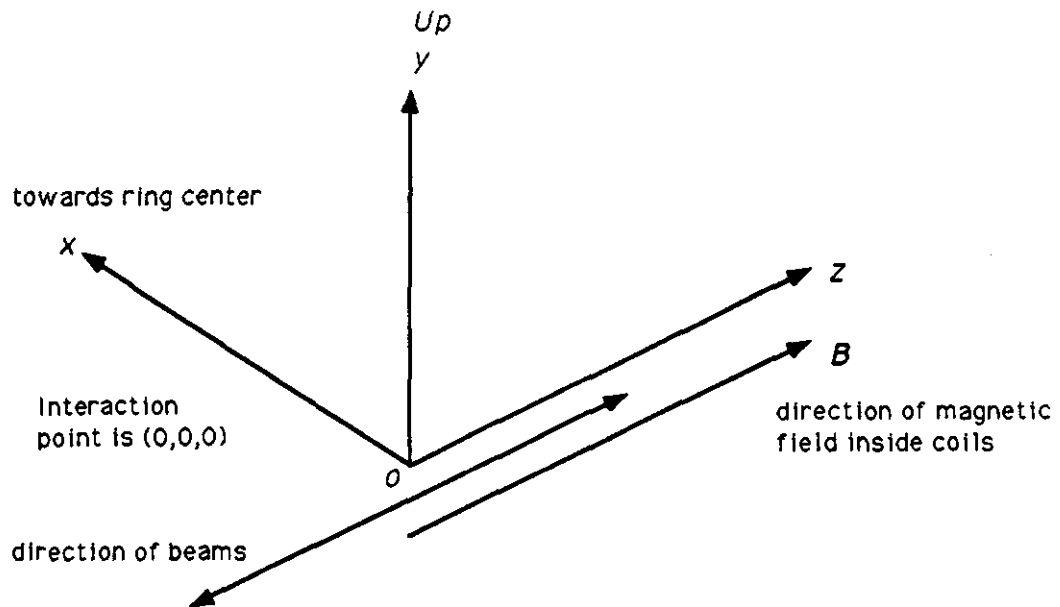




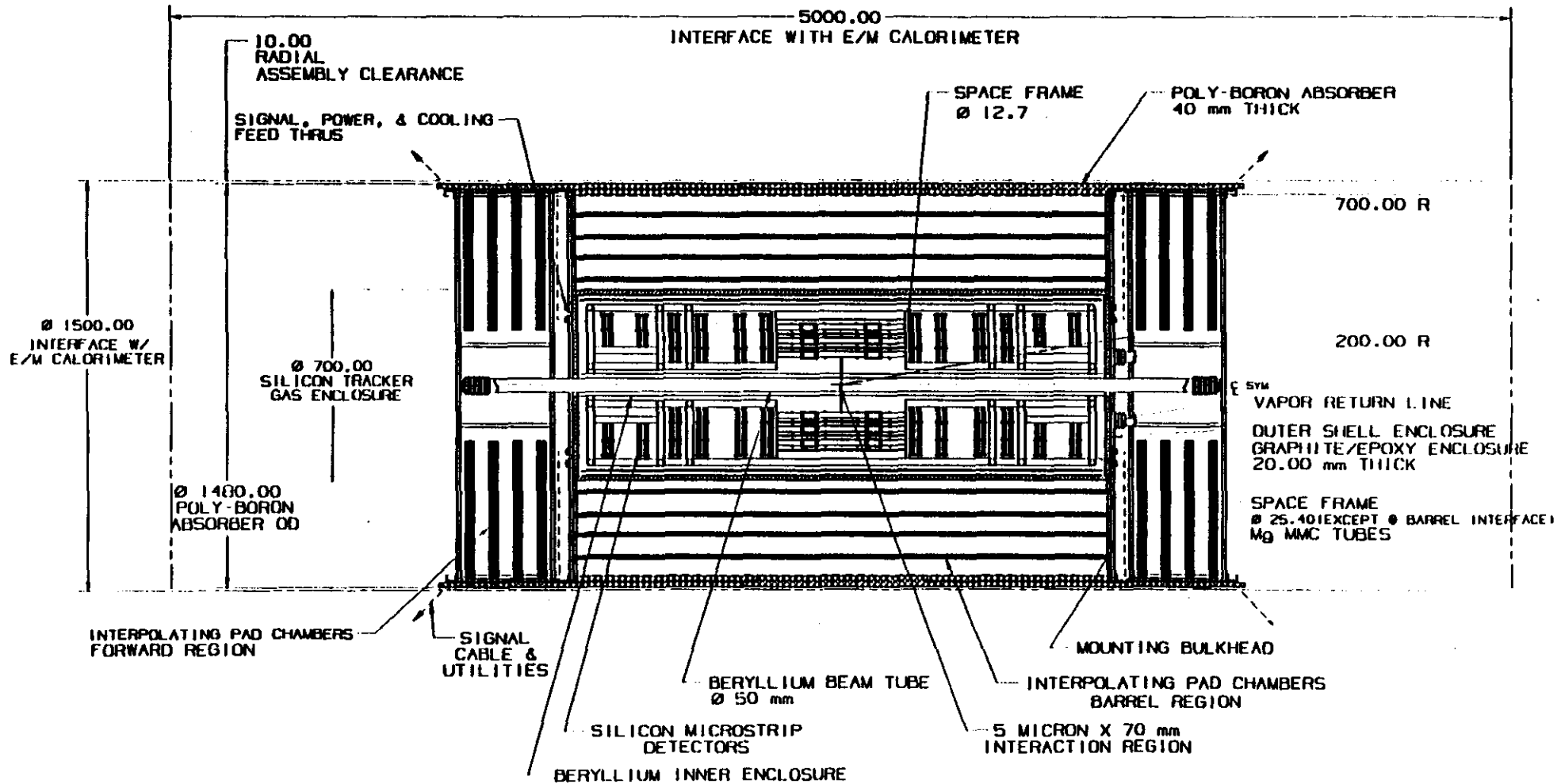
TYPICAL AZIMUTHAL CUT IN BARREL REGION

INTRODUCTION

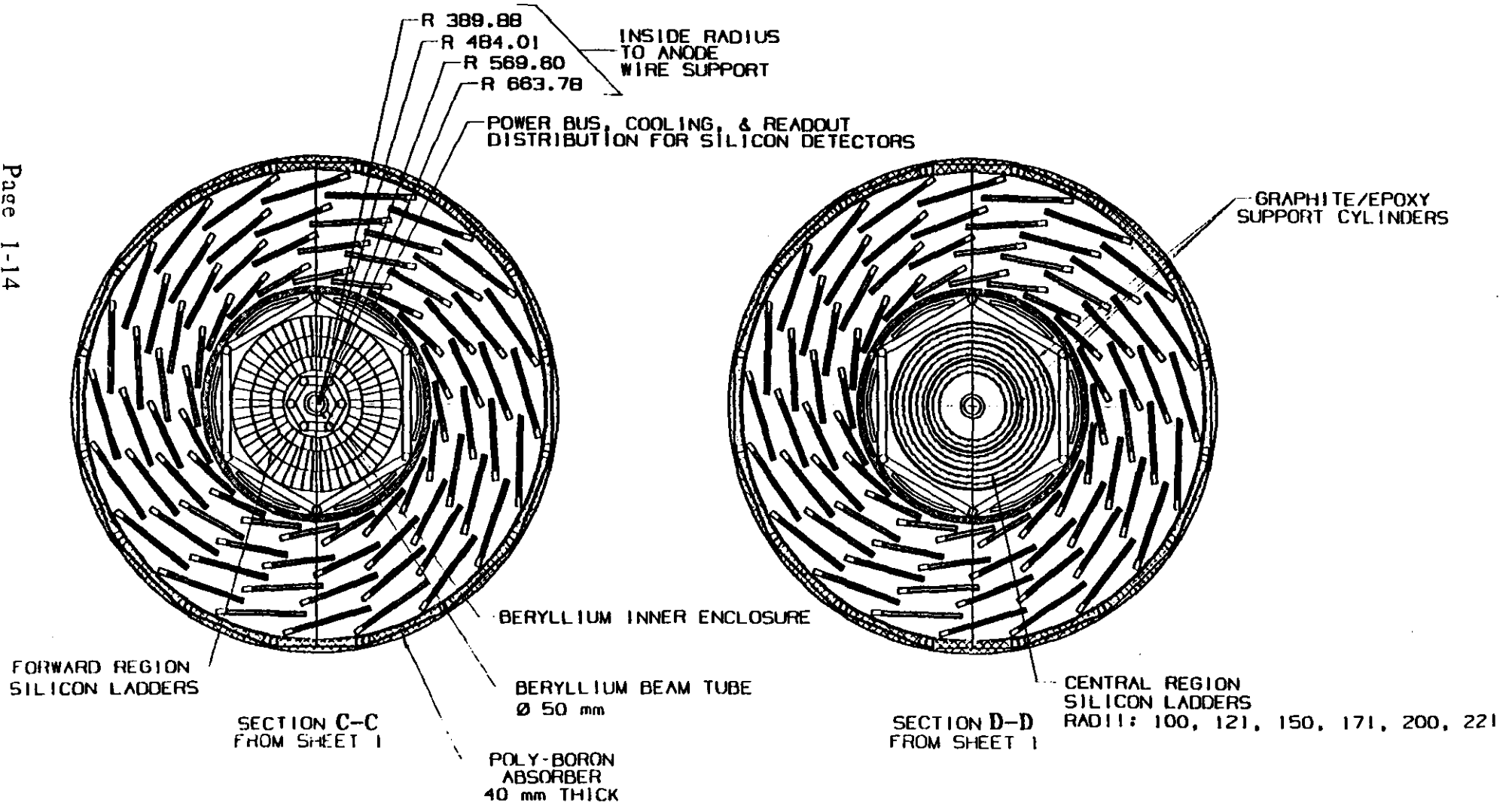
GEM Coordinate System and Field Direction



The GEM coordinate system is right-handed with its origin at the nominal interaction point, the z direction is along the beam direction and positive z is North. The positive x direction is towards the machine center and y is up. The magnetic field is parallel to the z axis, roughly in the same direction as the Earth's field.

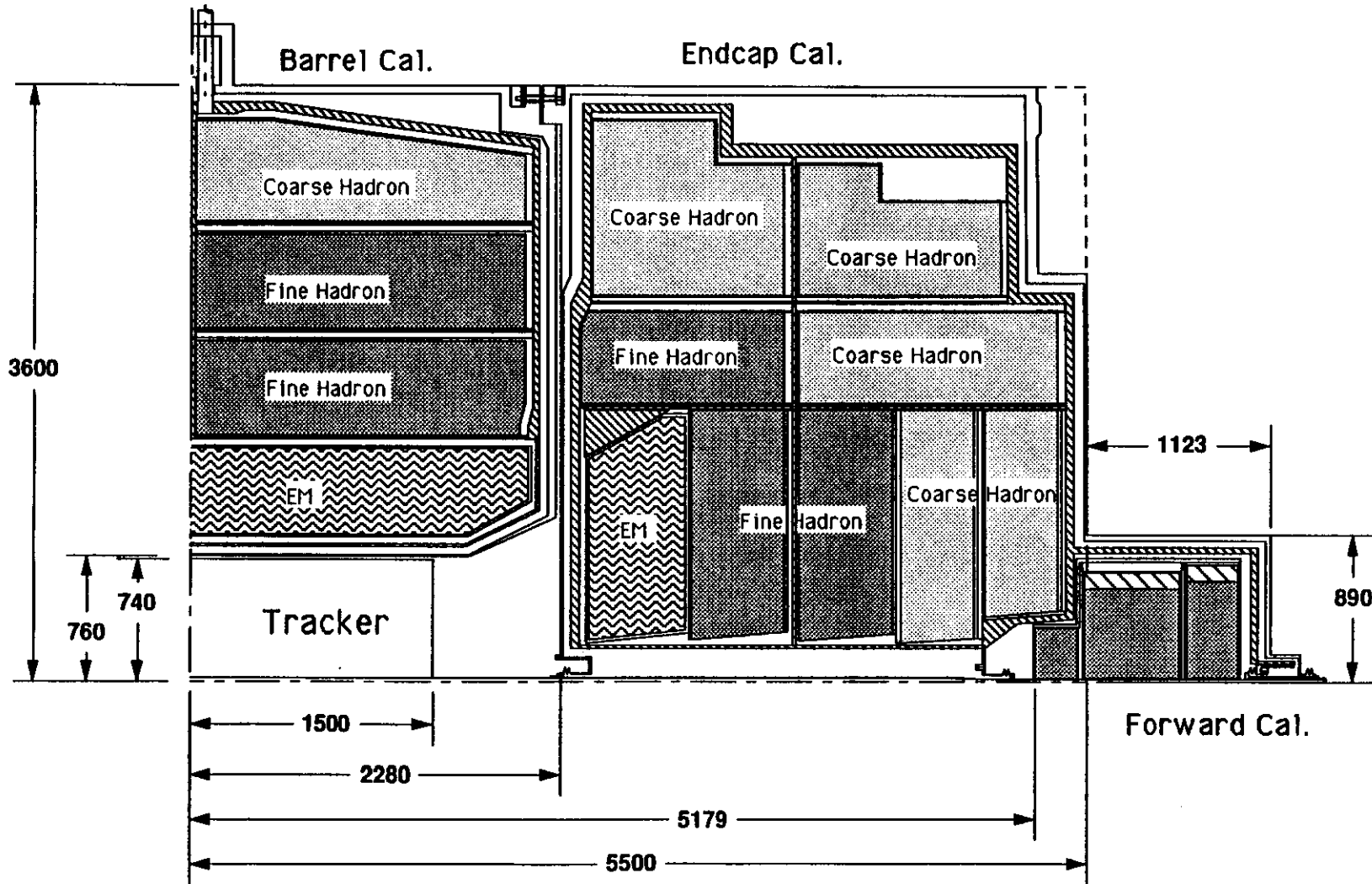


GEM CENTRAL TRACKER



LIQUID ARGON CALORIMETER - 12 X 14 LAMBDA, FLAT ENDCAP HEAD

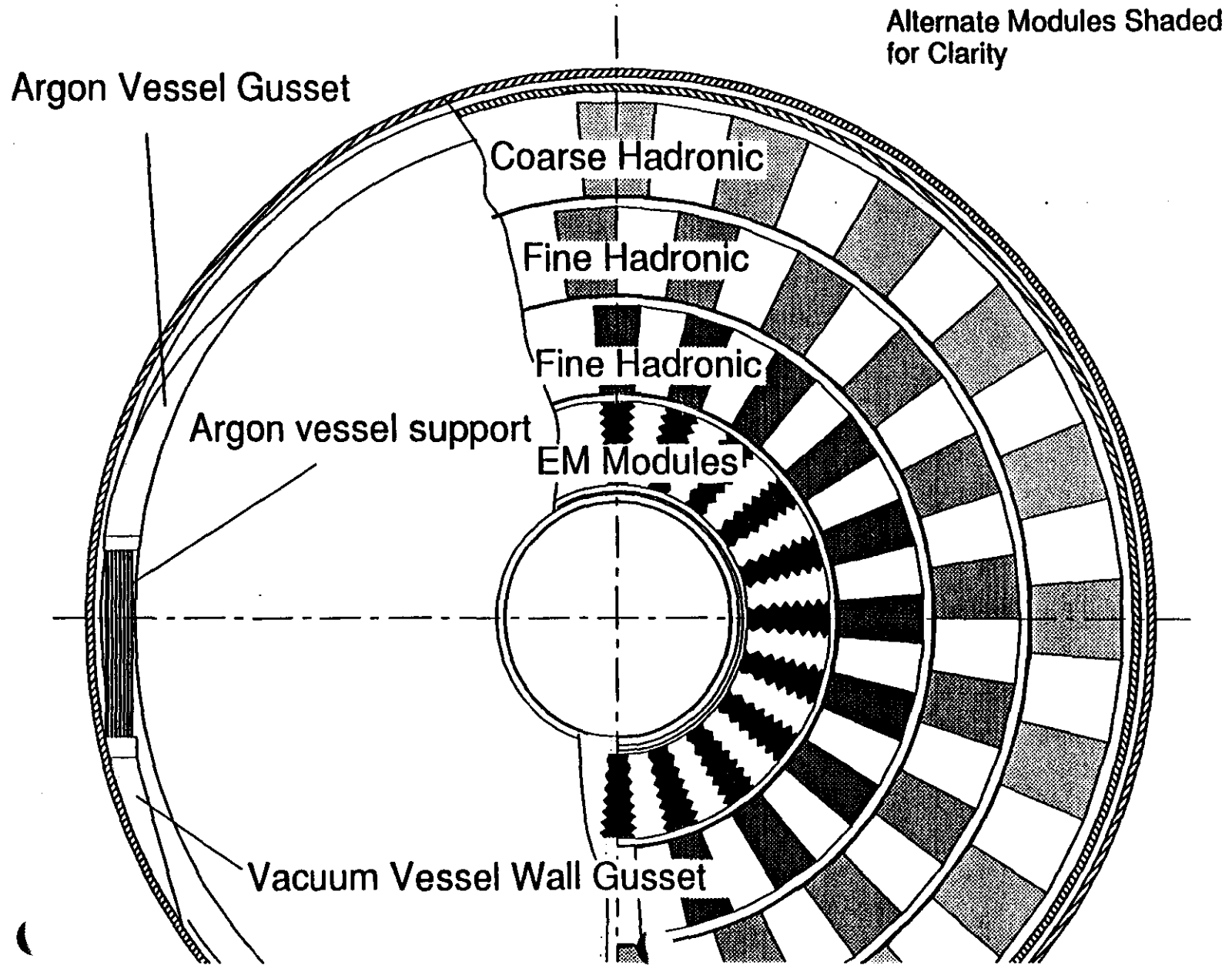
Page 1-15



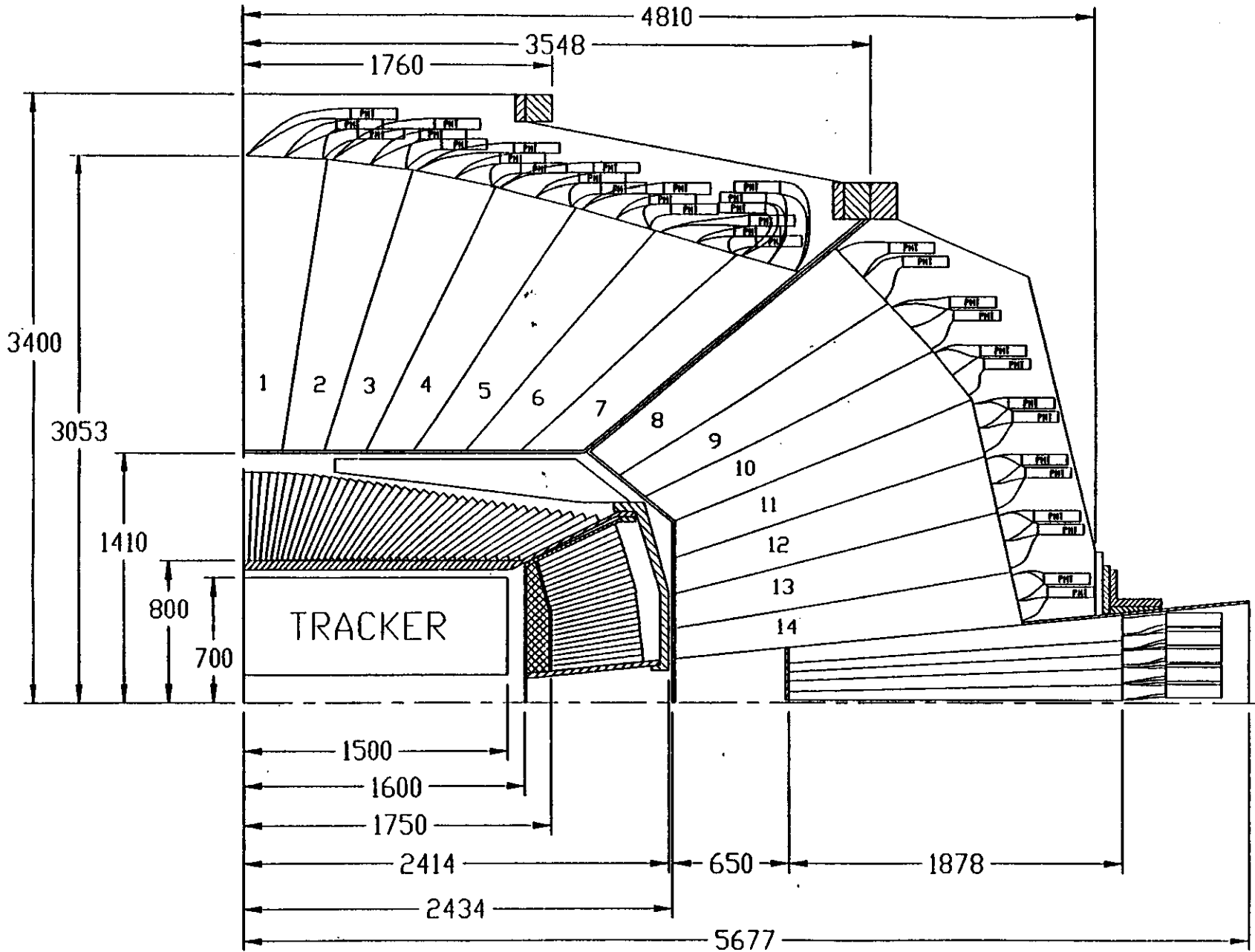
Dimensions in millimeters

LLMASON 920620 BASELINE.LAC

Barrel Cross-Section (looking down beam line)



GEM DETECTOR
 Fiber Hadron Calorimeter
 Fiber with BaF2 Design

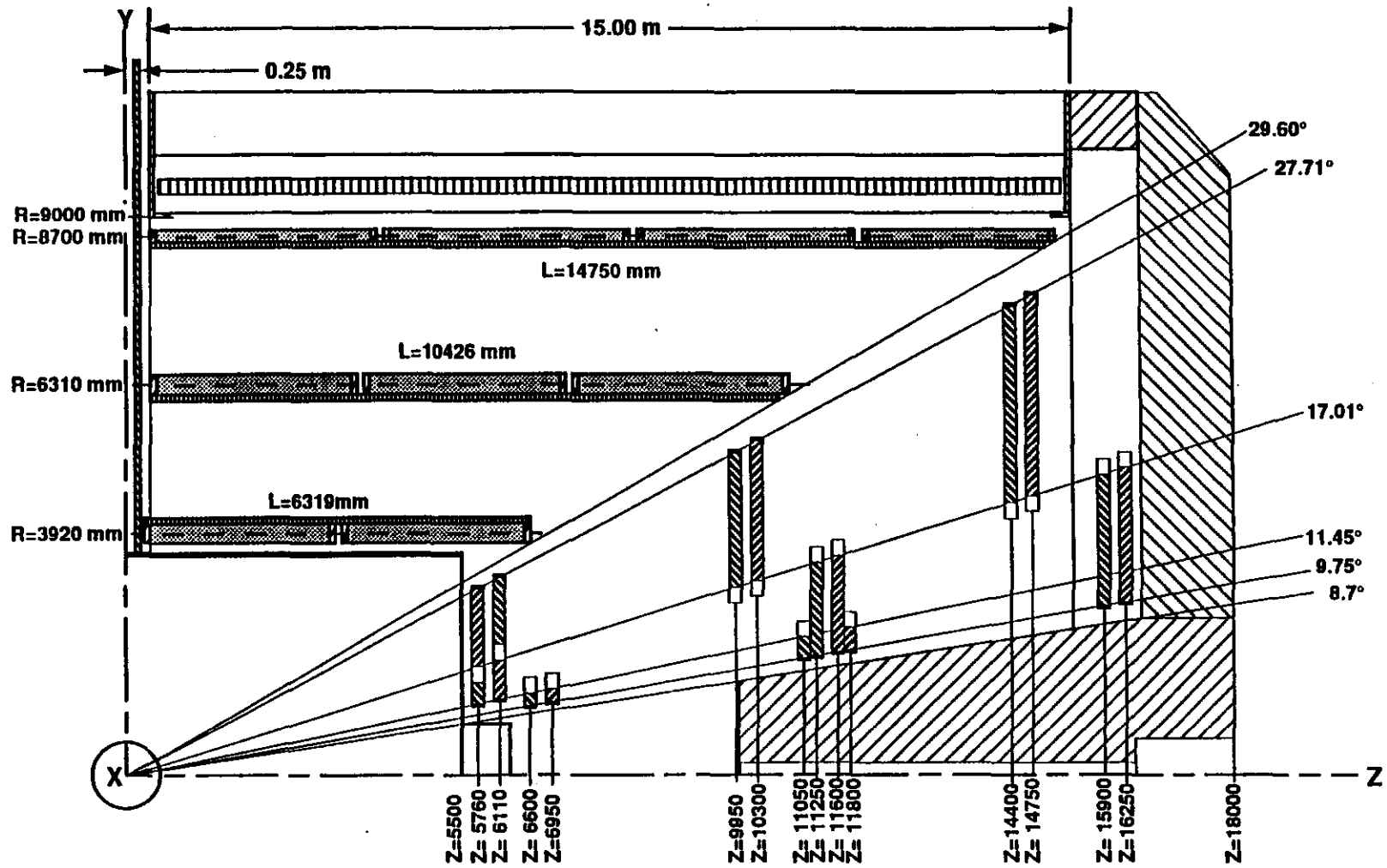


Page 1-17

A. SMIRNOV

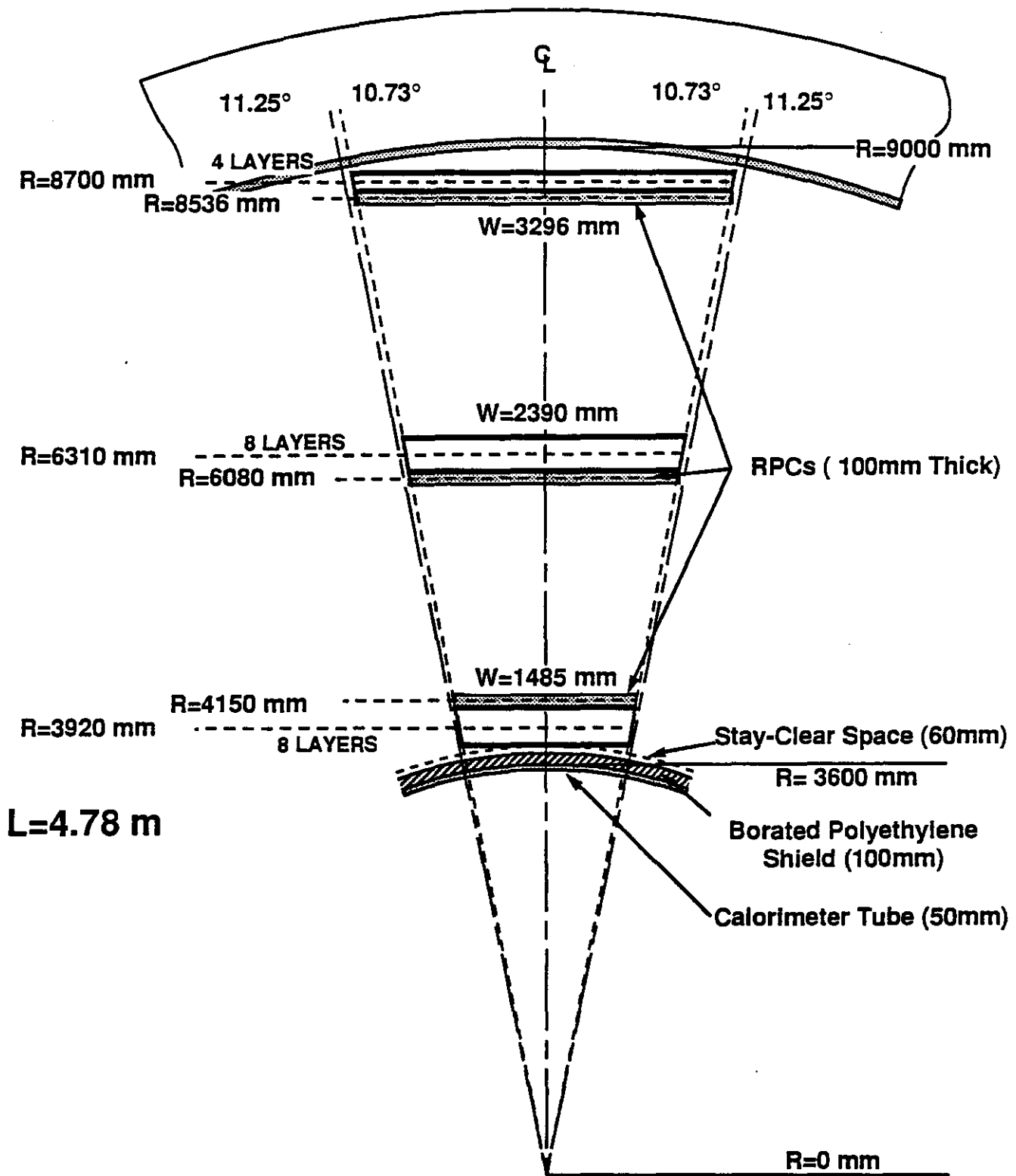
**GEM DETECTOR CALORIMETER
 FIBER HADRON & BARIUM FLUORIDE EM**

DRNL 6/30/92



GEM MUON SYSTEM CHAMBER LAYOUT BASELINE I

Draper Laboratory	
GEM Muon System Chamber Layout	
Drawn By: F. Nimblett	Rev (1)
Dwg. No: GMU0010	6/25/92
Approved by:	



GEM BARREL REGION (PDT)

(Chamber Endview)

BASELINE I

Draper Laboratory	
GEM Muon System (endview)	
Drawn By: F. Nimblett	Rev (2)
Dwg. No: GMU0002	6/26/92
Approved by:	

SCHEDULES/MILESTONES

TABLE OF CONTENTS

OVERVIEW

TABLES:

GEM Milestones
Installation Sequence Requirements
Subsystem Site Building Beneficial Occupancy Requirements
Magnet Development, Assembly and Installation
Central Tracker Development, Assembly and Installation
Calorimeter Manufacture, Assembly and Installation
Muon System Development, Assembly and Installation
Electronics and Data Acquisition Requirements

SCHEDULES/MILESTONES

SCHEDULE/MILESTONES

OVERVIEW

All milestones shown in this section have been extracted from a preliminary master schedule for the GEM detector. The master schedule was constructed based on previous experience on other detectors, discussions with the principle physicists and engineers from the various subsystems, and on certain assumptions regarding funding of the project as well as construction progress. For these reasons, the dates for many of the activities shown may be subject to revisions as the project becomes better defined. In particular, the availability of the various surface and underground facilities may be affected by funding profile restrictions. Perturbations in the availability of facilities will have serious repercussions on assembly of subsystem components into completed subsystems on-site. Although some contingency planning has been built into the schedule, substantial slips in availability of key facilities could result in serious schedule delays.

This section is organized to present top-level events and activities for the overall GEM detector first, followed by the activity sequence for installation of the detector into the underground hall. The site availability dates (Beneficial Occupancy Dates, BOD) for the various facilities are presented next. Finally, lists of significant events during the development, fabrication, assembly and installation of the different detector subsystems are presented.

SCHEDULE/MILESTONES

GEM MILESTONES

1	PAC Review	July, 1992
2.	Title 2 Coil Winding Building	August, 1992
3.	Magnet RFP	August, 1992
4.	Calorimeter Option Choice	September, 1992
5.	Title 1 Other Surface Facilities	September, 1992
6.	Muon Option Choice	October, 1992
7.	Technical Design Report	December, 1992
8.	Magnet Prime Contract	January, 1993
9.	DOE Review	January, 1993
10.	Subsystem Final Design	April, 1993
11.	BOD Coil Winding Building	February, 1994
12.	JOD Underground Experiment Hall	April, 1996
13.	Start Detector Installation	April, 1996
14.	BOD Underground Experiment Hall	August, 1996
15.	Complete Detector Installation	April, 1999
16.	Detector Ready for Physics	October, 1999

Legends:

PAC Program Advisory Committee
RFP Request For Proposals
DOE Department of Energy
BOD Beneficial Occupancy Date
JOD Joint Occupancy Date

SCHEDULE/MILESTONES

INSTALLATION SEQUENCE REQUIREMENTS

1.	Underground Hall ready (unequipped)	January, 1996
2.	Install Magnet Rails	January, 1996
3.	Underground Hall completed	April, 1996
4.	Install Magnet Flux Concentrator (south)	May, 1996
5.	Install Magnet Half Coil (south)	May, 1996
6.	Install Central Detector Support	June, 1996
7.	Install Magnet Half Coil (north)	June, 1996
8.	Install Magnet Flux Concentrator (north)	June, 1996
9.	Test Magnet Systems	November, 1996
10.	Map Magnet Field	January, 1997
11.	Install Calorimeter	May, 1997
12.	Install Muon Barrel	May, 1997
13.	Cold Test Calorimeter	August, 1997
16.	Install Muon Endcaps	November, 1997
17.	Close Magnet Halves & Test Muon System	January, 1998
18.	Open Magnet for Tracker Installation	May, 1998
19.	Install Tracker	June, 1998
20.	Close Magnet Coil Halves	November, 1998
21.	Complete Subsystem Connections	April, 1999
22.	Install Collider Components	April, 1999
23.	Complete Tests and Checkouts	March, 1999
24.	Commission Detector	July 1999
25.	Detector Ready for Physics	October 1999

SCHEDULE/MILESTONES

SUBSYSTEM SITE BUILDING BENEFICIAL OCCUPANCY REQUIREMENTS

- | | | |
|-----|---|-----------------|
| 1. | Magnet Coil Winding Building | February, 1994 |
| 2. | Magnet Assembly Building | August, 1994 |
| 3. | Magnet Vessel Construction Pad | August, 1994 |
| 4. | Magnet Steel Assembly Pad | October, 1994 |
| 5. | Muon Assembly Building | January, 1995 |
| 6. | Operations and Office Building | January, 1995 |
| 7. | Calorimeter Assembly Building | March, 1995 |
| 8. | Utilities Building | January, 1996 |
| 9. | Central Tracker Building (Central Facility) | January, 1996 |
| 10. | Electronics Rooms in Cable Shaft | July, 1996 |
| 11. | Gas Mixing Building | September, 1996 |

Source: MH
Updated:

SCHEDULE/MILESTONES

MAGNET DEVELOPMENT, ASSEMBLY AND INSTALLATION

- | | | |
|-----|---|-----------------|
| 1. | BOD Coil Winding Building | February, 1994 |
| 2. | Complete Magnet Design | April, 1994 |
| 3. | BOD Magnet Assembly Building | August, 1994 |
| 4. | Complete Winding First Coil | September, 1994 |
| 5. | Start Assembly of First Magnet Half Section | October, 1994 |
| 6. | Start Assembly of Forward Field Shapers | June, 1995 |
| 7. | Start Magnet Installation Underground | April, 1996 |
| 8. | Complete Magnet Installation | November, 1996 |
| 9. | Complete Magnet Cold Testing & Mapping | March, 1997 |
| 10. | Reclose Magnet After Tracker Installation | December, 1998 |

Source: L Parlier
Updated: 6/26/92

SCHEDULE/MILESTONES

CENTRAL TRACKER DEVELOPMENT, ASSEMBLY AND INSTALLATION

1. Research and Development Complete April, 1994

Silicon Tracker

1. Start Prototype Development January, 1993
2. Start Electronics Production January, 1994
3. Start Silicon Detector Production March, 1994
4. Start Ladder Assemblies June, 1995

IPC Tracker

1. Start Electronics Production March, 1994
2. Start Module Fabrication June, 1994
3. Start Module Assembly April, 1995

System Assembly and Installation

1. Start Equipment Installation in Facility January, 1996
2. Beneficial Occupancy of Facility June, 1996
3. Start Module Beam Testing at SSCL June, 1996
4. Start Silicon/IPC Assembly October, 1997
5. Start Installation in Underground Hall June, 1998
6. Complete Underground Installation September, 1998
7. Complete Tracker Testing December, 1998
8. Tracker Ready for Commissioning April, 1999

Source: K Morgan
Updated: 6/22/92

SCHEDULE/MILESTONES

CALORIMETER MANUFACTURE, ASSEMBLY AND INSTALLATION

- | | | |
|----|-----------------------------------|----------------|
| 1. | Complete Final Design | April, 1994 |
| 2. | Start Component Manufacture | May, 1994 |
| 3. | BOD Calorimeter Assembly Building | March, 1995 |
| 4. | Complete Subsystem Assembly | August, 1996 |
| 5. | Complete Subsystem Testing | November, 1996 |
| 6. | Start Installation | April, 1997 |
| 7. | Complete Installation | August, 1997 |
| 8. | Complete System Testing | October, 1997 |

Source: C Eberle
Updated: 6/24/92

SCHEDULE/MILESTONES

MUON DEVELOPMENT, ASSEMBLY AND INSTALLATION

- | | | |
|---|--|----------------|
| 1 | Complete CDR Barrel/Endcap | August 1994 |
| 2 | Complete Manufacture Barrel
and Endcap Prototype | June 1995 |
| 3 | Complete Test & Evaluate Barrel
and Endcap Prototype | September 1995 |
| 4 | Finalize Barrel/End Cap Design | January 1996 |
| 5 | Complete Manufacture Barrel
and End Cap Components | December 1996 |
| 6 | Complete Assembly Barrel
and End Cap Muon systems | November 1997 |
| 7 | Complete Installation Barrel
and End Cap Muon systems | March 1999 |

Source: H Baker
Update: 6/29/92

SCHEDULE/MILESTONES

ELECTRONICS & DATA ACQUISITION

TO BE PROVIDED

Source:
Updated:

FACILITIES

TABLE OF CONTENTS

OVERVIEW

FIGURES:

IR-5 Site Plan
IR-5 Site Isometric
Magnet Assembly Building Floor Plan
Magnet Assembly Building Cross Section
Magnet Assembly Building Converted for Muon Module Storage
Coil Winding Building Floor Plan
Coil Winding Building Cross Section
Coil Winding Building Crane Coverage Plan
Coil Winding Building Converted for Muon Module Storage
Central Tracker Assembly and Maintenance Facility
Calorimeter Assembly Building Floor Plan
Calorimeter Assembly Building Cross Section
Calorimeter Assembly Building Crane Coverage Plan
Muon Assembly Building Floor Plan
Muon Assembly Building Cross Section
Muon Assembly Building Crane Coverage Plan
GEM Experimental Hall (3-D view)
[GEM Experimental Detector] Hall Floor Plan
Experimental Detector Hall Roof Plan
Experimental Detector Hall (center line transverse section)
Experimental Detector Hall (transverse section through North
Assembly Shaft)
Experimental Detector Hall (longitudinal center line section facing
away from ring center)
Experimental Detector Hall (longitudinal center line section facing
ring center)
Cable Electronics Shaft Floor Plan
Typical Rack Room, Cable Electronics Shaft
Transverse Section, Cable Electronics Shaft
Electronic Rack Room Iron Shield [Requirements]

TABLES:

East Complex and Central Facility Buildings
Tracker Assembly Building Facility Specification
Underground Facilities Requirements

FACILITIES

FACILITIES

OVERVIEW

1. Introduction

The GEM detector will be assembled, installed and operated at the interaction region #5 (IR-5), located on the east side of the main collider ring in Ellis County near the town of Palmer.

2. Surface Facilities

Drawings of the collider and the east experimental areas are shown in this section. The proposed layout of GEM surface facilities is displayed in the IR-5 Site Plan. The IR-5 site is in close proximity to major transportation routes, municipal services, and utilities.

Attention is being paid to road improvements leading to the site, ensuring that the wide and heavy components can be transported in a reasonable way. A rail head is available at Palmer for off-loading detector components or materials which may be brought by rail to the site.

The site layout will mainly be determined by the assembly requirements of the large components that may require difficult maneuvers during the assembly process and attention must be paid to assure that these components can be lowered with the minimum of effort into the underground hall. The alignment of the load paths to the shafts plays a vital role in this consideration.

The dedicated detector site buildings will be the magnet coil winding, magnet assembly, muon assembly, calorimeter assembly and operations. The magnet buildings will be used for muon chamber module storage after magnet construction is complete. The present plan is to assemble the central tracker at the Central Facility and transport it to IR-5. Shaft headhouses are also desirable if economically feasible.

3. Underground Facilities

The GEM detector will be housed in an underground hall whose foundation rests on Austin Chalk. The dominant factors driving the general configuration and size of the underground facilities are the configuration, installation, and maintenance requirements of the detector and accelerator systems in addition to their radiation shielding requirements.

Source: MH
Updated: 6/29/92

FACILITIES

The hall will be situated to allow for the positioning of the long axis of the detector parallel to the beam line, so that it is centered around the interaction region. The hall floor is level but not parallel with the beam pipe which drops over 0.2 meters between the north and south ends of the hall. The length and the width of the hall are determined by the detector installation and maintenance access requirements.

Two large shafts are required for the installation of the detector within the time span allowed by the present collider start up schedule. Each assembly shaft will be closed with a minimum 8 meter thick removable radiation shield after detector installation is complete.

The detector cable and fiber readout services will exit the underground hall via the electronic room access shaft situated on the west side of the hall. This will also contain several levels of shielded modules equipped with racks of electronics equipment. The electronics rooms are positioned underground to minimize delay between detector electronics and trigger electronics. A utility shaft on the opposite side of the hall will permit the routing of the technical and conventional utility systems to the hall and detector.

Each wall of the experimental hall will have gangways for access around the detector and the survey monuments. This complex will be connected to the various elevator and stair systems contained in the utility and electronics shafts for access and egress. For emergency egress the collider tunnel may also be used.

Two identical 100/20 metric ton bridge cranes are required in the experimental hall to install the detector. The cranes must be capable of being operated simultaneously, but independently, from separate portable control stations. They must also be capable of tandem operation from a single control. In addition, the surface will be equipped with the necessary heavy lift cranes that will lower the detector components down the proper assembly shaft.

FACILITIES

East Complex

Building Identification	Dim (meters)			Area m ²	Area ft ²	Required Occ
	L	W	H			
IR5 Coil Winding Building						Feb-94
Assembly	105	30	16	3,150	33,888	
Gantry Crane - 30 t						
Gantry Crane - 30 t						
Shops	17.5	8.5	4	149	1,601	
Offices	42.5	8.5	4	361	3,887	
IR5 Magnet Assembly Building						Aug-94
Assembly	30	60	20	1,800	19,368	
Shops	17.5	8.5	4	149	1,601	
Offices	42.5	8.5	4	361	3,887	
IR5 Muon Assembly Building						Jan-95
Assembly	100	30	12	3,000	32,280	
Crane - 30/10 ton						
Crane - 10 ton						
Shops	17	8	4.5	136	1,463	
IR5 Calorimeter Assembly Building						Mar-95
Assembly	50	15	14	750	8068	
Crane - 50/10						
Clean Rms and Test area	50	15	10	750	8068	
IR5 Detector Operations Building	40	28	2 lvl	2,240	24,102	Jan-95
IR5 Utility Building	80	24	8	1,920	20,659	Jan-96
IR5 Intallation Gantry Crane - 50/20 tons						Mar-96
IR5 Installation Shaft Cover (north)	26	18	n/a	468	5,036	Jan-96
IR5 Installation Shaft Cover (south)	26	18	n/a	468	5,036	Jan-96
IR5 Personnel Headhouse	16	16	4	256	2,755	Mar-96
IR5 Equipment Headhouse	22	16	4	352	3,788	Mar-96
IR5 Gas Mixing Building	17	10	4	170	1,829	Aug-97

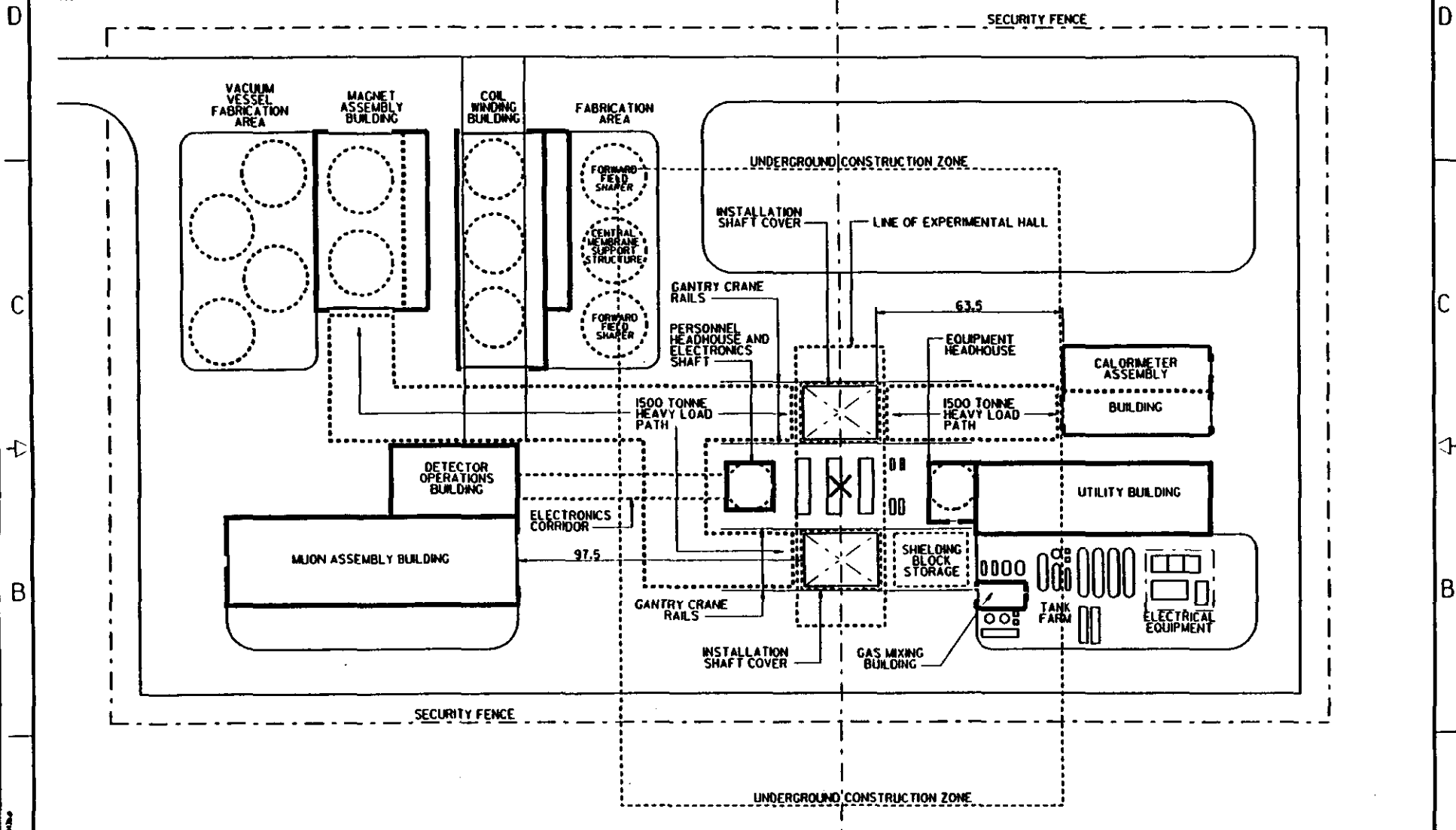
Central Facility

CF Tracker Facility (GEM)	30	20	6	600	6456	Jan-96
----------------------------------	----	----	---	-----	------	--------

Source: TVP/jng
Updated: 6/23/92



4 3 2



SITE PLAN

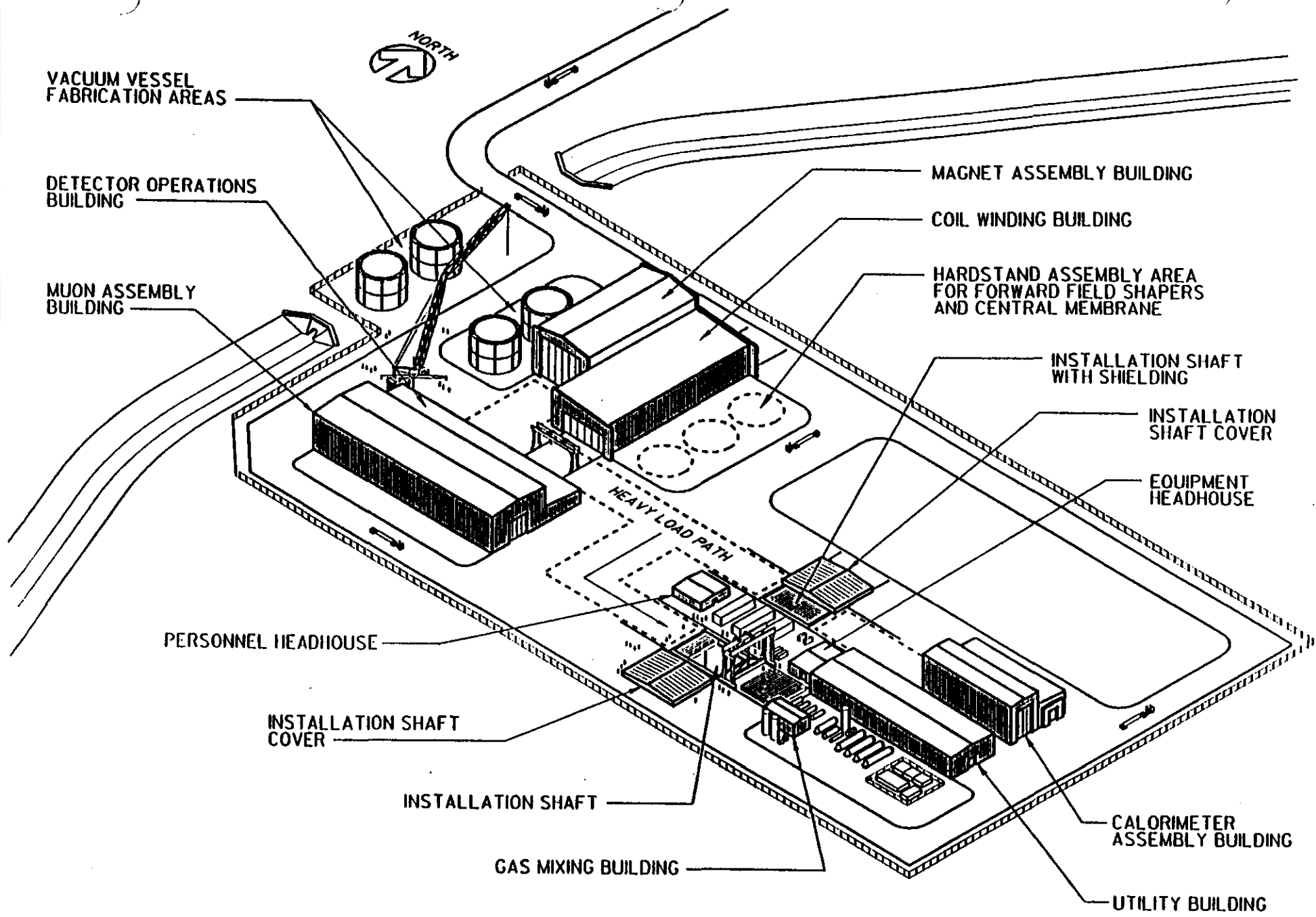
DIMENSIONS ARE SHOWN IN METERS UNLESS NOTED OTHERWISE.

THIS IS A CAD GENERATED DRAWING. DO NOT MAKE MANUAL REVISIONS OR ALTERATIONS.

PHYSICS RESEARCH DIVISION 		GEM EXPERIMENTAL FACILITIES IR-5 SITE PLAN		SCALE NONE DATE 6-15-99 BY C	PROJECT NUMBER DRAWING NUMBER SHEET NUMBER B 1
DESIGNER K. HAWKES	CHECKED APPROVED IN CHARGE T. PROSAPPO	CONTRACT NUMBER DE-AC35-97R0406	DRAWING CONTROL NUMBER GCD-00043		

REF. FILES ATTACHED
 /home/nava/pru/kenton/gem/gcd00042.b

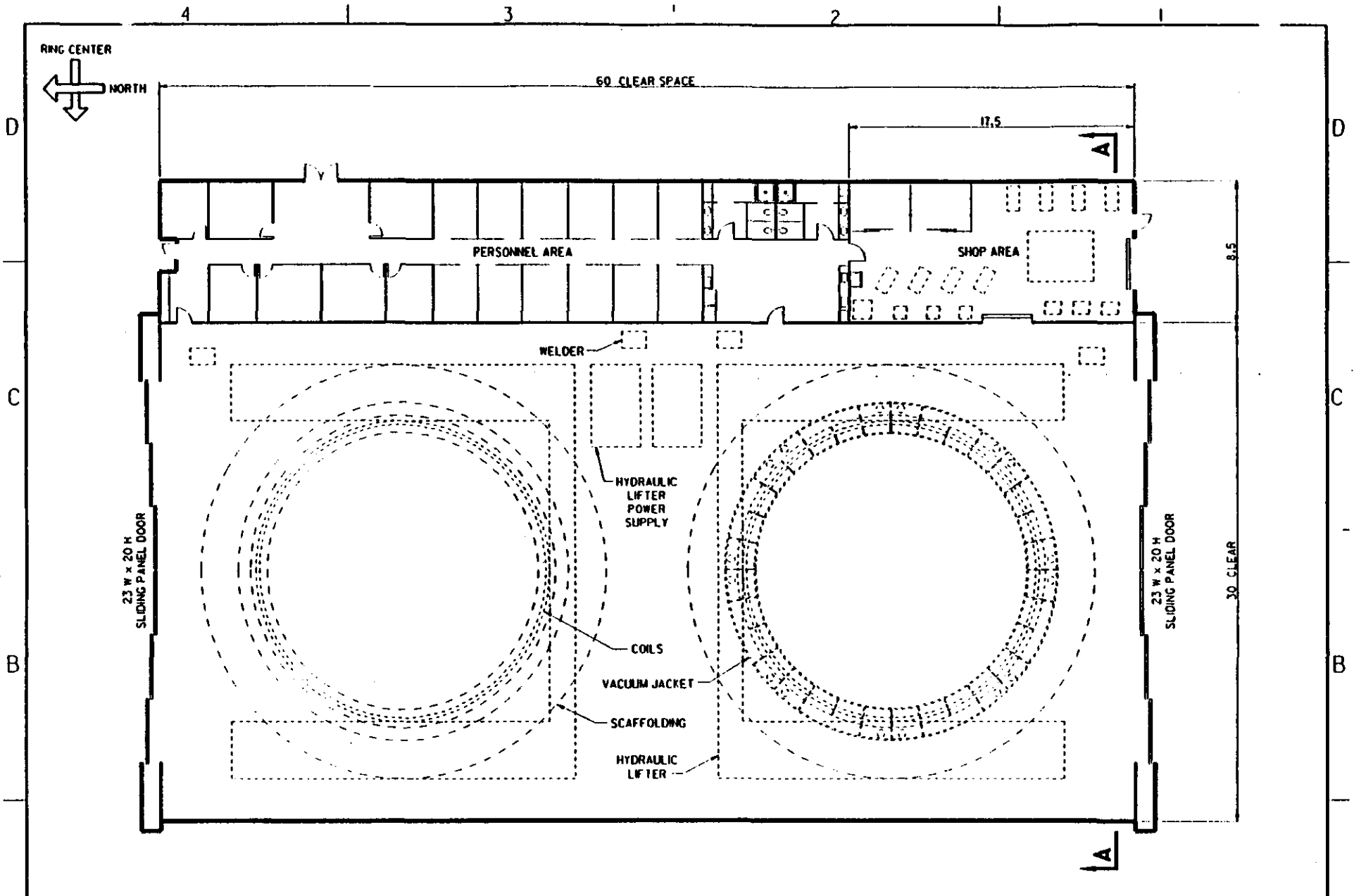
4 3 2



Page 2.5

IR-5 SITE

TVP/kh/hh - 5/14/92 - GC0000157



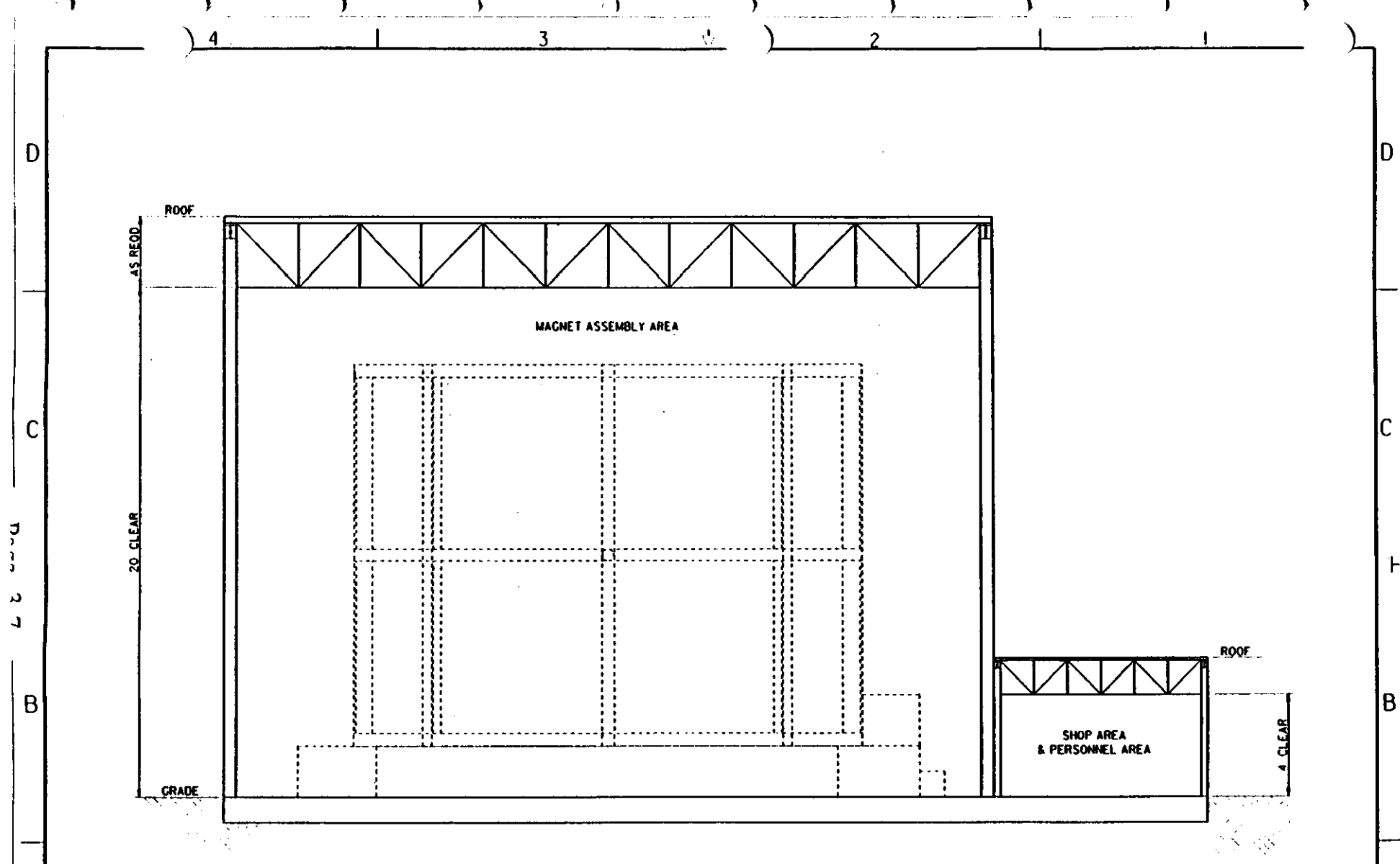
FLOOR PLAN

THIS IS A CAD GENERATED DRAWING. DO NOT MAKE MANUAL REVISIONS OR ALTERATIONS.

DIMENSIONS ARE SHOWN IN METERS UNLESS NOTED OTHERWISE.

	HAZLETT READ	PHYSICS RESEARCH DIVISION		GEM EXPERIMENTAL FACILITIES		PROJECT NUMBER
	PROSAPRO	CONTRACT NUMBER DE-25-X-000006		MAGNET ASSEMBLY BUILDING		DRAWING NUMBER
	GCD-000130	SHEET 1 OF 1		FLOOR PLAN		DATE 04-08-92

FIGURE 7-2



SECTION A-A

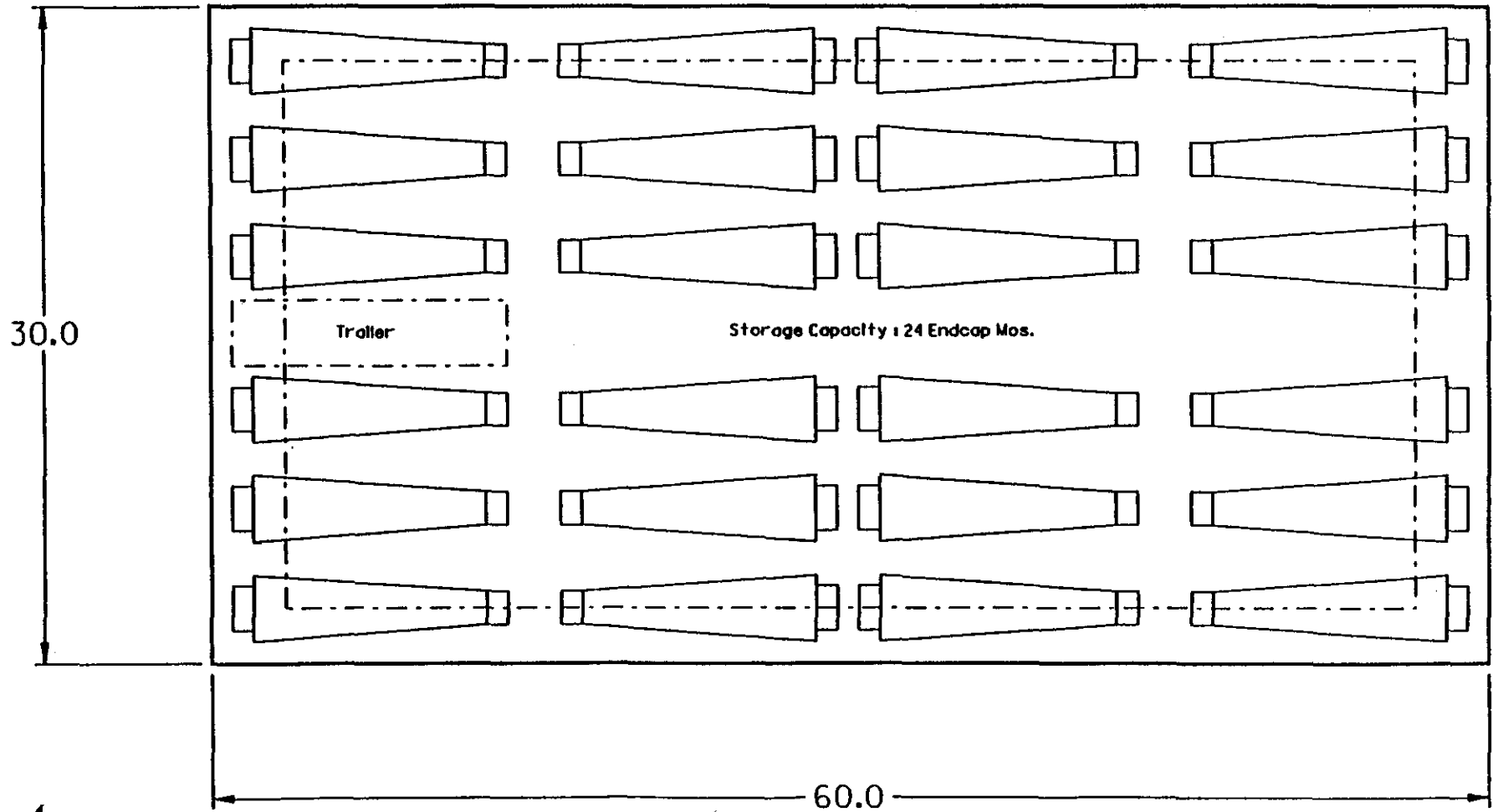
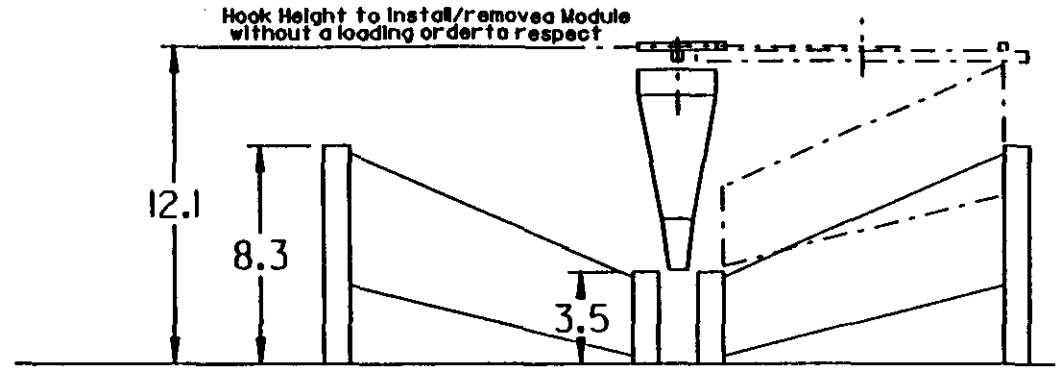
DIMENSIONS ARE SHOWN IN METERS UNLESS NOTED OTHERWISE.

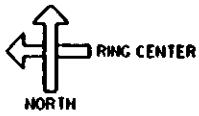
THIS IS A CAD GENERATED DRAWING. DO NOT MAKE MANUAL REVISIONS OR ALTERATIONS.

	DESIGNER H HAZLETT	CHECKED T PROSAPRO	 PHYSICS RESEARCH DIVISION	 SUPERCONDUCTING SUPERCELLULAR LABORATORY OAK RIDGE	CONTRACT NUMBER DE-AC05-87OR21400	GEM EXPERIMENTAL FACILITIES		SCALE 1:50	PROJECT NUMBER
	MAGNET ASSEMBLY BUILDING					DATE 04-08-92	DRAWING NUMBER		
	SECTION A-A					SHEET C	TOTAL SHEETS 1		
	NO OTHER COPIES ISSUED GCD-00031					REVISIONS	DATE		

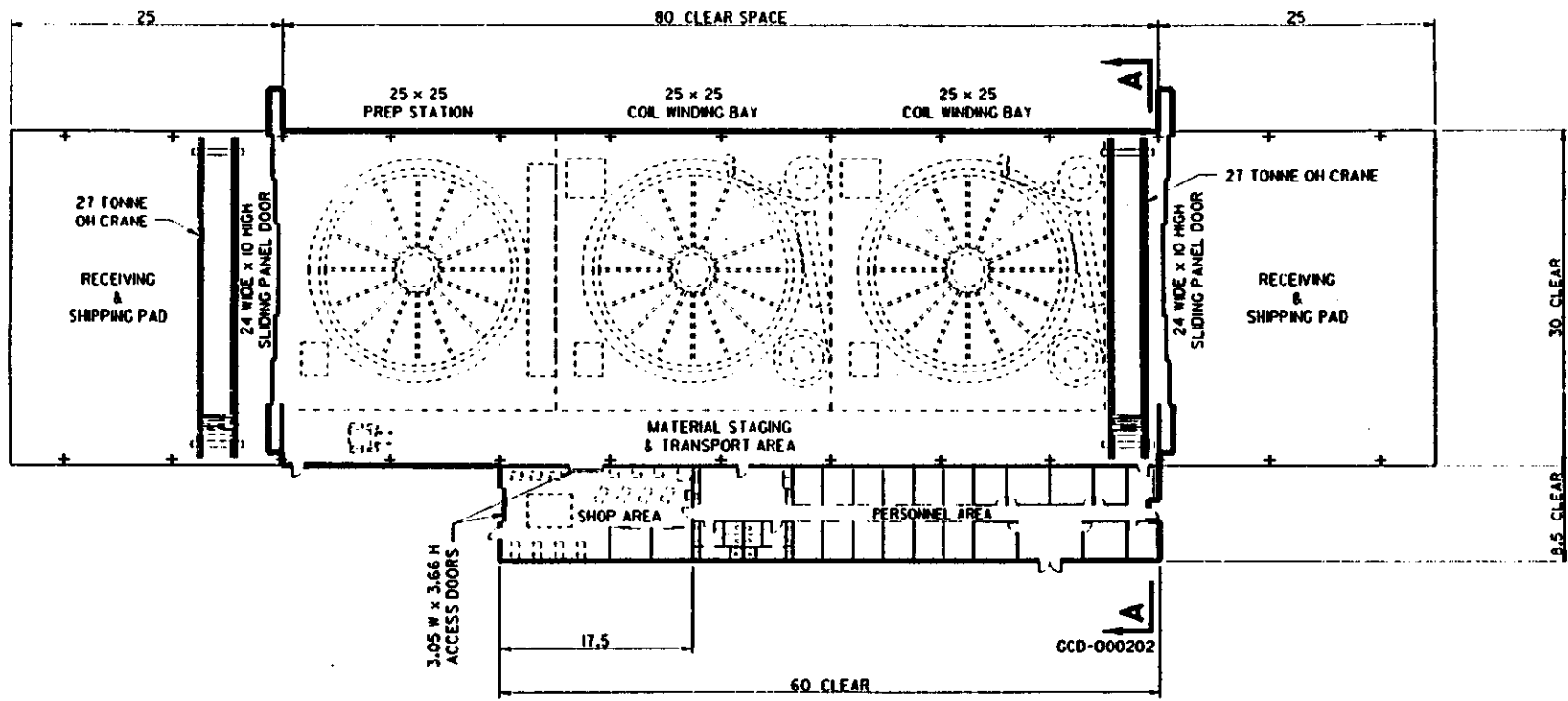
FIGURE 7-3

MAGNET ASSY BLDG.





Page 3-0



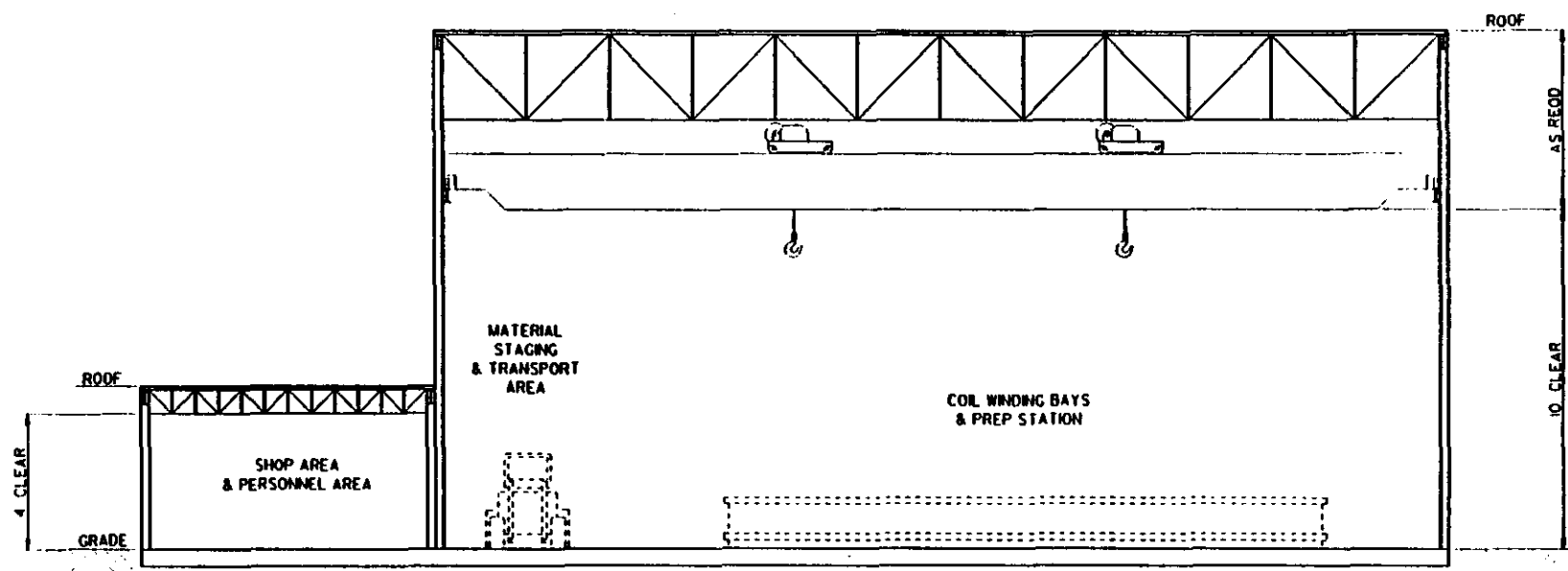
FLOOR PLAN

DIMENSIONS ARE SHOWN IN METERS UNLESS NOTED OTHERWISE.

THIS IS A CAD GENERATED DRAWING. DO NOT MAKE MANUAL REVISIONS OR ALTERATIONS.

	H HAZLETT T PROSAPIO			GEM EXPERIMENTAL FACILITIES COIL WINDING BUILDING FLOOR PLAN	PROJECT NUMBER DRAWING NUMBER GCD-000201
--	-------------------------	--	--	--	--

FIGURE 6-2



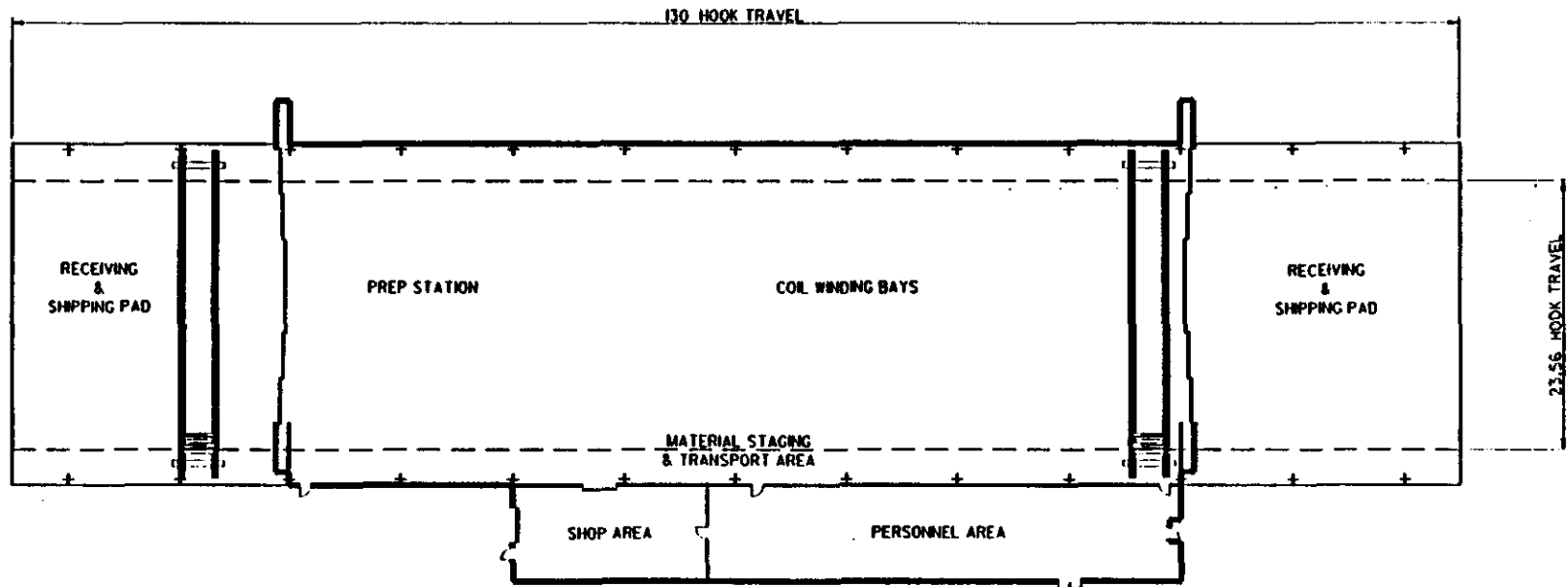
SECTION A-A

DIMENSIONS ARE SHOWN IN METERS UNLESS NOTED OTHERWISE.

THIS IS A CAD GENERATED DRAWING. DO NOT MAKE MANUAL REVISIONS OR ALTERATIONS.

	NO. 1 DATE BY CHECKED APPROVED	DESIGNED H. HAZLETT DRAWN T. PROSAPRO	PHYSICS RESEARCH DIVISION	SSC SUPPLEMENTARY SUPERFINDER LABORATORY BULLS HEAD	GEM EXPERIMENTAL FACILITIES COIL WINDING BUILDING SECTION A-A	SCALE 1/8" = 1'-0" DATE 04-12-92 DRAWN C	PROJECT NUMBER DRAWING NUMBER
	CONTRACT NUMBER H-218-92A4006	SHEET NUMBER 10 OF 10	DRAWING NUMBER GCD-000202	PROJECT NUMBER DRAWING NUMBER	SHEET NUMBER 10 OF 10	DRAWING NUMBER GCD-000202	PROJECT NUMBER DRAWING NUMBER
	CONTRACT NUMBER H-218-92A4006	SHEET NUMBER 10 OF 10	DRAWING NUMBER GCD-000202	PROJECT NUMBER DRAWING NUMBER	SHEET NUMBER 10 OF 10	DRAWING NUMBER GCD-000202	PROJECT NUMBER DRAWING NUMBER

FIGURE 6-3



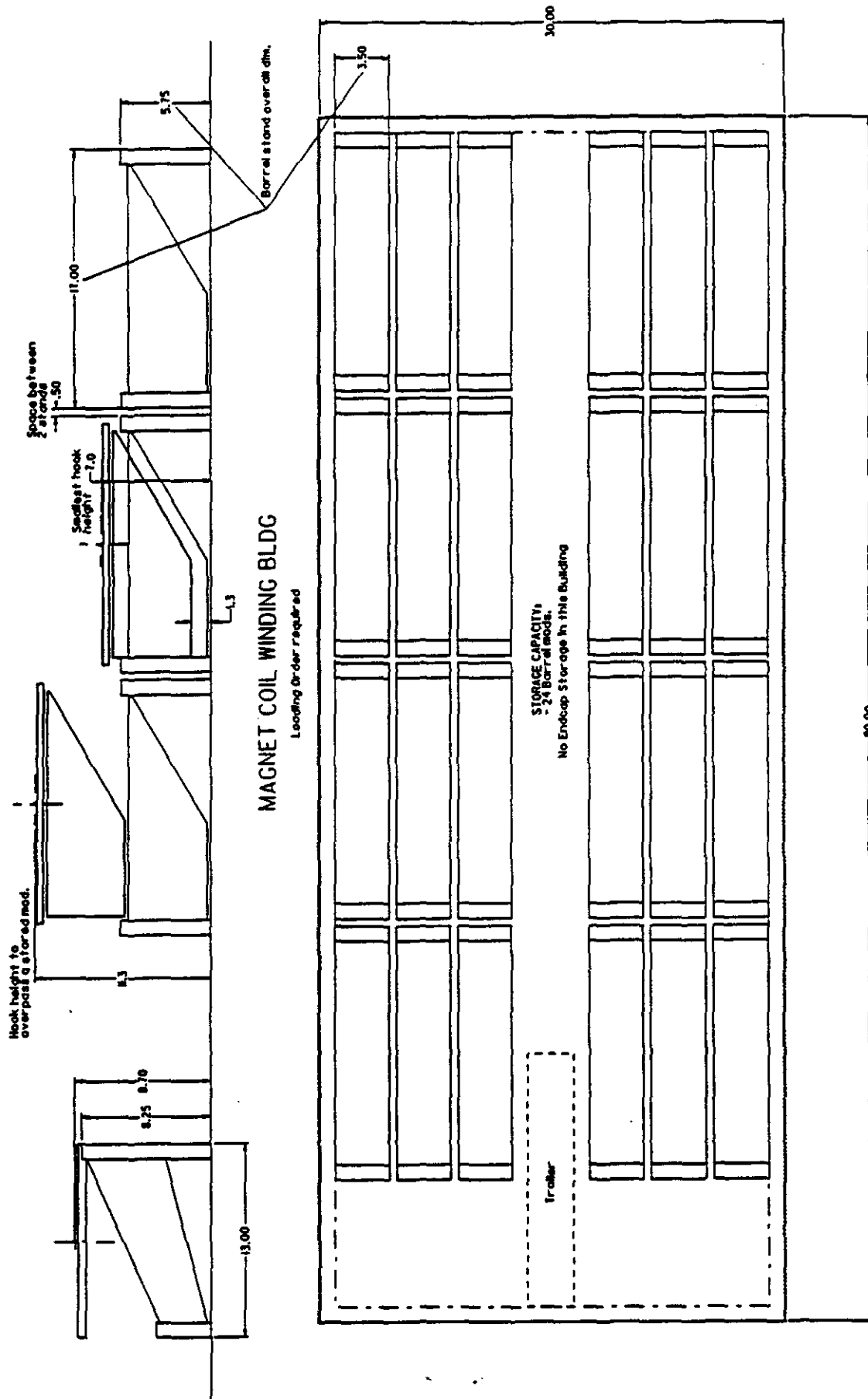
CRANE COVERAGE PLAN

DIMENSIONS ARE SHOWN IN METERS UNLESS NOTED OTHERWISE.

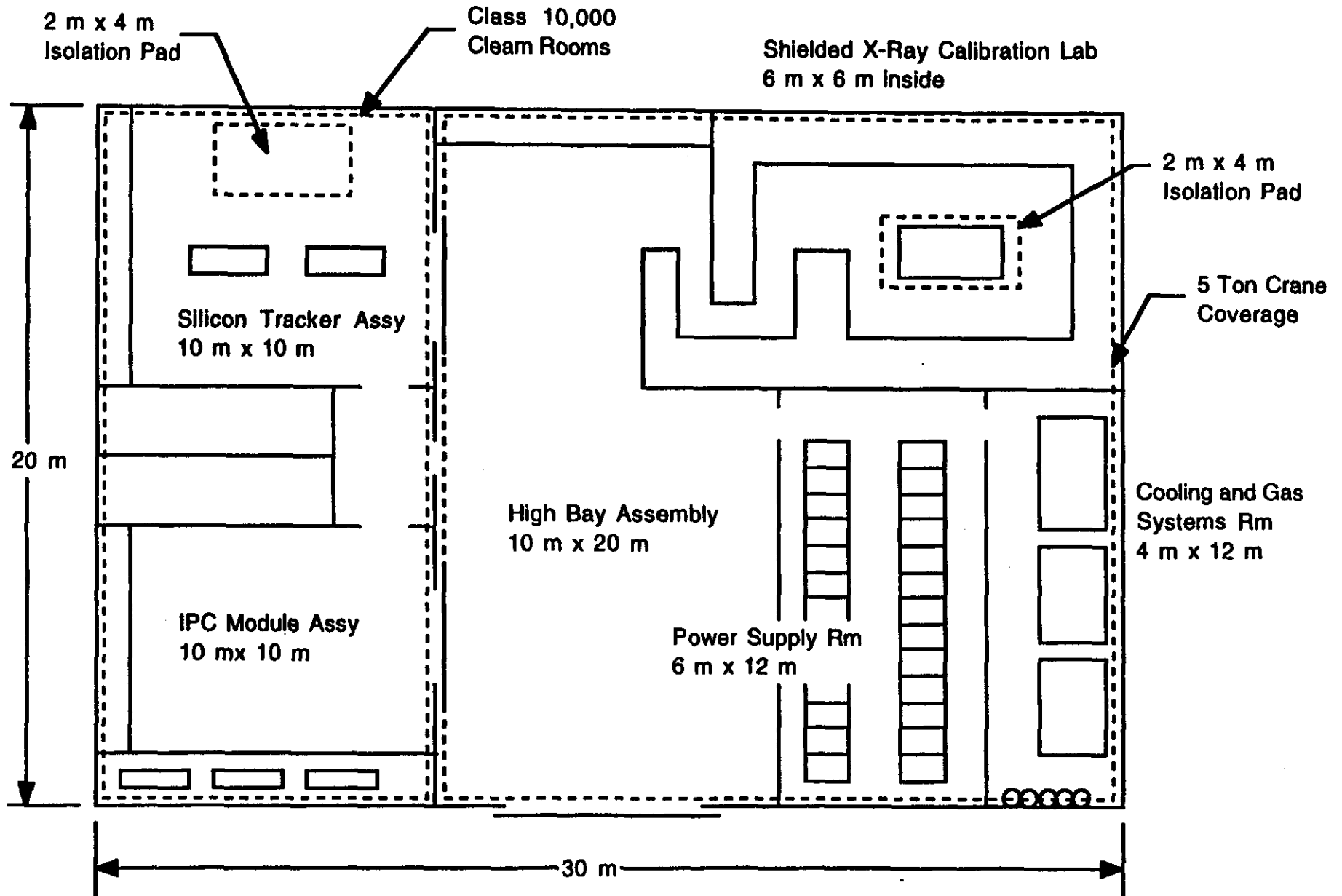
THIS IS A CAD GENERATED DRAWING. DO NOT MAKE MANUAL REVISIONS OR ALTERATIONS.

	DESIGNED BY H. HAZLETT	DRAWN BY F. PROSAPIO			GEM EXPERIMENTAL FACILITIES COIL WINDING BUILDING CRANE COVERAGE PLAN	SCALE 1:200	PROJECT NUMBER
	CHECKED BY F. PROSAPIO	DATE 04-03-92				DRAWING NUMBER	
	APPROVED BY F. PROSAPIO	SHEET C				TOTAL SHEETS 1	
	CONTRACT NUMBER DE-ACB-SPER-0006	GCD-000204				SHEET OF 1	

FIGURE 6-4



Central Tracker Assembly and Maintenance Facility



FACILITIES

TRACKER ASSEMBLY BUILDING FACILITY SPECIFICATION (Located at SSC Central Facility)

General: All areas to be temperature and humidity controlled

Silicon Assembly Class 10,000 Clean Room

Space: 10 x 10 m
Vibration isolated floor: 2 x 4 m
Storage: 10 m of wall space
Compressed air for air balance hoists

IPC Assembly Class 10,000 Clean Room

Space: 10 x 10 m
Storage: 10 m of wall space
Plumbed with bottled N₂

High Bay Areas

Central:

Space: 20 x 20 m
Storage: 10 m of wall space
5 ton crane coverage

X-Ray Calibration Laboratory:

Space: 6 x 6 m (free)
Vibration isolated floor: 2 x 4 m
5 ton crane coverage
HV, gas and cooling supplies
Personnel shielding

Electronics Area:

Space: 20 x 20 m
Clean electric power TBD A

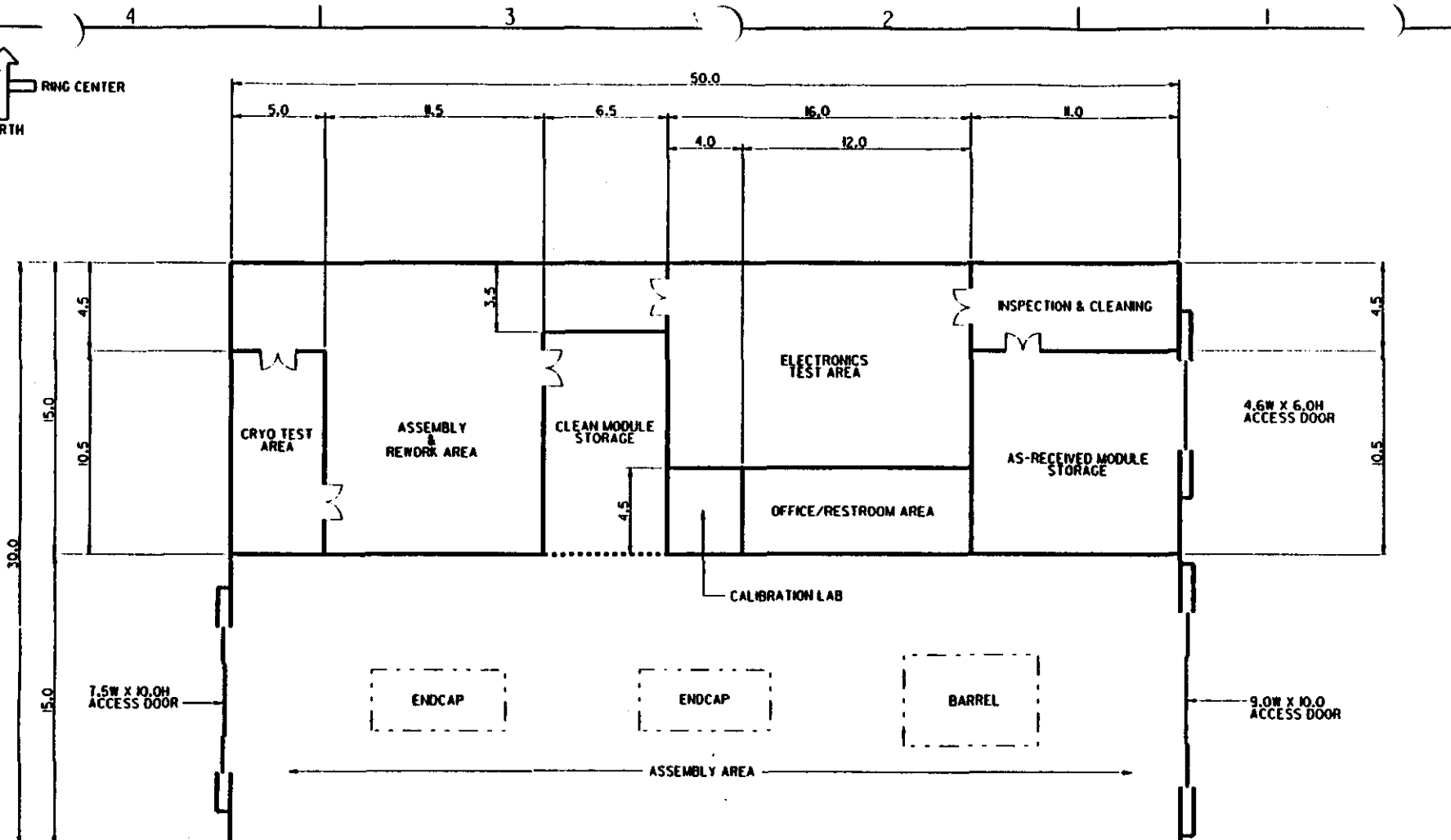
Cooling/Gas Area:

Space: 20 x 20 m
Storage for N₂, CO₂, CF₄, Butane and water cooling systems

Storage:

Space: 15 x 5 m

SOURCE: RB/KM
UPDATED: 4/9/92
JNG



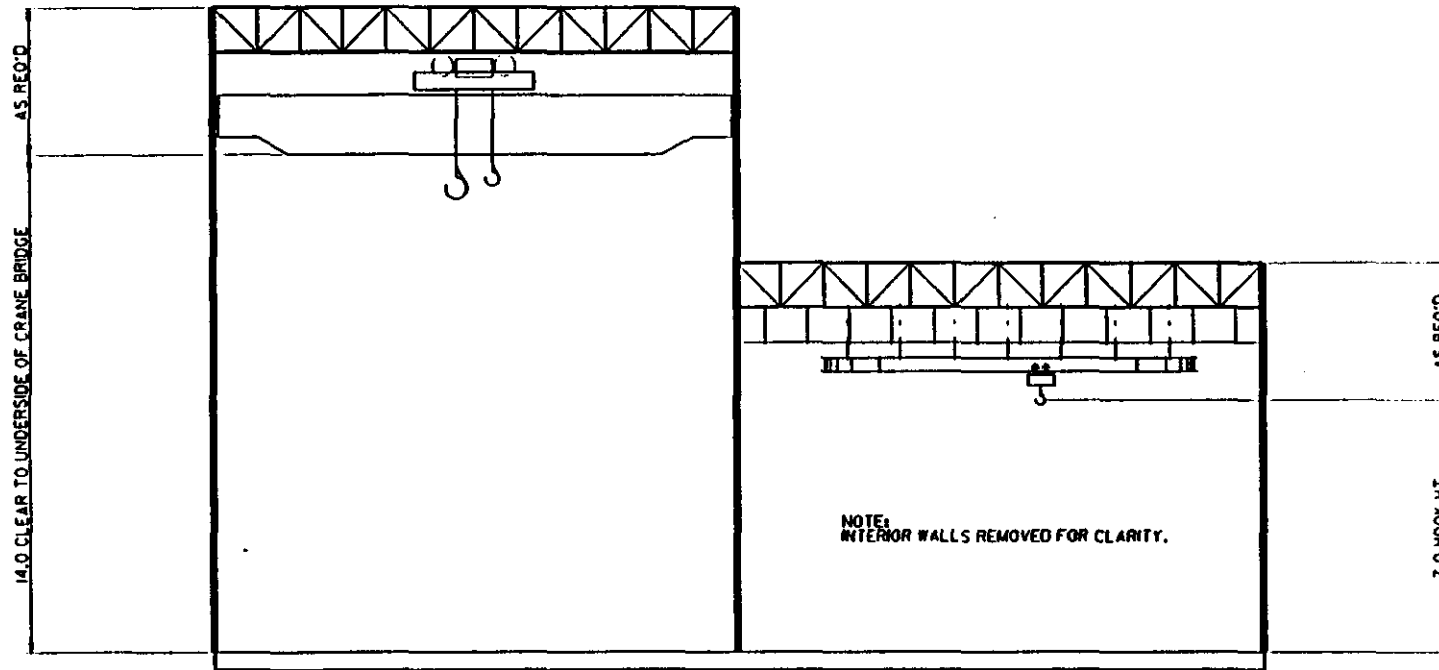
FLOOR PLAN

DIMENSIONS ARE SHOWN IN METERS UNLESS NOTED OTHERWISE.

THIS IS A CAD GENERATED DRAWING. DO NOT MAKE MANUAL REVISIONS OR ALTERATIONS.

	DESIGNED DRAWN CHECKED IN CHARGE APPROVED	MARKES F. PROSAPIO		 SUPERCONDUCTIVE SUPER COLLIDER LABORATORY DRIEHL, TEXAS	GEM EXPERIMENTAL FACILITIES CALORIMETER ASSEMBLY BUILDING FLOOR PLAN	SCALE DATE 4/27/92 THE C	PROJECT NUMBER DRAWING NUMBER	REVISION GCD-000145	
	CONTRACT NUMBER BE-ACV-890048	SHEET 1 OF 2	REVISION 1 OF 0	4 3 2 1	D C B A	4 3 2 1	1 2 3 4	1 2 3 4	
	PHYSICS RESEARCH DIVISION								GEM EXPERIMENTAL FACILITIES CALORIMETER ASSEMBLY BUILDING FLOOR PLAN
	CONTRACT NUMBER BE-ACV-890048								SHEET 1 OF 2 REVISION 1 OF 0 GCD-000145

FIGURE 10-2



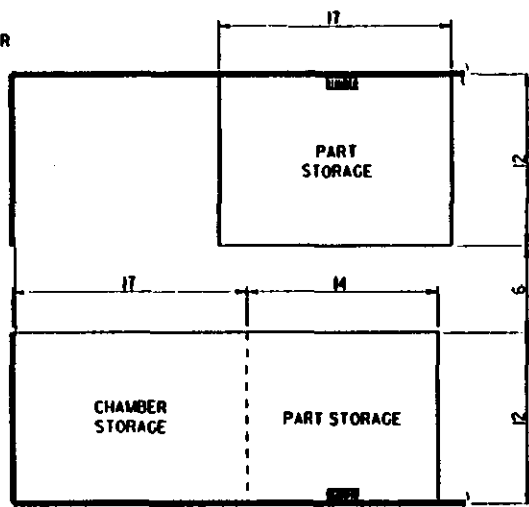
SECTION

DIMENSIONS ARE SHOWN IN METERS UNLESS NOTED OTHERWISE.

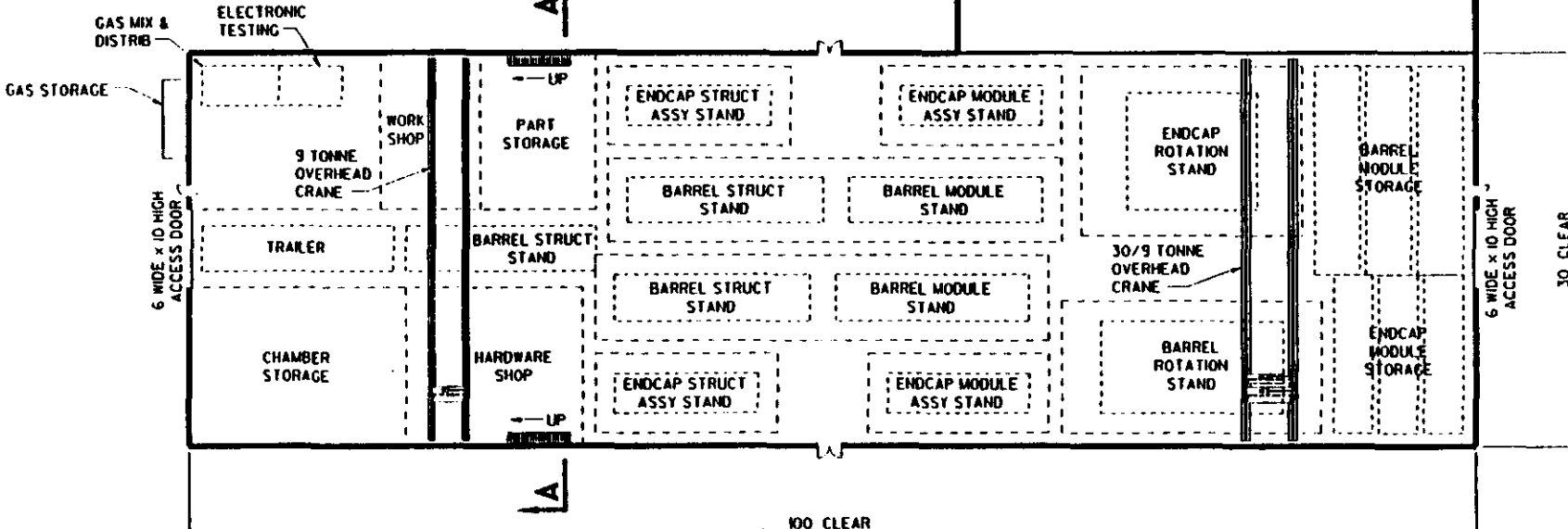
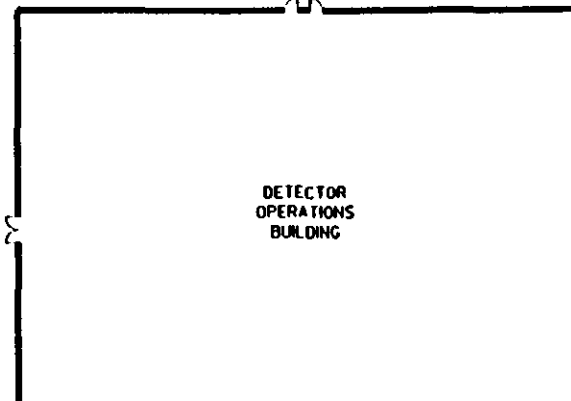
THIS IS A CAD GENERATED DRAWING. DO NOT MAKE MANUAL REVISIONS OR ALTERATIONS.

	<table border="1"> <tr> <td>DESIGNED</td> <td>DATE</td> </tr> <tr> <td>DRAWN</td> <td>DATE</td> </tr> <tr> <td>CHECKED</td> <td>DATE</td> </tr> <tr> <td>APPROVED</td> <td>DATE</td> </tr> <tr> <td>RESPONSIBLE ENGINEER</td> <td>DATE</td> </tr> <tr> <td>NAME</td> <td>DATE</td> </tr> <tr> <td>T. PROSAPRO</td> <td></td> </tr> </table>	DESIGNED	DATE	DRAWN	DATE	CHECKED	DATE	APPROVED	DATE	RESPONSIBLE ENGINEER	DATE	NAME	DATE	T. PROSAPRO		<p>PHYSICS RESEARCH DIVISION</p>		<p>GEM EXPERIMENTAL FACILITIES</p>	SCALE	PROJECT NUMBER
		DESIGNED	DATE																	
DRAWN	DATE																			
CHECKED	DATE																			
APPROVED	DATE																			
RESPONSIBLE ENGINEER	DATE																			
NAME	DATE																			
T. PROSAPRO																				
BY	DATE	DRAWING NUMBER																		
				SECTION	C															
					ISSUED FOR CONSTRUCTION	DATE														
					GCD-000147	1														

FIGURE 10-3



MEZZANINE PLAN



FLOOR PLAN

DIMENSIONS ARE SHOWN IN METERS UNLESS NOTED OTHERWISE.

THIS IS A CAD GENERATED DRAWING. DO NOT MAKE MANUAL REVISIONS OR ALTERATIONS.

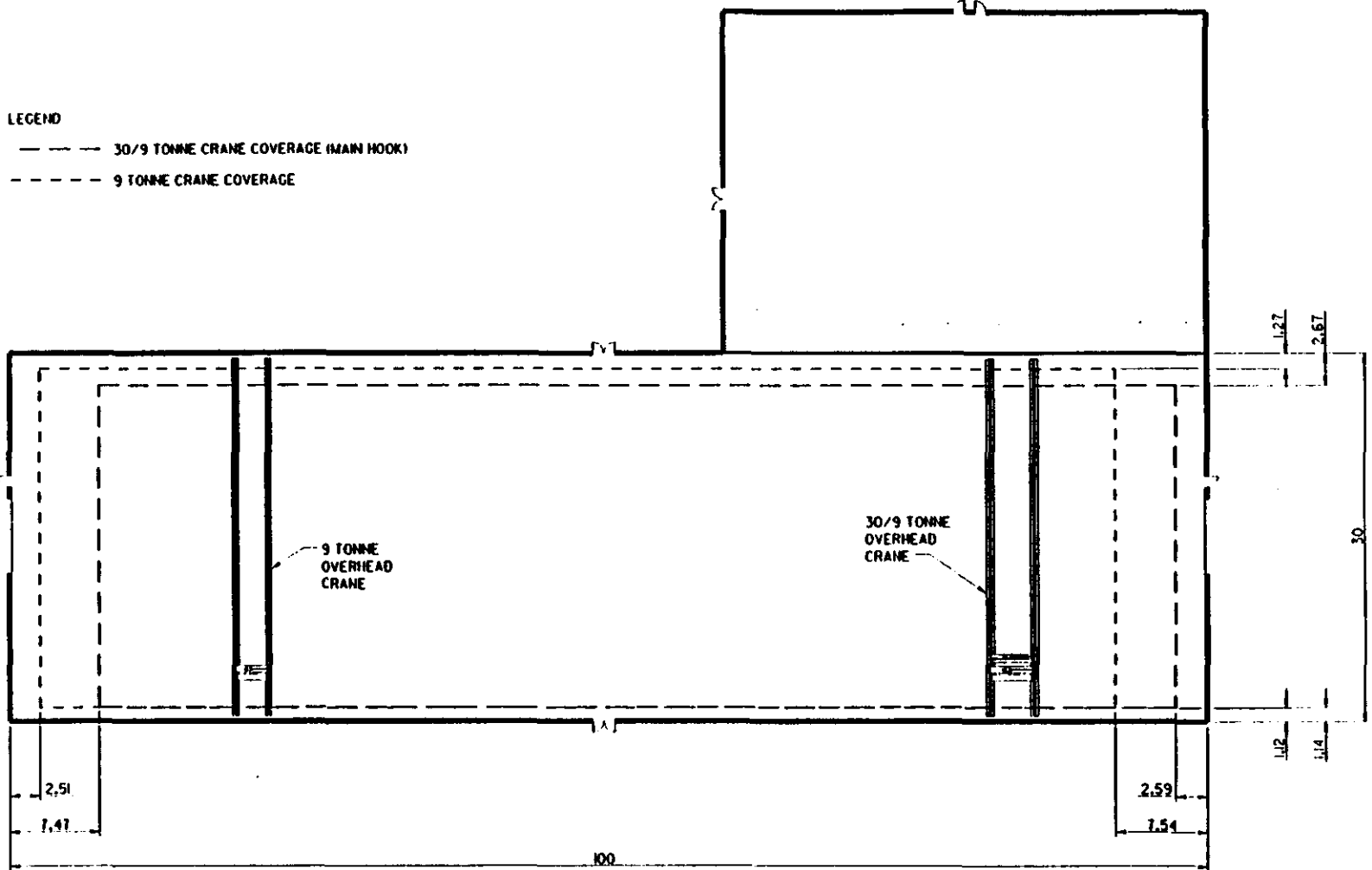
	DESIGNED H. HAZLETT	DRAWN I. PROSAPPO			GEM EXPERIMENTAL FACILITIES MUON ASSEMBLY BUILDING FLOOR PLANS	SHEET NO. 04-5-02	PROJECT NUMBER
						CONTRACT NUMBER DE-AC 75-80ER0005	GRAPHIC NUMBER
						DRAWING NUMBER GCD-00038	SHEET 1

FIGURE 9-2



LEGEND

- 30/9 TONNE CRANE COVERAGE (MAIN HOOK)
- - - 9 TONNE CRANE COVERAGE



CRANE COVERAGE PLAN

DIMENSIONS ARE SHOWN IN METERS UNLESS NOTED OTHERWISE.

THIS IS A CAD GENERATED DRAWING. DO NOT MAKE MANUAL REVISIONS OR ALTERATIONS.

	DESIGNER M HAZLETT	CHECKER T PROSAPID	SUPERCONDUCTING SUPERGRAVITY LABORATORY DULUTH, NEB.	GEM EXPERIMENTAL FACILITIES		TITLE CRANE COVERAGE PLAN	PROJECT NUMBER
	PHYSICS RESEARCH DIVISION			MUON ASSEMBLY BUILDING		DATE 04-10-92	DRAWING NUMBER
	CONTRACT NUMBER 88-0675-PER-0006			CRANE COVERAGE PLAN		NO. OF SHEETS GCD-000205	SHEET NO. 1

FIGURE 9-4

UNDERGROUND FACILITIES REQUIREMENTS

HALL

Length	100 m
Width	30 m
Distance Between Floor and Beam	13 m
Lift Clearance Above the IP	18 m

ASSEMBLY SHAFTS

Length	18 m
Width	27 m

ELECTRONICS SHAFT and ROOM

Diameter	16 m
----------	------

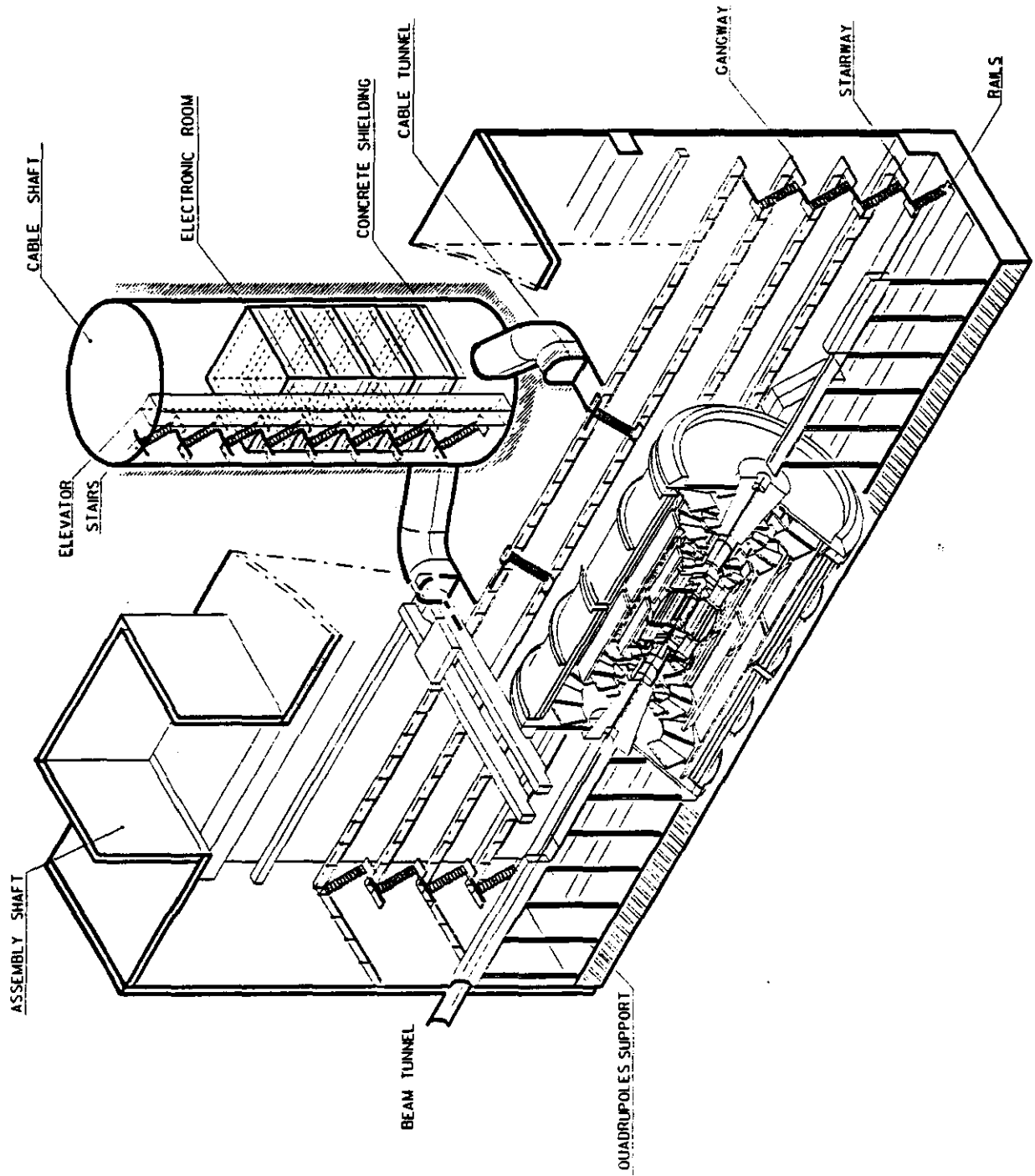
UTILITIES SHAFT

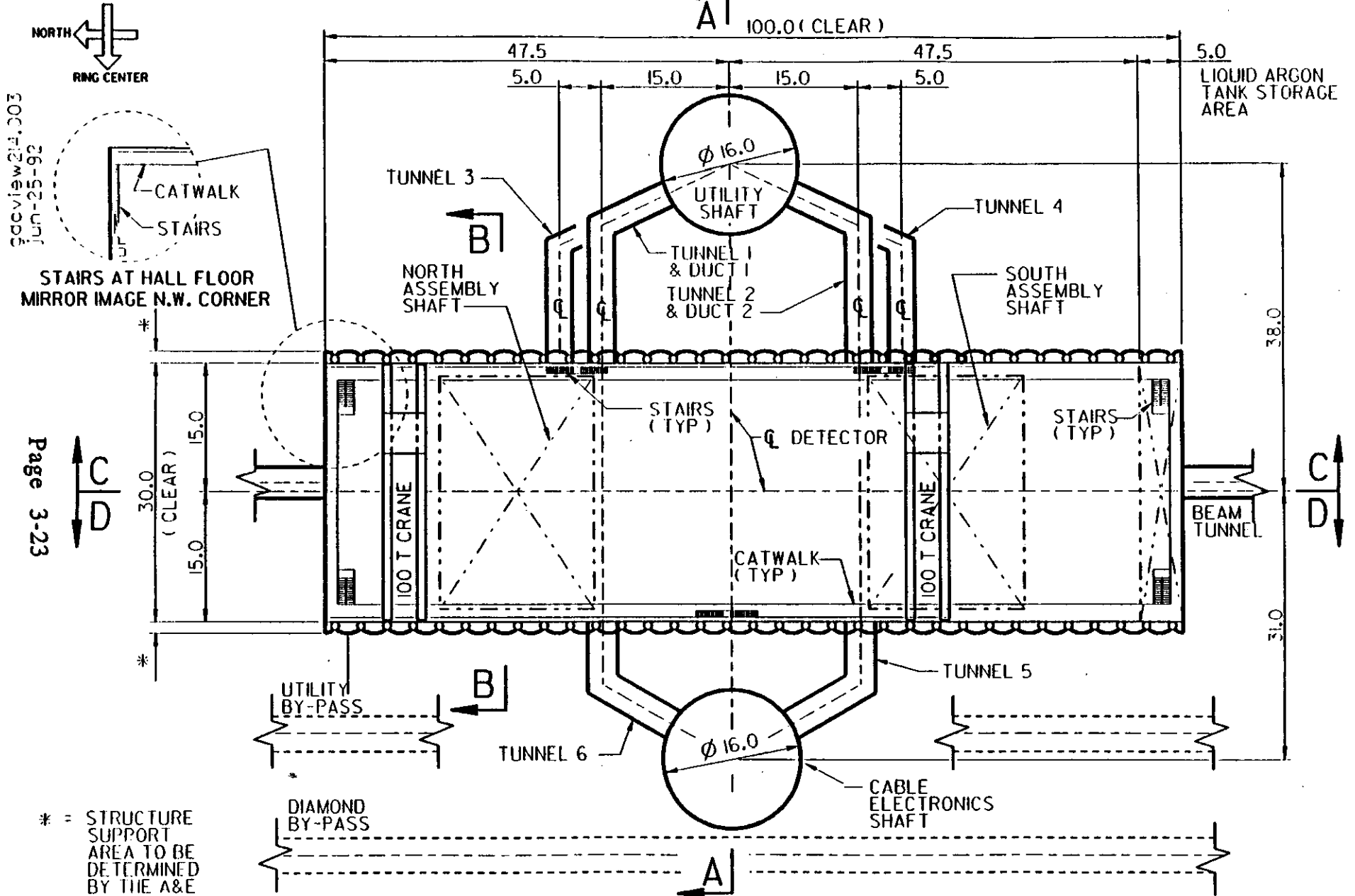
Diameter	16 m
----------	------

BRIDGE CRANES 2

Load Capacity - Main Hoist	100,000 kg
- Auxilliary Hoist	20,000 kg

GEM EXPERIMENTAL HALL - CABLE SHAFT SIDE

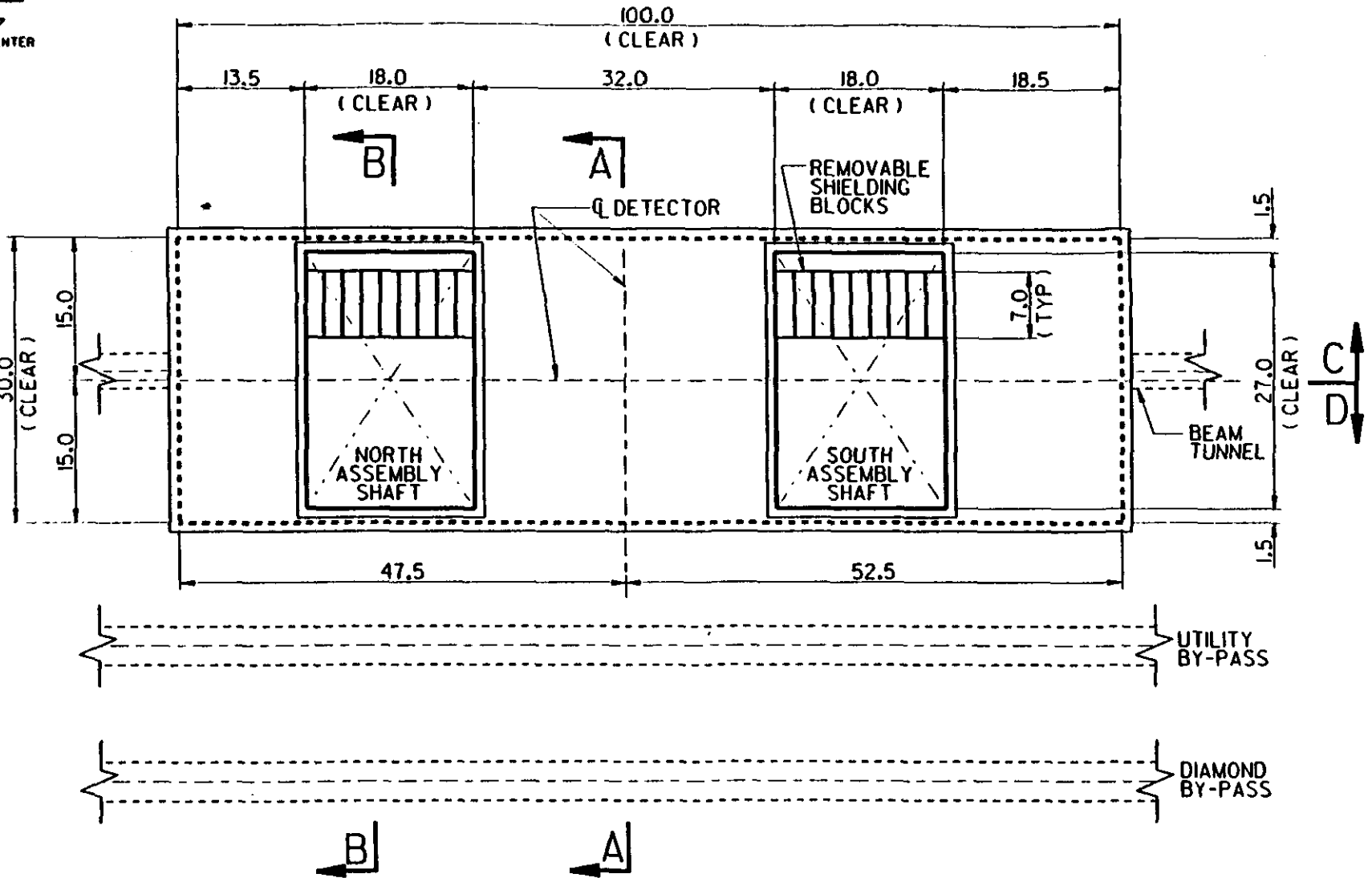
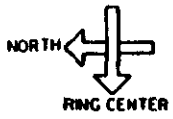




HALL FLOOR PLAN



26-55-25-92
 214,003



DRAFT

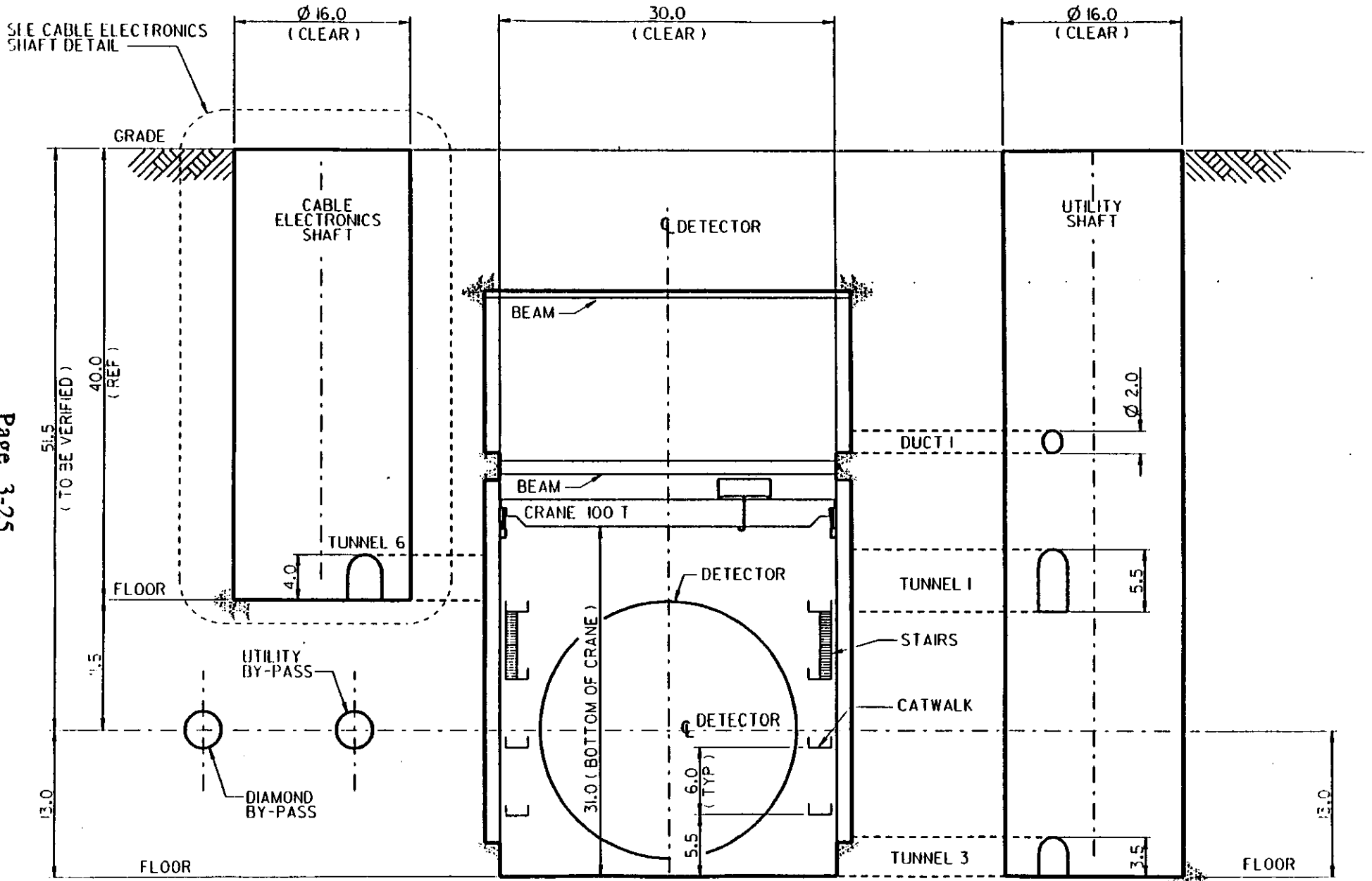
ROOF PLAN

DIMENSIONS ARE SHOWN IN METERS UNLESS NOTED OTHERWISE.

THIS IS A CAD GENERATED DRAWING. DO NOT MAKE MANUAL REVISIONS OR ALTERATIONS.

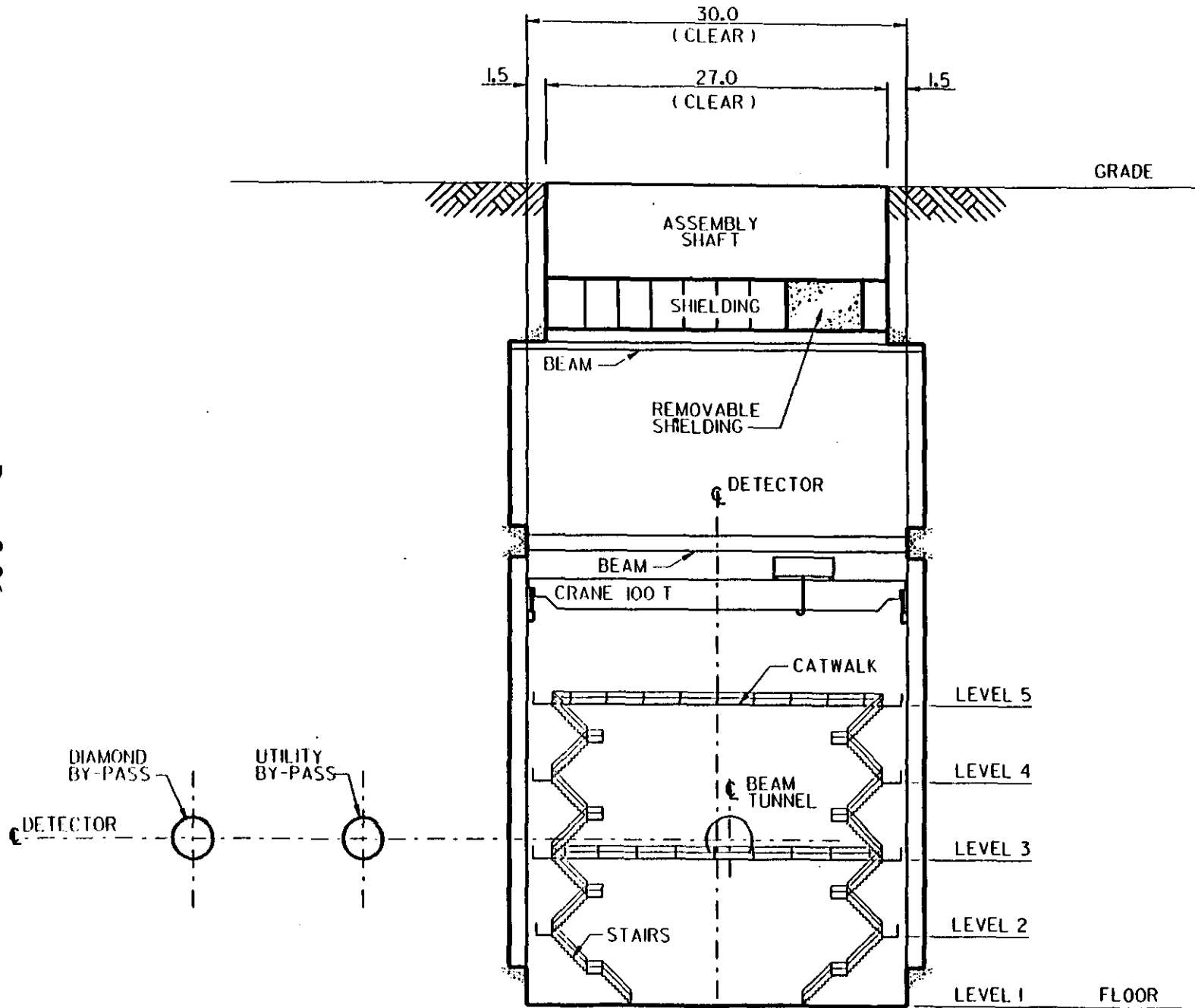
					SCALE	PROJECT NUMBER
					DATE	DRAWING NUMBER

Page 3-24
 B
 A

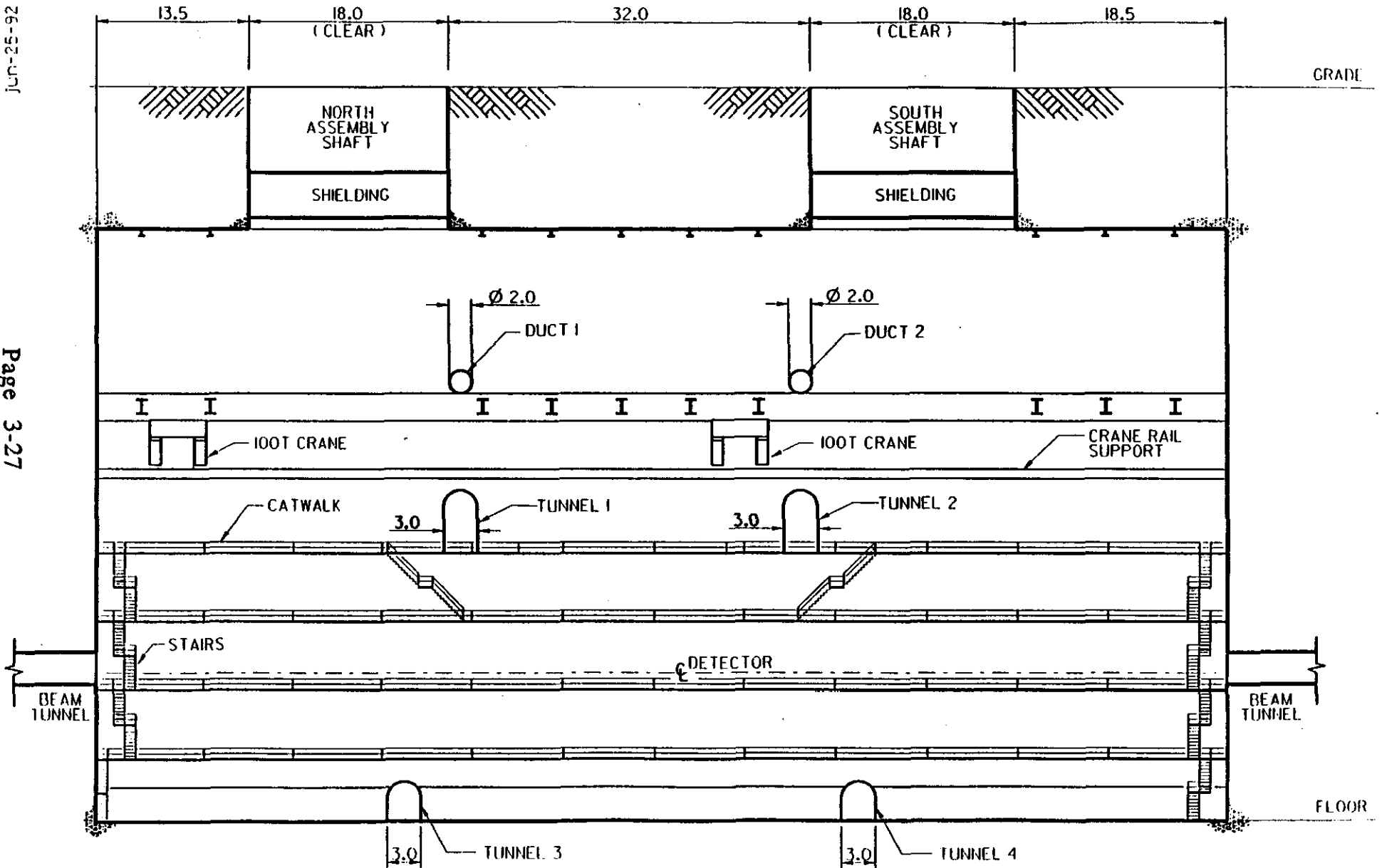


SECTION A-A



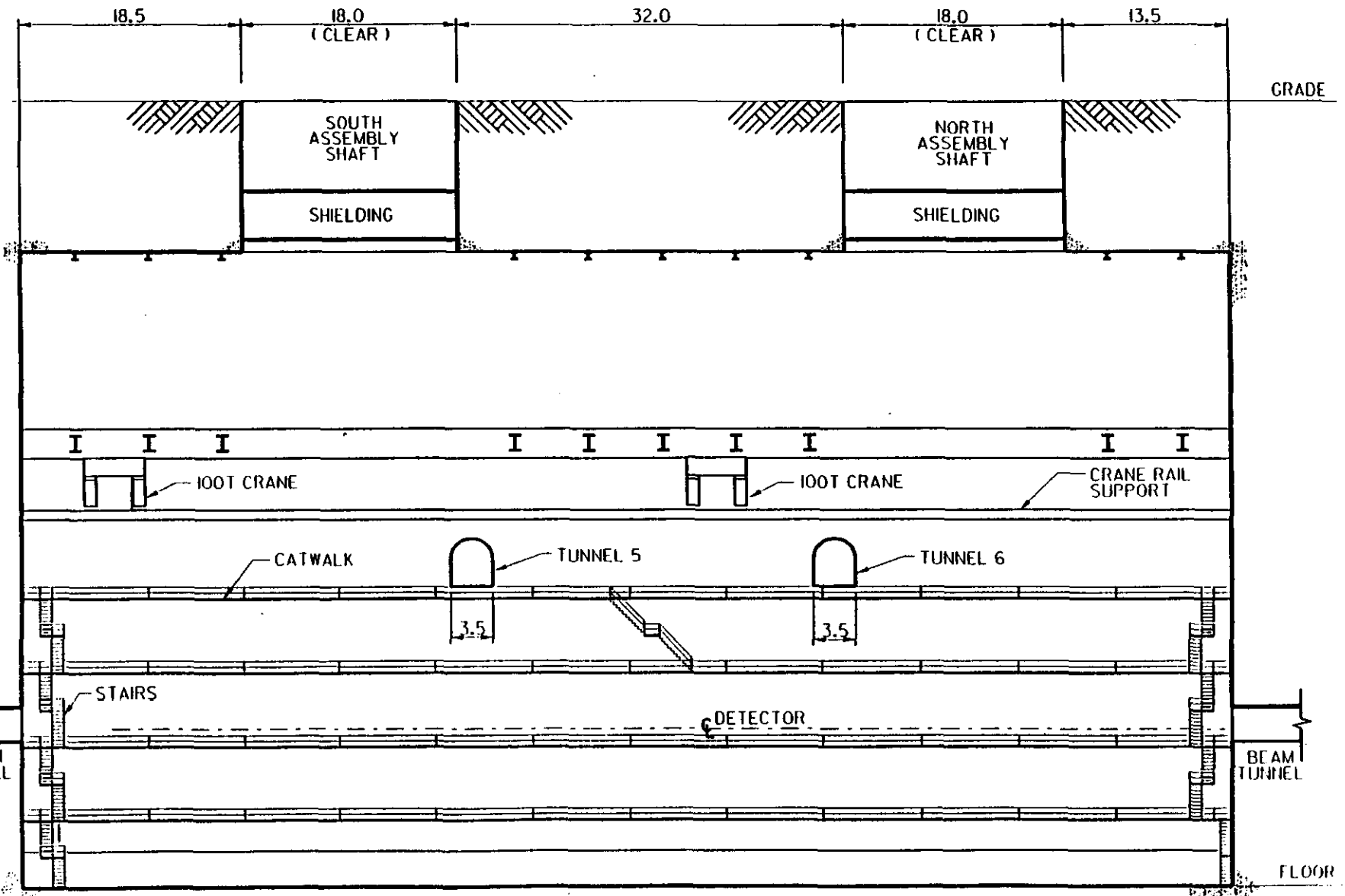


SECTION B-B



SECTION C-C



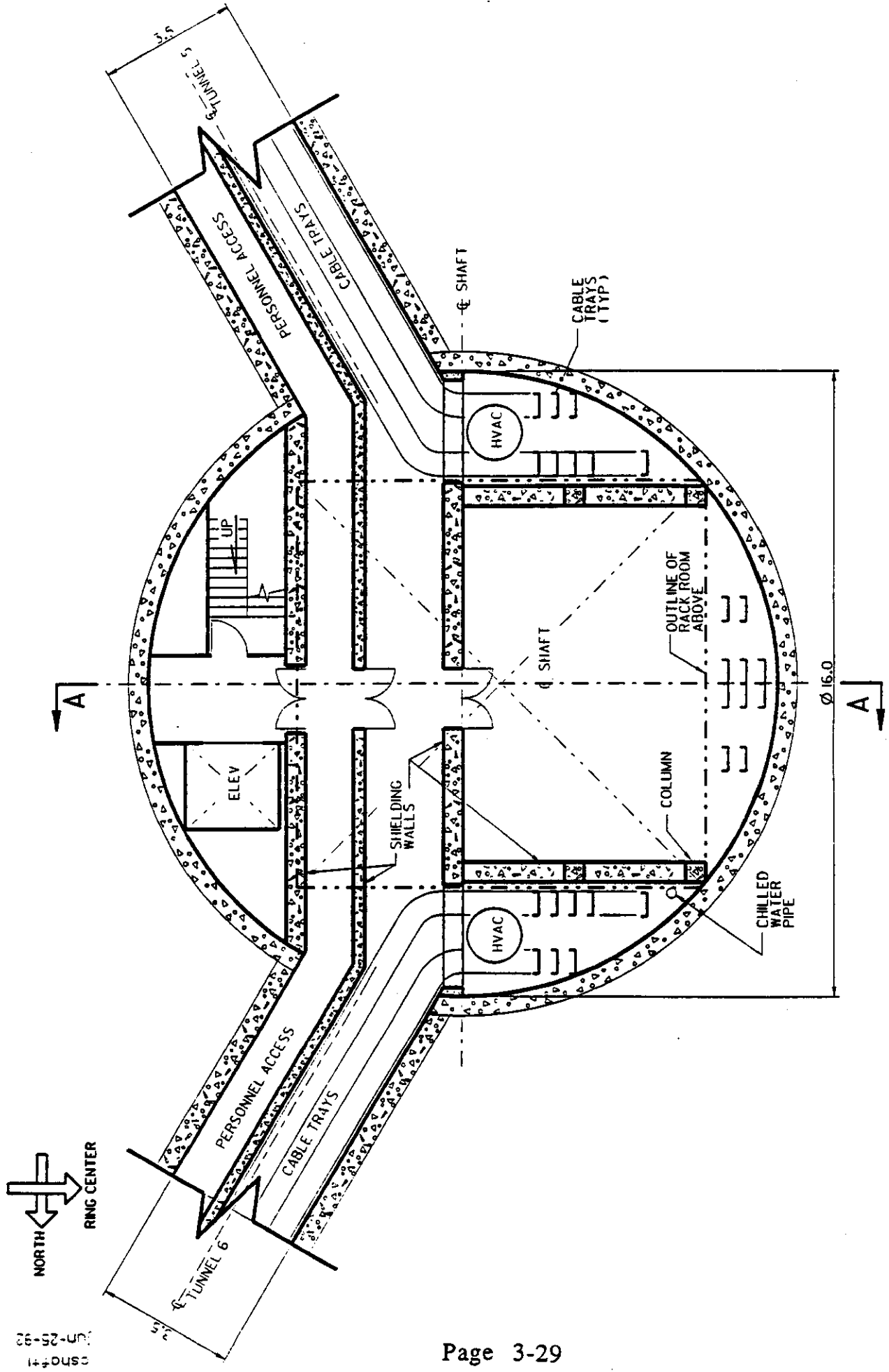


SECTION D-D



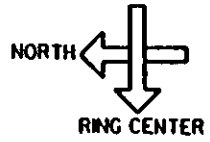


FLOOR PLAN CABLE ELECTRONICS SHAFT

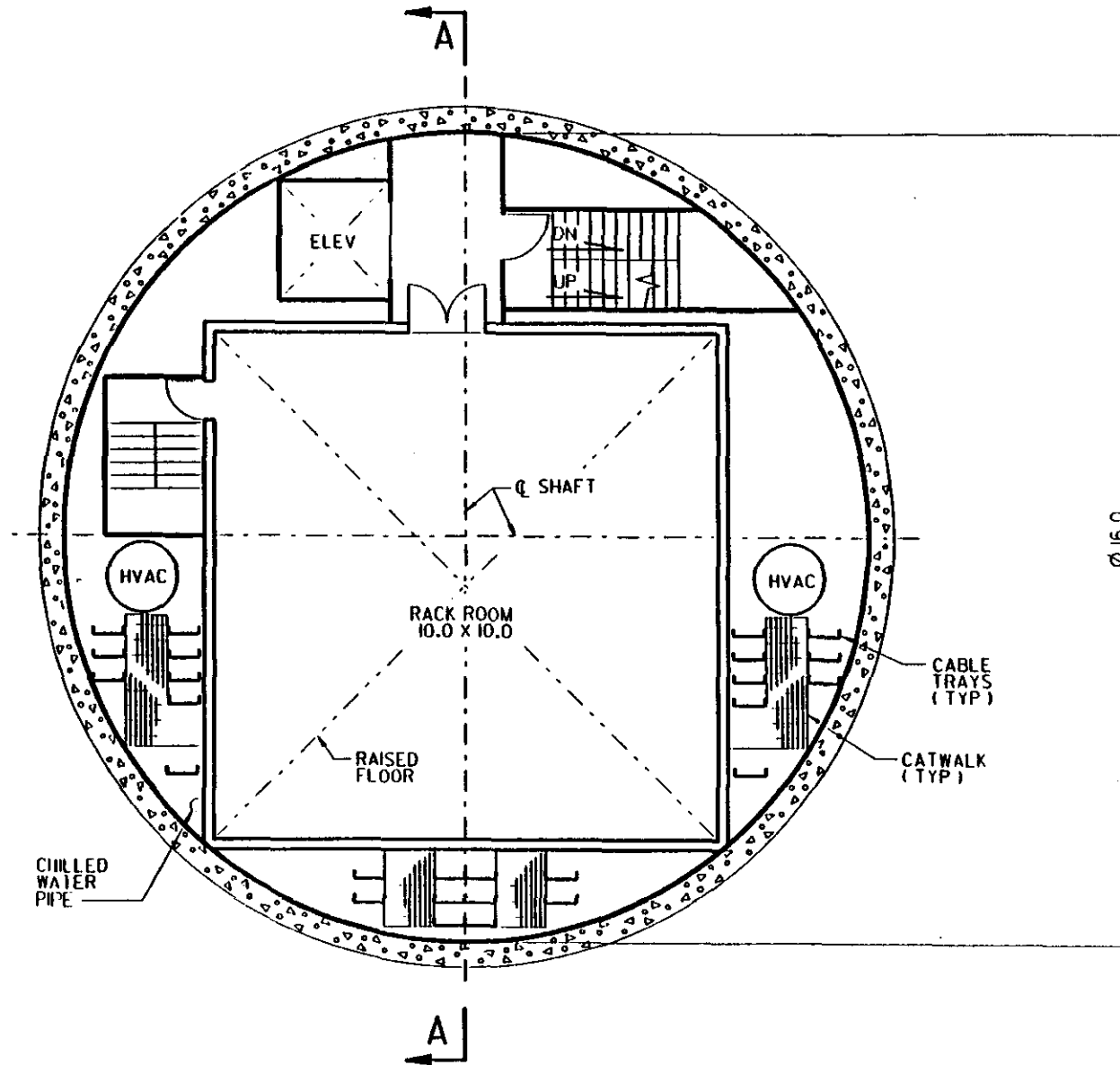


csno 41
Jun-25-92

CSHAFT1
JUN-25-92

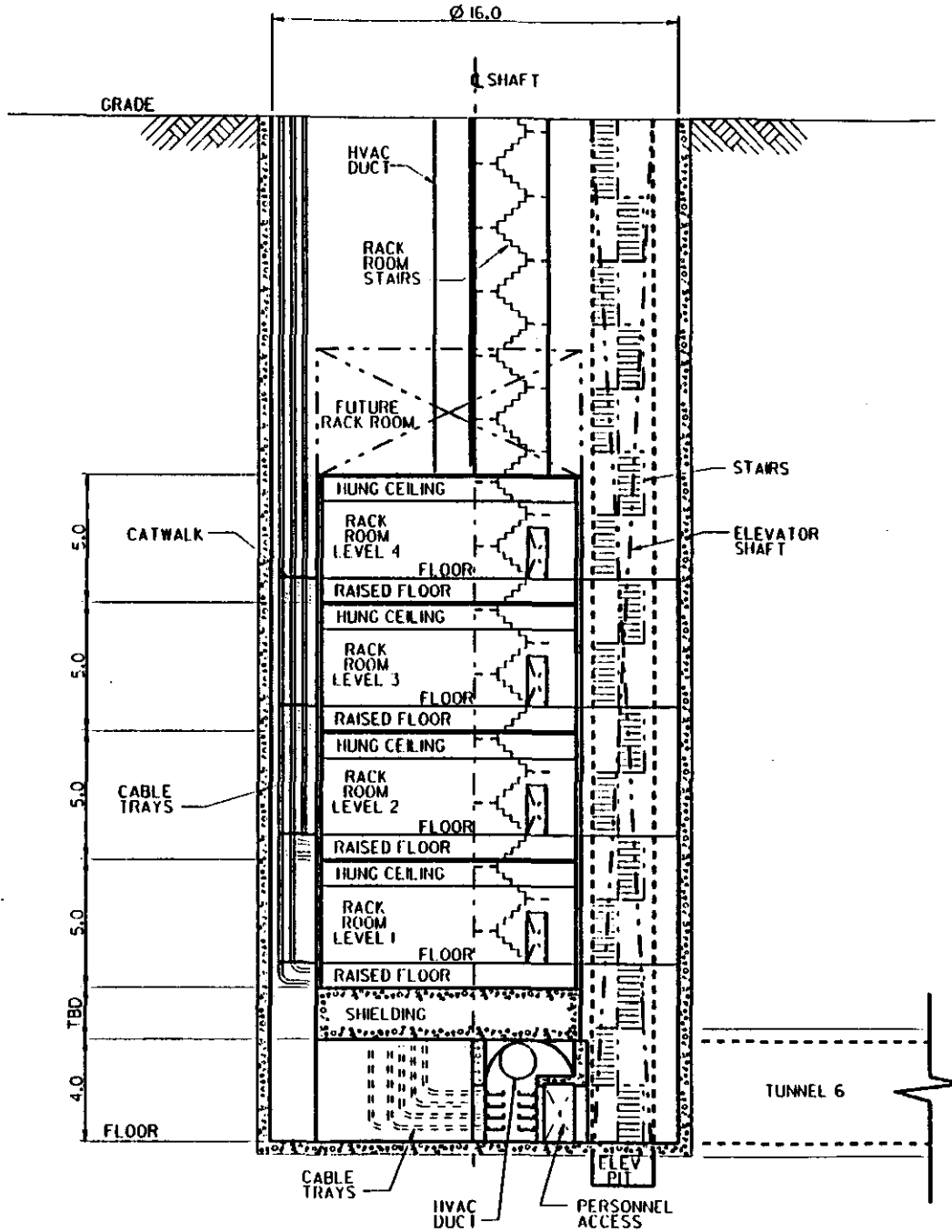


Page 3-30

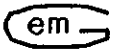


TYPICAL RACK ROOM
CABLE ELECTRONICS SHAFT

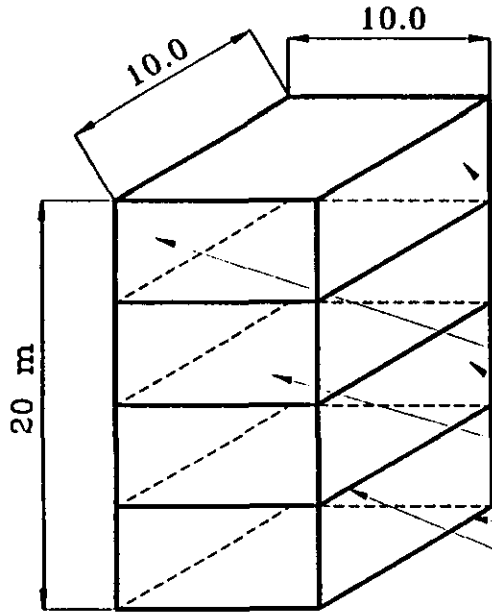
em



SECTION A-A
CABLE ELECTRONICS SHAFT



Electronic Rack Room Iron Shield (for max B < 50 G)



Thicknesses
of the shield's
walls, cm

- Easterly facing - 6.3
- Westerly facing - 2.5
- North and south - 2.5
- ERR bottom floor - 6.3
- Level 1 Ceiling - 5

Beamline

N

E

DRAFT

DETECTOR INSTALLATION

TABLE OF CONTENTS

OVERVIEW

DETECTOR INSTALLATION

Magnet Subsystem
Calorimeter Subsystem
Muon Subsystem
Tracker Subsystem
GEM Detector

FIGURES:

Group of related drawings showing baseline GEM installation
sequence (16 drawings total)
Drawing showing alternate installation of magnet utilizing second
shaft
Drawing showing tracker maintenance/installation
Drawing showing GEM Detector Maintenance Access
Group of related drawings showing Beamline Installation
(3 drawings total)

DETECTOR INSTALLATION

DETECTOR INSTALLATION

OVERVIEW

The GEM detector schedule must conform to the Collider start up milestone date since the Collider cannot be completed without having the detector in position. The critical path in the installation schedule is largely determined by the logic of the detector component installation sequence which is driven by the timeliness of design approval, the efficiency of procurement actions, the manufacturing process, the availability of facilities, and surface assembly operations (not necessarily in that order).

The overall installation period in the underground hall is estimated as approximately 3.5 years. The large superconducting magnet is planned as the first subsystem to be lowered during the first half of 1996. Assuming that a first contract could be placed in the beginning of 1993, this would leave a period of three years to build one of the world's largest superconducting magnets, containing 24 coil sections, each almost 19 m in inner diameter and 1.3 m high. The time to wind, insulate and test each section is estimated to take an average of one month. The magnet surface assembly process is expected to take at least 6 months and the subsequent tests another three. This would indicate that the magnet could be ready for installation if the procurement strategy is pursued as a top priority critical action item and that key contracts are placed no later than the beginning of next year.

The detector installation schedule is based on a series of sequential operations except in the case of the muon barrel chambers which could be installed at the same time as the calorimeter. The installation sequence begins with the south forward field shaper being lowered down the north construction shaft. Magnet installation continues over a nine month period. Assuming that further analysis confirms its feasibility, this would be followed by a magnet system test and a field mapping process.

During the next 4 month period the magnet is then reopened and the calorimeter is installed with the use of rail structures partly situated at a convenient point under the north construction shaft. The calorimeter is then closed up, tested and reopened to permit the central tracker to be installed. During this time the barrel muon chamber modules are being lowered through the south construction shaft and placed inside the completed magnet half sections.

Source: M. Harris/A. Gober
Updated: 6/26/92

DETECTOR INSTALLATION

The tracker installation and checking is expected to last 7 months. There is currently a conflict between the time of estimated tracker readiness for installation, and the baseline schedule. After tracker installation the calorimeter is again closed up and the muon barrel installation is completed. This permits the magnet half sections to be brought together so that, during the following 5 month period, the muon module endcaps can be installed using both construction shafts. The magnet forward field shapers are then closed and final connections and tests are carried out. Throughout the period of installation there would be a continuous laying and connecting of services, power busses, cables and fibers.

The two large construction shafts permit flexibility in the case of schedule changes and provides the option of first lowering the calorimeter, followed by the magnet, through both shafts. Surface facility heavy-load transport paths will be laid out to accommodate use of both shafts.

DETECTOR INSTALLATION

Since most of the detector subsystems consist of massive components, movement of these components from their initial position at the bottom of the assembly shaft to their final position in the detector requires a system of heavy duty rails and supporting equipment which will be completed in phase 1 of the installation process, before the first large component is lowered into the hall.

Magnet Subsystem

The magnet subsystem will be the first of the detector components installed into the underground hall. In order to minimize the cost of providing heavy lift cranes, only the north assembly shaft will be used initially for the heavy magnet components. Clearance considerations require that large components be installed at the opposite end of the hall before those for the near end can be installed. The southern field shaper will be the first magnet component lowered into the underground hall. (Phase 2) It will be lowered via the surface crane into position at the bottom of the assembly shaft where hydraulic transport equipment will be attached. The field shaper will then be moved into its normal mounting location. Installation will continue in a similar fashion as the south magnet half, central detector support structure, north magnet half, and northern field shaper are lowered into the hall and connected together. (Phases 3-6)

Source: M. Harris/A. Gober
Updated: 6/26/92

DETECTOR INSTALLATION

When all the magnet components have been lowered and installed, the northern shaft cover will be moved back into position over the shaft to protect it from the elements. In the meantime, the cryogenic plumbing and power busses will be installed onto the magnet system. All the connections will be tested before the magnet is cooled to operating temperature for final testing. After proper magnet operation has been verified, the magnetic field will be mapped. (Phase 7-8) Following magnetic field mapping, all the non-essential connections will be removed to allow for the separation of the magnet halves. (Phase 9) The magnet halves will be separated and parked at opposite ends of the hall to permit installation of the remaining detector subsystems. There will be space left in between the field shapers and the magnet halves to allow for connection of the barrel muon system.

Calorimeter Subsystem

Once the magnet has been completed, tested, and opened, the installation of the calorimetry system can begin. (Phase 9) The calorimeter will consist of three sections, a barrel and two endcaps. Each section will contain both the hadronic and electromagnetic calorimetry subsystems. These subsystems will be assembled on the surface prior to being lowered into the underground hall. While the calorimeter sections are being assembled above ground, support rails will be installed in the underground hall to assist in their installation. The rails will connect with the central detector support structure so that the weight of the calorimeter sections can be applied uniformly onto the support structure as they are installed. These rails will extend far enough from the central detector support to store the endcaps temporarily while the barrel section is being installed. The rail on the northern side of the central detector support will have an additional extension that reaches the length of the floor from the central support to the assembly shaft for transferring the subsystems after they are lowered.

While the rail system is being completed, the shaft cover will be removed to allow the calorimeter sections to be lowered into the hall. When the rail system and each of the calorimeter sections are ready, they will be lowered down the north assembly shaft and placed onto the installation rails. The south endcap will be the first of the sections to be lowered. It will be moved through the central detector support and placed out of the way on the support rail while the barrel section is being lowered. When the south endcap is safely out of the way, the barrel section will be moved into position within the central support

Source: M. Harris/A. Gober
Updated: 6/26/92

DETECTOR INSTALLATION

and its installation will begin. While the barrel section is being installed, the north endcap will be lowered and moved into position on the main support rail so that the extension can be removed. (Phase 10) This will leave room for the muon barrels to be installed into the north half of the magnet. Once the barrel section is secured, the two endcaps can be moved and joined simultaneously with the barrel section. (Phase 10)

While the final connections are being made on the calorimeter, the installation of the south muon barrel modules will have been completed. This will allow the liquid argon tanks to be lowered down the south assembly shaft and installed at the south end of the hall. (Phase 11) When the calorimeter has been successfully joined together, all the final electrical and data gathering cabling can be attached. Finally, the calorimeter will be cold tested to make sure all the connections have been made properly. (Phase 11)

Muon Subsystem

For this part of the detector installation, the south assembly shaft will be opened. This will allow the muon subsystem installation to begin while the calorimeter installation is being completed. The installation of the muon subsystem will begin on the southern end of the detector. (Phase 10) First, the inside walls of the separated magnet halves will be prepared for muon module insertion. A rail system will be installed to provide for both the insertion and support of the modules during their installation into the magnet.

One by one, working up from the bottom, the sixteen barrel modules designated for the southern magnet half will be lowered into the underground hall. They will be picked up by the hall crane and rotated into a position parallel to the beam line. They will then be placed onto a transport/support fixture that has been set to deliver the module to the magnet at its final height. The fixture will then be moved adjacent to the magnet where the module will be rotated to its final orientation. The fixture will be equipped with adjusting jacks so that the height of the module can be fine tuned for ease of installation. When the module is properly aligned, it will be inserted into the magnet barrel via the rail system. It will then be rechecked for alignment and adjusted. This process will repeat until all sixteen barrel modules have been installed.

Once the northern calorimeter endcap has been lowered and the rail extension removed, the north assembly shaft can be used to begin the installation of the muon barrel modules into the northern end of the

Source: M. Harris/A. Gober

Updated: 6/26/92

DETECTOR INSTALLATION

detector. (Phase 11) The process will be the same as the one used to install the muon barrels at the south end of the hall. When all sixteen barrel modules have been installed the shaft covers will again be closed to protect them from the elements. In addition, each module assembly will be fastened to the magnet half at both ends by a system of support fixtures.

When the installation of the calorimetry system and the central tracker has been completed and all the necessary tests performed, the calorimetry support rails will be removed and the magnet halves will be closed, leaving the field shapers in position at the ends of the hall. (Phase 12) This will allow the installation of the muon endcap modules to commence. The shaft covers will be removed and the endcap modules will be lowered and installed onto the field shaper. (Phase 13) Because of the overlap of the individual end chambers, installation must be done radially, rather than axially as for the barrel chambers.

When all of the modules have been installed, the magnet halves will then be separated and parked at the ends of the hall so that the tracker can be installed. (Phase 14) Final testing of the muon system can take place at this time.

Tracker Subsystem

When the installation of the muon endcap modules has been completed, the magnet halves will be separated far enough so that the tracker can be installed. (Phase 14) The calorimeter support rails will be reinstalled so that the calorimeter endcaps can be removed. This will allow access into the center of the barrel region. At this time, the tracker can be lowered into the hall and installed into the center of the barrel calorimeter section. All the necessary electronics and plumbing connections will be made while the vacuum pipe is being installed into the tracker. When all the components have been properly attached, the calorimeter endcaps will be reclosed. Final testing and checkout will commence on the tracker while the support rails are removed and the assembly shafts covered.

GEM Detector

The tracker subsystem will be the last subsystem of the detector to complete its installation. Once the tracker has been inserted, any final connections and adjustments can be made before the detector is closed. The magnet halves and field shapers will be moved back into position and bolted in place. In addition, the last part of the vacuum pipe will

Source: M. Harris/A. Gober
Updated: 6/26/92

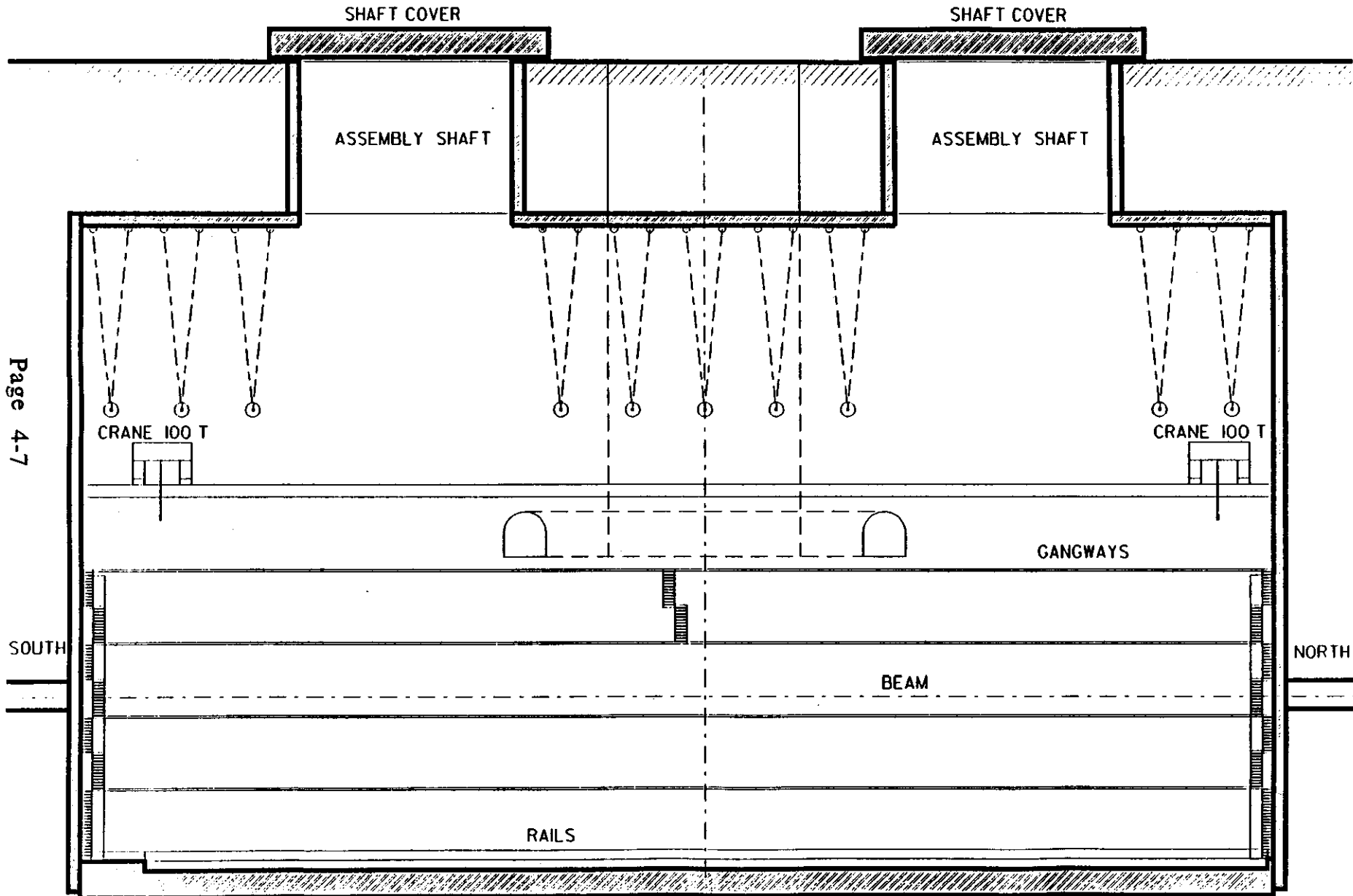
DETECTOR INSTALLATION

be installed while the magnet system is brought to operational temperature and pressure. (Phase 15-16) Finally, the beam line and quadrupoles will then be completed. In addition, the concrete shielding sealing both assembly shafts can be inserted and the shaft covers closed while all the final connections are being made on the detector. (Phase 17-18) All final tests and checkouts will be performed before the detector is commissioned ready for physics. (Phase 19-21)

Source: M. Harris/A. Gober
Updated: 6/26/92

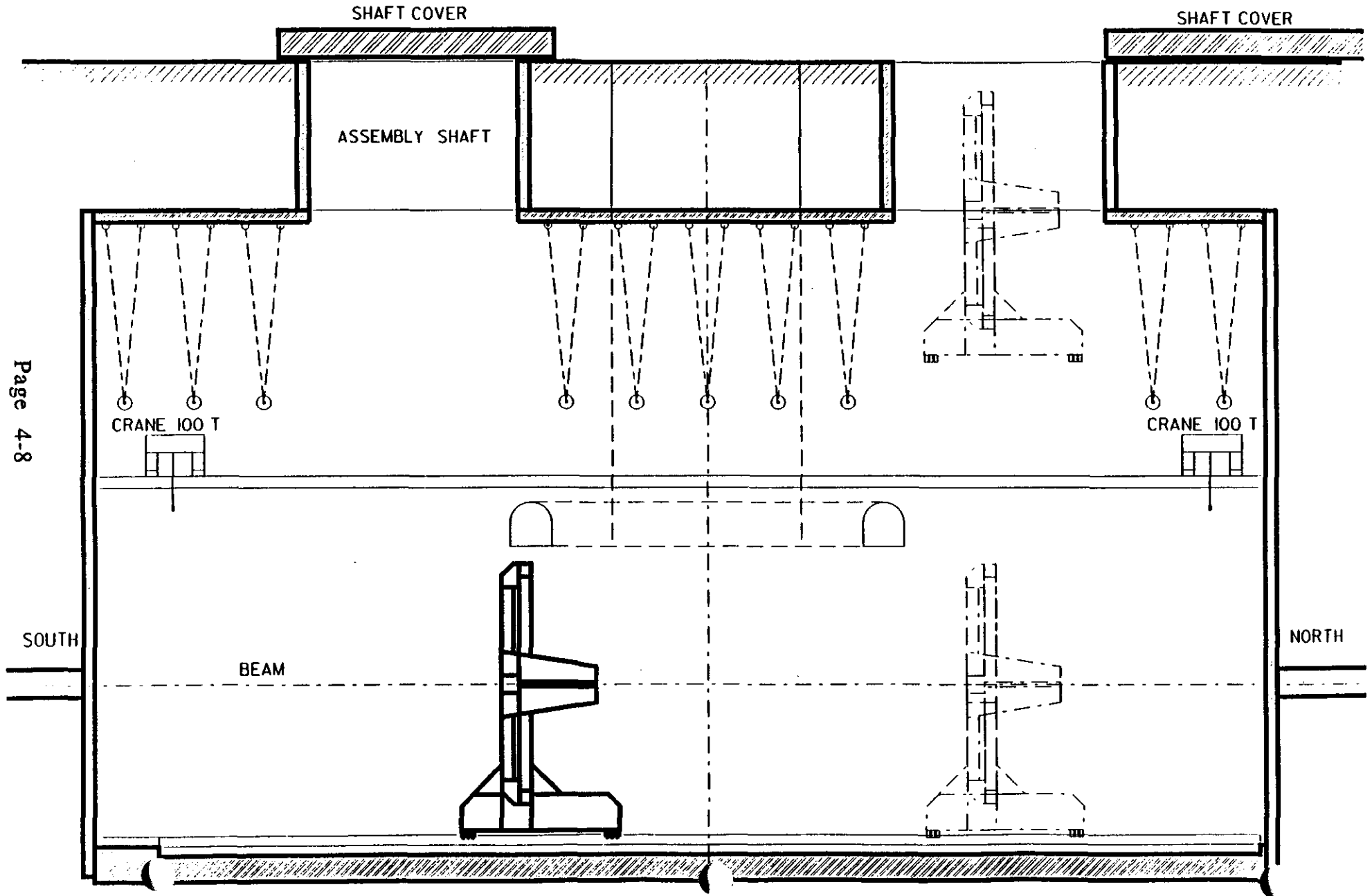
PHASE I

UNDERGROUND HALL COMPLETED



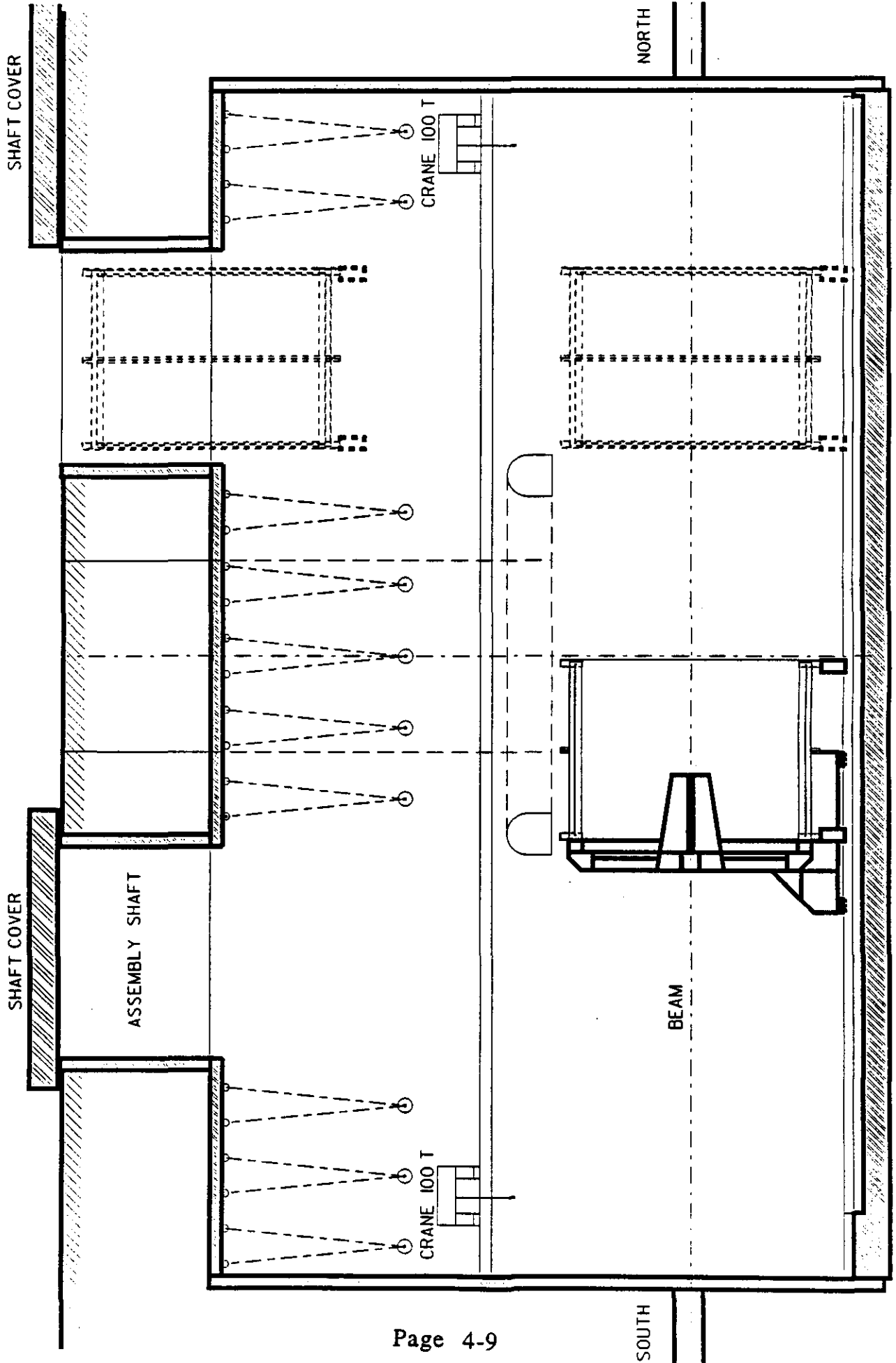
PHASE 2

INSTALL FORWARD FIELD SHAPER SOUTH



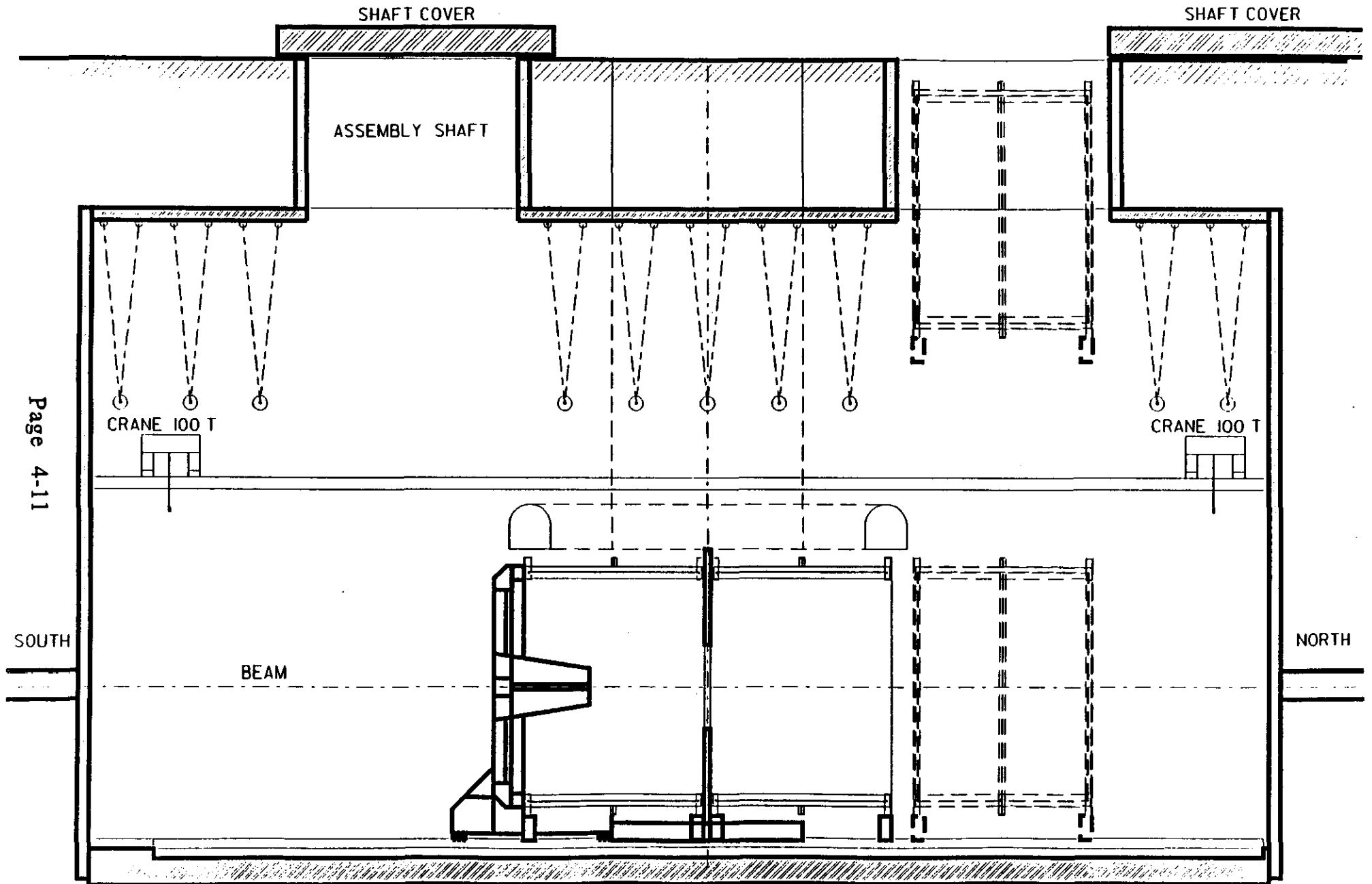
PHASE 3

INSTALL MAGNET HALF COIL SOUTH



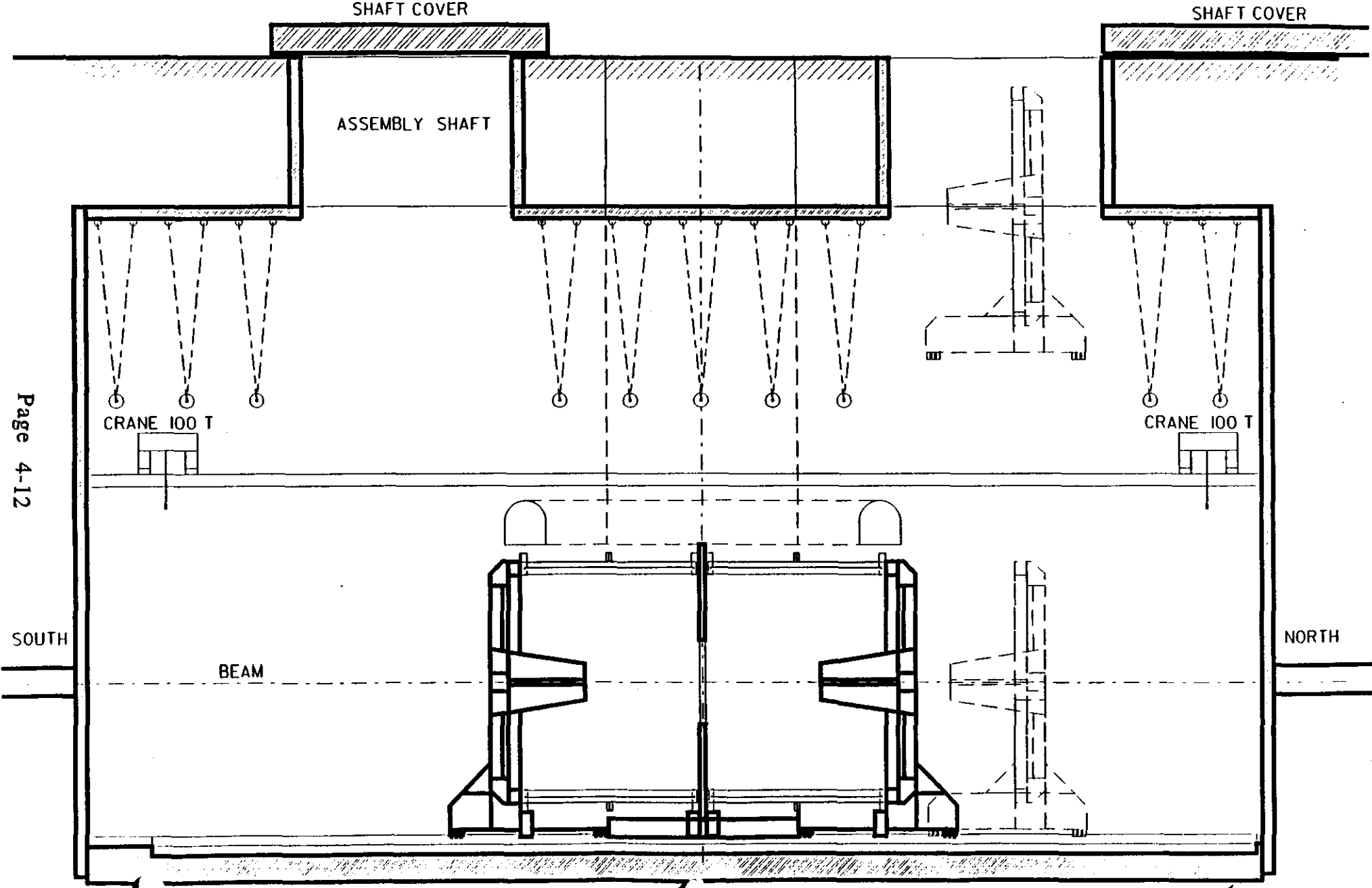
PHASE 5

INSTALL MAGNET HALF COIL NORTH



PHASE 6

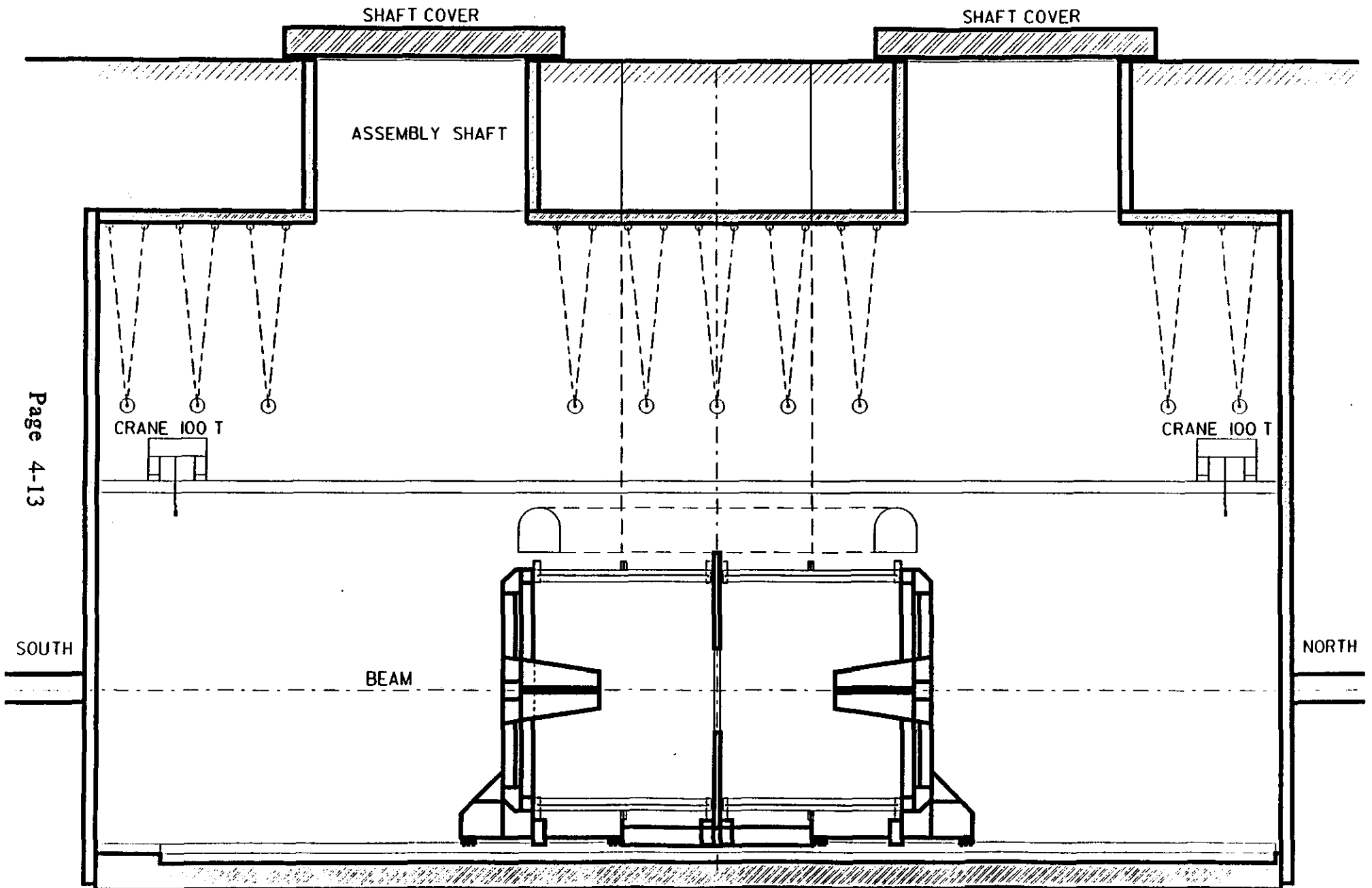
INSTALL FORWARD FIELD SHAPER NORTH



Page 4-12

PHASE 7 - 8

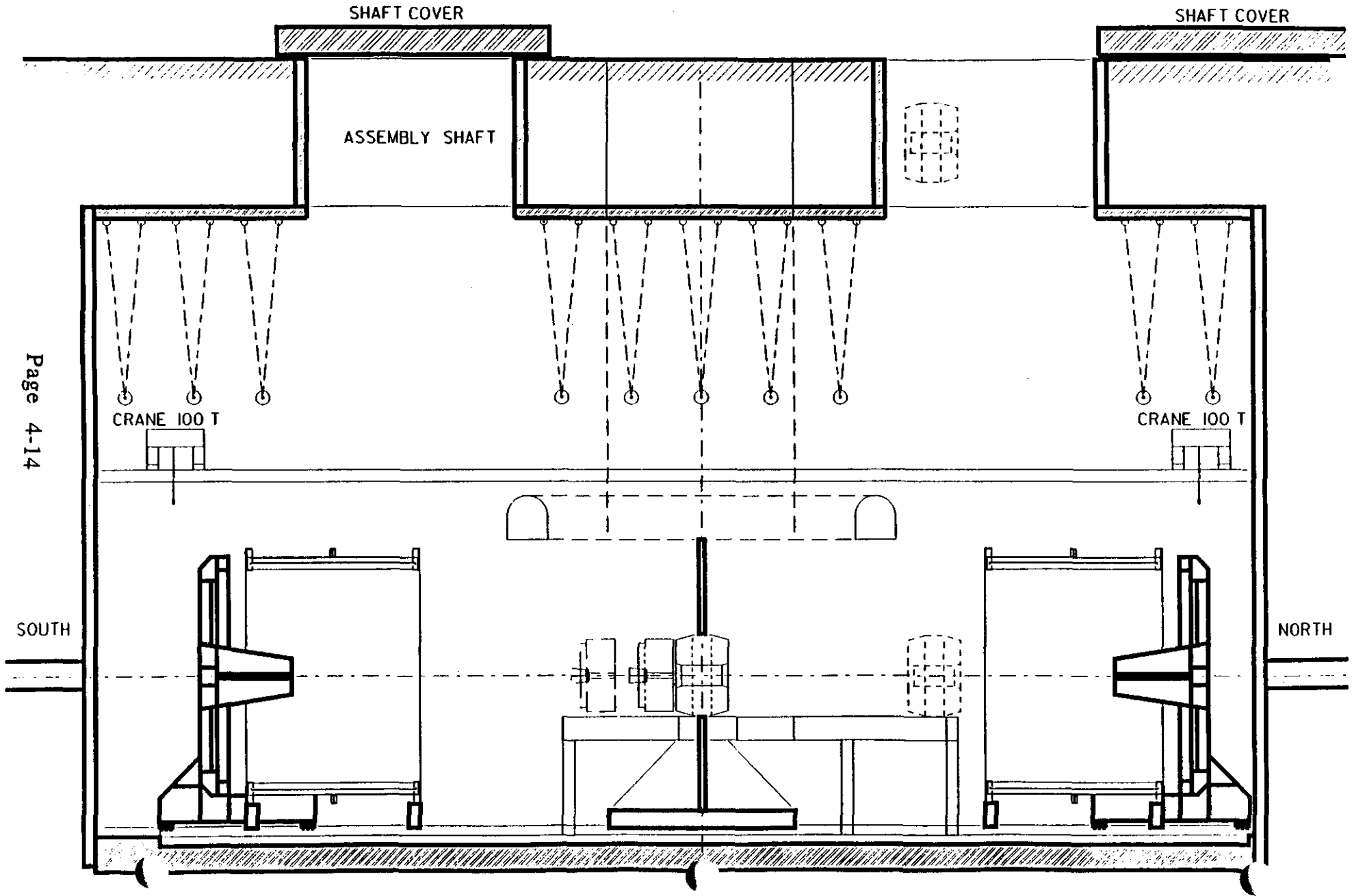
TEST MAGNET SYSTEMS - MAP MAGNET FIELD



Page 4-13

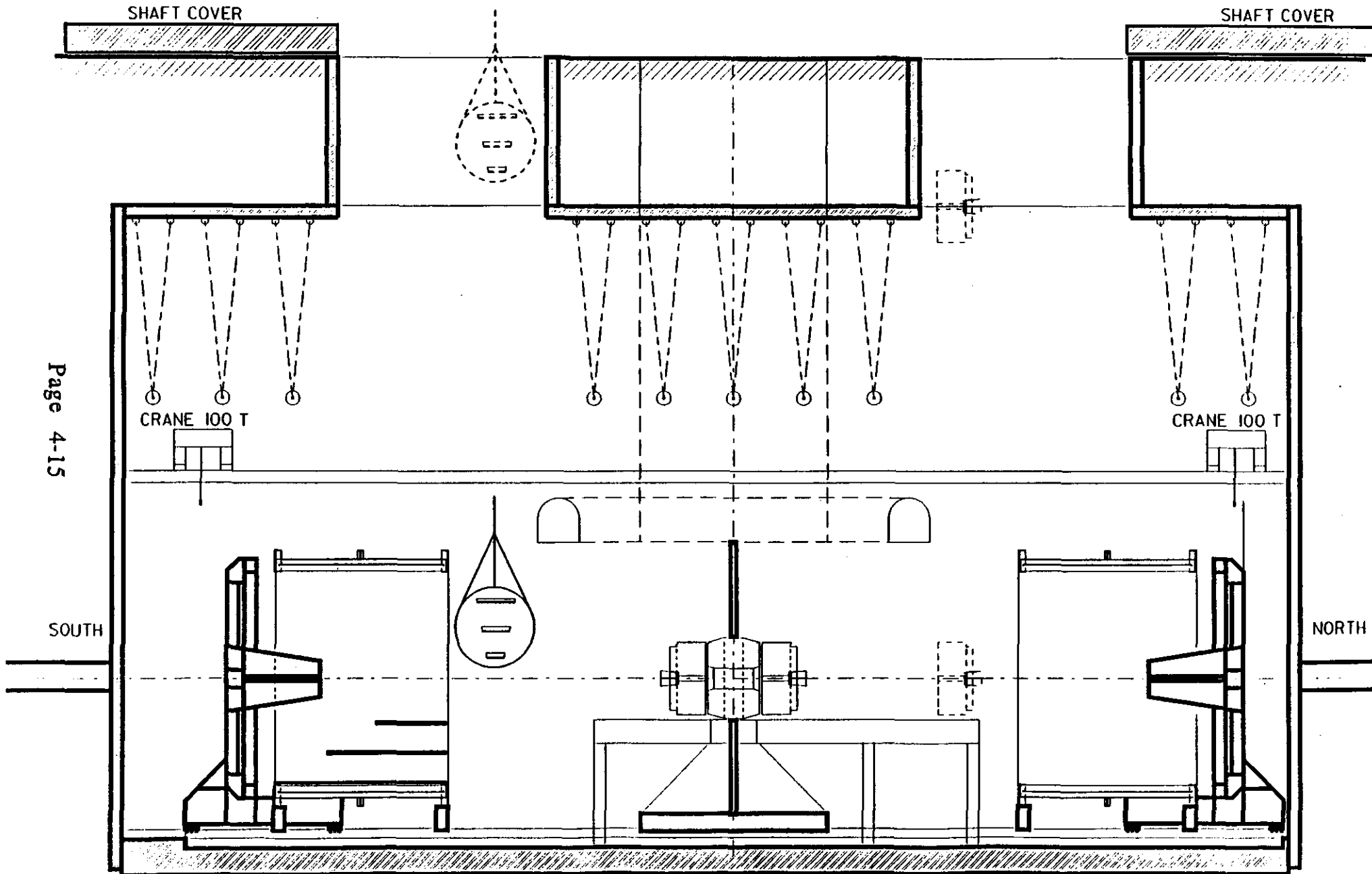
PHASE 9

OPEN MAGNET - INSTALL SUPPORT AND CALORIMETER



PHASE 10

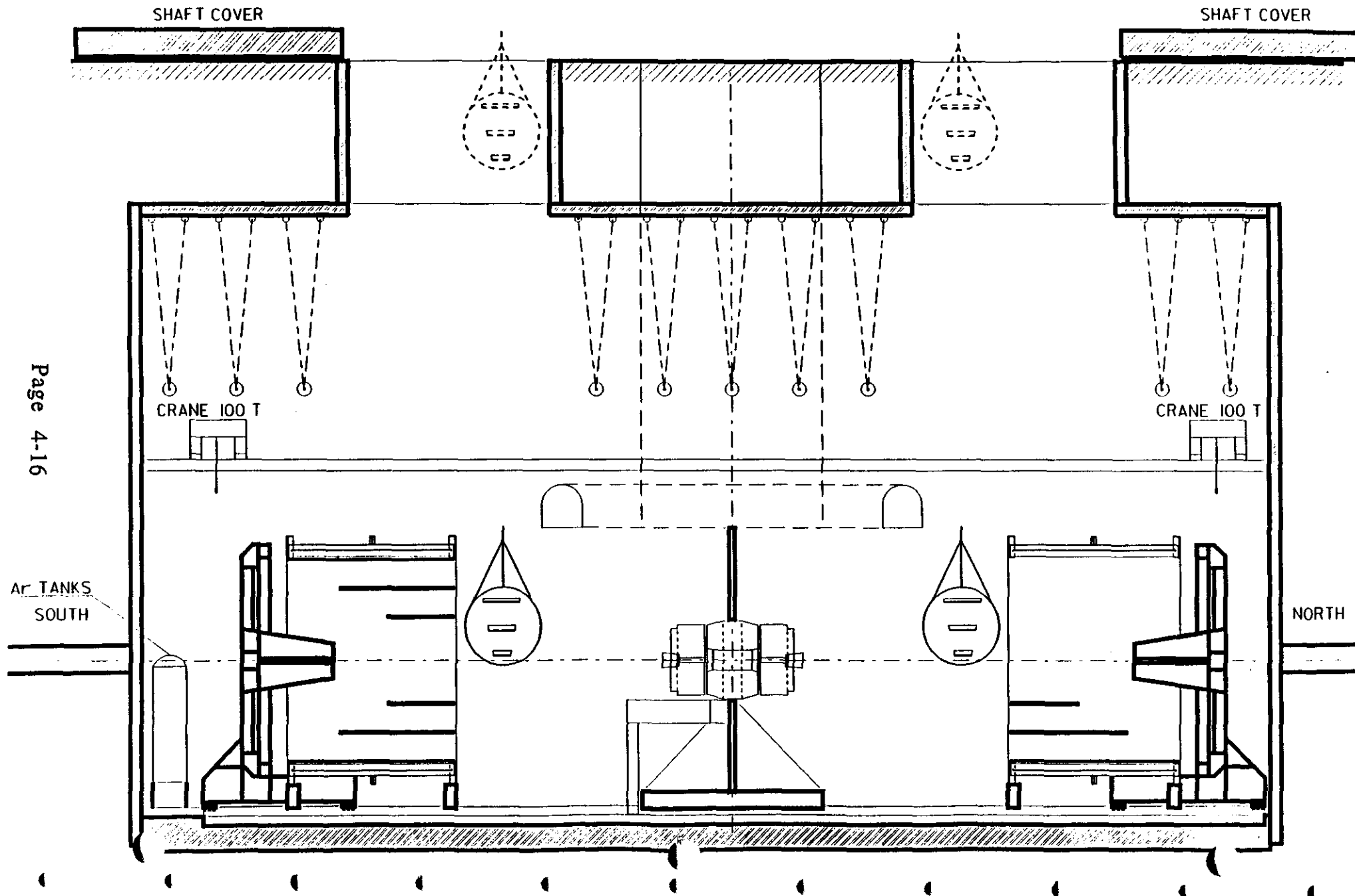
INSTALL MUON BARREL SOUTH - END CAP CALORIMETER



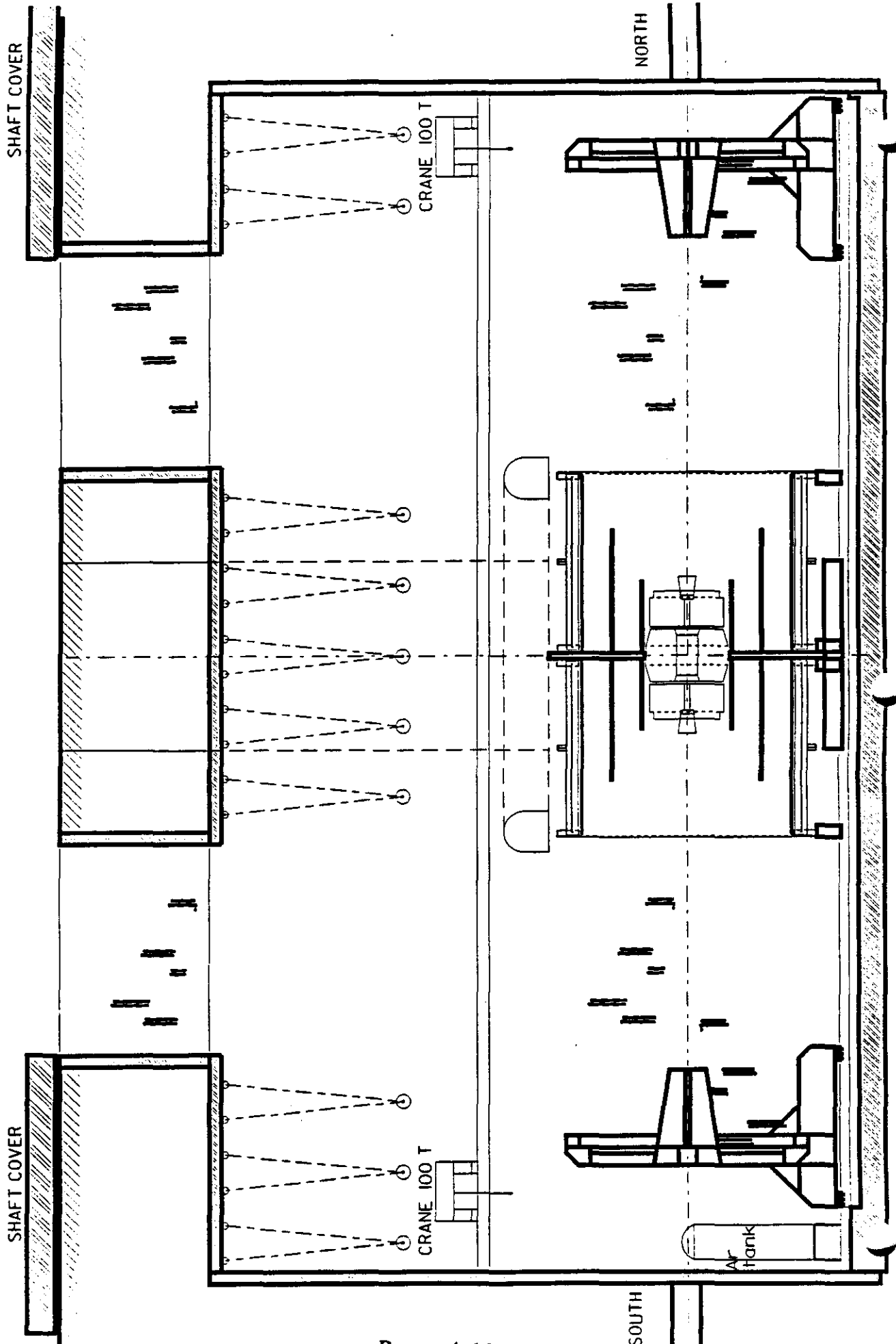
PHASE II

INSTALL MUON BARREL - SOUTH - NORTH

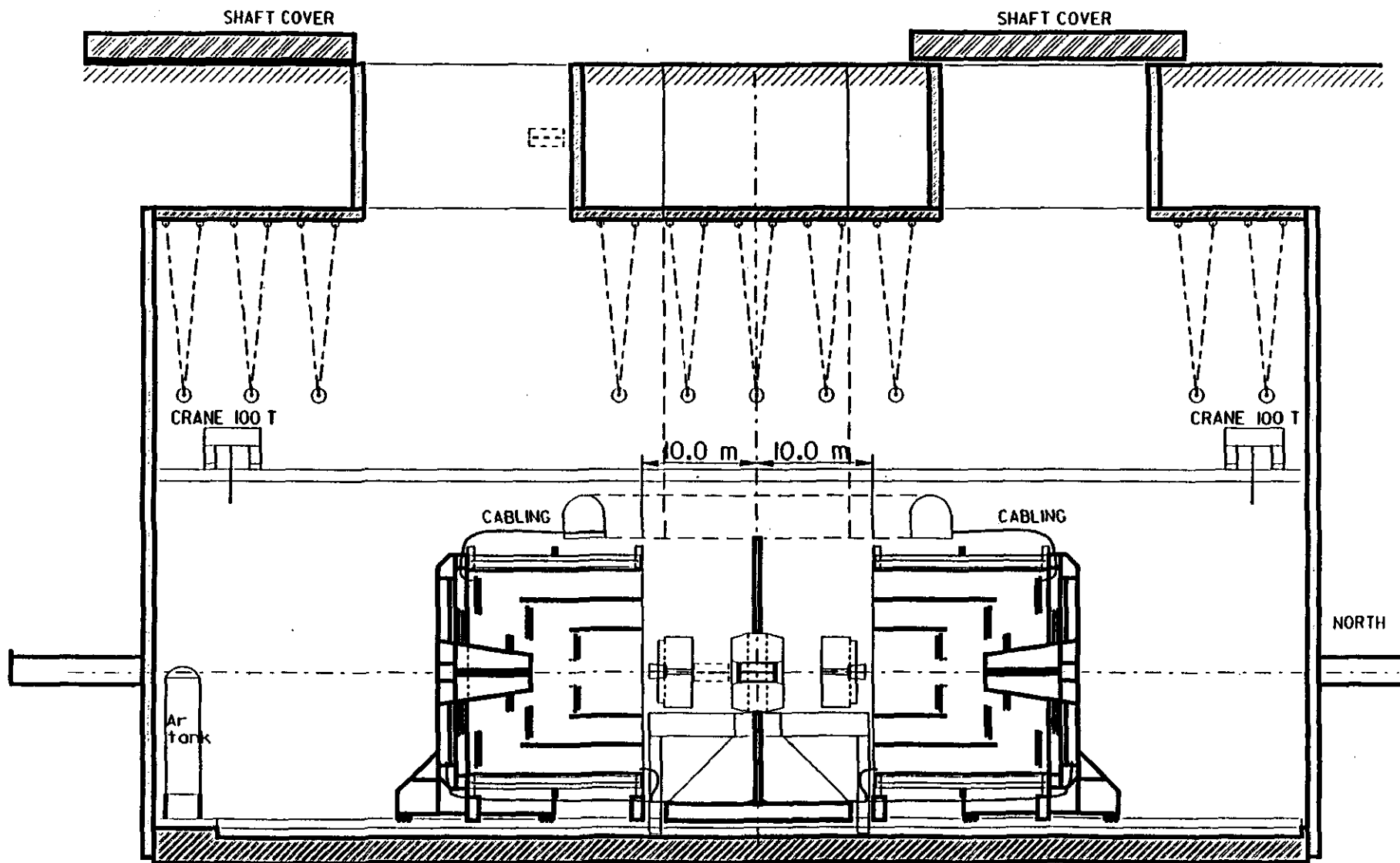
COLD TEST CALORIMETER



PHASE 13 INSTALL MUON ENDCAP

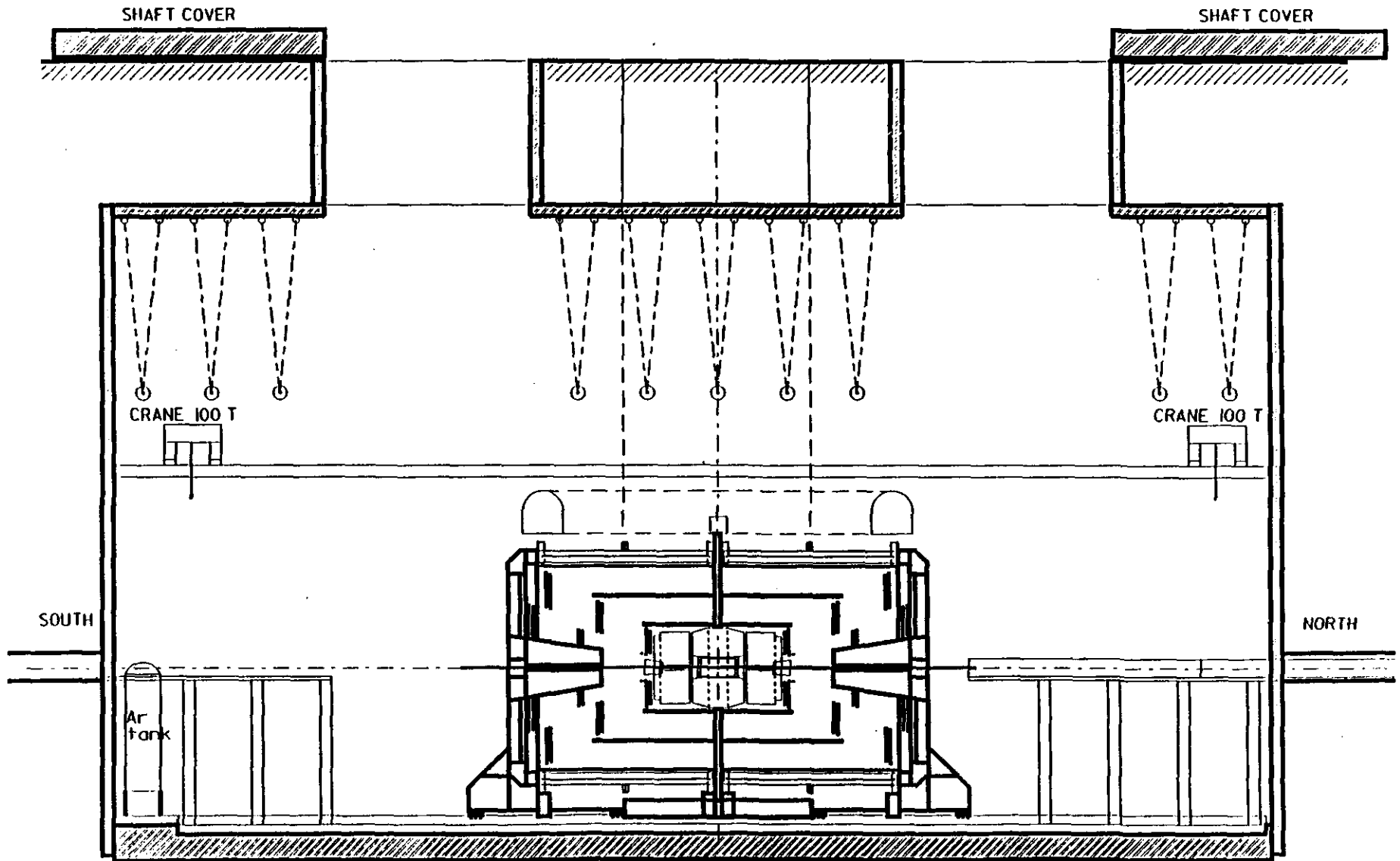


PHASE 14 INSTALL TRACKER - VACUUM PIPE



PHASE 15 - 16

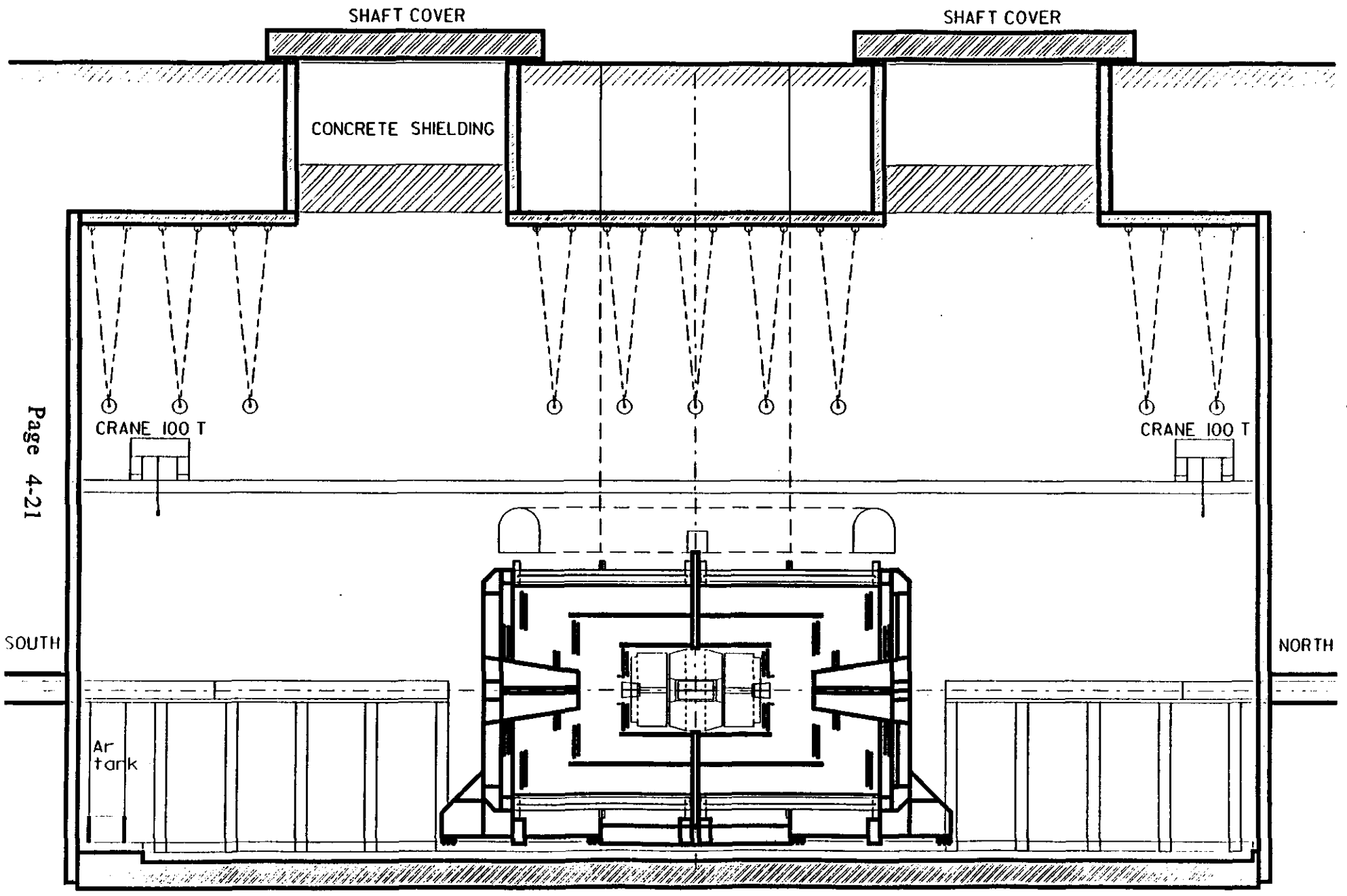
COMPLÈTE SUBSYSTEM CONNECTIONS-LAST PART VACUUM PIPE
INSTALL QUADRAPOLES-CLOSE DETECTOR



PHASE 7 - 18

INSTALL CONCRETE SHIELDING - COLLIDER COMPONENTS

COMPLETE BEAM LINE

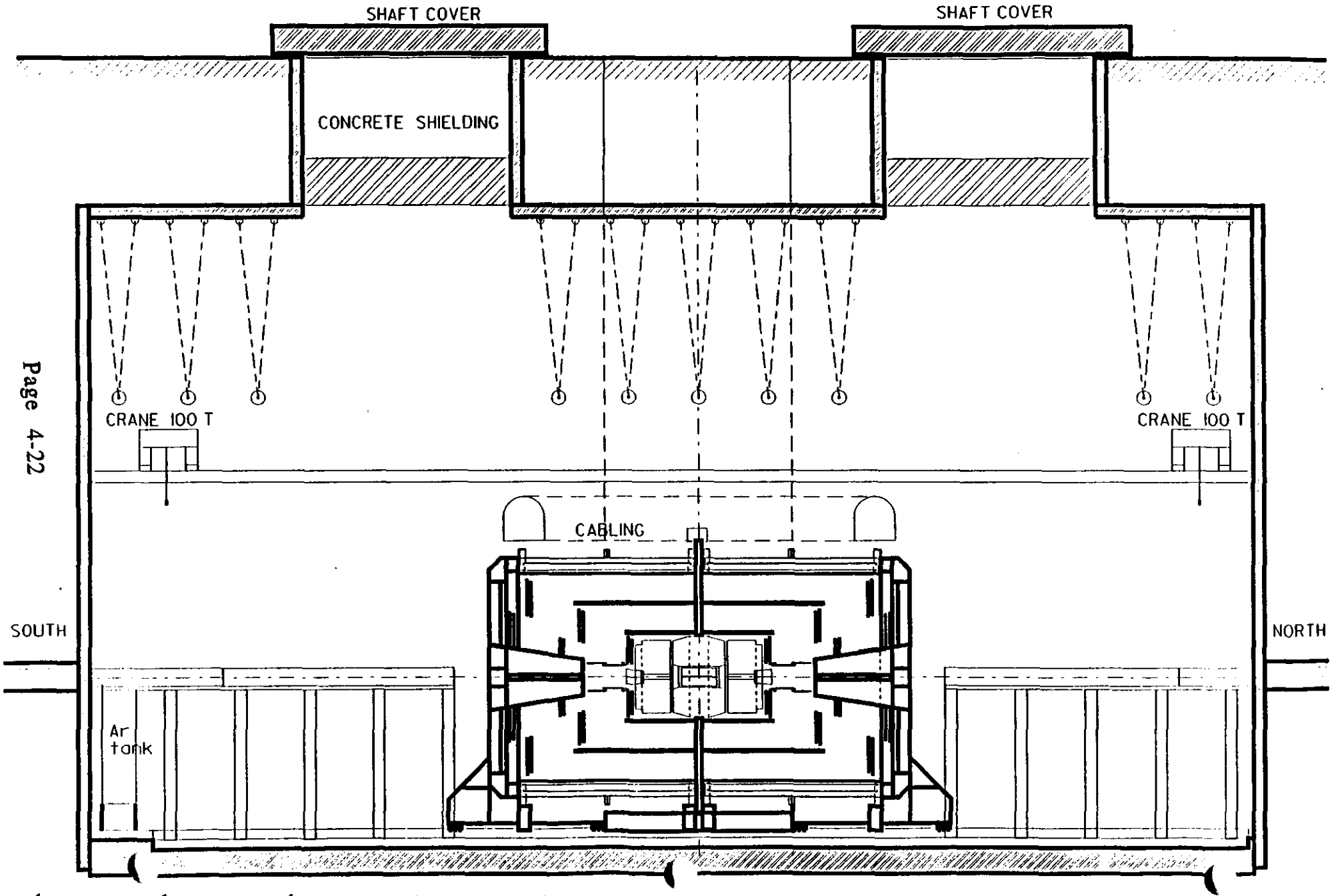


Page 4-21

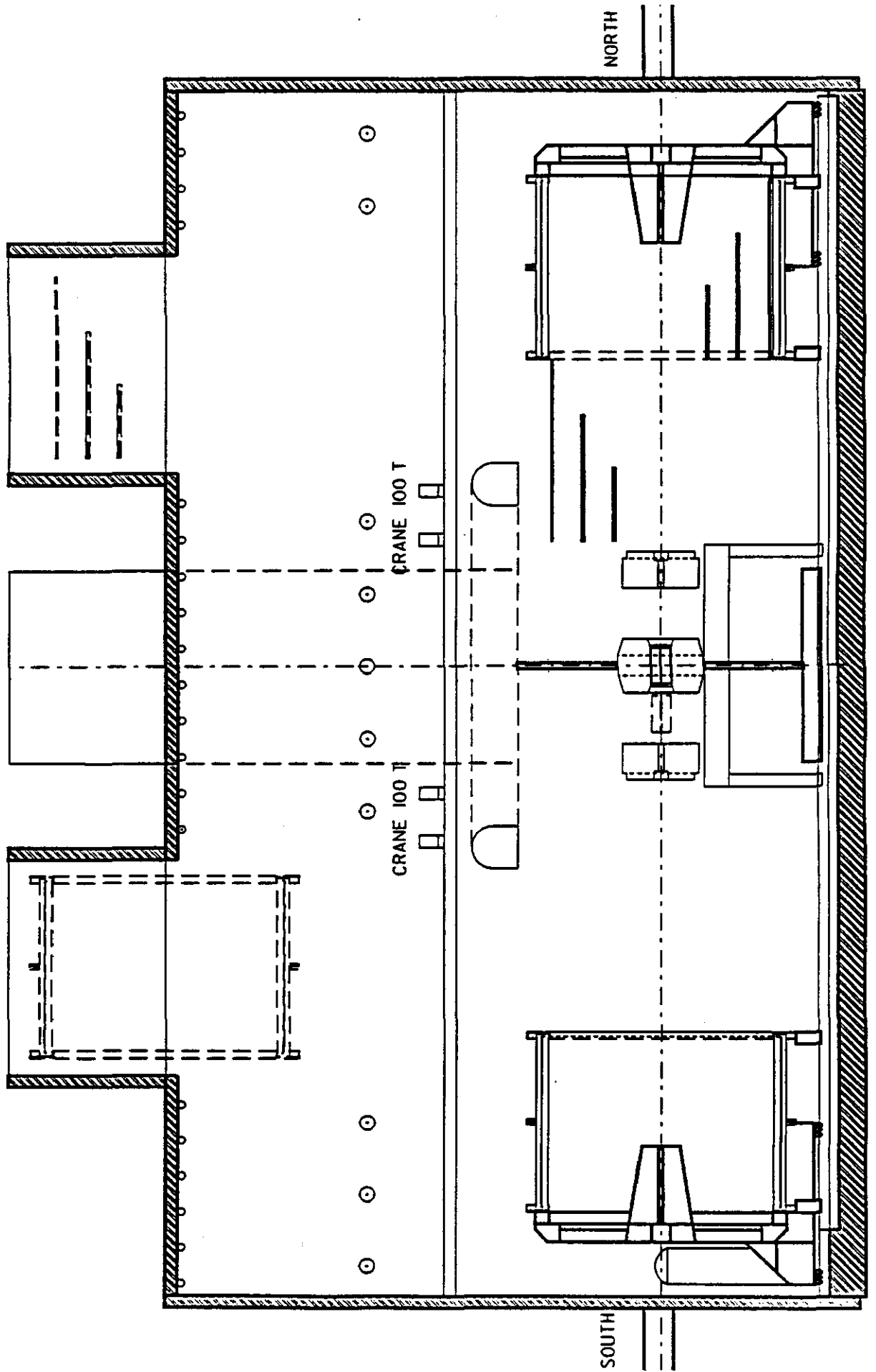
PHASE 1) -20 - 21

COMPLETE TESTS AND CHECKOUTS

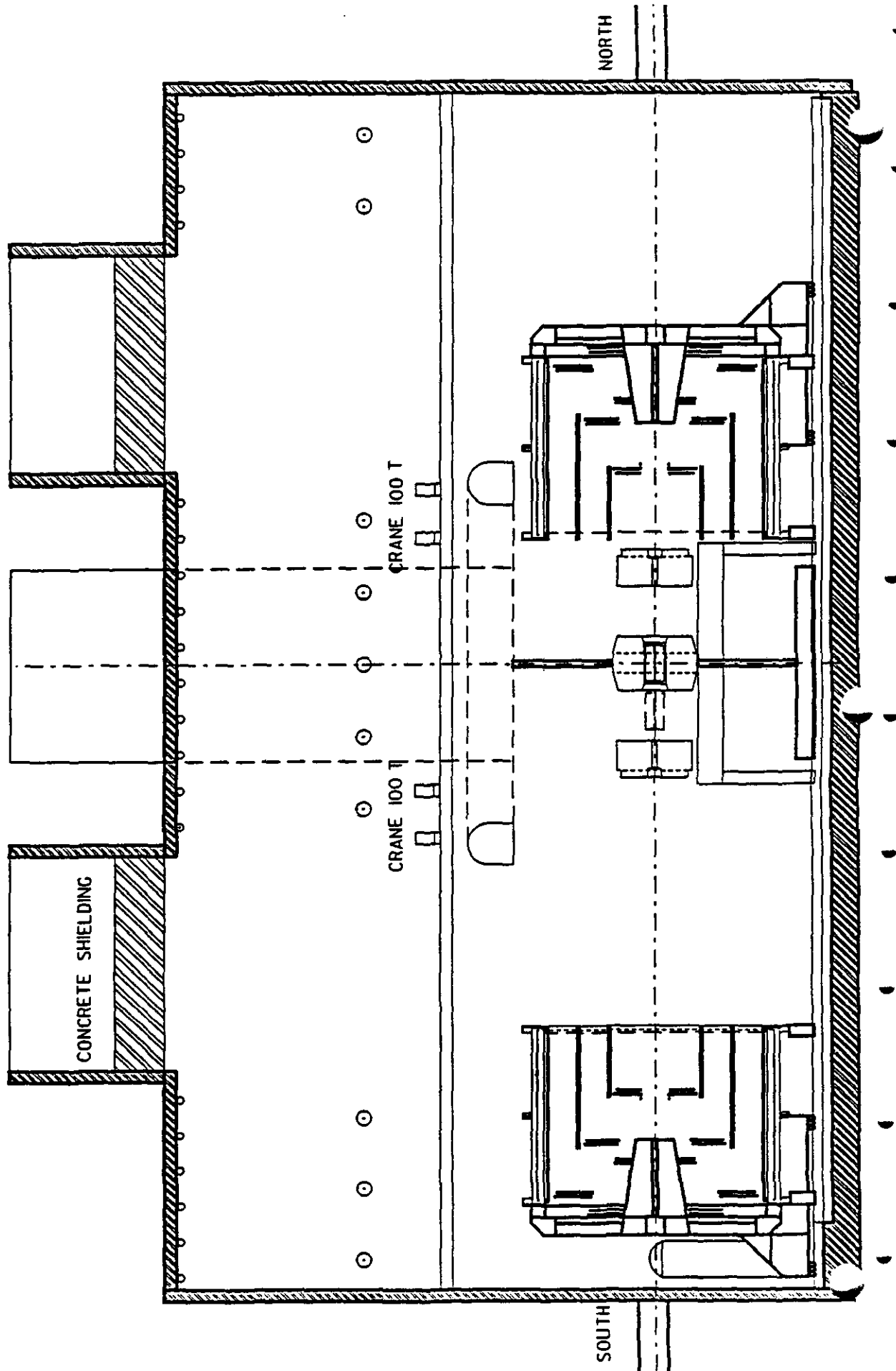
COMMISSION COLLIDER DETECTOR READY FOR PHYSICS



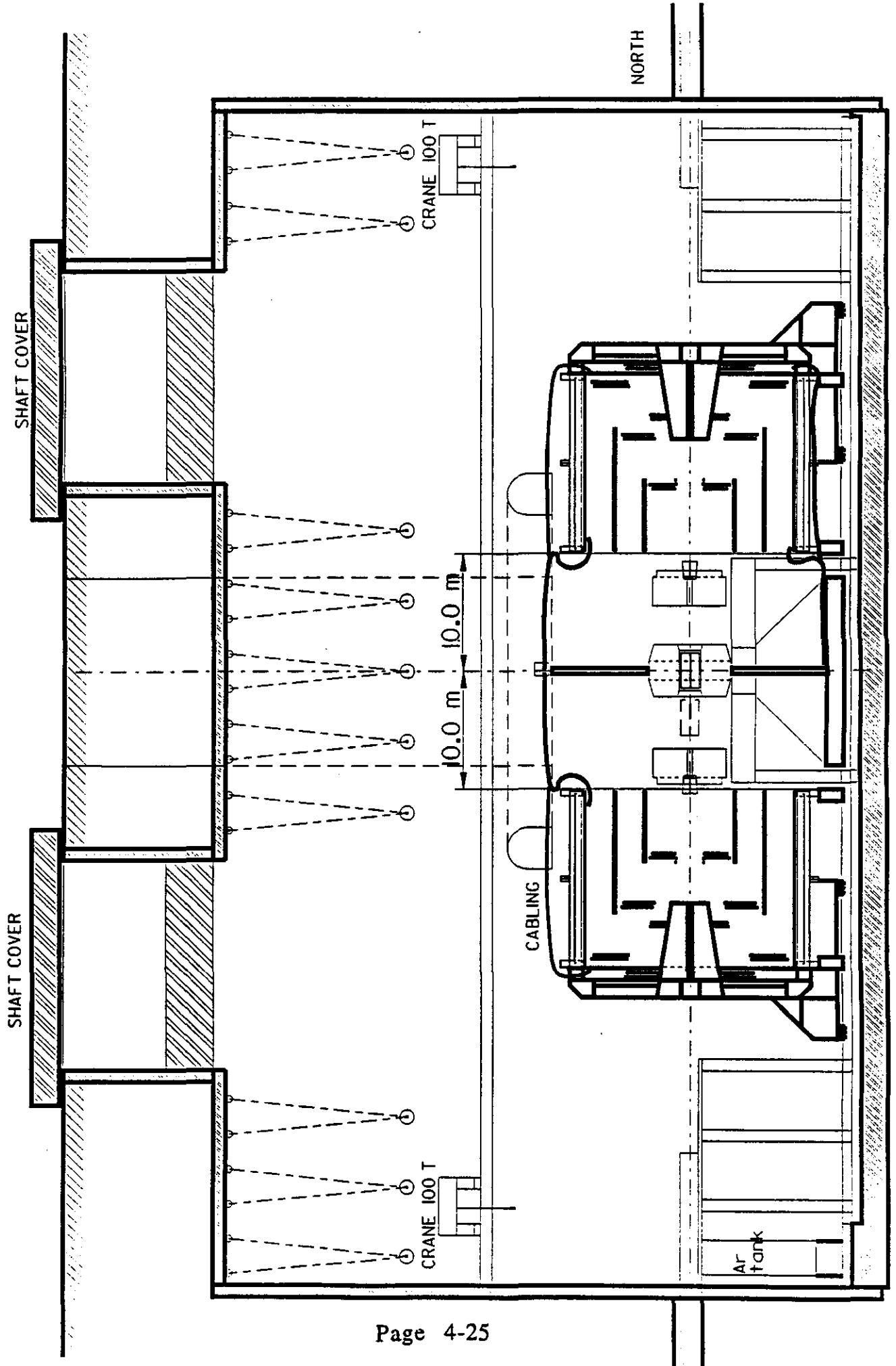
ALTERNATE MAGNET INSTALLATION



TRACKER MAINTENANCE / INSTALLATION

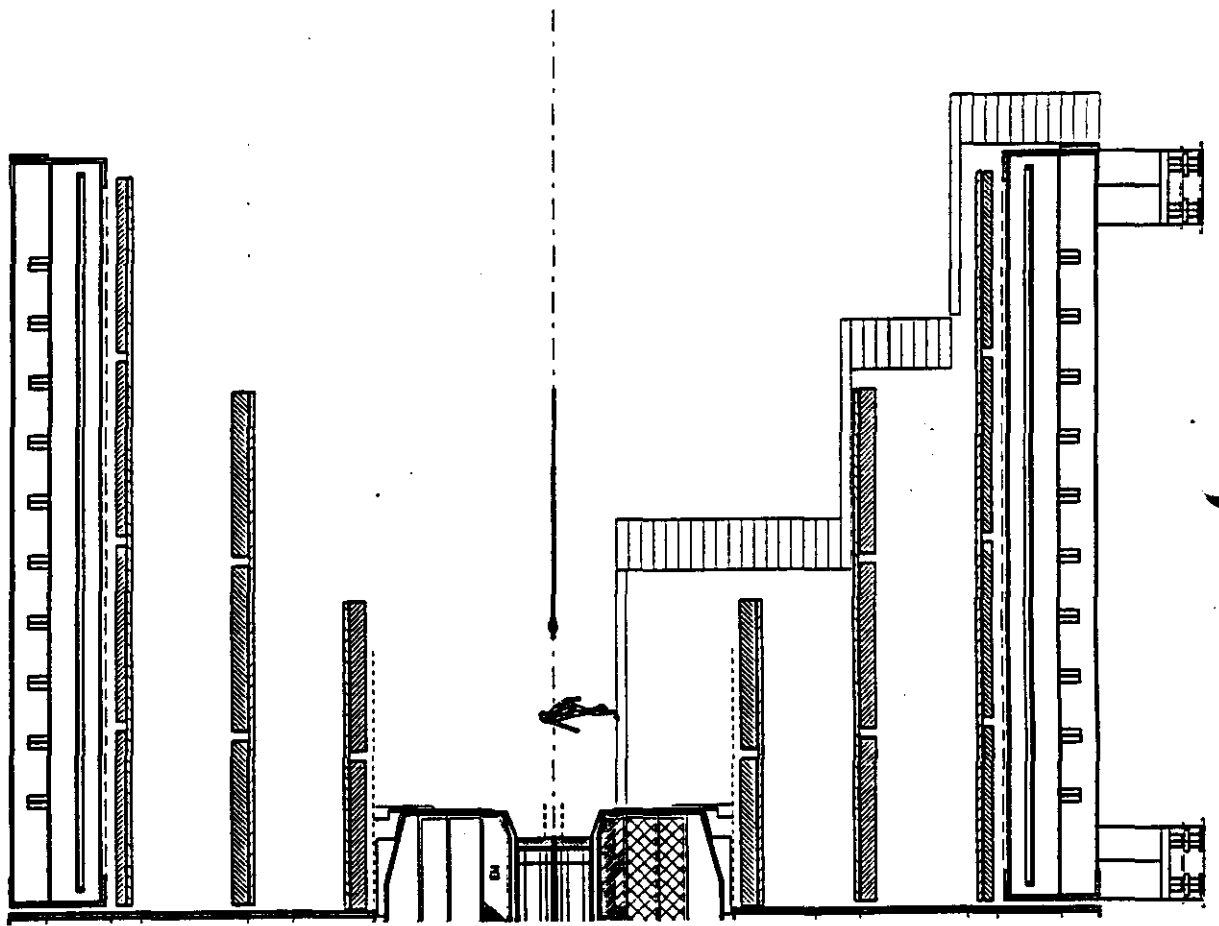


DETECTOR MAINTENANCE



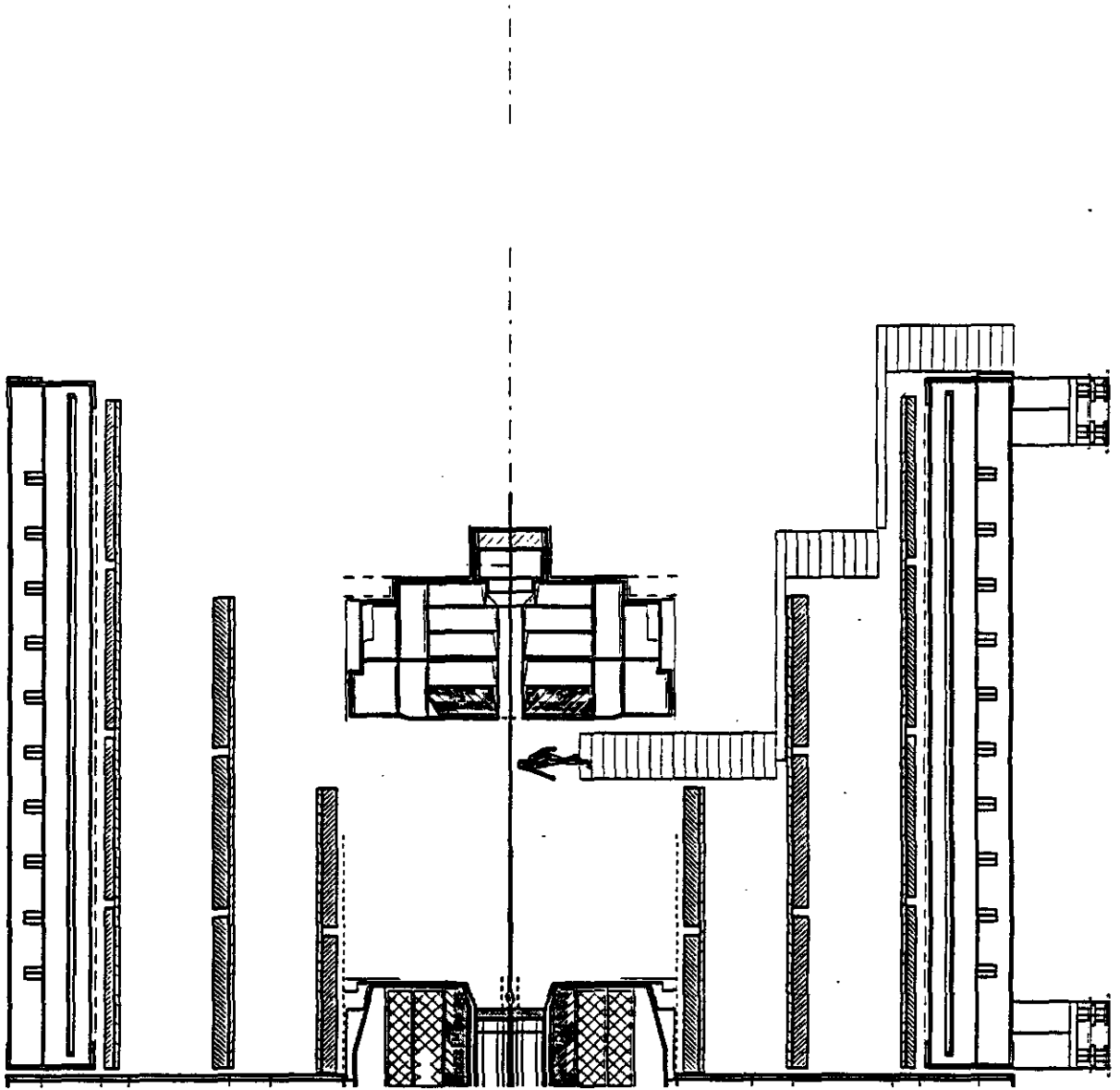
BEAM LINE INSTALLATION - PHASE 1

FIRST PART BEAM PIPE



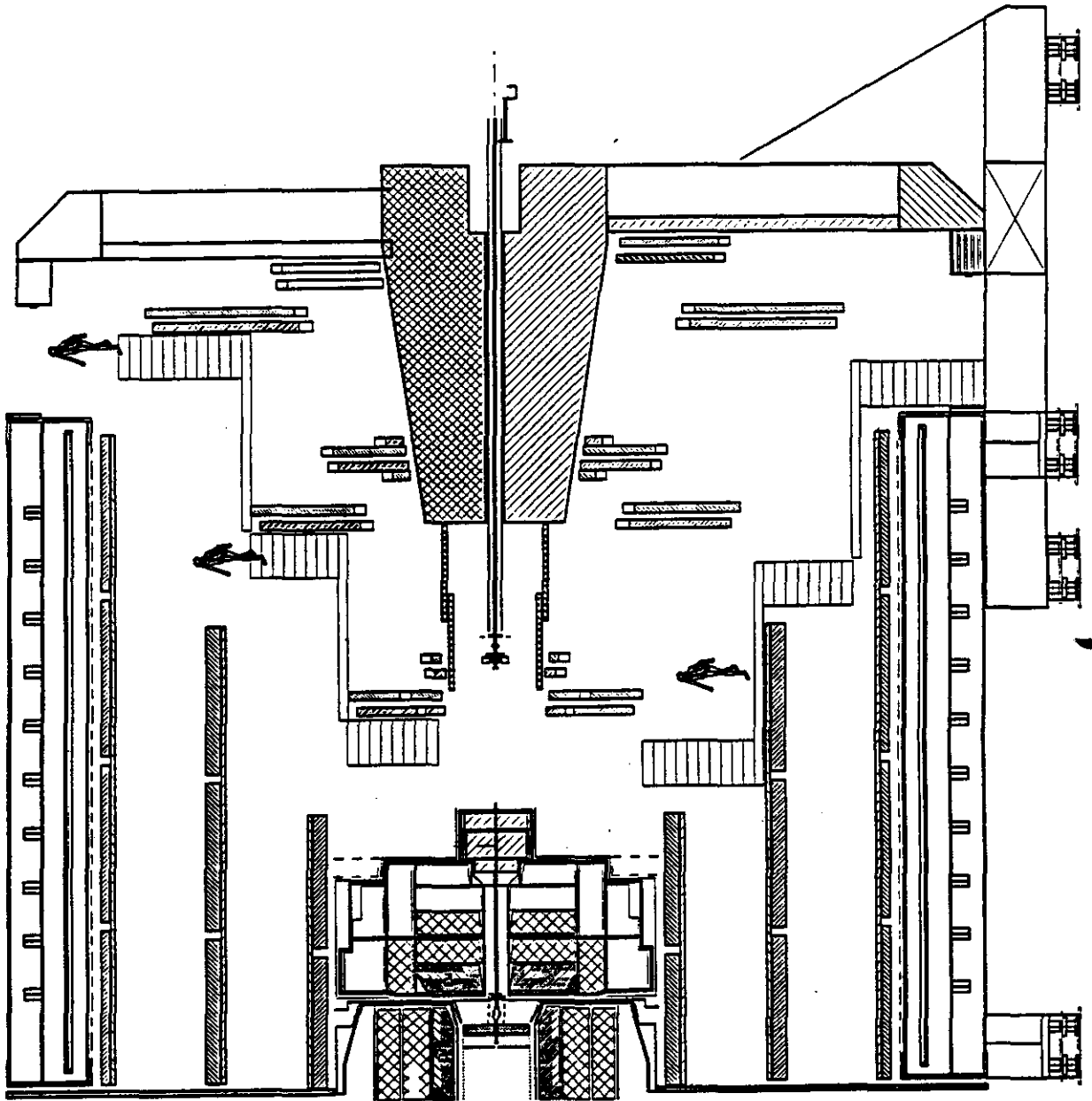
BEAM LINE INSTALLATION - PHASE 2

END - CAP CALORIMETER



BEAM LINE INSTALLATION - PHASE 3

LAST PART VACUUM PIPE WITH FFS



DETECTOR ACCESS

TABLE OF CONTENTS

OVERVIEW

Installation
Commissioning
Operation and Maintenance
Terminology

FIGURES:

Electronics System Layout
GEM Beam Pipe Subsystem Utilities Layout
GEM LAr Calorimeter Subsystem Utilities Layout
GEM Muon Subsystem Utilities Layout
GEM Magnet Subsystem Utilities Layout
GEM Tracker Subsystem Utilities Layout
Access Level (Unrestricted Access)
Access Level (Restricted Access)
Access Level (Beam/Field Off)
Access Level (Beam/Field Off, FFS Open)
Access Level (Beam/Field Off, Magnet Halves Separated)
Access Level (Beam/Field Off, Calorimeter Endcaps Open)
Access Level (Beam/Field Off, Tracker Disassembled)
Detector Access Plan View (FFS withdrawn 2.6 m)
Maintenance Access (Showing Access Scaffolding)
[GEM Maintenance Access] with FFS Withdrawn
Drawing showing detector opened for tracker access

TABLES:

GEM Detector Maintenance Access (2 pages)

DETECTOR ACCESS

DETECTOR ACCESS

OVERVIEW

Four stages of access are required during the life-cycle of the GEM Detector -- installation, commissioning, operation and maintenance. This overview addresses some of the access considerations during each of these stages.

Access is defined as the ability to move personnel and equipment from various staging areas to some point on (or inside) the detector. This includes the ability to reach areas located at varying heights above a floor level as well as access to areas normally obstructed by detector subsystems or services. Typical equipment for this purpose will be scaffolding, hydraulic elevators, mobile platforms and gangways. Throughout the installation of the detector, a large variety of types of access will be required, both in the underground experimental hall shafts and in the surface facilities.

Installation

The magnet will be the first item to be installed. Access to the magnet is required to connect power, cryogenic systems, vacuum systems, mechanical compression members between the two coil units, control and monitoring systems. Because of its large size, access at different levels will require installation of extensive equipment to ensure safe operation. The highest point at which access will be required will be approximately 23 m from the floor. The present concept incorporates bridging between the magnet structure and the gangways fixed to the hall walls.

A major portion of the detector electronics will be attached to the magnet end faces and the central detector support. To access these items permanent or removable gangways will be installed linking the electronics access platforms with the hall wall system or to the floor.

The Baseline 1 schedule includes the mapping of the field inside the magnet. To achieve this, access at beam level may be necessary in the central region. It is assumed that any equipment needed for access will be designed to spread support loads in order to avoid point loads on the inner wall of the cryostat.

The next item to be installed, after the magnet has been separated and moved away from the central detector support structure, is the calorimeter. The weight of the calorimeter will necessitate a heavy platform and rail system, placed on each side of the central detector

Source: M Harris
Updated: 6/26/92

DETECTOR ACCESS

support. This platform will be large enough to accommodate scaffolding or elevators to reach the upper level of the calorimeter--reaching over 3.5 m above the beam line, which is, in turn, some 13 m above the floor level--in order to mate the endcaps to the barrel and make connections to the calorimeter subsystem.

During the latter stages of the calorimeter installation, the barrel muon modules can be lowered and fitted to the ends of the magnet coil units. To access the attachment points around the magnet flanges, a combination of scaffolding and hydraulic elevators will be necessary.

Similarly, the muon end caps are lowered and attached around the periphery of the forward field shapers. This requires structures to enable access to the periphery of the field shapers, which reach some 25 meters above the floor level. The design of the access equipment used for installing the barrel section will enable reuse of this equipment to install the endcaps.

The last item to be installed is the tracker, which requires reopening the magnet and withdrawal of the calorimeter endcaps on the heavy rail platform system. Special access scaffolding and support equipment is needed to connect and disconnect cryogenic and power services to the terminating subsystem racks and connectors via the central detector support structure.

Commissioning

During the detector commissioning process, access to the experimental hall will be coordinated with powering of the magnet since access will not be permitted when the magnetic field is present. When the magnet is not powered, normal access to items such as electronics will be required. In some cases it will be necessary to penetrate the interior of the magnet via well defined paths to specific locations.

Studies to date indicate that it may be plausible to withdraw the forward field shaper and muon end cap assembly by approximately 2 m to allow access to the inside of the detector. This would greatly enhance access during the commissioning and maintenance periods.

Operation and Maintenance

During beam runs, there will be no access to the below ground experimental hall, although there may be limited access to the shielded electronic rooms adjacent to the experimental hall. When short shut-

Source: M Harris
Updated: 6/26/92

DETECTOR ACCESS

down periods occur and the magnet is de-energized, the access conditions are similar to the commissioning stage.

The current SSC Level 2 Specifications for Experimental Systems (11/25/91) describes an operations scenario with scheduled down times of 940 hours at one day per week, and a maximum of 2190 hours for long term repairs. The current GEM access philosophy, which impinges strongly on the design, assumes that short accesses will only allow maintenance to components outside the magnet. This will permit access to much of the calorimeter electronics located at the periphery of the support membrane. In addition there is limited access to the muon volume through the ends of the magnet through the support structure for the FFS, or by opening the detector slightly as discussed above. This will allow access in the plane of the beam along a walkway, and more limited access to modules out of the plane. This route provides access also to the periphery of the calorimetry where some electronics can also be located. The vacuum pumps located downstream of the forward calorimetry are also accessible here.

All access to other components in the interior of the detector requires a once-per-year down time of 3 months (2160 hrs) which allows for detector disassembly, including rolling apart the magnet halves, and permits access and removal of the inner tracker. This can be accomplished in various stages which are illustrated in this section. First, the IR quads and collimators, which are currently located directly behind the FFS, must be removed. (There is serious consideration of moving these quads further upstream to avoid this problem and the attendant issues of activation and magnetic shielding). The FFS can then be moved for better access to the barrel muon chambers, one or both magnet halves, with the muon chambers and FFS attached, can be moved. This provides access to the calorimetry and also the muon chambers. With the magnet halves open, the end calorimeters can be moved to provide access to the inner tracker. This operation of opening and closing the magnet halves is estimated to require approximately two months.

Further study is in progress to understand the impact of limited access on the performance of GEM. The location of critical elements, the redundancy of systems for greater reliability, and the reliability studies of components all must be validated. The use of movable carriers for the service cables will allow the services to remain connected to the detector subsystems, thus eliminating the time normally needed to disconnect the detector components. Temporary platforms, scaffolding

Source: M Harris
Updated: 6/26/92

DETECTOR ACCESS

and hydraulic elevators may then be transported to the maintenance area over the top of the magnet using the hall crane.

The following tables lists for each GEM subsystem hardware which can be repaired at a specified access level. Access levels are listed in order of increasing difficulty, e.g., equipment located on the surface will be continually accessible, but equipment located in the detector hall will be accessible only when the beam and field are off, with perhaps other restrictions as well. Much hardware, e.g., cabling, is listed at almost every access level; clearly the access level required to repair such hardware depends on the location of the failure. Generally hardware is listed only at the least difficult access level unless the next level of access exposes additional surface.

Terminology

Electronics includes racks, crates, cards and chips but excludes cables and power supplies.

Process cooling includes both water and air cooling.

Slow control instrumentation includes such items as thermocouples, pressure sensors, etc and associated equipment.

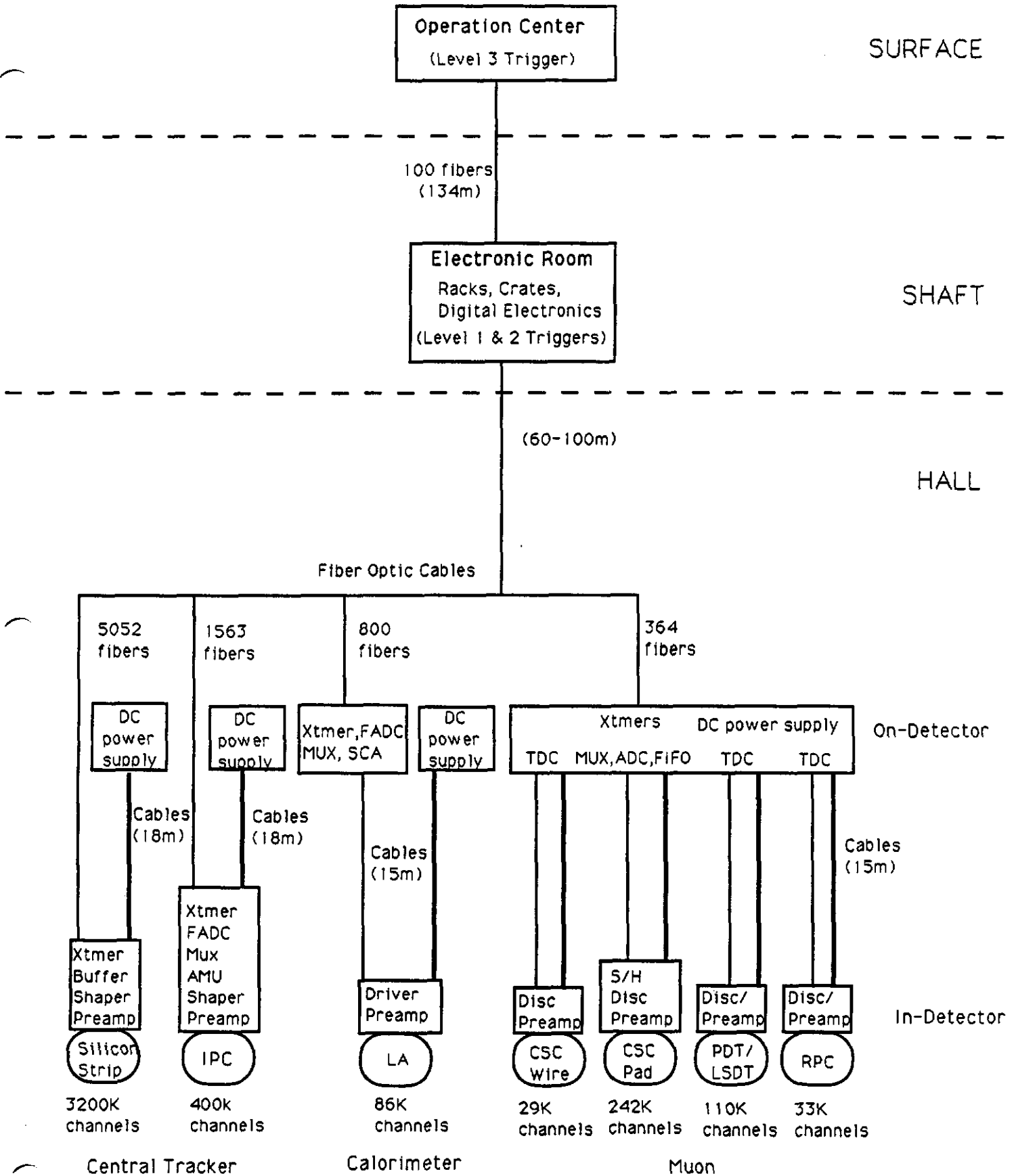
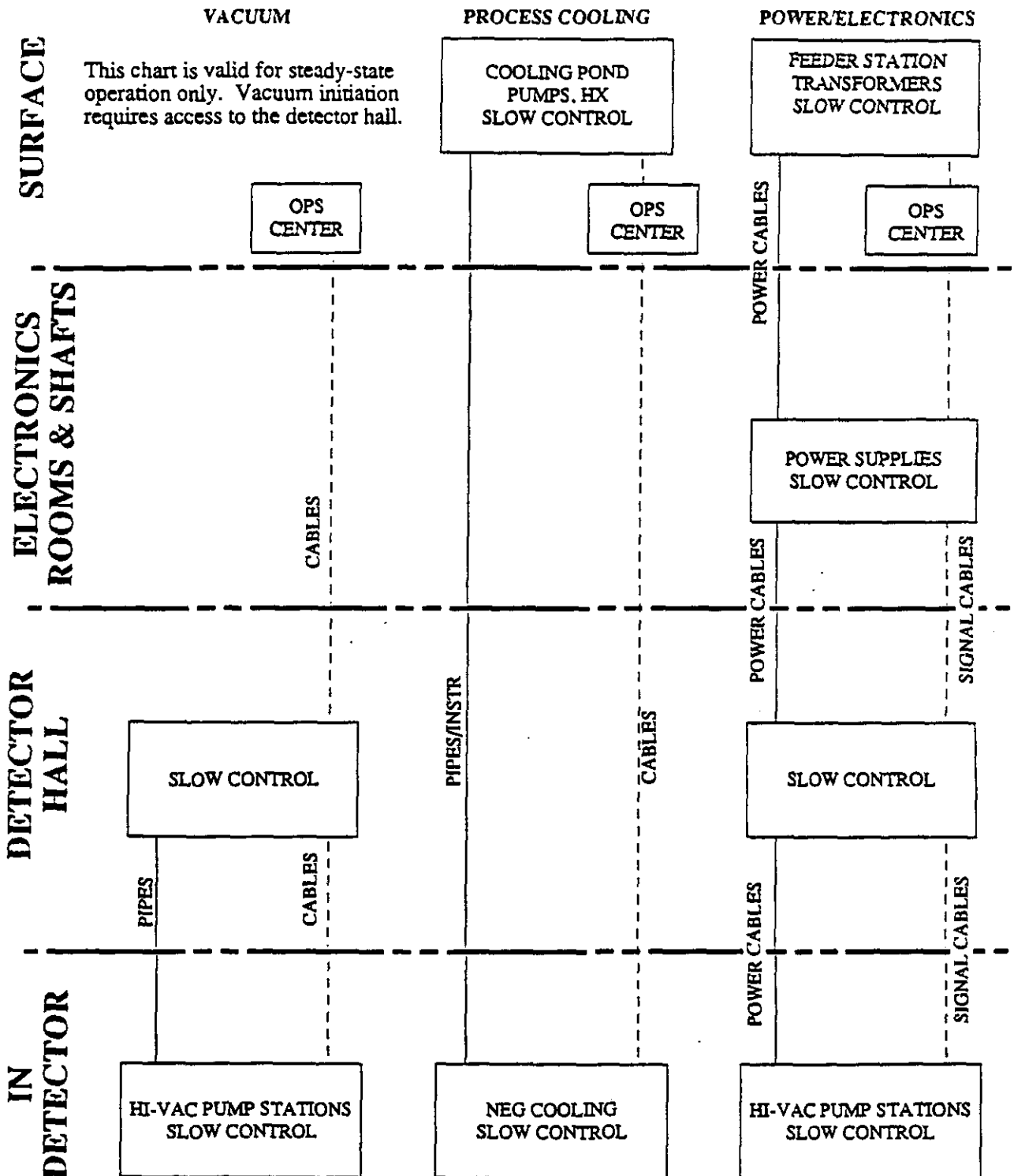
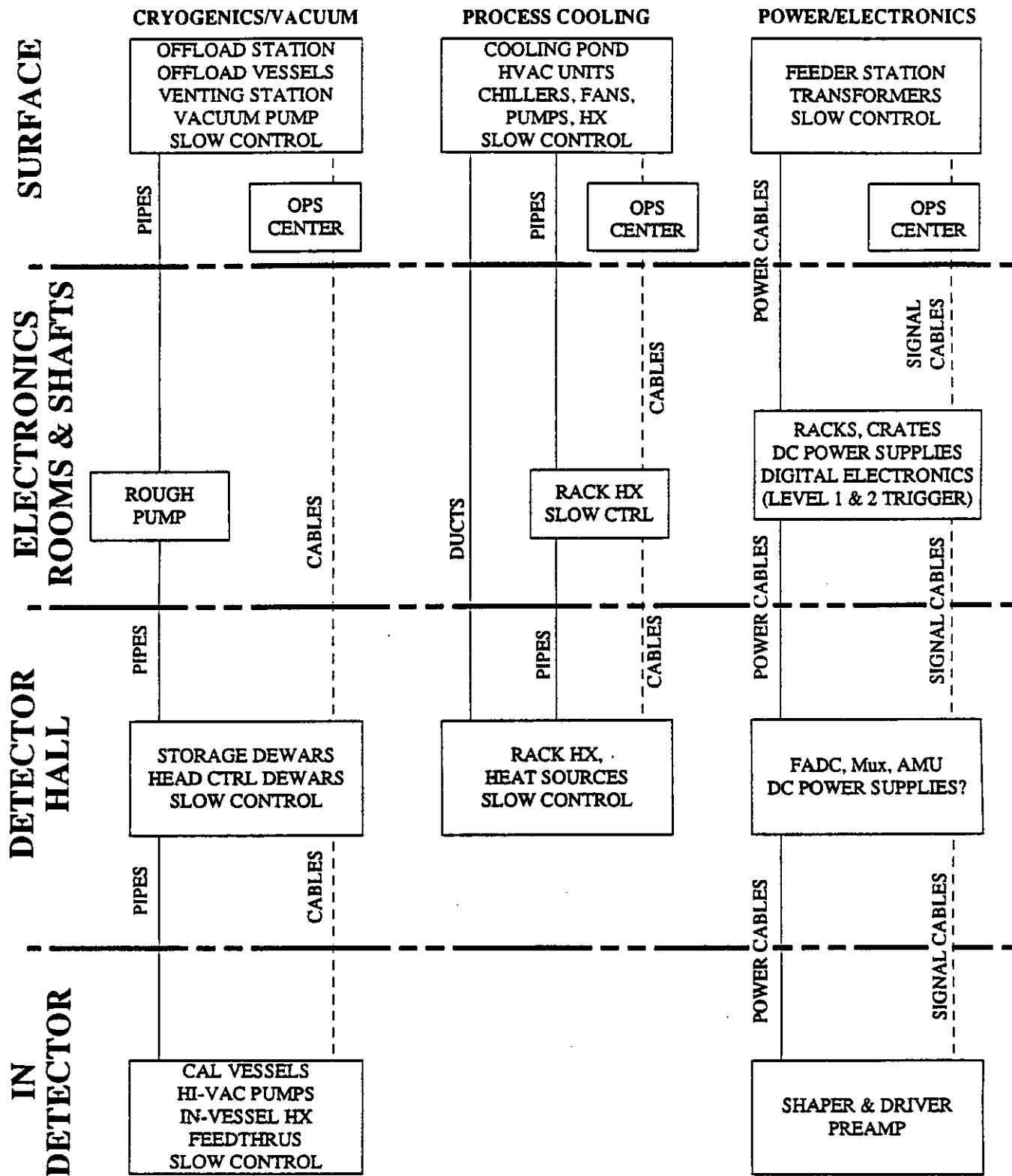


Figure 5-1. Electronics System Layout



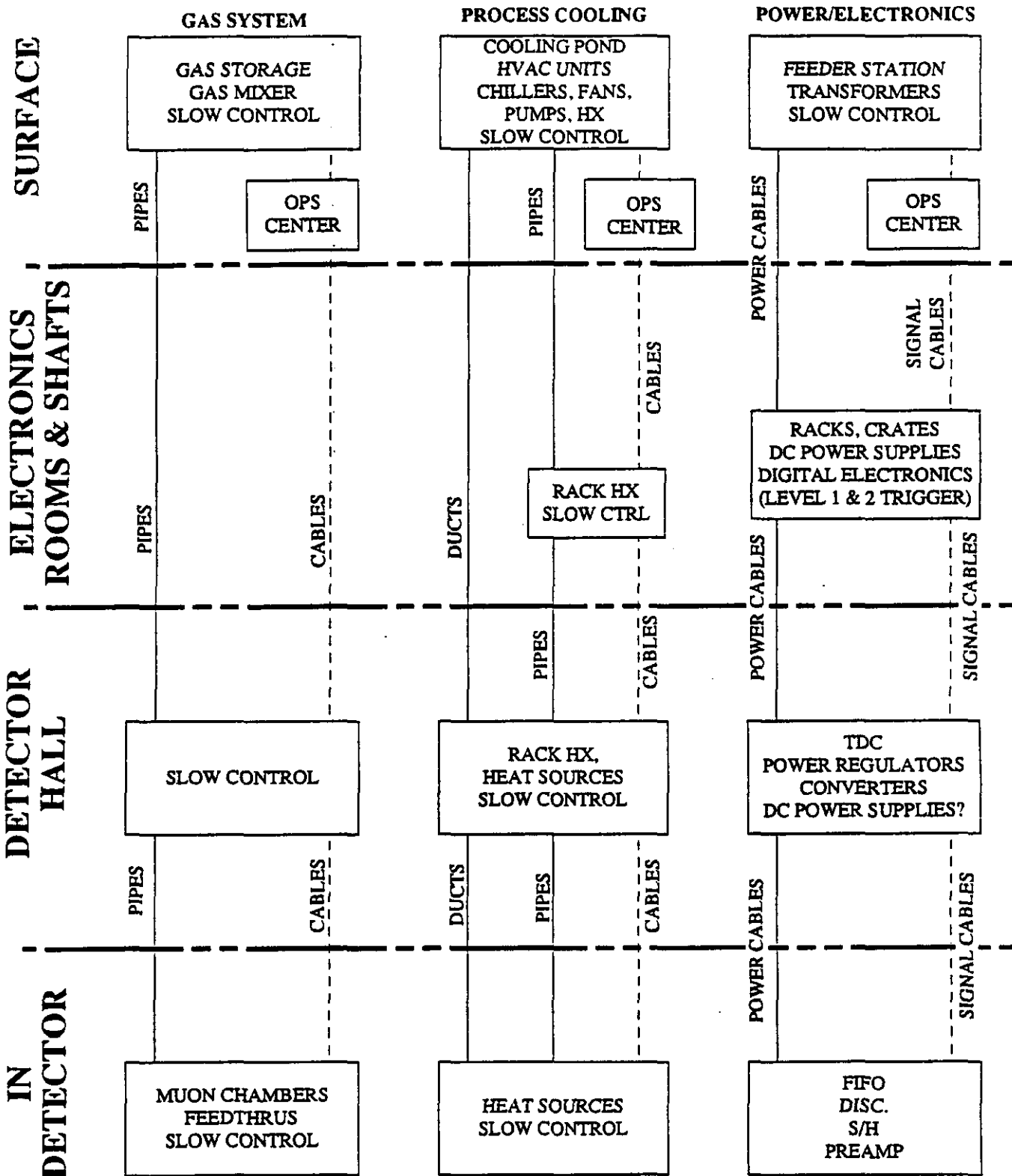
GEM BEAM PIPE SUBSYSTEM UTILITIES LAYOUT
 EBERLE 07/01/92

KEY: HV = HIGH VOLTAGE
 HX = HEAT EXCHANGER
 NEG = NONEVAPORABLE GETTER PUMP
 OPS = OPERATIONS



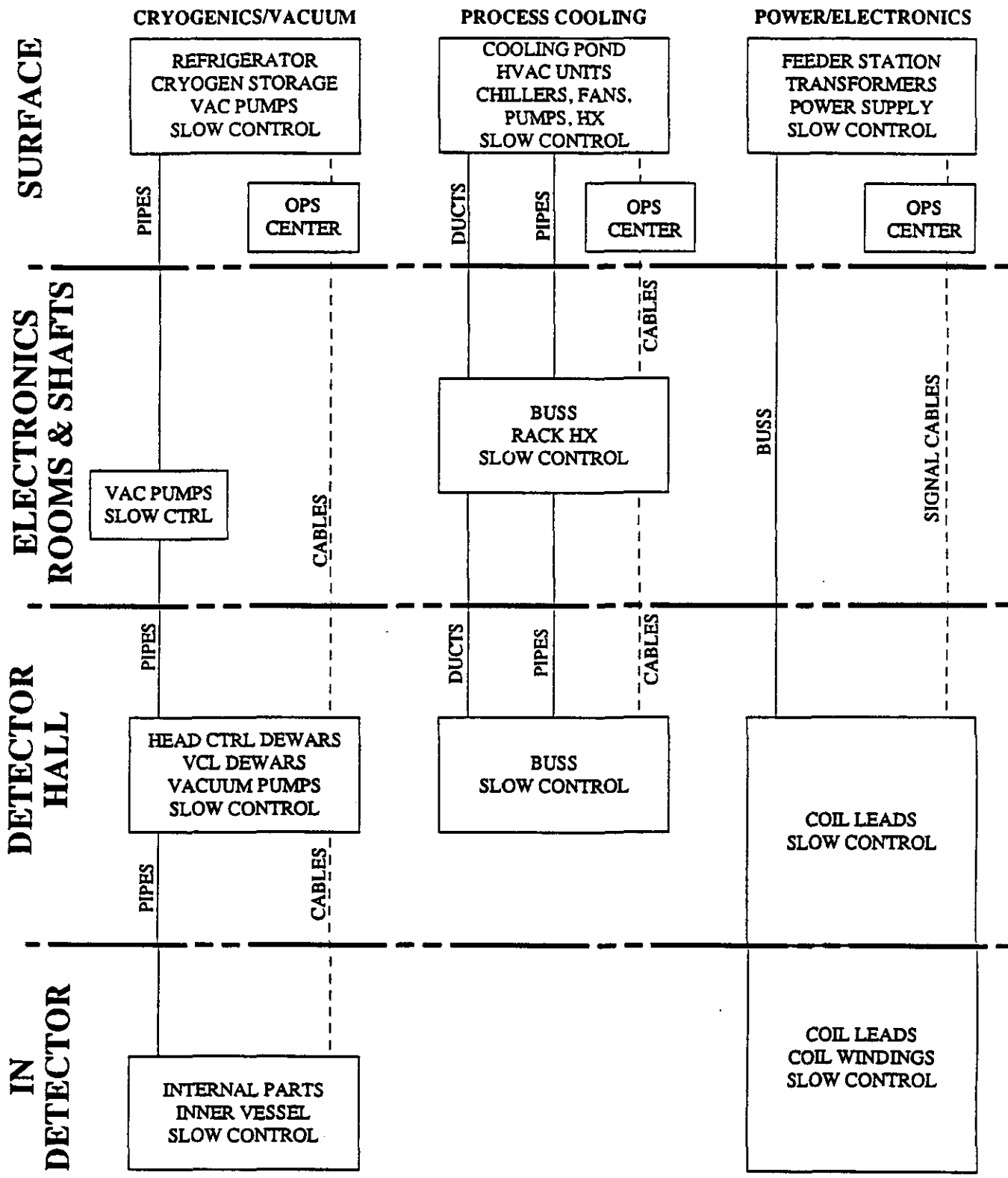
**GEM LAr CALORIMETER SUBSYSTEM
UTILITIES LAYOUT**
EBERLE 07/01/92

KEY: HV = HIGH VOLTAGE
HX = HEAT EXCHANGER
OPS = OPERATIONS



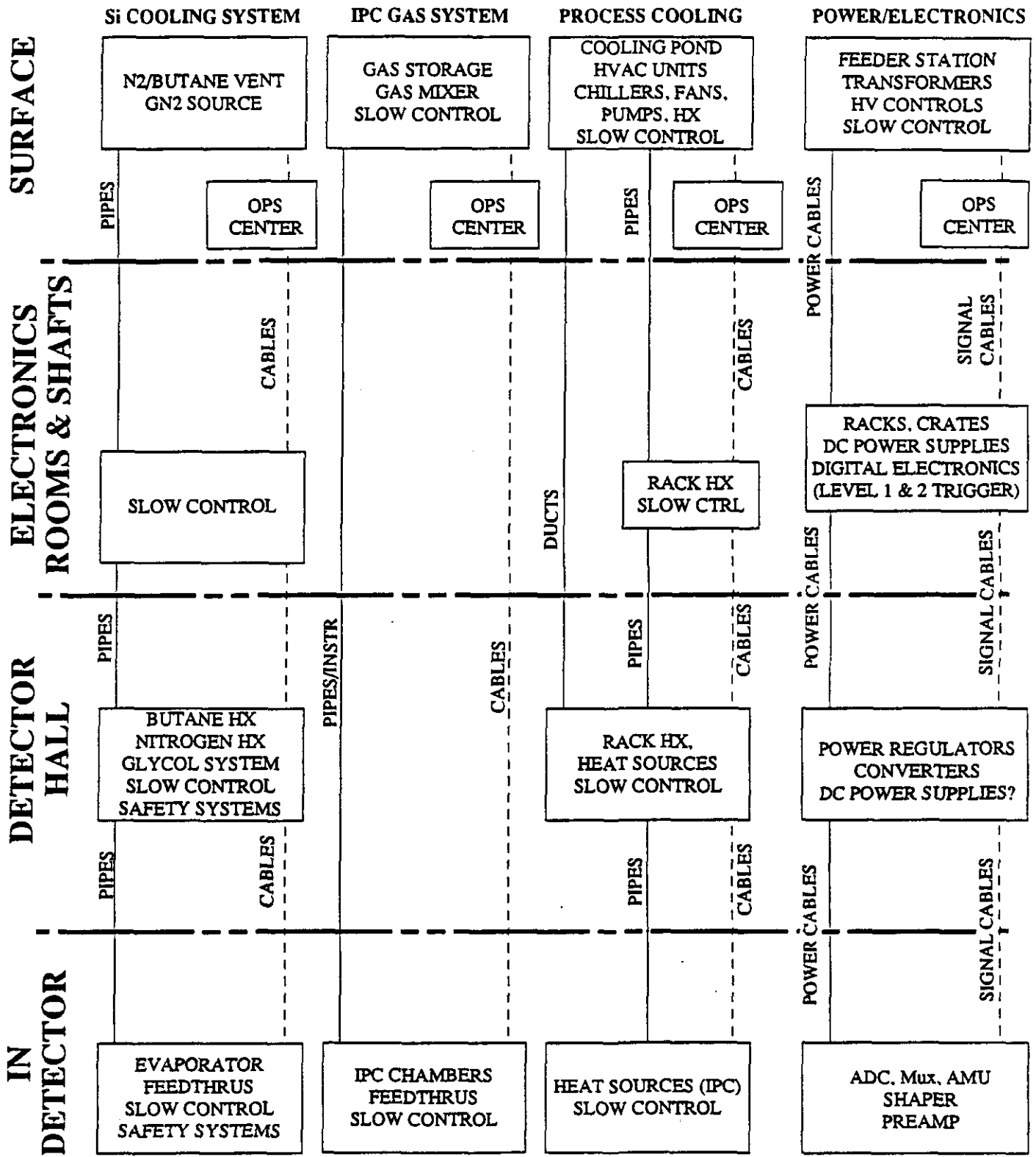
**GEM MUON SUBSYSTEM
UTILITIES LAYOUT**
EBERLE 07/01/92

KEY: HV = HIGH VOLTAGE
HX = HEAT EXCHANGER
OPS = OPERATIONS



**GEM MAGNET SUBSYSTEM
UTILITIES LAYOUT
EBERLE 07/01/92**

KEY: HV = HIGH VOLTAGE
HX = HEAT EXCHANGER
OPS = OPERATIONS
VCL = VAPOR-COOLED LEAD



GEM TRACKER SUBSYSTEM UTILITIES LAYOUT
 EBERLE 07/01/92

KEY: GN2 = GASEOUS NITROGEN
 HV = HIGH VOLTAGE
 HX = HEAT EXCHANGER
 OPS = OPERATIONS

GEM DETECTOR MAINTENANCE ACCESS

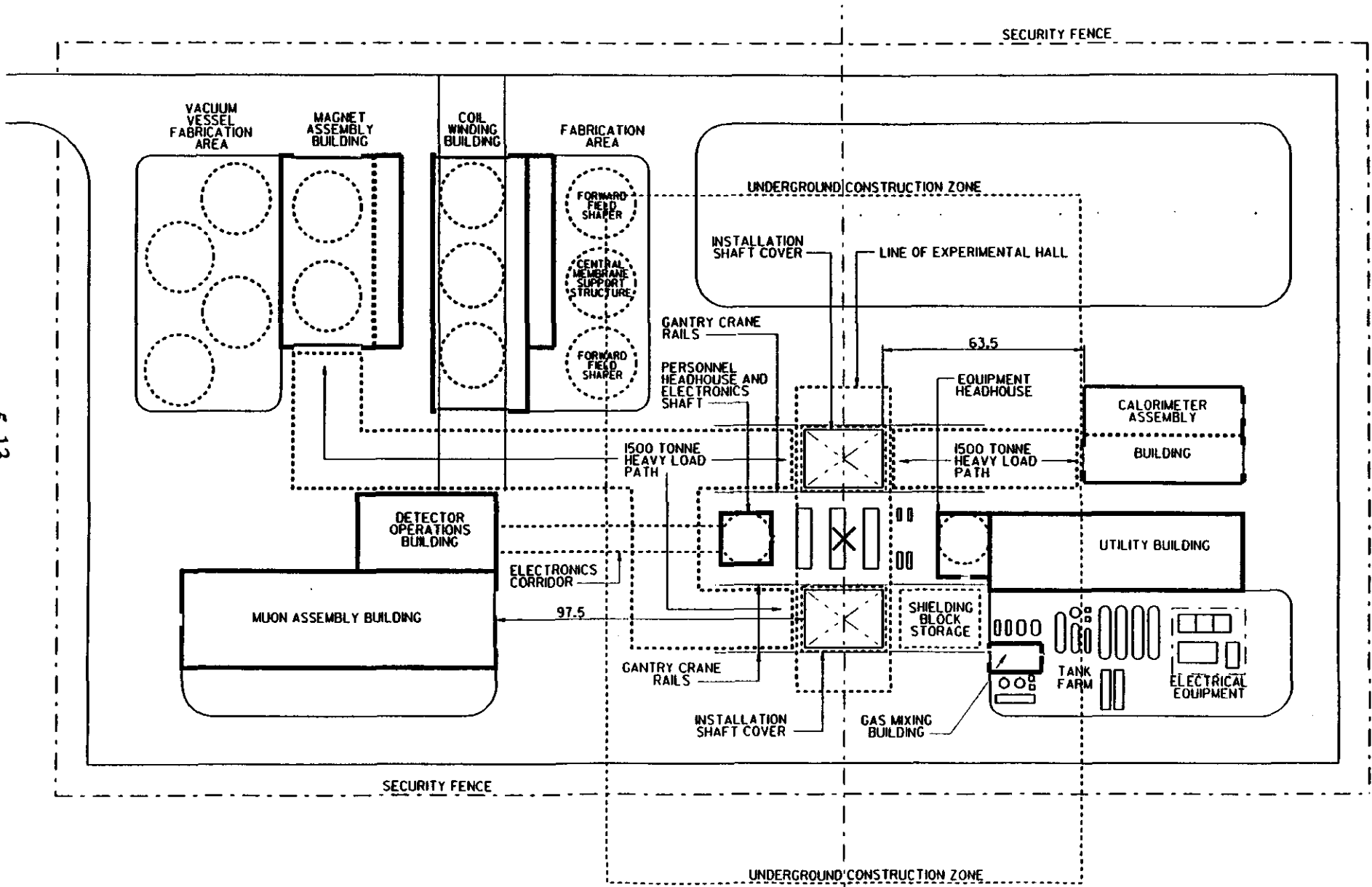
ACCESS LEVEL	Hardware Description				
	<i>At the specified access level, the listed types of hardware can be accessed for repair</i>				
	Magnet	Muons	Calorimeters	Tracker	Beam Pipe
Surface Unrestricted Access	Ops center	Ops center	Ops center	Ops center	Ops center
	Power supply	Gas storage	Pipes	Gas storage	UHV controls
	Buss	Gas mixer	Slow control	Gas mixer	Cables
	Slow control	Slow control		Slow control	
	Process cooling	Process cooling	Process cooling	Process cooling	
	Refrigerator	Pipes		Pipes	
	Helium storage		Cryogen storage	N2 & Butane vents	
	Pipes			HV controls	
Electronics Rooms, Cable Shaft & Utilities Shaft Restricted Access	Buss	Electronics	Electronics	Electronics	N2 pipes
	Slow control	Cables	Cables	Cables	Vac interlocks
	Pipes	Slow control	Slow control	Slow control	Vac terminals
	Process cooling	Process cooling	Process cooling	Process cooling	(State of vac system)
	Cables	Pipes	Pipes	Gas storage	Cables
	Vac pumps		Valves	HV supplies	
			Rough pump	Pipes	
			ODH monitor		
Detector Hall Beam & Field Off for Access	Buss	Electronics	Electronics	Electronics	Sector valves
	Leads	Power supply	Power supply	Power supply	
	Cables	Cables	Cables	Cables	Cables
	External vac vessel	Process cooling	Process cooling	Process cooling	External ion pump station
	Head control dewars	Slow control	Cryogen storage	Slow control	Sublimation pump
	Slow control	Pipes	Pipes	HV	
	VCL dewars		Valves	Gas storage	
	Pipes		Slow control	Pipes	
	Vac pumps		ODH monitor		
In-Detector, Closed Beam & Field Off, Access between Coils & FFS		Electronics	Electronics	Minimal Accessible Hardware	Nitrogen Pipes
		Cables	ODH monitor		Valves
		Process cooling	Vac vessel (endcap head)		Internal ion pump station
		Slow control			
		Small gas leak			
		Alignment			
		Pipes			

GEM DETECTOR MAINTENANCE ACCESS

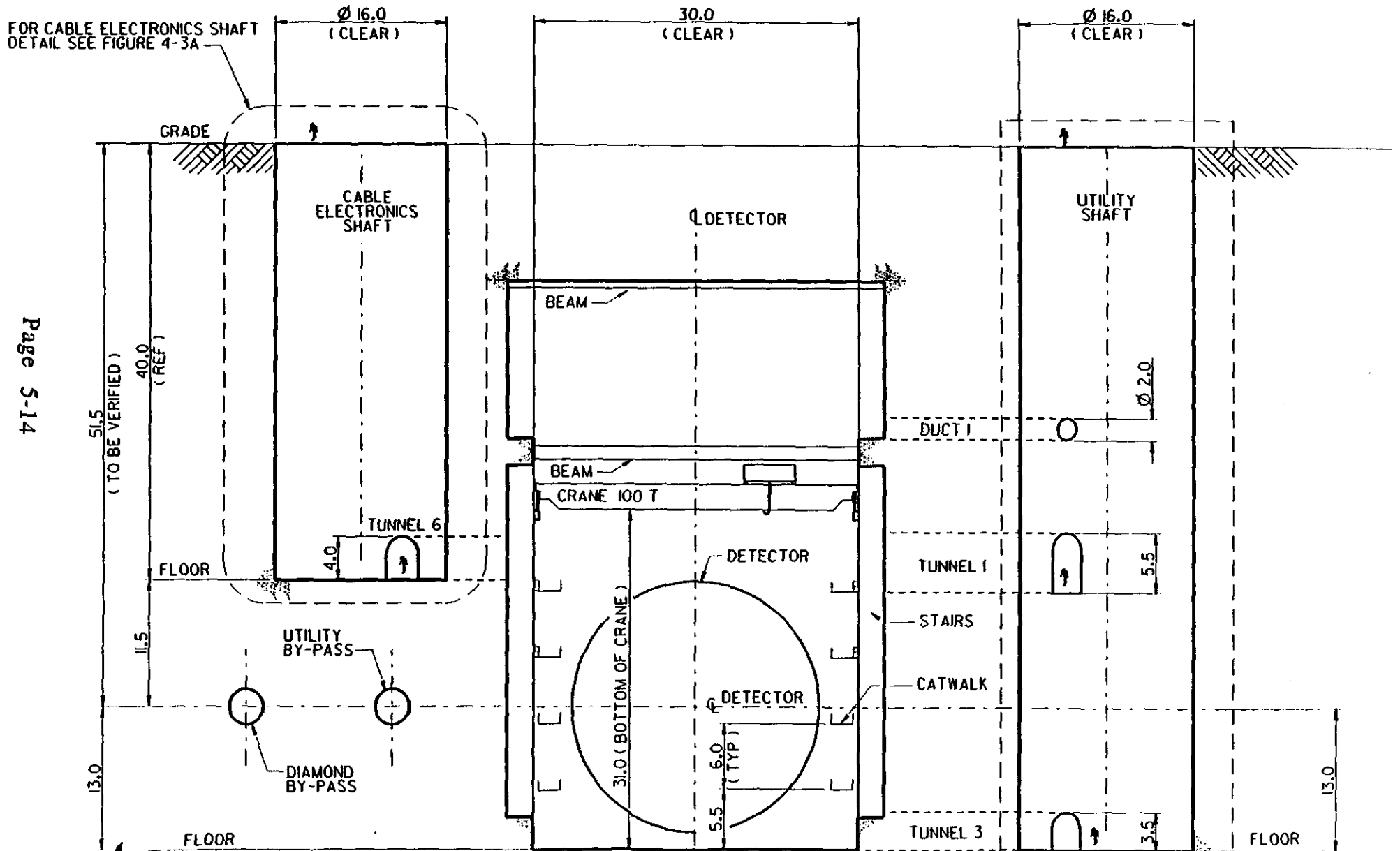
ACCESS LEVEL	Hardware Description				
	<i>At the specified access level, the listed types of hardware can be accessed for repair</i>				
	Magnet	Muons	Calorimeters	Tracker	Beam Pipe
In-Detector, Coils Retracted Beam & Field Off, Coils Moved for Access		Electronics	Electronics	Minimal Accessible Hardware	Pipe thru FFS
		Cables	Cables		
		Process cooling	Vac vessel minor repair		
		Small gas leak	Hi vac pump		
		Alignment	Feedthrus		
		Pipes			
		Slow control			
In-Detector, End Cals Retracted Beam & Field Off, Coils & End Cals Moved for Access		Same as Coils Retracted	Same as Coils Retracted, with more vac vessel surface areal exposed	IPC Detectors	NEG
				Electronics	Cables
				Cables	Pipe thru calorimeters
				Process	Bakeout equip
				Pipes	Nitrogen pipes
				Slow control	
				HV	
				Gas leaks	
				Gas enclosure	
Subsystem Removal Beam & Field Off, Coils (& End Cals) Moved, Subsystem Disassembled for Access	Major vessel repair	Structural repair	Pressure vessel repair	Internal components	Pipe thru tracker
	Coil windings	Broken wires	Module repair	Electronics	Supports
		Major gas leak	Pre-amps	Cables	
	Internal components		Vac vessel major repair	Process cooling	
			Internal cables	Slow control	
			N2 HX repair	HV	
			Feedthrus	Pipes	

ACCESS LEVEL FIGURE 1 UNRESTRICTED ACCESS

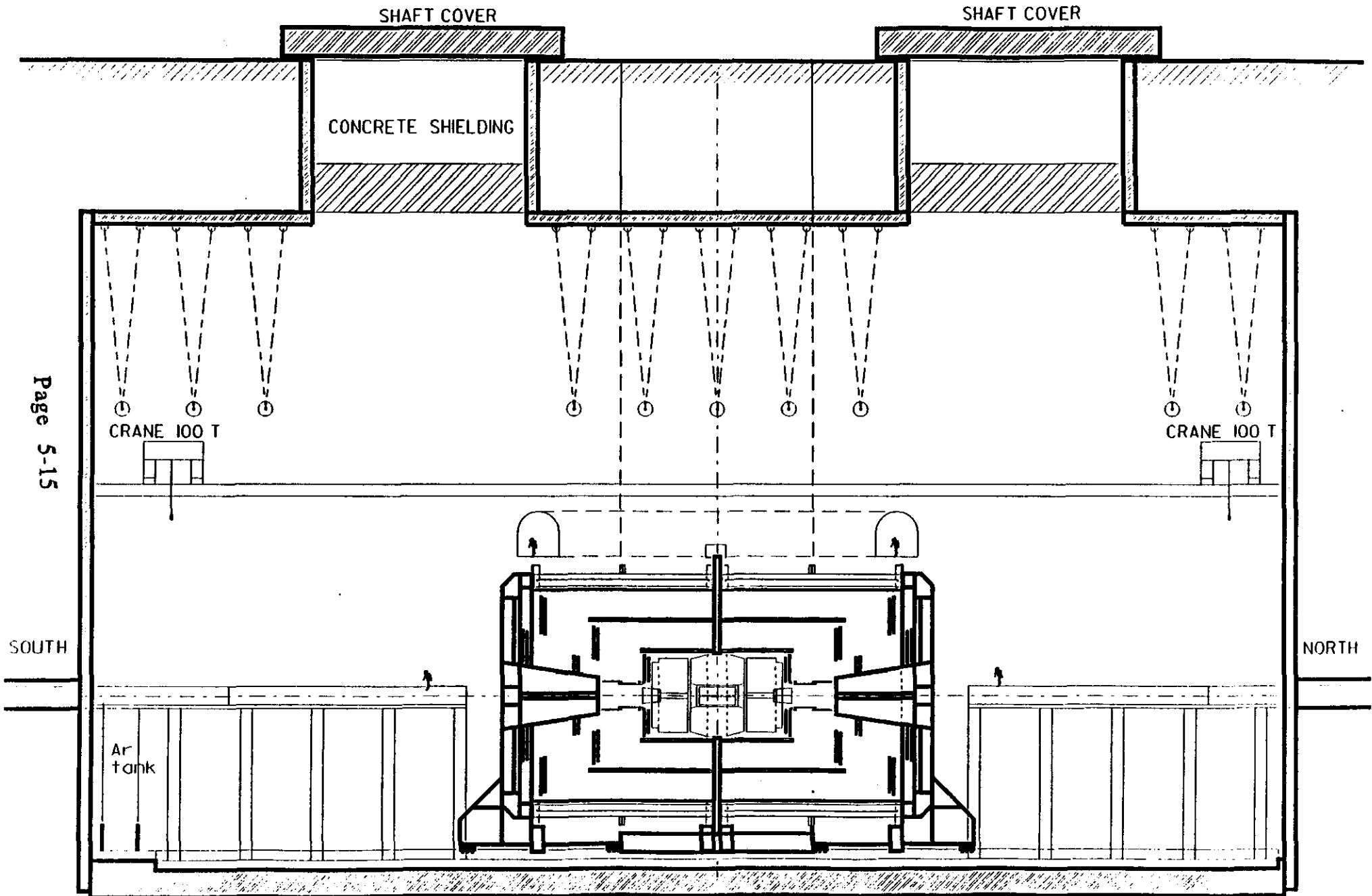
Page 5-13



ACCESS LEVEL FIGURE 2 RESTRICTED ACCESS

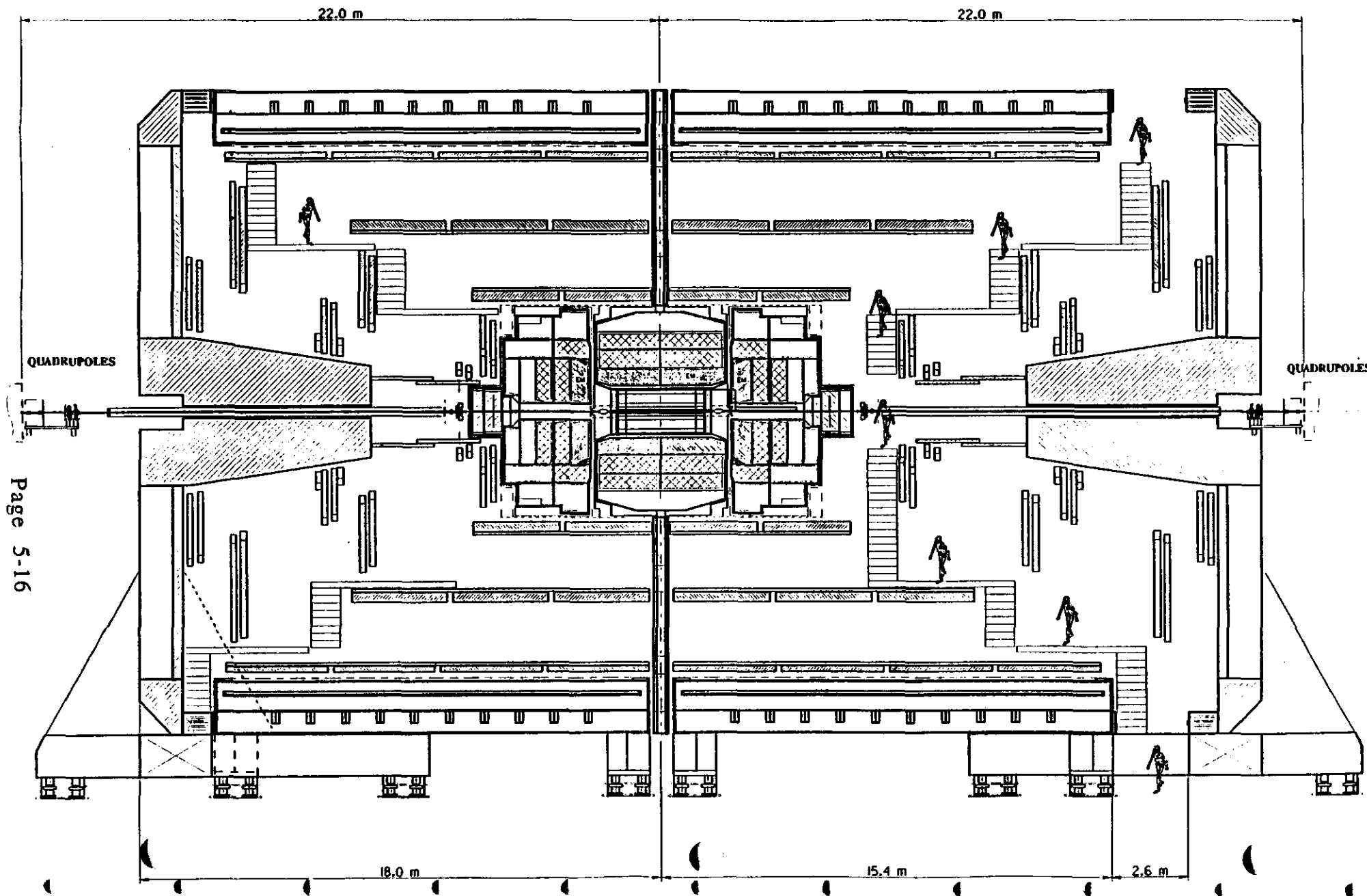


ACCESS LEVEL FIGURE 3 BEAM - FIELD OFF FOR ACCESS

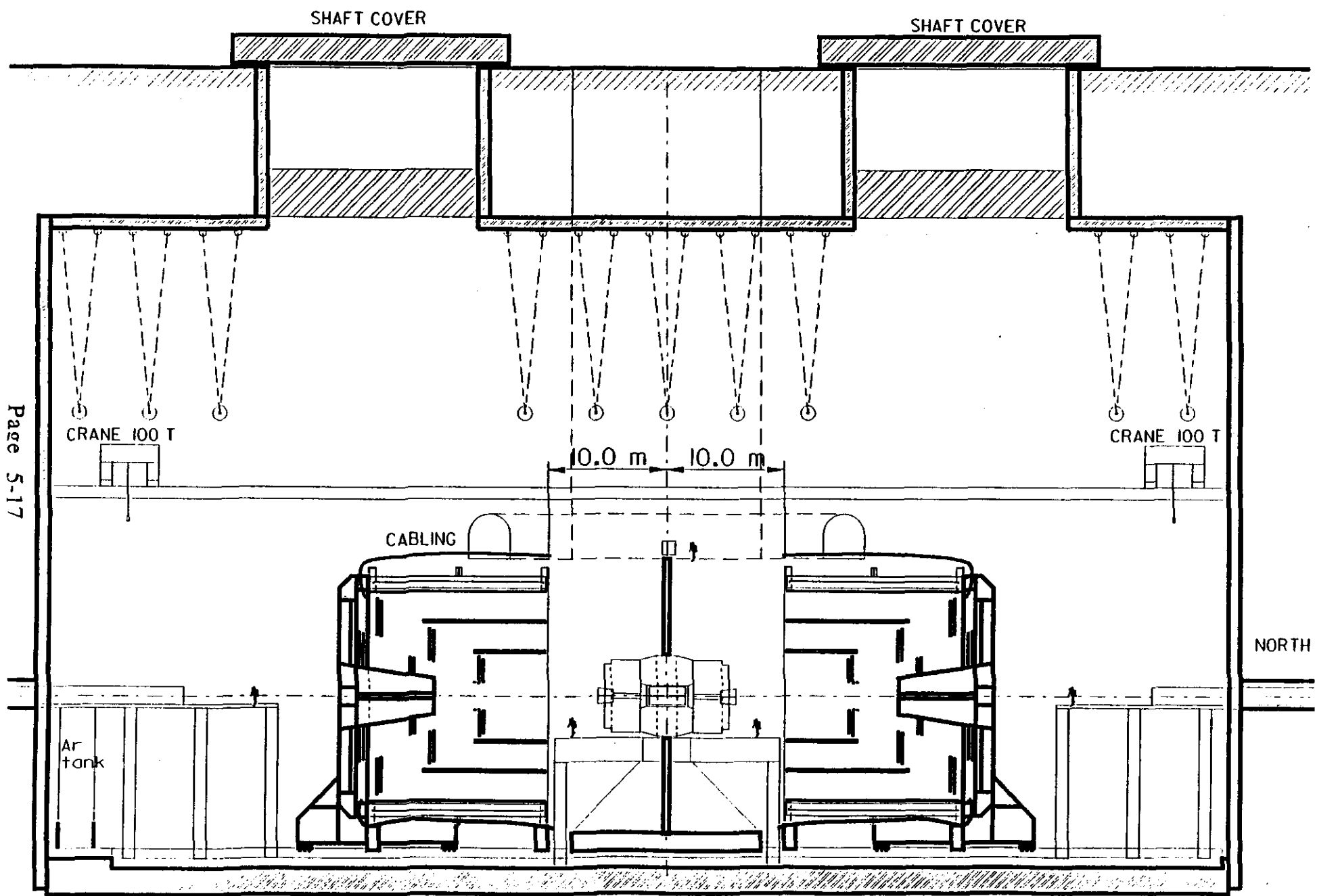


ACCESS LEVEL FIGURE 4

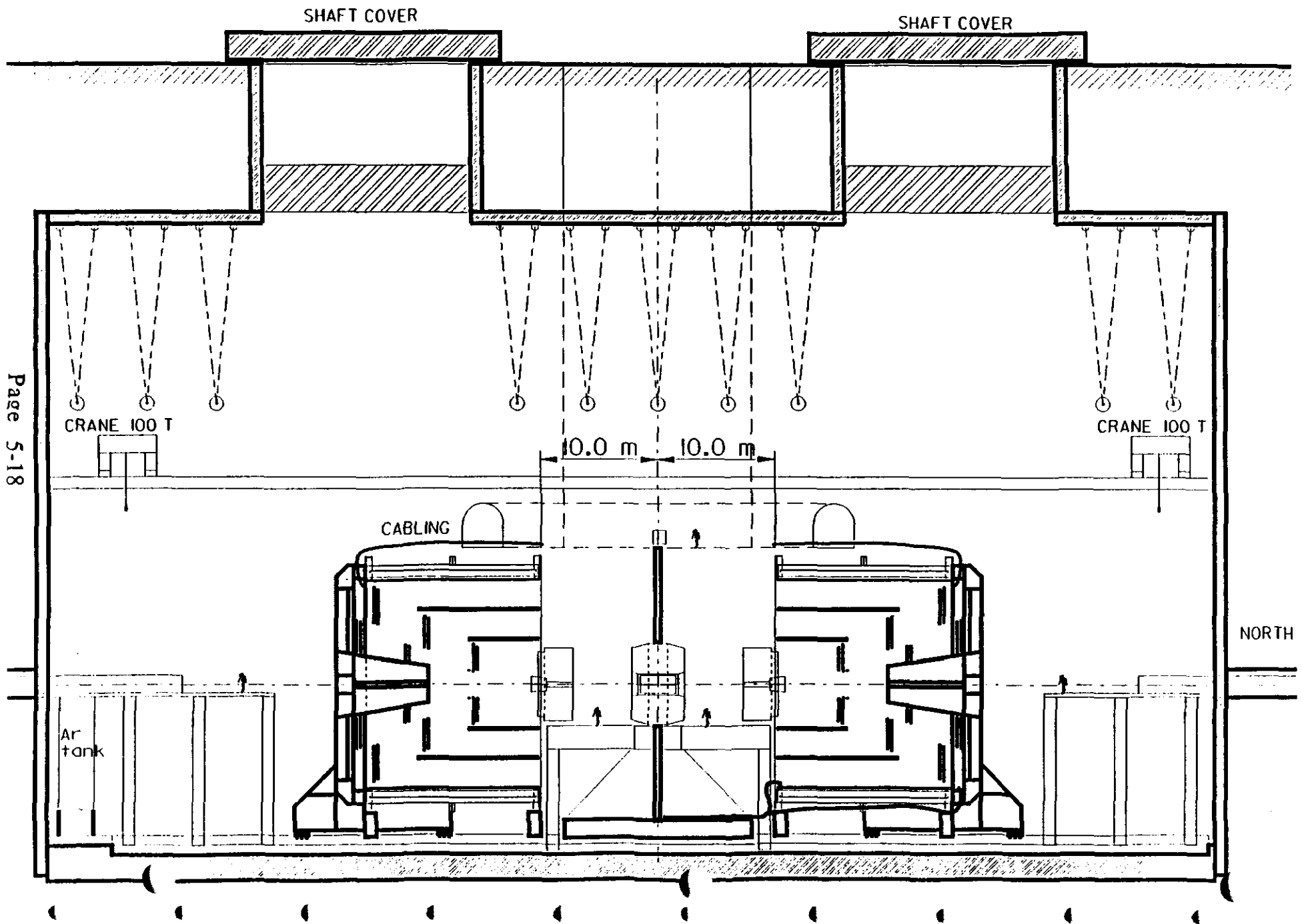
BEAM - FIELD OFF ACCESS BETWEEN COILS - FFS



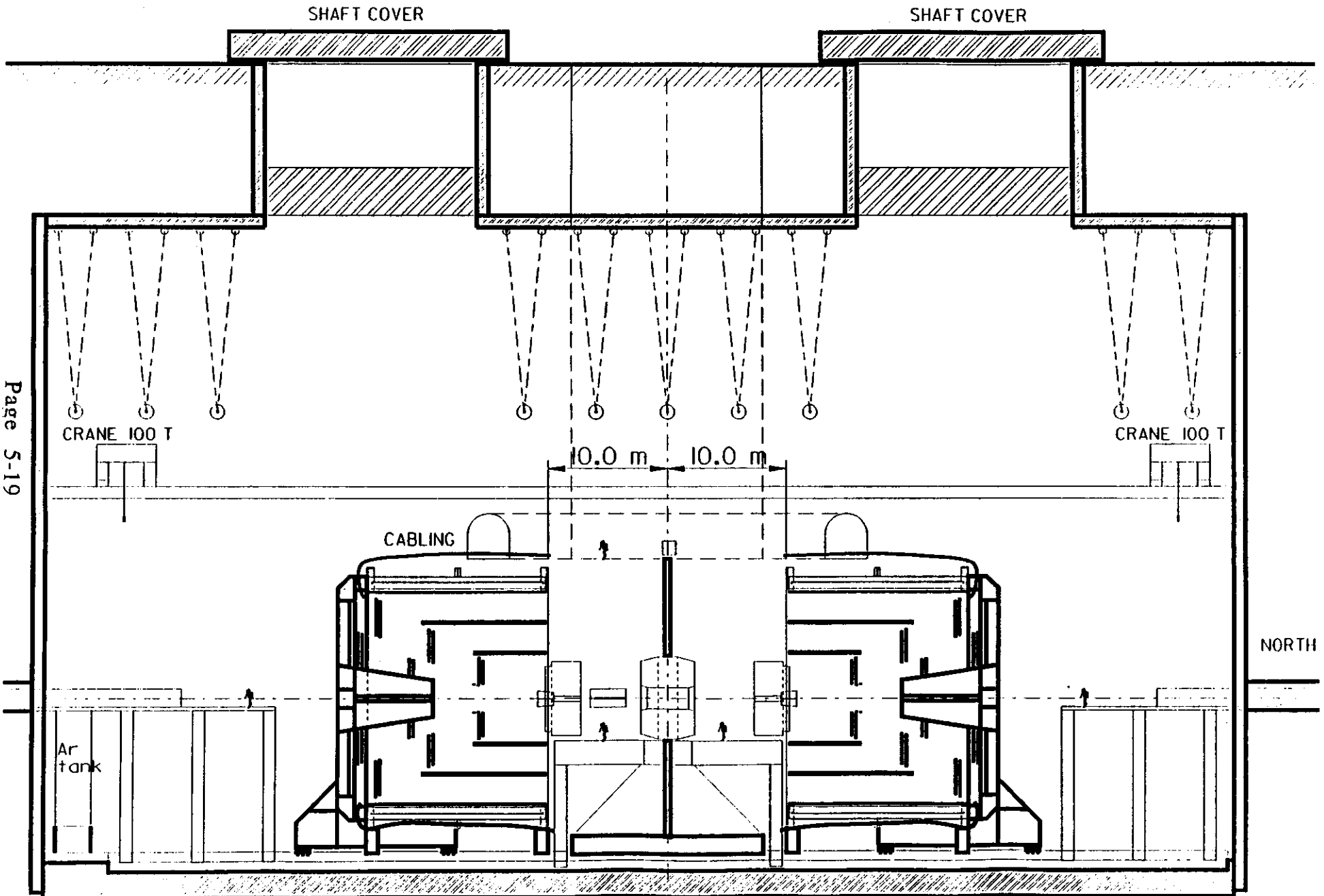
ACCESS LEVEL) FIGURE 5 BEAM - FIELD OFF COILS MOVED FOR ACCESS



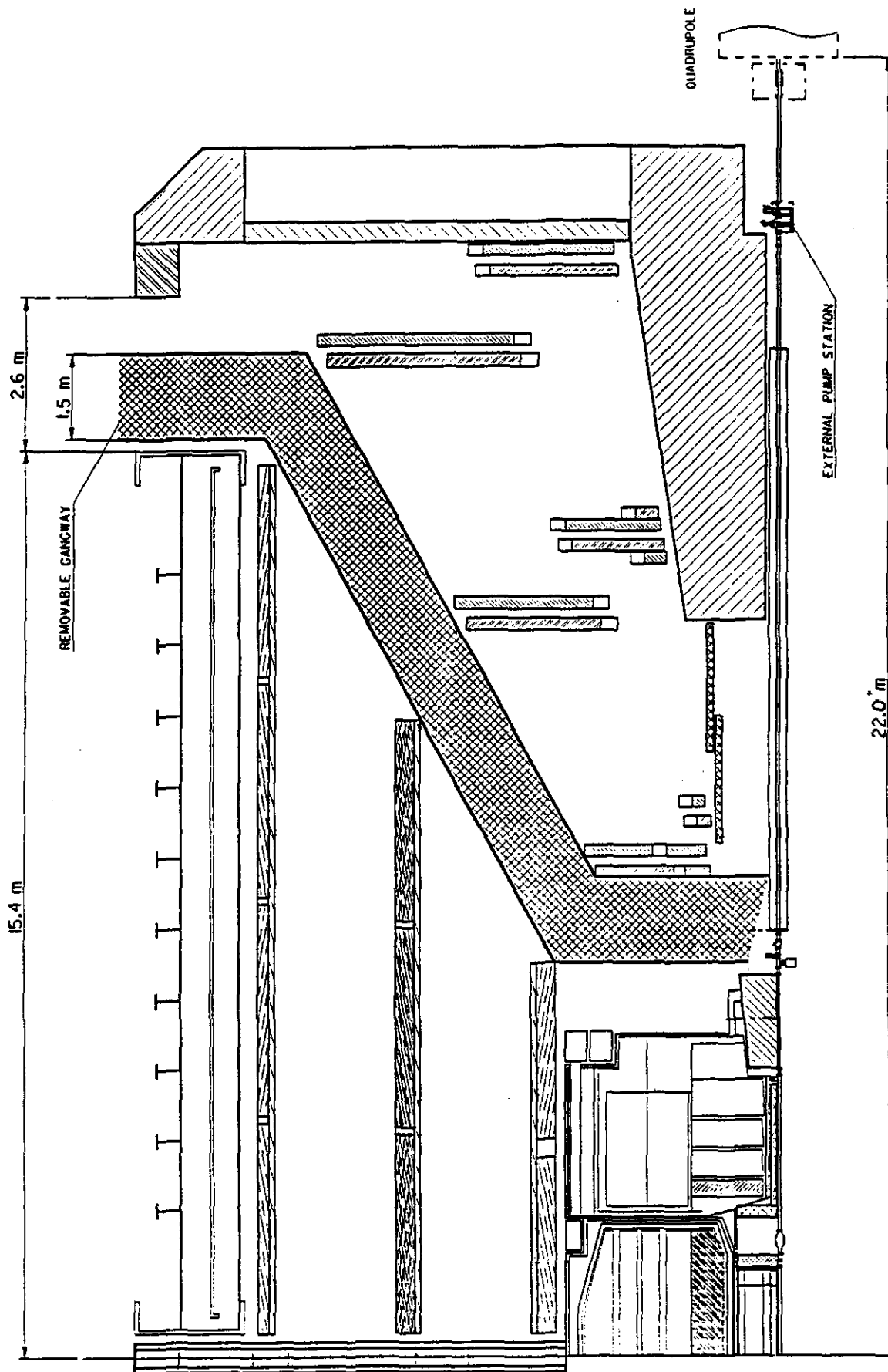
ACCESS LEVEL FIGURE 6 BEAM - FIELD OFF COILS - END CAP CALORIMETER MOVED FOR ACCESS



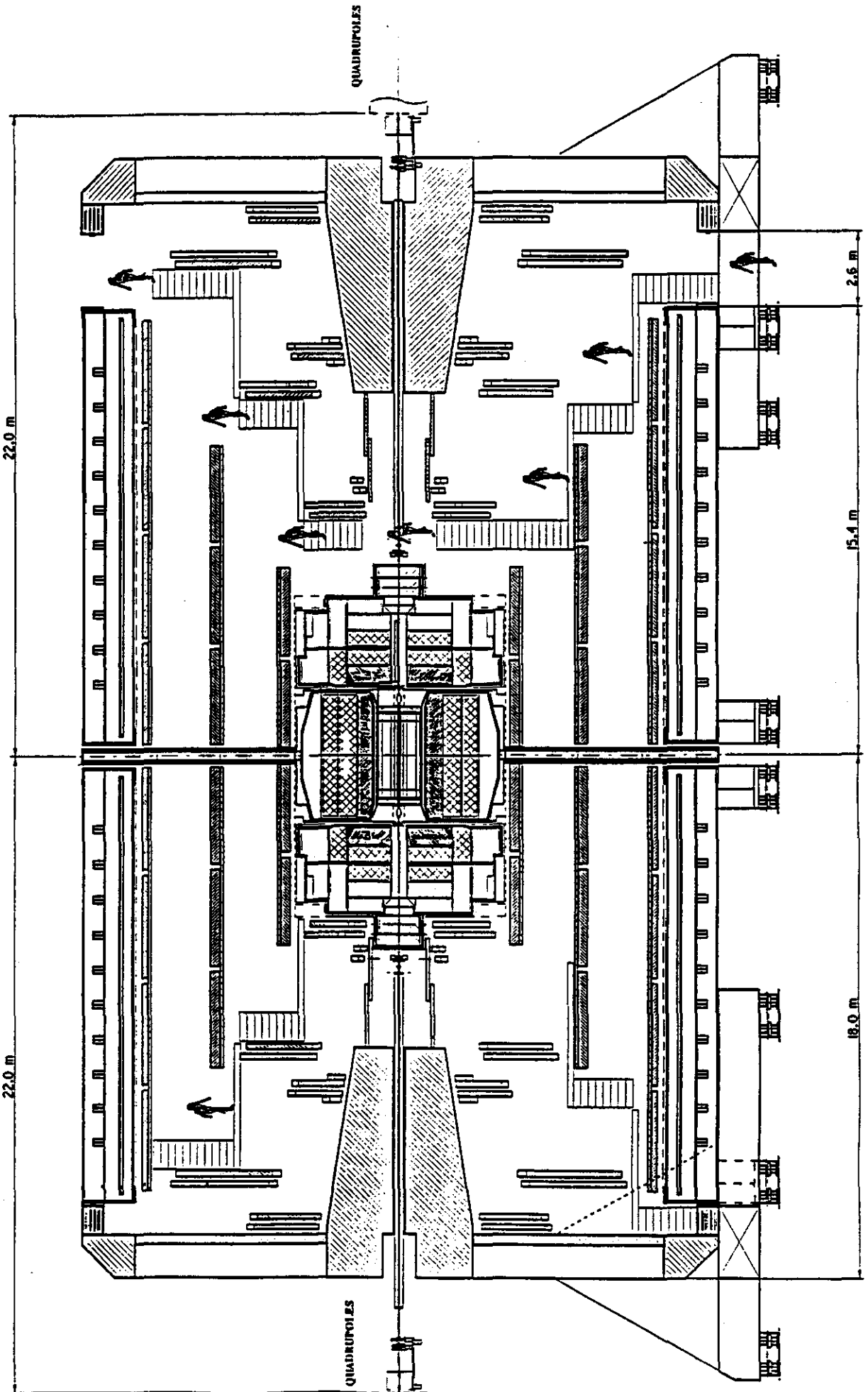
ACCESS LEVEL) FIGURE 7
BEAM - FIELD OFF COILS - END CAP CALORIMETER
MOVED - SUBSYSTEM DISASSEMBLED



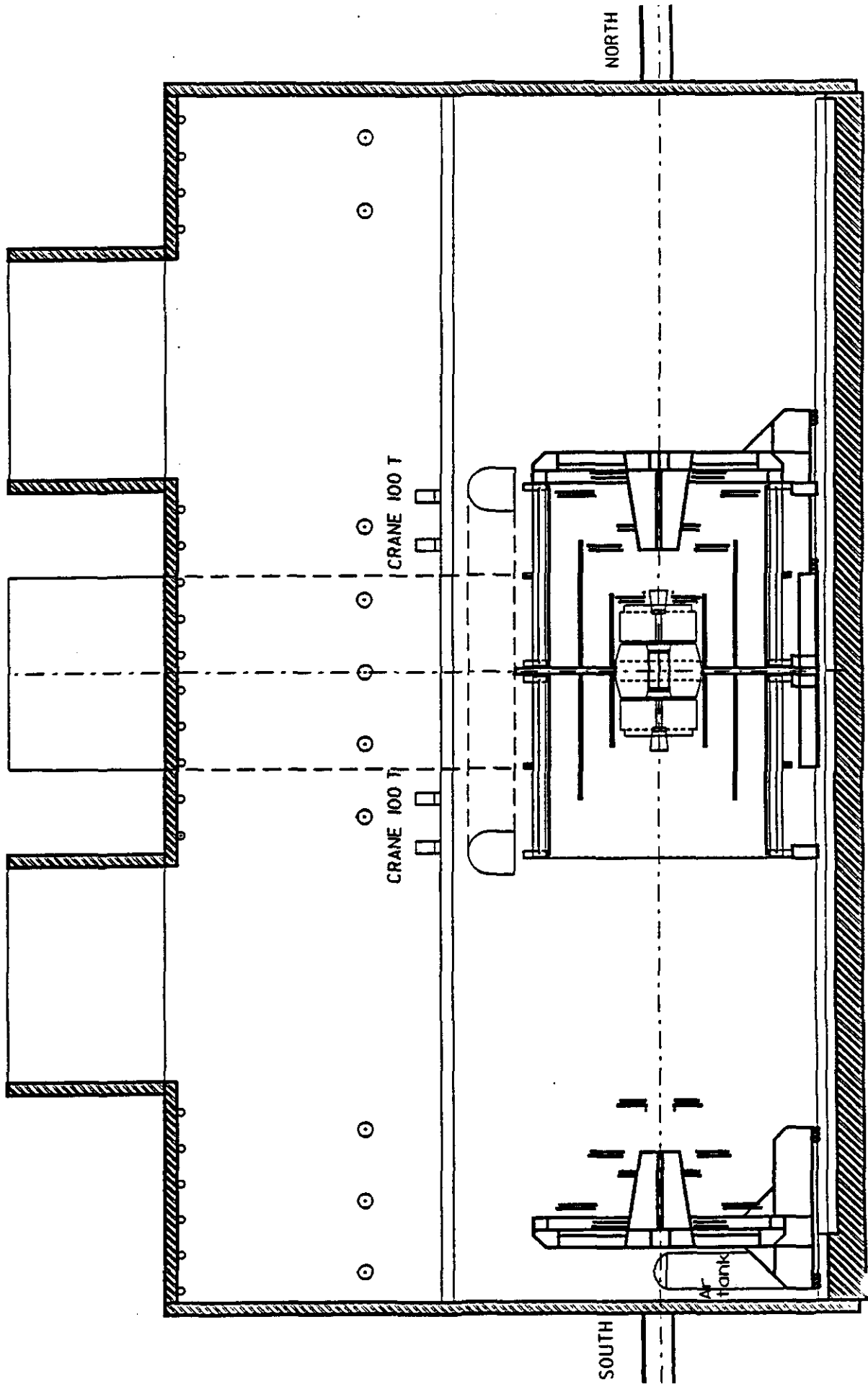
DETECTOR ACCESS PLAN VIEW
FFS WITHDRAWN BY 2.6 m



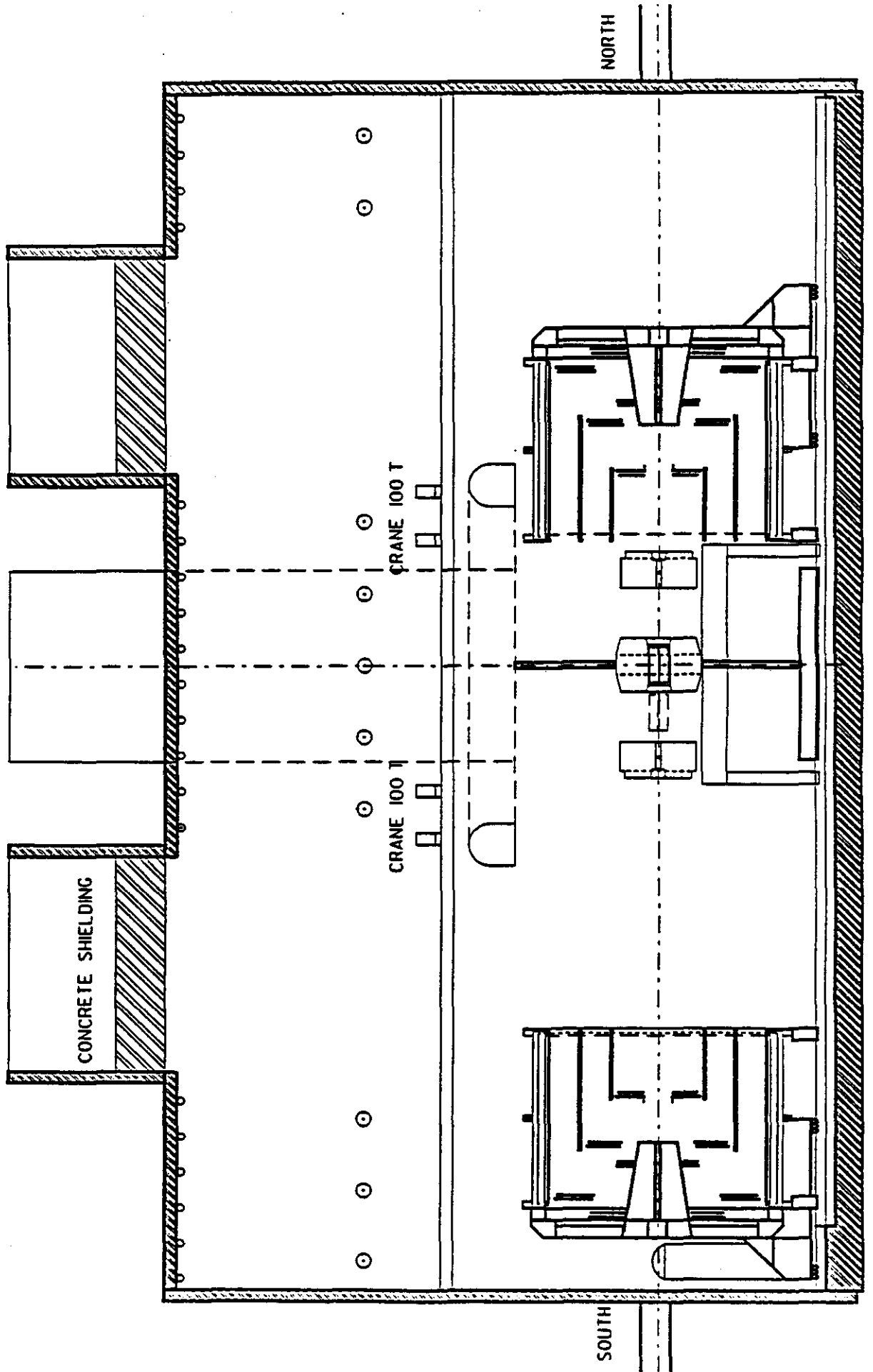
MAINTENANCE ACCESS



FFS WITHDRAWN



TRACKER MAINTENANCE / INSTALLATION



BEAM LINE

TABLE OF CONTENTS

OVERVIEW

FIGURES:

GEM Central Tracker Beryllium Beam Tube
Beam Line Layout
Transverse Excursion of the Beam in the Experiments

TABLES:

Beam Tube Dimensions (Through Tracker)
Beam Slope at IR-5
Accelerator Parameters for Detector Designers

BEAM LINE

BEAM LINE

OVERVIEW

The design of the beam line within the GEM experimental area has begun. The following describes our current thinking.

Diameter: The section of the beam pipe running through the Central Tracker is fixed at 50 mm in diameter. In the Forward Calorimeter we are studying the effect of decreasing the diameter to about 33mm to allow more hermetic calorimetry. In all other areas the pipe is nominally 50 mm, although this may grow to increase our pumping efficiency if needed.

Material: The beam pipe in the Central Tracker consists of Beryllium less than 1 mm thick. Both Stainless Steel and Aluminum are being considered for the subsequent sections of pipe. Vacuum quality and bake-out temperatures argue for stainless steel while activation results and total material in the beam line indicate the advantages of aluminum. Thicknesses will depend on the choice of material. Simulations must be done to study the effect of the material in the pipe, pumps, and flanges.

Vacuum: We are currently designing the system to a specification of 10^{-9} torr/l/sec with the expectation that real operating conditions will degrade that figure at least to 10^{-8} torr/l/sec. To achieve this value under perfect conditions requires ion pumps located immediately outside the Forward Calorimeters and again immediately after the Forward Field Shapers. In addition, a heat activated gettering pump is necessary at either end of the Central Tracker to compensate for the reduced pumping efficiency caused by the small diameter pipe through the Forward Calorimeters.

An *in situ* bake-out of the vacuum line appears to be difficult to effect in certain areas of the experiment. However it may be required. A more detailed set of vacuum calculations assuming less perfect conditions will be done in the near future to address this issue as well as pipe diameter and pumping locations.

We require ion pumps which can operate in our magnetic field. Design studies for the gettering pump are in progress. Two different methods of heat activation are under consideration; direct current and convection. Prototypes will be constructed and tested to determine the optimum design.

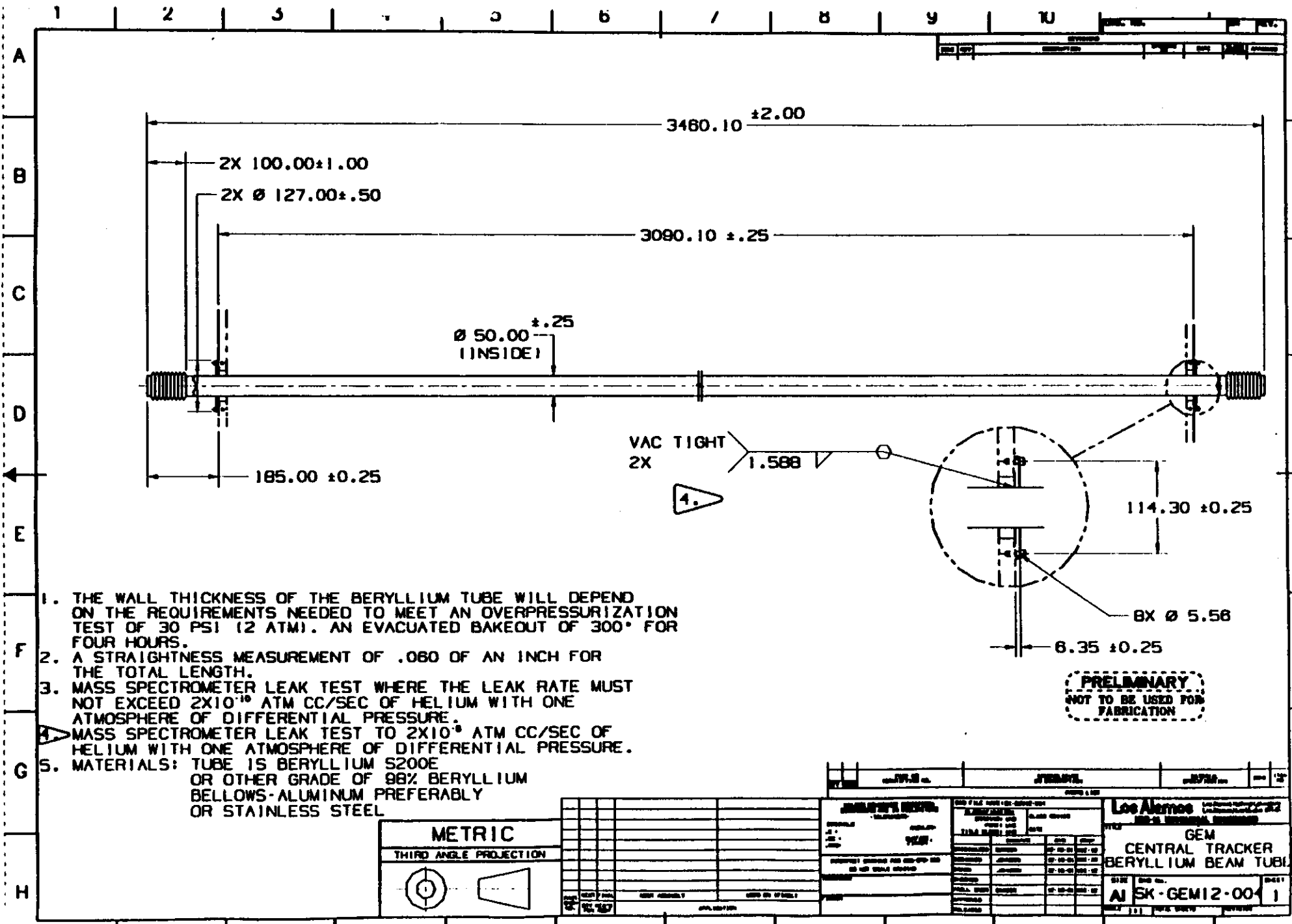
Source: KM
Updated: 4/9/92

BEAM LINE

IR Quadrupoles/Machine Interface: The Final Focusing Quadrupoles are nominally located at $\pm 20\text{m}$ from the IP with a 2m long Iron or Tungsten collimator located directly in front of the quads beginning at $\pm 18\text{m}$. The design of the lattice in the Interaction Regions is not complete. There are indications that these quads may be moved further away from the IP with limited effect on the maximum luminosity of the machine. Moving the quads has numerous benefits for the experiments as well as for the machine; and Physics Research is requesting that the accelerator group seriously consider the possibility of moving the quads further from the IP. Previous studies on activation levels at the quadrupoles indicate that after one year of operation, the innermost portions of the quads will be activated to more than 100 Rads/h. This result argues in favor of placing the quads further from the experiment for access and shielding purposes.

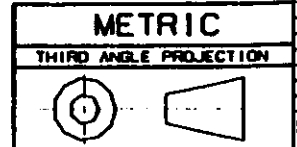
Installation/Access: The installation of the beam line will proceed in sections beginning at the Central Tracker and adding each successive section of pipe and the associated pumping stations as the detectors are installed. Each section will be aligned to the theoretical beam line and then vacuum tested before the next section is installed. The couplings are presently considered to be a combination of welded joints and traditional bolted flanges, depending on the assembly scenario for a given section. Permanent access to the ion pumps must be maintained even with the detector closed. However, access to the gettering pumps will require disassembly of the entire detector and beam line.

Source: KM
Updated: 4/9/92



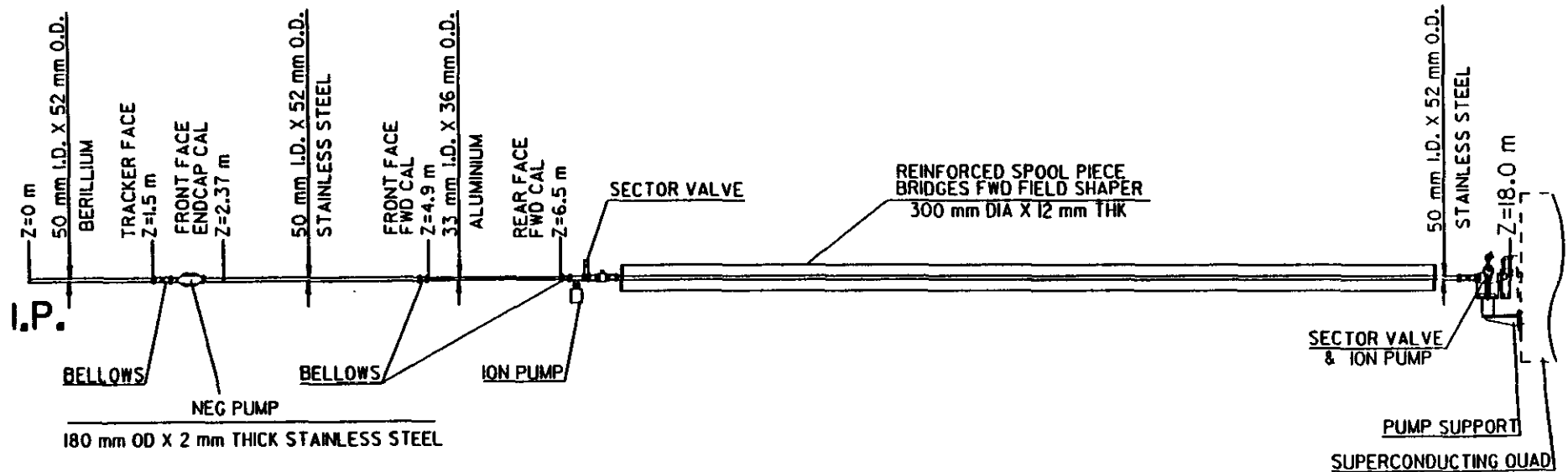
1. THE WALL THICKNESS OF THE BERYLLIUM TUBE WILL DEPEND ON THE REQUIREMENTS NEEDED TO MEET AN OVERPRESSURIZATION TEST OF 30 PSI (2 ATM). AN EVACUATED BAKEOUT OF 300° FOR FOUR HOURS.
2. A STRAIGHTNESS MEASUREMENT OF .060 OF AN INCH FOR THE TOTAL LENGTH.
3. MASS SPECTROMETER LEAK TEST WHERE THE LEAK RATE MUST NOT EXCEED 2×10^{-10} ATM CC/SEC OF HELIUM WITH ONE ATMOSPHERE OF DIFFERENTIAL PRESSURE.
4. MASS SPECTROMETER LEAK TEST TO 2×10^{-9} ATM CC/SEC OF HELIUM WITH ONE ATMOSPHERE OF DIFFERENTIAL PRESSURE.
5. MATERIALS: TUBE IS BERYLLIUM S200E OR OTHER GRADE OF 98% BERYLLIUM BELLOWS-ALUMINUM PREFERABLY OR STAINLESS STEEL

PRELIMINARY
NOT TO BE USED FOR
FABRICATION



Los Alamos	GEM	CENTRAL TRACKER	
BERYLLIUM BEAM TUBE			
SK-GEM12-00	1		

BEAM LINE LAYOUT FOR GEM DETECTOR



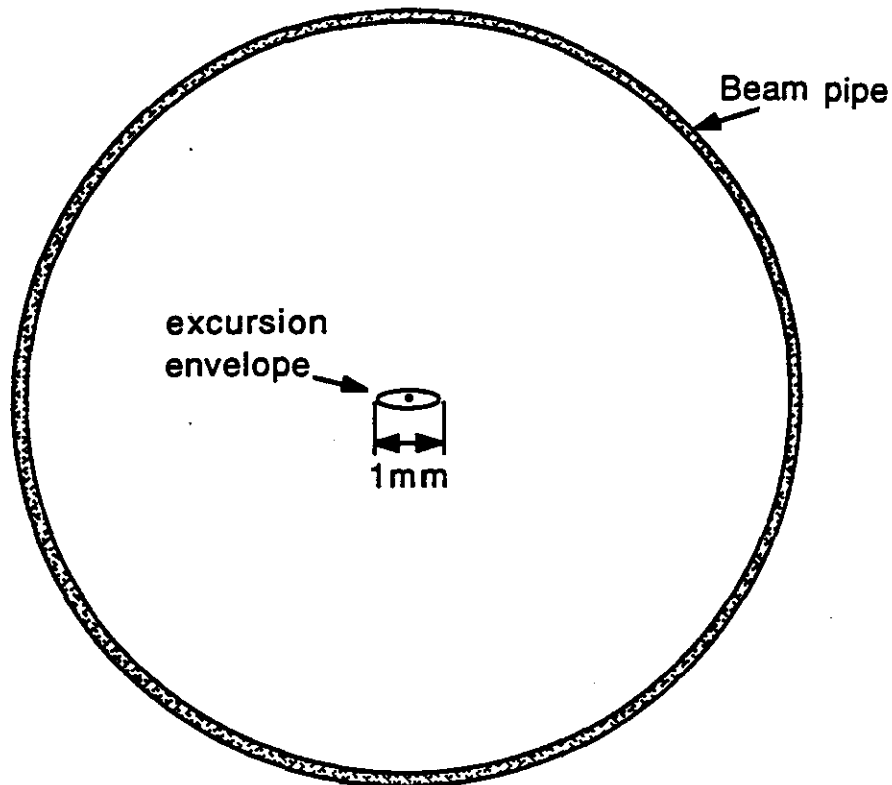
Beam Tube	
Inside Diameter	5 cm
Material	
Beryllium	Z = ±158 cm
Stainless Steel	Z ≥ ±304 cm
Wall Thickness	0.5 mm

Table 6-1
Beam Tube Dimensions

Hall Orientation	Beam Slope
North-to-South	-1.73 mm/m
East-to-West	1.05 mm/m

Table 6-2
Beam Slope at IR-5

Transverse Excursion of the Beam in the Experiments*



(50 mm inside diameter)

The beam can be moved transversely about 1mm in the experiments. The two experiments are coupled, so displacement of the beam in one experiment will cause displacement in the other. More than 1mm motion is possible, but will result in loss of luminosity.

The beam can be positioned in the 1mm envelope to less than 100 μ m precision and this position is expected to be reproducible to less than 100 μ m even from fill to fill.

*Information from the Accelerator/Experiment Interface Meetings
K. Morgan 6.9.92

Accelerator Parameters for Detector Designers

TABLE 1

No. particles/bunch		$N = 0.80 \times 10^{10}$
No. bunches/ring		1.60×10^4
Filling factor		$F = 92\%$
Bunch collision frequency		$f = 60 \text{ MHz}$
Bunch separation		5.0 m
Avg. beam current per beam		71 mA
Bunch length (68% of bunch)		$2\sigma_z = 12.0 \text{ cm}$
Amplitude function at IP		$\beta^* = \begin{cases} 0.5 \text{ m at 2 IRs}^\dagger \\ 10.0 \text{ m at IRs}^\dagger \end{cases}$
Beam radius (68% of bunch)	$\sigma = \sqrt{4.69 \times 10^{-11} \beta^*}$	$\begin{cases} 4.8 \mu\text{m} (\beta^* = 0.5 \text{ m}) \\ 21.7 \mu\text{m} (\beta^* = 10 \text{ m}) \end{cases}$
Crossing angle		$\alpha = 0-150 \mu\text{rad (adjustable) typical } 75 \mu\text{rad}$
Length of luminous region (68% of interactions)		$\begin{cases} \frac{12.0}{\sqrt{2+7.8 \times 10^7 \alpha^2}} & \text{cm } (\beta^* = 0.5 \text{ m}) \\ \frac{12.0}{\sqrt{2+3.8 \times 10^6 \alpha^2}} & \text{cm } (\beta^* = 10 \text{ m}) \end{cases}$
Crossing time (68% of interactions)		0.28 ns
Standard luminosity (Initial luminosity = average)	$\mathcal{L} = \frac{fN^2}{4\pi\sigma^2} \frac{F^2}{\sqrt{1+\alpha^2\sigma_z^2/(4\sigma^2)}} 10^{-4} (\text{m}^2/\text{cm}^2) =$	$\begin{cases} 10^{33} \text{ cm}^{-2}\text{s}^{-1} & (\beta^* = 0.5 \text{ m at } \alpha = 75 \mu\text{rad}) \\ 5.5 \times 10^{31} \text{ cm}^{-2}\text{s}^{-1} & (\beta^* = 10 \text{ m at } \alpha = 75 \mu\text{rad}) \end{cases}$
Avg. no. interactions/collision		$\begin{cases} 1.8 & (\beta^* = 0.5 \text{ m}) \\ 0.09 & (\beta^* = 10 \text{ m}) \end{cases}$
Power radiated from collisions		$\begin{cases} 580 \text{ J/s} & (\beta^* = 0.5 \text{ m}) \\ 30 \text{ J/s} & (\beta^* = 10 \text{ m}) \end{cases}$
Luminosity lifetime		$\sim 24 \text{ hr}$
Free space at IP		$\begin{cases} \pm 20\text{m} & (\beta^* = 0.5 \text{ m}) - \text{ may be larger: } \pm 25 \text{ m} \\ \pm 120\text{m} & (\beta^* = 10 \text{ m}) \end{cases}$

[†]Low- β^* regions are paired together in series in the same diamond; similarly for high- β^* regions.

MAGNET, FIELD SHAPER & CENTRAL DETECTOR SUPPORT

TABLE OF CONTENTS

OVERVIEW

FIGURES:

GEM Magnet Subsystem Envelope/Major Dimensions
GEM Magnet, Vessel and Support Structure
GEM Magnet Vessel and Coil Support Structure
GEM Magnet Vessel and Coil Support Details
GEM Magnet Vacuum Vessel Support Concept
GEM Magnet Vacuum Vessel Support Detail
GEM Magnet Conductor
Conductor Splice Access Concept
Coil and Bobbin Cross Section (Preliminary)
GEM Magnet Forward Field Shaper Assembly Concept
GEM [Forward] Field Shaper Support Structure End View
GEM Magnet, Helium Flow Schematic
Central Detector Support

TABLES:

General Physical [Parameters]
Superconducting Coil [Parameters]
Vacuum Vessel [Parameters]
Forward Field Shaper (FFS) [Parameters]

MAGNET, FIELD SHAPER & CENTRAL DETECTOR SUPPORT

MAGNET, FIELD SHAPER & CENTRAL DETECTOR SUPPORT

OVERVIEW

The GEM magnet is a large superconducting solenoid 30.8 m long with 18 m diameter inner bore and a central field of 0.8 T. It consists of two half-length coils each 14.44 m long, separated by a distance of 1.5 m. The detector subsystems are completely enclosed in the magnet, with the possible exception of a future upgrade to the muon system which adds chambers outside. The central tracker and both the electro-magnetic and hadronic calorimeters are supported by a free-standing fixed central membrane situated between the two coil halves. Muon system modules for the central barrel are mounted on the magnet cryostat. In the forward direction the muon modules are mounted on the Forward Field Shaper.

The two coil halves are designed to be mobile along the beam axis, allowing for their separation from the central detector support for the initial installation of the detector subsystems and for the access to the calorimeters and central tracker after the detector is put together. The magnet does not have a return yoke and has a substantial fringe field outside of the volume of the solenoid. Inside the coil, the magnetic field is shaped in the forward direction by two large iron field shapers. The field change introduced by this iron provides the baseline momentum resolution for the measurement of muons emitted in the rapidity range of $\eta = 1.5$ to 2.5. The iron field shapers are also designed to be mobile with an independent support system. Coupling the support of the coil halves to that of the Field Shapers is still being explored.

Each coil half is constructed in 12 identical segments of conductor wound on the inside of the 1.2 m long aluminum bobbin. Each segment has 19 turns of the "cable-in-conduit" conductor consisting of 450 braided strands of NbTi superconducting alloy enclosed in a 2.0 cm ID stainless steel tube which is filled with liquid helium. The stainless steel tube is surrounded by an aluminum stabilizer. The baseline design of the conductor joints between individual segments has resistive coupling with separate cooling system for each joint. The cooling is provided by a natural convection flow of liquid helium provided by a thermo-syphon system. The design of the procedure of winding and assembly of the coil is still preliminary. Several options are being considered. The choice of the winding process will depend on the feasibility study to be conducted by industry.

Source: R Stroynowski
Updated:

MAGNET, FIELD SHAPER & CENTRAL DETECTOR SUPPORT

The magnet coils will be constructed above ground in a specially designed surface building. They will be completely assembled and tested above ground for electrical continuity and for gas leaks of the cryogenic systems. They will be then lowered to the experimental hall and assembled together with the central membrane and Forward Field Shapers. A full cold test of the magnet and a measurement of the field map will follow the underground installation.

The magnet is designed for a normal charge and discharge time of about 8 hours with an emergency discharge time of 5 minutes.

Source: R Stroynowski
Updated:

MAGNET AND FIELD SHAPER

General Physical

Central induction	0.80	T
Inner radius, magnet subsystem	9.00	m
Total mass of magnet assy (each half)	1,300,000	kg
Total mass of magnet support (each half)	110,000	kg
Total mass of FFS + support (each half)	1,265,000	kg
Overall outer radius (outside ribs)	10.9	m
Depth of outer ribs	750	mm
Number of coil/cryostat assemblies	2	
Number of ribs per coil assembly	3	
Central membrane maximum Z	250	mm
Mass of one muon sector	11,400	kg
Number of barrel muon sectors (per half)	16	
Radius of CG of barrel muon sectors	6.22	m
Location of barrel muon sectors CG in Z	3.89	m
Magnet axis height above hall floor	13.0	m
Module and Coil Weights		
Bobbin	14,882	kg
Compression flanges	13,875	kg
Conductor aluminum sheath	7,986	kg
Conductor conduit	1,607	kg
Conductor cable	1,352	kg
Turn insulation	1,846	kg
Ground wrap	1,819	kg
Number turns per module	19	
Total module weight	43,367	kg
Number of modules per magnet half	12	
Magnet half weight	520,404	kg
Magnet weight	1,040,808	kg

Source:
Updated:
jng

MAGNET AND FIELD SHAPER

Superconducting Coil

Coil length, end-to-end (per half)	14.438	m
Conductor length (total)	27,219	m
Total mass of coil windings (per half)	153,000	kg
Mean radius of windings	9.50	m
Axial force on conductor (each half)	52	MN
Operating current	50.2	kA
Stored energy	2.5	GJ
Inductance	1.98	H
Number of turns	456	
Inner radius of conductor	9.466	m
Mean radius of conductor	9.5	m
Outer radius of conductor	9.534	m
Inner radius of inner ground wrap	9.456	m
Actual axial winding length/assembly	14.25	m
Outer radius of bobbin	9.544	m
Actual axial winding length (per assy)	14.25	m
Bobbin inner radius	9.544	m
Bobbin outer radius	9.620	m
Bobbin minimum Z	656	mm
Bobbin maximum Z	15.094	m
Winding minimum Z	750	mm
Winding maximum Z	15	m

Vacuum Vessel

Cryostat vessel length (each half)	15	m
Outer radius of outer cryostat vessel	10.15	m
Inner radius of inner cryostat vessel	9.10	m
Total mass cold 4.5° K structure (per half)	520,404	kg
Total mass of cryostat vessel (each half)	851,000	kg
Thickness of inner thermal shield	4.8	mm
Thickness of inner cryostat	25.5	mm
Thickness of outer cryostat vessel	50.7	mm
Thickness of cryostat vessel ends	76.2	mm
Outer radius of inner cryostat vessel	9.1255	m
Inner radius of inner LN shield (avg)	9.295	m
Outer radius of inner LN shield (avg)	9.298	m
Inner radius of outer LN shield (avg)	9.8	m
Outer radius of outer LN shield (avg)	9.803	m
Inner radius of outer cryostat vessel	10.0993	m
LN shield minimum Z	562	mm
LN shield maximum Z	15.192	m
Cryostat outer end minimum Z	15.323	m
Cryostat outer end maximum Z	15.4	m
Cryostat inner end minimum Z	400	mm
Cryostat inner end maximum Z	476.2	mm

Source:

Updated:

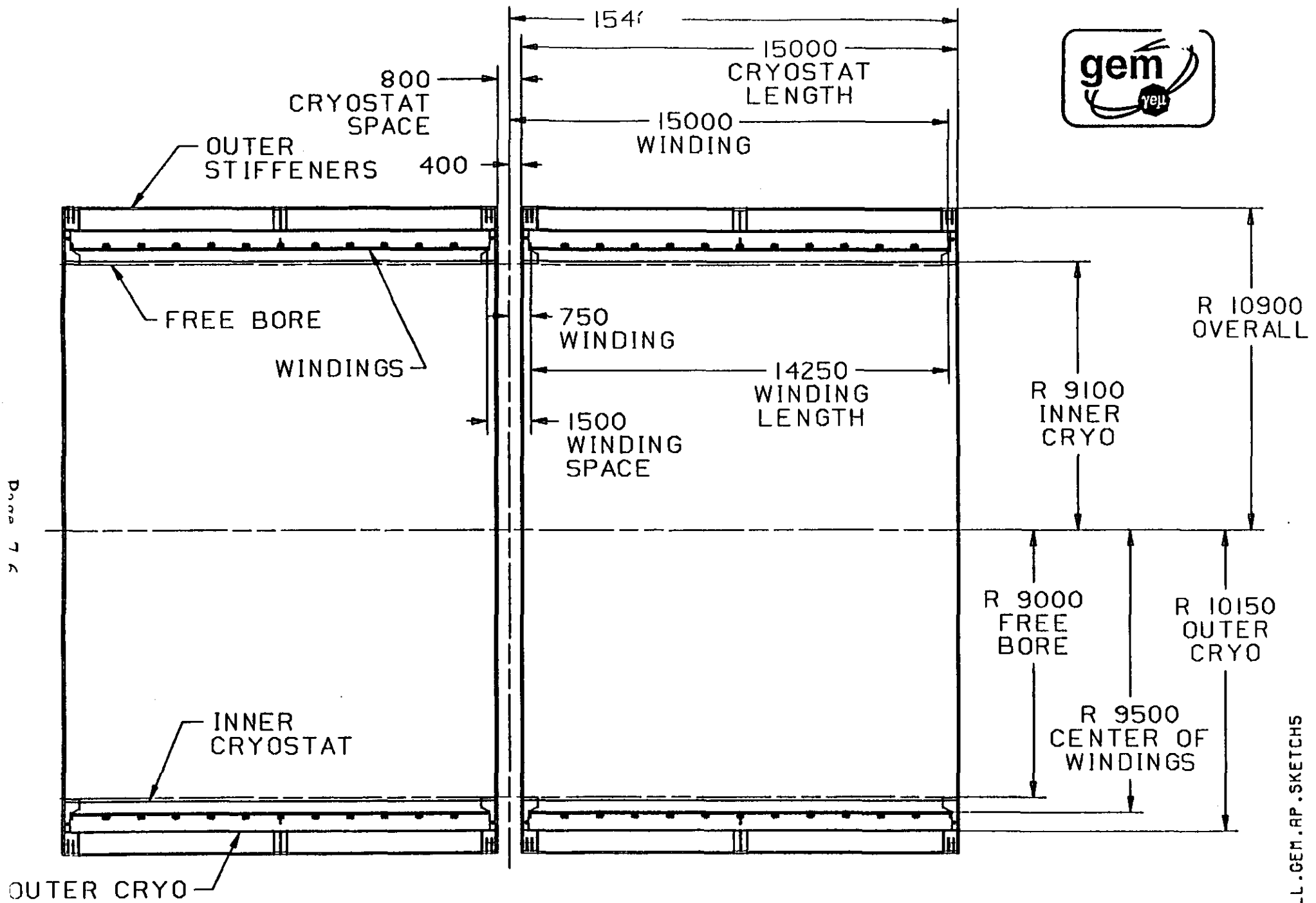
jng

MAGNET AND FIELD SHAPER

Forward Field Shaper (FFS)

Forward field shaper minimum Z	10	m
Forward field shaper maximum Z	18	m
Forward field shaper included angle	17.4	deg
Forward field shaper mass	899,000	kg
Forward field shaper support mass	366,000	kg
Axial force on forward field shaper	12.2	MN
FFS notch minimum Z	16.5	m
FFS notch maximum Z	18	m
FFS notch diameter at minimum Z	1.175	m
FFS notch diameter at maximum Z	1.251	m

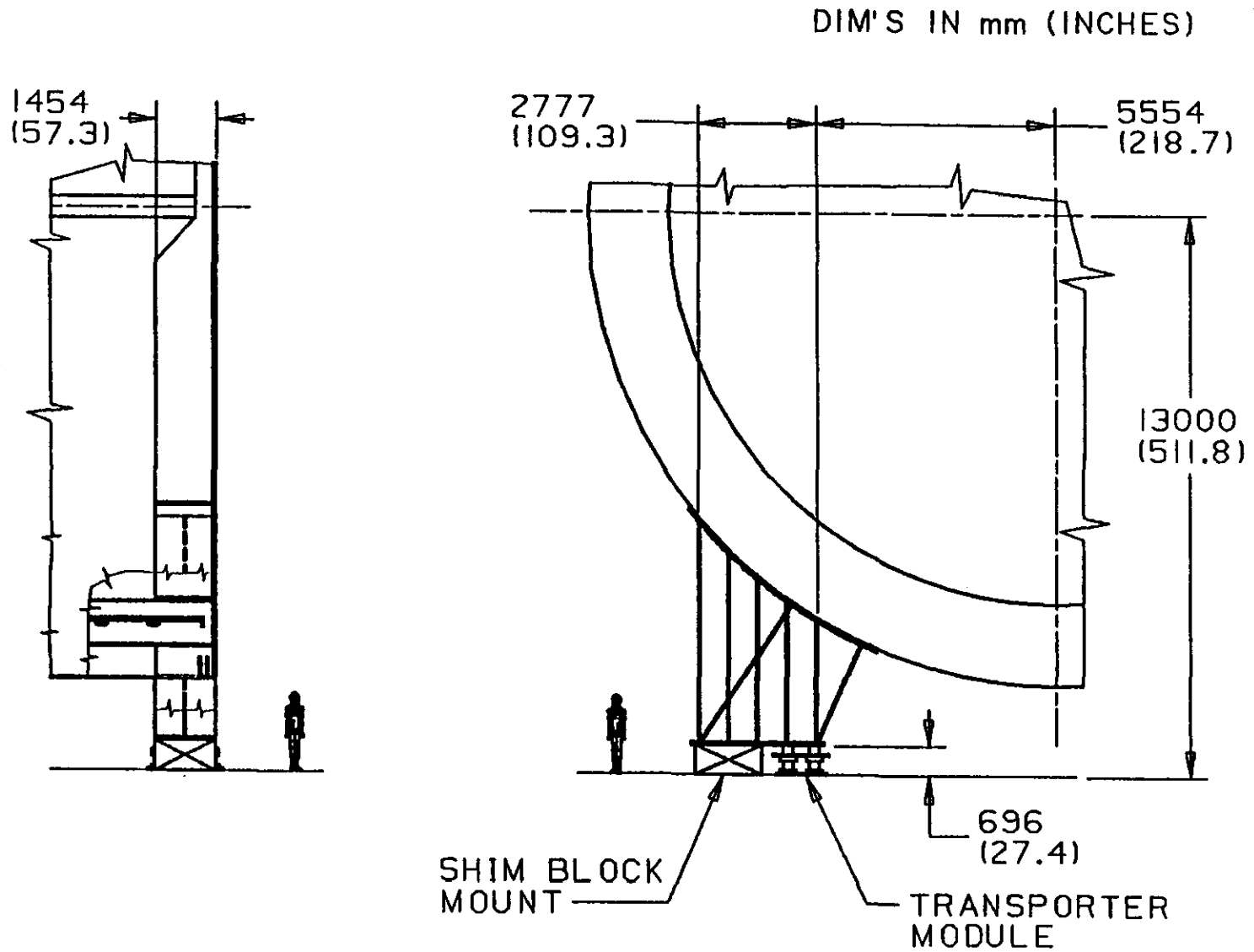
Source:
Updated:
jng



GEM MAGNET SUBSYSTEM ENVELOPE / MAJOR DIMENSIONS

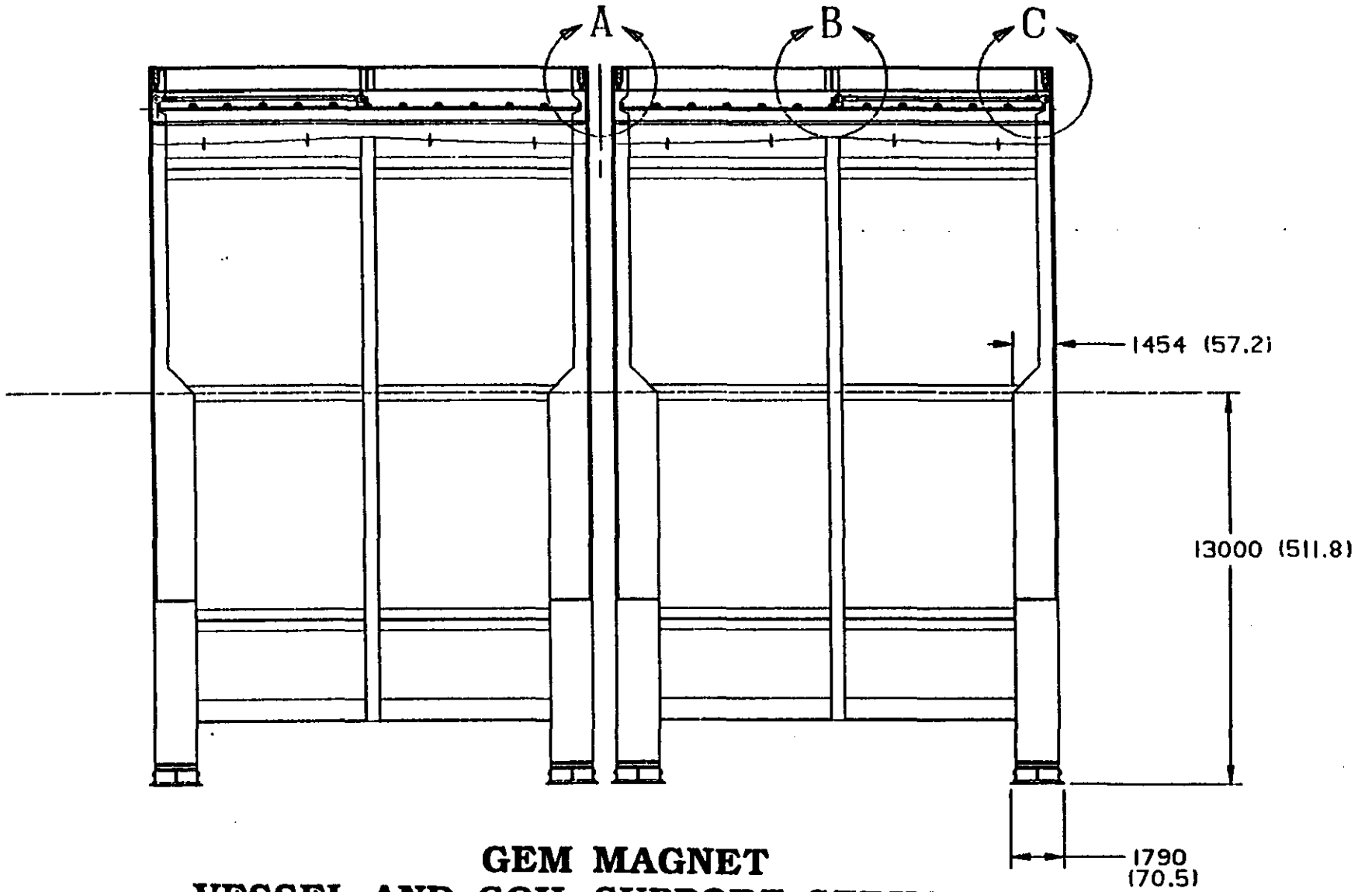
(ALL DIMS IN MM)

Done 7/8

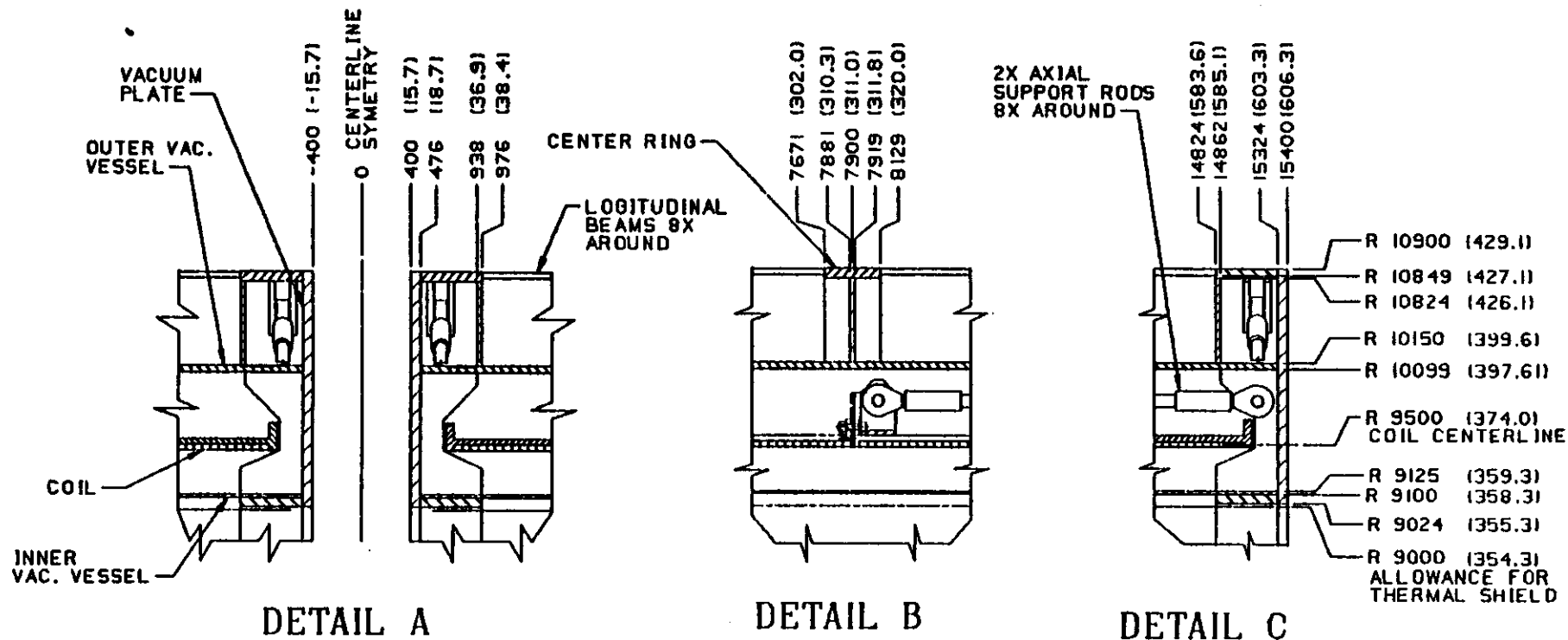


GEM MAGNET, VESSEL AND SUPPORT STRUCTURE

3/6/92

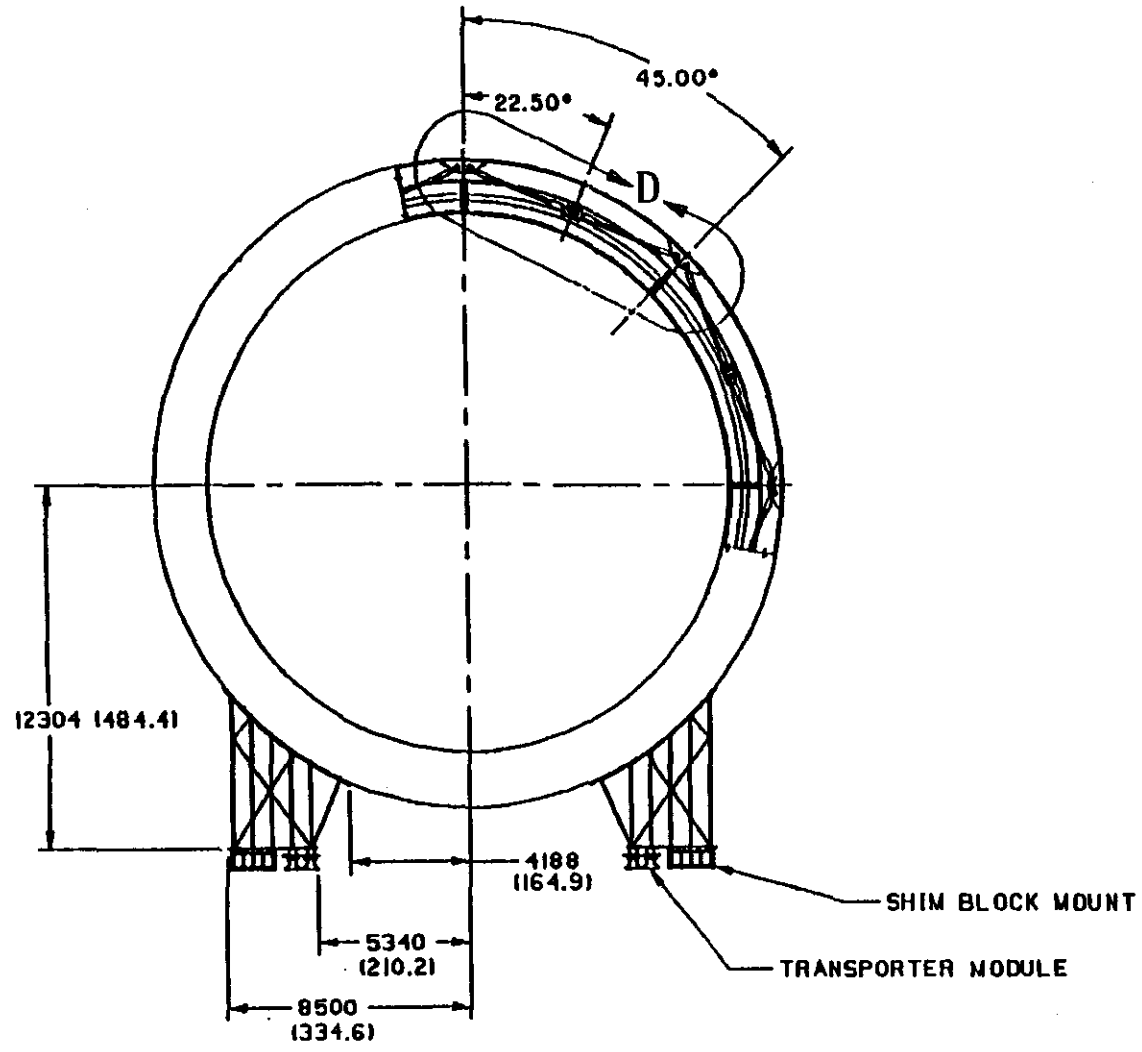


**GEM MAGNET
VESSEL AND COIL SUPPORT STRUCTURE**



**GEM MAGNET
 VESSEL AND COIL SUPPORT DETAILS**

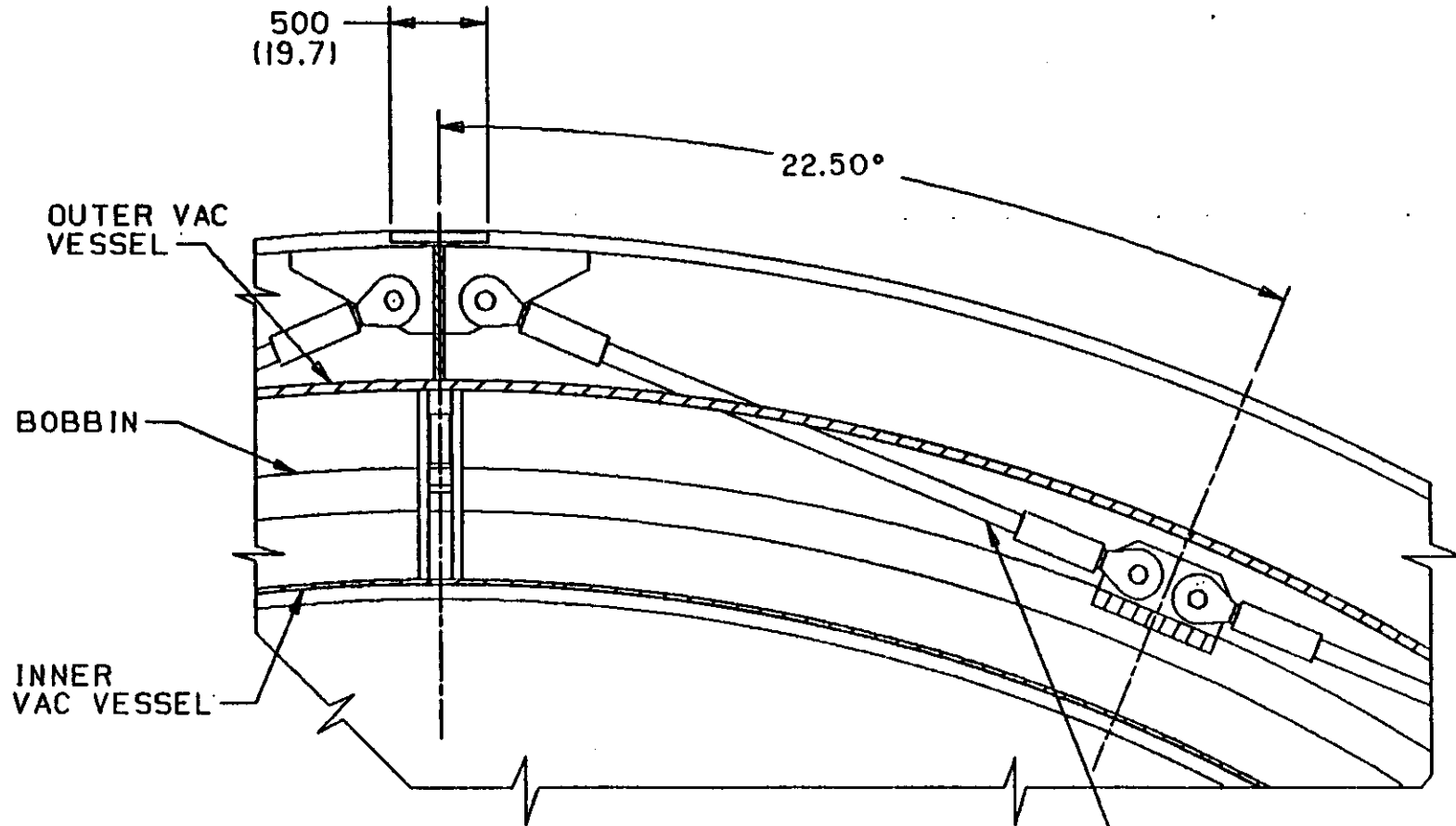
**GEM MAGNET
 VACUUM VESSEL SUPPORT CONCEPT**



NO	REQD	PART/LIN	STR NO	DESCRIPTION/MATERIAL	SPEC NO	ITEM
		DWN V. WILLIAMSON	4/92	CLASSIFICATION	MAJOR UNIT GEM COIL ASSEMBLY	
		CHK		THIS DOCUMENT IS THE PROPERTY OF THE UNIVERSITY OF CALIFORNIA LAWRENCE LIVERMORE NATIONAL LABORATORY. REPRODUCTION PROHIBITED WITHOUT THE PERMISSION OF THE MECHANICAL ENGINEERING DEPARTMENT.	SUBASSY VAC. VESSEL & COIL ASSY	
		APVD			DETAIL VESSEL CONCEPT	
		CLASIFIED BY:			DRAWING NO AAA92-102656-00	
		TITLE	DATE		COPY	
LAWRENCE LIVERMORE NATIONAL LABORATORY MECHANICAL ENGINEERING DEPT UNIVERSITY OF CALIFORNIA				ACT 0027-66	SCALE	1/5000 SHEET OF

LTR	DWG	CHK	DATE	ZONE	CHANGE

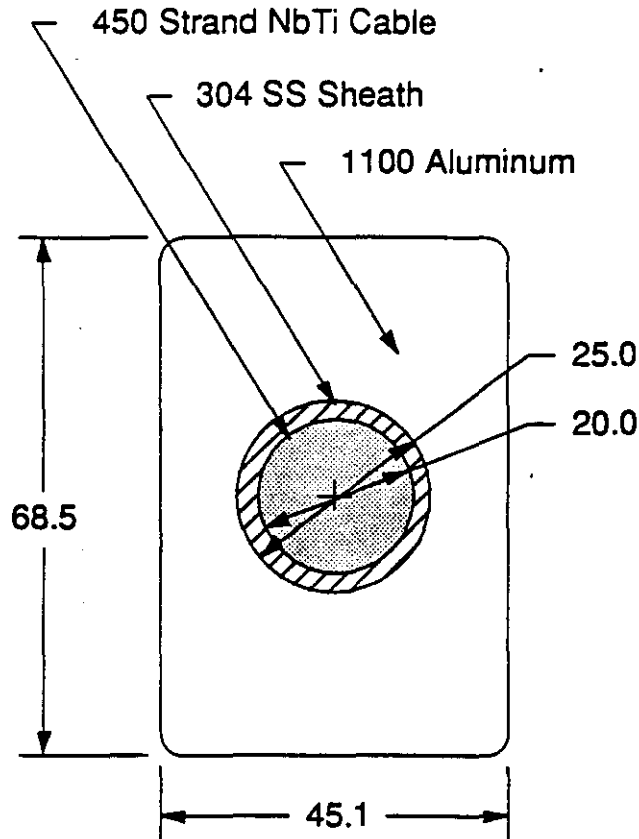
FILE NAME : LLL.V.M.GEM.COIL.ASSY



DETAIL D

**GEM MAGNET
VACUUM VESSEL SUPPORT DETAIL**

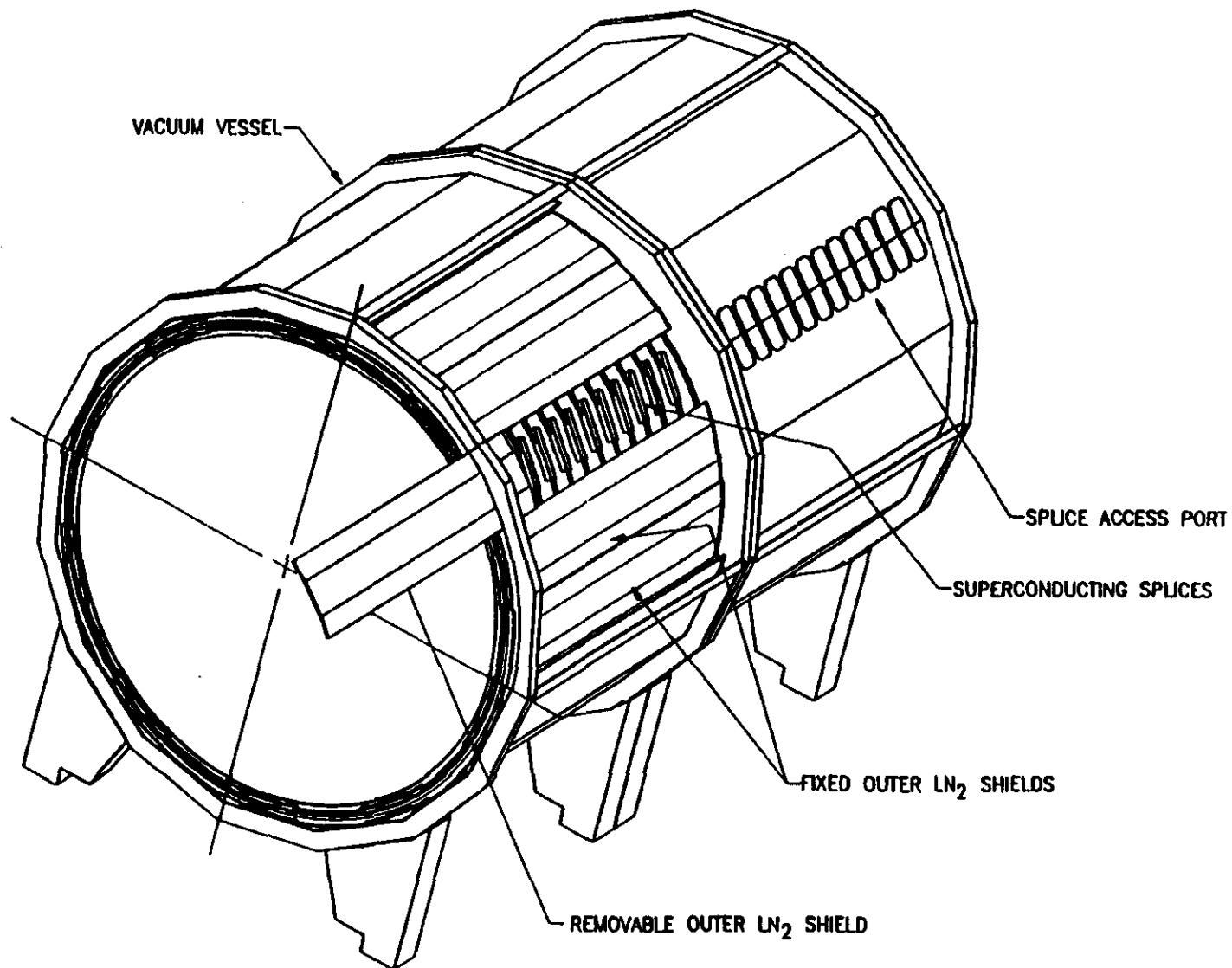
Page 7 11



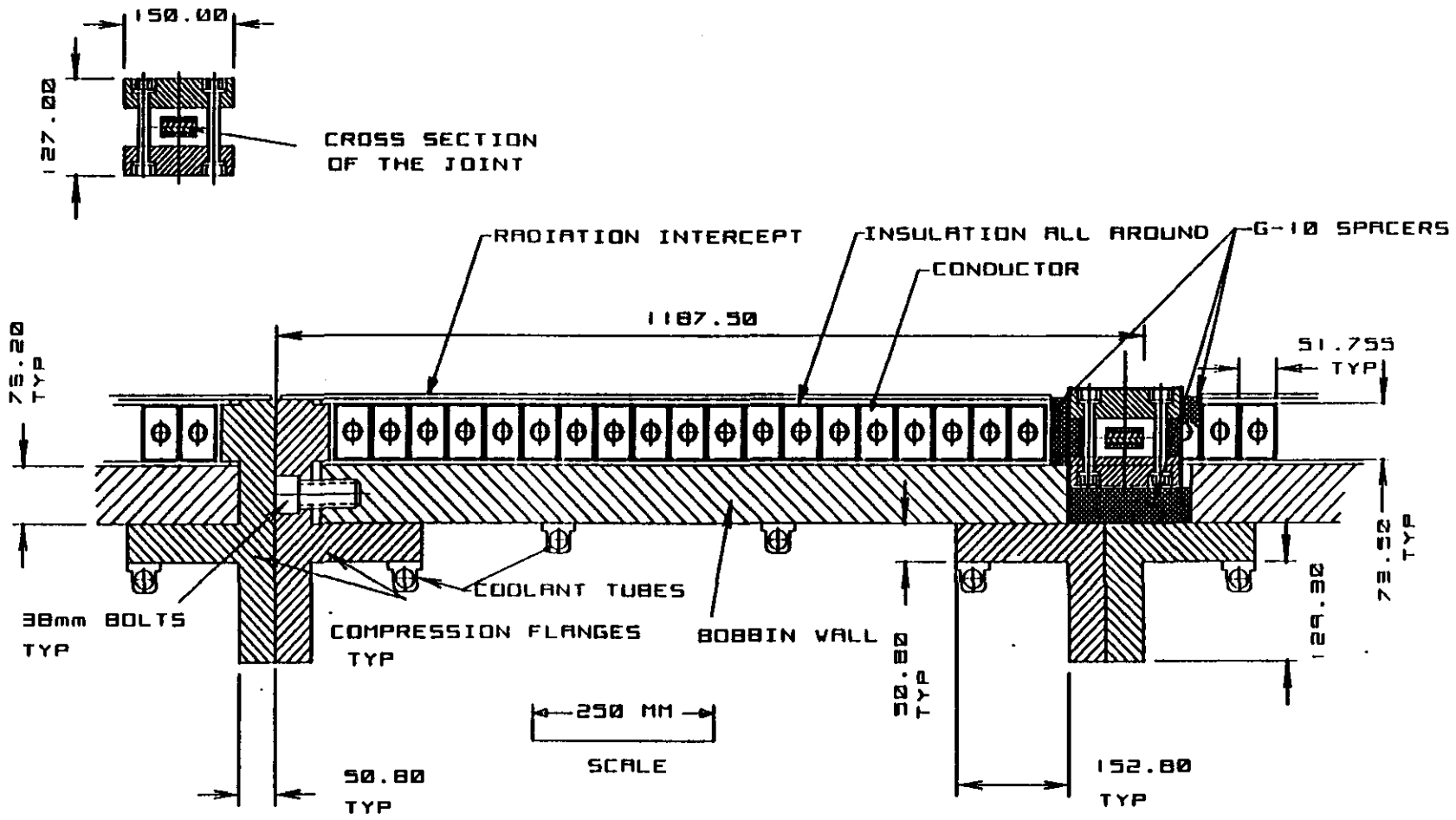
GEM Magnet Conductor

Sheath Material	Aluminum Alloy 1100
RRR	14
Hole Diameter (mm)	25.0
Width (mm)	45.1
Height (mm)	68.5
Corner Radii. (mm)	3.0
Conduit Material	Type 304 SS
Outer Diameter (mm)	25.0
Inner Diameter (mm)	20.0
Cable	
Cable Pattern	3x5x5x6
Strand Diameter (mm)	0.73
Cu:Non-Cu	3
Number of Strands	450
Operating Current (A)	50,000

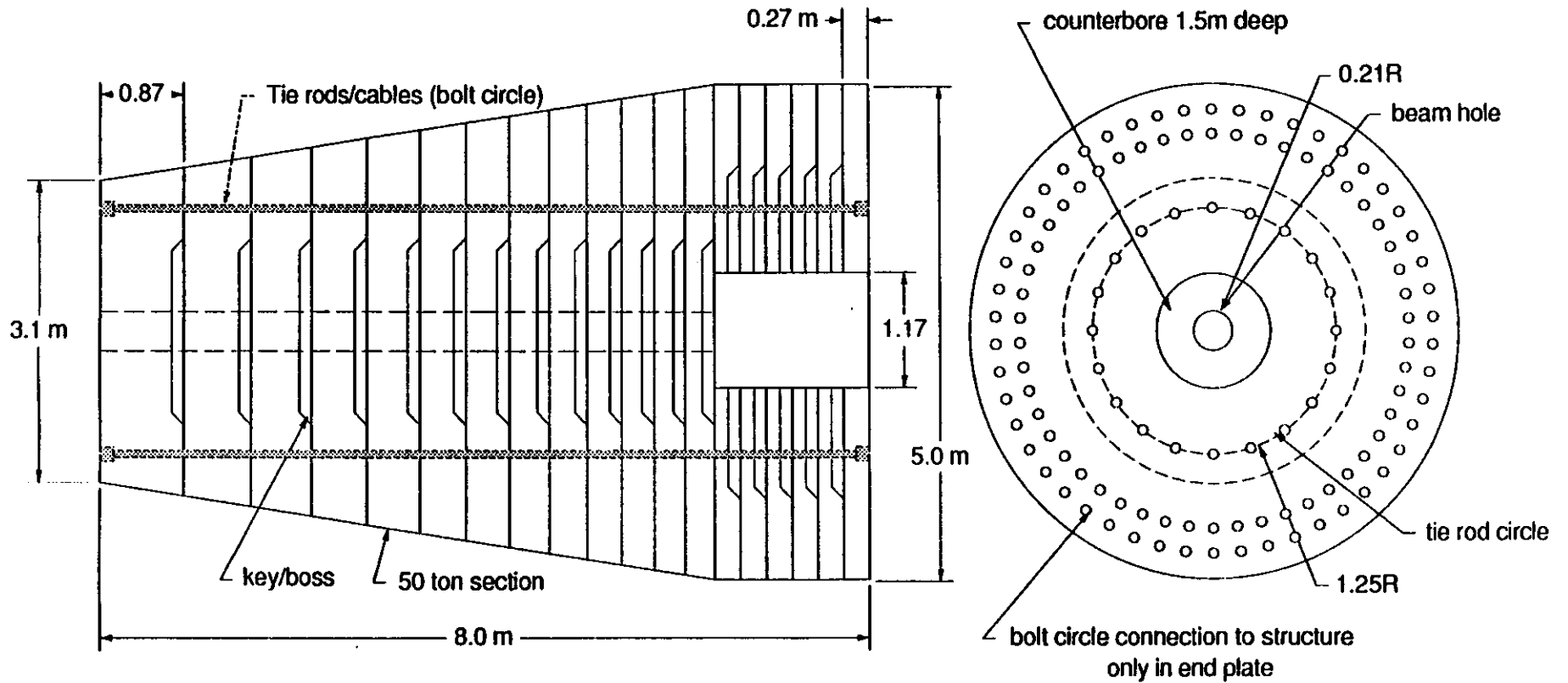
Conductor Splice Access Concept



COIL & BOBBIN CROSS SECTIONS

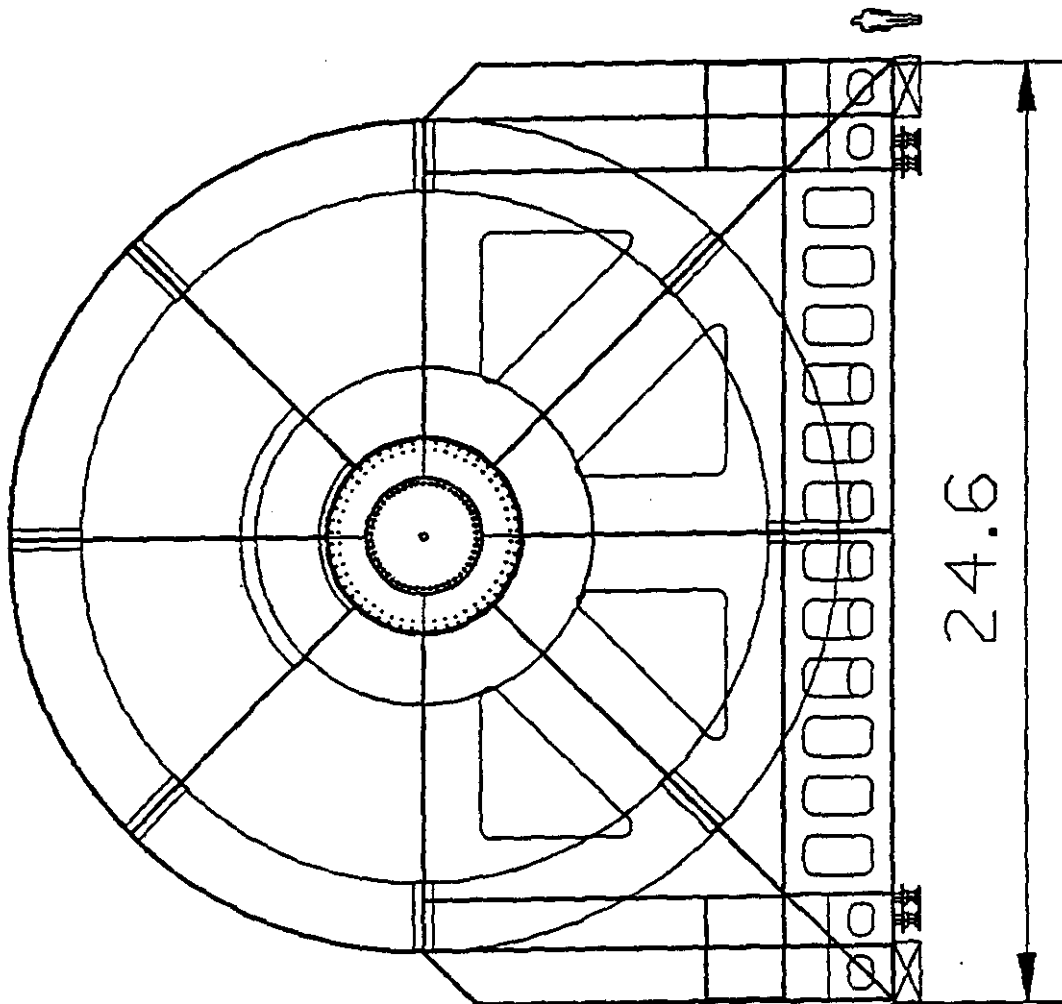


PRELIMINARY



(each section has roughly equal weight)
total weight = 970 English tons

Forward field shaper



GEM FIELD SHAPER
SUPPORT STRUCTURE
END VIEW

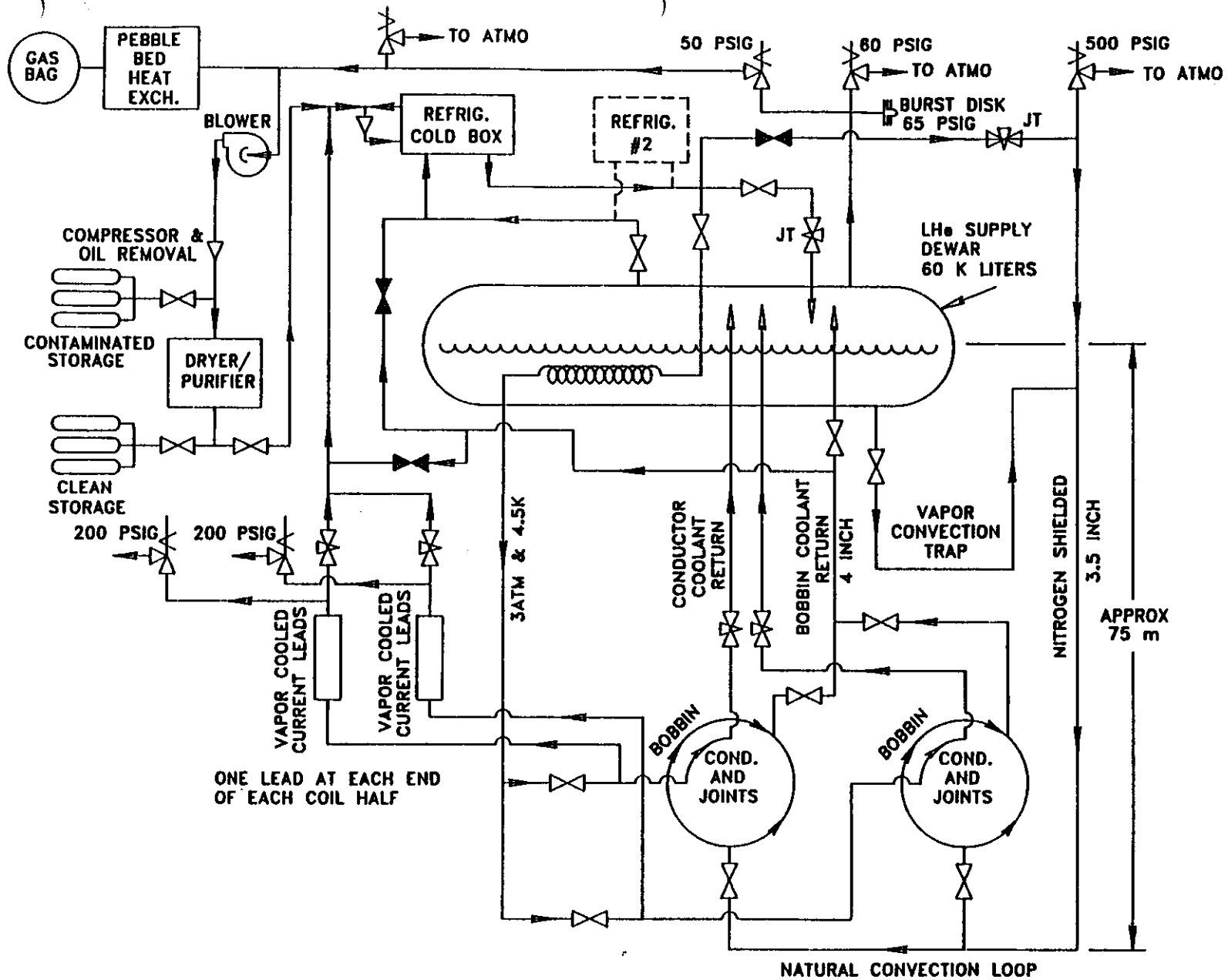
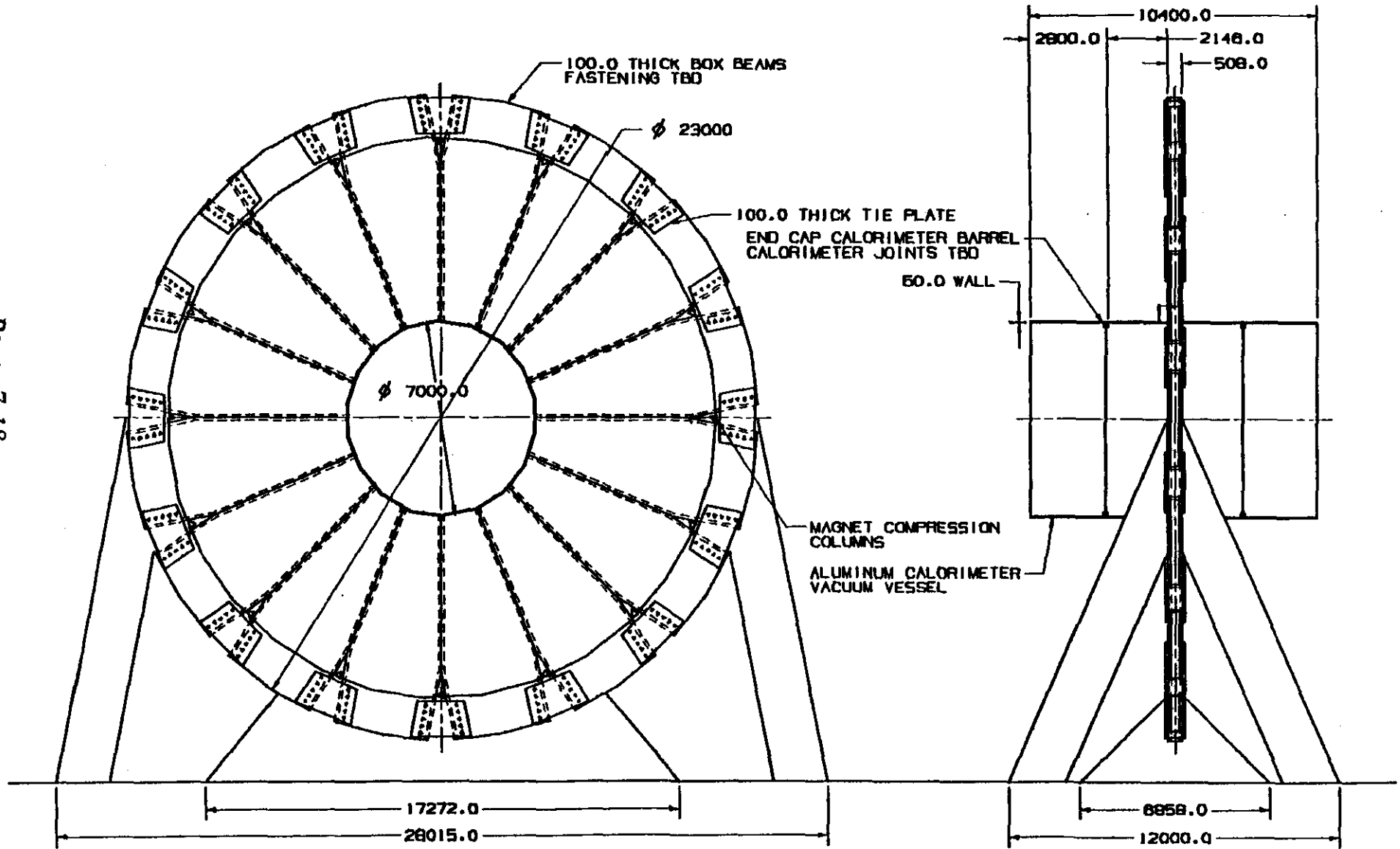


Fig. 1 GEM Magnet, Helium Flow Schematic

CENTRAL DETECTOR SUPPORT

Page 7-18



MAGNETIC FIELD

TABLE OF CONTENTS

OVERVIEW

FIGURES:

- Contours of Constant Flux
- Contours of Constant B (3 figures)
- Magnetic Field Pattern at Surface of IR-5
- Magnetic Field Pattern Section Through Detector Hall
- B versus Axial Distance, Barrel Muon Chambers
- B versus Transverse Distance, End Cap Muon Chambers (3 figures)

MAGNETIC FIELD

MAGNETIC FIELD

OVERVIEW

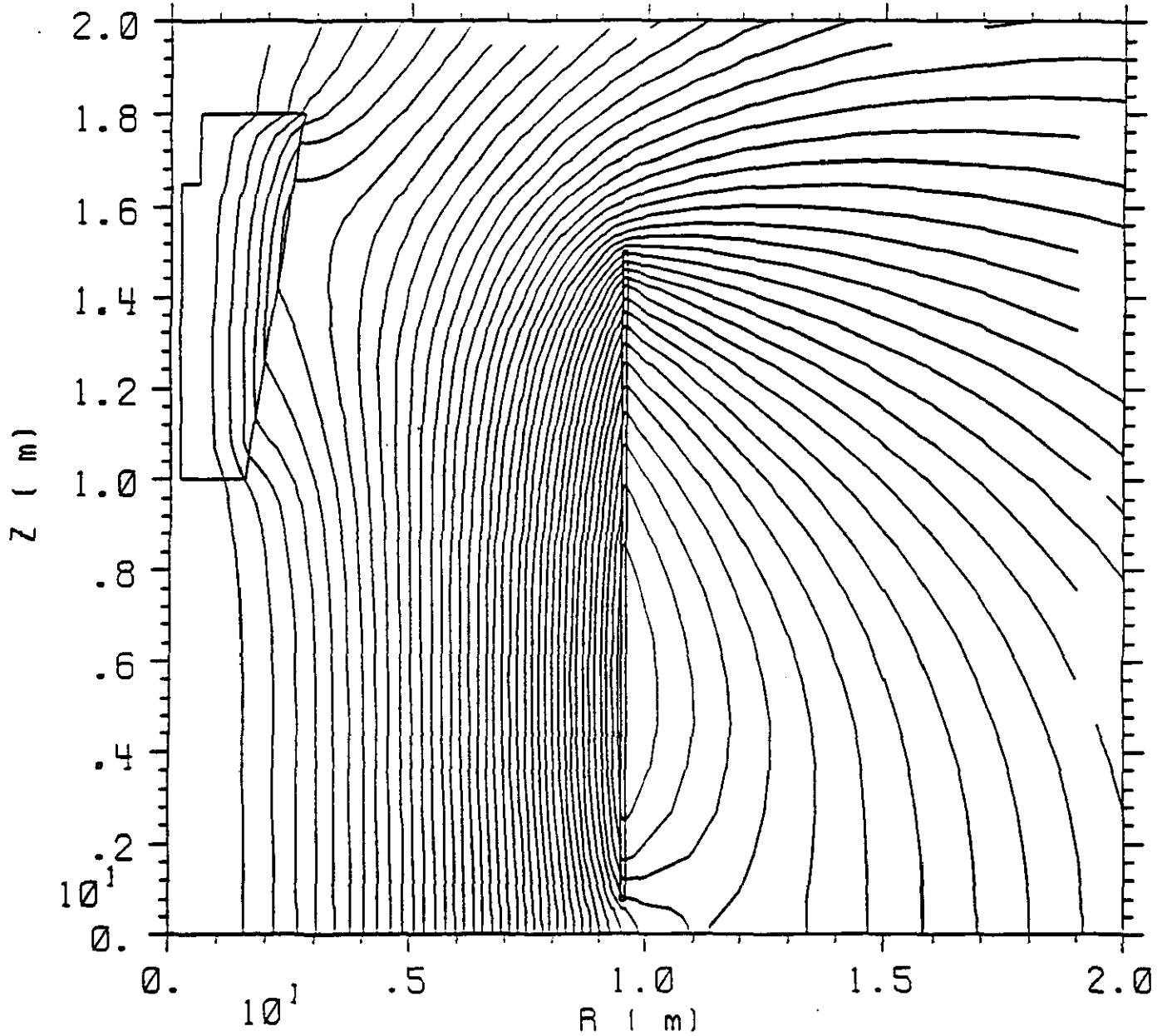
The size of the GEM magnet and the value of its central field result from a cost optimization procedure required to satisfy physics goals of the experiment. A baseline design with a 9 m radius of the inner bore and 0.8 T central field satisfy the requirements of 5% momentum resolution for 500 GeV/c transverse momentum muons in the rapidity range of $\eta = 0 - 1.5$. In the forward direction requirements necessitate addition of field shaping iron, which provides flux concentration and a rapid field gradient in the forward region.

The magnitude and direction of the magnetic field must be known in order to measure muon and electron momenta. In addition to inducing a curvature of charged particle trajectories, the field also influences the drift of ionization electrons towards the sense wires of tracking chambers affecting position measurement resolution. Furthermore, the field and its direction affect placement and performance of photo-sensitive devices considered for the signal readout of the calorimetric devices.

As a result of cost and construction schedule considerations, the GEM magnet does not have a return yoke. The substantial fringe field is present at all points of the experimental hall and a residual field remains at the surface. Precise knowledge of the field is needed to estimate and correct its influence on the beam, the IR quadrupoles and to mitigate its effects on any mechanical or electronic component in the hall, the electronic counting house or in the operations center.

Procedures and requirements for field mapping and monitoring during GEM operations are under development. These will include a full field map measurement, directional placement of sensitive equipment and local shielding.

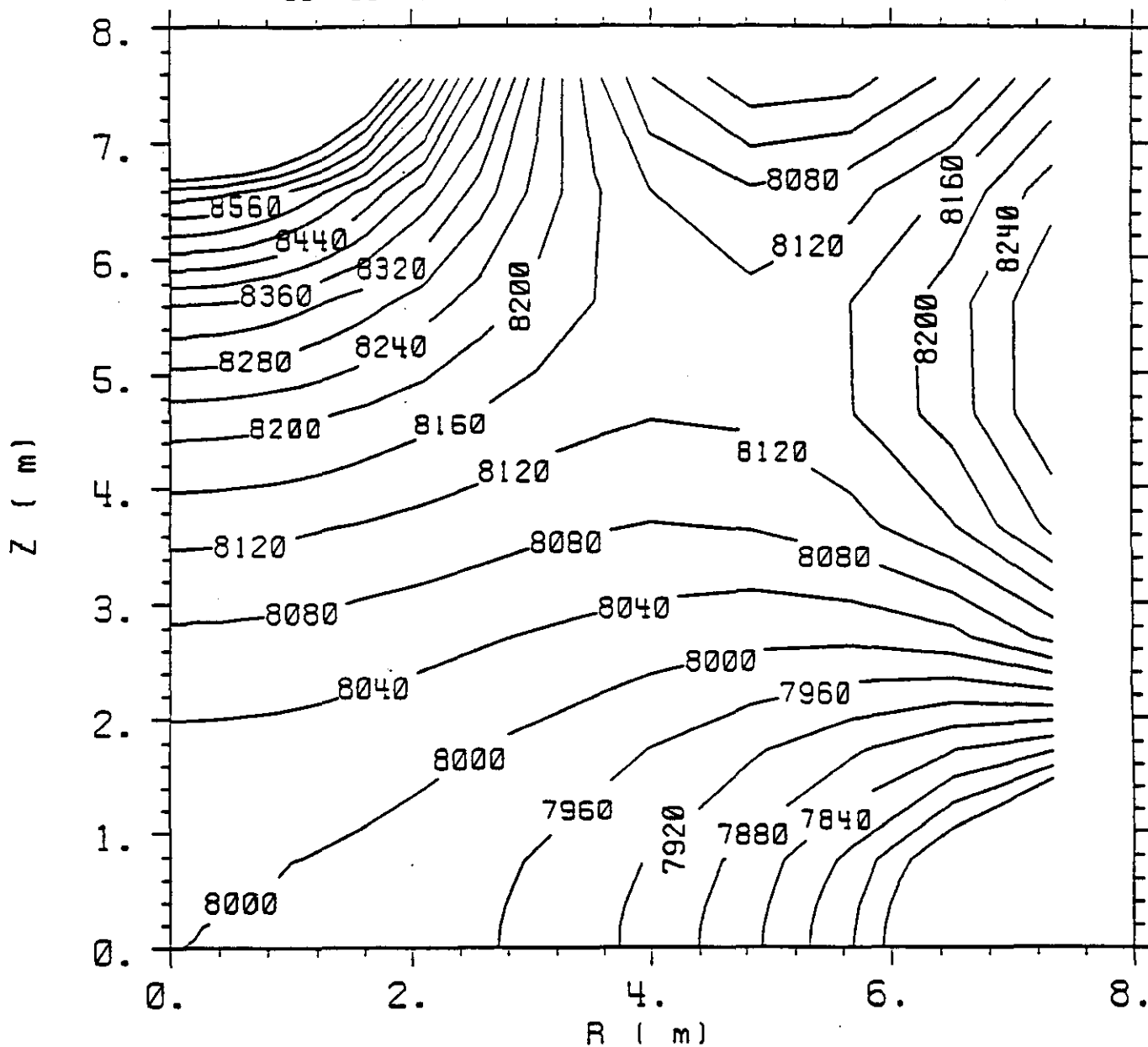
MITMAP V1.0 3/30/92 17:29
Contour 1 * 0.000E+00 Delta * 5.884E+00



CONTOURS OF CONSTANT FLUX

Figure 1: Lines of constant magnetic flux in a meridional half-plane; the figure is rotationally symmetric about the horizontal axis and has mirror symmetry about $Z = 0$. Note: the beam axis, Z , is vertical while the transverse axis, R is horizontal. Both axes extend from 0 to 20 m and the field is in gauss. A sketch of the superconducting winding and the forward field shaper is also shown.

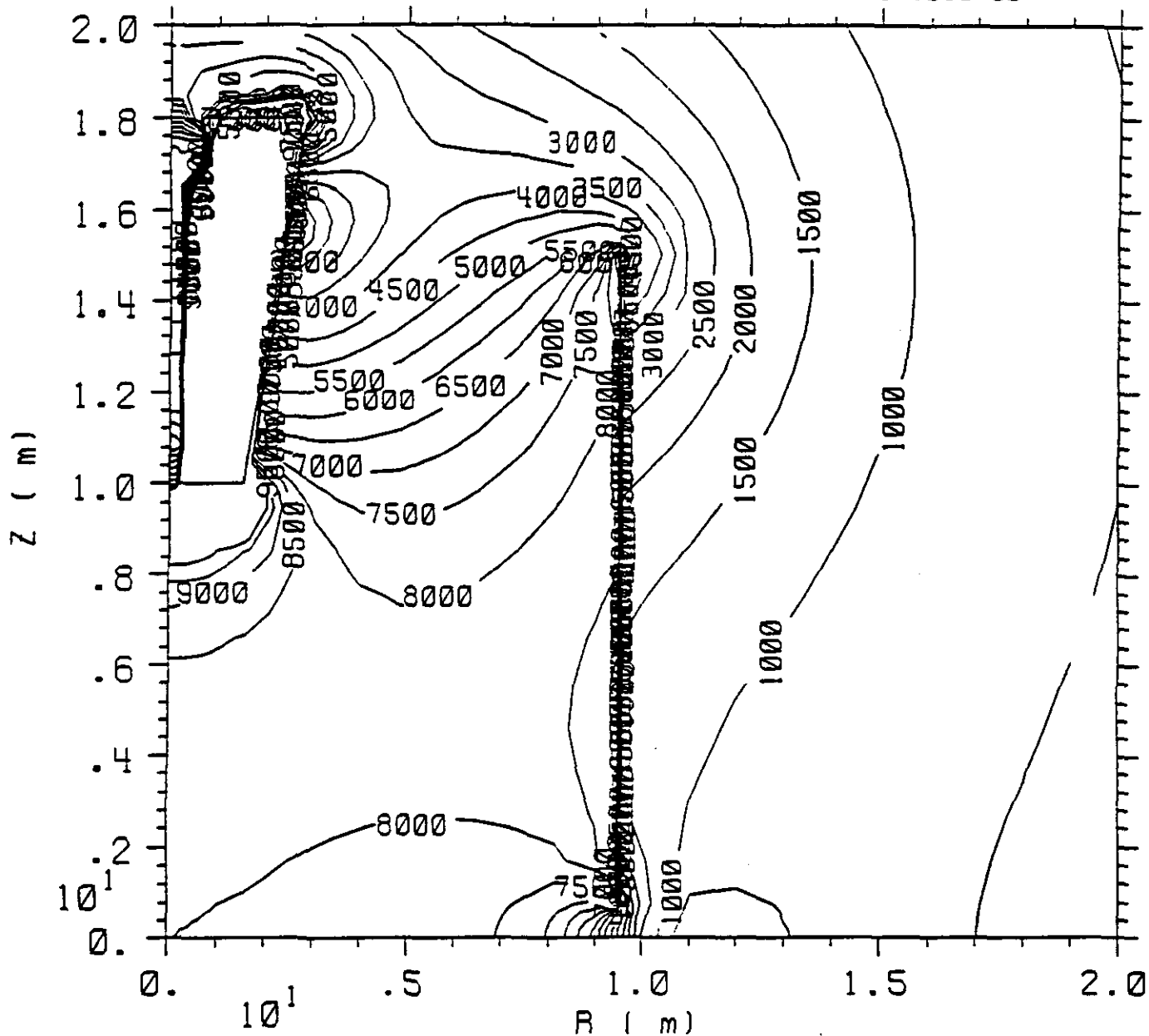
MITMAP V1.0 3/30/92 17:34
 Contour 1 • 7.720E+03 Delta • 4.000E+01



CONTOURS OF CONSTANT B

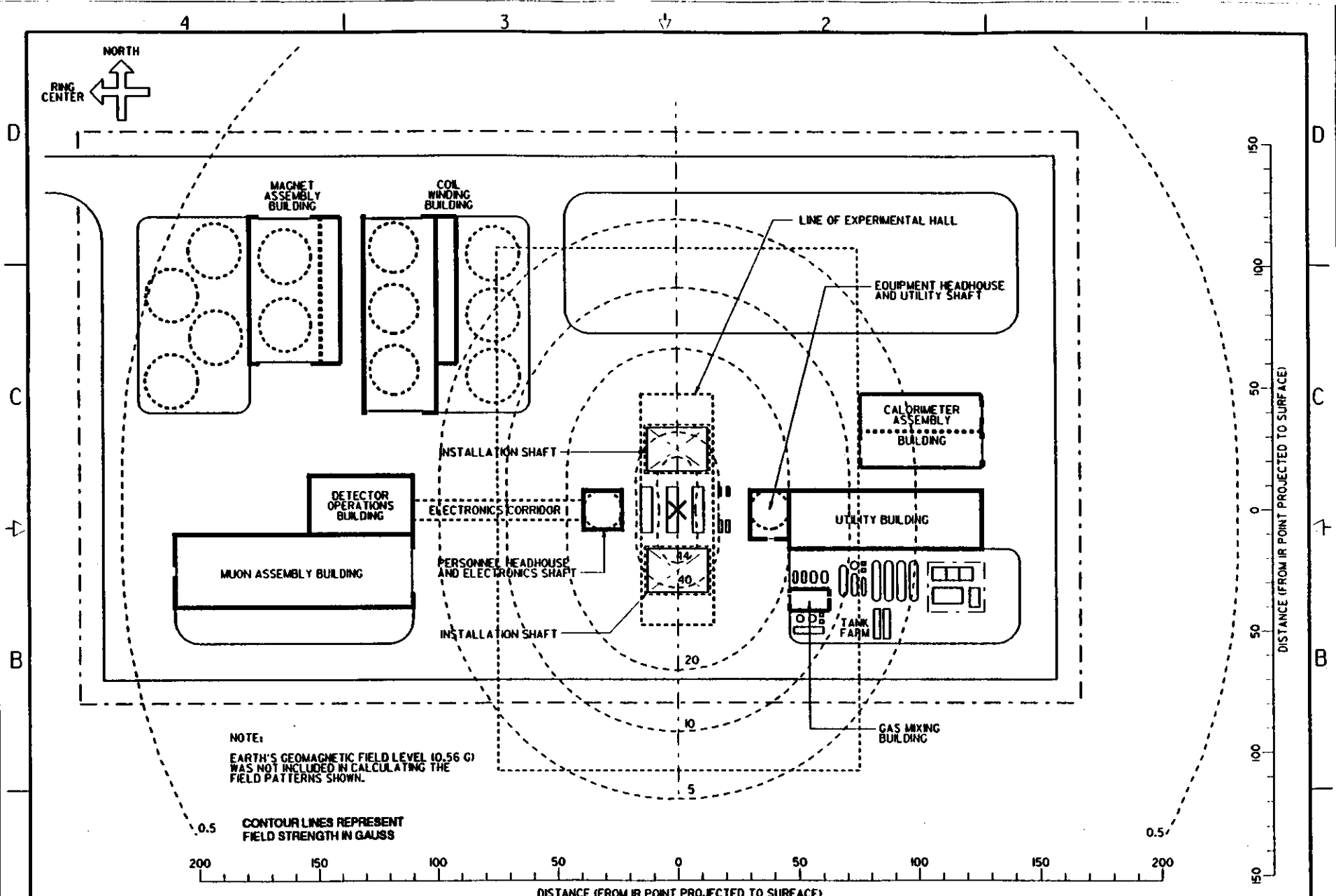
Figure 2: Isopleths of the magnetic field in a meridional half-plane for the central detector volume; the figure is rotationally symmetric about the horizontal axis and has mirror symmetry about $Z = 0$. Note: the beam axis, Z , is vertical while the transverse axis, R is horizontal. Both axes extend from 0 to 8 m and the field is in gauss. A sketch of the superconducting winding and the forward field shaper is also shown.

MITMAP V1.0 3/30/92 17:35
 Contour 1 - 7.000E-04 Delta - 5.000E+02



CONTOURS OF CONSTANT B

Figure 3: Isopleths of the magnetic field in a meridional half-plane for the muon detector volume; the figure is rotationally symmetric about the horizontal axis and has mirror symmetry about $Z = 0$. Note: the beam axis, Z , is vertical while the transverse axis, R is horizontal. Both axes extend from 0 to 20 m and the field is in gauss. A sketch of the superconducting winding and the forward field shaper is also shown.



NOTE:
EARTH'S GEOMAGNETIC FIELD LEVEL (0.56 G)
WAS NOT INCLUDED IN CALCULATING THE
FIELD PATTERNS SHOWN.

0.5 CONTOUR LINES REPRESENT
FIELD STRENGTH IN GAUSS

DISTANCE (FROM IR POINT PROJECTED TO SURFACE)

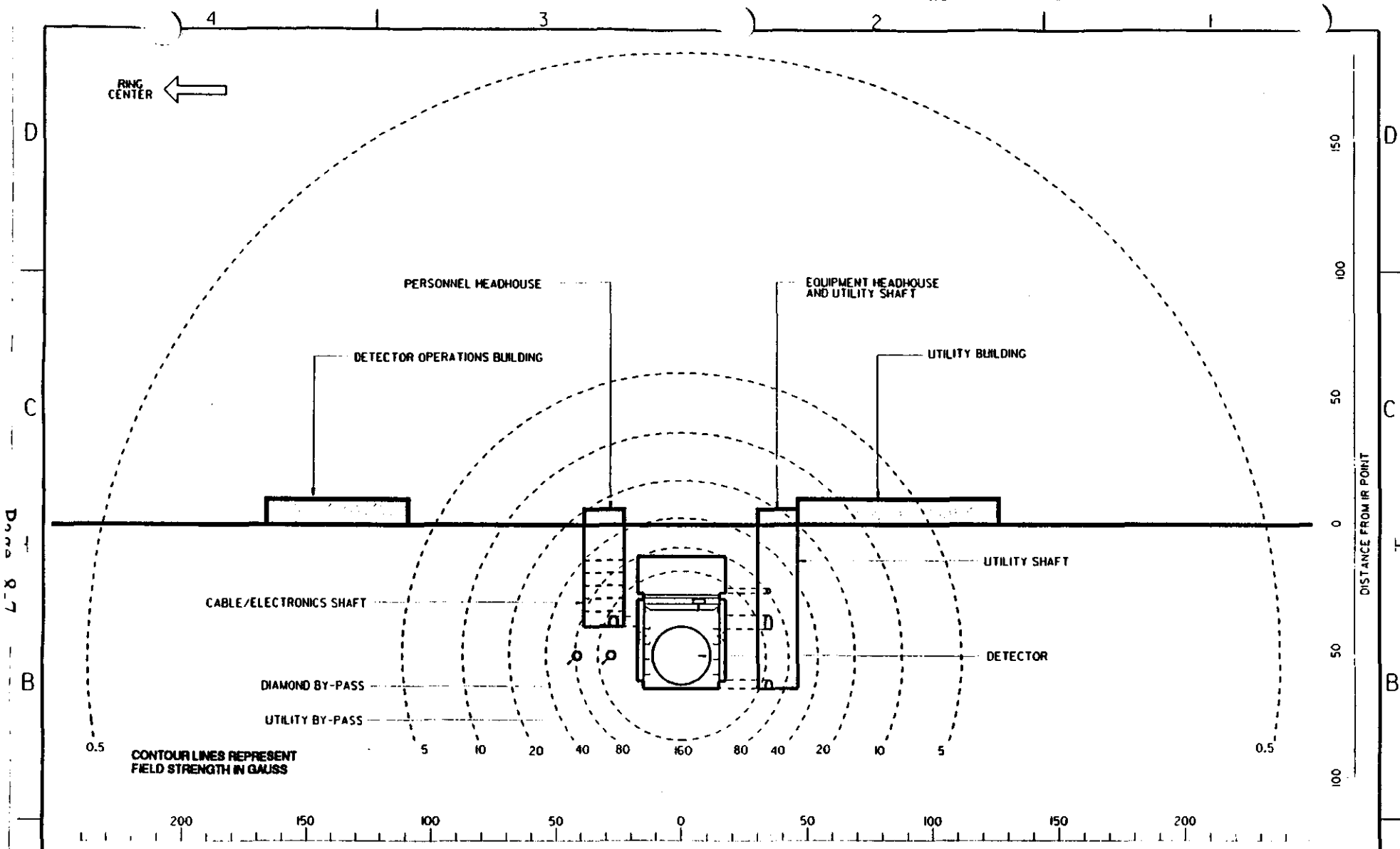
A DIMENSIONS ARE SHOWN IN METERS UNLESS NOTED OTHERWISE.

PLAN AT SURFACE

THIS IS A CAD GENERATED DRAWING. DO NOT
MAKE MANUAL REVISIONS OR ALTERATIONS.

RECORD NAME: HAWKES DESIGN: [] RESPONSIBLE ENGINEER: R. WOOLLEY		PHYSICS RESEARCH DIVISION		 SUPERCONDUCTING SUPERTECHNOLOGY LABORATORY DALLAS, TEXAS CONTRACT NUMBER: DE-AC25-97ER4006		GEM EXPERIMENTAL FACILITIES IR-5 MAGNETIC FIELD PATTERN PLAN AT SURFACE		SCALE: NONE DATE: 6-9-92 SHEET: C		PROJECT NUMBER: DRAWING NUMBER:	
REF. FILES	HED:	4	3	2	1	REVISION CONTROL NUMBER:	REV:	DATE:	BY:	APP:	
/home/rnd	d/kanton/gcd00042.b					GCD-000153	A				

REF. FILES /home/rnd HED: d/kanton/gcd00042.b



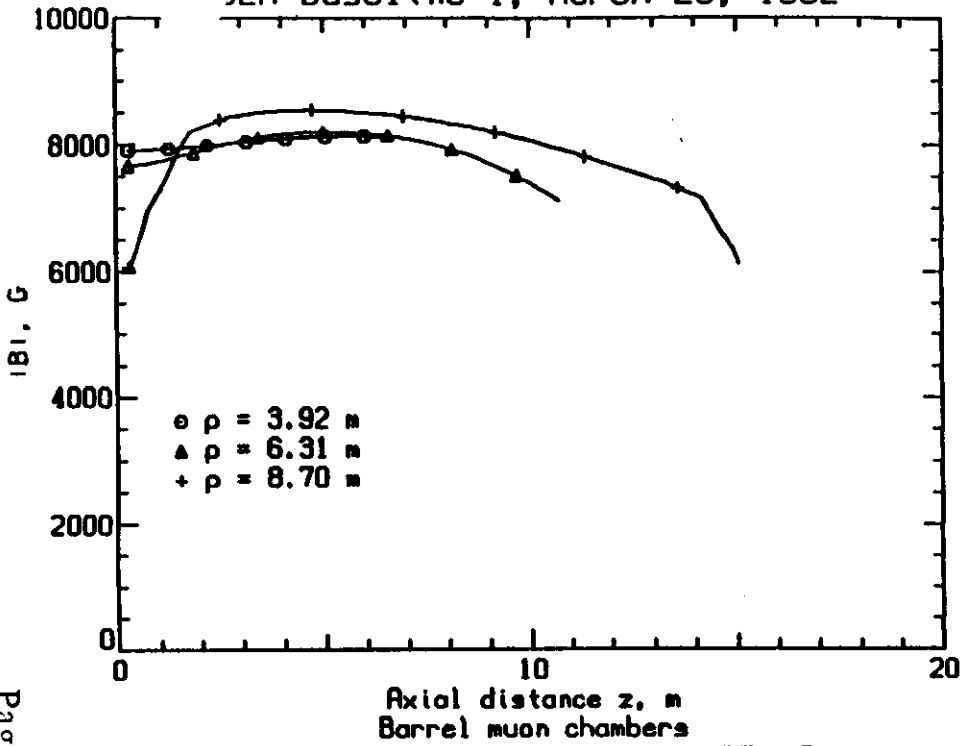
NOTE:
 EARTH'S GEOMAGNETIC FIELD LEVEL (0.56 G)
 WAS NOT INCLUDED IN CALCULATING THE
 FIELD PATTERNS SHOWN.

THIS IS A CAD GENERATED DRAWING. DO NOT
 MAKE MANUAL REVISIONS OR ALTERATIONS.

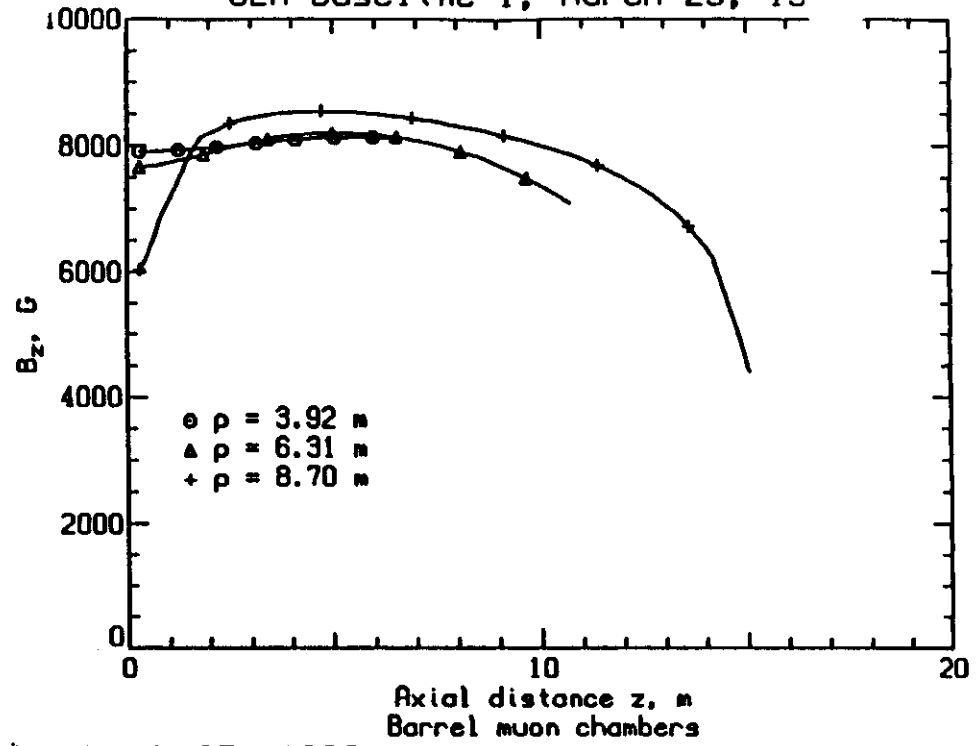
A DIMENSIONS ARE SHOWN IN METERS UNLESS NOTED OTHERWISE.

REVISIONS 1 2 3 4	DATE BY CHK APPR	NAME HAWKES DESIGNED R. WOOLLEY	APPROVED APPROVED APPROVED APPROVED	PHYSICS RESEARCH DIVISION	 SUPERCONDUCTING SUPERCOLLIDER LABORATORY DALLAS, TEXAS CONTRACT NUMBER DE-AC35-89-RD0046	GEM EXPERIMENTAL FACILITIES MAGNETIC FIELD PATTERN AT SURFACE SECTION VIEW AT IR-5	SCALE NONE	PROJECT NUMBER
							DATE 4/17/92	DRAWING NUMBER
NET PAGES ATTACHED: 4 NAME: HAWKES, R. WOOLLEY							DRAWING CONTROL NUMBER GCD-000156	SHEET 1 OF 1

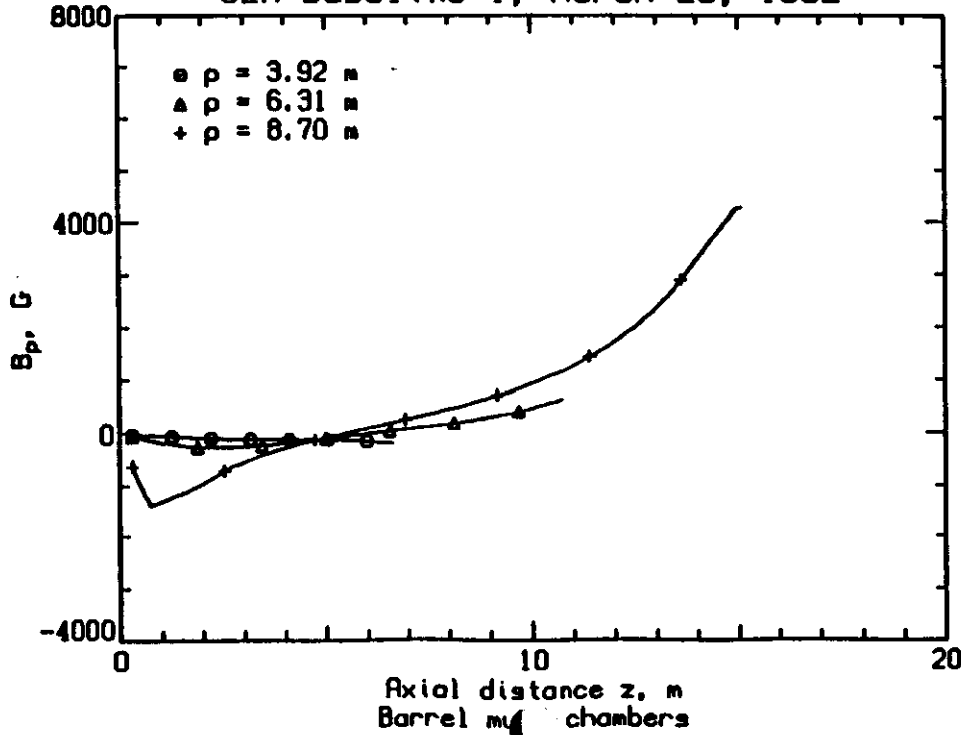
GEM Baseline 1, March 25, 1992



GEM Baseline 1, March 25, 19

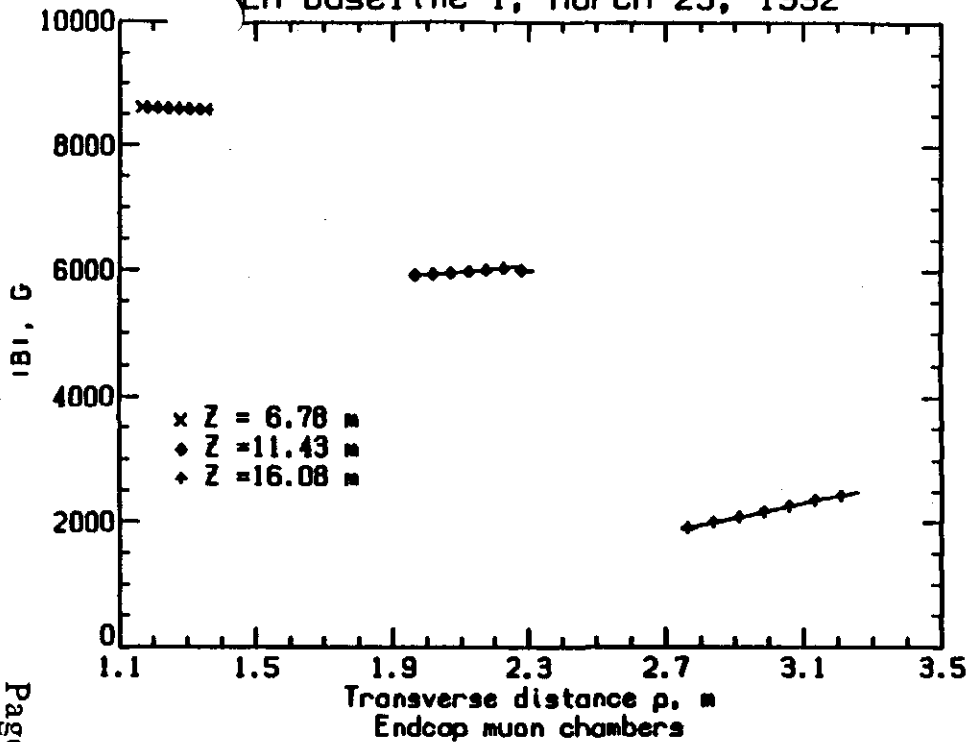


GEM Baseline 1, March 25, 1992

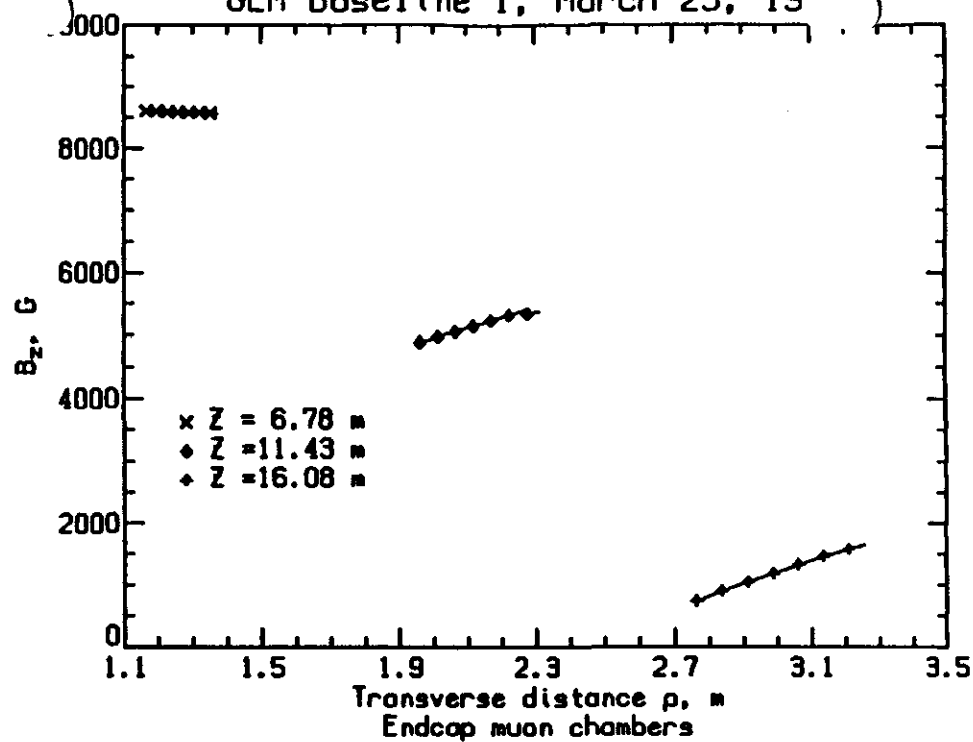


Plots of the magnetic field along the barrel muon chambers; the total field B , axial component B_z , and radial component B_r are shown.

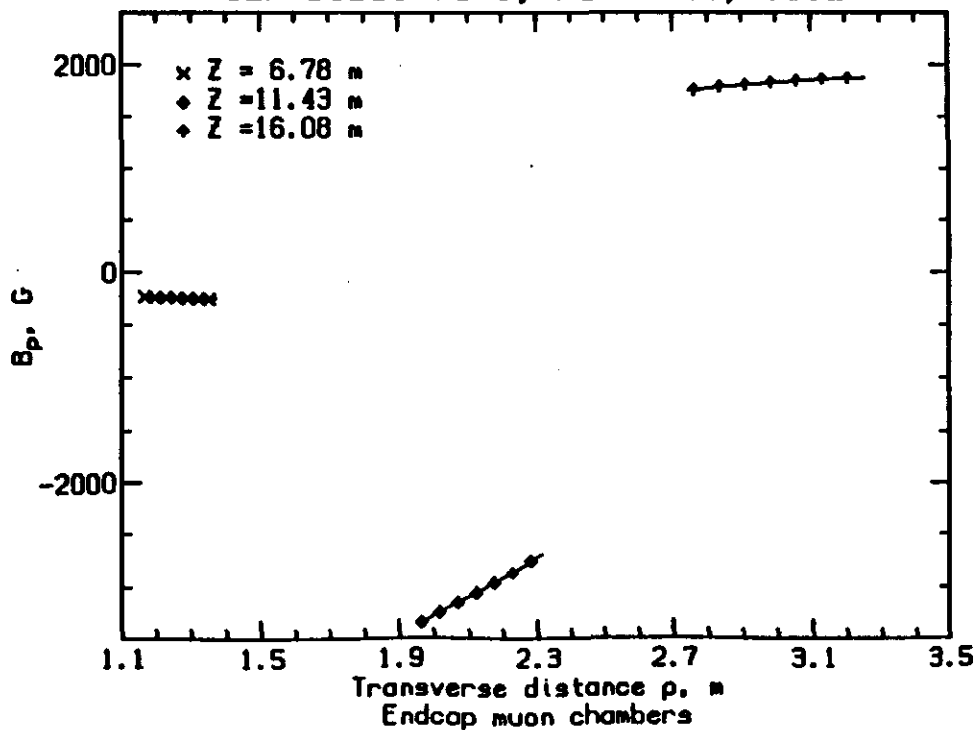
GEM Baseline 1, March 25, 1992



GEM Baseline 1, March 25, 1992

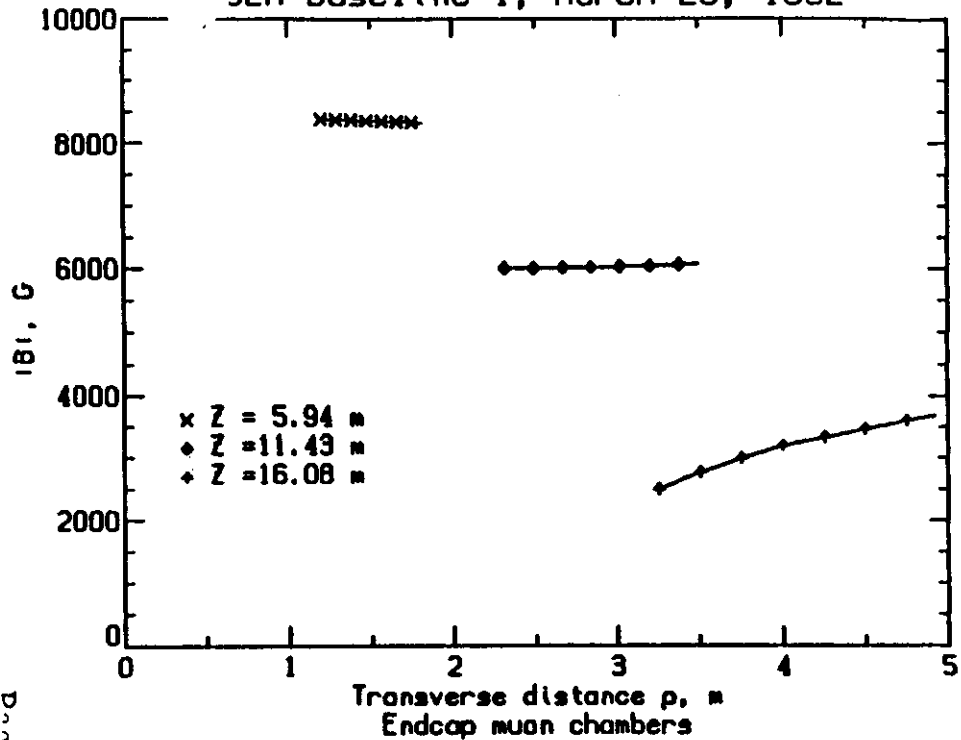


GEM Baseline 1, March 25, 1992

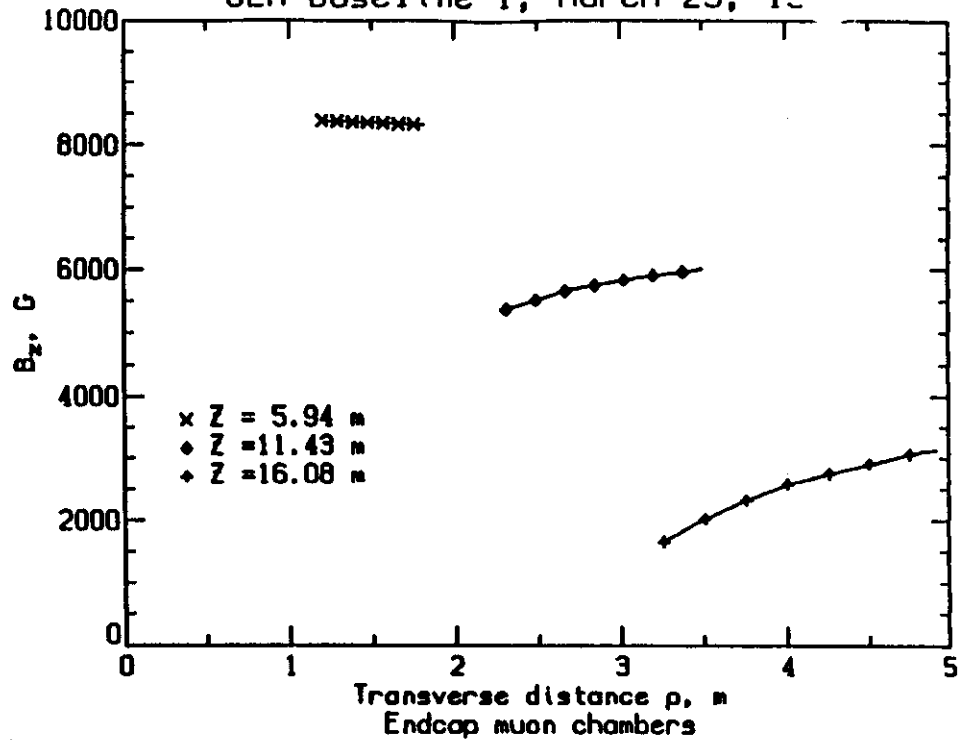


Plots of the magnetic field along the endcap muon chambers (17.0-27.7): the total field B , axial component B_z , and radial component B_ρ are shown.

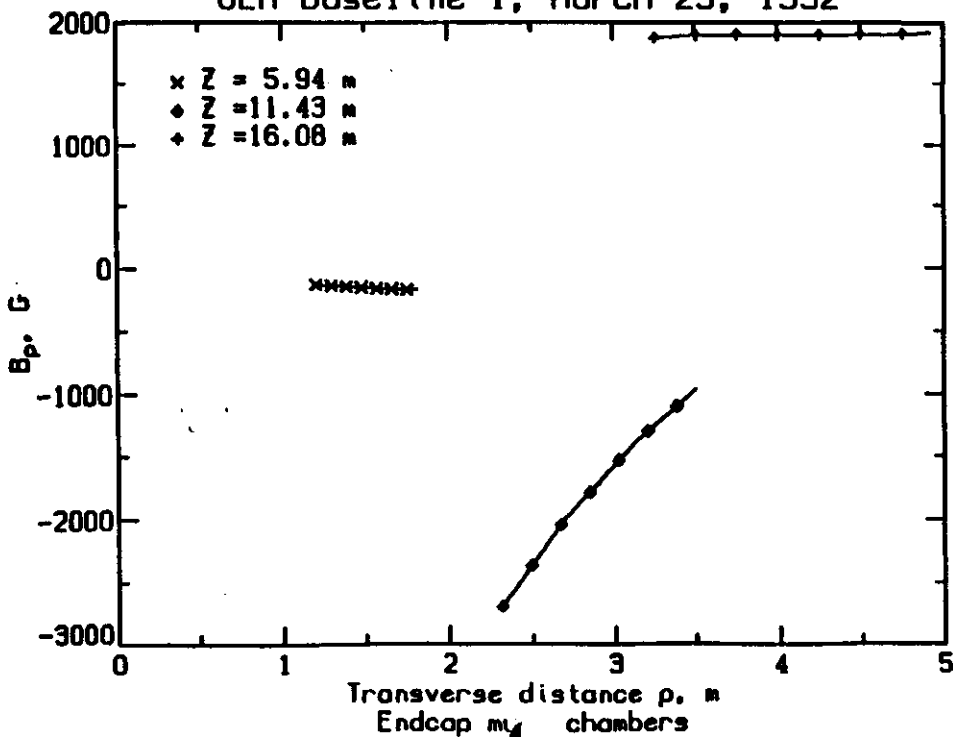
GEM Baseline 1, March 25, 1992



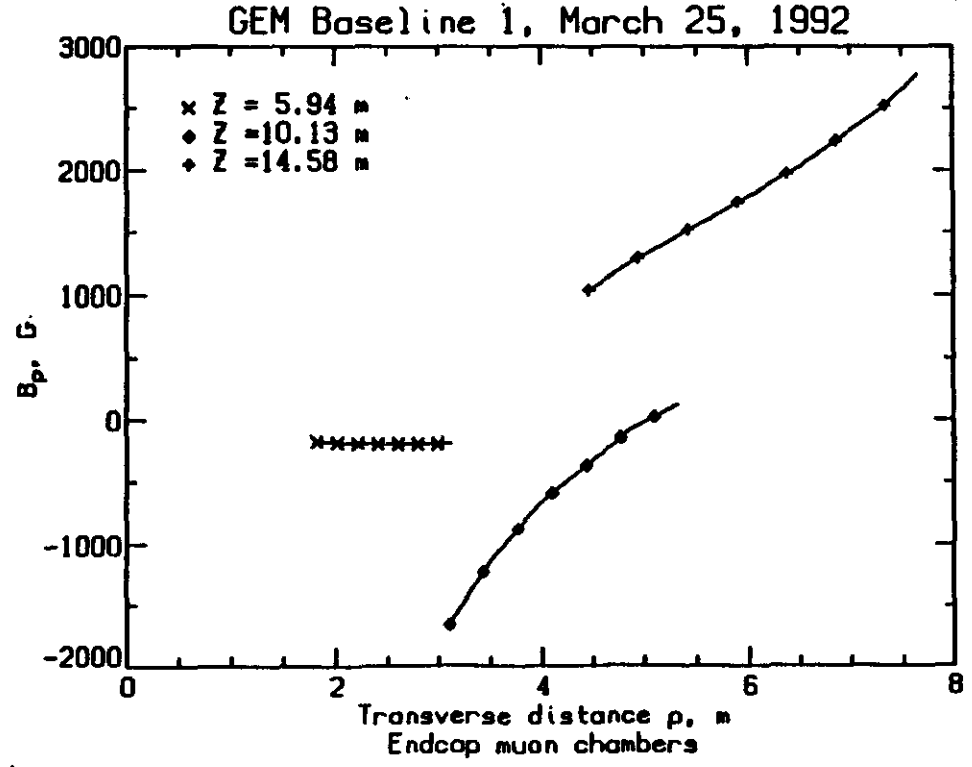
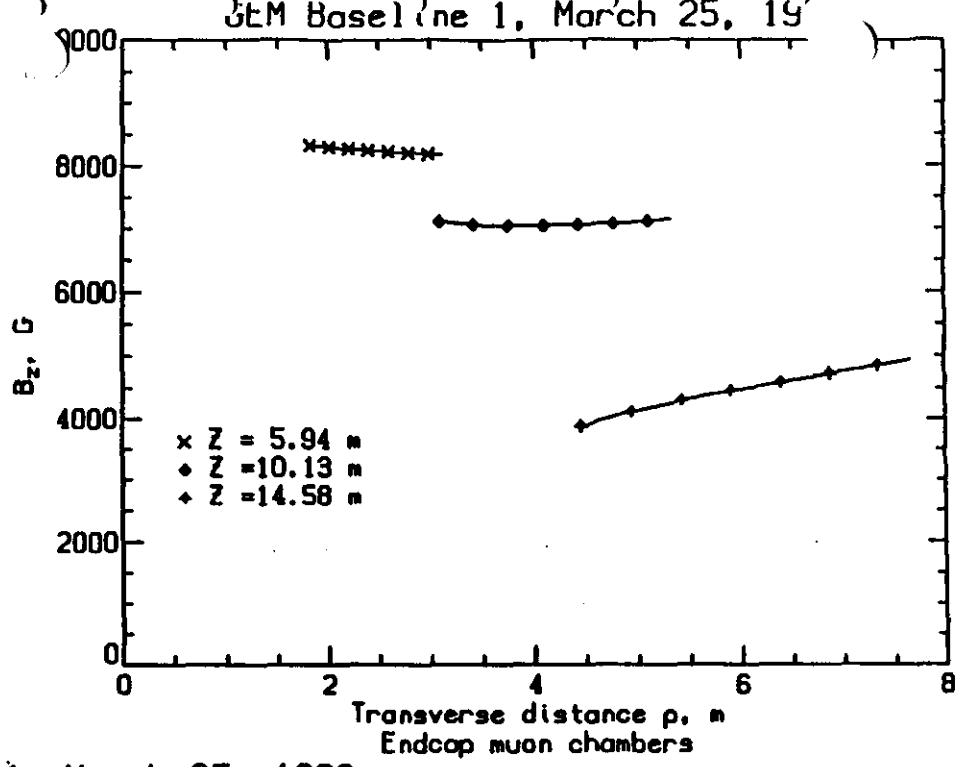
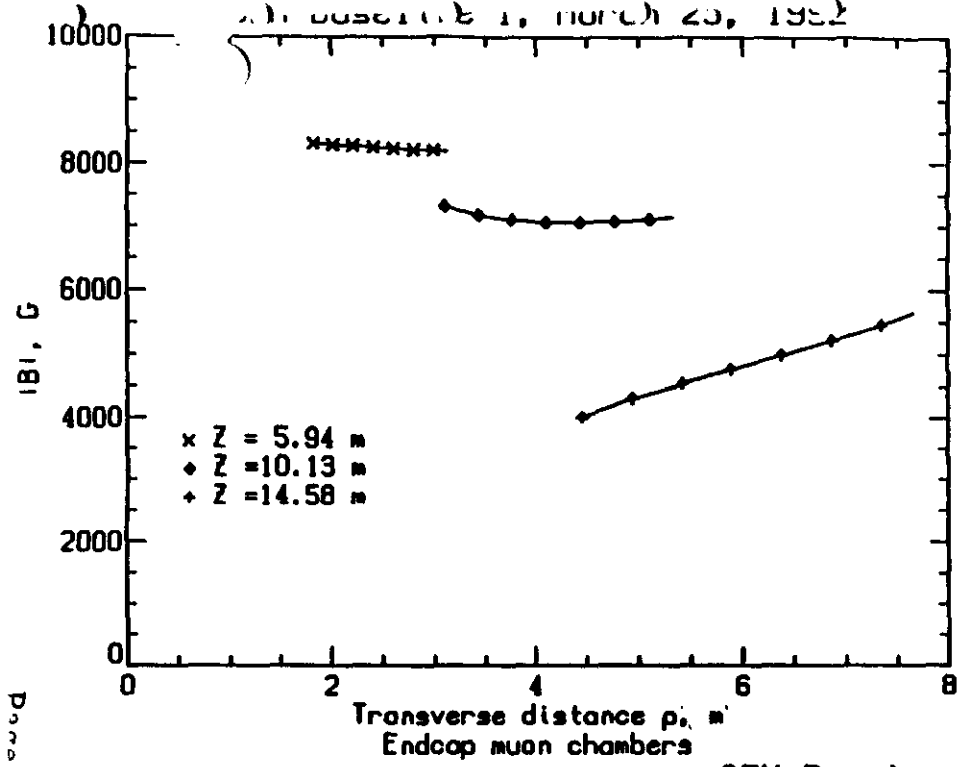
GEM Baseline 1, March 25, 19



GEM Baseline 1, March 25, 1992



Plots of the magnetic field along the endcap muon chambers (11.5-17.0°): the total field B , axial component B_z , and radial component B_p are shown.



Plots of the magnetic field along the endcap muon chambers (9.75-11.5'); the total field B , axial component B_z , and radial component B_ρ are shown.

TRACKING SYSTEM

TABLE OF CONTENTS

OVERVIEW

FIGURES:

95% Confidence Level Charge Separation
GEM Central Tracker Assembly
GEM Central Tracker Sections
Silicon Tracker Assembly
Typical Silicon Wafer X-Layer
Silicon Ladder Assembly
Silicon Tracker Space Frame Assembly
Butane Gas Enclosure
IPC Superlayer (Section)
IPC Superlayer
GEM IPC Tracker Barrel Module
Cell Geometry View Along the Wire
Pad Arrangement in the Barrel Chambers
Pad Arrangement in the End Cap Chambers
Phi Across One Module
Material in Central Tracker
Momentum Resolution verses Eta
Transverse Momentum verses Eta
Impact Parameter Resolution verses Momentum
Impact Parameter verses Eta
Tracker/Calorimeter Interface

TABLES:

[Tracker] Design Parameters
Central Tracker Physics Studies
Occupancy
Resolution and Stability
Silicon Wafer Design Parameters
Silicon Detector Parameters
IPC Design Parameters
IPC Array Design Parameters
IPC Array Stability Requirements
IPC Radiation Length Budget

TRACKING SYSTEM

CENTRAL TRACKER

OVERVIEW

The Central Tracker of the GEM detector is designed to operate in the 0.8 Tesla magnetic field of the large GEM superconducting solenoid. The tracker is compact, with a 75 cm outer radius and a total length of 300 cm. It covers a pseudorapidity range of ± 2.5 units. The present baseline design consists of a Silicon Microstrip (SM) inner tracker and an Interpolating Pad Chamber (IPC) outer tracker. The geometry of the Central Tracker in this design is shown in Figure 9.1 (a).

Since the submission of the GEM Expression of Interest, a variety of technologies were considered for use in the GEM Central Tracker. For the inner tracker silicon microstrips, silicon pixels and long drift length silicon detectors were discussed. Silicon pixel and long drift silicon detectors were considered to be too immature, with large uncertainties of performance, radiation resistance, and costs, to be a sensible choice at this time. Silicon microstrip detectors were chosen as the baseline design for the following reason:

1. The very fine segmentation possible combined with proven high radiation resistance make this detector ideal as the element closest (~ 10 cm) to the interaction point.
2. Very high spatial resolution allows very precise vertex position and track impact parameter measurement.
3. It is a mature technology, which is presently in use in a number of fixed target and collider experiments with relatively well understood performance, radiation resistance and cost.

Silicon detectors were considered to be too expensive for the outer tracker. Technologies under serious discussion for outer tracker were Straw Tubes, Scintillating Fibers and interpolating Cathode Pad Chambers. The Interpolating Pad Chambers were chosen for the baseline design for the following reasons:

1. Pad sizes of the order of a few cm^2 are easily achieved. This allows for a low occupancy even at a luminosity of $10^{34} \text{ cm}^{-2}\text{sec}^{-1}$. Thus, this technology is suitable even at the highest proposed luminosities of the SSC. The other technologies would result in considerably higher occupancies.
2. The pads, in some approximation, approach 3 dimensional points, which is quite important for good tracking in the high rate and multiplicity environment of the SSC. The two other technologies

Source: K Morgan
Updated:

CENTRAL TRACKER

produce stereo images i.e., all tracks projected onto a plane, which make pattern recognition more difficult.

3. Interpolating Pad Chambers are not a new technology; they have been demonstrated to have the resolution needed with chamber sizes similar to those required for the GEM tracker design.

The Silicon Microstrip inner tracker consists of six layers of silicon strip ladders. The geometrical layout of the silicon is shown in Figure 9.2. Each ladder is composed of two back-to-back single sided silicon sensors with a 5 mrad stereo angle between the two sensors. Each sensor is 300 μm thick with a strip pitch of 50 μm . Each pair of sensors provides a space point with a resolution of 10 μm in the $r - \phi$ plane and 3 mm in the $r - z$ projection. The six layers of ladders are organized into three superlayers, each of which provides a track stub to a track finding algorithm. In the forward region, the silicon sensors are mounted into disks with the strips projecting radially inward toward the beam axis. The Silicon Tracker is ~200 cm long and extends in a radius from 10 to 35 cm. The total area of silicon ladders in the detector is about 7 m^2 with about 3.2×10^6 strips to be read out. The read-out will be highly multiplexed, with 640 strips to one fiber optic readout channel, for a total readout channel count of 5,052.

The outer tracker consists of 8 layers of pad chambers, both in the barrel region at radii between 35 and 70 cm, and in the forward region which extends from 20 to 70 cm in radius. The 8 layers are arranged in 4 superlayers with 2 layers each. Each barrel layer will consist of 20 chambers, each covering 18° in azimuth, with the largest chamber being 30 cm wide \times 200 cm long. The forward layers will be disks divided into ten trapezoidal chambers about 50 cm \times 50 cm each.

The IPC's in this system will be very similar in concept and performance to chambers which have been constructed and are now taking data in experiment E-814 at Brookhaven AGS [2]. These chambers have various sizes up to 50 cm \times 200 cm and have obtained a resolution of ~50 μm , or ~1% of the pad size, which is what the GEM design calls for.

Each of the chambers will be tilted in azimuth by the Lorentz angle of the gas (~6 to 9°) so that the $E \times B$ effect in the 0.8 T field does not degrade the resolution. This tilt also allows the chambers to be overlapped, eliminating dead regions due to electronics and structural elements (see Figure 9.1b).

Source: K Morgan
Updated:

CENTRAL TRACKER

The direction of good resolution in these pad chambers is along the anode wire. Thus, the wires in the barrel chambers will run across the chambers, in the " ϕ direction", keeping the wire length between 15 and 30 cm. In the forward chambers the wires will also run in the " ϕ direction", with wire length between 10 and 40 cm. The wire spacing will be 2 mm in both the barrel and the forward chambers.

In the present design pad sizes are a uniform $\Delta\eta \times \Delta\phi = 0.0007$ in all parts of the tracker. This results in a total of just under 400,000 pads for the entire device.

In the present design the pads are 2.5 mm wide (in the ϕ direction) and a few centimeters long (in the z direction, which is the direction along the beams). With an analog readout we expect to interpolate to obtain a precision in the ϕ direction of $\sim 50 \mu\text{m}$. To obtain better precision than the pad length in the z direction, the pads will be tilted by ± 30 mrad in the two layers of each superlayer, respectively. This stereo angle will provide a z resolution of $\sim 700 \mu\text{m}$, which is good enough to provide a vertex z resolution of ≤ 1 mm from the IPC's alone, so that this vertex z resolution will be available at the highest luminosities at the SSC.

The IPC readout electronics for each pad include a fast front end amplifier and shaper feeding an analog pipeline which is multiplexed at the output by a factor of 256, giving a total of 1600 channels. The present design calls for on board digitization using an 8 bit flash ADC system, multiplexed to optical drivers.

CENTRAL TRACKER

Primary Physics Goals

- Identify the primary vertex of an event of interest, so that it can be separated from other pileup events in the memory time of the detector.
- Separate electrons and gammas using the presence or absence of a charged track pointing to an electromagnetic shower in the calorimeter.
- Provide track information for e, μ or γ isolation cuts, and help with rejection of conversions and Dalitz pairs.
- Help with electron-hadron separation by providing a momentum measurement that can be compared with the energy deposition in the calorimeter.
- Help with rejection of background by matching the muon momentum measured in the central tracker with the momentum measured in the muon chambers.
- Determine the electron sign up to 400 GeV/c.

Secondary Physics Goals

- Full reconstruction of the charged tracks in the event.
- Secondary vertex finding.
- Tracking at low momenta with good resolution.

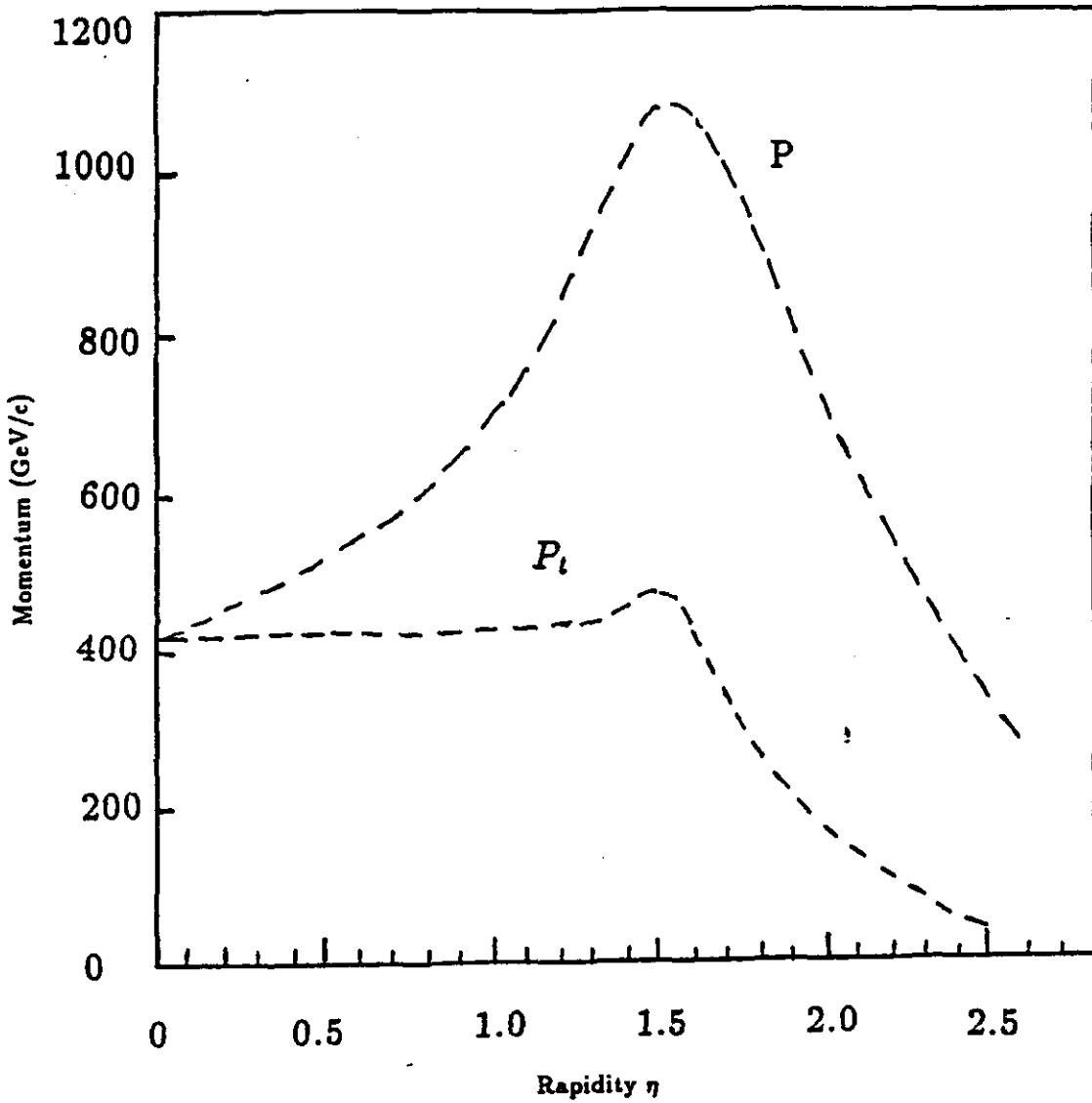
Design Parameters	
Outer radius	70 cm
Length (from IP to outer face)	± 150 cm
Rapidity Coverage	$ \eta \leq 2.5$
Magnetic field	0.8 T
Occupancy	$\leq 1\%$
at $L = 10^{33}$ cm ⁻² s ⁻¹	$\leq 10\%$
at $L = 10^{34}$ cm ⁻² s ⁻¹	$p \leq 400$ GeV/c
Charge separation at 95% c.l.	
Momentum Resolution at 90°	
High momenta	$\Delta p/p^2 \sim 1.5 \times 10^{-3}$ (GeV/c) ⁻¹
(measurement limited)	
low momenta	$\Delta p/p \sim 4\%$
(multiple scattering limited)	
Vertex resolution	
Along beam direction	$\delta z \sim 1$ mm
Impact parameter	$\delta b \sim 30$ μ m
	above 10 GeV/c

Source: K. Morgan/R. Barber

Updated: 6/25/92

Physics Processes	Id. Primary Vertex	e, μ , γ Separation	e/h Separation	Muon Separation	e \pm Sign Momentum Check	Secondary Separation	Low Momentum Vertex	Full Event Reconst.
$H^0 \rightarrow \gamma + \gamma$	X	X	X					
$H^0 \rightarrow e^+e^-l^+l^-, e^+e^-\nu\bar{\nu}, e^+e^- jetjet$	X	X	X	X			X	
$H^0 \rightarrow \mu^+\mu^-l^+l^-, \mu^+\mu^-\nu\bar{\nu}, \mu^+\mu^- jetjet$	X		X			X		
Gluino Pair Prod $\tilde{g}\tilde{g} \rightarrow e^\pm e^\pm, \mu^\pm e^\pm$	X	X	X	X	X	X		
Techni eta $\eta_T \rightarrow b + \bar{b}$ or $t + \bar{t}$	X		X				X	
WW Scattering $W^\pm W^\pm \rightarrow e^\pm e^\pm, \mu^\pm e^\pm$	X	X	X	X	X	X		
$Z^1 \rightarrow e^+e^-$ Asymmetry	X	X	X	X		X		
B Physics, e.g. $B \rightarrow \Psi$, etc.	X						X	X
Top Physics $t \rightarrow W + b$, etc.	X		X				X	X

CENTRAL TRACKER PHYSICS STUDIES



**95% Confidence Level
Charge Separation**

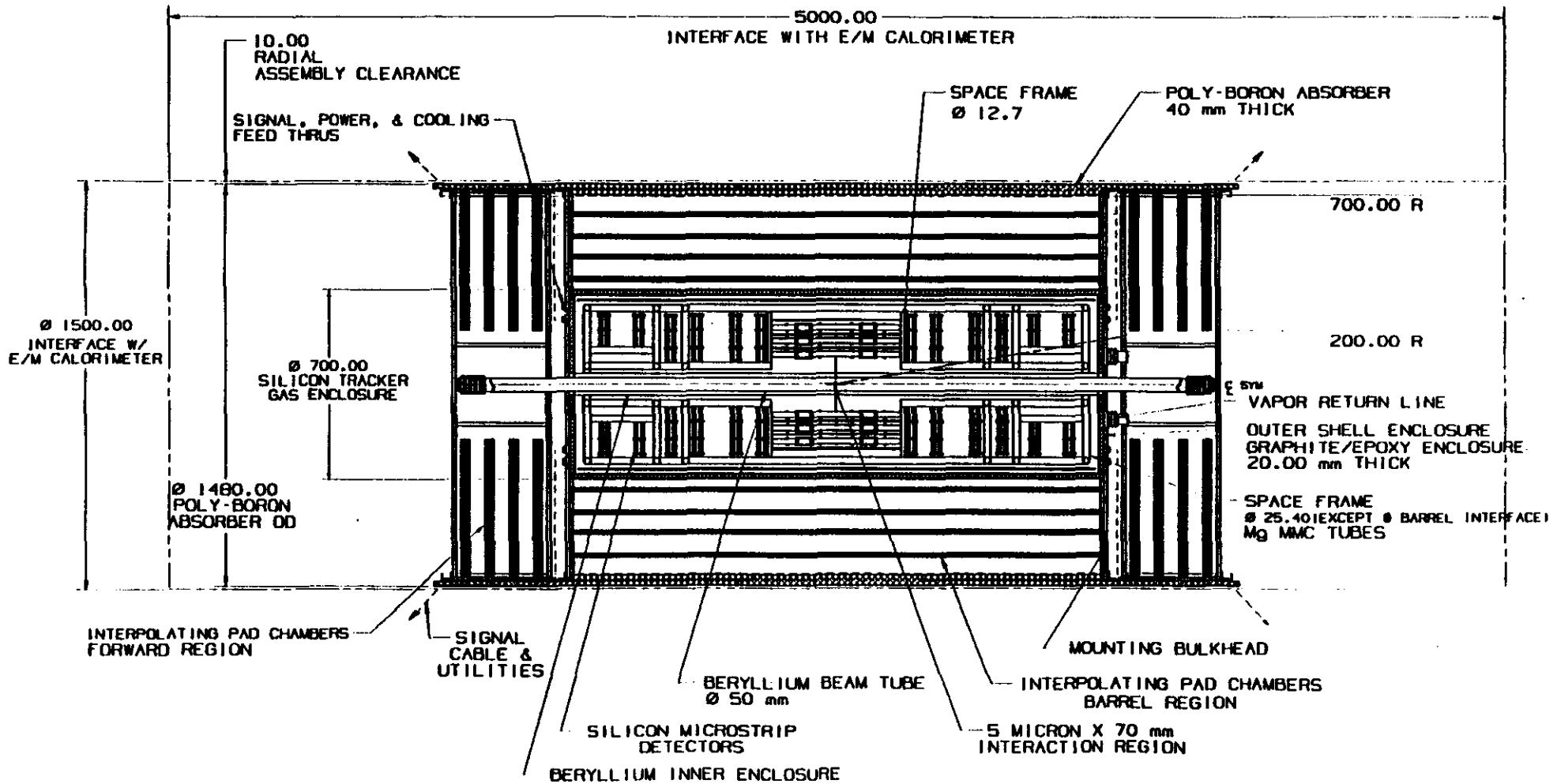
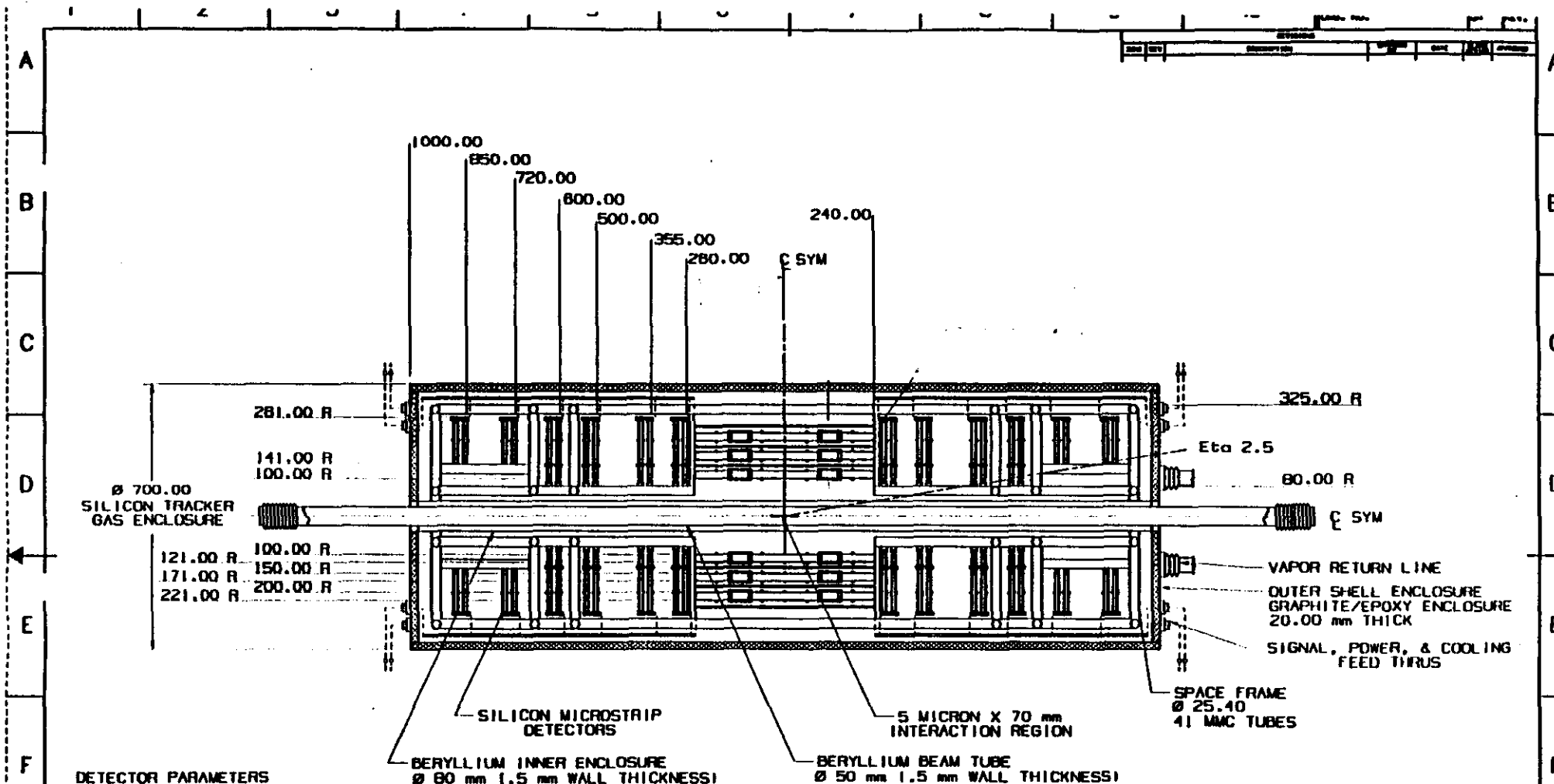


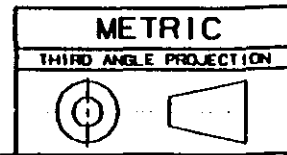
Fig. 9.1 (a) GEM CENTRAL TRACKER ASSEMBLY



DETECTOR PARAMETERS

	CENT. REGION	FWD REGION
WAFERS	3227	5987
MC MODULES	1814	3438
DETECTOR STRIPS	1.03E+08	2.20E+08
WAFER AREA	3.25	4.37
(M ² FRONTAL AREA)		

Fig. 9-2 SILICON TRACKER ASSEMBLY



<table border="1"> <tr> <th>REV</th> <th>DATE</th> <th>DESCRIPTION</th> </tr> <tr> <td> </td> <td> </td> <td> </td> </tr> <tr> <td> </td> <td> </td> <td> </td> </tr> </table>	REV	DATE	DESCRIPTION							<table border="1"> <tr> <th>NO</th> <th>DATE</th> <th>BY</th> <th>CHKD</th> <th>APP'D</th> </tr> <tr> <td> </td> <td> </td> <td> </td> <td> </td> <td> </td> </tr> <tr> <td> </td> <td> </td> <td> </td> <td> </td> <td> </td> </tr> </table>	NO	DATE	BY	CHKD	APP'D											<table border="1"> <tr> <td> Los Alamos NATIONAL LABORATORY GEM CENTRAL TRACKER SILICON TRACKER </td> <td> SIZE: 11x17 SHEET NO.: AI SK-06M12-020A REV: 1 </td> </tr> </table>	Los Alamos NATIONAL LABORATORY GEM CENTRAL TRACKER SILICON TRACKER	SIZE: 11x17 SHEET NO.: AI SK-06M12-020A REV: 1
REV	DATE	DESCRIPTION																										
NO	DATE	BY	CHKD	APP'D																								
Los Alamos NATIONAL LABORATORY GEM CENTRAL TRACKER SILICON TRACKER	SIZE: 11x17 SHEET NO.: AI SK-06M12-020A REV: 1																											

CENTRAL TRACKER

Occupancy			
Silicon	$\Delta\eta\Delta\Phi$ cell	Occupancy (%)	Fraction of Time Dead (%)
$L = 10^{33} \text{ cm}^{-2}\text{s}^{-1}$	$0.9-8.0 \times 10^{-4}$	0.06-0.22	0.6-2.2
$L = 10^{34} \text{ cm}^{-2}\text{s}^{-1}$	$0.9-8.0 \times 10^{-4}$	0.26-0.96	2.6-9.6
IPC			
$L = 10^{33} \text{ cm}^{-2}\text{s}^{-1}$	0.0007	≤ 1	0
$L = 10^{34} \text{ cm}^{-2}\text{s}^{-1}$	0.0007	≤ 10	0

Resolution and Stability	
Silicon microstrips resolution	10 μm
Silicon alignment stability	5 μm
Pad chamber resolution	50 μm
Pad chamber alignment stability	25 μm

Silicon Wafer Design Parameters	
Thickness	300 $\mu\text{m} \pm 15 \mu\text{m}$
Number of strips	640
Strip pitch	50 μm
Number of readouts	640
Readout pitch	50 μm
Substrate	n type high resistivity silicon, 4 - 8 $\text{k}\Omega$
C (interstrip)	$5 \times C(\text{backplane}) < C < 1.5 \text{ pf/cm}$
C (coupling)	$> 10 \times C(\text{interstrip})$
Depletion voltage	60 volts max. prior to irradiation 140 volts max. after 5 MRads of irradiation
Breakdown voltage	150 volts min. prior to irradiation 180 volts min. after 5 MRads of irradiation
Leakage/strip	10 nA max. prior to irradiation 90% strips $\leq 2 \text{ nA}$ prior to irradiation
Leakage/Wafer	3.5 μA max. prior to irradiation (assume 90% @ 2nA + 7% @ 10 nA + 3% @ 100 nA)
Metalization	Aluminum
Radiation Hardness	$5 \times 10^{13} \text{ neutrons/cm}^2$; 5 Mrad
Strip faults/wafer	Maximum of 3% of the strips (19 strips) due to a combination of capacitive coupling faults or P-N junction faults. No more than 3 faulty strips in 10 adjacent strips.

Source: K. Morgan/R. Barber

Updated: 6/25/92

CENTRAL TRACKER

Silicon Detector Parameters		
	Central Region	Forward Region
SI Microstrip Wafers	3228	5977
Multi-chip Modules (MCM)	1614	3438
Detector Strips	1,030,000	2,200,000
Strips per MCM	640	640
MCM Heat Load per Strip	3 mW	3 mW
FO Driver and Receiver Heat Load	250 mW	250 mW
MCMs per FO Driver	1	1
Total Heat Load (kW)	3.5	7.5
Central Region Width	±240 mm	
1st Layer Radius	10 cm	
2nd Layer Radius	12.1 cm	
3rd Layer Radius	15 cm	
4th Layer Radius	17.1 cm	
5th Layer Radius	20 cm	
6th Layer Radius	22.1 cm	
Forward Region Inner Radius		10 cm
Forward Region Outer Radius		26.1 cm
1st Superlayer Z		26 cm
2nd Superlayer Z		35.5 cm
3rd Superlayer Z		50 cm
4th Superlayer Z		60 cm
5th Superlayer Z		72 cm
6th Superlayer Z		85 cm

Source: K. Morgan/R. Barber
 Updated: 6/25/92

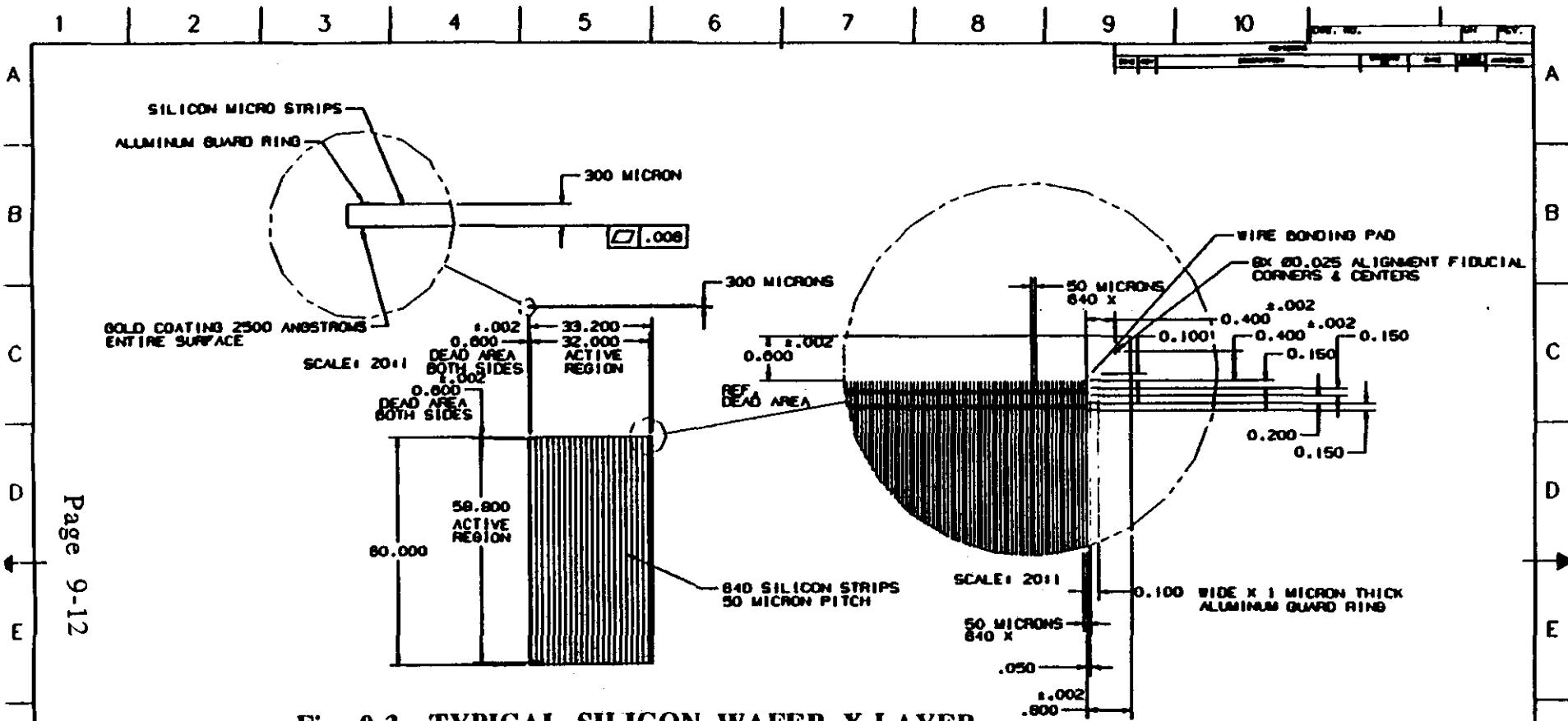
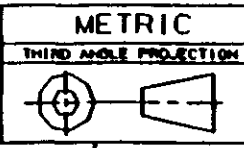


Fig. 9-3 TYPICAL SILICON WAFER X-LAYER

Page 9-12

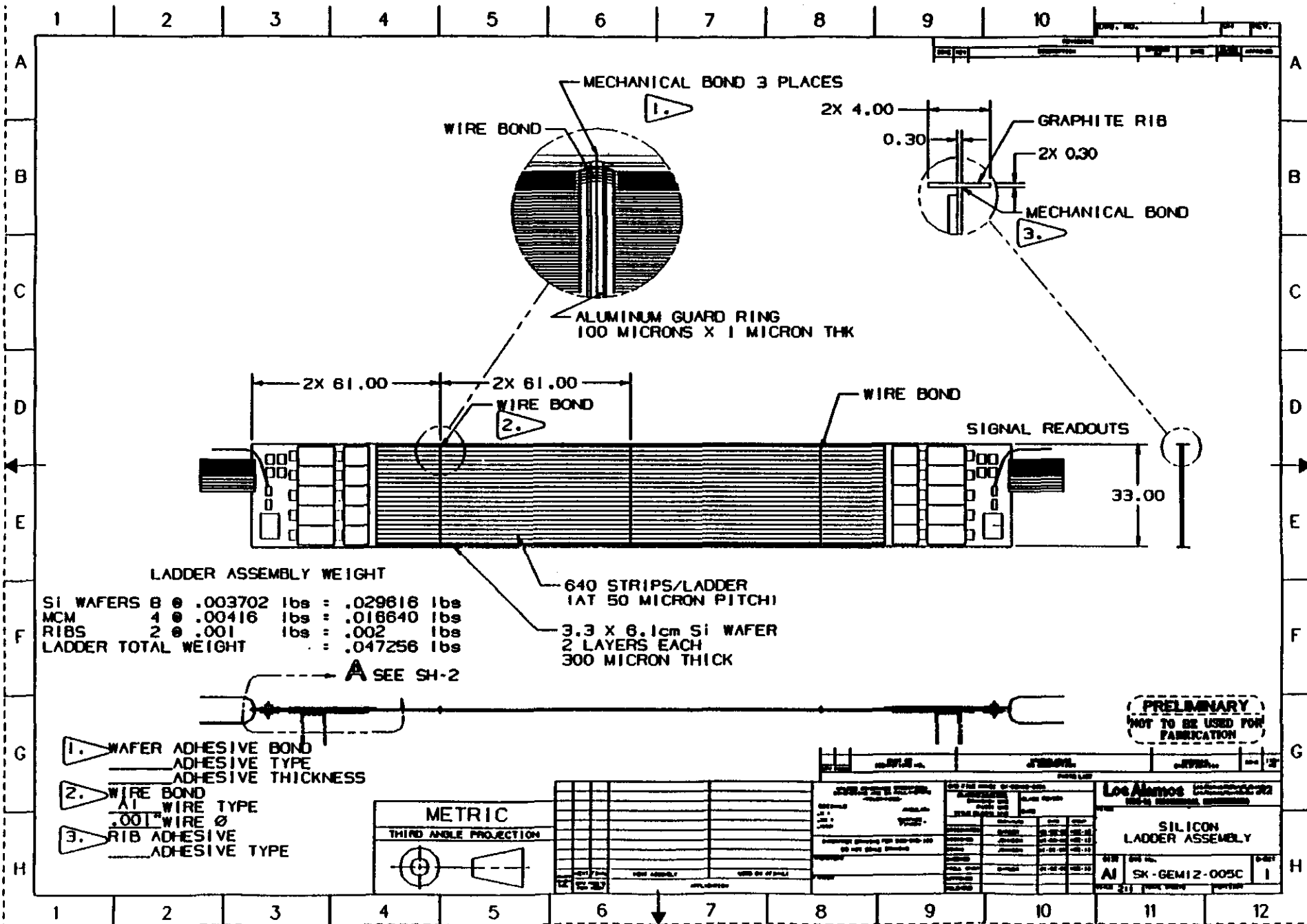
WEIGHT OF SILICON WAFER
 $\rho = 2.33 \text{ g/cm}^3$
 VOLUME/WAFER = 0.5978 cm^3
 $0.5978 \text{ cm}^3 \times 2.33 = 1.392408 \text{ grams}$
 $1 \text{ gram} \times 2.205 \times 10^{-6} = \text{pounds}$
 WAFER WEIGHT = .0030702 lbs.

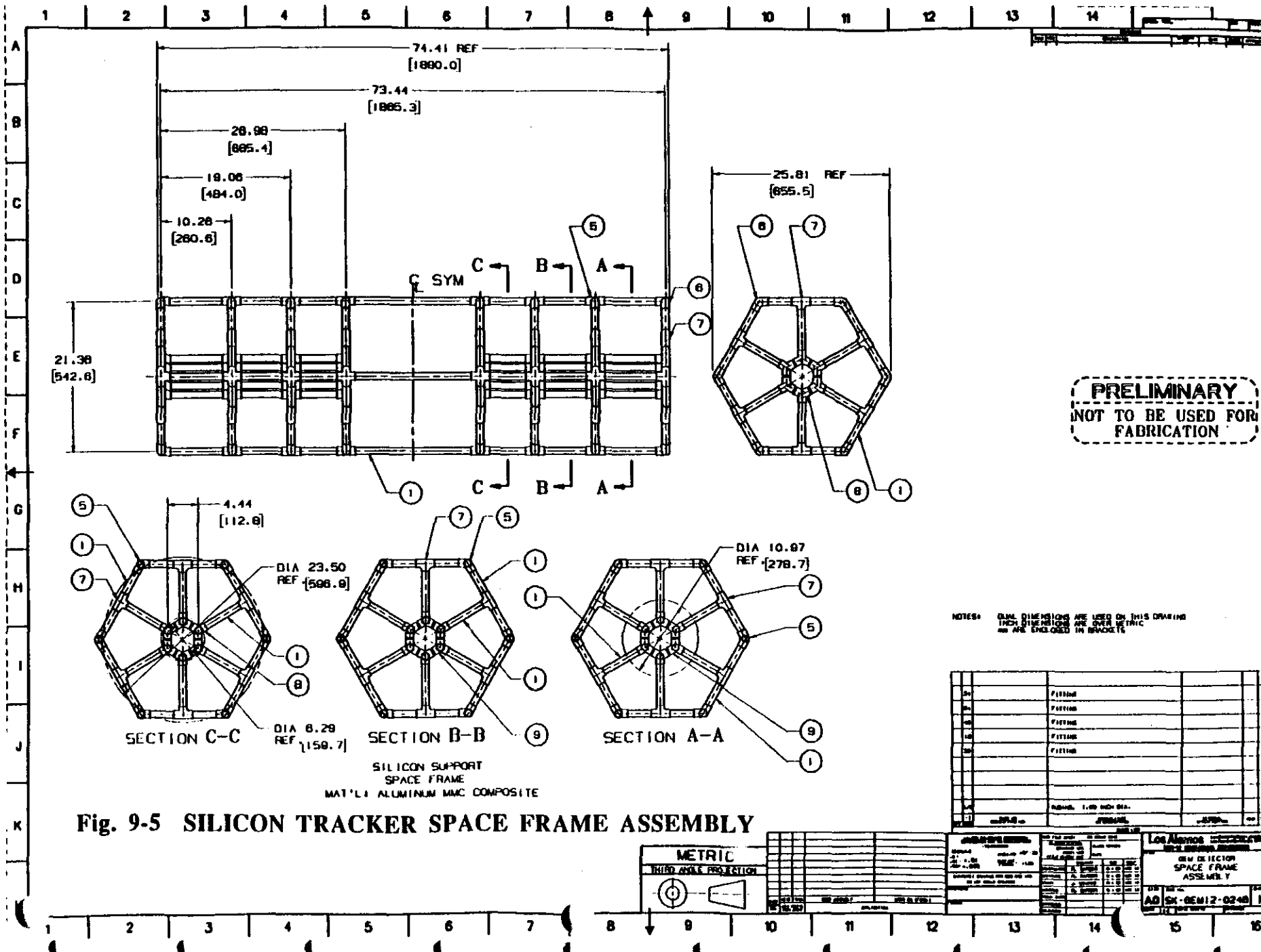
PRELIMINARY
 NOT TO BE USED FOR
 FABRICATION



DESIGNER'S CHECK		DATE	

Los Alamos GEM DETECTOR TYPICAL SILICON WAFER WITH X LAYER CONFIGURATION AI SK-GEM12-001C		11 1
---	--	---------





CENTRAL TRACKER

IPC Design Parameters	
Parameter	Quantity
Beam crossing rate	60 Mhz
Charged track density/min bias event	$dN/d\eta d\phi = 1.2$
Number min bias events/crossing@ 10^{34} Lum	16
Tracks/sec-mm wire @ 10^{34}	$1 \times 10^4 \text{ s}^{-1} \text{ mm}^{-1}$
Integrated charge/yr-cm wire @ 10^{34}	1.4 C/cm-yr
Position resolution (pads)	50 μm
Position resolution (Wires)	600 μm
Occupancy @ 10^{34}	< 10 %
Wire spacing	2 mm
Anode-Cathode spacing	2 mm
Wire diameter	40 μm
Voltage	3000 volts
Gas	50-50 CO ₂ -CF ₄
Barrel channel count	16000

IPC Array Design Parameters	
Parameter	Quantity
Lorenz angle	12 degrees
Number of sectors - barrel superlayer	20
Number of sectors - endcap superlayer	10
Number of superlayers - barrel and endcap	4
Number of chambers per superlayer	2
Chamber depth (cathode to cathode)	4 mm
Anode wire pitch - barrel and endcap	2 mm
Anode wire diameter	$25 \leq d \leq 40 \mu\text{m}$
Anode wire potential	3 Kv
Barrel IPC superlayer length	200 cm
Barrel IPC array inner radius boundary	35 cm
Barrel IPC array outer radius boundary	70 cm
Endcap IPC minimum axial boundary	110 cm
Endcap IPC maximum axial boundary	140 cm
Chevron pad width in ϕ	0.5 cm
Number of barrel pads	222360
Number of pads (each endcap)	87280
Electronics power dissipation - barrel	13.6 Kw
Electronics power dissipation - each endcap	5.2 Kw

IPC Array Stability Requirements	
Parameter	Quantity
Between superlayer modules in ϕ	25 μm
Between superlayers modules in z	100 μm
Between endcaps and barrel in ϕ	25 μm
Between endcaps and barren in z	100 μm
Maximum superlayer module deflection	1000 μm
Module transverse flatness	160 μm
-or-	20 μm over adjacent pads

Source: K. Morgan/R. Barber

Updated: 6/25/92

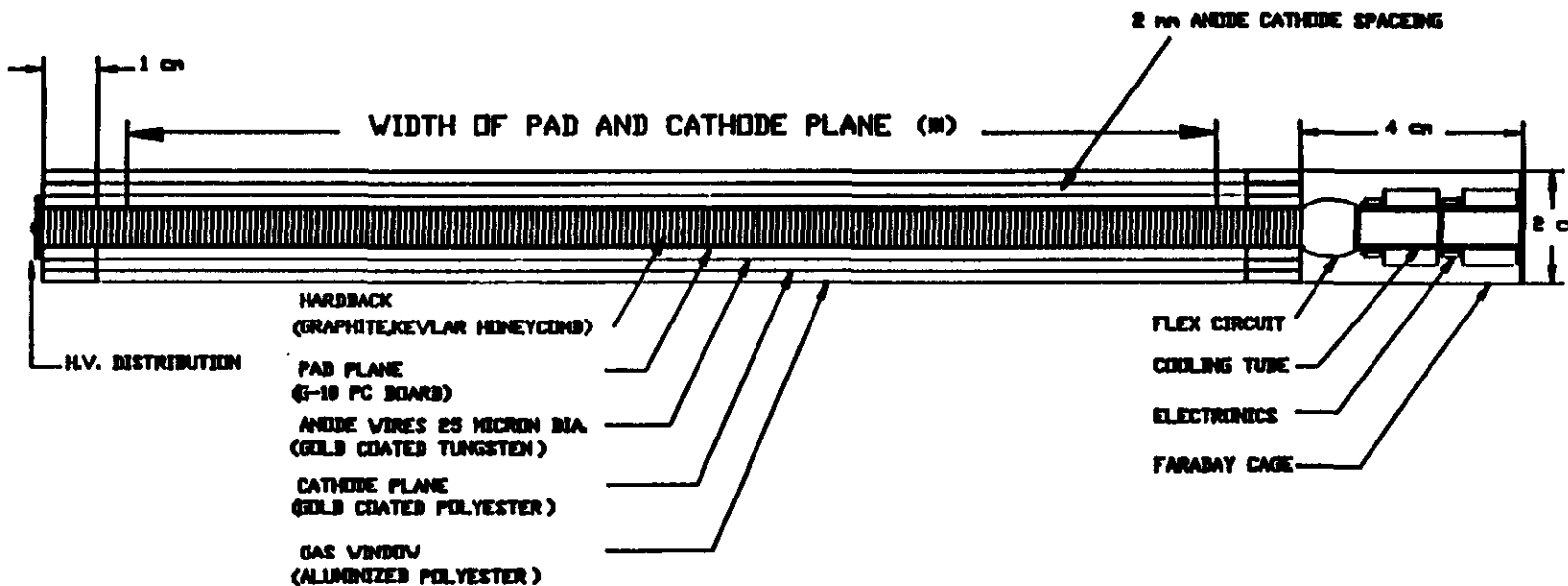
IPC SUPERLAYER

SECTION A-A

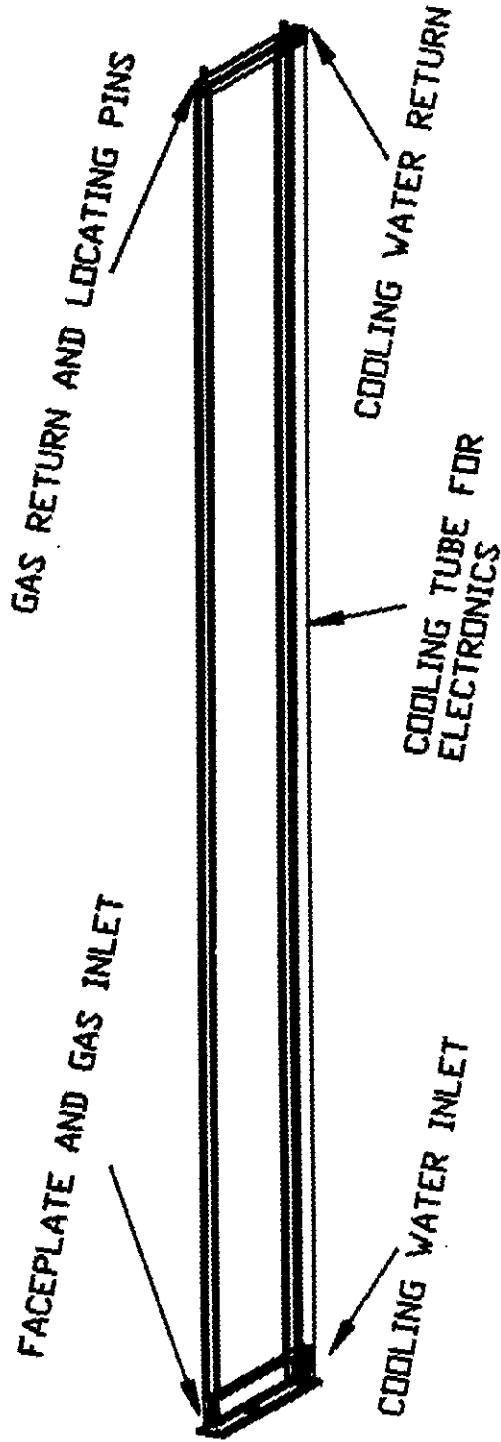
NOTE WIDTH VARIES BY LAYER

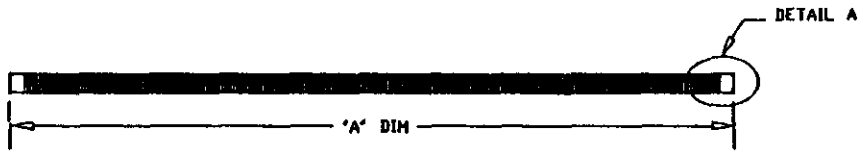
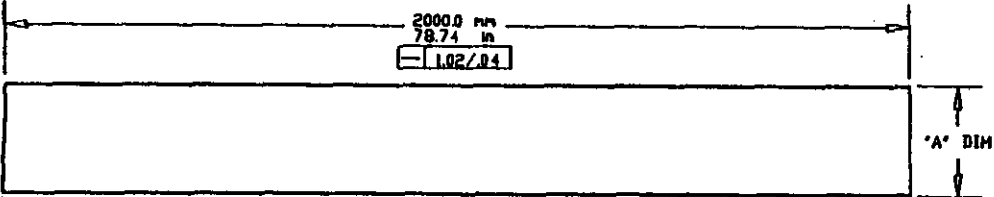
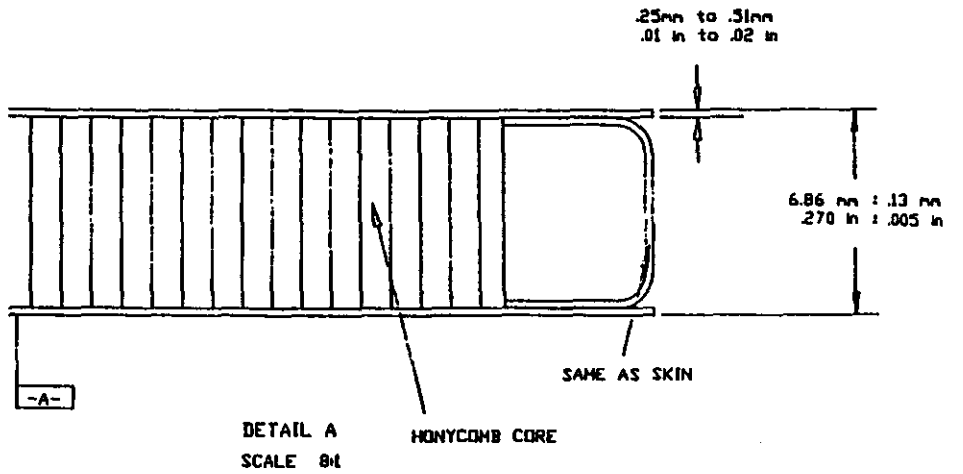
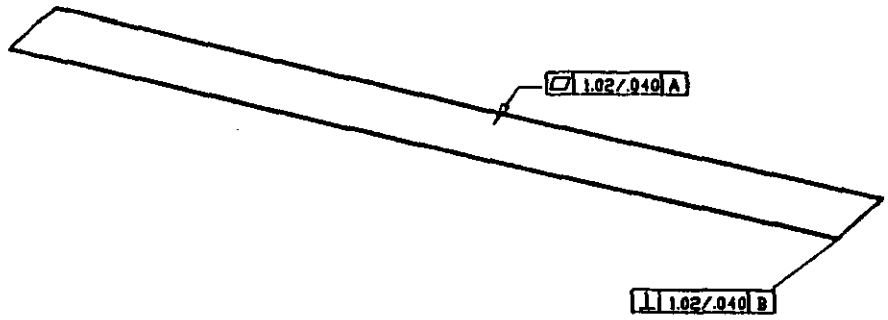
LAYER 1 = 14 CM
 LAYER 2 = 17 CM
 LAYER 3 = 20 CM
 LAYER 4 = 23 CM

Page 9-17



IPC SUPERLAYER





BONDED ASSEMBLY
SCALE 1:4

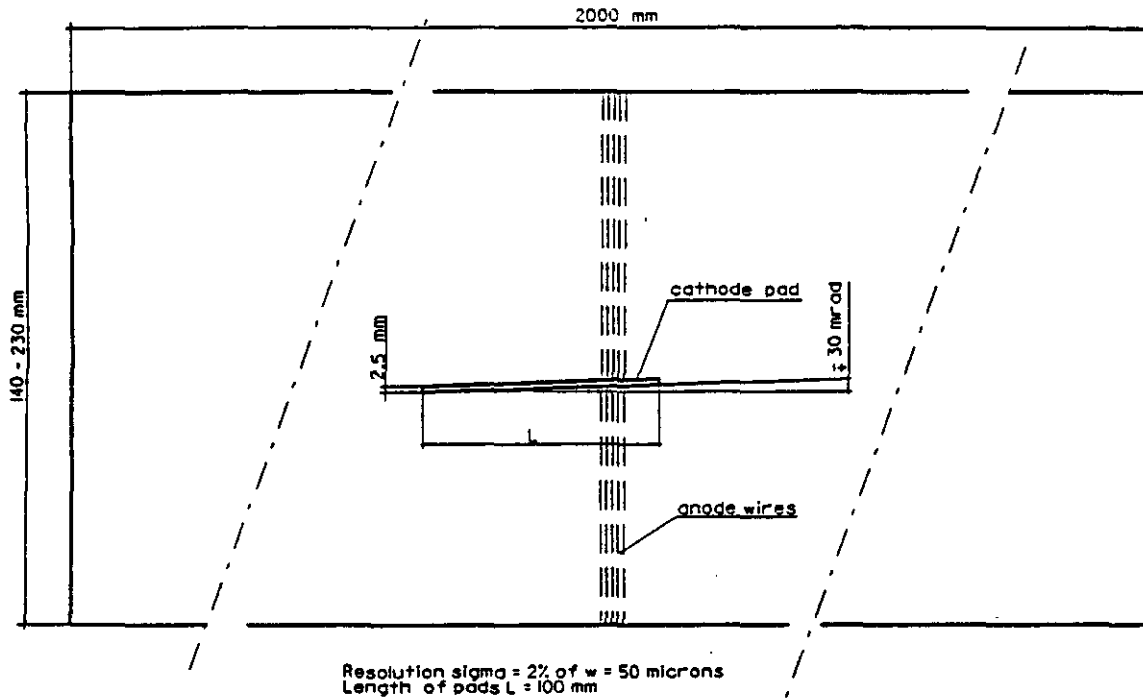
BONDED PANEL END VIEW
SCALE 2:1

ITEM	'A' DIM
1 - 243.8 mm - 9.60 in	-.13/.005
2 - 214.4 mm - 8.44 in	-.13/.005
3 - 187.8 mm - 7.39 in	-.13/.005
4 - 150.9 mm - 5.94 in	-.13/.005

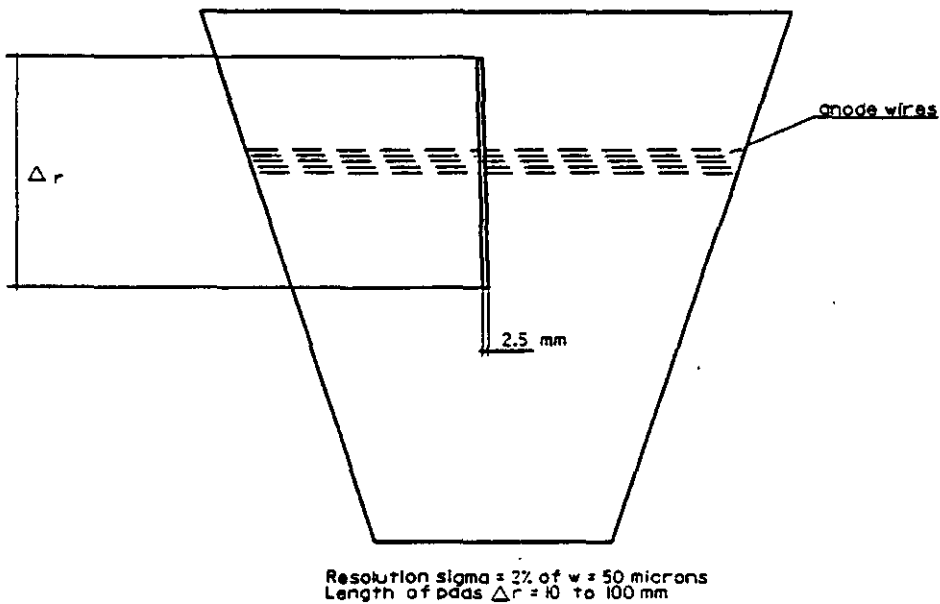
ALL DIMENSIONS ARE IN MILLIMETERS/INCHES	GATE UNIVERSITY		
	TITLE GEM IPC TRACKER BARREL MODULE		
CHECKED V.EMMET	NAME J.SINNOTT	SECTION P.P.G	
APPROVED V.EMMET	SCALE SHOWN	INST	SHEET 1



a) Cell geometry viewed along the wire



b) Pad arrangement in the Barrel Chambers



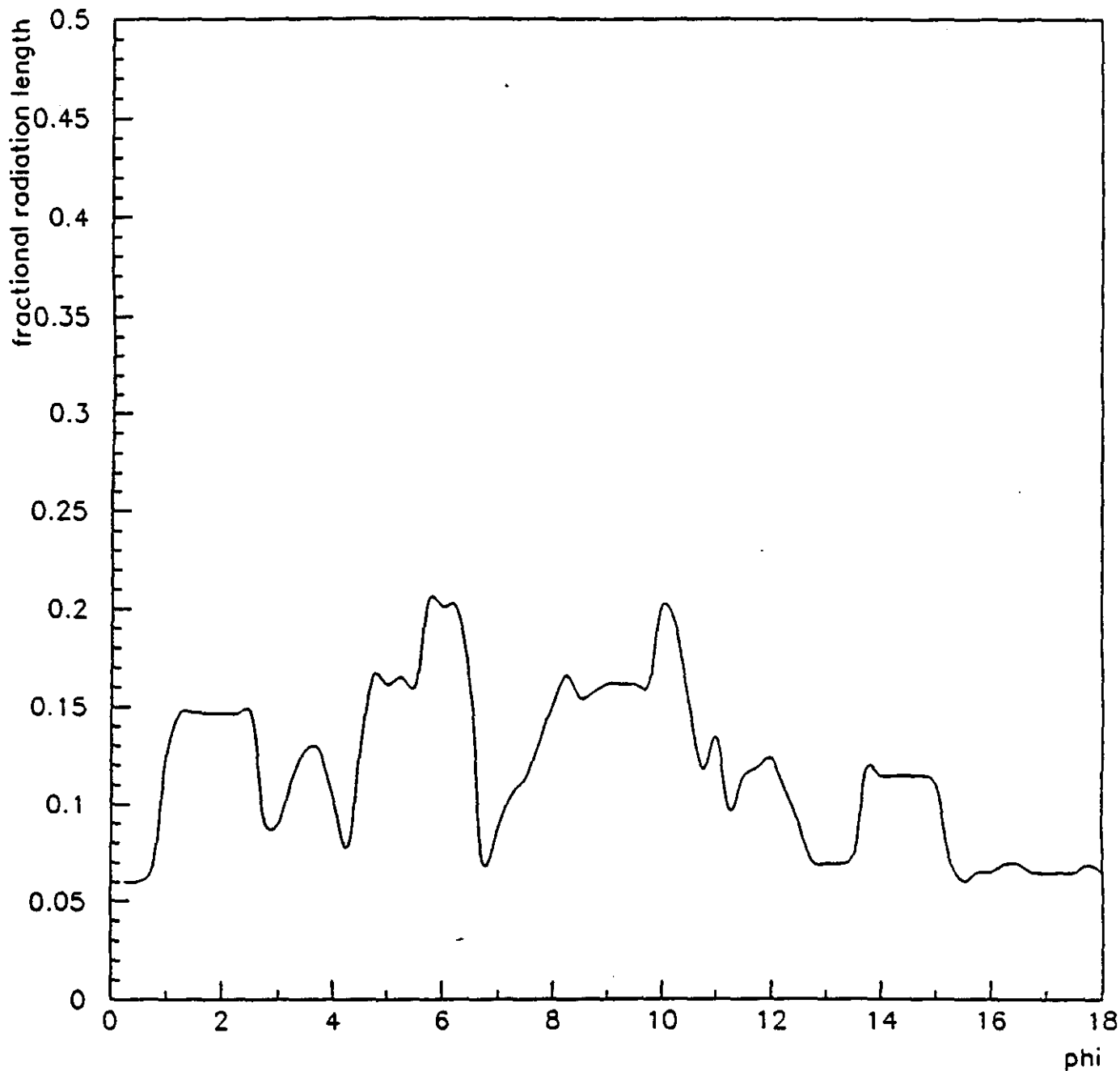
c) Pad arrangement in the End Cap Chambers

CENTRAL TRACKER

IPC Radiation Length Budget			
Layer Material	Thickness (cm)	Lrad (cm)	%Lrad
Hardback			
Graphite/Epoxy (skin)	0.0508	25.00	0.203
Graphite/Epoxy (corrugated core)	0.0508	25.00	0.203
Graphite/Epoxy (skin)	0.0508	25.00	0.203
Upper Chamber			
Chevron cathode pads (0.5 mil alum.)	0.0013	8.9	0.0146
Foam insulator (10 mil)	0.0254	150.0	0.0169
Signal plane (0.5 mil alum.)	0.0013	8.9	0.0146
Mylar insulator (2 mil)	0.0051	28.7	0.0178
Outer cathode plane	0.0013	8.9	0.0146
Mylar insulator (2 mil)	0.0051	28.7	0.0178
Lower Chamber			
Chevron cathode pads (0.5 mil alum.)	0.0013	8.9	0.0146
Foam insulator (10 mil)	0.0254	150.0	0.0169
Signal plane (0.5 mil alum.)	0.0013	8.9	0.0146
Mylar insulator (2 mil)	0.0051	28.7	0.0178
Outer cathode plane	0.0013	8.9	0.0146
Mylar insulator (2 mil)	0.0051	28.7	0.0178
Gas Envelope Windows			
Upper chamber (5 mil mylar)	0.0127	28.7	0.0443
Lower chamber (5 mil mylar)	0.0127	28.7	0.0443
Subtotal per superlayer:			0.891
% due to hardback:			68.44
% due to pad material:			9.84
% due to insulator material:			21.72
Module sides (anode supports, etc):			5.13
Average of module side effects:			
Superlayer I:			0.8
Superlayer II:			0.65
Superlayer III:			0.55
Superlayer IV			0.47
Average of electronics:			
Superlayer I:			1.22
Superlayer II:			1.0
Superlayer III:			0.85
Superlayer IV			0.75
Grand Total			
			9.82
- or - at 12 degree Lorenz angle			10.04

Source: K. Morgan/R. Barber

Updated: 6/25/92



**Phi Across One Module
(in degrees)**

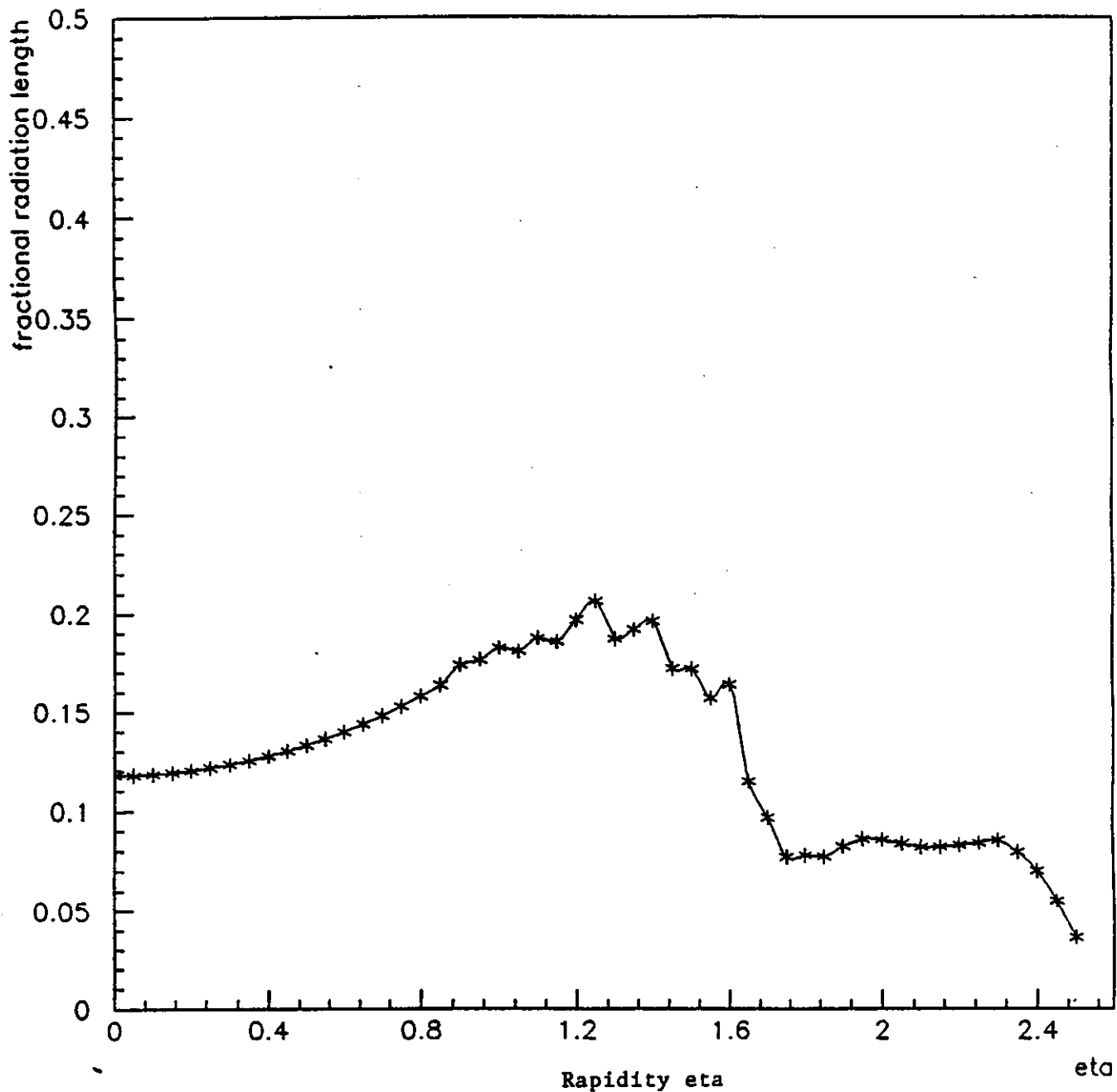
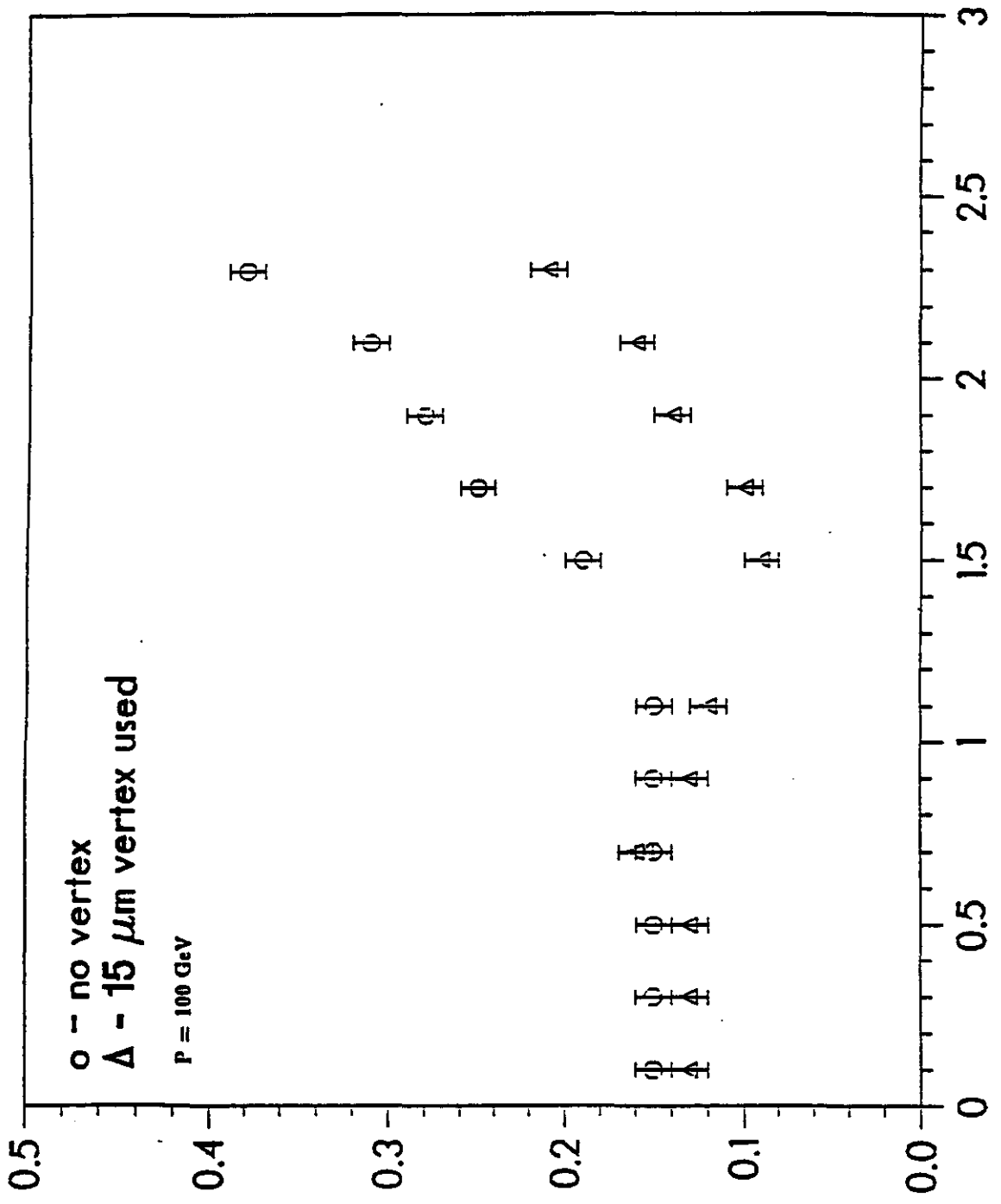


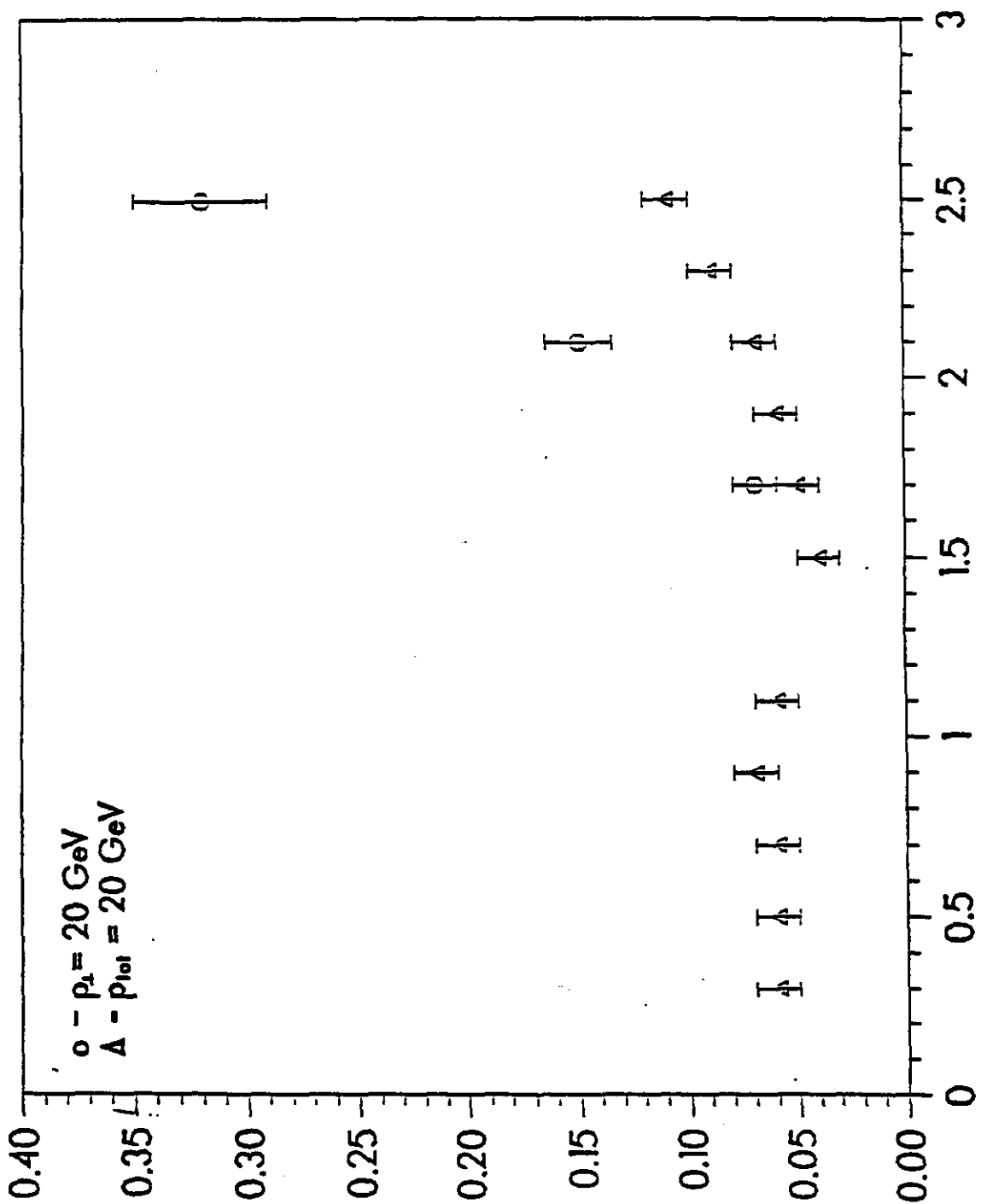
**Fig 9-12 MATERIAL IN CENTRAL TRACKER
EXCLUDING OUTERMOST PAD CHAMBERS AND
FORWARD OUTERMOST ELECTRONICS**



MOMENTUM RESOLUTION VERSUS ETA
 FOR 100 GeV PARTICLES (measurement limited case)

M. BROOKS, LOS ALAMOS
 ETA

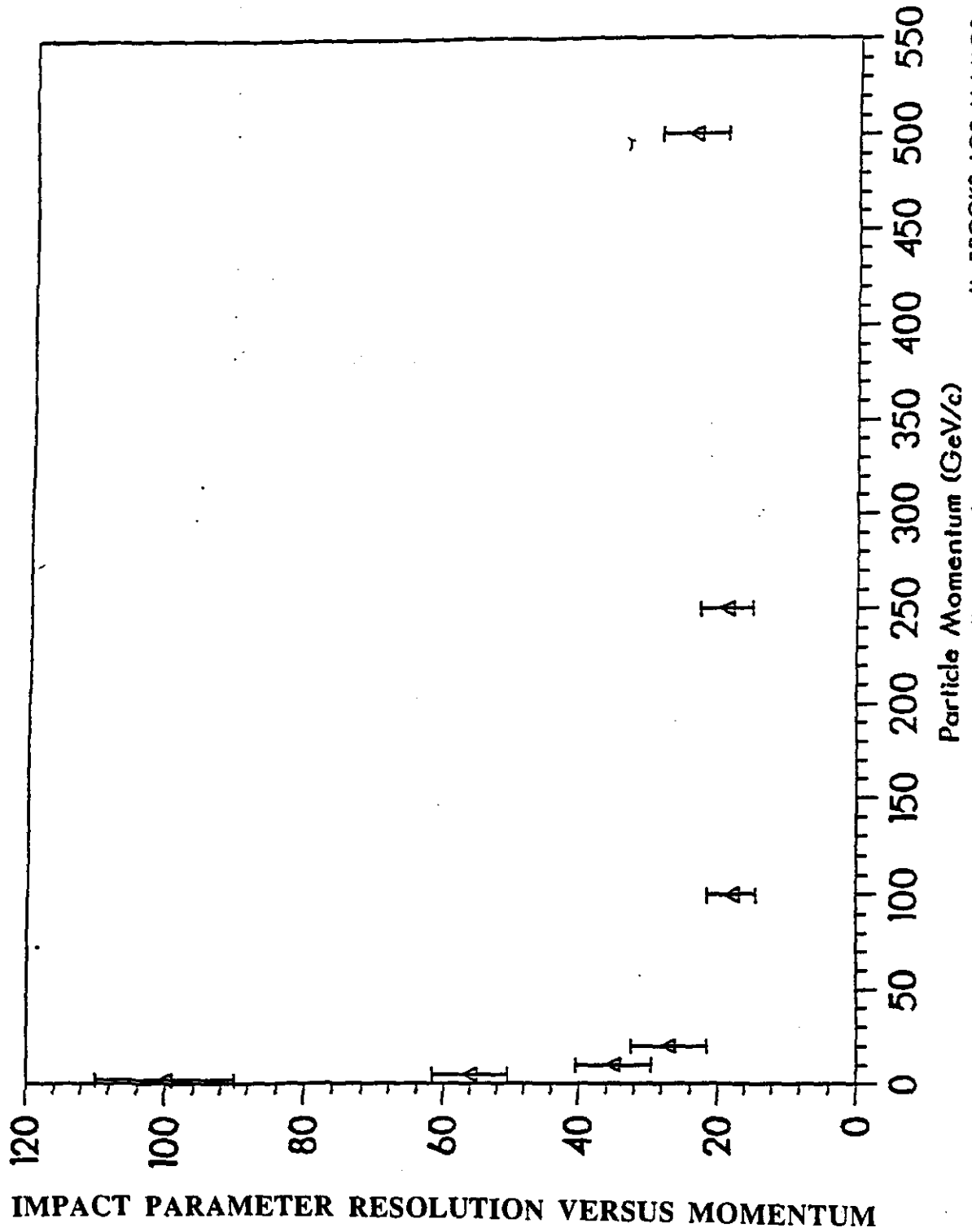
Figure 2.3b



TRANSVERSE MOMENTUM RESOLUTION VERSUS ETA
 FOR 20 GeV PARTICLES (multiple scattering limited)

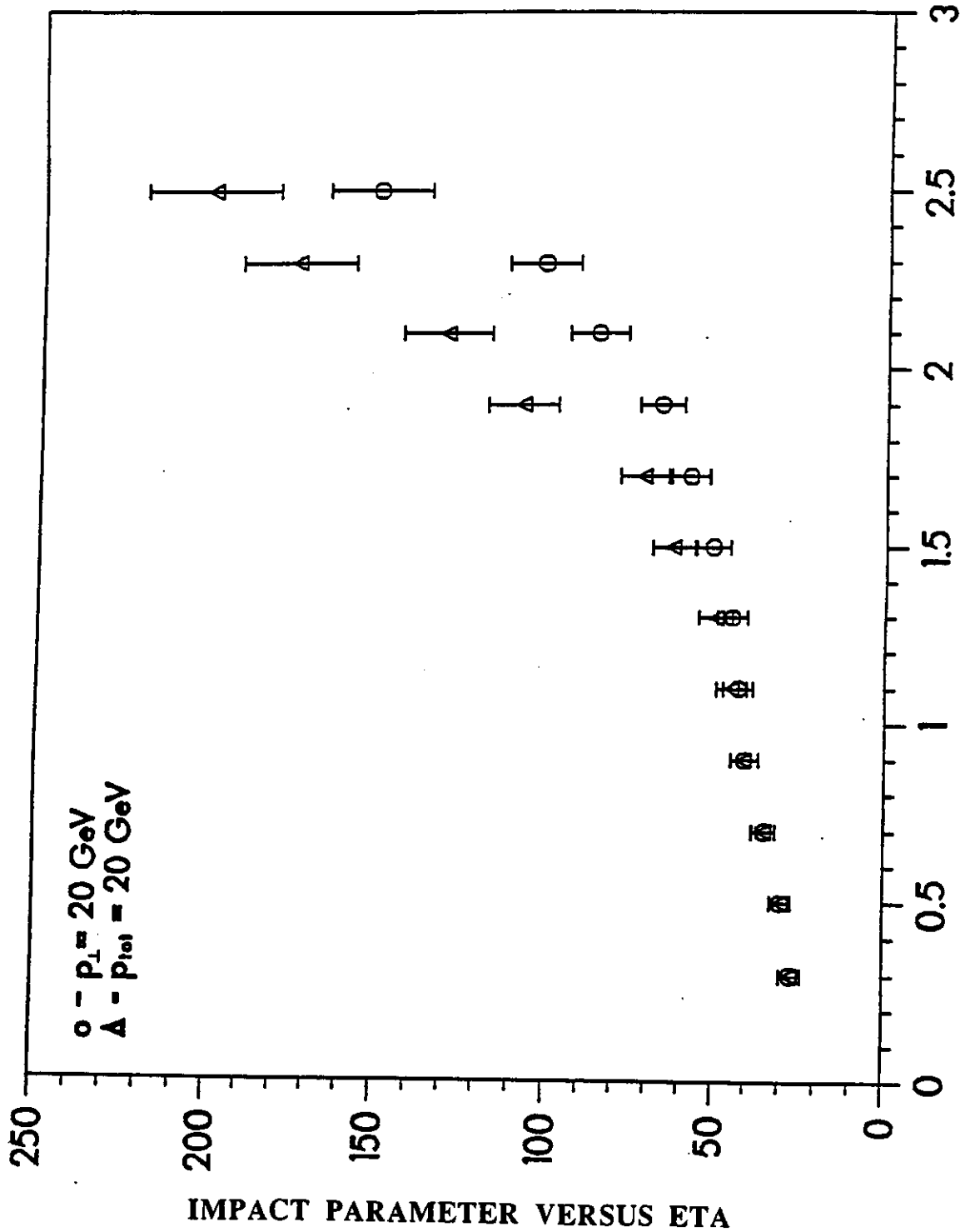
M. BROOKS, LOS ALAMOS
 ETA
 Figure 2.4

Barrel Region



M. BROOKS, LOS ALAMOS

Figure 7.3.3



M. BROOKS. LOS ALAMOS

ETA
Figure 7.3.7

CALORIMETER/TRACKER ASSEMBLY

Page 9-28

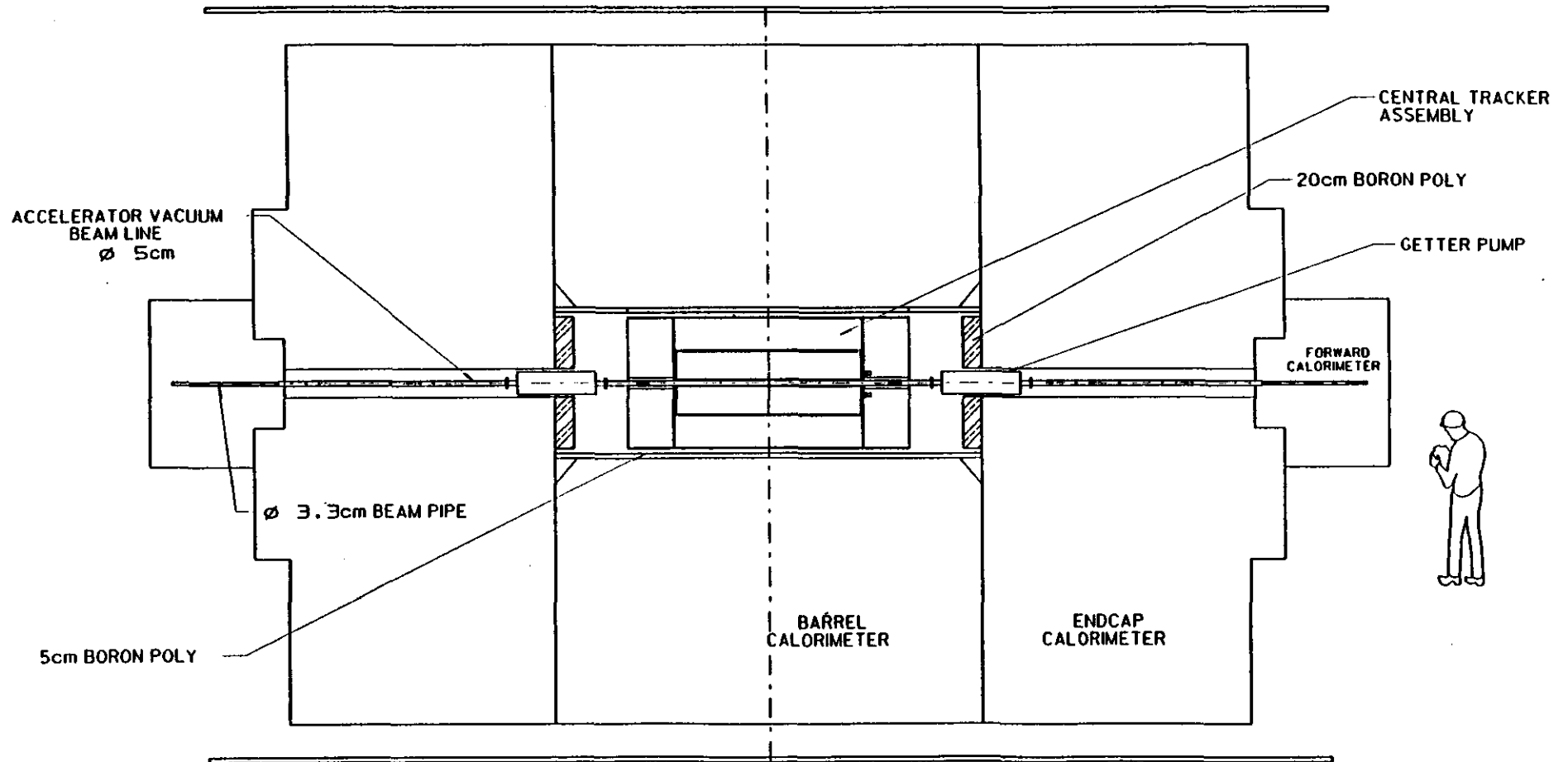


Fig. 9-17 TRACKER/CALORIMETER INTERFACE

CALORIMETER

TABLE OF CONTENTS LIQUID ARGON OPTION

OVERVIEW

Electromagnetic Calorimeter
Hadronic Calorimeter

FIGURES:

Liquid Argon Calorimeter (1/4 Elevation)
LAr Barrel Cross Section
Electrode Structure for 1 mm and 2 mm option
EM Barrel Module with Electronics and Cables
Accordion Mini-Module Barrel Section
Endcap Accordion EM
Endcap Accordion EM (isometric)
Cell Structure for Hadronic EST Cell
Hadron Module #2
Composite Shell Module Concept (Module #2)
Module Stack-up Cross Section (Module #2)
Sensing Plate (Module #2)
Absorber Plate (Module #2)
Ground Plate (Module #2)
Assembly Position (Module #2)
Absorption Length verses Eta
Liquid Argon Calorimeter 1/4 Elevation with Dimensions
Calorimeter Endviews (Barrel and Endcap)
Endcap Calorimeter Side View
Endcap Calorimeter End View
Liquid Argon Calorimeter Argon Supply System
Liquid Argon Calorimeter Nitrogen Supply System
Liquid Argon Calorimeter Electronic Feed-Through Cross Section
View with 10x Expansion in Vertical Direction
Tube Position Arrangement Detail

TABLES:

Primary Physics Goals
Secondary Physics Capabilities
Unique Physics Capabilities
Physics Performance
Physical Parameters

CALORIMETER

TABLE OF CONTENTS SCINTILLATING OPTION

OVERVIEW

Electromagnetic Calorimeter
Hadron Calorimeter
Forward Calorimeter

FIGURES:

GEM Scintillator Hadron & BaF EM Calorimeter System
GEM Detector - Barium Fluoride/Scintillating Fiber Calorimeter
End Section View at 90 Degrees
GEM Detector Barium Fluoride EM Calorimeter
Forward Calorimeter - Liquid Scintillating Option
Spaghetti FCal Layout Concept
GEM Scintillating Calorimeter Depth
Scintillating Fiber Hadron Calorimeter
End View of Tower Quarter Section
Fiber Hadron Calorimeter - Partially Assembled, Axial View
GEM Calorimeter/Central Tracker Interface
BaF/Fiber Calorimeter Option
GEM Detector Barium Fluoride Calorimeter Theta Crystals/PMT
Barium Fluoride Readout
Barium Fluoride Crystal Configuration

TABLES:

Primary Physics Goals
Barium Fluoride EM Calorimeter
Scintillating Fiber and Copper Hadron Calorimeter
Liquid Scintillator and Tungsten Forward Calorimeter
Secondary Physics Capabilities
Unique Physics Capabilities
Physics Performance
Physical Parameters
Barium Fluoride EM Calorimeter
Scintillating Fiber and Copper Hadron Calorimeter
Liquid Scintillator and Tungsten Forward Calorimeter
Quantities and Dimensions for One Side of Forward Calorimeter

CALORIMETER LIQUID ARGON OPTION

OVERVIEW

This section describes the present baseline parameters for the liquid argon calorimeter system. Liquid argon calorimetry has inherent stability and uniformity of the system over time as well as linearity enabling calibration of the system to 0.2-0.3%. Using fast shaping, time resolution of the order of nanoseconds can be obtained with signal to noise many times larger than that of minimum ionizing particles.

The calorimeter is divided into three cylindrical sections: a barrel and two endcap sections including the forward calorimeters. The total weight of the barrel section is 891 Mg and each endcap is 626 Mg, including 19 Mg for each of the forward calorimeters.

Electromagnetic Calorimeter

The goal for the electromagnetic calorimeter(EM) is to achieve an energy resolution of better than $7.5 \text{ } \%/ \sqrt{E} \oplus 0.5\%$. There are $25 X_0$ in the barrel and $28 X_0$ in the endcap since the mean energy is higher there. The absorber plates are a composite of lead, prepreg and stainless steel skins. The plate thickness is kept constant in eta, but the fraction of lead is decreased at higher eta to maintain resolution. The EM calorimeter covers the region $-3 < \eta < 3$.

Electrode Structure: The EM calorimeter will utilize the accordion design with signals collected on electrodes (which are transmission lines) and sums the signal longitudinally. In the GEM design there are 4 cells per tower and the granularity in the η, ϕ directions is 0.032×0.032 . Each tower will be segmented into two sections longitudinally: 8 and 17 X_0 at $\eta = 0$. The transverse and longitudinal segmentation allows one to get a position resolution at the face of the calorimeter of $5 \text{ mm} / \sqrt{E}$ and to be able to point back to the vertex with an angular resolution of $\sim 6 \text{ mrad}$ at 120 GeV. The small transverse segmentation will also be beneficial in improving the π^0 to γ separation using shower shape analysis. There will be $\sim 60,000$ EM channels.

We are investigating the use of krypton as the sampling medium to improve the resolution further. For the same density, one will be able to increase the sampling ratio by reducing the plate thickness and increasing both the density and volume of the sensitive material.

Source:

Update: 6/26/92

CALORIMETER LIQUID ARGON OPTION

Readout: The readout chain for the calorimeter will consist of a JFET pre-amp that will be placed inside the LAr calorimeter, and able to survive more than 200 Mrad. The shaping amplifiers will be located in standard crates on the central membrane outside the magnet coil. For the electromagnetic section we are planning to use shaping time of 40 ns. This shaping time minimizes the total contribution to the noise from both beam related pileup and thermal noise. For a typical tower at $\eta = 0$ we will get thermal noise of 20 to 30 MeV and pileup noise of 15 MeV at $10^{33}\text{cm}^{-2}\text{s}^{-1}$. The noise in the EM section does not significantly affect energy resolution and/or isolation criteria using cluster algorithms to reconstruct the energy. The output of the shaper is sampled every 16 ns and stored in dual range AMU. Each AMU should have a dynamic range of 12 bits. The AMU output is multiplexed into a 12 bit ADC.

To achieve the required dynamic range of 10^5 with the accuracy required, we are planning to use a nonlinear pre-amp that will have a linear response up to an energy of about 200 GeV and then condense the upper end of the dynamic range. Twenty-five towers (5×5) are added together for an EM trigger tower (0.16×0.16).

Hadronic Calorimeter

The requirements on the hadronic calorimeter are less stringent than the electromagnetic calorimeter but it is still a formidable challenge to achieve the needed requirements. The physics objectives are to achieve an energy resolution of $60\% / \sqrt{E} \oplus 2\%$. The total number of λ at $\eta = 0$ is 12 rising to 14 at $\eta = 3$.

EST electrode structure: In order to match the detector capacitance to that of the pre-amp, we are planning to use the "electrostatic transformer" configuration in the hadronic section, by adding layers in series. The absorber material will be copper tiles. The transformer ratio is 4.

Segmentation: The hadronic segmentation is determined by the size of the hadronic shower and the need to match up with the EM granularity. We have thus selected a granularity of 0.08×0.08 in η and ϕ . There are three longitudinal modules with the following number of absorption lengths: $\lambda_1=3.2$, $\lambda_2= 3.2$, $\lambda_3= 3.7$. The middle module is divided into two readout sections to reduce the noise. Sixteen non-overlapping towers (4

Source:
Update: 6/26/92

CALORIMETER LIQUID ARGON OPTION

× 4) will be added together for a hadron veto for each EM trigger tower. Four of these veto towers will be added together for a jet trigger tower.

Readout: The readout for the hadronic section follows the EM very closely. There will be ~27,000 channels in the hadronic section.

Forward calorimeter: The forward calorimeter will be an integral part of the LAr endcap. It will be built out of tungsten rods and tubes creating a small drift distance which is needed to minimize the positive charge buildup. The forward calorimeter will cover the region of $3 < \eta < 5.5$. The E_T resolution is expected to be 10% independent of the energy since the error will be dominated by the angular resolution. There will be a total of ~2,000 channels in both forward calorimeters.

Cryostat: The cryostat will be an aluminum alloy with a thickness $0.3 X_0$ at the entrance at $\eta = 0$. For the endcap, the total thickness will be $0.7 X_0$. The interface between the barrel and the endcap, from $1.42 \leq \eta \leq 1.64$, will have degraded EM resolution but will have useful comparable hadronic resolution.

Installation and Assembly: The hadronic granularity leads naturally to hadronic modules. In the EM section, we envision building mini-modules consisting of about 5 towers or 9° in ϕ . The full barrel will have 200 towers in ϕ . There would be 20 modules in ϕ for the hadronic modules, while the EM in the endcap would be a monolith. The 40 EM mini-modules and hadronic modules will be assembled at the SSC Lab inside the cryostat. The cryostat itself will then be welded shut. The calorimeter will be fully assembled above ground and tested before being installed in the experimental hall.

Source:
Update: 6/26/92

**CALORIMETER
LIQUID ARGON OPTION**

Revision 2.0; June 26, 1992

10.1.0 Liquid Argon Calorimeter Baseline

10.1.1.0 Primary Physics Goals

10.1.1.1 Lead/Liquid Argon EM Calorimeter (EM)

- Precision energy measurement of isolated photons or electrons.
- Precision impact coordinate measurement at the front surface of the calorimeter for isolated photons and electrons; momentum vector determination, using two longitudinal segments of the EM calorimeter.
- e/π separation using longitudinal and transverse segmentation.
- Search for narrow resonances by reconstructing the invariant mass of multi-photons or electrons.

10.1.1.2 Liquid Argon/Copper Hadron Calorimeter (HAD)

- Electron and photon identification (hadron veto).
- Muon identification, isolation, and pattern recognition.
- Muon energy loss measurement.
- Jet energy measurement.
- Missing energy measurement (using also EM and Forward calorimeters).

10.1.1.3 Forward Liquid Argon/Tungsten Calorimeter (FWD)

- Missing energy measurement (using also EM and HAD calorimeters).
- Jet tagging.

10.1.2.0 Secondary Physics Capabilities

- Provide a fast trigger for tagging the beam crossing.
- Rejection of backgrounds with isolation cuts at the trigger level.

Source: H Gordon
Updated: 6/26/92

CALORIMETER LIQUID ARGON OPTION

10.1.3.0 Unique Physics Capabilities

- Higgs searches:
 - $H^0 \rightarrow \gamma\gamma$
 - $t\bar{t} H^0 / WH^0 \rightarrow \gamma\gamma$
 - $H^0 \rightarrow e^+e^-e^+e^-$ (including ZZ*).
- Z' searches: $Z' \rightarrow e^+e^-$.
- Search for unknown narrow resonances which decay to multi-photons and/or electrons.
- Jet energy measurements up to the highest energies.
- Missing energy at the 100 GeV level.

10.1.4.0 Physics Performance

Time resolution

$$E_{EM} \geq 20 \text{ GeV}, \Delta t \leq 1 \text{ ns}$$

$$E_{jet} \geq 50 \text{ GeV}, \Delta t \leq 3 \text{ ns}$$

Speed shaping time

EM	40	ns
HAD	50-200	ns
FWD	16	ns

Noise (thermal/pileup)

EM	20/32 MeV/channel
HAD	130/118 MeV/channel

Hermeticity (E_t Measured)

$$0 < \eta < 5.5$$

EM energy resolution

$$7.5\% / \sqrt{E} \oplus 0.5\%$$

EM position resolution

$$4.4\text{mm} / \sqrt{E}$$

EM dynamic range

$$-10^5 \text{ (up to 10 TeV/tower)}$$

Hadron energy resolution (Jets)

$$60\% / \sqrt{E} \oplus 2\%$$

Hadron dynamic range

$$10^5 - 50 \text{ MeV to } 5 \text{ TeV}$$

Source: H Gordon
Updated: 6/26/92

CALORIMETER LIQUID ARGON OPTION

Number of absorption lengths	
at $\eta = 0$	12
at $\eta = 3.0$	14.0
Barrel Dimensions	
inner radius	0.76 m
outer radius	3.60 m
Lateral segmentation ()	
EM	0.032 x 0.032
HAD	0.08 x 0.08
Longitudinal segmentation	2 EM, 4 HAD

10.1.5.0 Physical Parameters

10.1.5.1 Lead Liquid Argon/EM Calorimeter

Absorber material	0.2mm SS/0.1mm prepreg/1.3mm Pb 0.1mm prepreg/0.2mm SS
Readout Board Sense Material	0.4mm (kapton/Cu/kapton) 2 x 2 mm argon
Lateral segmentation (η, ϕ)	0.032 x 0.032
Longitudinal segmentation	2(8 X ₀ , 17 X ₀)
Inner Radius (cryostat/accordion)	760/890 mm
Outer Radius (accordion)	1412 mm
Radiation Length	25 X ₀ at $\eta = 0$; 28 X ₀ at $\eta = 3$
Absorption Length	1.3 λ
Number of Channels-Total	62,000
Readout Device	JFET preamplifier (75 mW / channel)
Weight of Barrel	59 Mg
Weight of Each End Cap	19 Mg

Source: H Gordon
Updated: 6/26/92

CALORIMETER LIQUID ARGON OPTION

10.1.5.2 Liquid Argon/Copper Hadron Calorimeter

Lateral segmentation (η, ϕ)	0.08 x 0.08	
Longitudinal segmentation	4	
Dimensions		
Inner Radius (active)	1,489	mm
Outer Radius (active)	3,445	mm
Length (excluding forward)	11,000	mm
Copper Absorber Thickness	9/16	mm
Sense Material: Argon	2	mm
G10 Thickness	2 x 0.5	mm
Readout Channels - total hadron	20,000	
Assemblies (including EM and vessel)	3	each
Barrel Weight	891	Mg
End Cap Weight (each)	626	Mg
Forward (each)	19	Mg
Total	2,142	Mg
Liquid Volume		
Barrel	40,000	liters
End cap (each)	27,000	liters
Reserve in head vessel	3,600	liters
Reserve	6,000	liters
Total	104,000	liters
Total number of channels	87,000	

10.1.5.3 Liquid Argon Forward Calorimeter

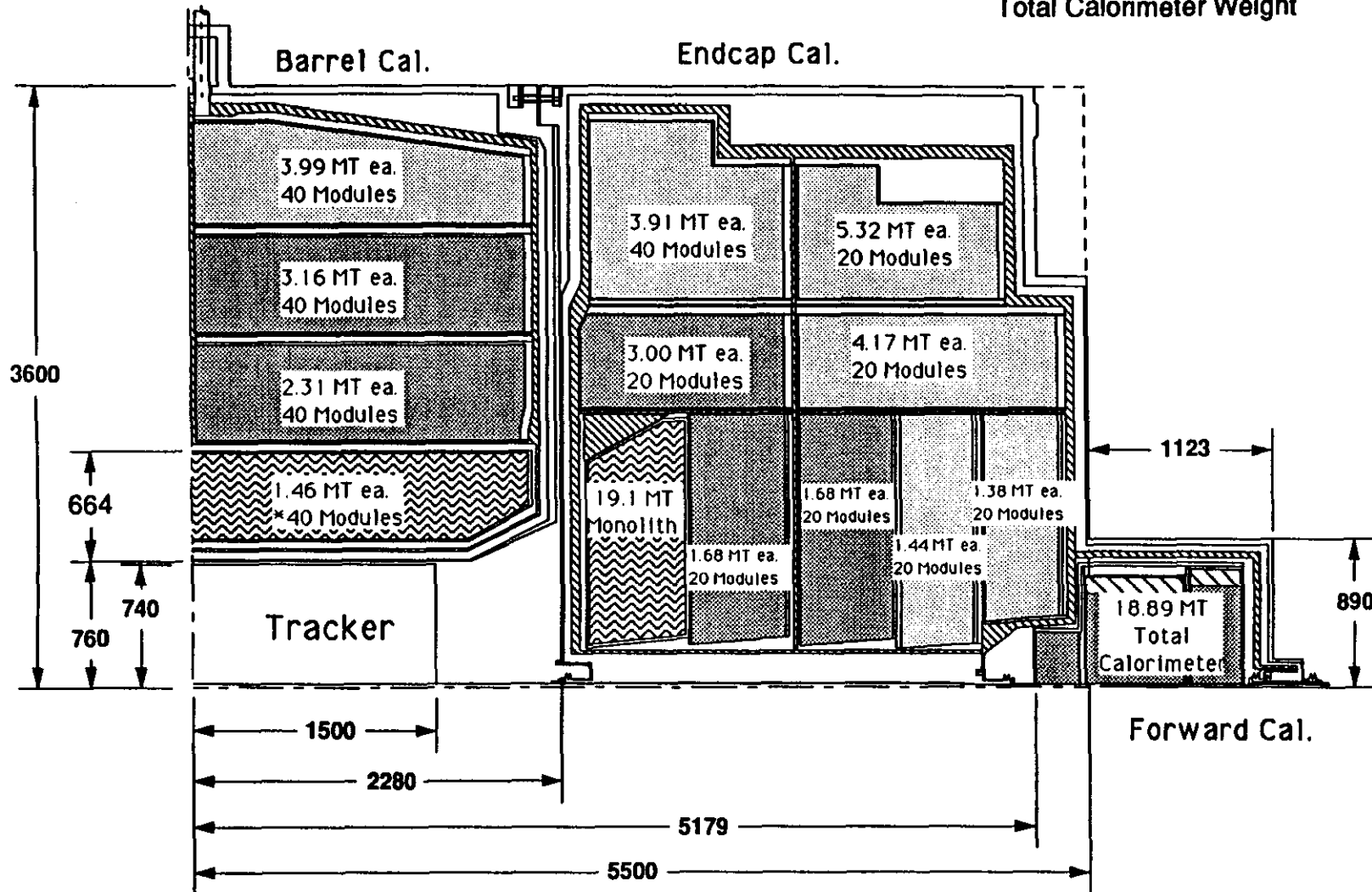
Distance from IP to near face	5,090	mm
Total Weight (per side)	28.1	Mg
Channels (per side)	1,070	
Active Absorption Length	10	λ
Dimensions		
Inner Radius	20	mm
Outer Radius	865	mm
Depth in Z	1120	mm
Integration Time		
EM Module	20	ns
Hadron/Tail Catcher	60	ns

Source: H Gordon
Updated: 6/26/92

LIQUID ARGON CALORIMETER - 12 X 14 LAMBDA, FLAT ENDCAP HEAD

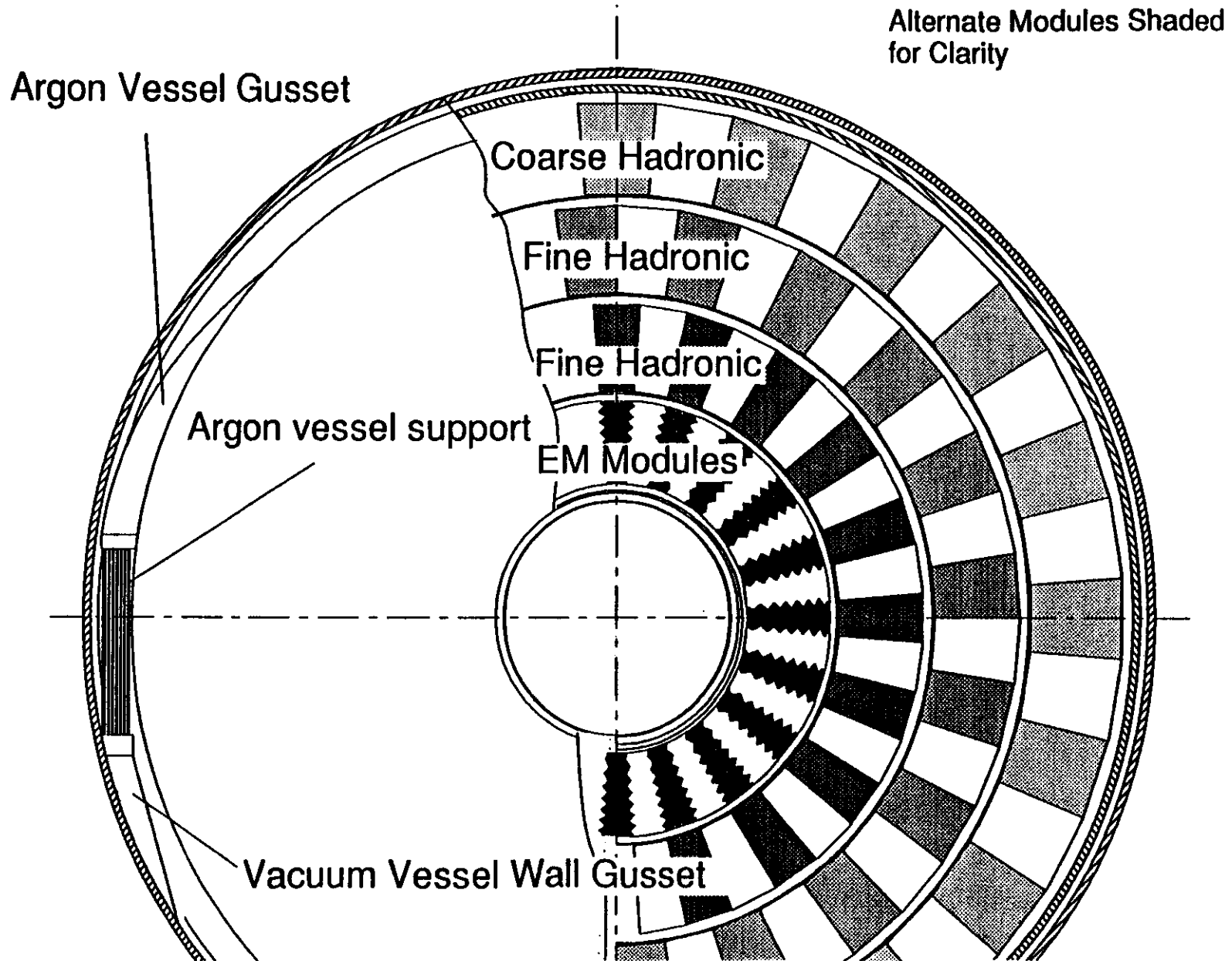
Central Barrel Calorimeter Weight	891 MT
Endcap Calorimeter Weight Each	626 MT
Total Calorimeter Weight	2,143 MT

Page 10-8



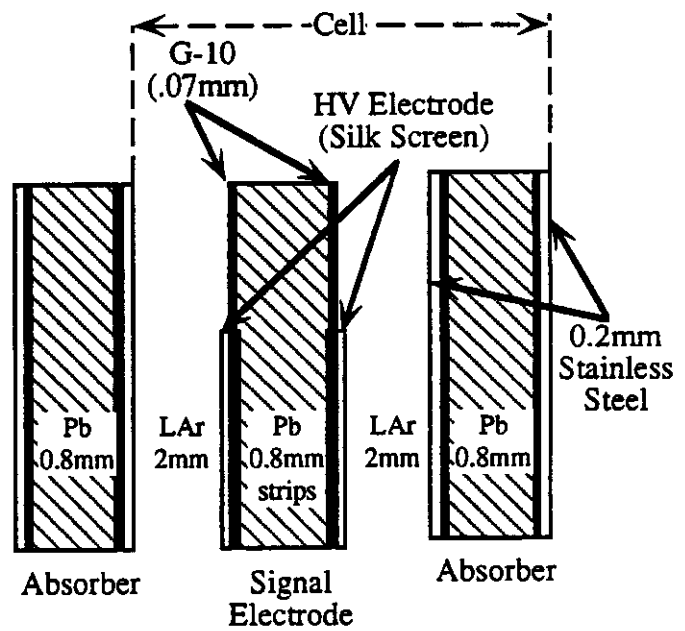
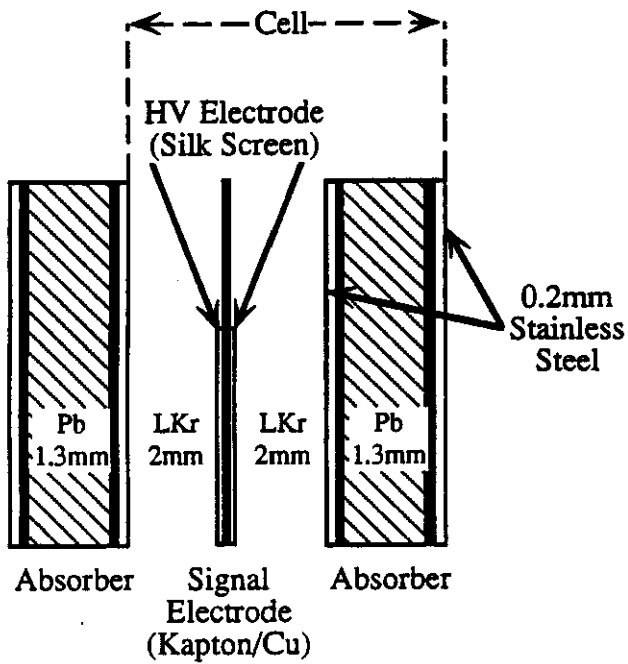
Dimensions in millimeters
 Module count is the number of modules
 in phi direction.
 * Half length of module shown

Barrel Cross-Section (looking down beam line)



2mm Option
 Rs = 21.1%
 Cell = 6.1mm

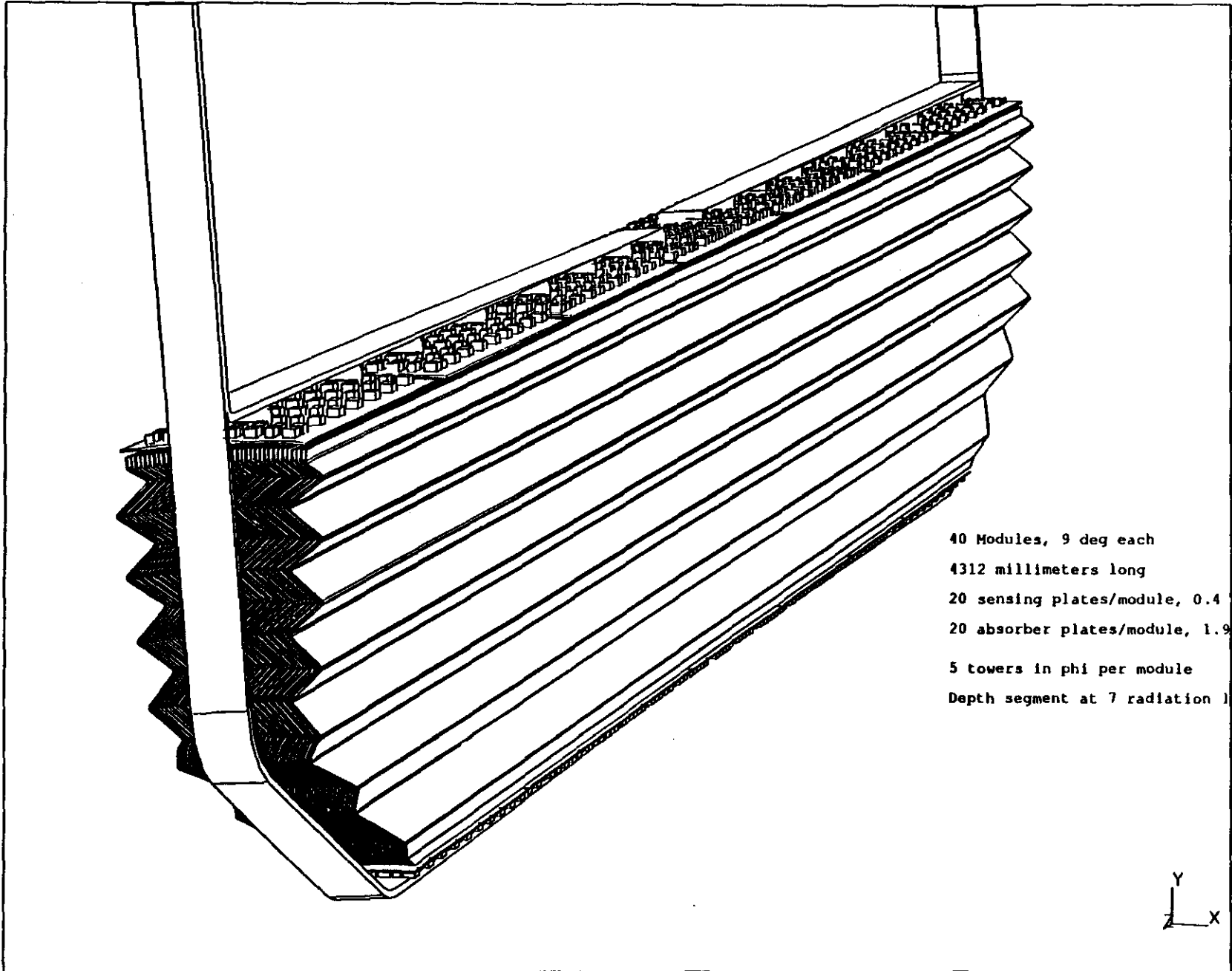
1mm Option
 Rs = 21.1%
 Cell = 6.1mm



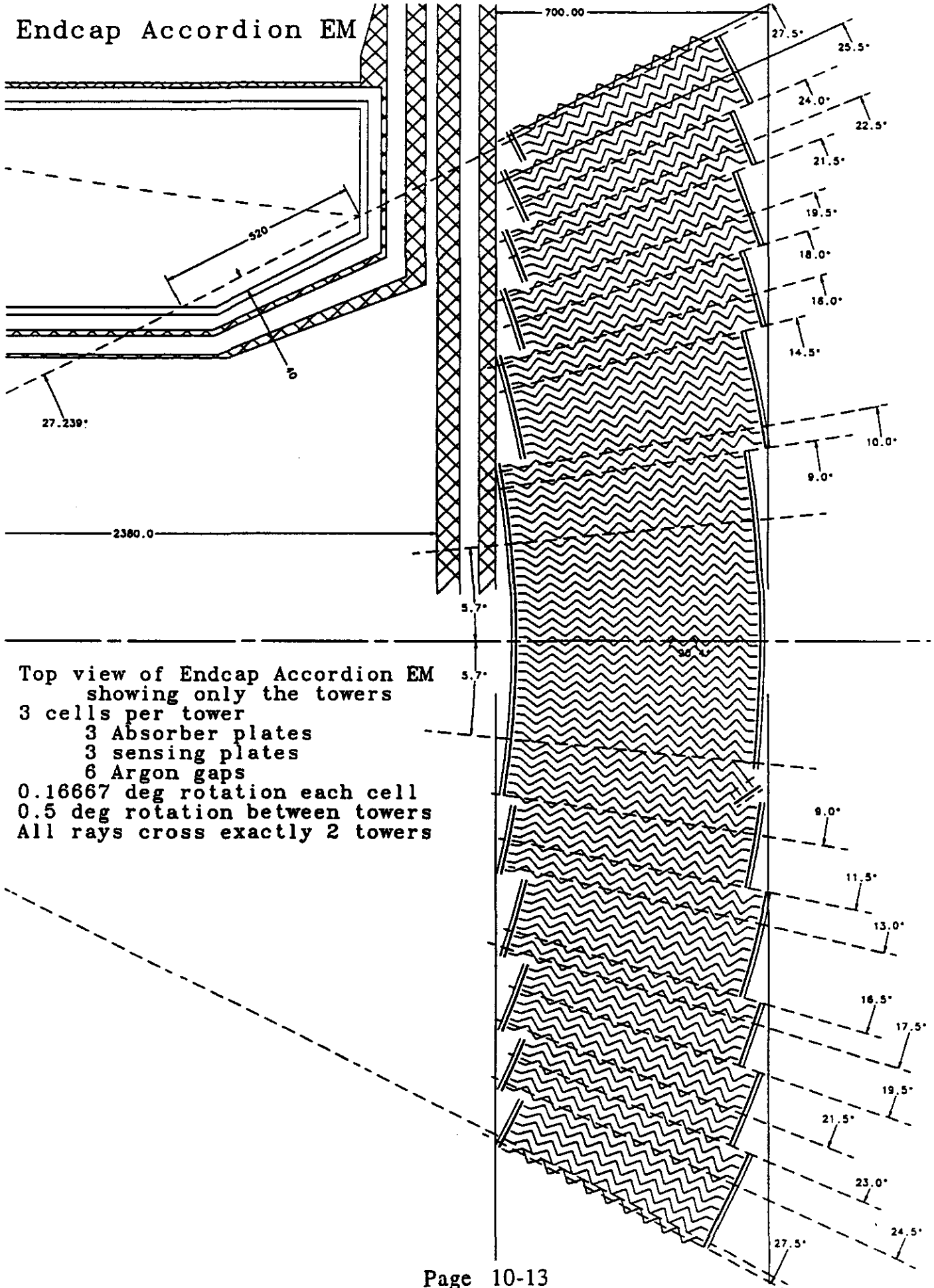
Electrode Structure for 1mm and 2mm Option

EM BARREL MODULE with Electronics and Cables

Page 10-11

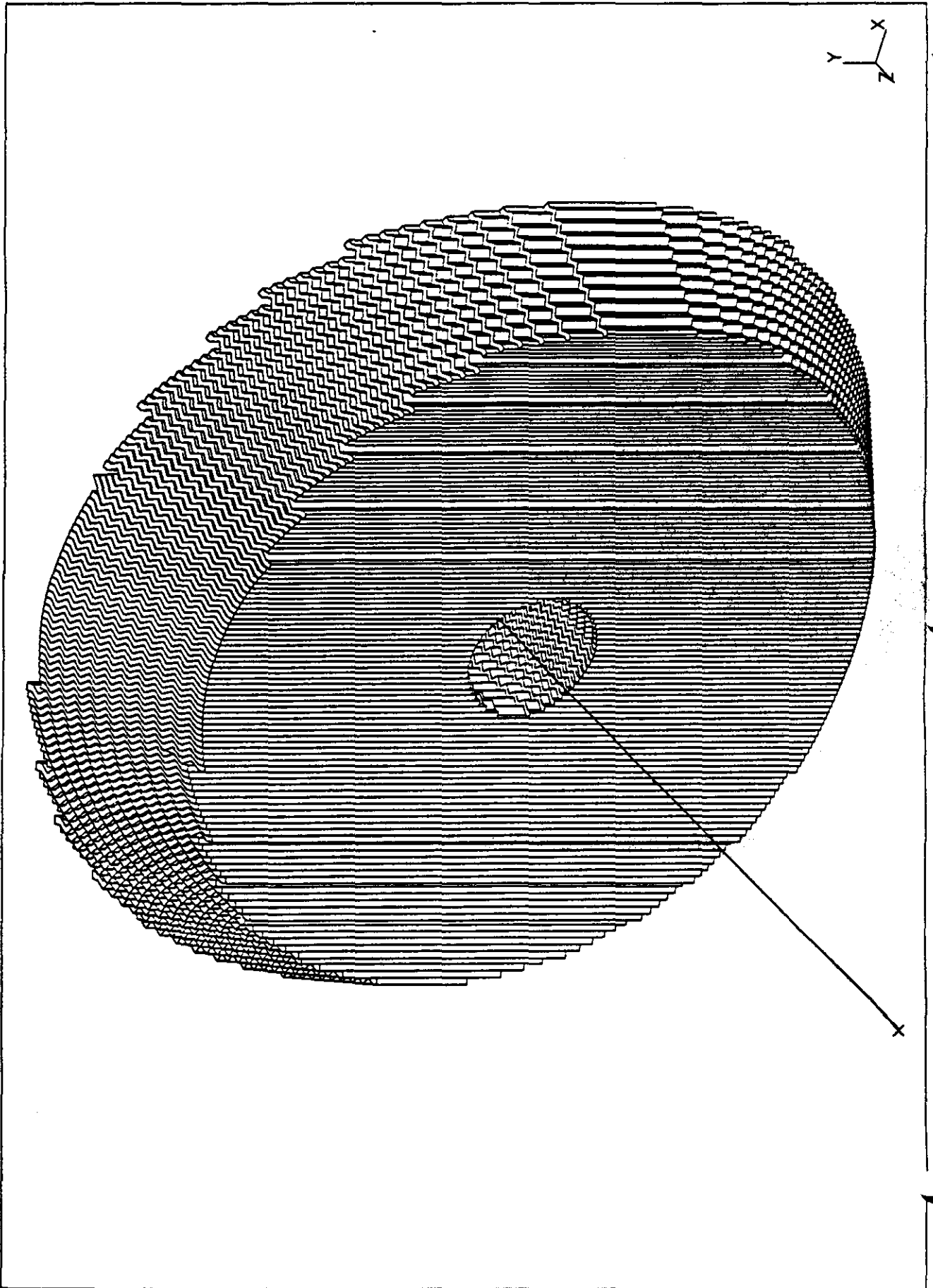


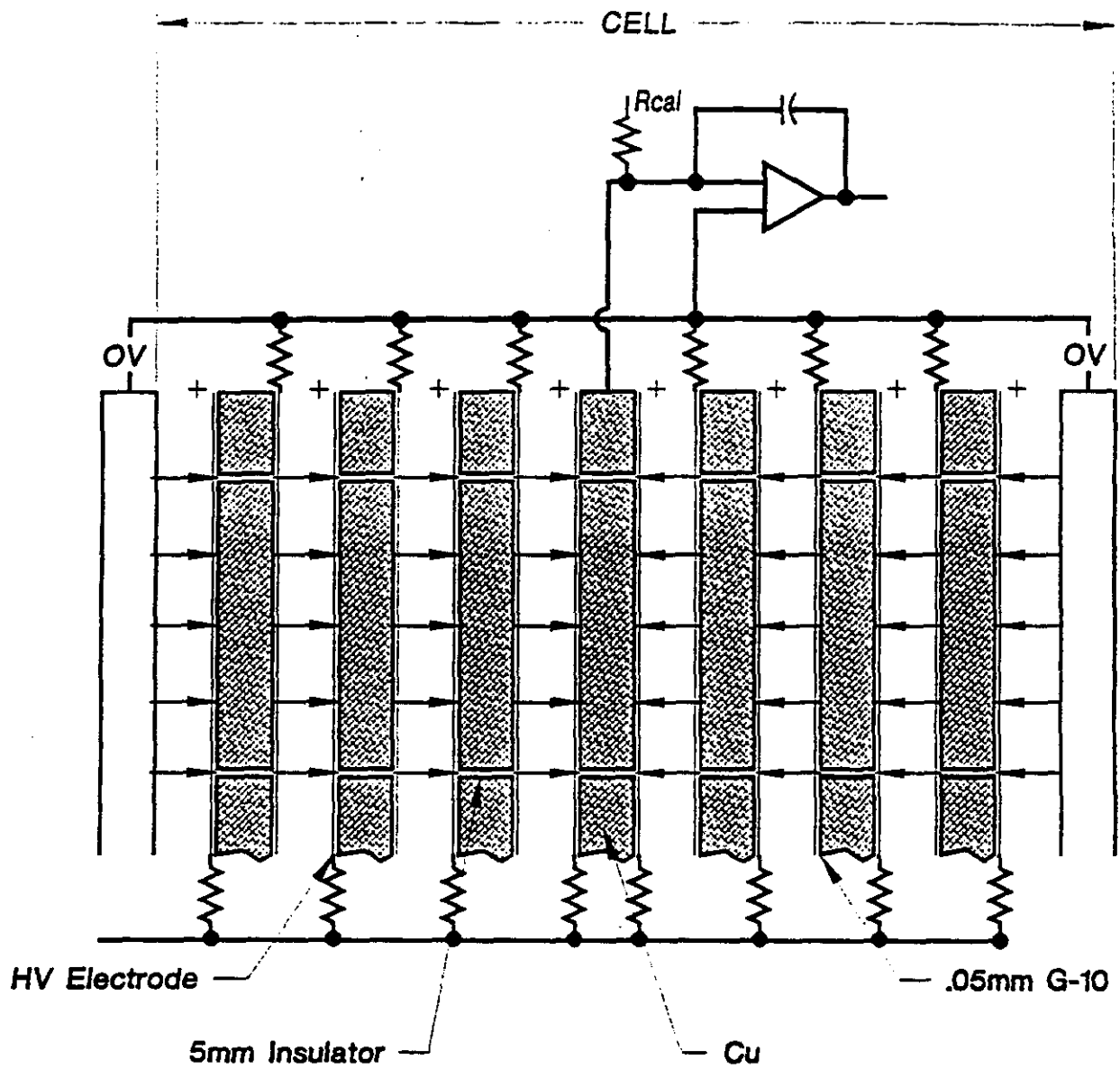
Endcap Accordion EM



Top view of Endcap Accordion EM
 showing only the towers
 3 cells per tower
 3 Absorber plates
 3 sensing plates
 6 Argon gaps
 0.16667 deg rotation each cell
 0.5 deg rotation between towers
 All rays cross exactly 2 towers

Endcap Accordion EM

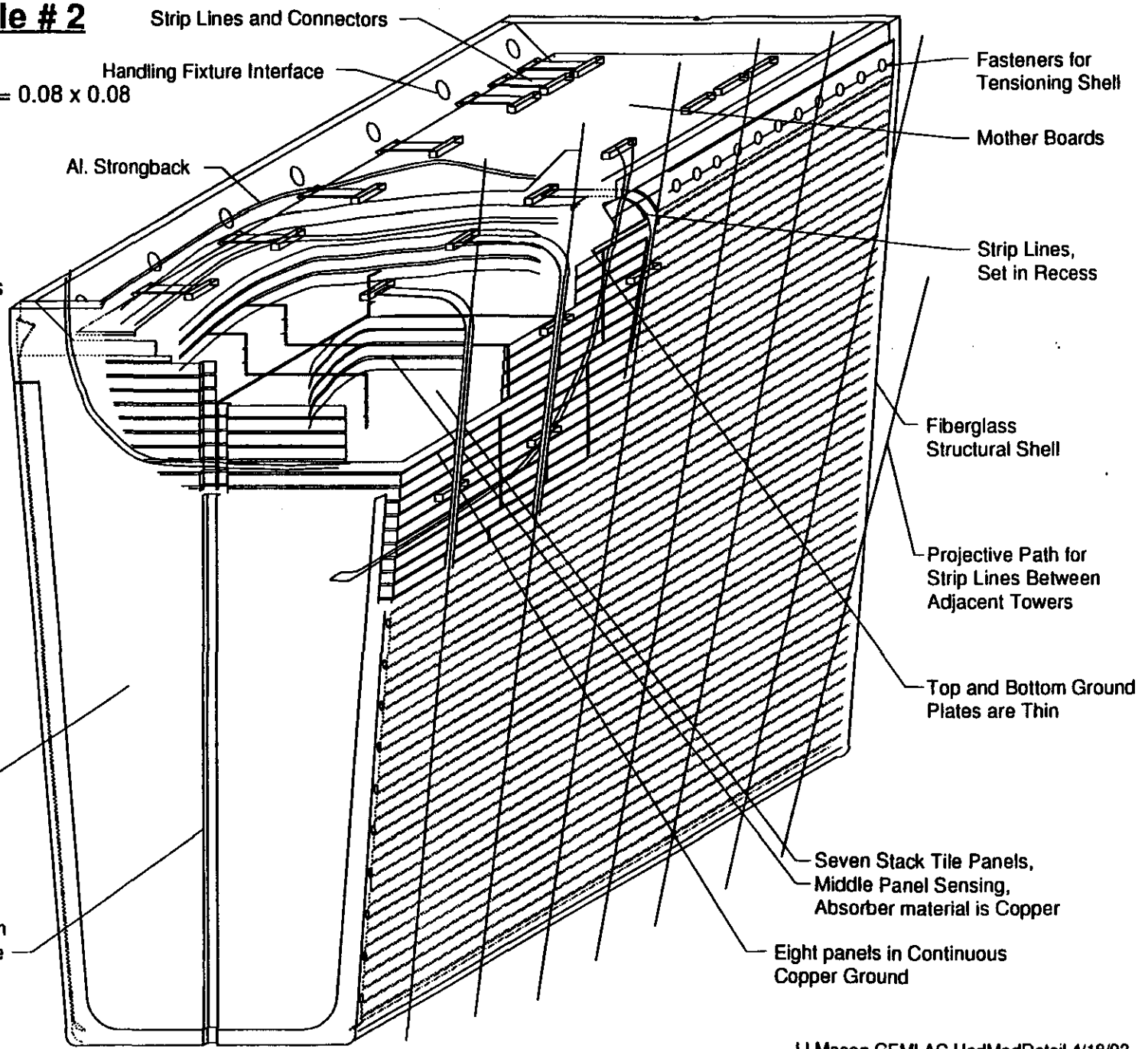




Cell Structure for Hadronic EST Cell

Hadron Module # 2

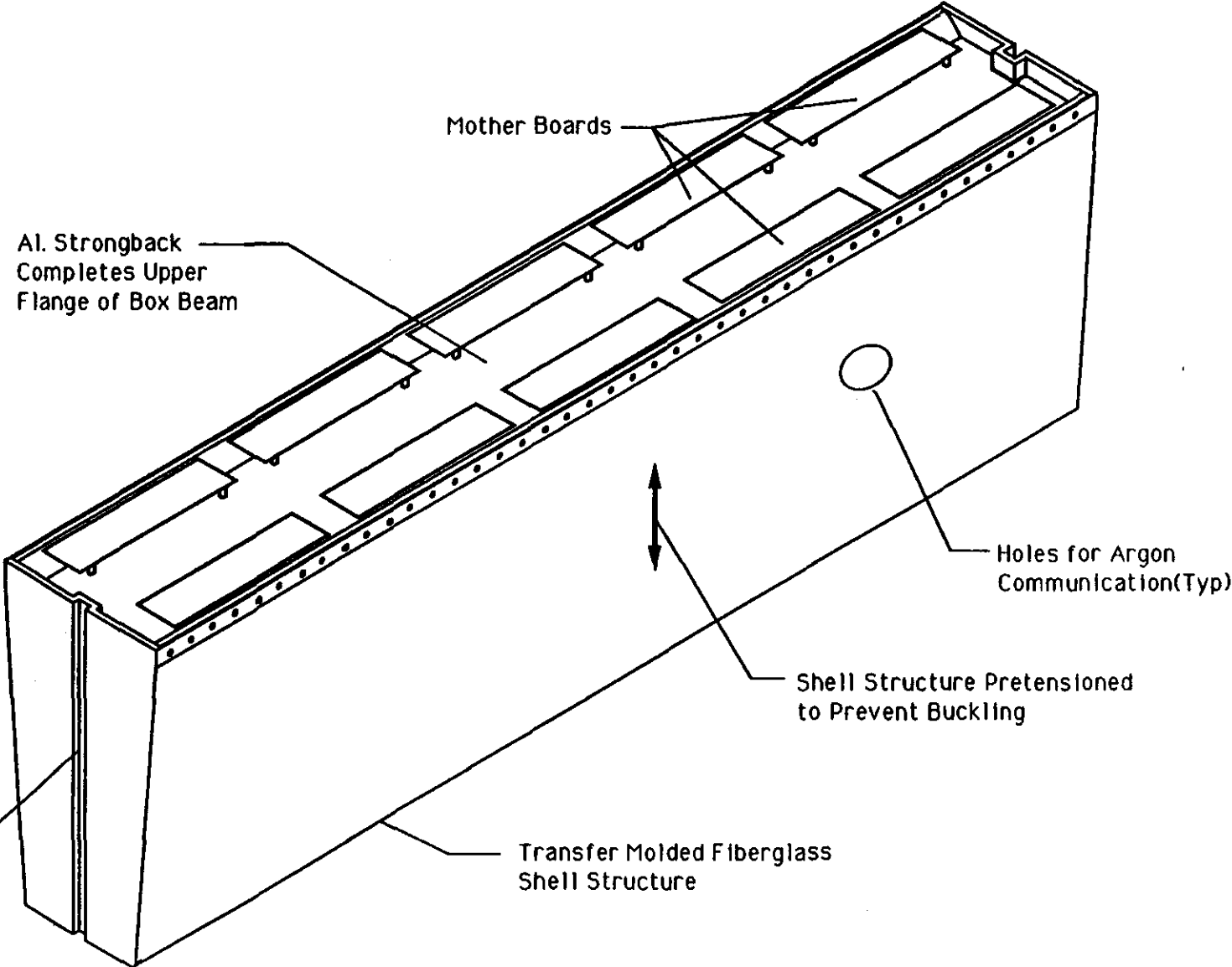
- Six Cells Depth
- Segmentation $\Delta\eta \times \Delta\phi = 0.08 \times 0.08$
- 80 Modules Required
- Wt. = 2.38 MT each
- Each Module Contains the Following:
- 1 - Top Ground Plate
- 1 - Bottom Gnd Plate
- 5 - Included Gnd Plates
- 36 - Tile Plates
Containing 948 Tile
- 6 - Sensing Plates
Containing 258 Tile
- 1 - Strongback
- 1 - Structural Shell
- 2 - End Plates
- 28 - Towers with Strip Lines and Electronics
- X - Mother Boards



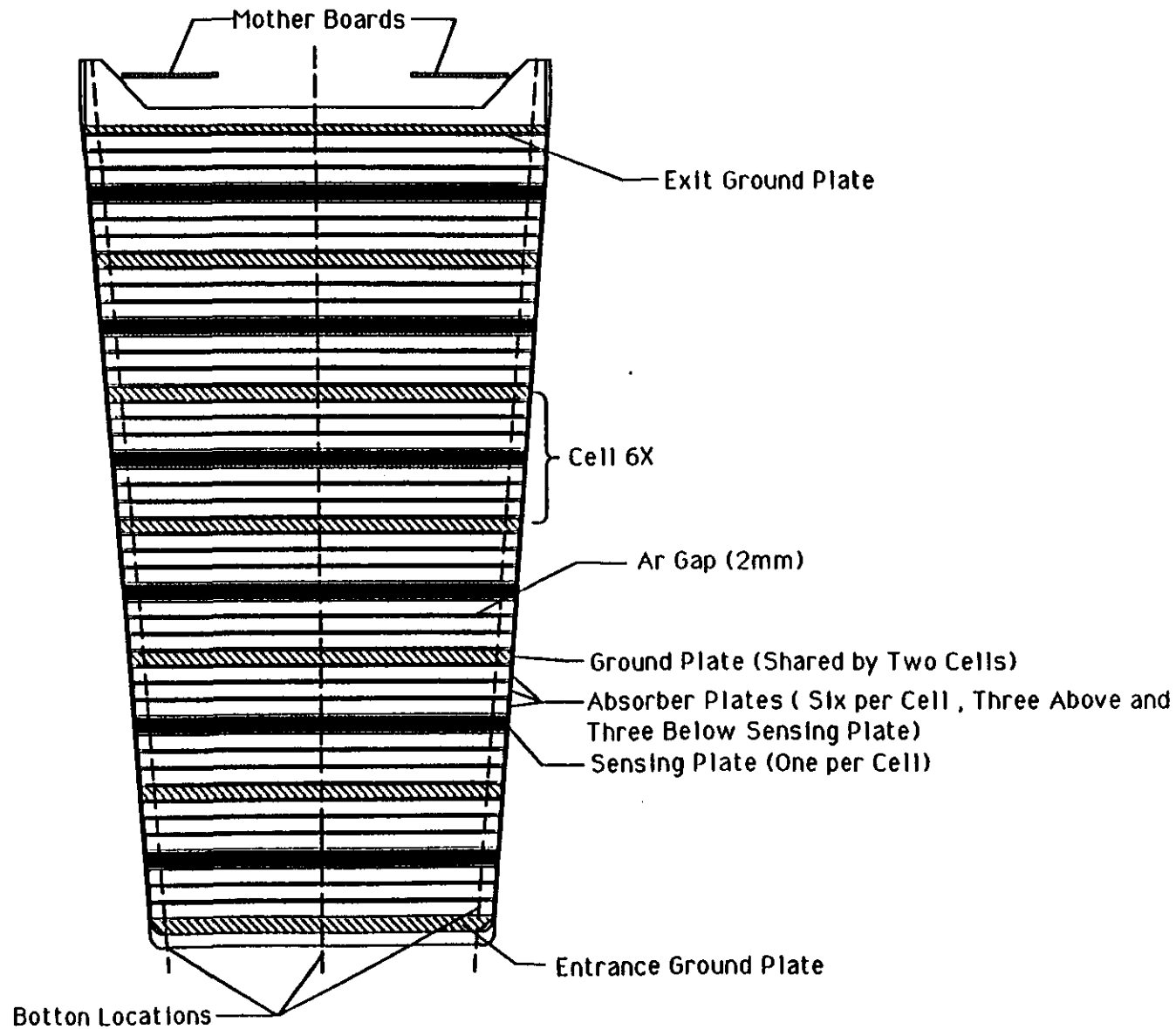
Page 10-16

COMPOSITE SHELL MODULE CONCEPT (Module #2)

9 degree Included Angle
2106 mm Length
570 mm Depth
2.38 MT
80 required

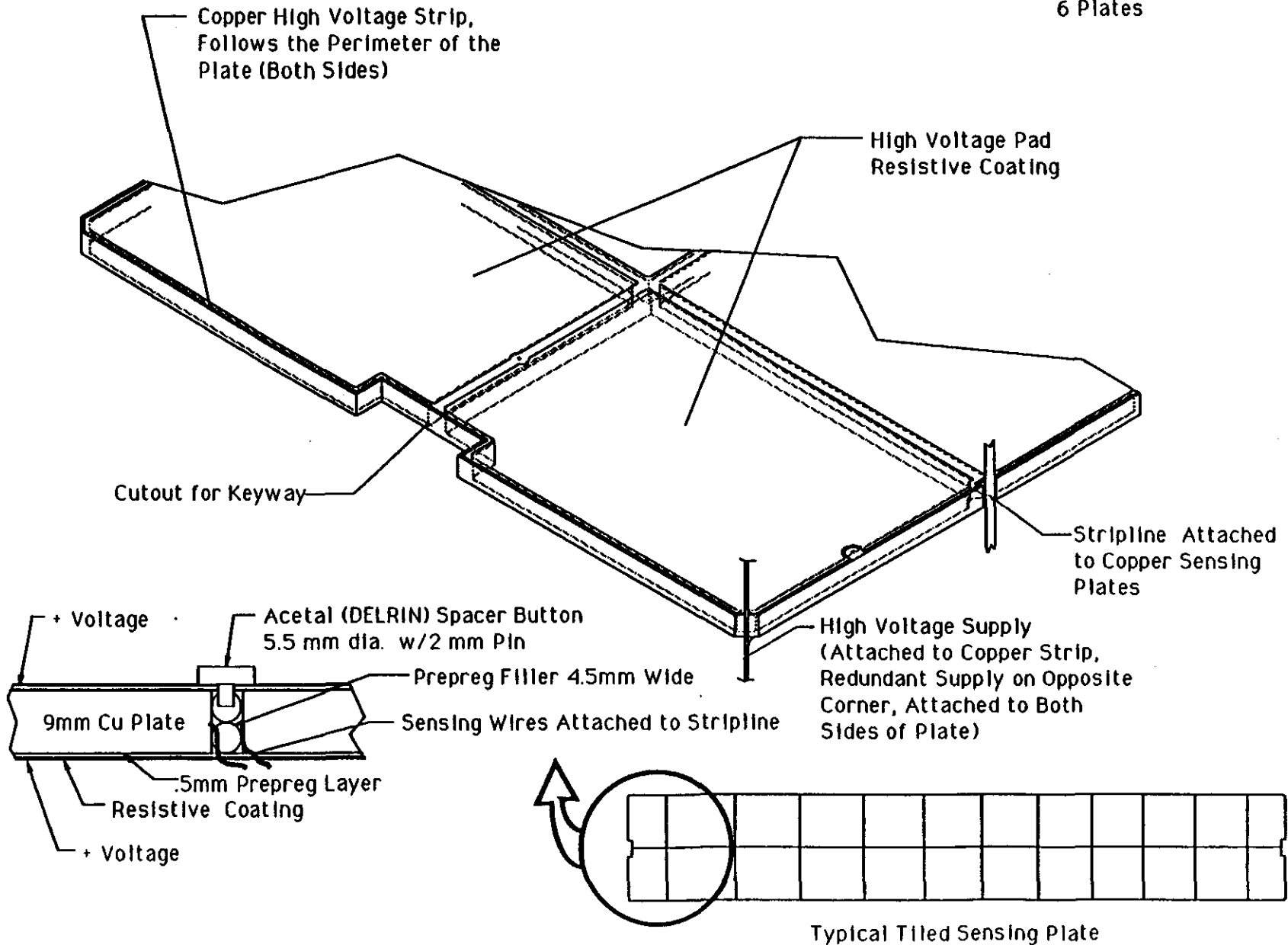


MODULE STACKUP CROSSSECTION (Module #2)



SENSING PLATE (Module #2)

6 Cell Depths
 6 Resistive Coating Template:
 6 Plates

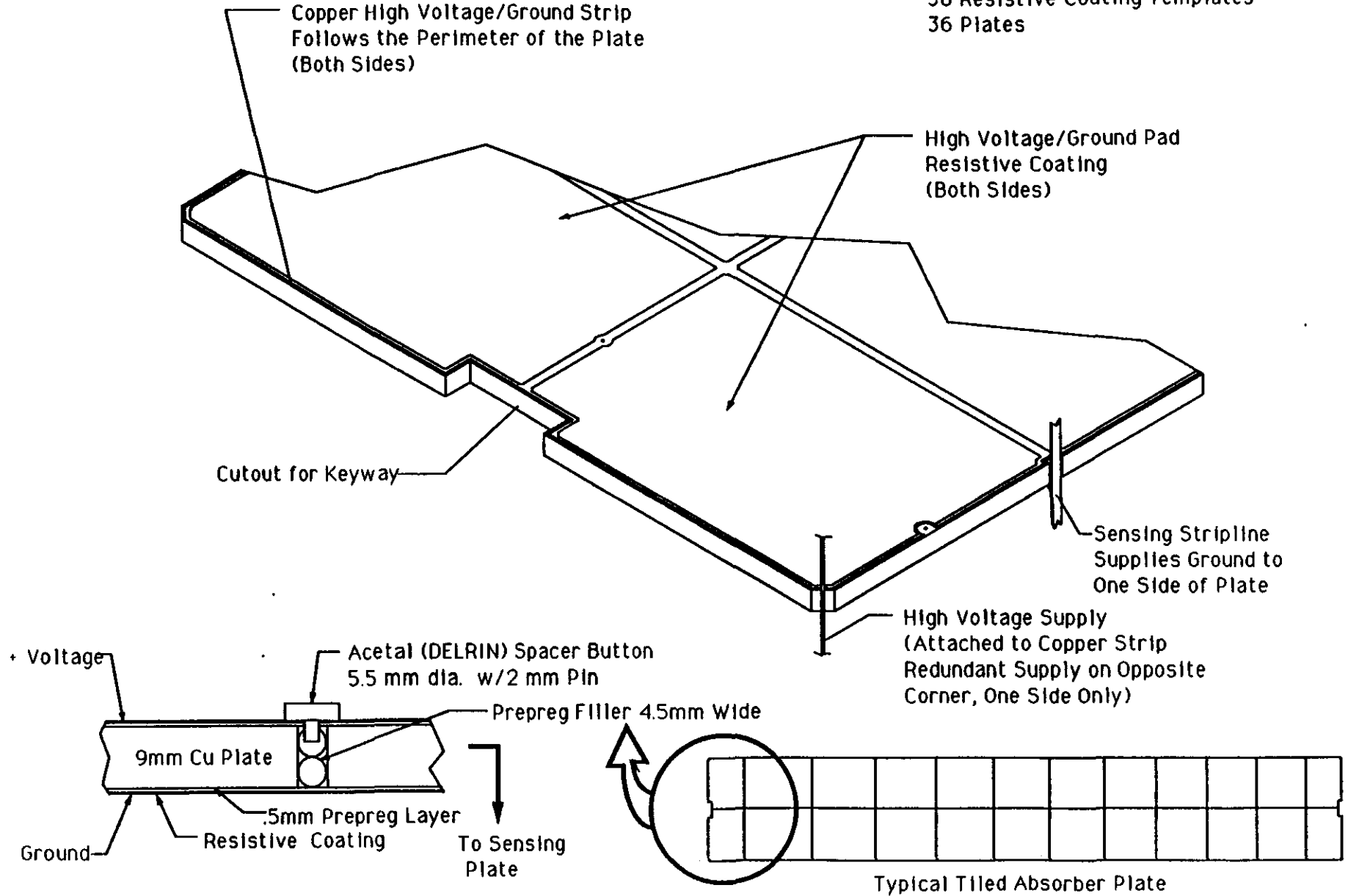


Page 10-19

ABSORBER PLATE (Module #2)

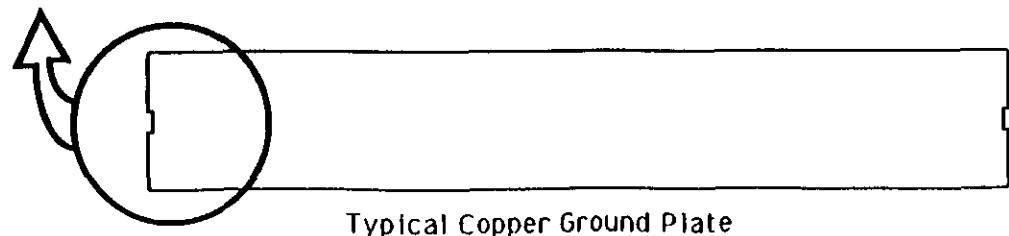
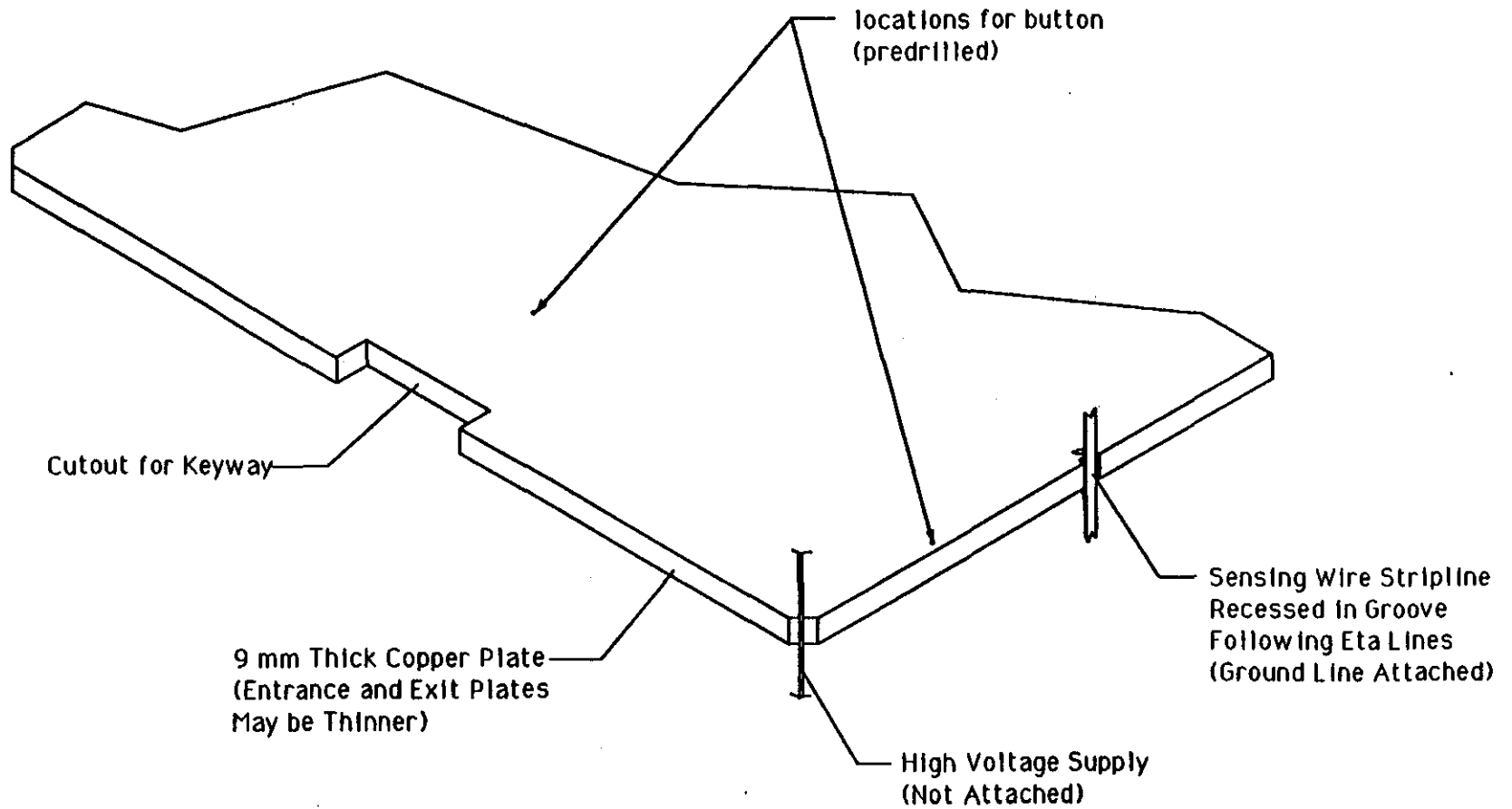
Page 10-20

6 Cell Depths
 36 Resistive Coating Templates
 36 Plates



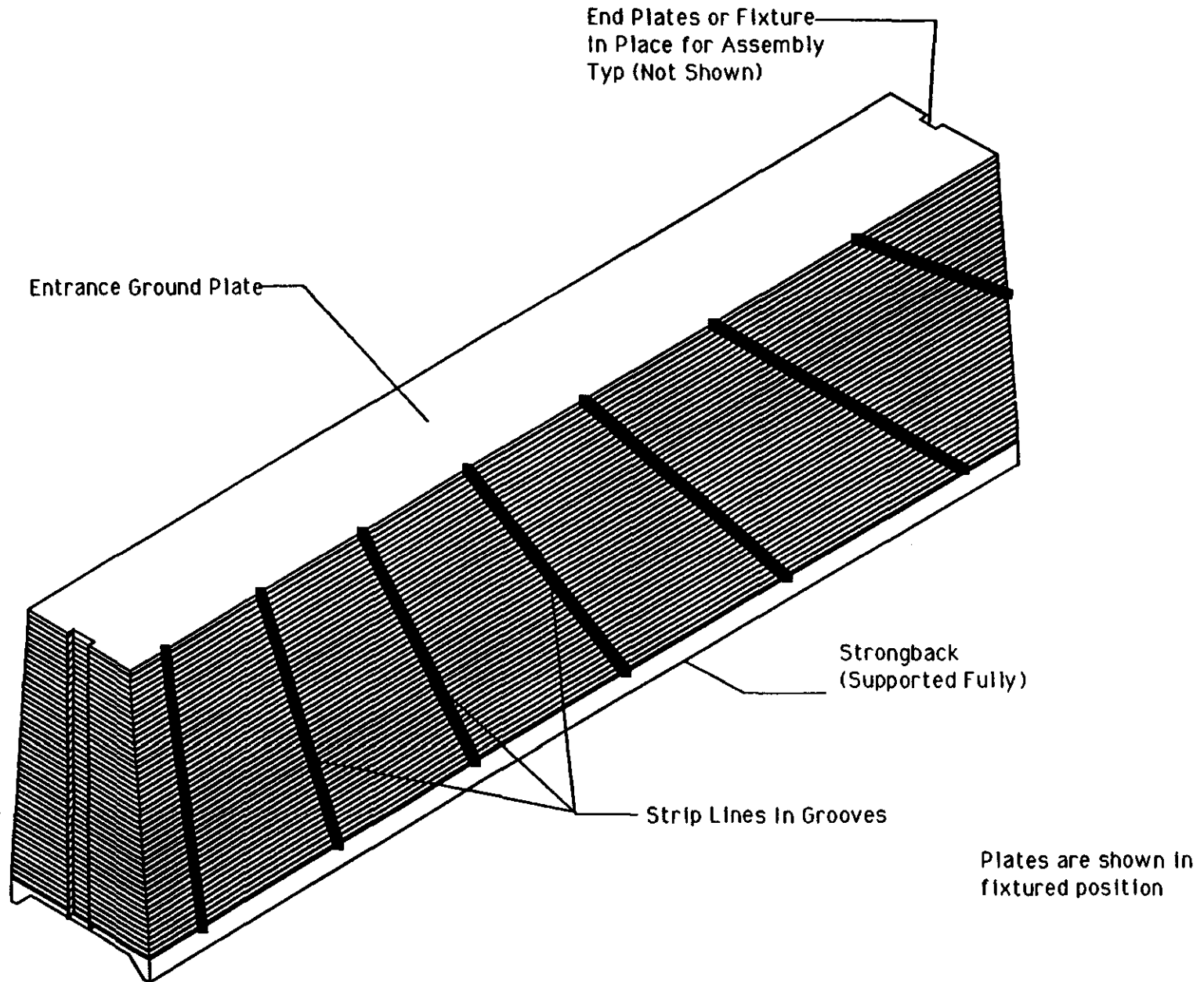
GROUND PLATE (Module #2)

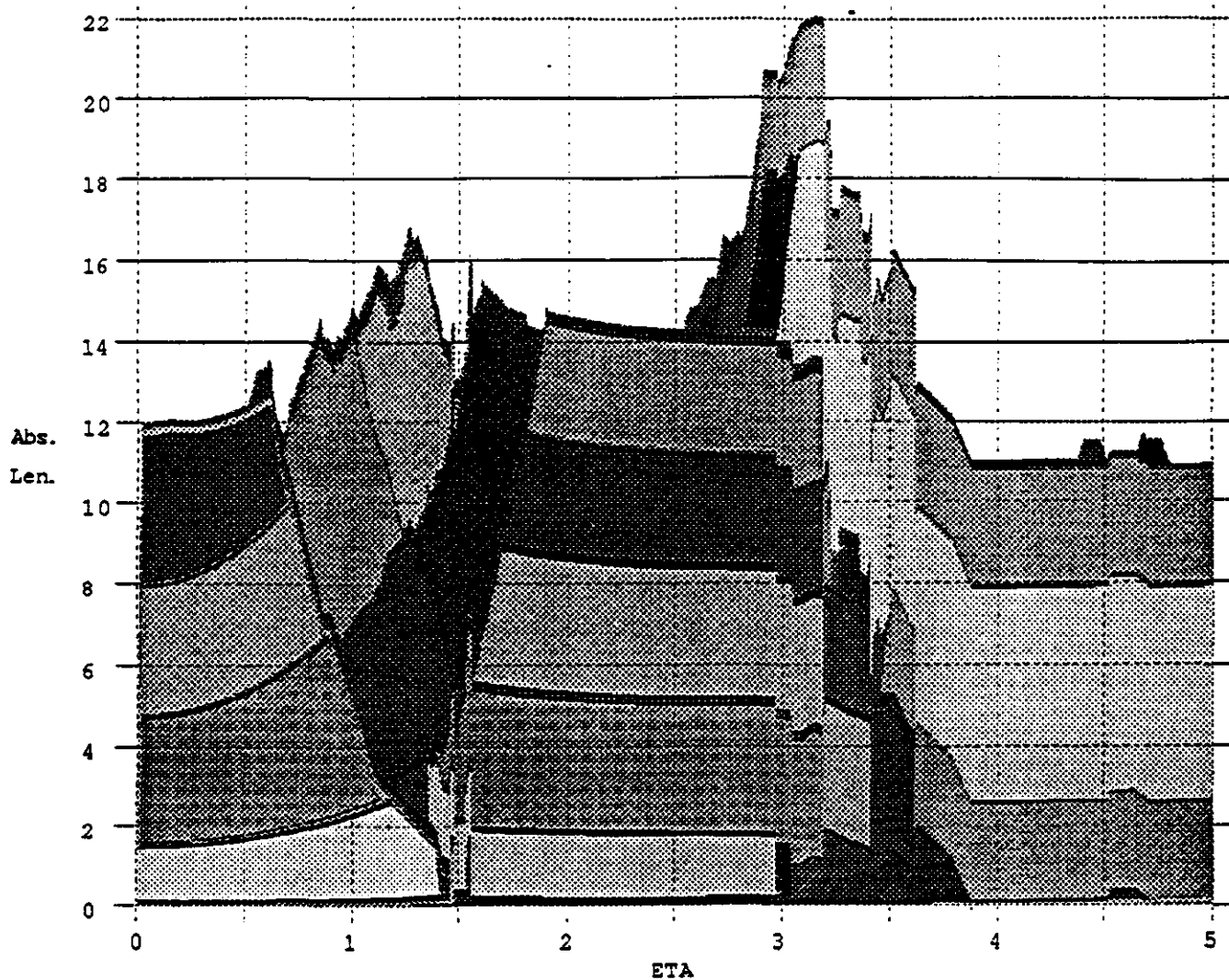
- 5 Plates
- 1 Entrance Plate
- 1 Exit Plate



Typical Copper Ground Plate

ASSEMBLY POSITION (Module #2)

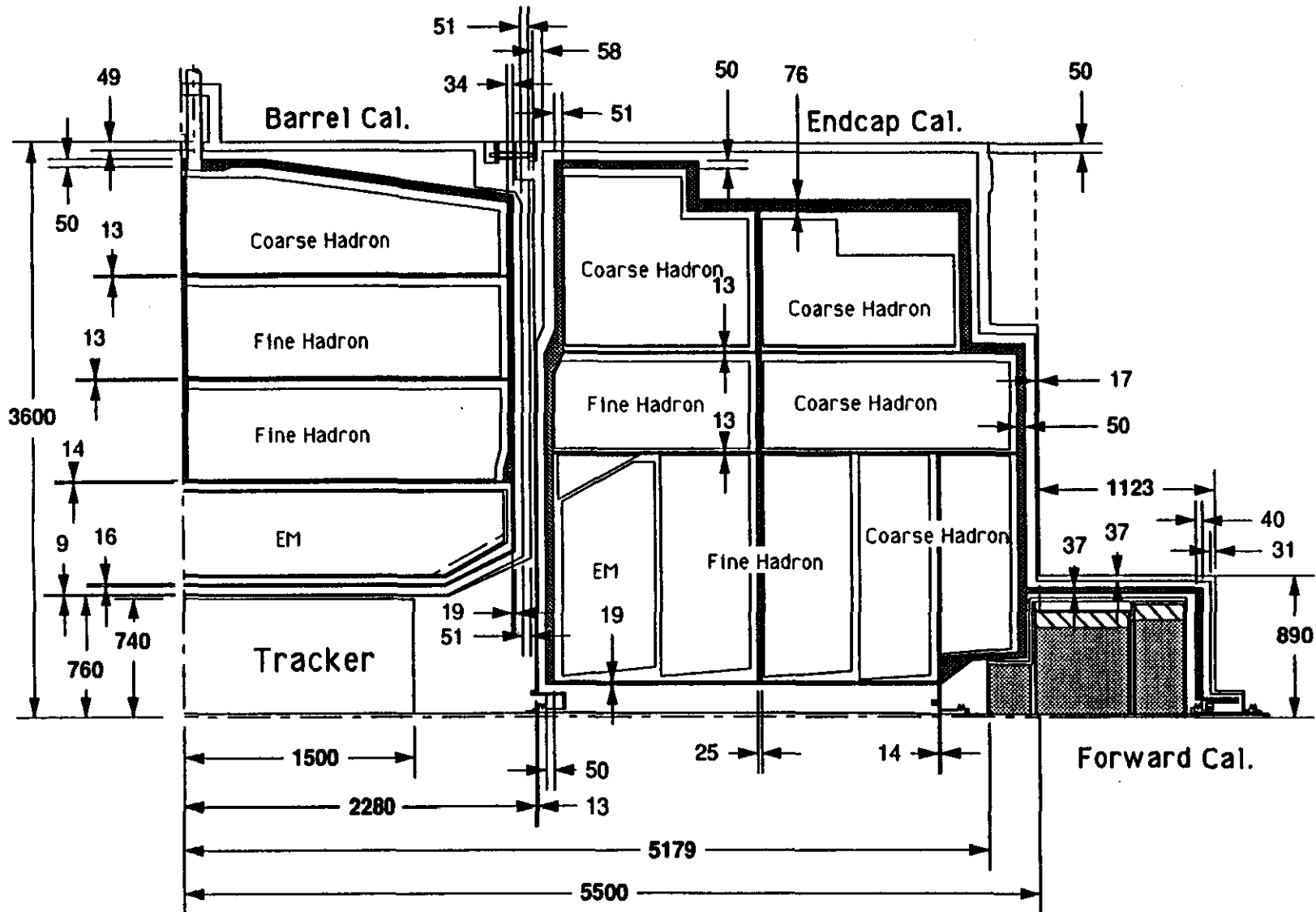




ABSORPTION LENGTH vs ETA
Showing Contribution of Each System Element

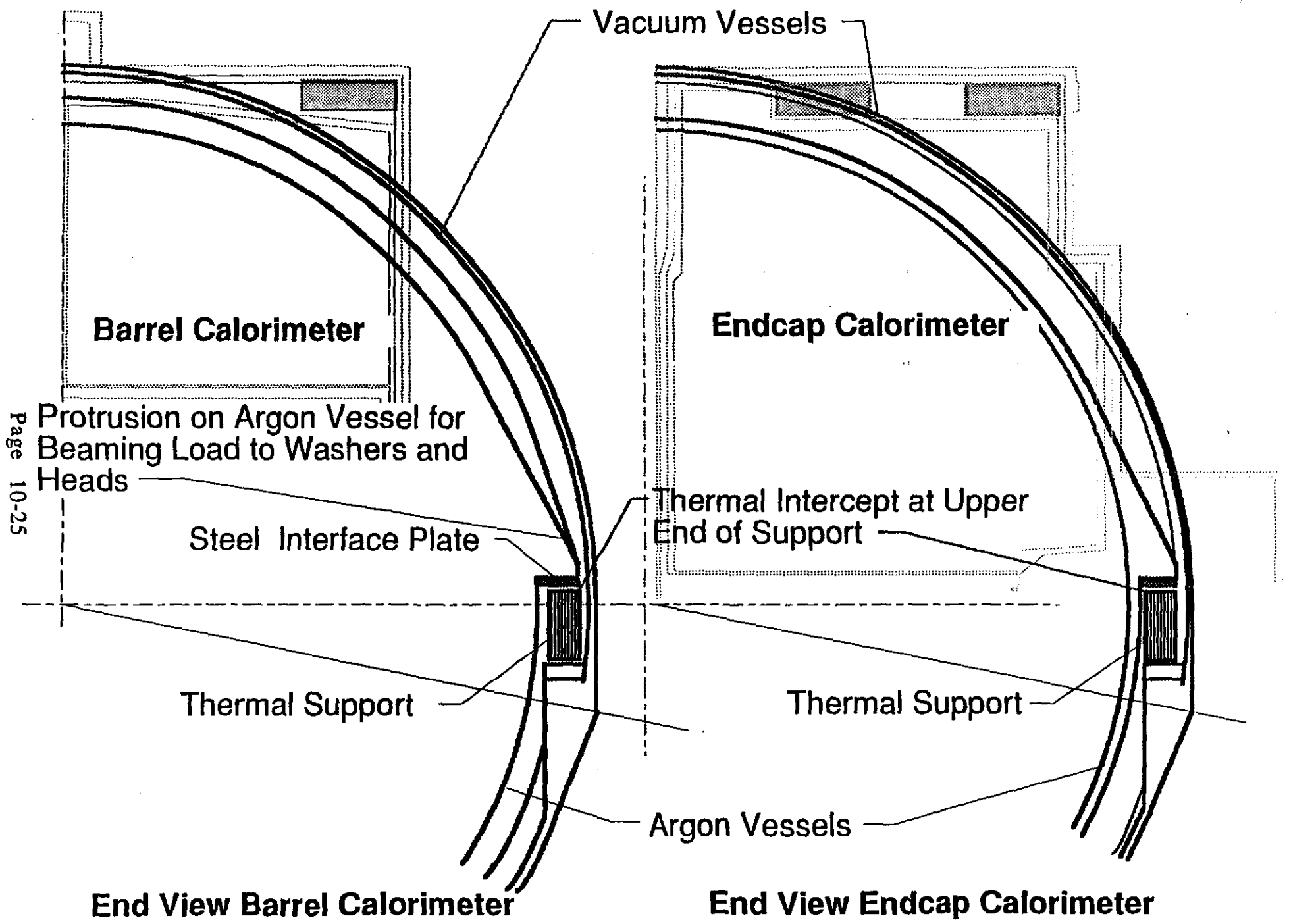
LIQUID ARGON CALORIMETER - 12 X 14 LAMBDA, FLAT ENDCAP HEAD

Page 10-24



Dimensions in millimeters

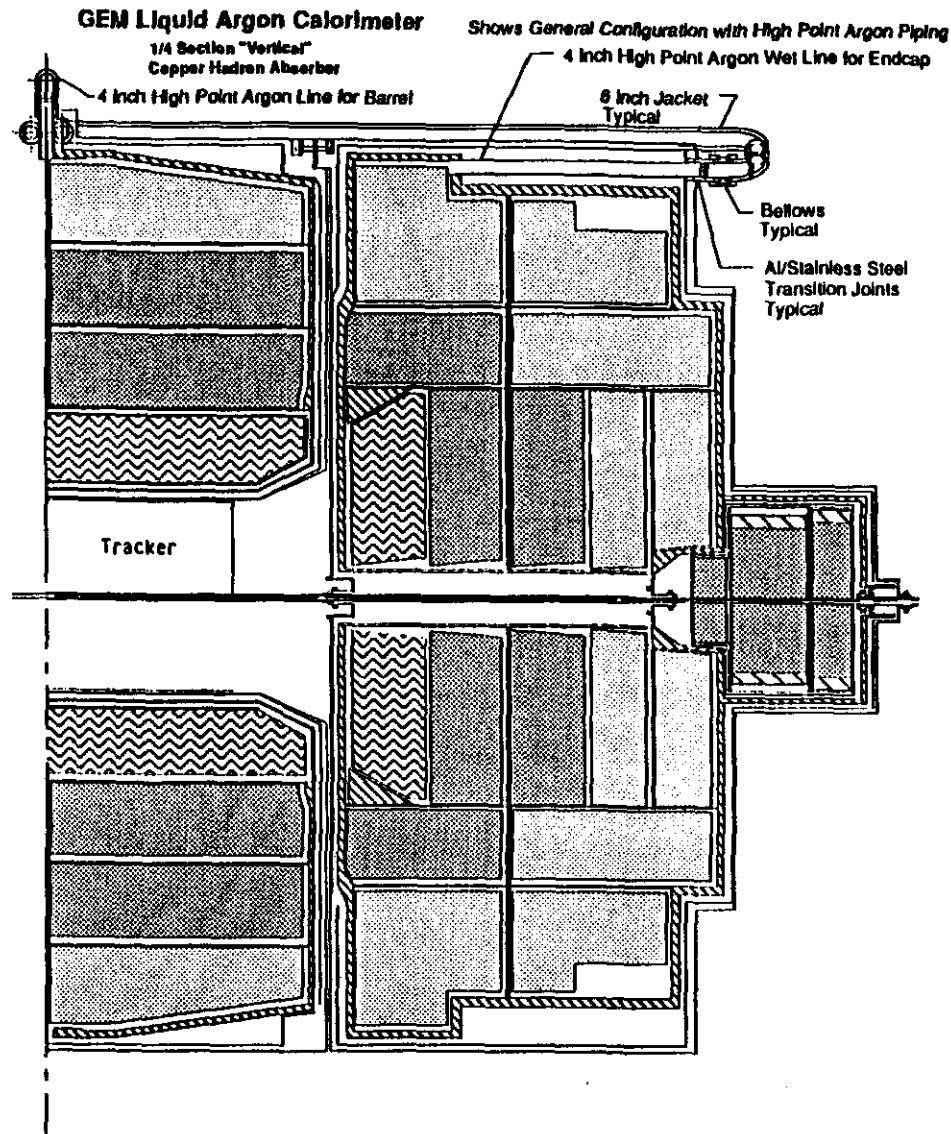
LLMASON 920620 B/L I LAC wall Thk



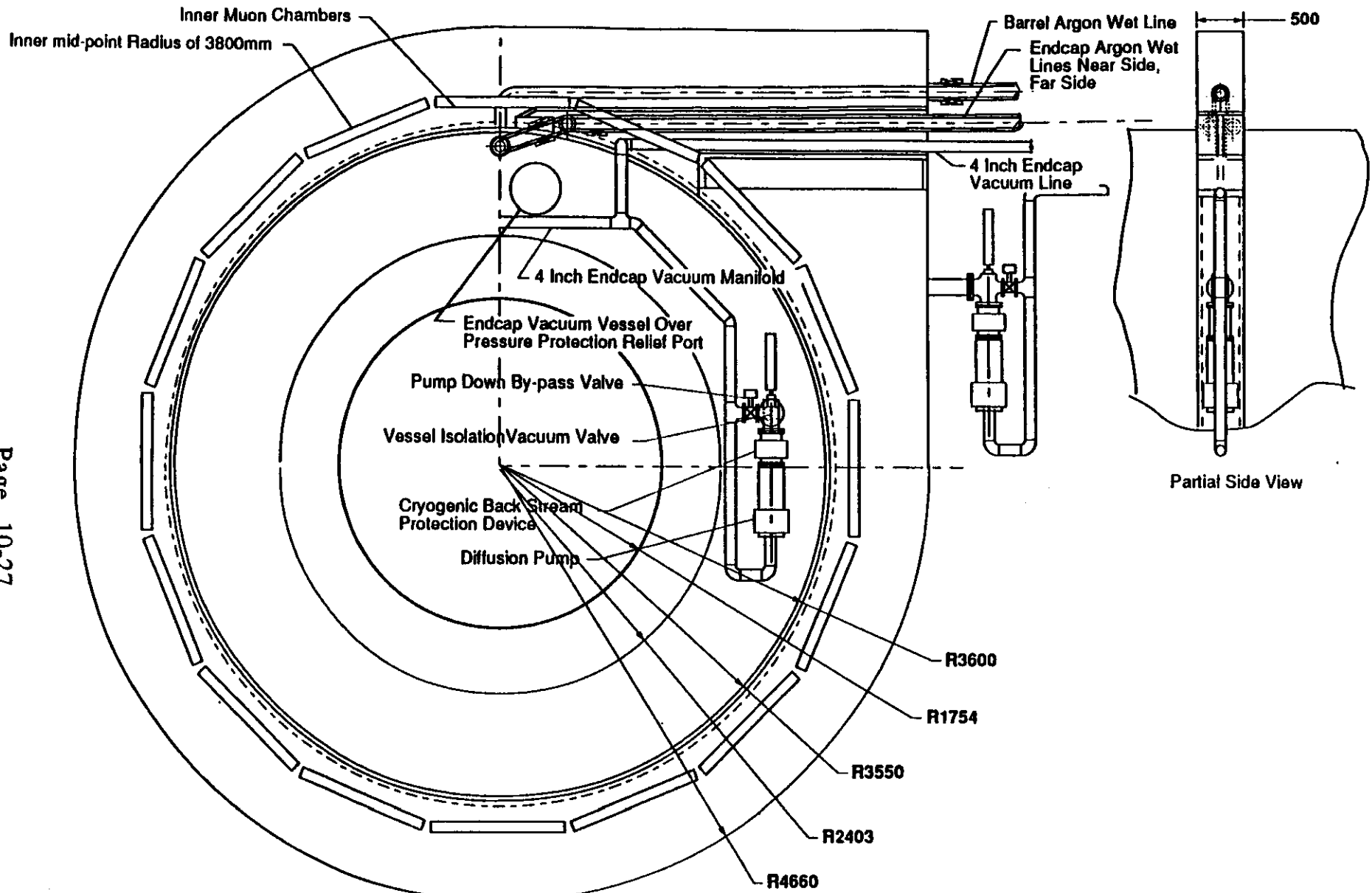
Page 10-25

End View Barrel Calorimeter

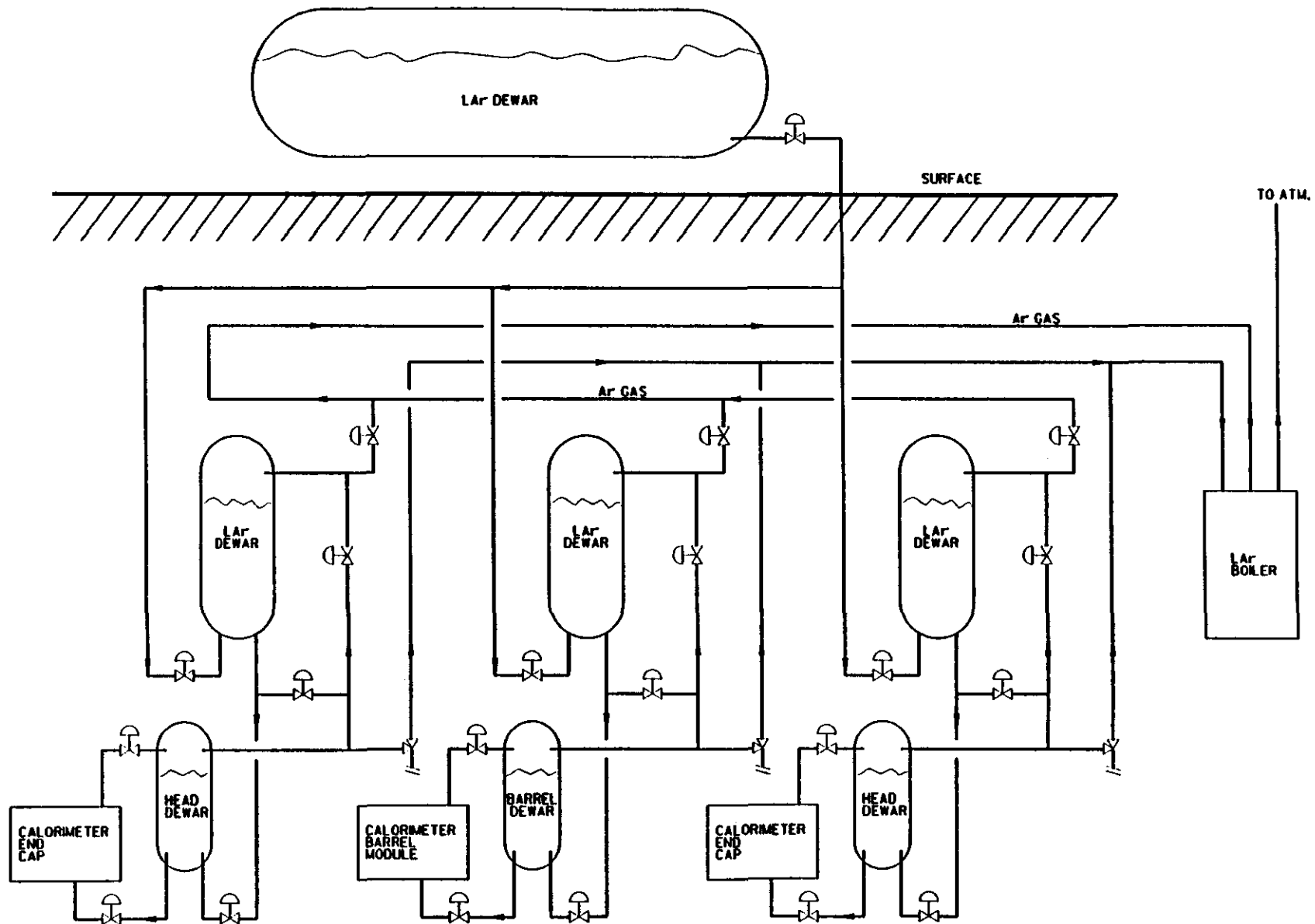
End View Endcap Calorimeter



Endcap Calorimeter SideView Showing Vacuum System and Argon Wet Line to Head Vessel

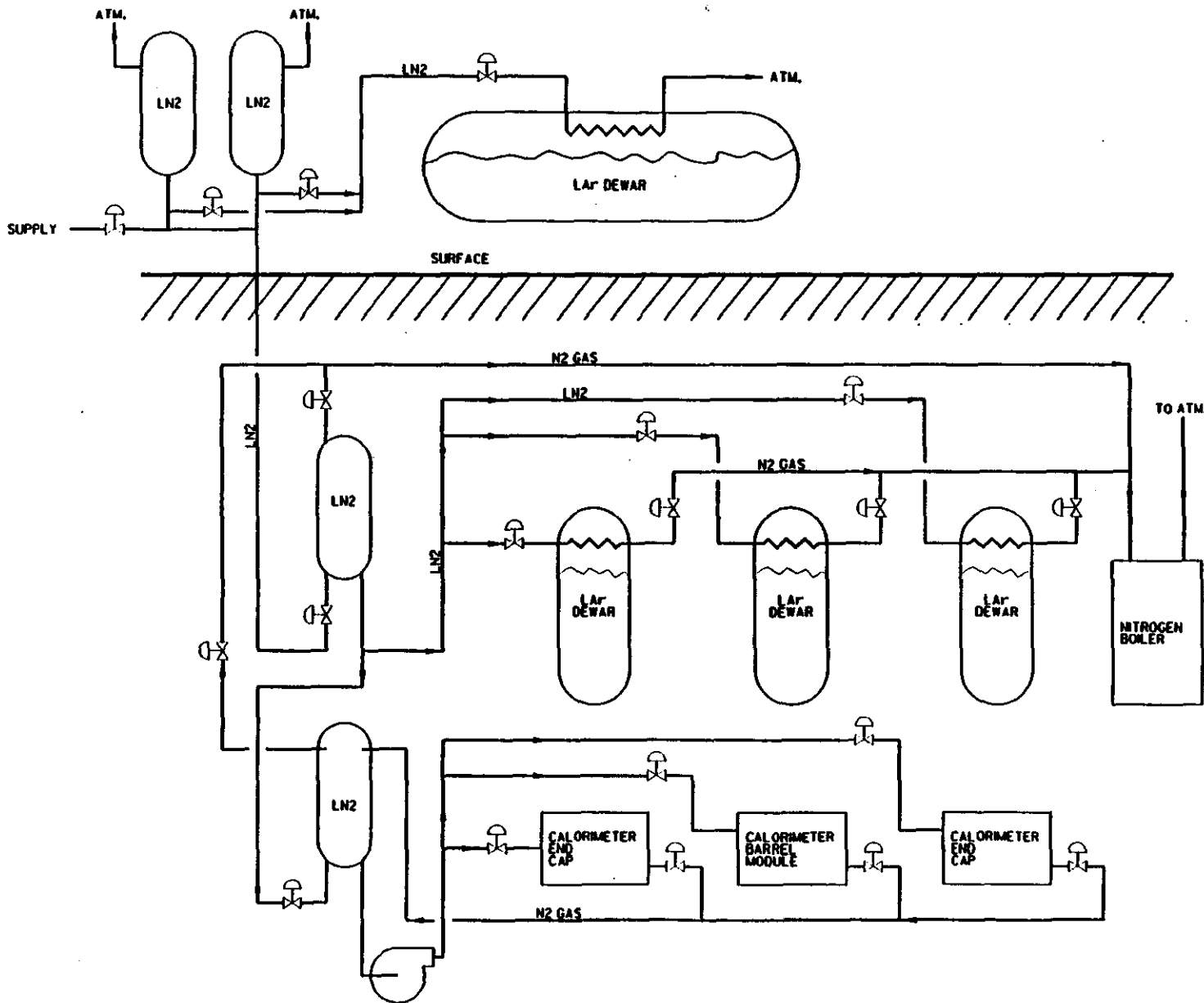


Endcap Calorimeter End View Showing Vacuum System and Argon Wet Line to Head Vessel



GEM
LIQUID ARGON CALORIMETER
ARGON SUPPLY SYSTEM

DRAWN BY: WILLIAM R. PETERSON
DATE: 6/25/92



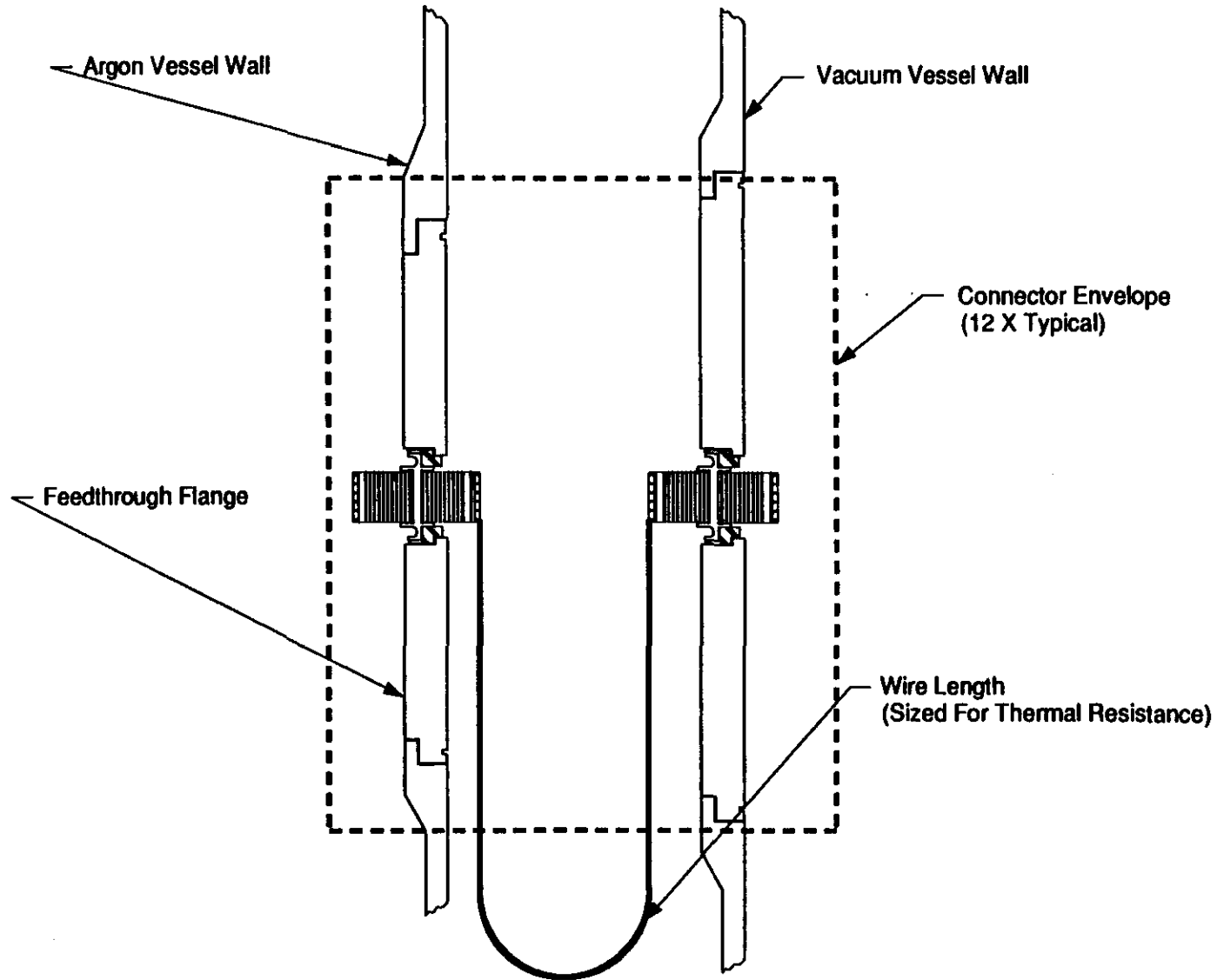
Page 10-29

GEM
LIQUID ARGON CALORIMETER
NITROGEN SUPPLY SYSTEM

DRAWN BY: WILLIAM R. PETERSON
DATE: 6/26/92

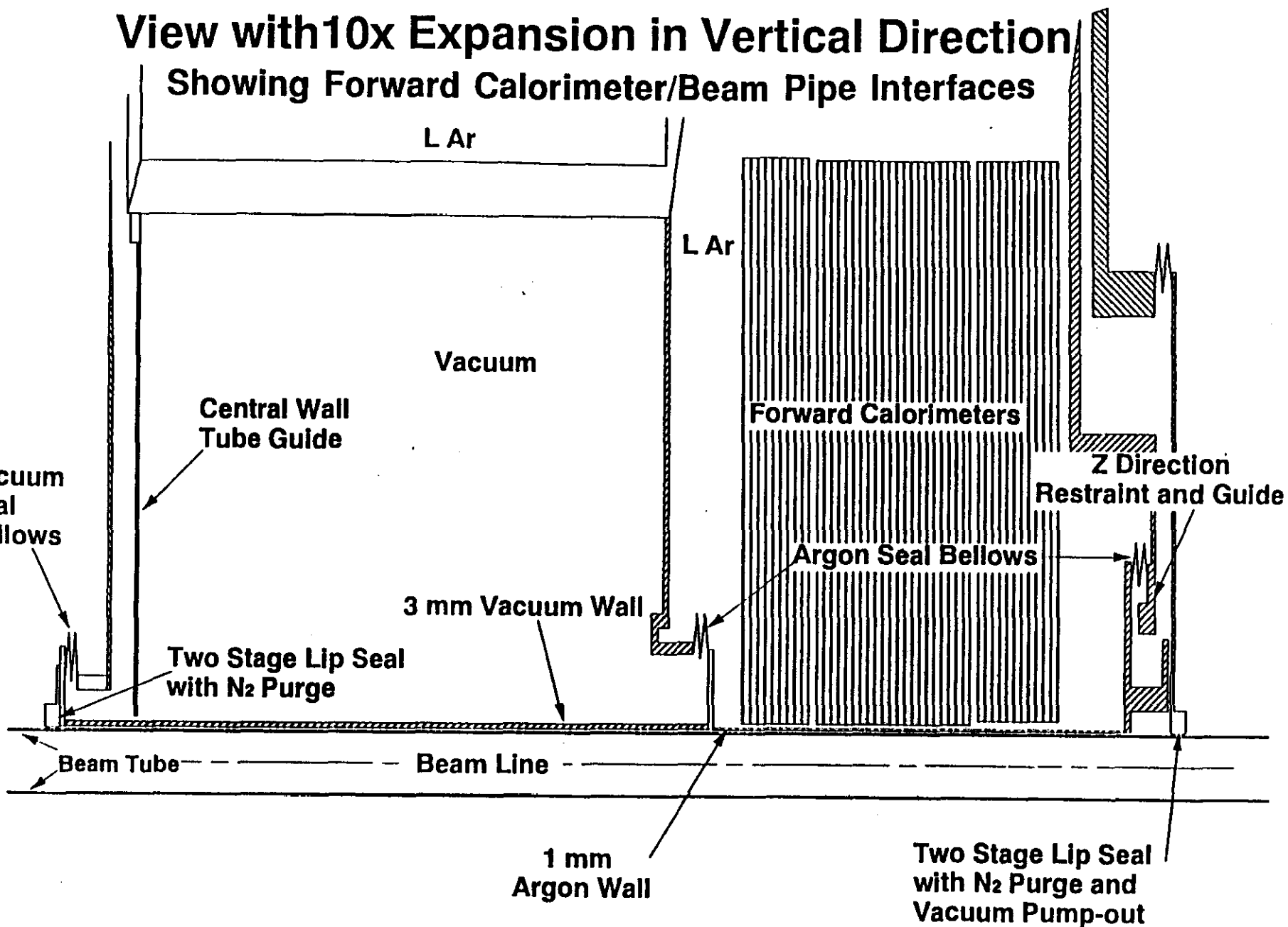
LIQUID ARGON CALORIMETER

Electronic Feedthrough Cross Section



View with 10x Expansion in Vertical Direction Showing Forward Calorimeter/Beam Pipe Interfaces

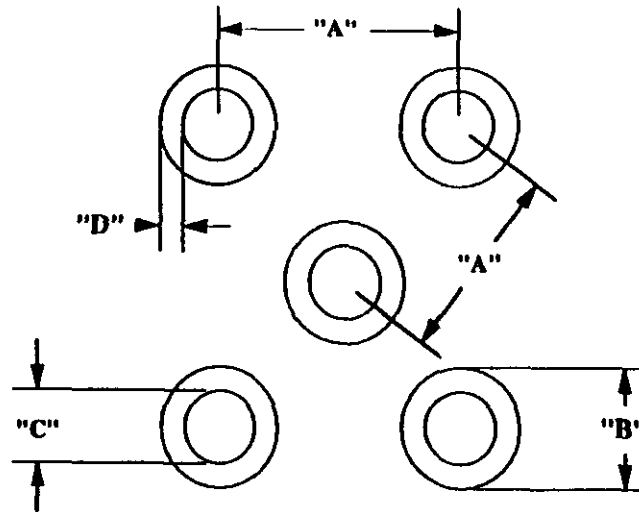
Page 10-31



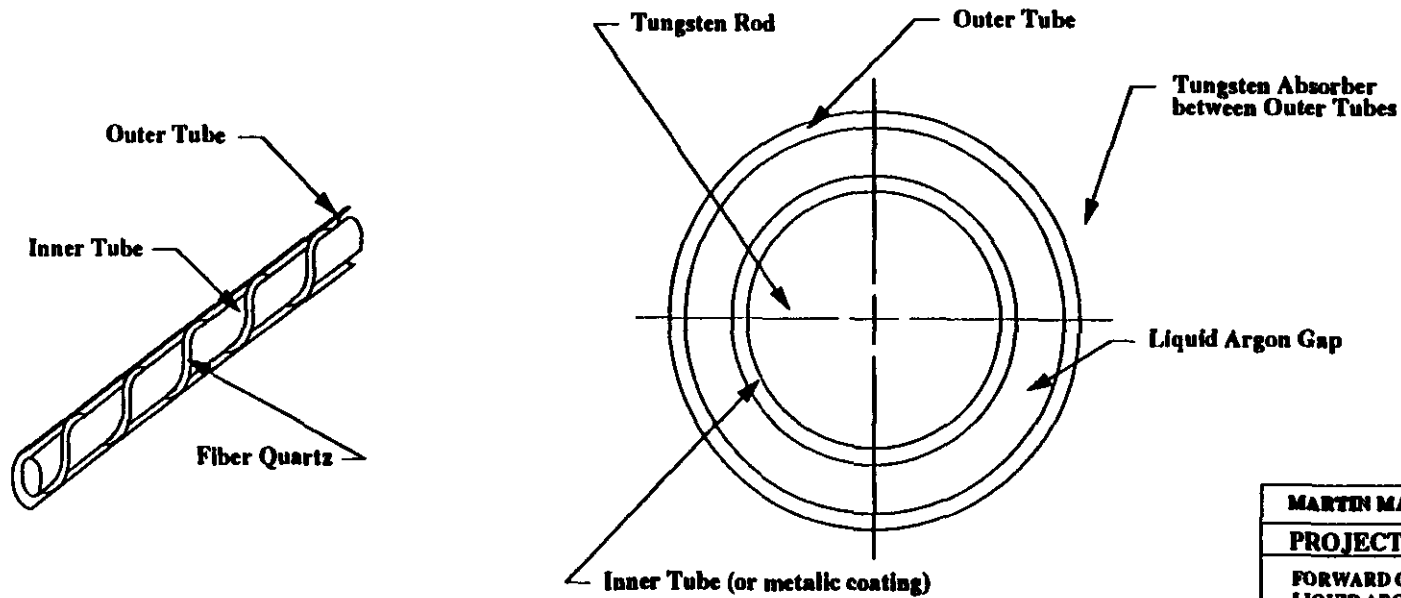
MODULES (units in mm)			
	EM	HADRONIC	Tail Catcher
A	7.50	8.13	8.80
B	5.00	5.39	5.82
C	4.80	4.79	5.22
D	0.10	0.30	0.30

Definitions:

- "A" = Center to Center Distance
- "B" = ID of Outer Tubes
- "C" = OD of Inner Tubes
- "D" = Liquid Argon Gap



GENERAL TUBE ARRANGEMENT



TUBE POSITION ARRANGEMENT DETAIL

MARTIN MARIETTA ENERGY SYSTEMS	
PROJECT: SSC GEM DETECTOR	
FORWARD CALORIMETER LIQUID ARGON OPTION TUBE ARRANGEMENTS IN MODULES	
PRINT NO: FCLAR-MD002	REV 2
DRAWN BY: S. M. CHAE	3/23/92
CHECKED & APPROVED BY:	

CALORIMETER SCINTILLATING OPTION

OVERVIEW

The other primary option for the GEM calorimeter system consists of a BaF2 crystal total absorption EM calorimeter and a scintillating fiber/copper sampling hadron calorimeter. In this section the Baseline 1 parameters of the scintillating calorimeter options are described.

The most important properties of a scintillating fiber hadron calorimeter are high speed, compactness, hermeticity and projective geometry, and "tunable" compensation.

Both the BaF2 EM and the scintillating fiber hadron calorimeters will be divided into cylindrical sections consisting of a barrel and two endcaps. The weights of the BaF2 barrel and of each BaF2 endcap are 43.96 and 6.61 metric tons respectively. The weight of the entire scintillating fiber calorimeter will be 1383 metric tons.

The forward calorimeter in the Baseline 1 scintillator option will consist of a liquid scintillator/tungsten sampling calorimeter. Other options (e.g. quartz fibers, high pressure gas etc) are under consideration.

Electromagnetic Calorimeter

The BaF2 electromagnetic calorimeter is expected to combine excellent energy resolution, $(2.0/\sqrt{E} \oplus 0.5)\%$, with high speed (16 ns gate width), good position resolution (dx and dy approx. 1 mm for EM showers), and very good e/pi, gamma/jet and e/jet separation characteristics (about 10^{-4}). It will cover a pseudorapidity range from -3 to +3.

The calorimeter will consist of 15,584 crystals each made up of two 250 mm-long crystals glued together to form crystals of 500 mm total length ($24.5 X_0$). Each crystal will be read out by a single photopentode. The granularity in both the η and in the ϕ direction is 0.04, corresponding to tapered crystals with sizes ranging from 31.4 x 31.4 mm (front face) - 51 x 51 mm (rear face) at $\eta = 0$ to 20.3 x 22.0 - 29.4 x 27.2 mm at $\eta = 2.5$. The Baseline 1 structure consists of a carbon composite based on the CERN L3 design, with a wall thickness of 0.3 mm. The option of a welded titanium structure with 0.1 mm walls is under study. Calibration options include the development of UV flash lamp monitoring, and by means of studies of in situ calibration options including the use of electrons generated by an RFQ (as in the L3 experiment), of minimum

Source: F. Plasil

Update:

CALORIMETER SCINTILLATING OPTION

ionizing particles and of the decay of known particles (e.g. upsilons and Z0's)

Hadron Calorimeter

The properties of a scintillating fiber hadron calorimeter are inherent speed (allowing a 32 ns gate width), compactness, adjustable compensation via the selection of an appropriate fiber/absorber ratio, hermeticity, simplicity of construction. The proposed fiber calorimeter will have two longitudinal segments. This will be achieved by means of an independent readout of 10% of the fibers located in a 2-lambda thick tailcatcher. The expected resolutions are $(90/\sqrt{E} \oplus 1.0)\%$ for hadrons, $(75/\sqrt{E} \oplus 1.0)\%$ for jets, and $(40/\sqrt{E})\%$ for hadrons propagating via electromagnetic showers. The entire EM plus hadron calorimeter will consist of 12 lambda at $\eta = 0$, rising to 14 lambda at $\eta = 3.0$.

Lateral segmentation of the scintillating fiber calorimeter is determined by the size of hadronic showers and by the need to match the segmentation of the BaF2 EM calorimeter. A segmentation of 0.08 in both η and ϕ has been selected. This results in a total of 3992 "physics" towers, corresponding to 998 mechanical towers (4 physics towers per mechanical tower). The total number of channels is 4990, corresponding to individual readout for each physics tower, plus one common tailcatcher readout for each physical tower. The sensing material consists of 1.5 mm diameter scintillating fibers, occupying 3% of available space. (Copper accounts for 93% of space with the rest, 4%, taken up by gaps.) The effective e/h ratio of the Cu/scintillating fiber hadronic section is expected to be 1.0 (+0.1, - 0.05).

Forward Calorimeter

The forward calorimeter, which will cover the region from $\eta = 3$ to $\eta = 5$, has been designed for installation in a location as close to the interaction region as possible. The present design calls for tungsten absorber material (to maximize transverse containment of hadronic showers) and for liquid scintillating readout material located in stainless steel tubes. The transverse η and ϕ segmentation will vary from 0.25 x 0.2 at $\eta = 3$ to 0.6 x 0.4 at $\eta = 5$. Options include the replacement of the stainless steel tubes with quartz tubes and the use of technologies such as quartz fibers and high pressure gases.

Source: F. Plasil
Update:

CALORIMETER SCINTILLATING OPTION

10.2.0 Scintillating Calorimeter Option

10.2.1.0 Primary Physics Goals

10.2.1.1 Barium Fluoride EM Calorimeter (EM)

- Precision energy measurement of isolated photons or electrons;
- Precision impact coordinate measurement at the front surface of the calorimeter for isolated photons and electrons; momentum vector determination, using the primary vertex determined from the central tracker;
- Search for narrow resonances by reconstructing the invariant mass of multi-photons or electrons.

10.2.1.2 Scintillating Fiber and Copper Hadron Calorimeter (HAD)

- Electron and photon identification (hadron veto);
- Muon identification, isolation, and pattern recognition;
- Muon energy loss measurement;
- Jet energy measurement (using EM and HAD Calorimeter);
- Missing energy measurement (using also EM and Forward calorimeters).

10.2.1.3 Liquid Scintillator and Tungsten Forward Calorimeter (FWD)

- Missing energy measurement (using also EM and HAD calorimeters).

10.2.2.0 Secondary Physics Capabilities

- Provide a fast trigger for tagging the beam crossing;
- Separate electrons and pions, by using the lateral and longitudinal shower distributions;
- Rejection of backgrounds with isolation cuts.

CALORIMETER SCINTILLATING OPTION

10.2.3.0 Unique Physics Capabilities

Higgs searches: $H^0 \rightarrow \gamma\gamma$
 $t\bar{t} H^0 / W H^0 \rightarrow \gamma\gamma$
 $H^0 \rightarrow e^+ e^- e^+ e^-$ (including $Z Z^*$);

Toponium searches: $\theta \rightarrow \gamma\gamma$,

Z^0 Searches: $Z^0 \rightarrow e^+ e^-$;

- Search for unknown narrow resonances which decay to multi-photons and/or electrons;
- Jet energy measurements up to the highest energies without model dependent corrections.
- Hermetic due to absence of intervening structure.

10.2.4.0 Physics Performance

Time resolution	
EM, HAD, and FWD	1 beam crossing
Speed (gate width)	
EM	16 ns
HAD	32 ns
FWD	32 ns
Noise	
EM	3 MeV / ch
HAD	3 MeV / tower
FWD	3 MeV / tower
Hermeticity (Et Measured)	$0 < \eta < 5$
EM energy resolution	$(2.0 / \sqrt{E} \oplus 0.5) \%$
EM position resolution	dx and dy approximately 1 mm
Expected e / h	1.0 (+0.1 -0.05)
Hadron energy resolution (Hadrons)	$(90 / \sqrt{E} \oplus 1.0) \%$
Hadron energy resolution (Jets)	$(75 / \sqrt{E} \oplus 1.0) \%$
Hadron energy resolution (Electromagnetic)	$(40 / \sqrt{E}) \%$
Hadron dynamic range	$10^5 \text{ @ } 50 \text{ MeV to } 5 \text{ TeV}$
Forward energy resolution	$(50 / \sqrt{E} \oplus 2) \%$
Number of absorption lengths	
at $\eta = 0$	12.0
at $\eta = 3.0$	14.0

Source: Y. Kamyshkov/M. Rennich
 Updated: 7/8/92

CALORIMETER SCINTILLATING OPTION

Compactness		
inner radius	0.75	m
outer radius	3.40	m
Total distance between absorber and muon system	0.65	m
Thickness of readout assembly	0.35	m
Total distance between structure and muon system	0.30	m

Density ~5.0 gm/cm³ in readout region (copper shot filled)

Lateral segmentation (η, ϕ)	
EM	0.04 x 0.04
HAD	0.08 x 0.08
FWD	0.25 x 0.2 at $\eta = 3$
	0.6 x 0.4 at $\eta = 5$
Longitudinal segmentation	1 EM, 2 HAD

10.2.5.0 Physical Parameters

10.2.5.1 Barium Fluoride EM Calorimeter

Absorber material	Barium fluoride	
Lateral segmentation (η, ϕ)	0.04 x 0.04	
Longitudinal segmentation	1	
Dimensions		
Inner Radius	750	mm
Outer Radius	1400	mm
Total Length of Assembly	4600	mm
Length of Crystals	500	mm
Glued Crystal Joint @	250	mm
Radiation Length	24.5	X ₀
Absorption Length	1.7	Lambda
Number of Crystals-Total	15584	each
Number of Crystals-Barrel	10880	each
Number of Crystals-One End Cap	2352	each
Crystal Sizes @ $\eta = 0.0$	31.4 x 31.4 to 51 x 51 mm	
Crystal Sizes @ $\eta = 2.5$	20.3 x 22.0 to 29.4 x 27.2 mm	
Number of Channels-Total	15584	each

Source: Y. Kamyshev/M. Rennich
 Updated: 7/8/92

CALORIMETER SCINTILLATING OPTION

Three Subassemblies:	Barrel	
	Two end caps	
Structure	Carbon Composite	
Wall Thickness	0.3	mm
Distance Between Crystals	0.75	mm
Readout Device	Photopentode (One/Crystal)	
Crystal Volume	10.59	M ³
Crystal Volume in Barrel	8.39	M ³
Crystal Volume in One End Cap	1.10	M ³
Weight of Assembly	57.18	Mg
Weight of Barrel	43.96	Mg
Weight of Each End Cap	6.61	Mg

Source: Y. Kamyshev/M. Rennich
Updated: 7/8/92

CALORIMETER SCINTILLATING OPTION

10.2.5.2 Scintillating Fiber and Copper Hadron Calorimeter

Lateral segmentation (η, ϕ)	0.08 x 0.08	
Longitudinal segmentation	2	
Dimensions		
Inner Radius	1400	mm
Outer Radius	3400	mm
Length	9620	mm
Sense Material: 1.5 mm dia. Fibers	3%	
Absorber: copper	93%	
Gaps	4%	
Unit Radiation length of active absorber	15	mm
Unit Absorption length of active absorber	157	mm
Absorption Thicknesses		
Hadronic @ $\eta = 0.0$	10.3	λ
Total with BaF2 @ $\eta = 0.0$	12.0	λ
Hadronic @ $\eta = 3.0$	12.3	λ
Total with BaF2 @ $\eta = 3.0$	14.0	λ
Hadronic Tail Catcher		
Depth	2.0	λ
Sampling	10% of Fibers	
Physics Towers	3992	Each
Mechanical Towers (4 physics towers each)	998	Each
Readout		
Channels (5 per 4 physics towers)	4990	Each
Light yield	> 40	pe/GeV
Noise	< 3	MeV/tower
Total Weight		
Copper	1328	Mg
Structural Components-St St	47	Mg
Inner Rings-St St	4.5	Mg
Quantities		
Photomultipliers (1 per channel)	4990	Each
Length of Fiber	3,128,160	Meters
Number of Fibers	1,960,000	Each
Length of Copper Tubes	2,352,000	Meters

Source: Y. Kamyshkov/M. Rennich
 Updated: 7/8/92

CALORIMETER SCINTILLATING OPTION

Assemblies	3	Each
Barrel Weight	927	Metric Tons
End Cap Weight (each)	228	Metric Tons
Absorber Volume	179	M ³

10.2.5.3 Liquid Scintillator and Tungsten Forward Calorimeter

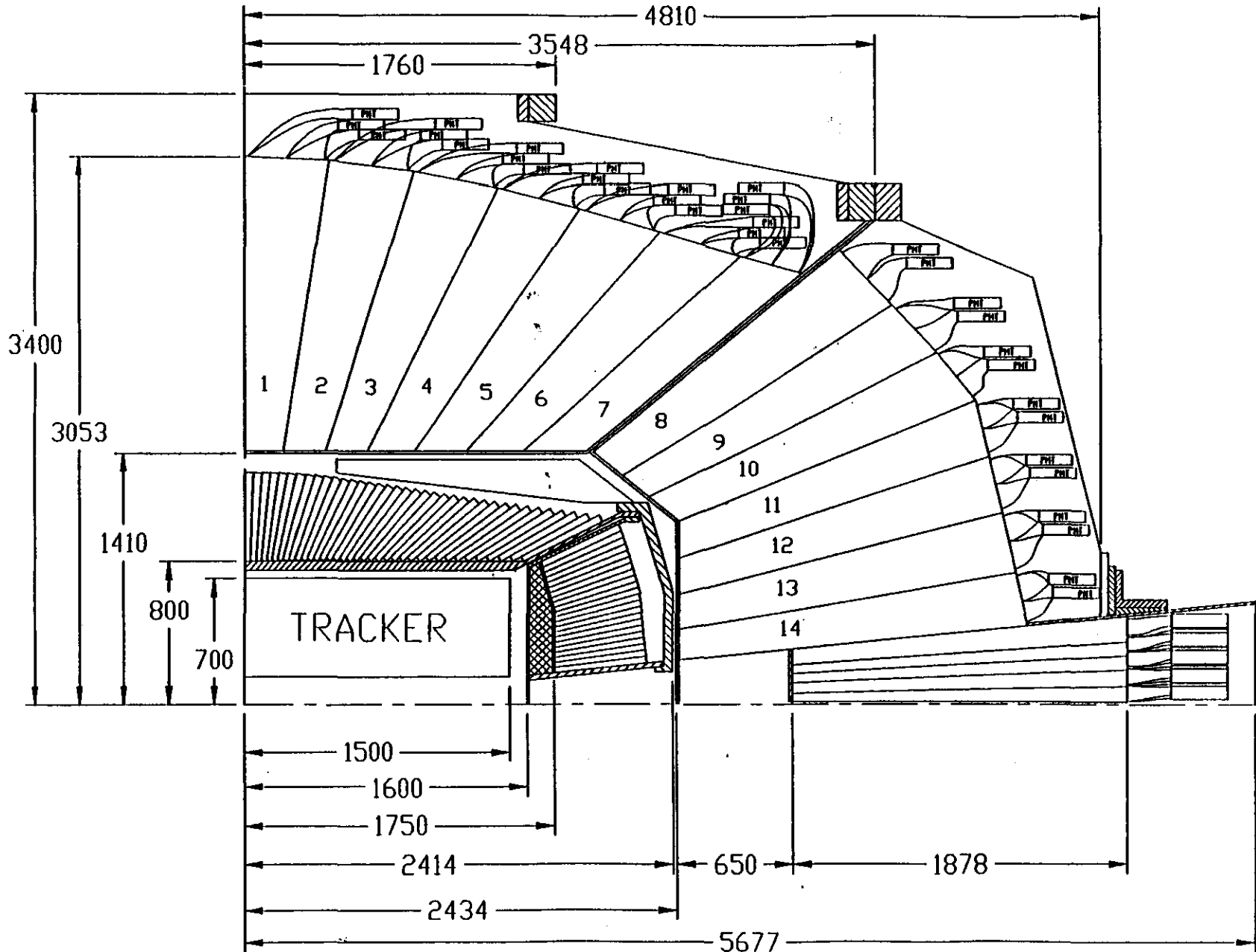
Segmentation		
Transverse	0.25 x 0.2 at $\eta = 3$	
	0.6 x 0.4 at $\eta = 5$	
Longitudinal (Each Tower)	2	
Scintillating Oil+Reflector	16.6%	
Absorber	79.6%	
Tungsten	50.0%	
Lead	11.2%	
Tin	8.6%	
Cadmium	5.5%	
Bismuth	24.2%	
Stainless Steel Tubes	3.8%	

Quantities and Dimensions for One Side of Forward Calorimeter:

Weight of Forward Calorimeter	50.1	Metric Ton
Number of Mechanical Towers	120	Each
Number of Channels	960	Each
Absorption Length	12.0	Lambda
Material Quantities		
Tungsten	26.4	Metric Ton
Eutectic	6.5	Metric Ton
Stainless Steel sheath	2.6	Metric Ton
Stainless Steel Tube	1.1	Metric Ton
Structural Components - SS	7.1	Metric Ton
Photomultiplier Tubes	960	Each
Length of Tubes	96,587	Meters
Length of fibers	16,064	Meters
Number of tubes & fibers	64,295	Each
Volume of Liquid+Reflector	0.56	M ³
Dimensions		
Inner Radius	25	mm
Outer Radius	945	mm
Active Length	1,822	mm
Total Length	~2200	mm

Source: Y. Kamyshev/M. Rennich
 Updated: 7/8/92

GEM DETECTOR
 Fiber Hadron Calorimeter
 Fiber with BaF2 Design

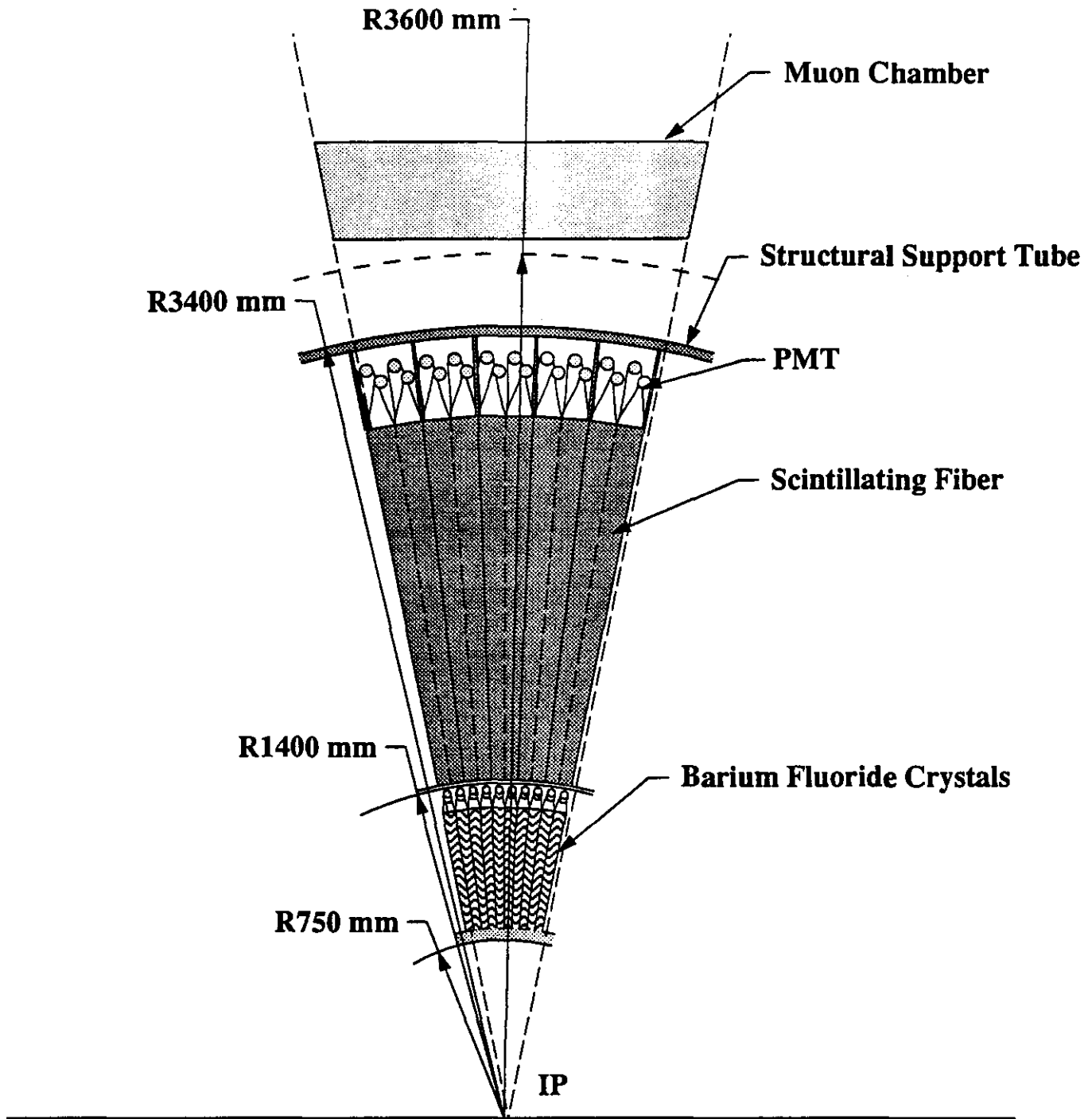


Page 10-41

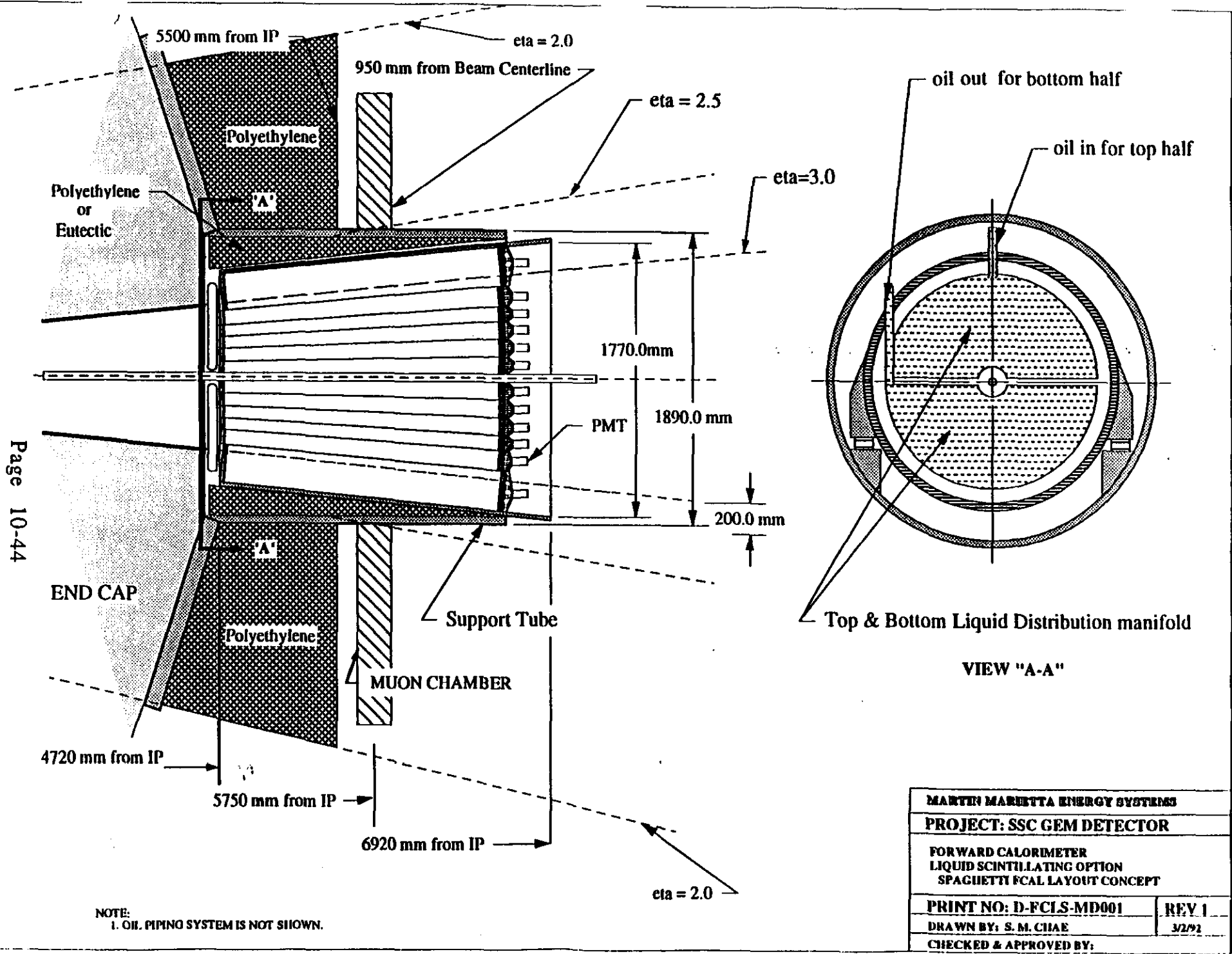
A. SMIRNOV

**GEM DETECTOR CALORIMETER
 FIBER HADRON & BARIUM FLUORIDE EM**

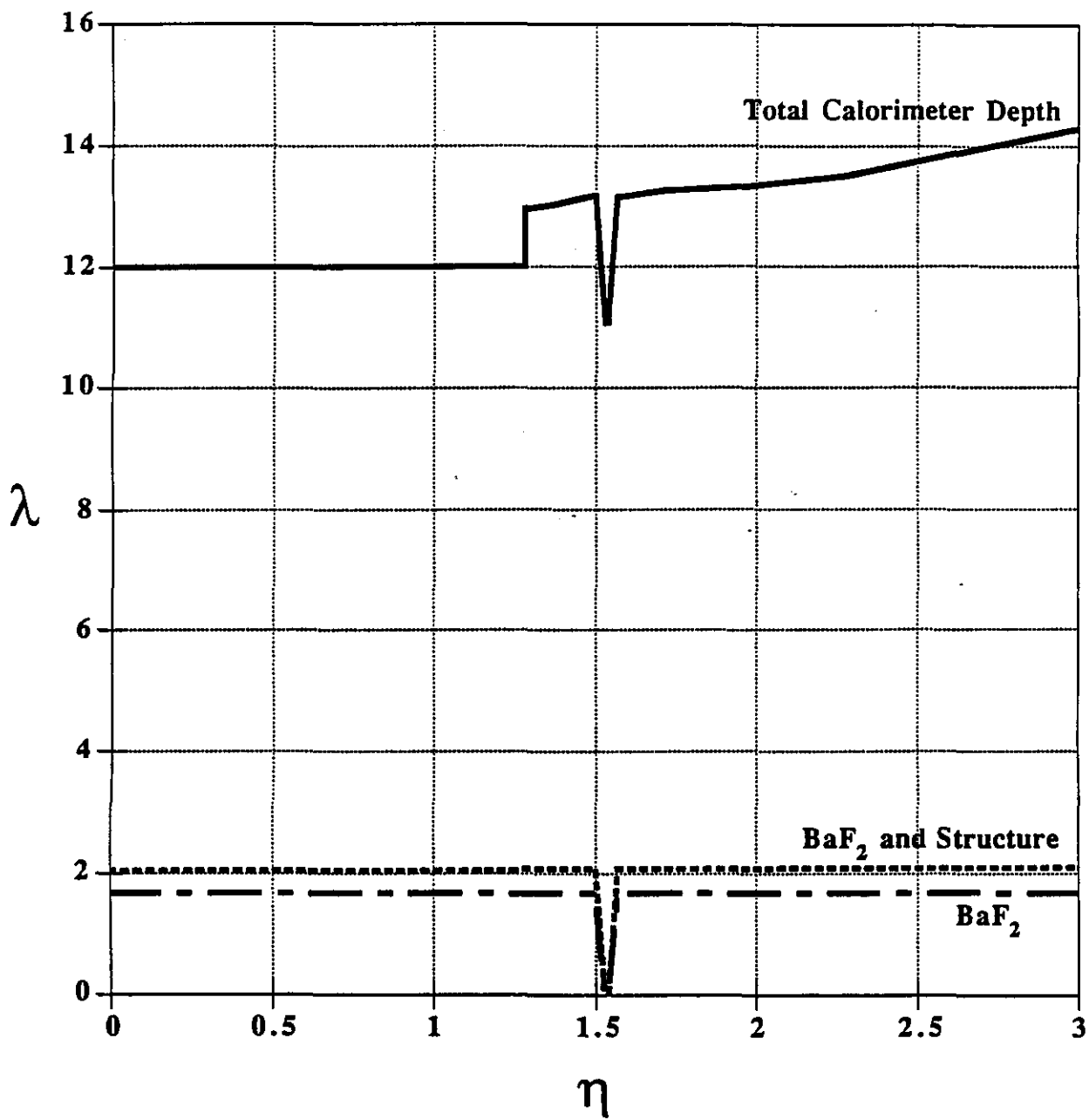
DRNL 6/30/92



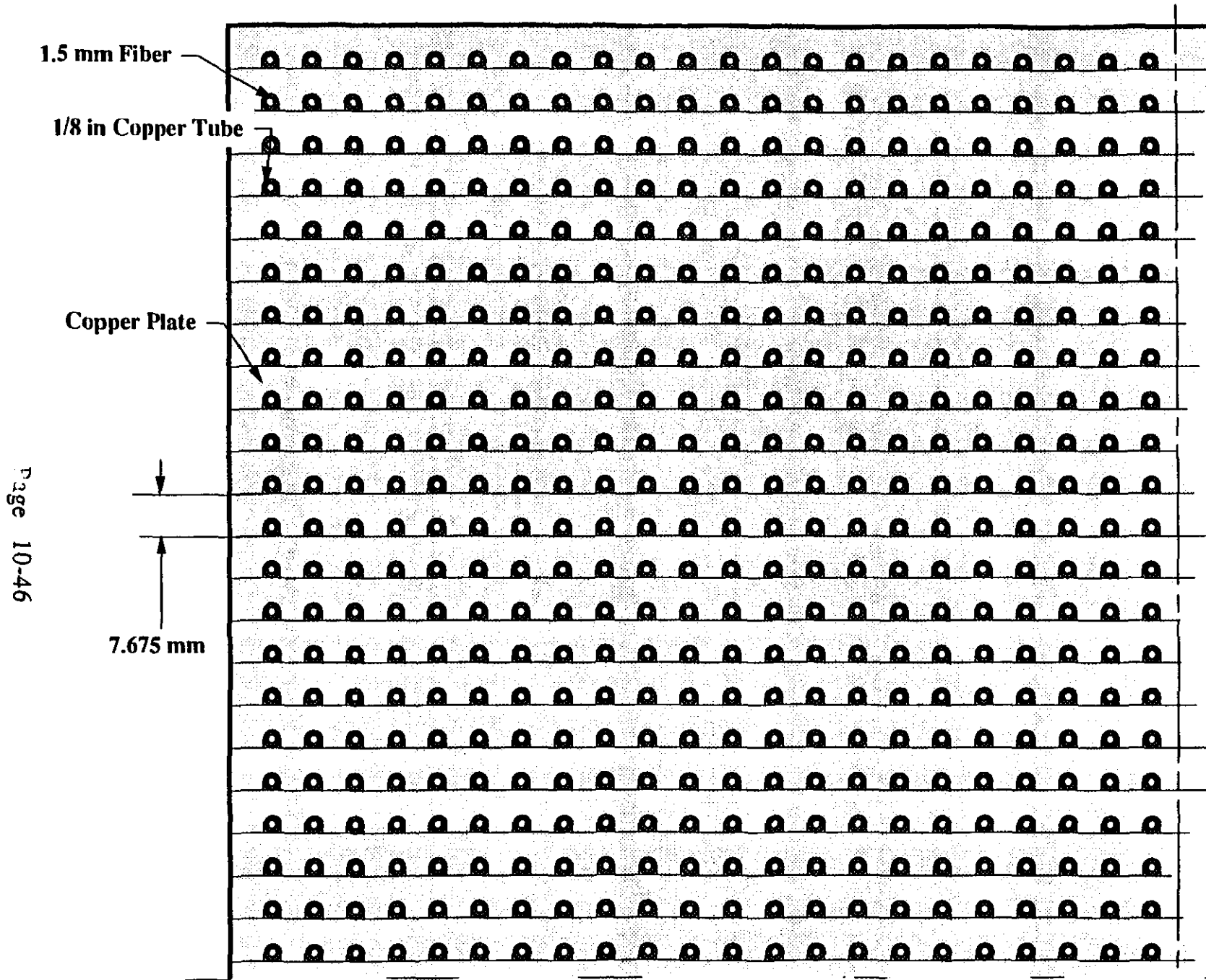
GEM Detector
Barium Fluoride/Scintillating Fiber Calorimeter
End Section View at 90 Degrees



MARTIN MARIETTA ENERGY SYSTEMS	
PROJECT: SSC GEM DETECTOR	
FORWARD CALORIMETER LIQUID SCINTILLATING OPTION SPAGHETTI FCAL LAYOUT CONCEPT	
PRINT NO: D-FCIS-MD001	REV 1
DRAWN BY: S. M. CHAE	3/2/92
CHECKED & APPROVED BY:	



GEM Scintillating Calorimeter Depth

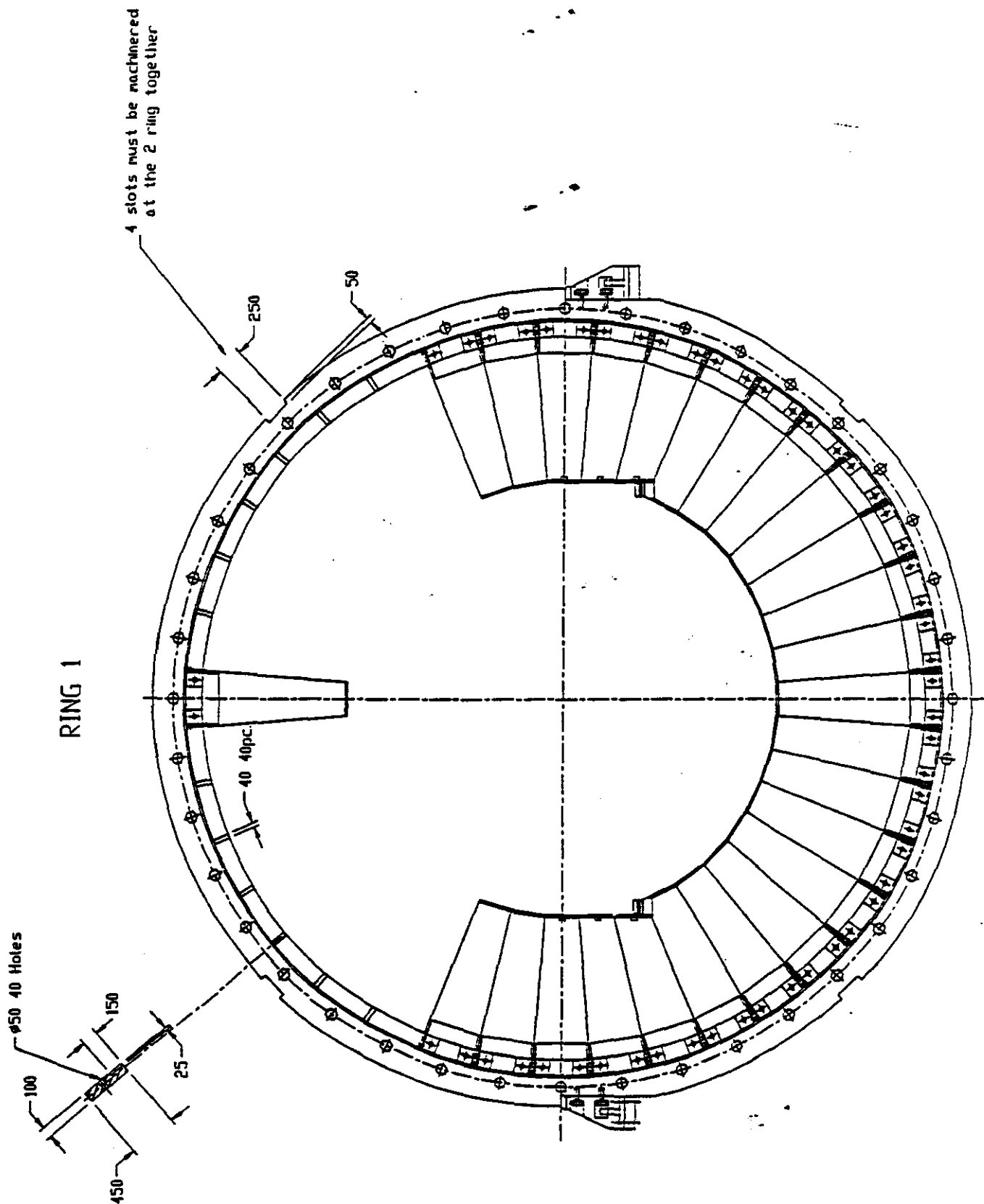


Page 10-46

G.03.CU.001

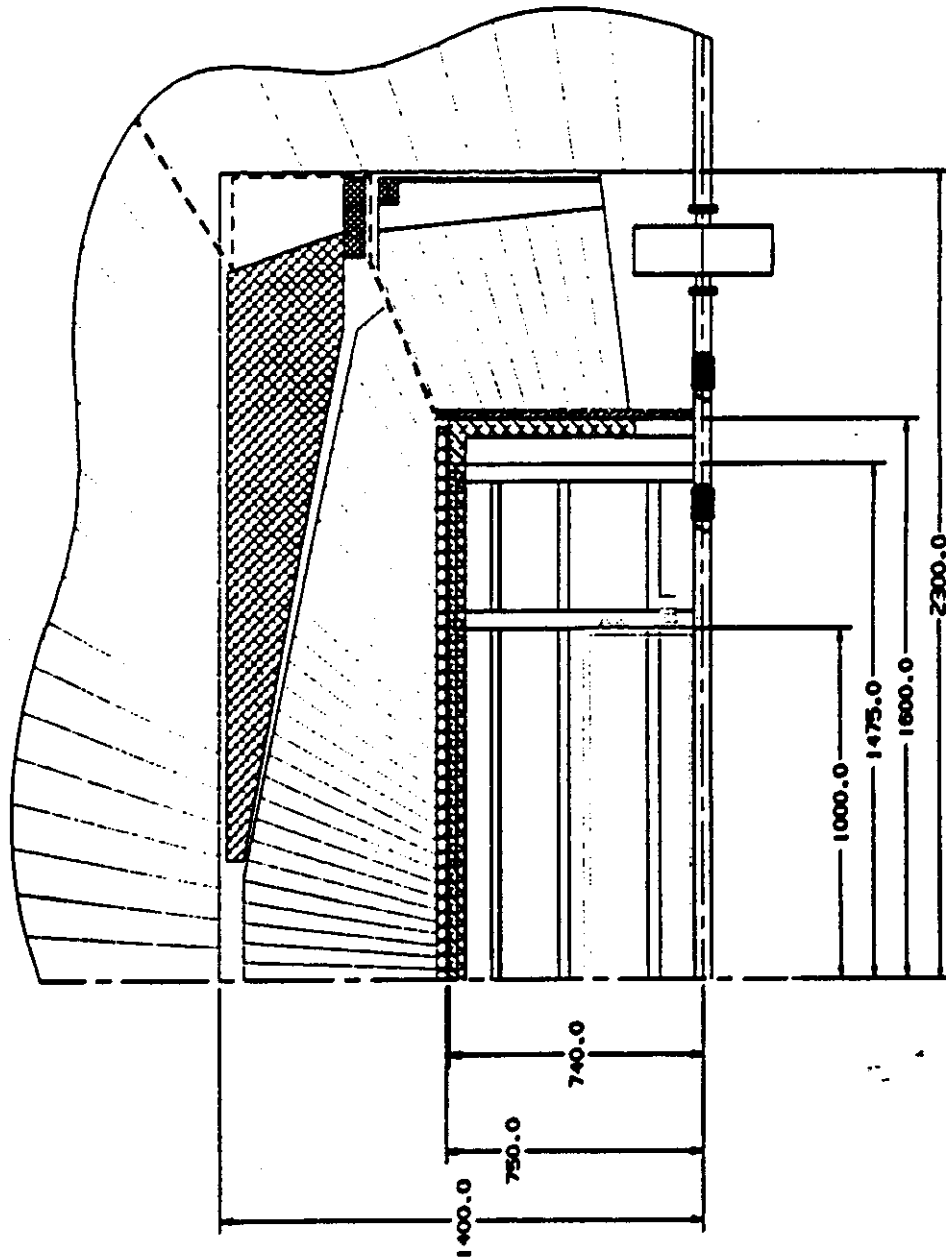
SCINTILLATING FIBER HADRON CALORIMETER
END VIEW OF TOWER QUARTER SECTION

RENNICH



Fiber Hadron Calorimeter
Partially Assembled, Axial View

GEM CENTRAL TRACKER



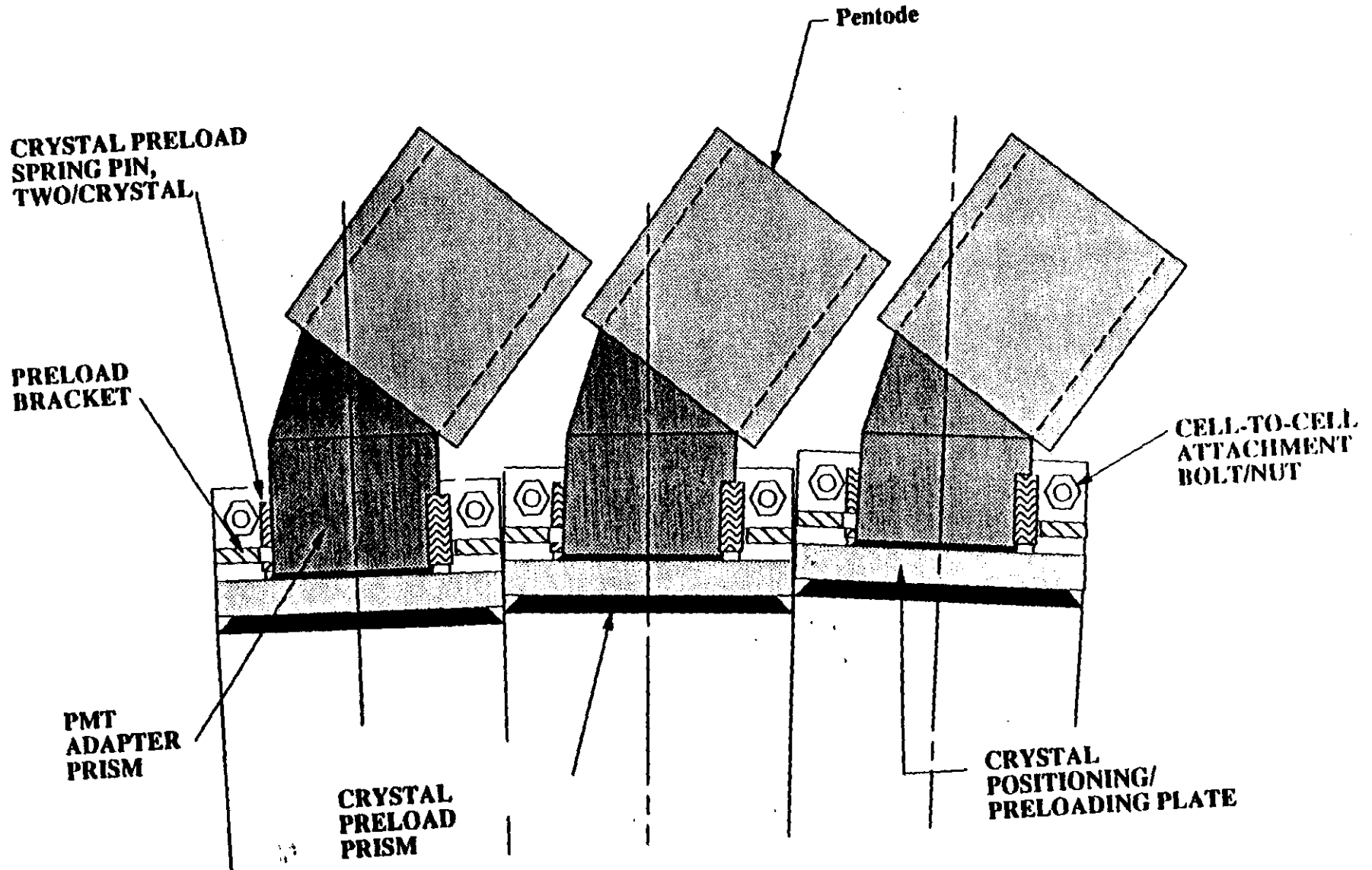
Bof/FIBER CALORIMETER OPTION

ALL DIMENSIONS ARE IN MM

LOS ALAMOS

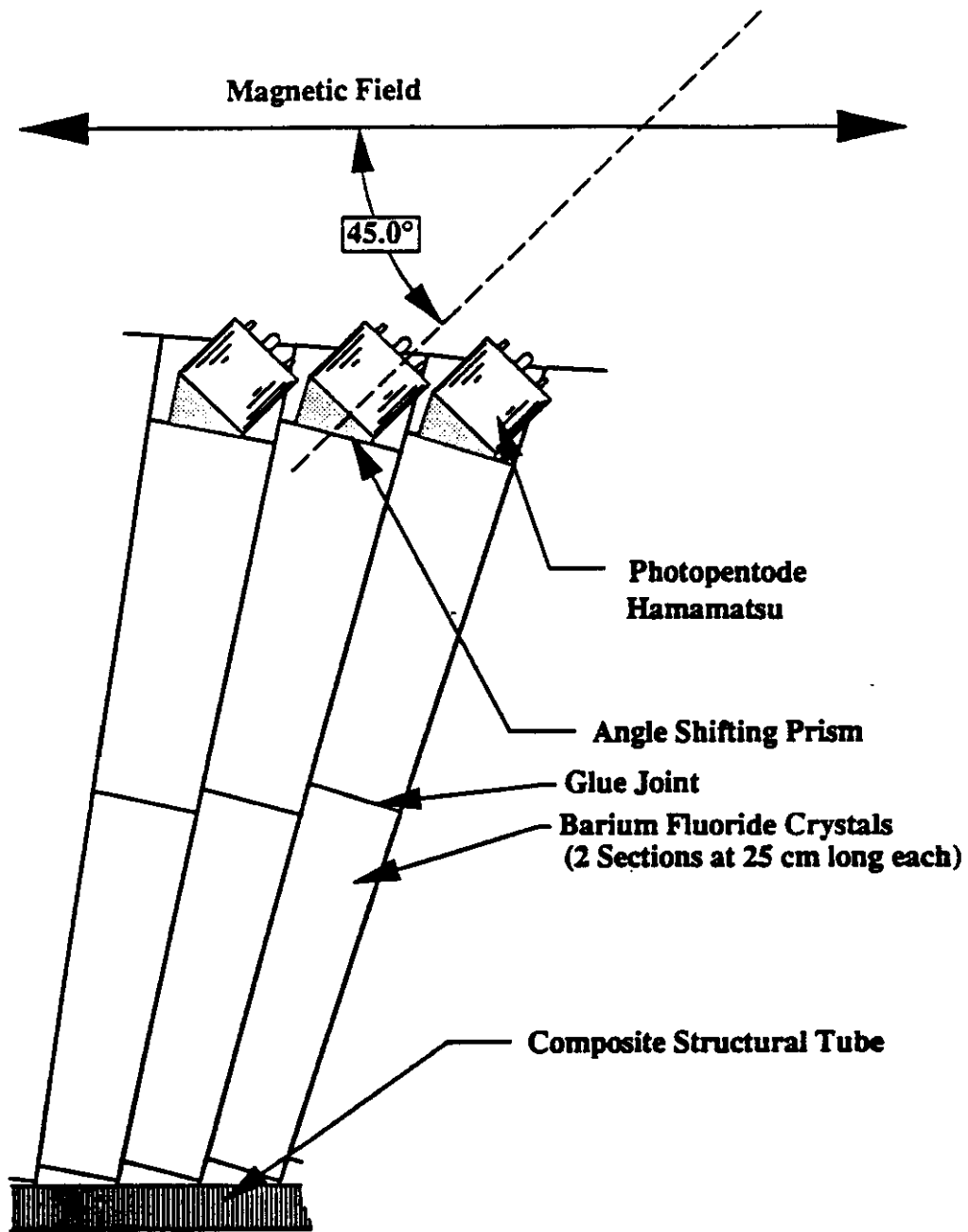
MECHANICAL AND ELECTRONIC
ENGINEERING DIVISION

FORM 100C-11 03-20-82

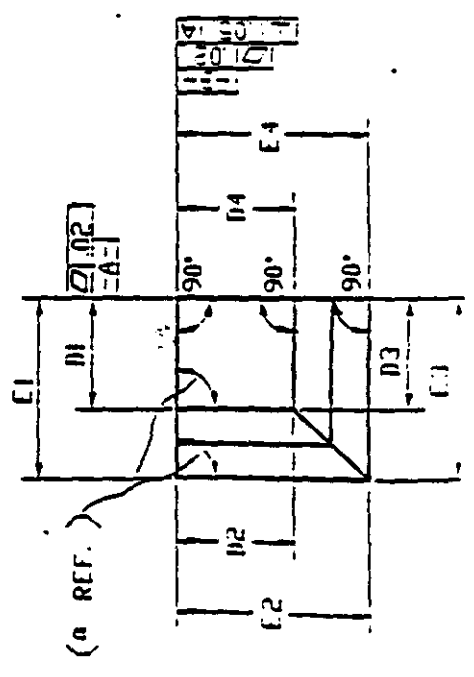
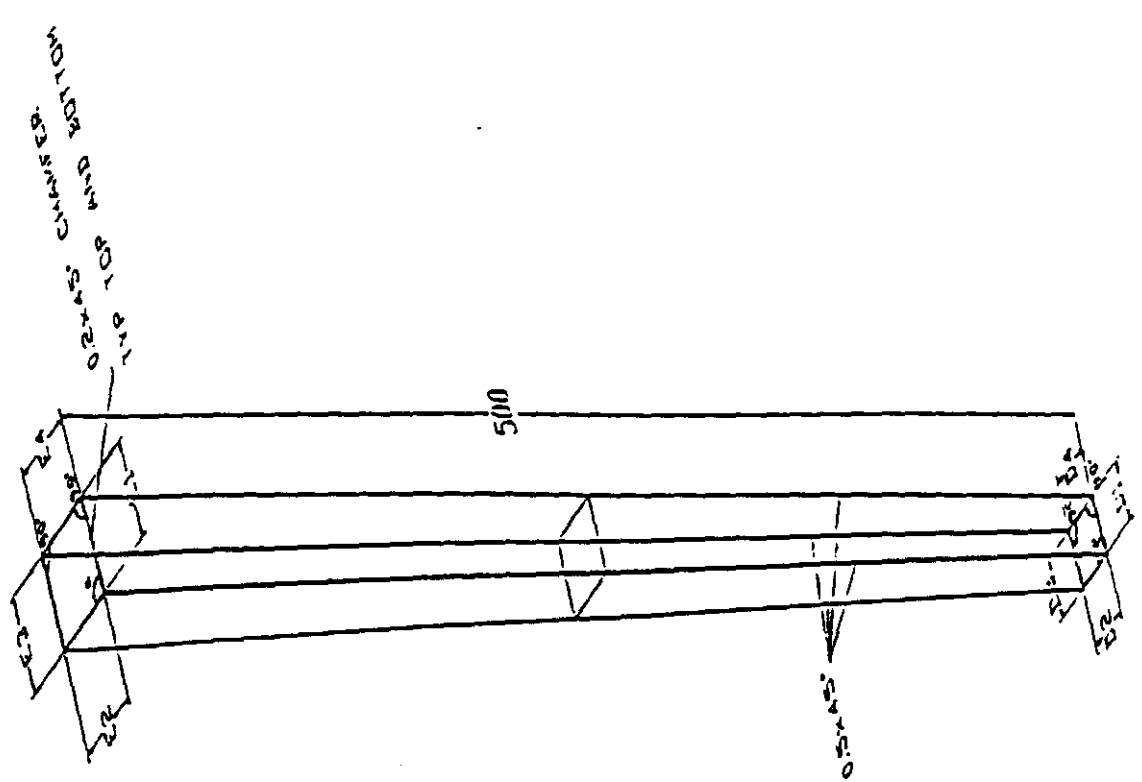
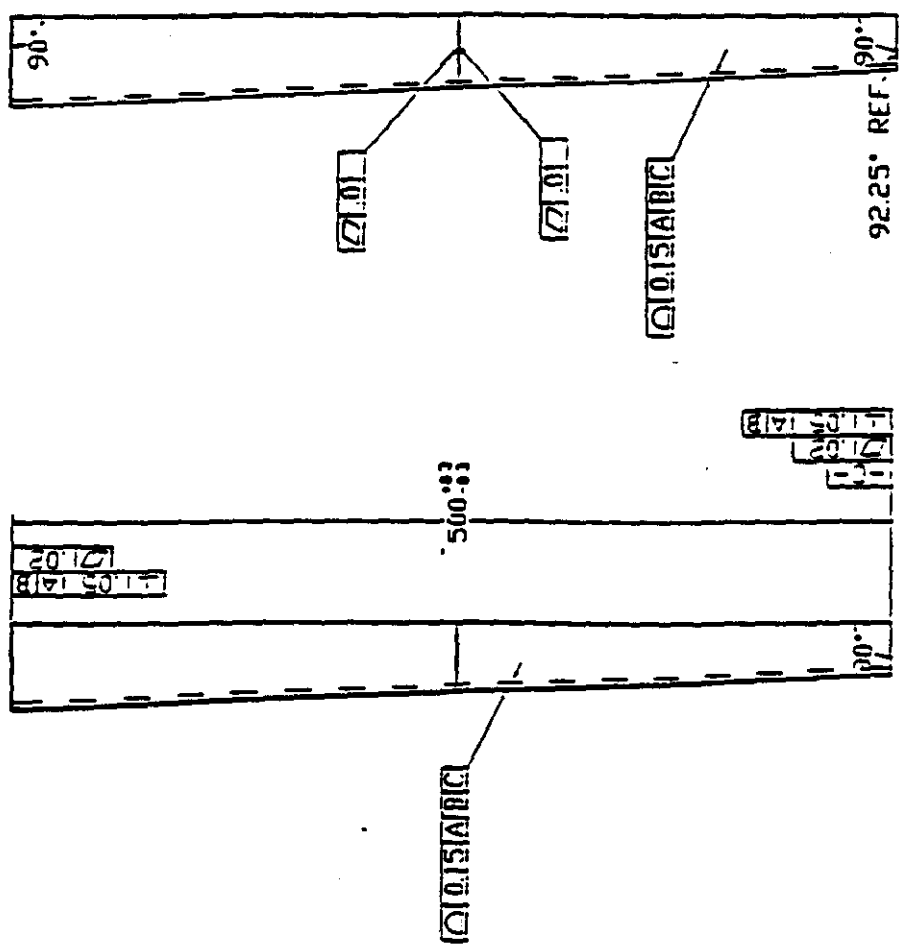


**GEM Detector
Barium Fluoride Calorimeter
Theta Crystals/PMT**

Rennich



Barium Fluoride Readout



Barium Fluoride Crystal Configuration

MUON SYSTEM

TABLE OF CONTENTS

OVERVIEW

FIGURES:

GEM Muon System (Quarter Elevation)
GEM Barrel Region Muon System (End View)
GEM Endcap Muon System Assembly
GEM Muon System Chamber Layout
GEM Barrel Region (PDT) (Chamber End View)
GEM Muon System Chamber Layout Showing Chamber Lengths
GEM Muon System (Alignment Line Layout)
GEM Endcap Muon Chambers
Theta Coverage (Non-Projective)
Theta Coverage (Projective)
Interface Hardware (Magnet/Barrel Muon Module)
Interface Hardware (Middle Chamber to Structure)
Middle Chamber/Structure Assembly (Alignment Lines)
Muon Chamber Installation Approach (Bottom-Up)
Barrel Region Installation (Elevation View)
Barrel Region Installation (Three O'Clock Position)
 p_t Resolution for Constant Transverse Momentum
Interaction Lengths (λ versus θ)
Typical Energy Loss Distribution
Muon Energy Loss versus Momentum
Muon Momentum Resolution versus P
Polar Angle Resolution versus η for fixed p_t
Momentum Resolution (4 figures)
Muon Trigger Strategies
Trigger Efficiency versus Transverse Momentum (3 figures)
Trigger Rates versus ΔN_{strips} (2 figures)
Trigger Logic Schematic
Particle Rates as a Function of Calorimeter Depth (4 figures)
Particle Rates as a Function of Rapidity
Interaction Lengths versus η
Charged Particle Flux as a Function of Rapidity (4 figures)
Charged Particle Flux as a Function of Polar Angle θ
(4 figures)
Charged Particle Rate in Forward Endcap versus Track ID for Four
Calorimeter Depths

MUON SYSTEM

TABLE OF CONTENTS (Continued)

FIGURES:

Charged Particle Rate verses Rapidity in the Barrel/Endcap
Charged Particle Rate verses Calorimeter Depth (2 figures)
GEM Muon Parameters Outside Magnet
Improvement of P_t Resolution with the Addition of an External
Superlayer
Prototype Cathode Strip Chamber
Cathode Strip Chambers Module
Outer Bakelite RPC Cross Section
LSDT Chamber Layout
LSDT Wire Alignment Detail
LSDT Insulating Wire Bridge Detail
8 Layer PDT Chamber
PDT Chamber Details

MUON SYSTEM

TABLE OF CONTENTS (Continued)

TABLES:

Physics Goals
System Parameters
Barrel Region
Geometry
Chamber Parameters
Tracking
Triggering
Channel Segmentation and Count
Tracking
Triggering
End Cap Region
Geometry
Chamber Parameters
Channel Segmentation and Count
Coverage
Total Radiation Length per Superlayer
Endcaps Tracking and Triggering
Forward Angle Region
Intermediate Angle Region
Outer Angle Region
Mechanical Layout of Muon System
PDT & RPC Chamber Data
LSDT & RPC Chamber Data
CSC Baseline Configuration
Momentum Resolution
Trigger
Hadron Punchthrough
System Upgrades
Chamber Technologies
Summary of RPC Properties
Summary of LSDT Properties
Summary of PDT Properties

MUON SYSTEM

MUON SYSTEM

OVERVIEW

The GEM Muon System is based on a large, open solenoidal magnet with an air flux return. Three superlayers of muon tracking chambers will be deployed between the calorimeter and magnet cryostat to reconstruct the sagitta in the magnetic field. Iron flux concentrators will be placed along the central axis of the magnet to create a radial component of the B-field, thereby increasing the bend power at small angles. Muon trajectories will be reconstructed from $|\eta| = 0$ to 2.5 over most of the azimuth. The design goals for the momentum resolution of the system are for $P_t = 500 \text{ GeV}/c$, $\delta P_t/P_t = 5\%$ at $\eta = 0$ and $\approx 12\%$ for $|\eta| = 2.5$. A P_t dependent trigger will be provided, allowing selective access to processes involving high transverse momentum muons.

The magnet will furnish a field at the IP of 0.8 T. It will consist of a superconducting coil of 9.5 m radius, constructed in two parts, each with a coil length of approximately 14.25 m. The coil halves will be separated by 1.5 m. The inner cryostat radius is 9.0 m and constrains the outer radius of the barrel muon chambers. The steel of the field shaper will be located in a cone of half-angle 8.7° , extending from 10 m to 18 m from the IP. There will be no pole pieces.

The resolution of the reconstructed muon momentum will be determined by the chamber resolution, alignment precision within a superlayer and between superlayers, bending power of the magnet (BL^2) and "unreconstructable" fluctuations of the energy loss in the calorimeter. For the barrel region the lever arm, L , at 90° will be ≈ 4.8 m, and in the endcaps, equal to, or larger than, 8.6 m (plus angle factors). Multiple layers of chambers will be required with exacting spatial resolutions (of order $100 \mu\text{m}$ per detector element) and systematic alignment (of order $25 \mu\text{m}$) to reach the desired momentum resolution.

At this time two technologies are being considered for the barrel region, each founded on the drift chamber concept, but differing in operating mode and construction philosophy. One design employs pressurized drift tubes (PDTs), consisting of long aluminum tubes, each supporting a $25\mu\text{m}$ wire anode operated at greater than atmospheric pressure in the proportional mode. The other will be constructed from "U" shaped cathodes, with $100 \mu\text{m}$ wire anodes, operating in the limited streamer mode (LSDT). Triggering in the barrel region will be provided by

Source: F. Taylor
Updated: 7/6/92

MUON SYSTEM

separate resistive plate counters (RPCs). Only cathode strip chambers (CSCs) are being considered for the endcap region. These chambers achieve good resolution by precise analog readout of finely segmented pickup strips. Triggering and beam cross tagging in the endcap region will be provided by the same technology.

An R&D program is underway to choose the best barrel tracking technology and to validate triggering, tracking, and alignment concepts. Full scale chamber prototypes will be tested with cosmic rays at the Texas Test Rig (TTR) in late summer of 1992.

Source: F. Taylor
Updated: 7/6/92

MUON SYSTEM

GEM MUON SYSTEM BASELINE

Source: Frank Nimblett
Charles Stark Draper Lab, Inc.
555 Technology Square
Cambridge, MA 02193
tel. (617) 258-1393
FAX (617) 258-1131
EMail NIMBLETT@DRAPER.COM

Frank E. Taylor
Laboratory of Nuclear Science
Massachusetts Institute of Technology
Cambridge, MA 02139
tel. (617) 253-7249
FAX (617) 253-1755
EMail FET@MITLNS.MIT.EDU

Date: June 28, 1992

Revision: 5

Source: F. Nimblett/F. Taylor
Update: 7/7/92

MUON SYSTEM

(1) Physics Goals:

- (1) Provide muon identification-track penetrating 12 to 14 λ of calorimeter
- (2) Charge assignment of muons
- (3) P_t trigger - both levels 1 and 2
- (4) Beam crossing time marker
- (5) Muon momentum determination from a few GeV/c to a few TeV/c.
Design goal: $\delta P_t/P_t = 5\%$ (12%) at $\eta = 0$ (2.5), for $P_t = 500$ GeV/c.

(2) System Parameters

Barrel Region:

Geometry:

Rmagnet (inner radius of cryostat)	9.0 m
B-field at the IP	0.8 T
Rcalorimeter (outer radius of calorimeter)	3.60 m
Calorimeter thickness at $h = 0$	12 λ
Assumed calorimeter material (hadronic section)	Cu
Number of sectors in F	16
Location of neutron shield	3.60 m < R < 3.70 m
Chamber stay-clear (from neutron shield or magnet cryostat)	6 cm

Chamber Parameters:

(a) Tracking:

Pressurized Drift Tubes (PDT), or
Limited Streamer Drift Tubes (LSDT)

Spatial resolutions:

Chamber single-layer resolution	100 μm (s)
Internal chamber alignment	50 μm
Superlayer-to-superlayer alignment	25 μm
Radiation length/chamber layer	1.1%
Chamber thickness	4 cm/layer
Chamber configuration	8:8:4
Radii of superlayer midplanes	SL 1 = 3.920 m SL 2 = 6.310 m SL 3 = 8.700 m
Barrel lever arm	4.78 m
Half-lengths of superlayers along axis of magnet (Z)	SL 1 = 6.319 m SL 2 = 10.426 m SL 3 = 14.750 m

Source: F. Nimblett/F. Taylor
Update: 7/7/92

MUON SYSTEM

Φ Widths of sectors
SL 1 = 1.485 m
SL 2 = 2.390 m
SL 3 = 3.296 m

Coverage:
Polar angle $29.6^\circ < \theta < 85.8^\circ$
Pseudorapidity $0.074 < \eta < 1.33$
Azimuthal angle 95.3%

(b) Tracking:

Resistive Plate Counters (RPC)
Nonbend plane segment widths
SL1 = 3.9 cm
SL2 = 6.5 cm
SL3 = 8.9 cm
Nonbend plane channel count 16,000

(c) Triggering:

Resistive Plate Counters (RPC)
Radial locations of RPCs (chamber midplane)
SL 1 = 4.15 m
SL 2 = 6.08 m
SL 3 = 8.54 m
Radiation length/RPC superlayer (2 gaps) 3 %
Chamber thickness for 2 gap package 3.3 cm
Total radiation length per superlayer
SL 1 = 11.8% (8-layer)
SL 2 = 11.8% (8-layer)
SL 3 = 7.4% (4-layer)

Channel segmentation and count:

(a) Tracking:

PDT Option
Bend plane segment width (all superlayers) 3.81 cm
Number bend plane tracking channels 110,000
LSDT Option
Bend plane segment width (all superlayers) 2.5 cm
Number bend plane tracking channels 91,000

(b) Triggering:

Resistive Plate Counters (RPC)
Bend plane segment width 1.3 cm
Number of bend plane trigger channels 17,000
Double hit rate at $L = 10^{33}/\text{cm}^2\text{sec}$ <10 % in bend plane

Source: F. Nimblett/F. Taylor
Update: 7/7/92

MUON SYSTEM

Endcap region:

Geometry:

B-field at IP	0.8 T
Length of magnet cryostat	15 m
Z-separation of coils	1.5 m
Flux concentrator (FC):	
Z _{front}	10.0 m
Z _{rear}	18.0 m
OD-half angle of steel	8.7° (may change)
ID	0.4 m
Z _{calorimeter} (half-length of calorimeter along beam axis)	5.50 m
Calorimeter thickness at $\eta = 2.5$	14 λ
Z _{max}	16.5 m
Number of sectors in Φ	16
Location of neutron shield 10 cm behind calorimeter	5.50 m < Z < 5.60 m
Chamber stayclear	6 cm

Chamber Parameters:

Cathode Strip Chambers (CSC for both tracking and triggering)	
Spatial resolutions:	
Chamber single-layer resolution	75 μm (σ)
Chamber internal alignment	50 μm
Superlayer-to-superlayer alignment	25 μm
Radiation length/chamber layer	3.75%
Chamber thickness	5 cm / layer
Timing resolution (for trigger)	< 10 ns for "OR" of 4

Channel segmentation and count:

For all θ -segments	
Bend plane segment width	5 mm (at middle)
Bend plane channel count	242,000
Nonbend plane segment width	2.5 cm
Nonbend plane channel count	30,000
Single channel rate at $L = 10^{33}/\text{cm}^2\text{sec}$	< 100 Hz
Occupancy for "OR" of 7 strips at $L = 10^{34}/\text{cm}^2\text{sec}$	< 3 %

Coverage:

Polar angle	$9.75^\circ < \theta < 27.71^\circ$
Pseudorapidity	$1.40 < \eta < 2.46$
Azimuthal angle	100%

Total radiation length per superlayer:

For non-overlap regions	SL 1 = 1.6%
	SL 2 = 1.6%
	SL 3 = 1.6%

Source: F. Nimblett/F. Taylor
Update: 7/7/92

MUON SYSTEM

Endcaps - Tracking and Triggering:

- (a) Forward angle region: $9.75^\circ < \theta < 11.45^\circ$ ($2.30 < \eta < 2.46$)
- | | |
|--------------------------------|----------------|
| Chamber configuration | 4:8:4 |
| Average Z location of chambers | SL 1 = 6.78 m |
| | SL 2 = 11.43 m |
| | SL 3 = 16.08 m |
| Average lever arm | 9.3 m |
- (b) Intermediate angle region: $1.45^\circ < \theta < 17.01^\circ$ ($1.90 < \eta < 2.30$)
- | | |
|--------------------------------|----------------|
| Chamber configuration | 4:4:4 |
| Average Z location of chambers | SL 1 = 5.94 m |
| | SL 2 = 11.43 m |
| | SL 3 = 16.08 m |
| Average Lever arm | 10.14 m |
- (c) Outer angle region: $17.01^\circ < \theta < 27.71^\circ$ ($1.40 < \eta < 1.90$)
- | | |
|--------------------------------|----------------|
| Chamber configuration | 4:4:4 |
| Average Z location of chambers | SL 1 = 5.94 m |
| | SL 2 = 10.13 m |
| | SL 3 = 14.58 m |
| Average lever arm | 8.64 m |

MUON SYSTEM

(3) Mechanical Layout of Muon System

(person responsible: Frank Nimblett - Draper Labs)

The Muon System of the GEM detector is constructed in two sections: the Barrel Region, covering polar angles in the range of 29° to 90° ; and the Endcap Region, covering angles down to 9.5° . The Barrel Region fills the volume bounded on the inside by the dimensions of the neutron shield surrounding the calorimeter, and the solenoid magnet inner dimensions. The Endcap region is bounded by the end the endcap calorimeter, the flux concentrator, and the end of the solenoidal magnet.

The three super-layers in each region are supported by structures partitioned in $1/16$ of full azimuth. Each of these regions is called a "sector". The sectors must be sufficiently rigid and instrumented with precision alignment devices such that the alignment tolerances and stability of the muon system can be met. At this time the details of the support structures and their attachment points to the magnet are being determined. Also at issue is the construction and installation concept.

Fig. 3-1 (a): The quadrant layout of the muon system is shown. Featured are the chamber support structures, the flux concentrator, and shielding for the endcap chambers.

Fig. 3-1 (b): Plan view of the support structure.

Fig. 3-1 (c): End view of support structure.

Fig. 3-2: The locations of barrel and endcap chambers are shown, (a) plan view, (b) endview.

Fig. 3-3: Deleted

Fig. 3-4: GEM muon system alignment line layout

Fig. 3-5: Endcap chambers showing the overlap petal arrangement. Note that this design is driven by the goal of obtaining full θ and Φ coverage.

Fig. 3-6 (a): θ -acceptance of GEM muon system (non-projective).

Fig. 3-6 (b): θ -acceptance of GEM muon system (projective).

Source: F. Nimblett/F. Taylor
Update: 7/7/92

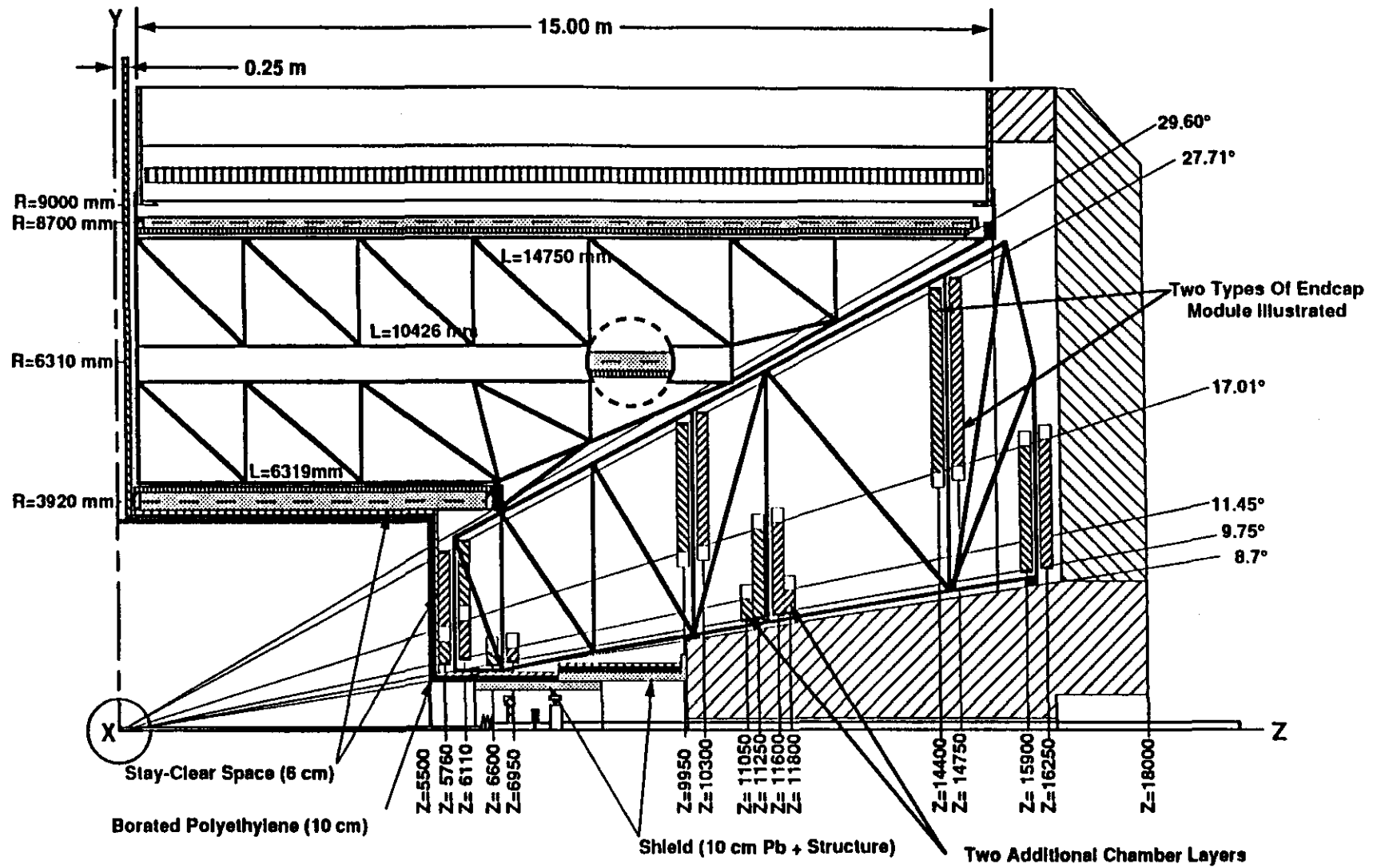
MUON SYSTEM

- Fig. 3-7: Details of mounting of the support structure to magnet and chamber connection to support structure.
- Fig. 3-8: Details of mounting of the middle chamber to support structure.
- Fig. 3-9: Middle chamber/structure assembly showing alignment lines on central detector support end.
- Fig. 3-10: Muon installation diagram showing "bottom up" approach.
- Fig. 3-11: Barrel region installation (elevation view)
- Fig. 3-12: Barrel region installation (three o'clock position)

Tables of Chamber Mechanical Specifications:

Barrel Region:

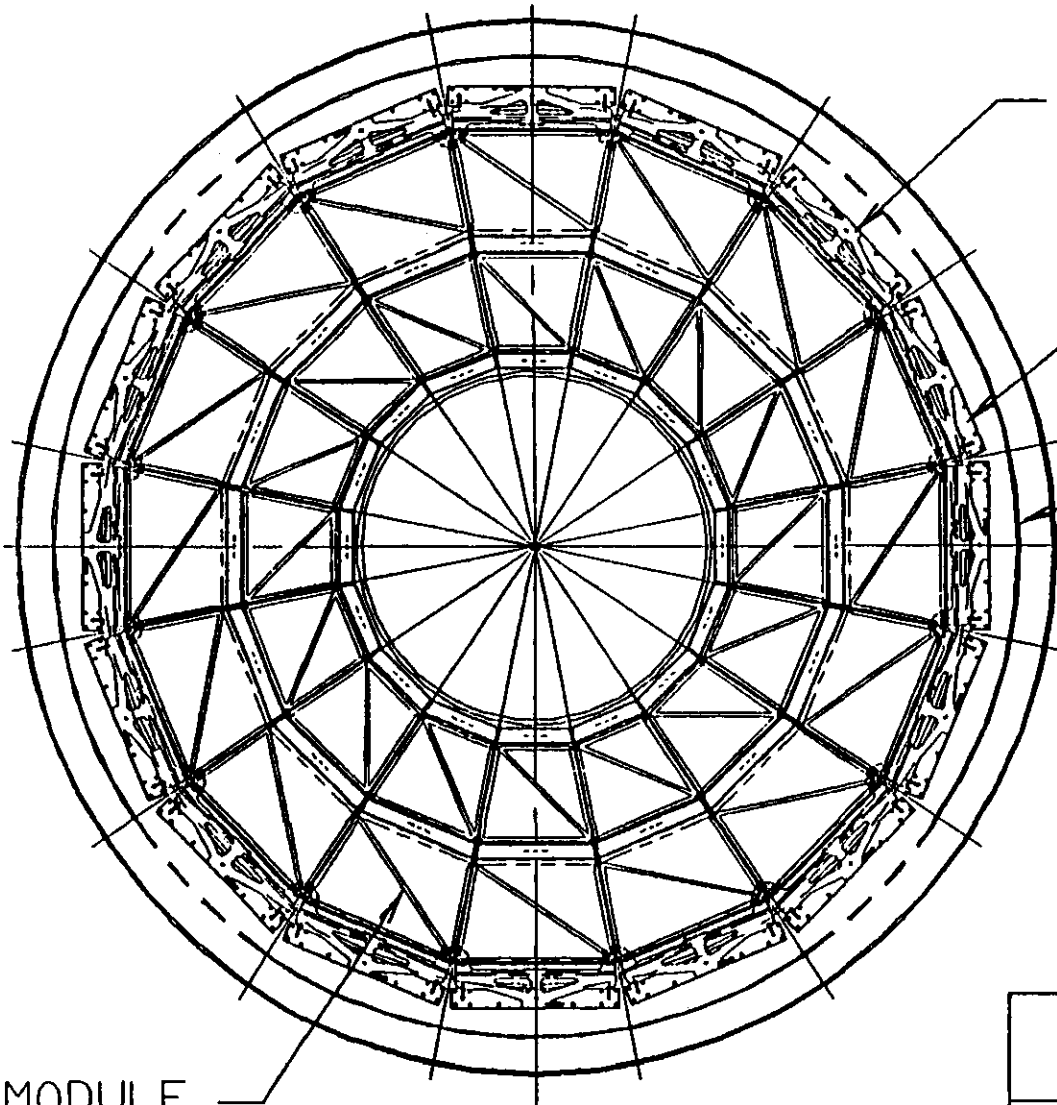
- (a) PDT and RPC
- (b) LSDT and RPC
- (c) CSC Endcaps: (Scott Whitaker - Boston U.)



GEM MUON SYSTEM (BASELINE I)

Fig. 3.1 a

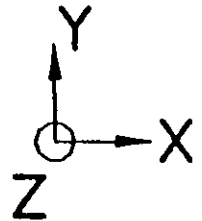
Draper Laboratory	
GEM Muon System (BASELINE) 4/8/4 Layers 9.75° to 11.45°	
Drawn By: F. Nimblett	Rev (1)
Dwg. No: GMU0009	6/25/92
Approved by:	



MODULE ATTACHMENT
PLATE

MAGNET INTERFACE
PLATE

MAGNET
END PLATE



MUON MODULE
(ONE OF 16)
INDEPENDENTLY
MOUNTED TO MAGNET
END PLATES

Fig. 3.1 b

THE CHARLES STARK DRAPER LABORATORY INC CAMBRIDGE, MASSACHUSETTS. 02139			
DRAWN BY B.D BIGGIO	APPD BY	DATE 30JUN92	
GEM BARREL REGION MUON SYSTEM (END VIEW)			
SIZE A	FSCM NO. 51993	DRAWING NO. 292932-01	REV -
SCALE NONE		SHEET 1 OF	

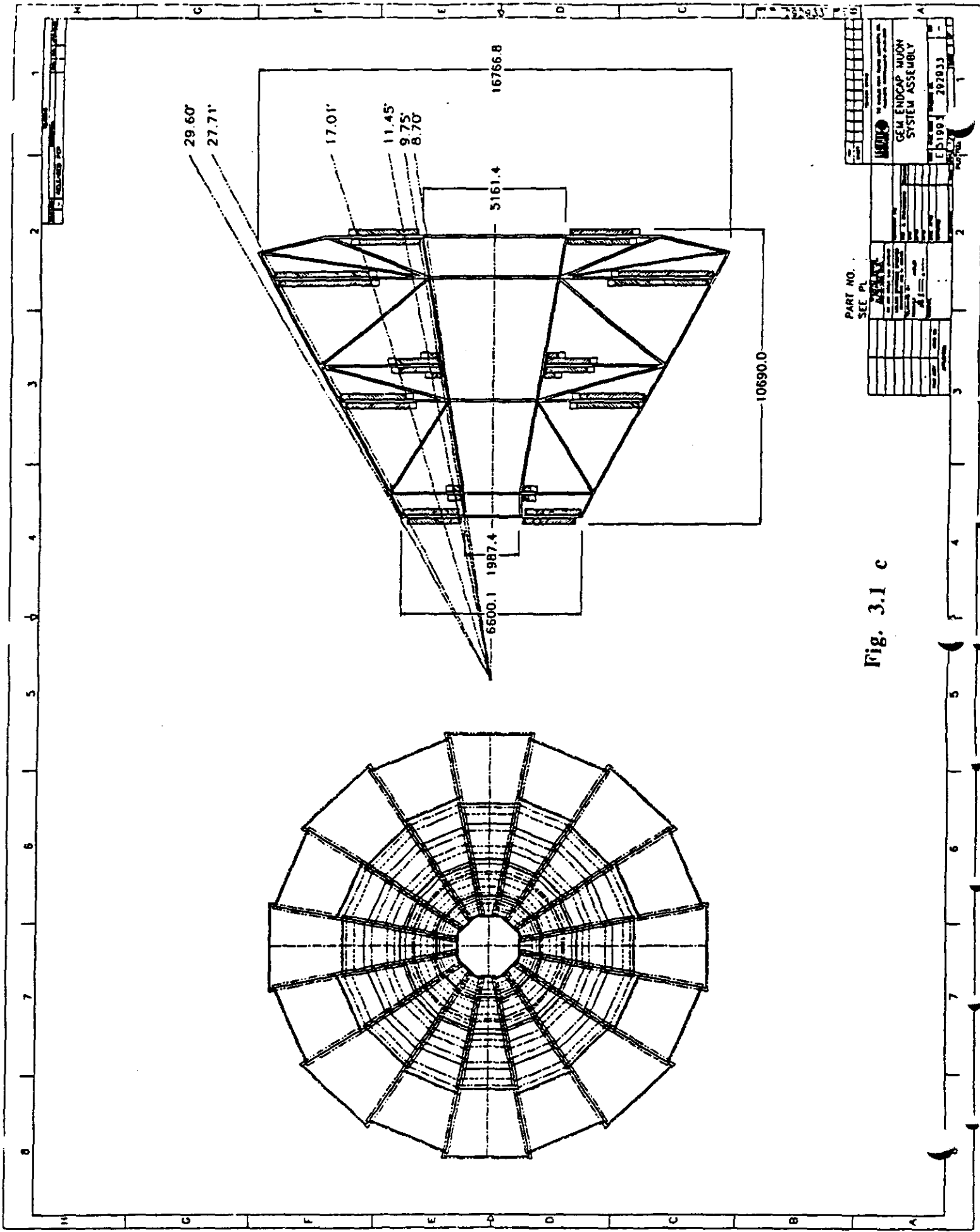
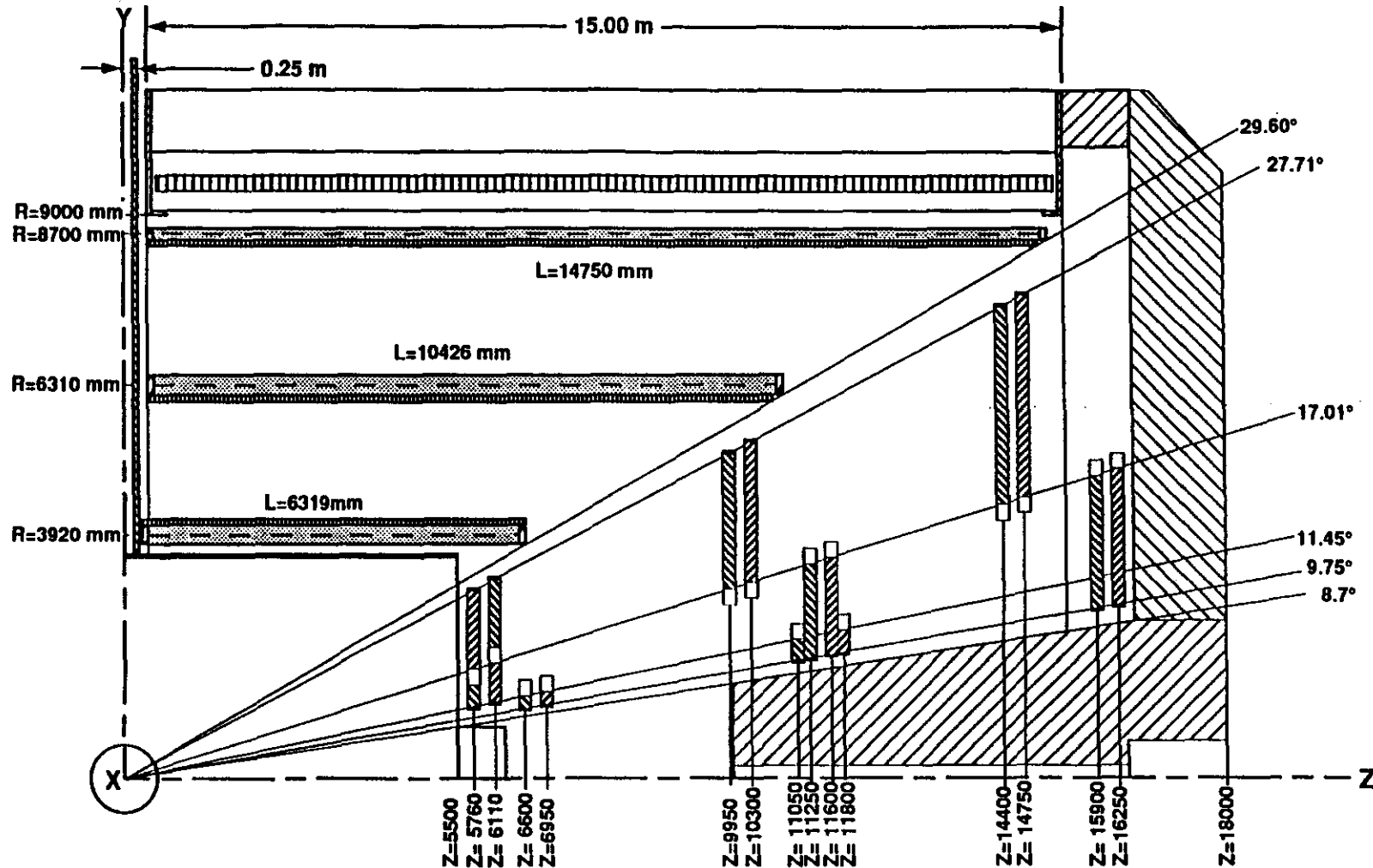


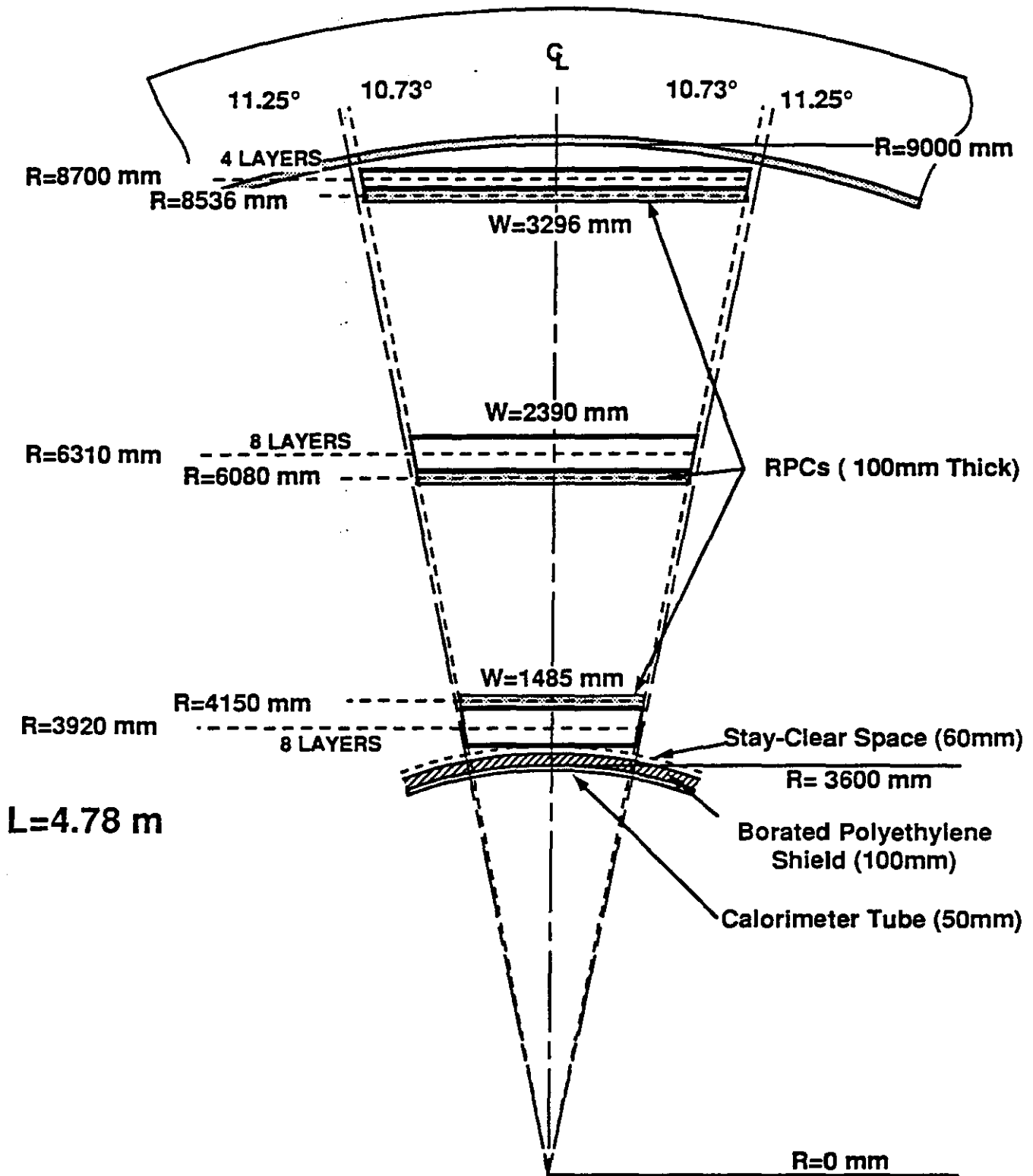
Fig. 3.1 c



**GEM MUON SYSTEM CHAMBER LAYOUT
BASELINE I**

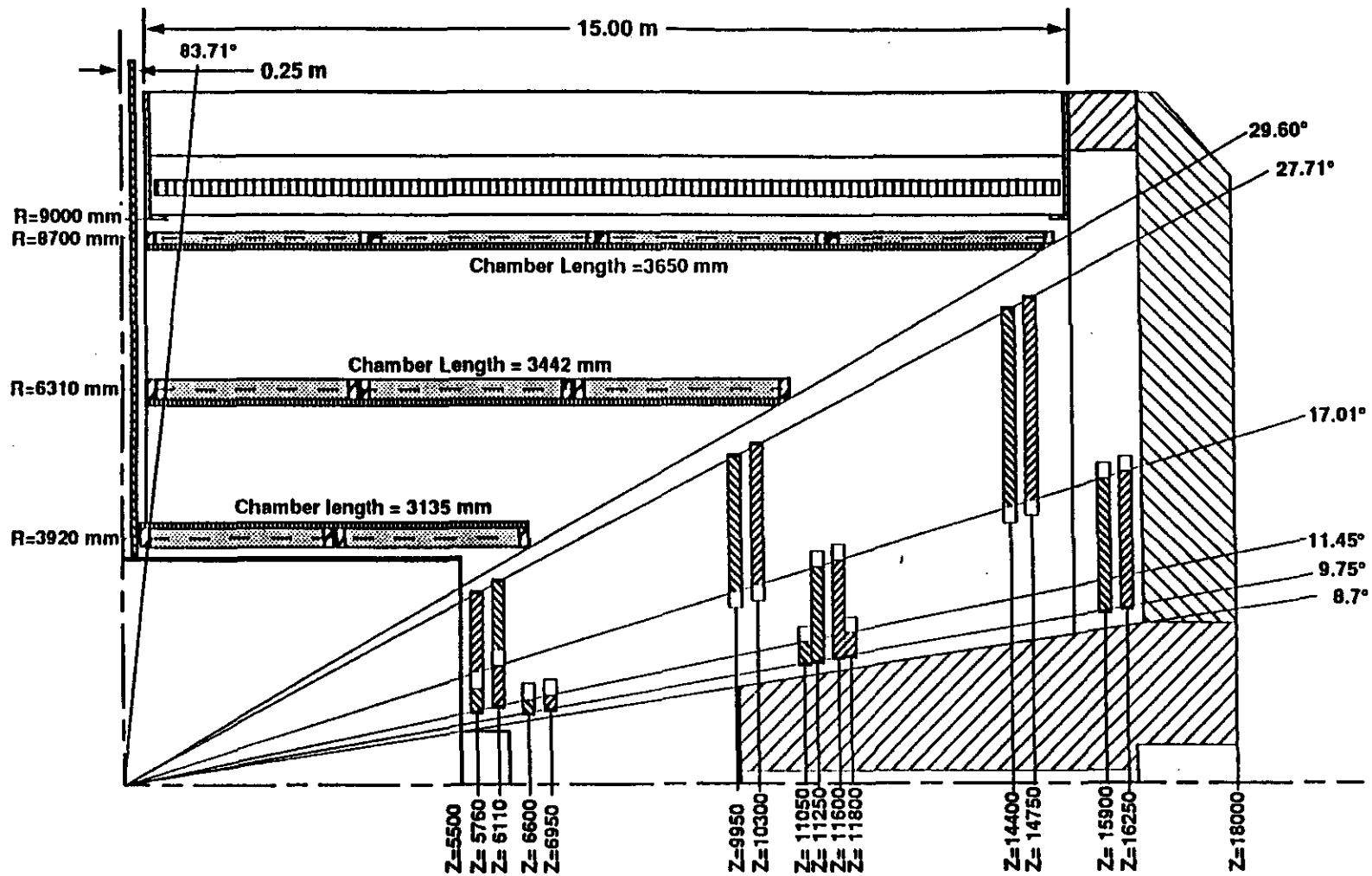
Fig. 3.2 a

Draper Laboratory	
GEM Muon System Chamber Layout	
Drawn By: F. Nimblett	Rev (1)
Dwg. No: GMU0010	6/25/92
Approved by:	



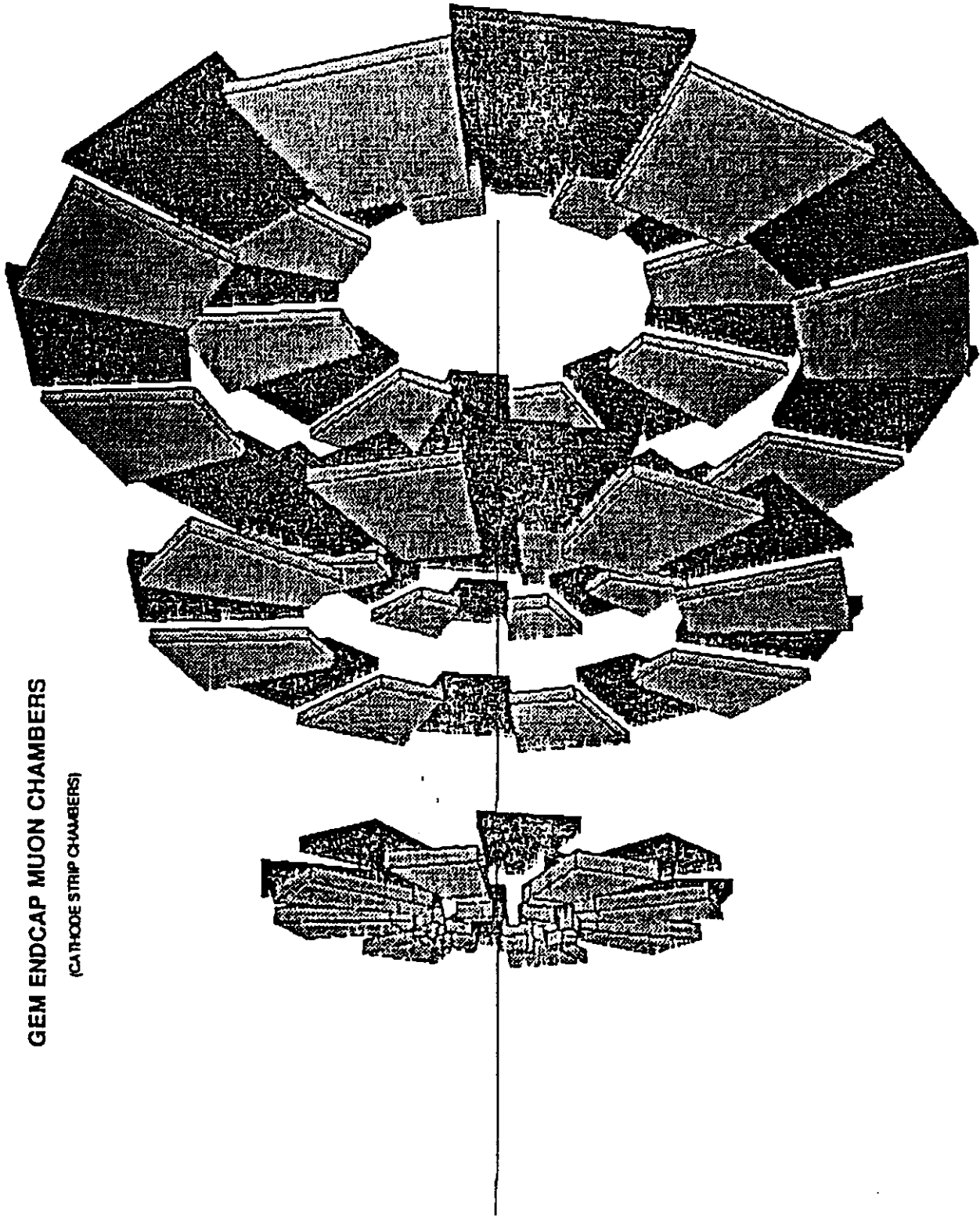
GEM BARREL REGION (PDT)
 (Chamber Endview)
BASELINE I

Drexler Laboratory	
GEM Muon System (endview)	
Drawn By: F. Nimblett	Rev (2)
Dwg. No: GMU0002	6/26/92
Approved by:	



**GEM MUON SYSTEM CHAMBER LAYOUT
 BASELINE I
 (2,3,4 PDT Chambers per Layer)**

Draper Laboratory	
GEM Muon System PDT Baseline Chamber Layout	
Drawn By: F. Nimblett	Rev (-)
Dwg. No: GMU0014	6/30/92
Approved by:	



GEM ENDCAP MUON CHAMBERS
(CATHODE STRIP CHAMBERS)

Fig. 3.5

Theta Coverage for 2,3,4 PDT Chambers per Layer (Non-Projective)

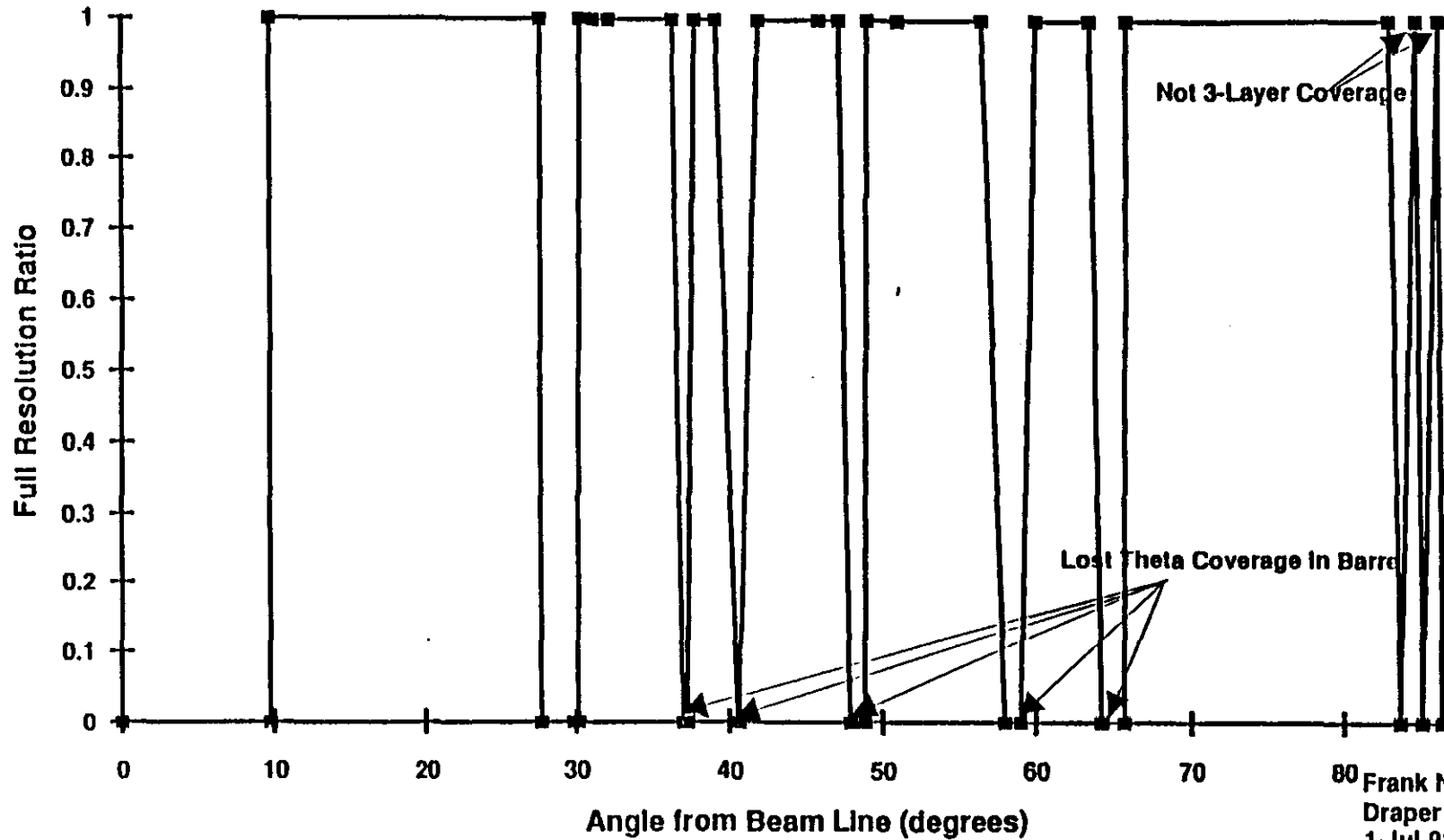


Fig. 3-6 a

Frank Nimblett
Draper Laboratory
1-Jul-92

Theta Coverage for 2,3,3 PDT Chambers per Layer (Projective)

Mechanics on Chamber Ends is 150 mm and space between Chambers is 50 mm

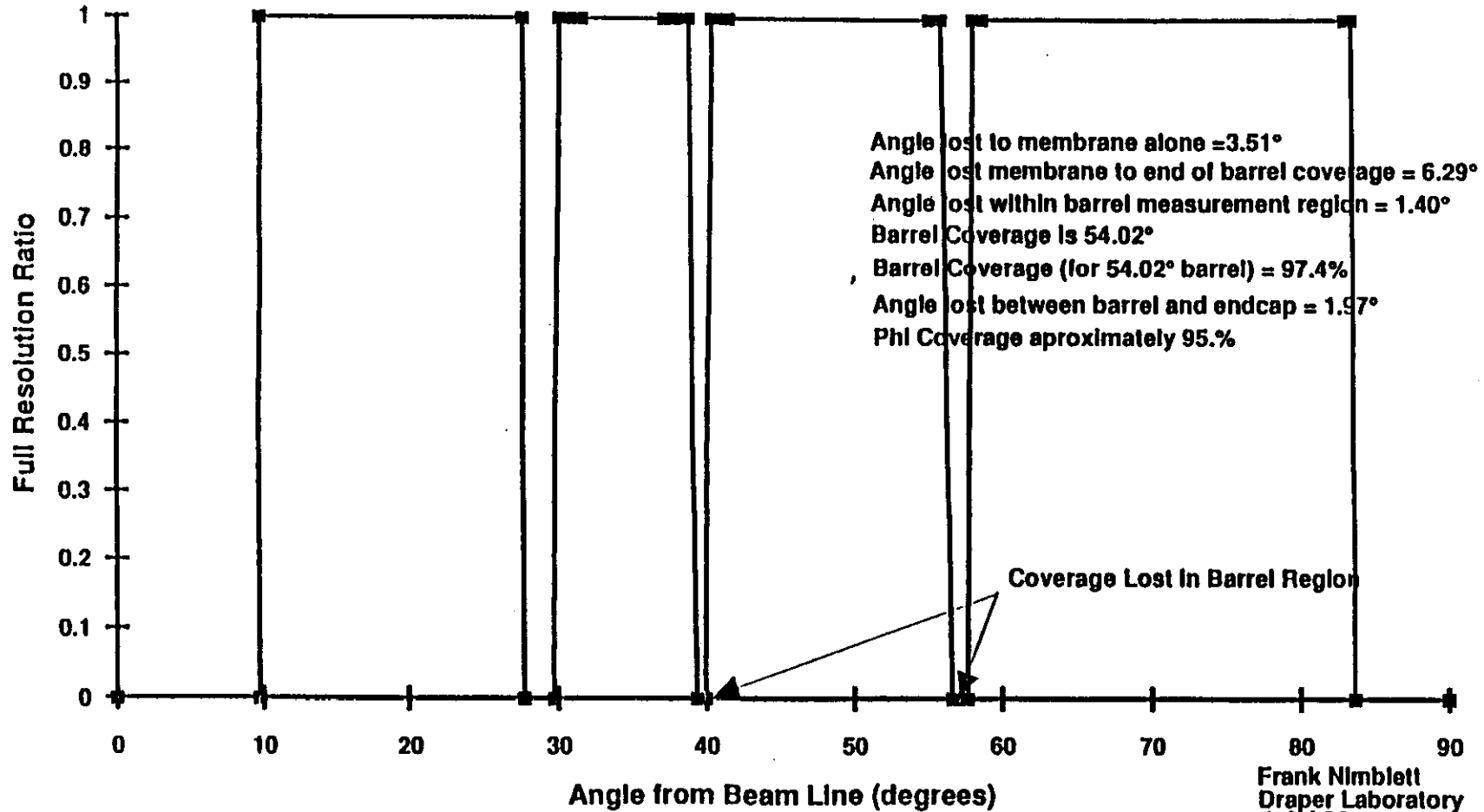


Fig. 3-6 b

Frank Nimblett
Draper Laboratory
1-Jul-92

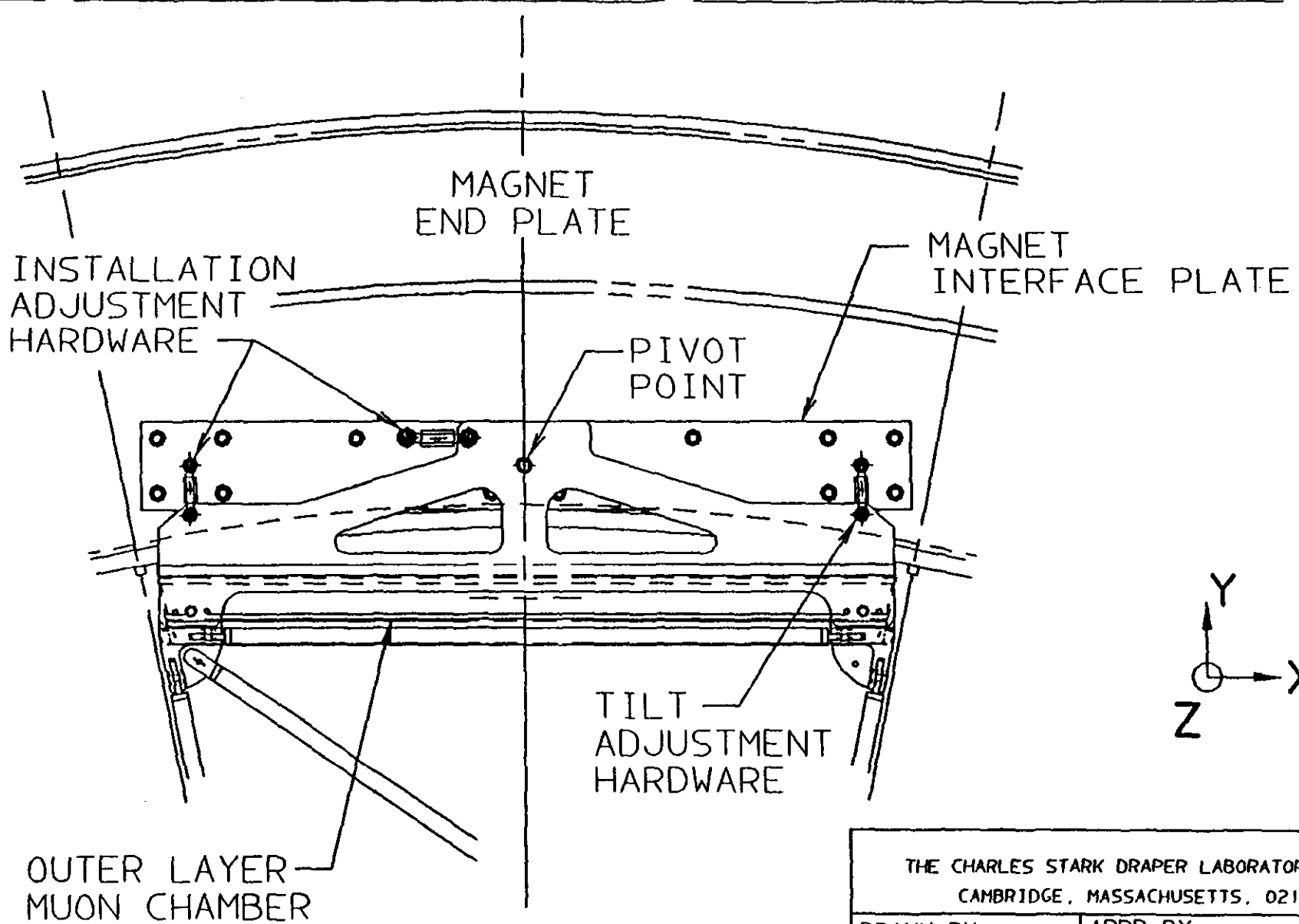
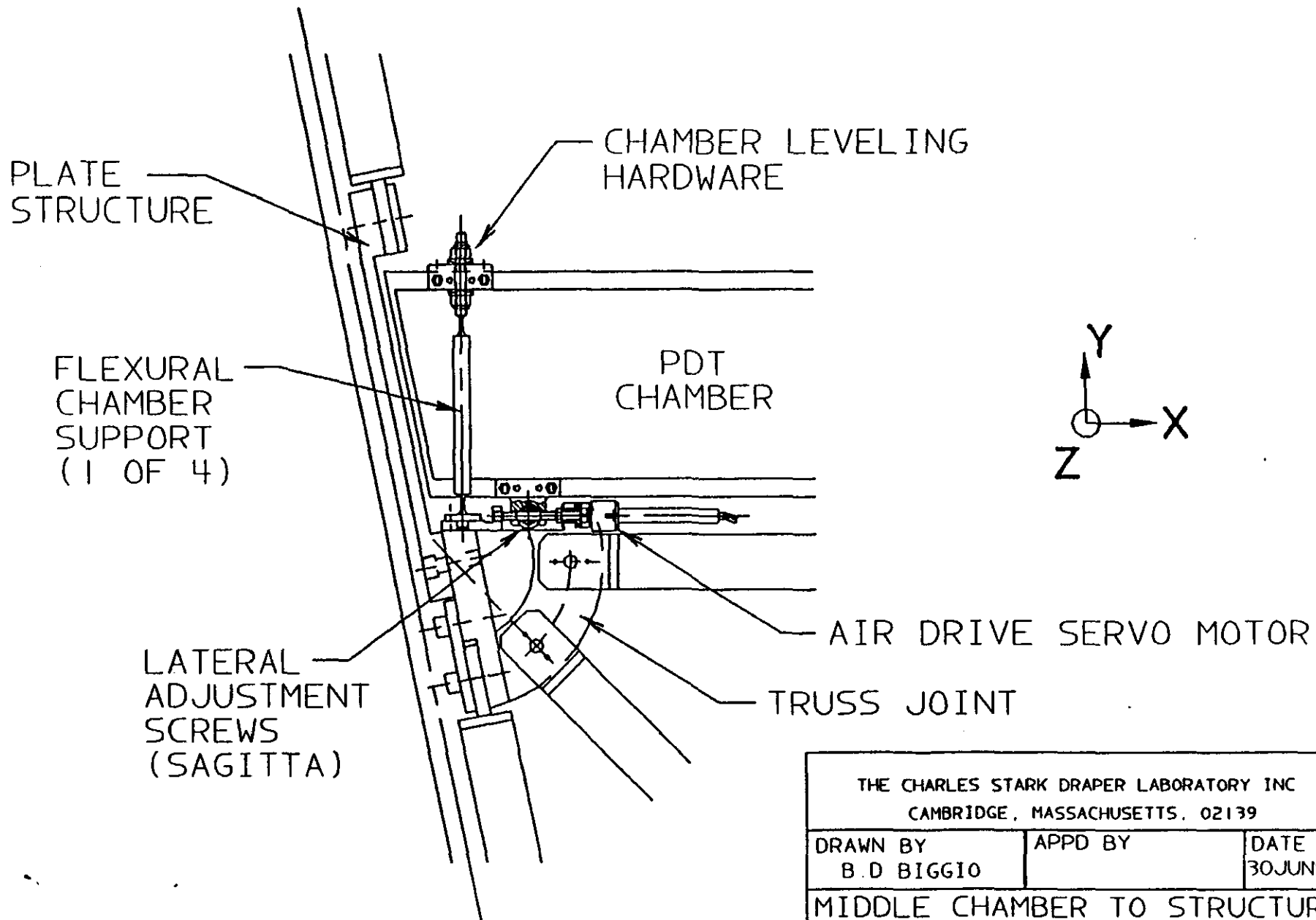
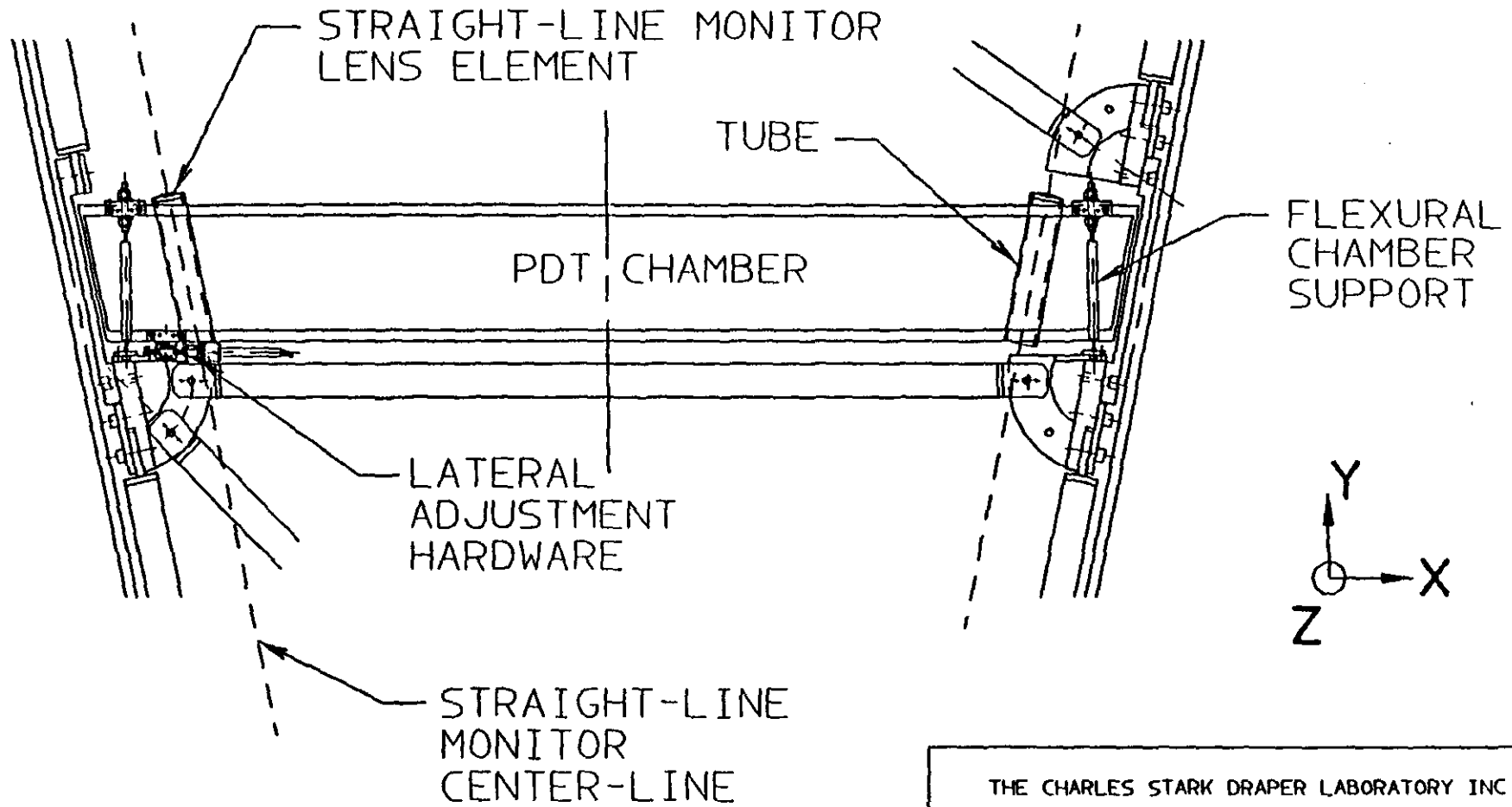


Fig. 3.7

THE CHARLES STARK DRAPER LABORATORY INC CAMBRIDGE, MASSACHUSETTS, 02139			
DRAWN BY B D BIGGIO	APPD BY	DATE 30JUN92	
INTERFACE HARDWARE (MAGNET/BARREL MUON MODULE)			
SIZE A	FSCM NO. 51993	DRAWING NO. 292932-02	REV -
SCALE NONE		SHEET	OF



THE CHARLES STARK DRAPER LABORATORY INC CAMBRIDGE, MASSACHUSETTS. 02139			
DRAWN BY B. D. BIGGIO		APPD BY	DATE 30JUN92
MIDDLE CHAMBER TO STRUCTURE (INTERFACE HARDWARE)			
SIZE A	FSCM NO. 51993	DRAWING NO. 292929-01	REV -
SCALE NONE		SHEET 1 OF	

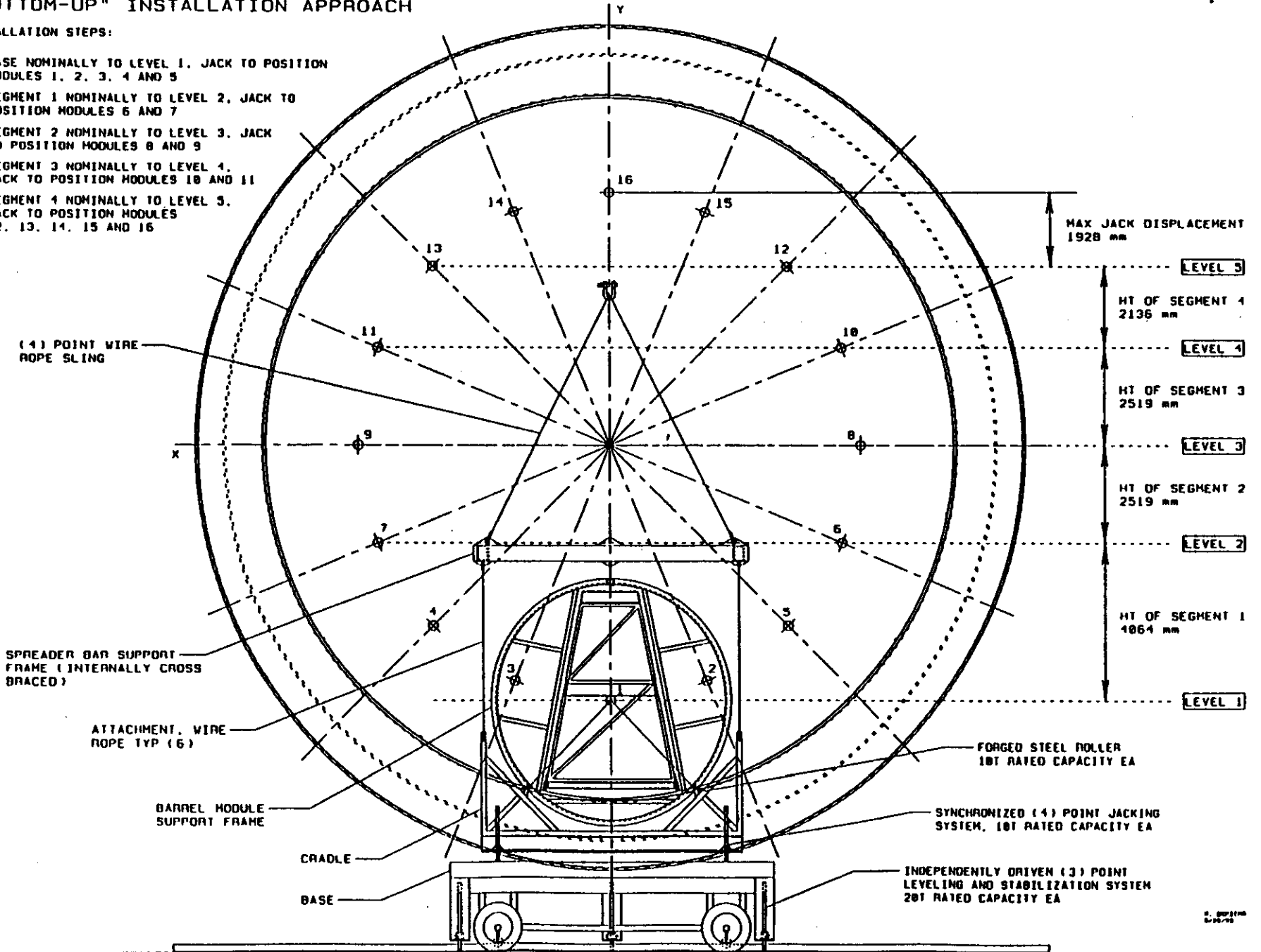


THE CHARLES STARK DRAPER LABORATORY INC CAMBRIDGE, MASSACHUSETTS. 02139			
DRAWN BY B. D. BIGGIO		APPD BY	DATE 30 JUN 92
MIDDLE CHAMBER/STRUCTURE ASSY (BARREL REGION-PDT CHAMBERS) ALIGNMENT LINES ON MEMBRANE END			
SIZE	FSCM NO.	DRAWING NO.	REV.
A	51993	292929-02	-
SCALE NONE			SHE 1 OF

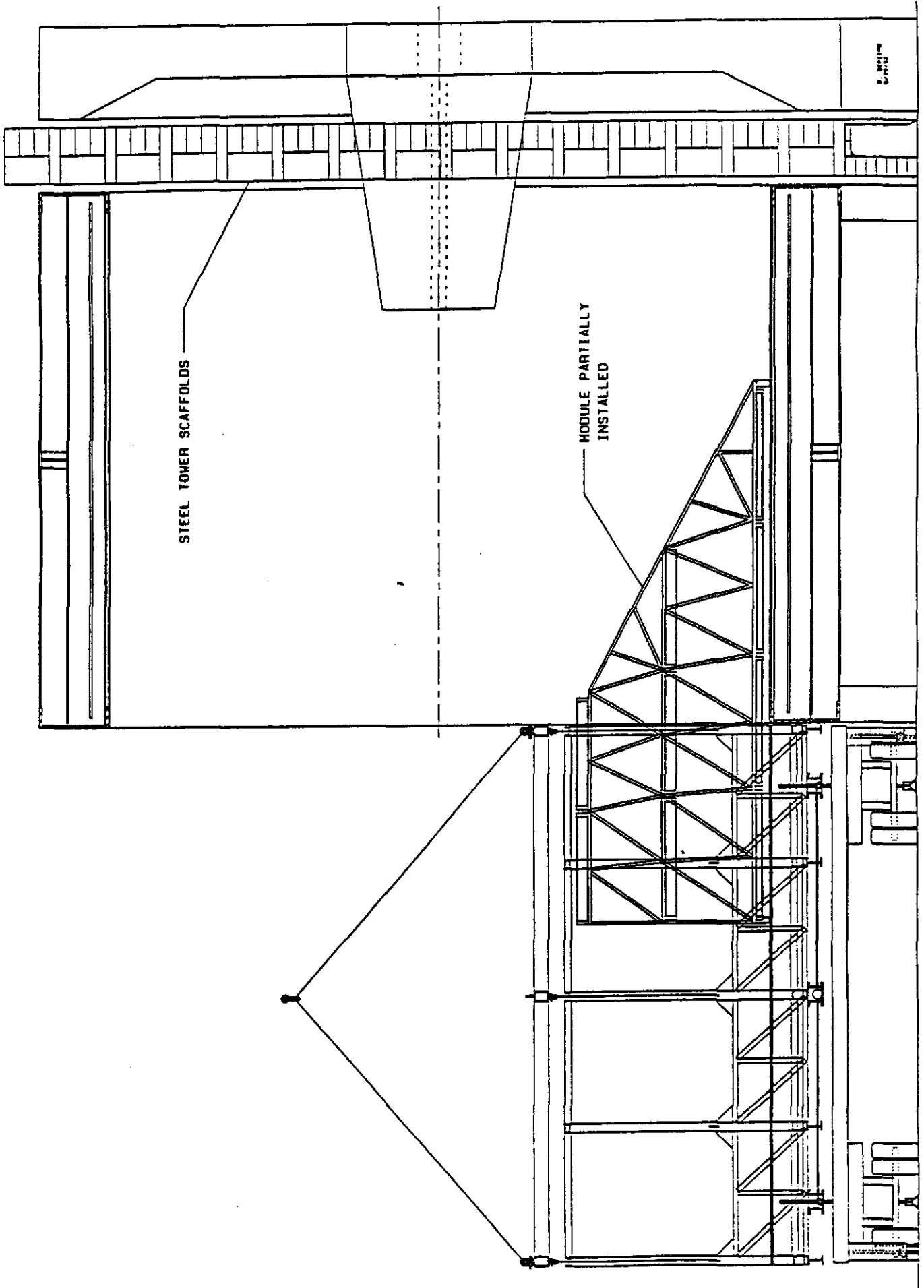
"BOTTOM-UP" INSTALLATION APPROACH

INSTALLATION STEPS:

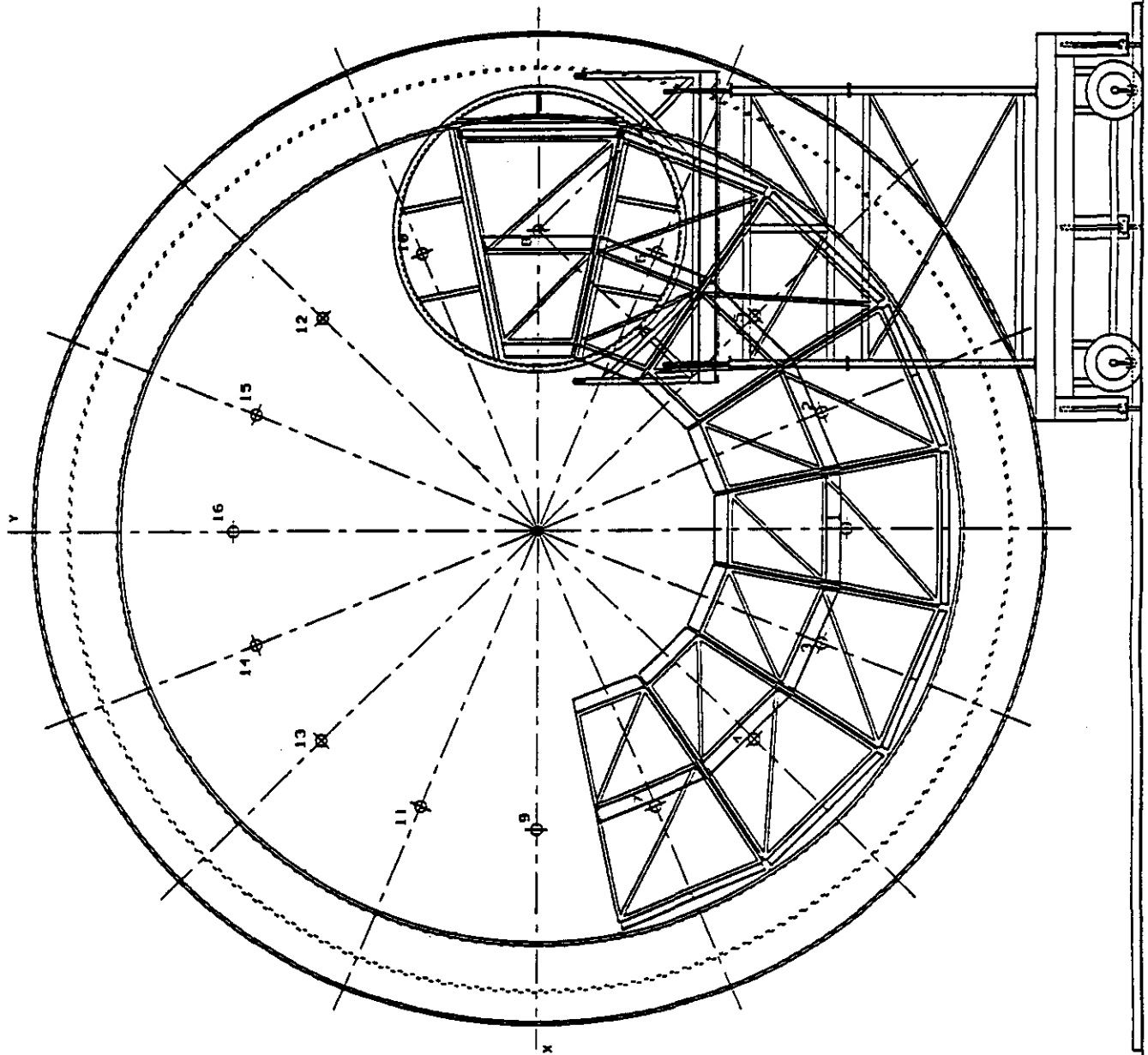
1. BASE NOMINALLY TO LEVEL 1. JACK TO POSITION MODULES 1, 2, 3, 4 AND 5
2. SEGMENT 1 NOMINALLY TO LEVEL 2. JACK TO POSITION MODULES 6 AND 7
3. SEGMENT 2 NOMINALLY TO LEVEL 3. JACK TO POSITION MODULES 8 AND 9
4. SEGMENT 3 NOMINALLY TO LEVEL 4. JACK TO POSITION MODULES 10 AND 11
5. SEGMENT 4 NOMINALLY TO LEVEL 5. JACK TO POSITION MODULES 12, 13, 14, 15 AND 16



BARREL REGION INSTALLATION
(ELEVATION VIEW)



BARREL REGION INSTALLATION
(3-0' CLOCK POSITION)



E. J. ...
S. ...

PDT & RPC CHAMBER DATA

PDT GAS VOLUME	METER^3	PDT CHAMBER WEIGHTS.	KILOS
LAYER 1 ONE MODULE (2 CHAMBERS)	1.99	LAYER 1 ONE MODULE (2 CHAMBERS)	843
LAYER 2 ONE MODULE (3 CHAMBERS)	5.82	LAYER 2 ONE MODULE (3 CHAMBERS)	2113
LAYER 3 ONE MODULE (4 CHAMBERS)	5.44	LAYER 3 ONE MODULE (4 CHAMBERS)	2249
TOTAL PER MODULE	13.25	TOTAL PER MODULE	5205
LAYER 1, 1 HALF	31.81	LAYER 1, 1 HALF	13492
LAYER 2, 1 HALF	93.13	LAYER 2, 1 HALF	33805
LAYER 3, 1 HALF	87.02	LAYER 3, 1 HALF	35986
TOTAL PER HALF	211.95	TOTAL PER HALF	83283
LAYER 1- TOTAL	63.61	LAYER 1- TOTAL	26984
LAYER 2 -TOTAL	186.25	LAYER 2 -TOTAL	67610
LAYER3 -TOTAL	174.04	LAYER3 -TOTAL	71972
TOTAL SYSTEM	423.90	TOTAL CHAMBER WEIGHTS	166567

PDT N2 GAS VOL	METER^3	PDT CHANNEL COUNT	CHANNELS
LAYER 1 ONE MODULE (2 CHAMBERS)	0.28	LAYER 1 ONE MODULE (2 CHAMBERS)	600
LAYER 2 ONE MODULE (3 CHAMBERS)	0.87	LAYER 2 ONE MODULE (3 CHAMBERS)	1464
LAYER 3 ONE MODULE (4 CHAMBERS)	0.88	LAYER 3 ONE MODULE (4 CHAMBERS)	1368
TOTAL PER MODULE	2.02	TOTAL PER MODULE	3432
LAYER 1, 1 HALF	4.43	LAYER 1, 1 HALF	9600
LAYER 2, 1 HALF	13.88	LAYER 2, 1 HALF	23424
LAYER 3, 1 HALF	14.05	LAYER 3, 1 HALF	21888
TOTAL PER HALF	32.36	TOTAL PER HALF	54912
LAYER 1- TOTAL	8.87	LAYER 1- TOTAL	19200
LAYER 2 -TOTAL	27.75	LAYER 2 -TOTAL	46848
LAYER3 -TOTAL	28.10	LAYER3 -TOTAL	43776
TOTAL SYSTEM	64.72	TOTAL CHANNEL COUNT	109824

RPC GAS VOLUME	METER^3	RPC CHAMBER WEIGHTS	KILOS
LAYER 1, 1 MODULE, 2 RPCs	0.036	LAYER 1, 1 MODULE 2 RPCs	84
LAYER 2, 1 MODULE, 3 RPCs	0.105	LAYER 2, 1 MODULE, 3 RPCs	243
LAYER 3, 1 MODULE, 4 RPCs	0.192	LAYER 3, 1 MODULE, 4 RPCs	442
TOTAL PER MODULE	0.334	TOTAL PER MODULE	769
LAYER 1, 1 HALF	0.582	LAYER 1, 1 HALF	1340
LAYER 2, 1 HALF	1.685	LAYER 2, 1 HALF	3880
LAYER 3, 1 HALF	3.075	LAYER 3, 1 HALF	7080
TOTAL PER HALF	5.342	TOTAL PER HALF	12300
LAYER 1- TOTAL	1.164	LAYER 1- TOTAL	7761
LAYER 2 -TOTAL	3.371	LAYER 2 -TOTAL	14160
LAYER3 -TOTAL	6.150	LAYER3 -TOTAL	24500
TOTAL RPC SYSTEM	10.684	TOTAL RPC WEIGHT	46520

LSDT & RPC CHAMBER DATA

LSDT GAS VOLUME	METER^3	LSDT CHANNEL COUNT	CHANNELS
LAYER 1 ONE SEGMENT (4 CHAMBERS)	1.48	LAYER 1 ONE SEGMENT (4 CHAMBERS)	429
LAYER 2 ONE SEGMENT (6 or 12 CHAMBERS)	4.19	LAYER 2 ONE SEGMENT (12 CHAMBERS)	1422
LAYER 3 ONE SEGMENT (4 or 8 CHAMBERS)	4.14	LAYER 3 ONE SEGMENT (8 CHAMBERS)	996
TOTAL PER SEGMENT	9.81	TOTAL PER SEGMENT	2847
LAYER 1 ONE HALF	23.67	LAYER 1 ONE HALF	6864
LAYER 2 ONE HALF	66.98	LAYER 2 ONE HALF	22752
LAYER 3 ONE HALF	66.31	LAYER 3 ONE HALF	15936
TOTAL PER HALF	156.97	TOTAL PER HALF	45552
LAYER 1 TOTAL	47.34	LAYER 1 TOTAL	13728
LAYER 2 TOTAL	133.97	LAYER 2 TOTAL	45504
LAYER 3 TOTAL	132.62	LAYER 3 TOTAL	31872
TOTAL SYSTEM	313.93	TOTAL CHANNELS	91104

LSDT CHAMBER WEIGHTS.	KILOS
LAYER 1 ONE SEGMENT (4 CHAMBERS)	952
LAYER 2 ONE SEGMENT (6 or 12 CHAMBERS)	2481
LAYER 3 ONE SEGMENT (4 or 8 CHAMBERS)	2371
TOTAL PER SEGMENT	5804
LAYER 1 ONE HALF	15227
LAYER 2 ONE HALF	39701
LAYER 3 ONE HALF	37936
TOTAL PER HALF	92863
LAYER 1 TOTAL	30453
LAYER 2 TOTAL	79401
LAYER 3 TOTAL	75871
TOTAL CHAMBER WEIGHTS	185726

RPC GAS VOLUME	METER^3	RPC CHAMBER WEIGHTS	KILOS
LAYER 1 1 SEG. 2 RPCs	0.019	LAYER 1 1 SEG. 2 RPCs	85
LAYER 2 1 SEG. 3 RPCs	0.034	LAYER 2 1 SEG. 3 RPCs	235
LAYER 3 1 SEG. 4 RPCs	0.049	LAYER 3 1 SEG. 4 RPCs	447
TOTAL PER SEG.	0.101	TOTAL PER SEG.	768
LAYER 1 1 HALF	0.297	LAYER 1 1 HALF	1368
LAYER 2 1 HALF	0.545	LAYER 2 1 HALF	3765
LAYER 3 1 HALF	0.776	LAYER 3 1 HALF	7149
TOTAL PER HALF	1.618	TOTAL PER HALF	12282
LAYER 1 TOTAL	0.594	LAYER 1 TOTAL	7530
LAYER 2 TOTAL	1.090	LAYER 2 TOTAL	14299
LAYER 3 TOTAL	1.553	LAYER 3 TOTAL	24565
TOTAL SYS.GAS	3.237	TOTAL RPC WEIGHT	46394

MUON SYSTEM

(4) Momentum Resolution

(Jim Sullivan, Larry Rosenson, Frank Taylor - MIT; Roger McNeil - LSU)

The muon momentum is reconstructed by the 3-point sagitta method (neglecting various angle factors), where the sagitta is given in terms of measured quantities as:

$$S = (y_1 + y_3)/2 - y_2 = qBL^2/8P.$$

y_1 , y_2 , and y_3 are the bend-plane locations of the muon trajectory in the three super-layers, B is the magnetic induction, L is the path length between super-layers 1 and 3, q is the muon charge, and P is the momentum. Hence good resolution is achieved for a large L even at a modest B . To set the scale for the momentum reconstruction, $S = 1.5$ mm for $P_t = 500$ GeV/c. If we are to achieve a 5% measure of this momentum our total error budget should be no larger than $75\mu\text{m}$. Hence the chambers should have good resolution and the should be aligned superlayer-to-superlayer to of order $25\mu\text{m}$.

Of importance to the resolution at low energies is the fluctuation of the energy loss in the calorimeter. This has been calculated by McNeil [1] and was used here to estimate the effect.

Figure Captions:

Fig. 4-1.1: The resolution for constant transverse momentum, P_t is shown as a function of pseudo-rapidity, $|\eta|$. Note that this configuration meets the design specification at $P_t = 500$ GeV/c for $\eta = 0$, but is somewhat worse than desired in the forward region. Further work is needed in this area to find a practical arrangement of chambers while maintaining sufficient bend power.

Fig. 4-2.1: The number of interaction lengths λ for our assumed calorimeter model. [Note that this model is a crude rendition based on the geometry of the LA calorimeter.]

Fig. 4-2.2: Typical energy loss distributions are shown. The calculation was performed over the muon energy range of 10 GeV to 1 TeV.

Fig. 4-2.3: Muon energy loss and fluctuations for 11.8 and 14.4 λ as a function of momentum. These were calculated with a cut to limit large fluctuations and therefore differ somewhat

Source: F. Nimblett/F. Taylor
Update: 7/7/92

MUON SYSTEM

at high energies from the quoted values in Fig. 4.2.2. The cut was $\Delta E_{\mu}/[\text{ave}\Delta E_{\mu}] < 2.5$.

Fig. 4-2.4: The estimated muon momentum resolution arising from the fluctuation of the energy loss in the calorimeter are shown for constant θ as a function of P .

Fig. 4-2.5: The polar angle resolution, $\sigma(\theta)$, is shown as a function of P_t and η . The resolution at high energies is determined by the nonbend-plane channel-segmentation, and at low momentum is dominated by multiple scattering in the calorimeter.

Fig. 4-3.1: The momentum resolution of the GEM muon system is shown with both resolution smearing effects combined. The response is shown separately for low and high momenta to highlight the different momentum dependence.

Reference:

[1] "Muon Energy Loss in GEM BaF₂/Scintillator Fiber Calorimeter", R. McNeil, GEM TN-92-69.

GEM Baseline 1, March 25, 1992

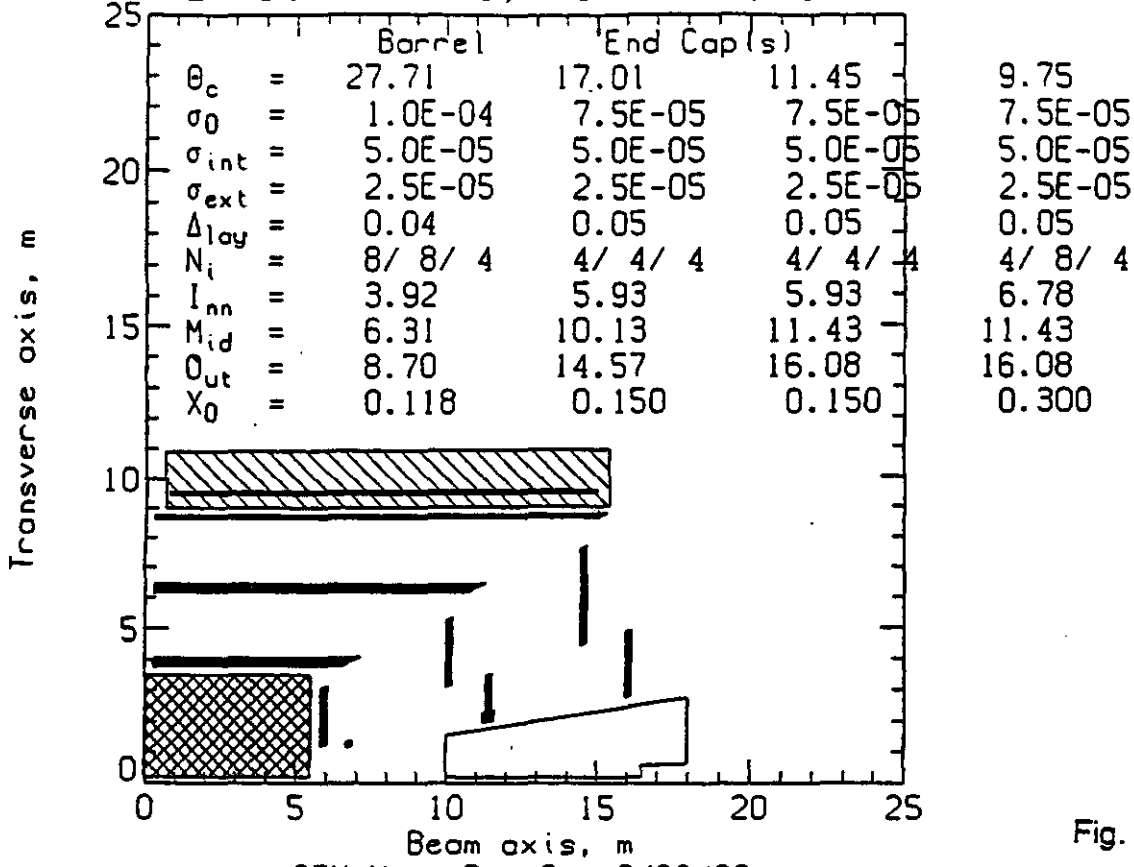
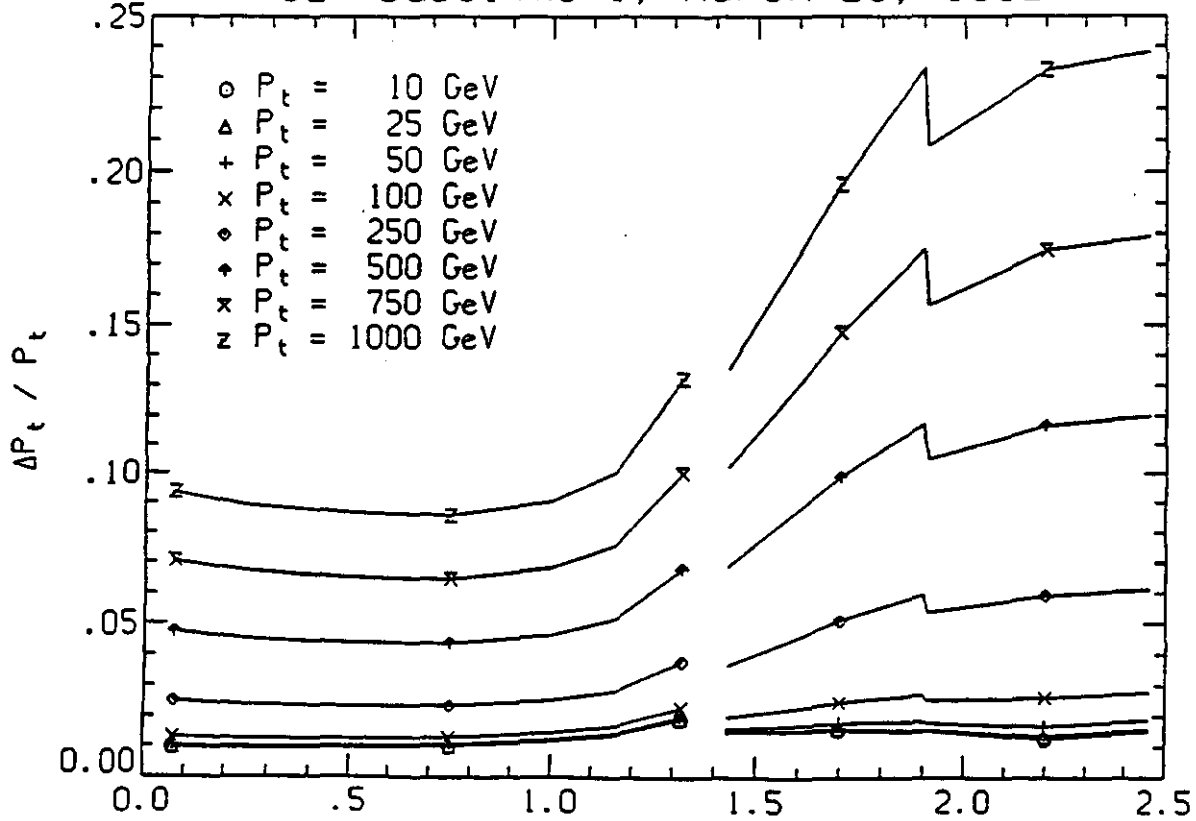


Fig. 4.1.1

GEM Muon Rev 2: 3/30/92

GEM Baseline 1, March 25, 1992



GEM Muon Rev 2: 3/30/92

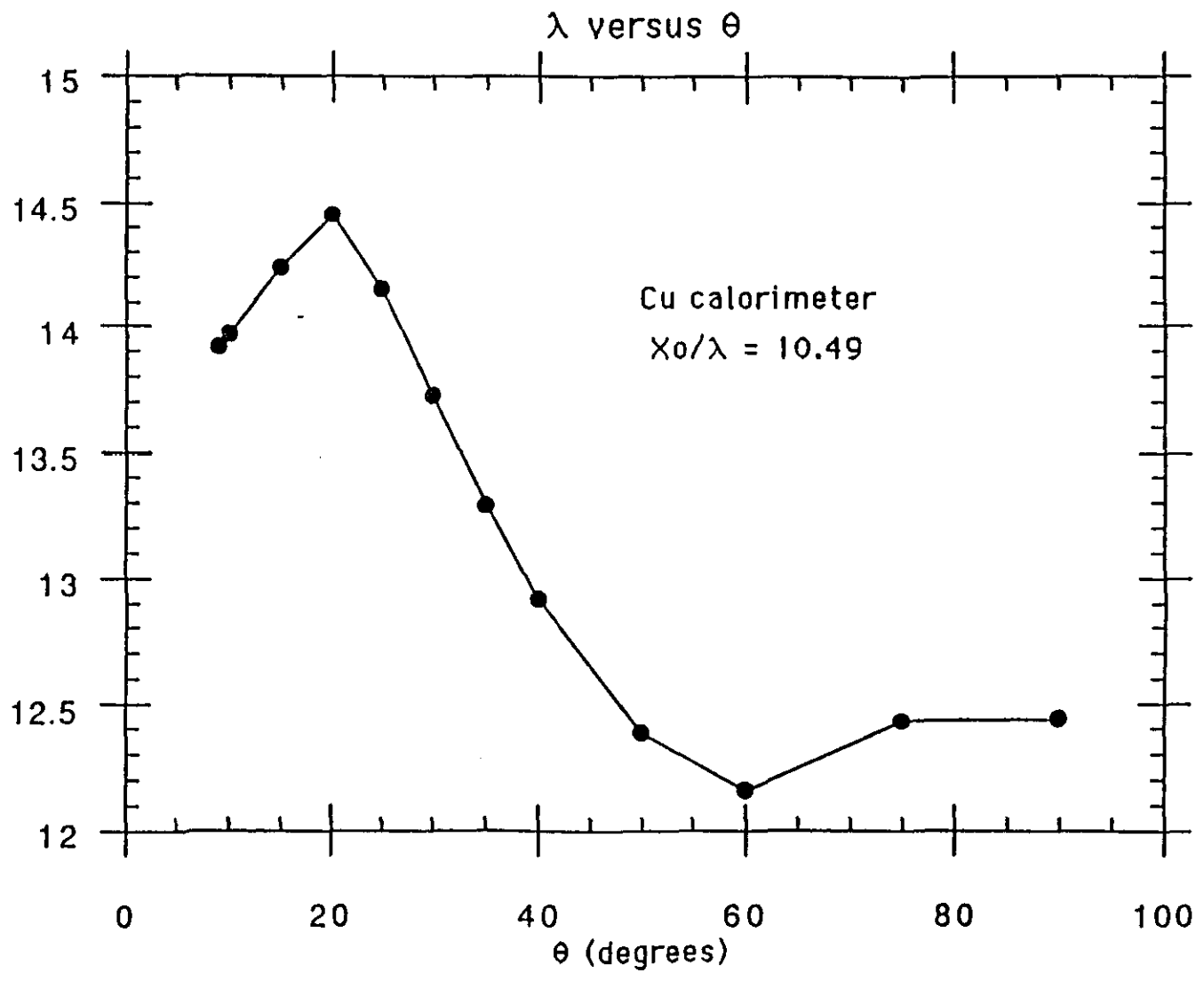


Fig. 4.2.1

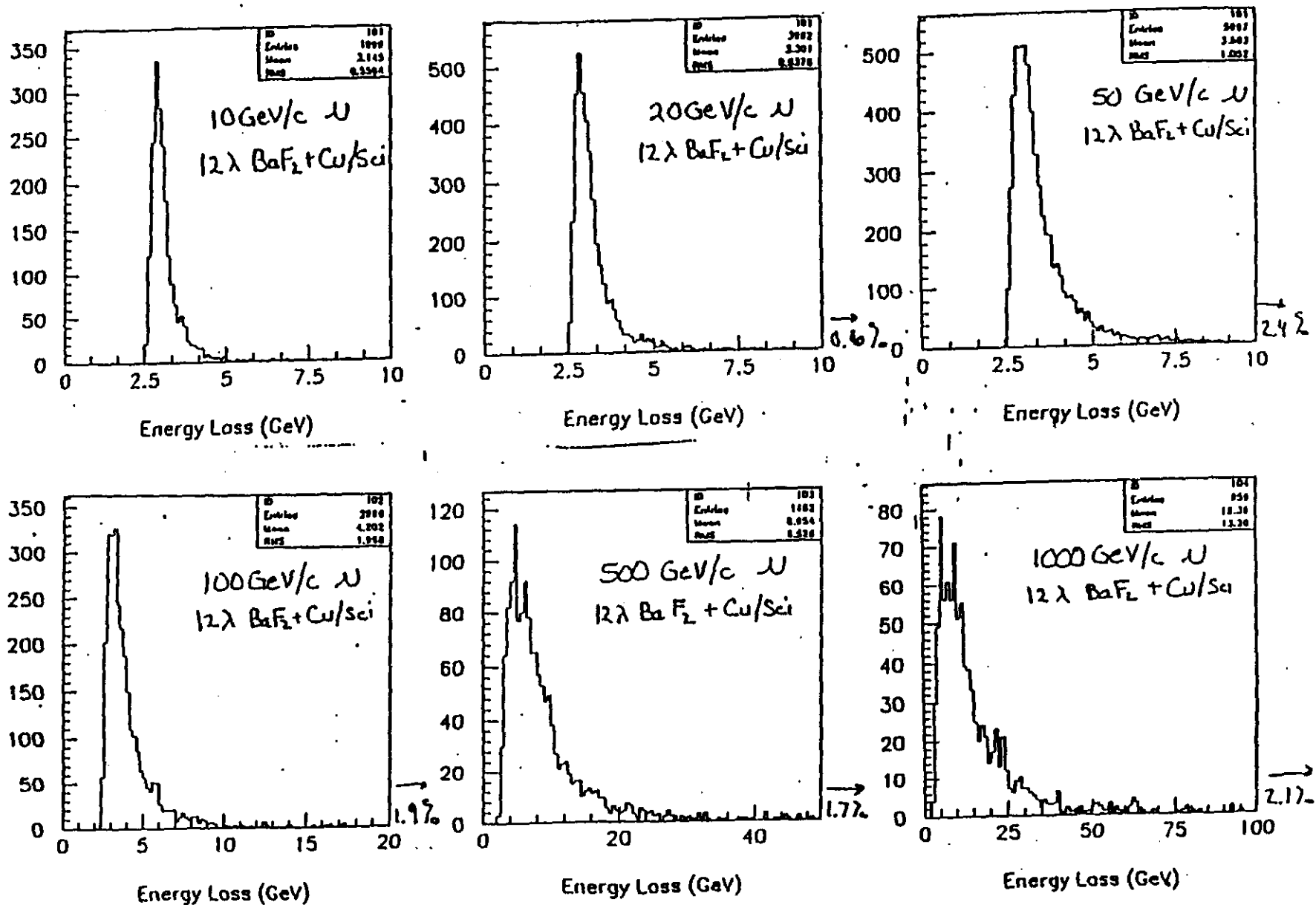


Fig. 4.2.2

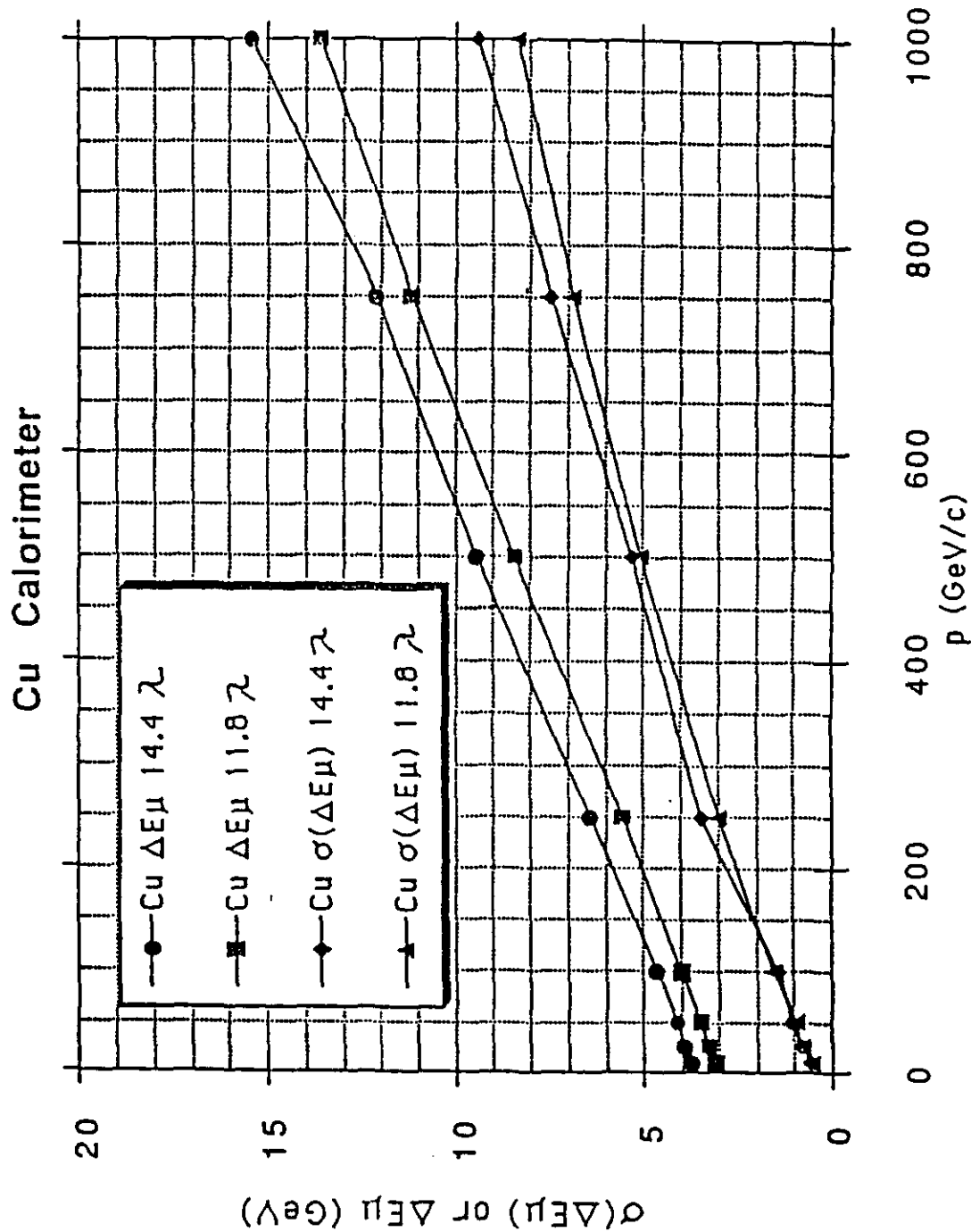


Fig. 4.2.3

Cu Calorimeter $\sigma(\Delta E\mu)$ only

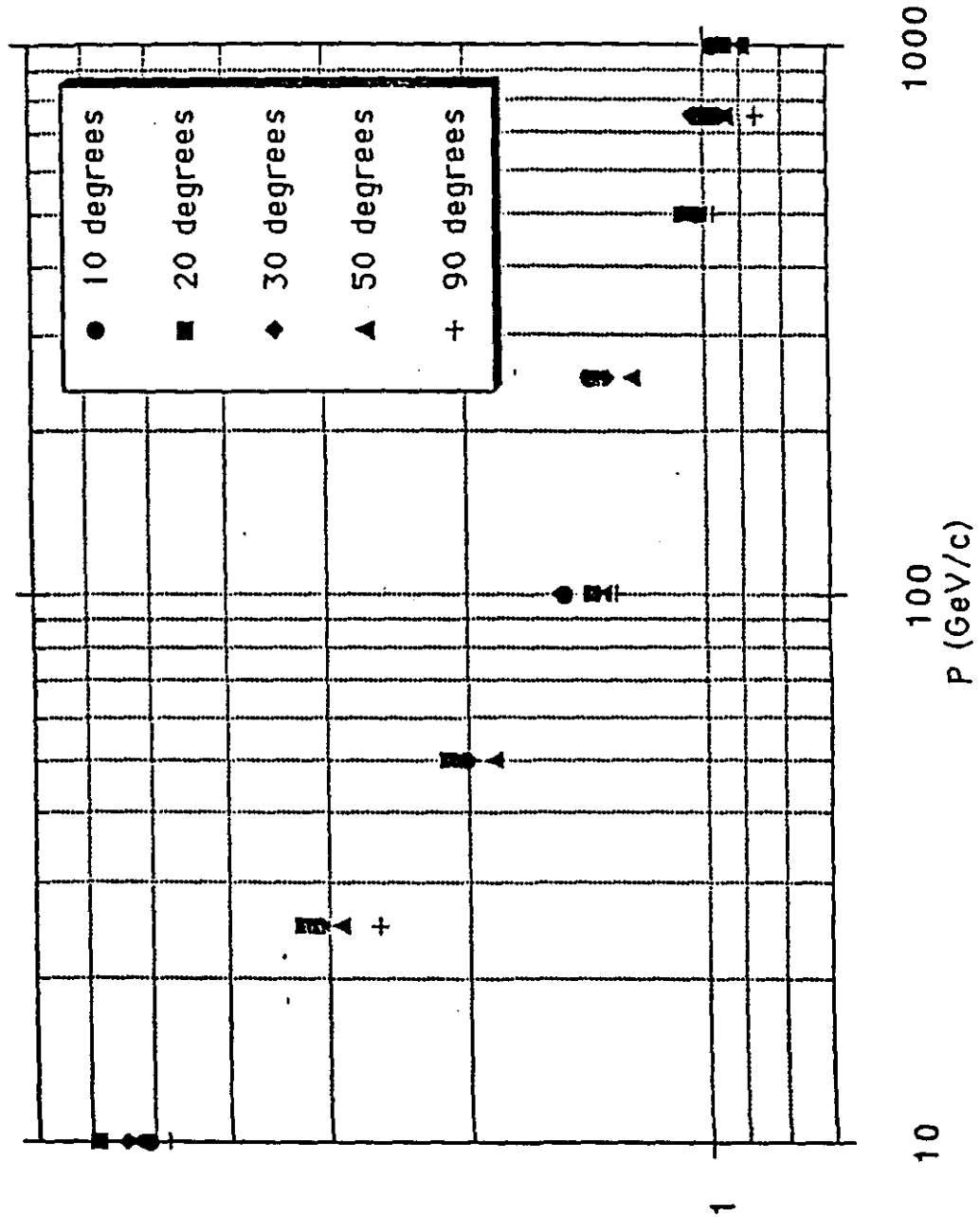


Fig. 4.2.4

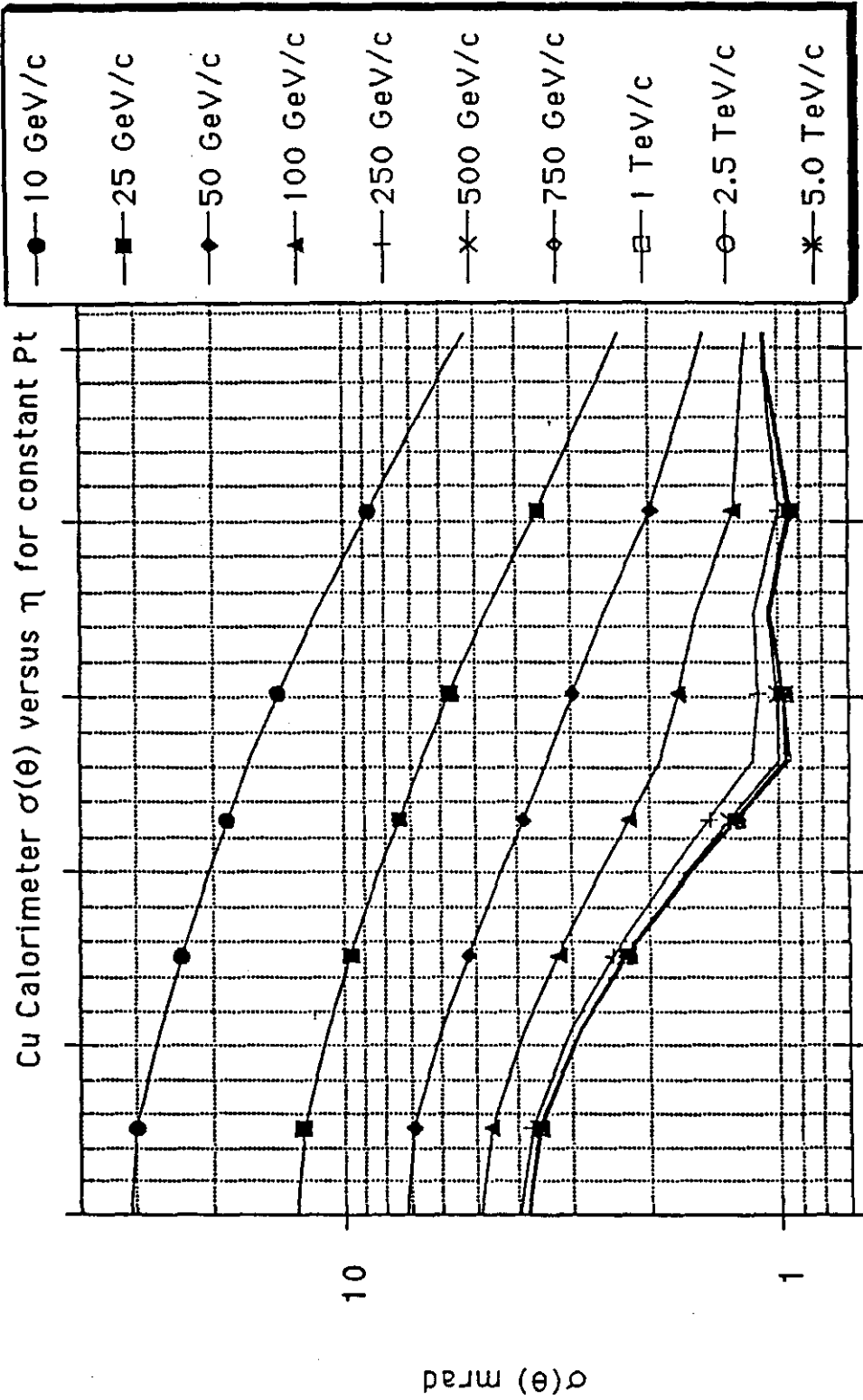


Fig. 4.2.5

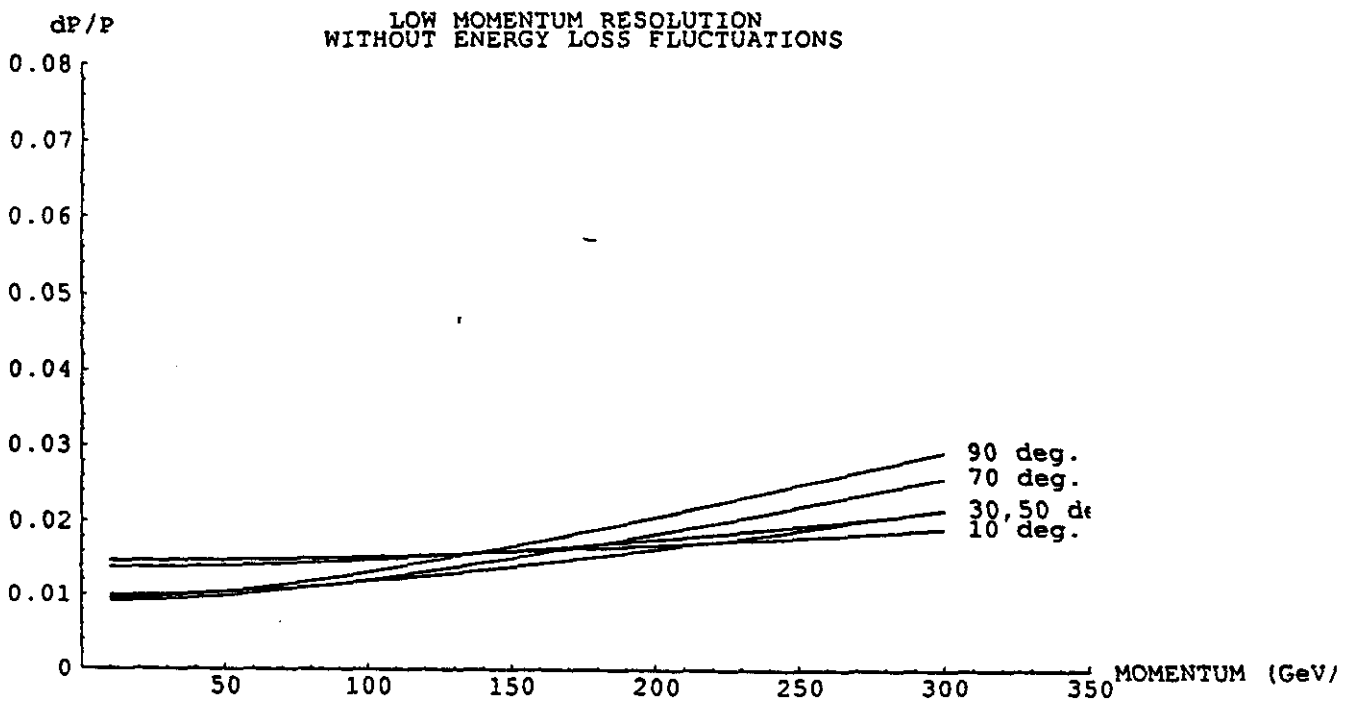
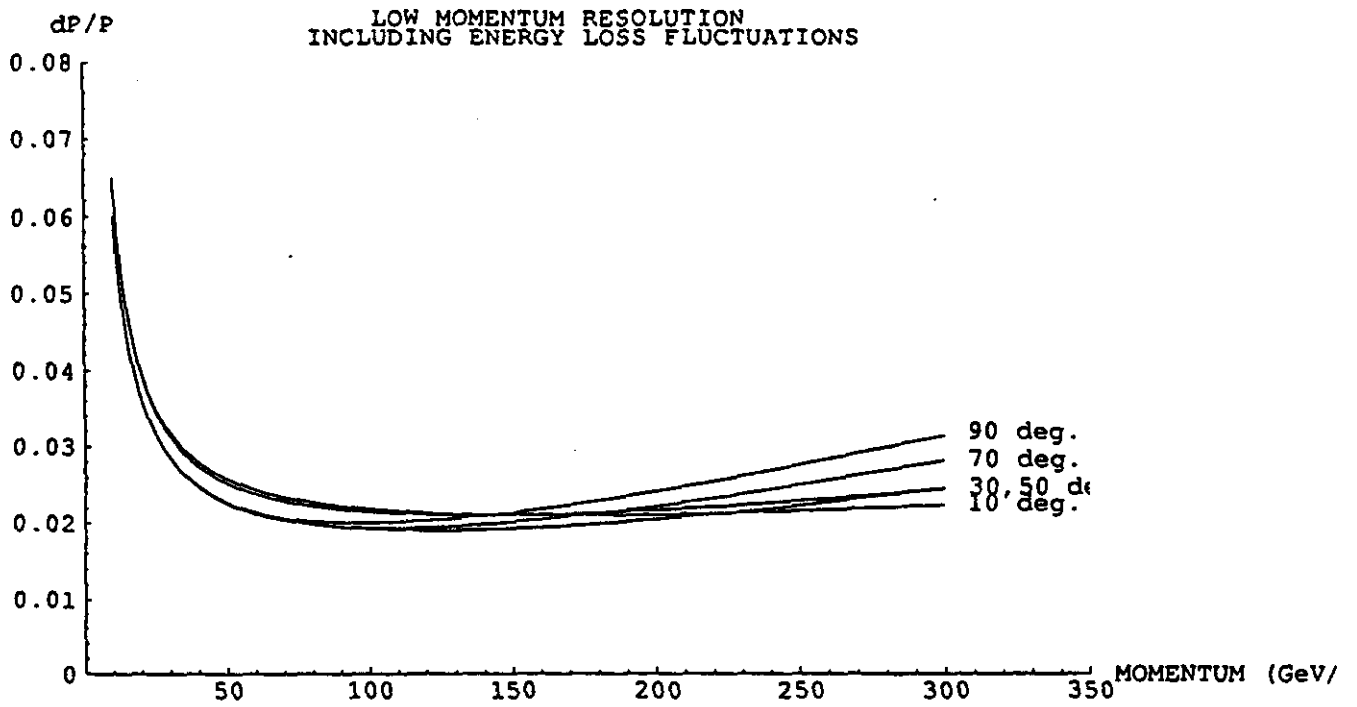
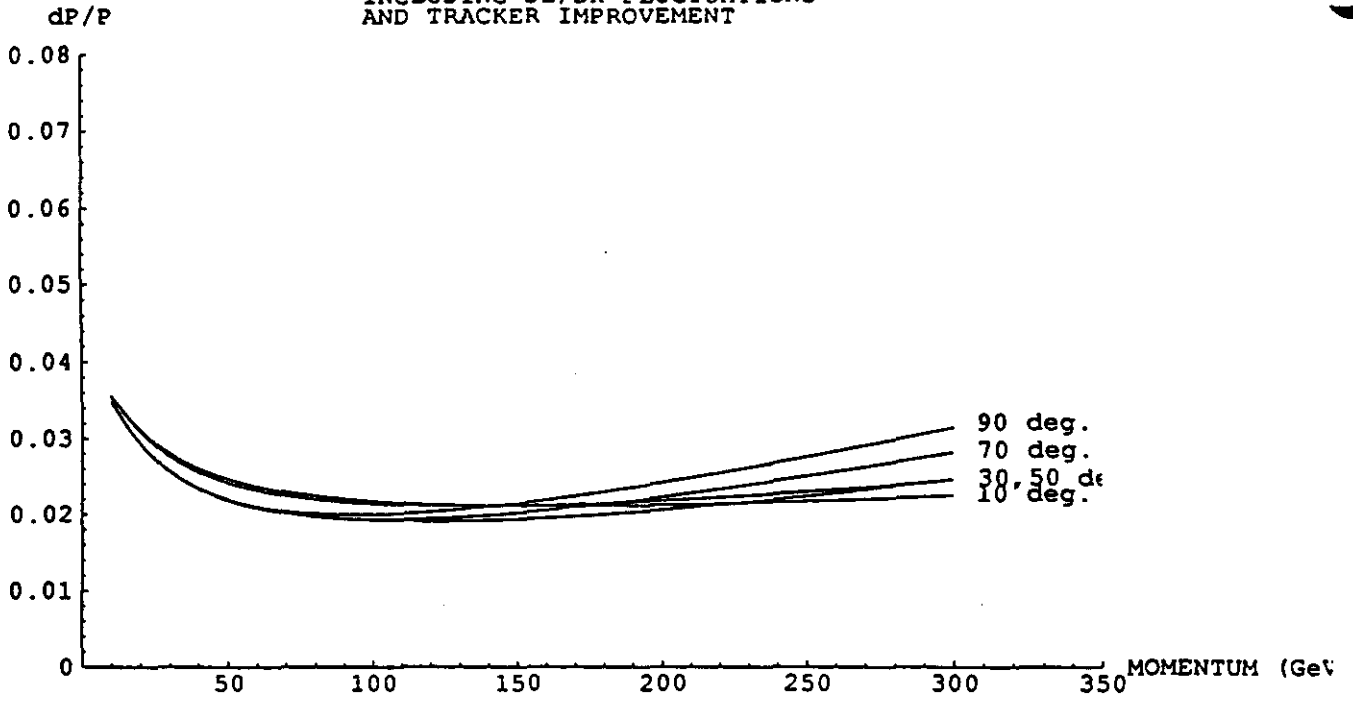


Fig. 4.3.1a

LOW MOMENTUM RESOLUTION
INCLUDING DE/DX FLUCTUATIONS
AND TRACKER IMPROVEMENT



P_T RESOLUTION INCLUDING ENERGY LOSS FLUCTUATIONS

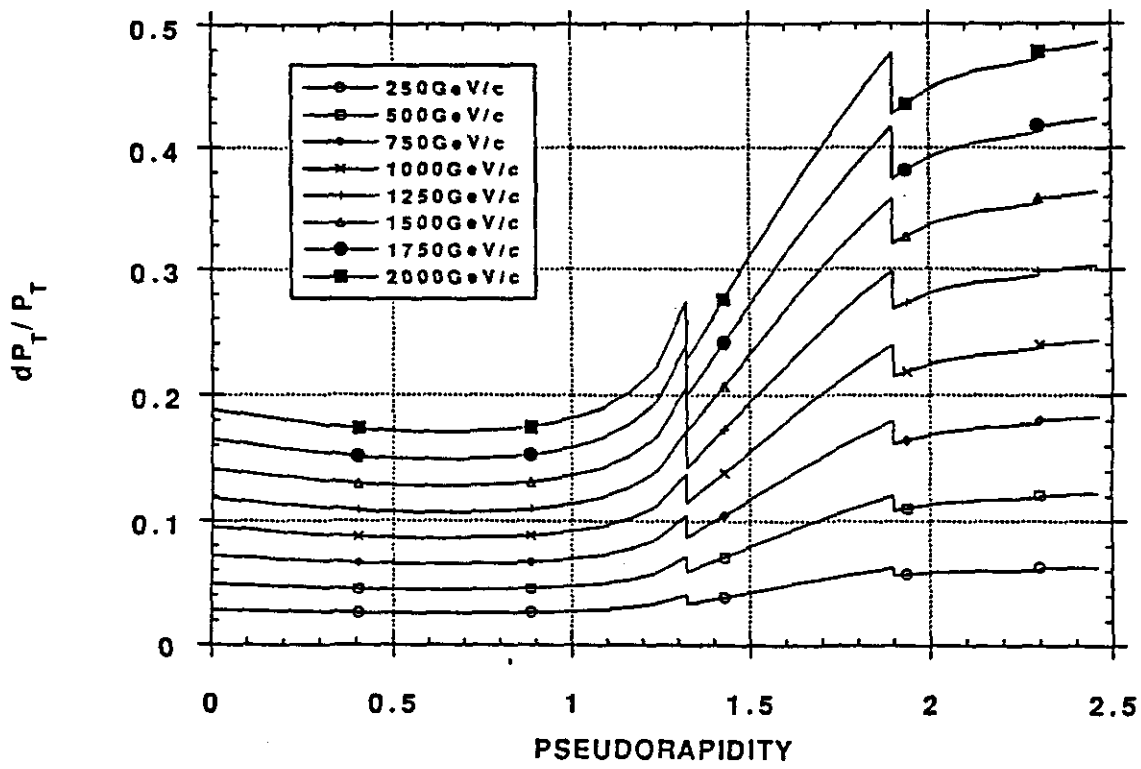


Fig. 4.3.1b

MUON SYSTEM

(5) Trigger

(persons responsible: Irwin Pless - MIT, Maged Atiya - BNL, Chiaki Yanagisawa - SUNY-SB)

The barrel trigger and beam crossing tag is based on RPCs, which will be instrumented with both Φ (bend plane) and Z (non-bend plane) coordinate readout. The RPCs will be constructed in two-gap modules and will be located in each of the three super-layers. This arrangement will enable both a momentum dependent trigger to be formed as well as a measurement of the orthogonal coordinate of the muon track. The RPCs have a measured time jitter of < 1.4 ns (I. Pless - private communication), which is sufficiently fast to unambiguously tag the beam crossing. The bend plane strips will be 1.3 cm wide, while the non-bend plane segmentation varies from 3.9 to 8.9 cm.

Both the endcap trigger and beam crossing tag will be provided by the CSCs. The bend plane strip segments which are used to form the trigger are the 0.5 cm wide strips readout digitally at trigger time. The non-bend plane measurement is provided by means of the anode wires which will be segmented in 5 cm wide electronic channels. Since the maximum drift time of the CSC is < 24 ns per plane, several planes in a superlayer must be "ORed" together to achieve sufficient resolution for the beam crossing tag.

The Level 1 muon trigger is based on hits in super-layers 2 and 3 (SL2 and SL3, respectively) which uses the change of the phi angle, $\Delta\phi$, to measure the curvature (momentum) of the track originating from the interaction point. $\Delta\phi$ is given in terms of the number of readout strips of the RPCs (1.3 cm wide) for a barrel muon, or the number of CSC pickup strips (0.5 cm wide) for an endcap muon. The line formed by the hit in SL2 and the interaction point extrapolated to SL3 gives the position of the muon track for infinite momentum. The difference measured in strips, ΔN_{strip} , between the hit in SL3 and the extrapolated point is a measure of the muon momentum. The concept is shown in Fig. 5.1.

Figs. 5.2 indicate the difference in the ϕ angle measured by strips in the RPC or CSC bend plane for various momenta. Figs. 5.3 indicate the counting rate for $L=10^{33}$ $\text{cm}^{-2}\text{s}^{-1}$ as a function of ΔN_{strips} . A possible logic circuit for the endcap region is shown in Fig. 5.4.

Source: F. Nimblett/F. Taylor
Update: 7/7/92

MUON SYSTEM

Figure Captions:

- Fig. 5-1 The trigger concept is shown schematically.
- Fig. 5-2 (a) The trigger efficiency is shown as a function of ΔN_{strip} for various values of Pt in the Barrel region.
- Fig. 5-2 (b) Same as Fig. 5-2 (a) for Endcap region 1.
- Fig. 5-2 (c) Same as Fig. 5-2 (a) for Endcap region 2.
- Fig. 5-3 (a) The trigger rate (Hz) for $L=10^{33}\text{cm}^{-2}\text{s}^{-1}$ is shown for the Barrel region as a function of ΔN_{strip} . To set the trigger for $P_t > 10$ GeV/c only muons with $\Delta N_{\text{strip}} < 20$ would be accepted.
- Fig. 5-3 (b) Same as Fig. 5-2 (a) for Endcap regions 1 and 2. Refer to Figs. 5- 2 (b) and 5-2 (c) for Pt cuts in these regions.
- Fig. 5-4 A schematic of the trigger electronics logic that could be employed to achieve the endcap trigger.

MUON TRIGGER STRATEGIES

($r-\phi$) PROJECTION

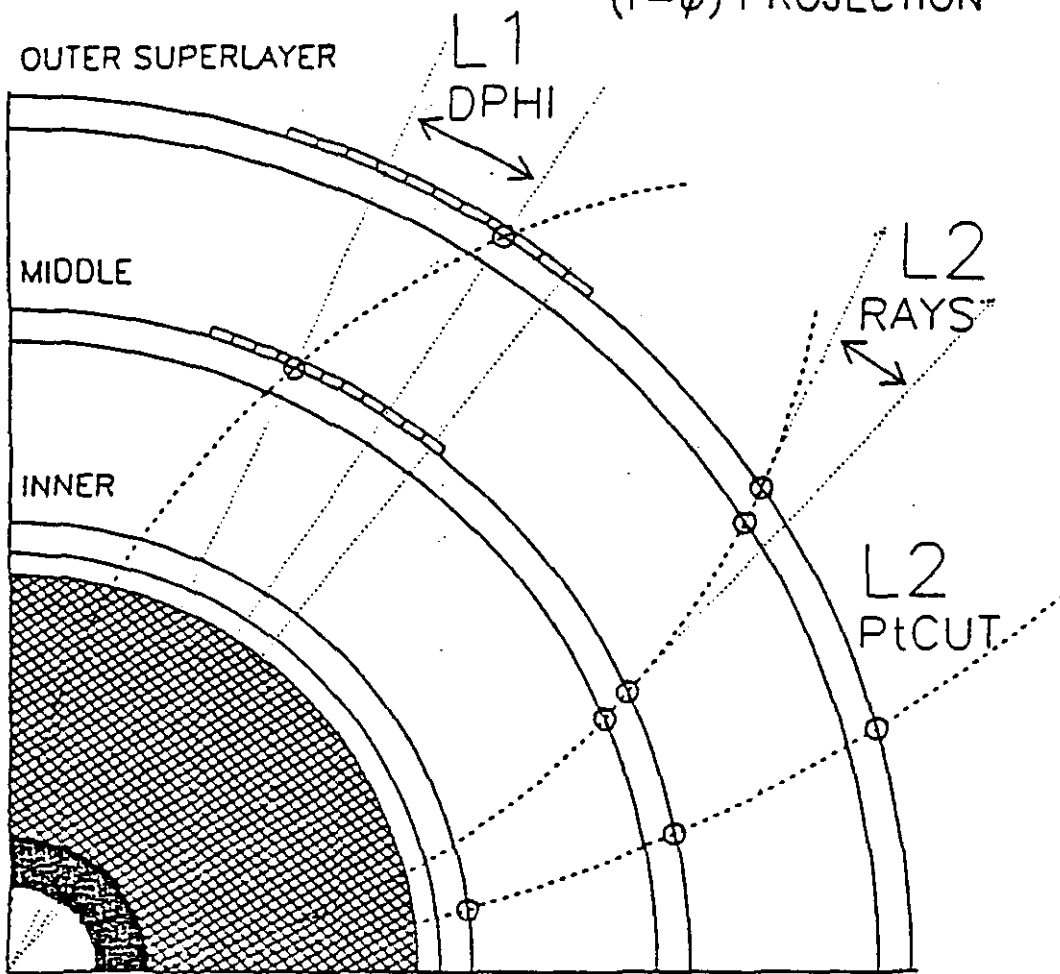
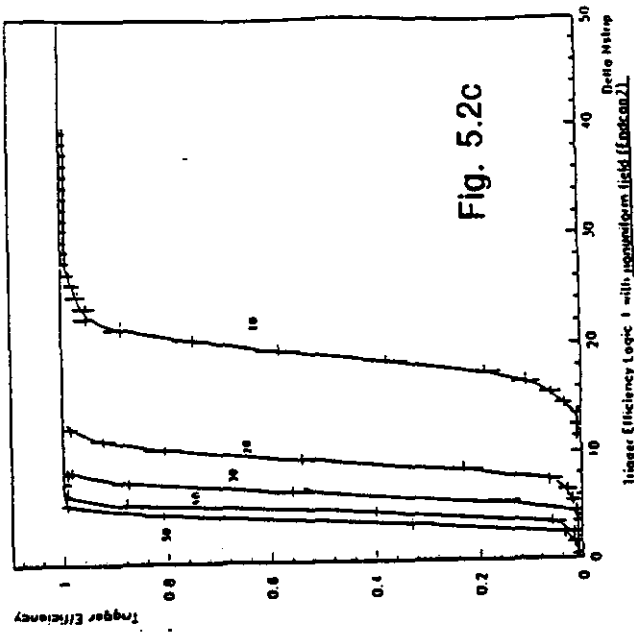
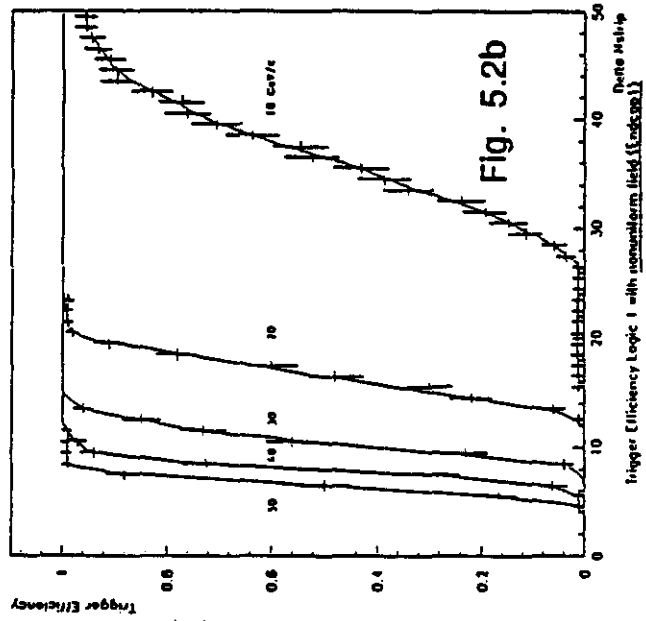
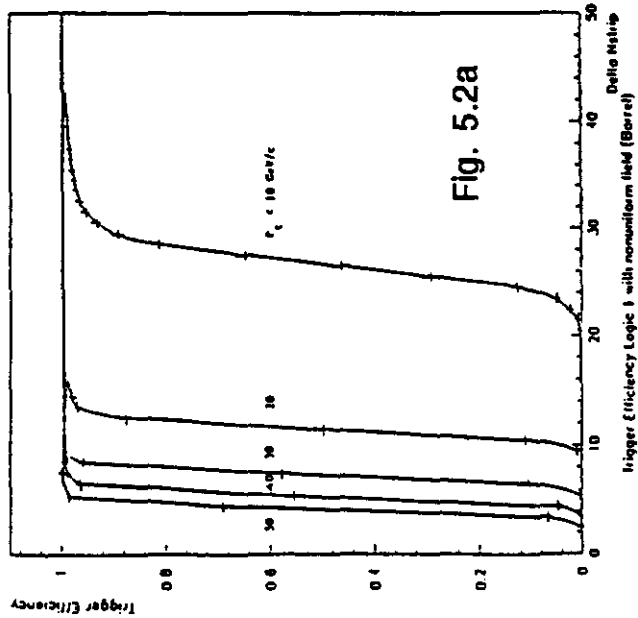
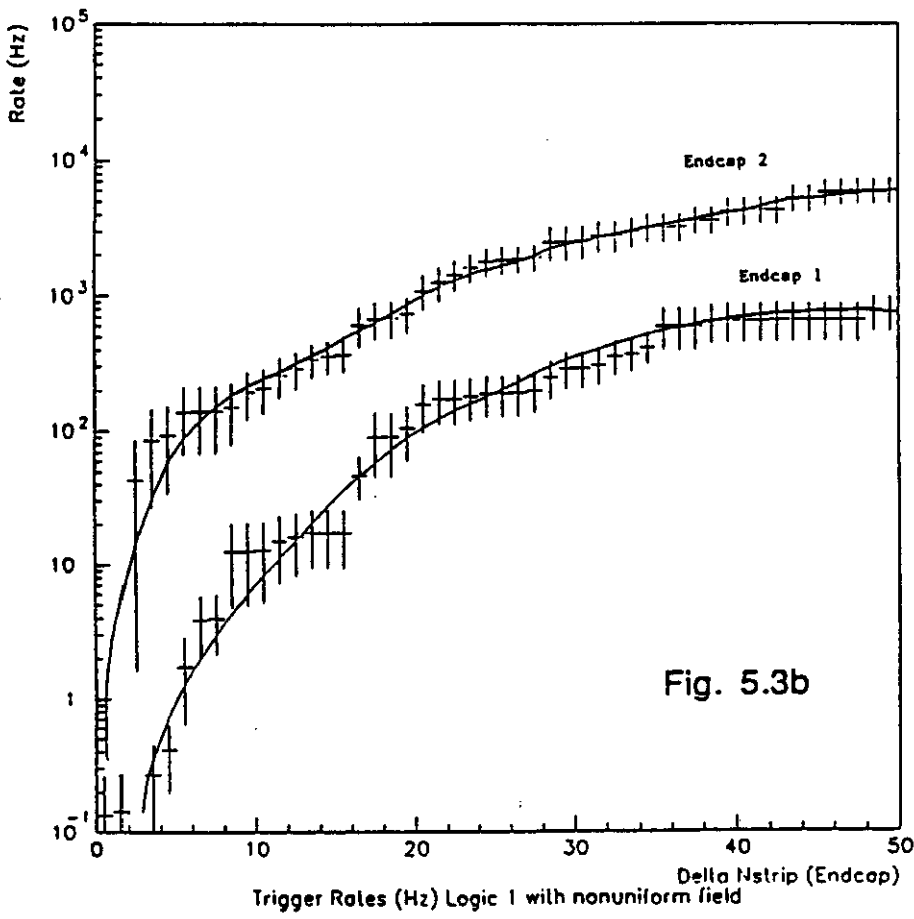
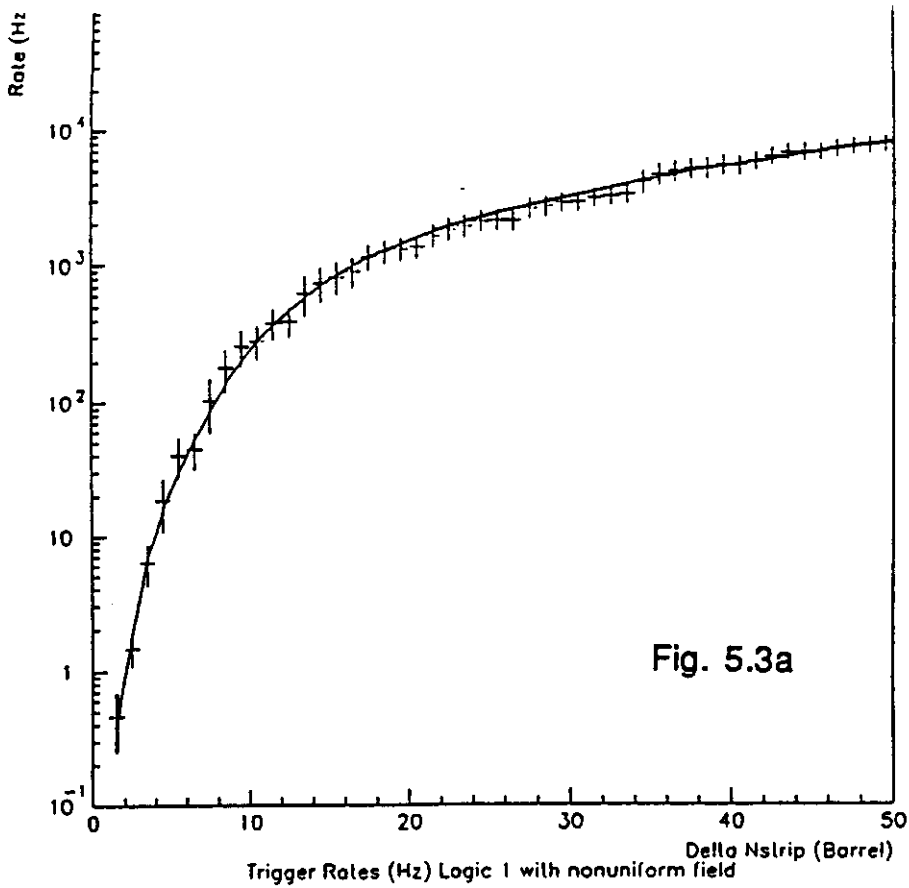
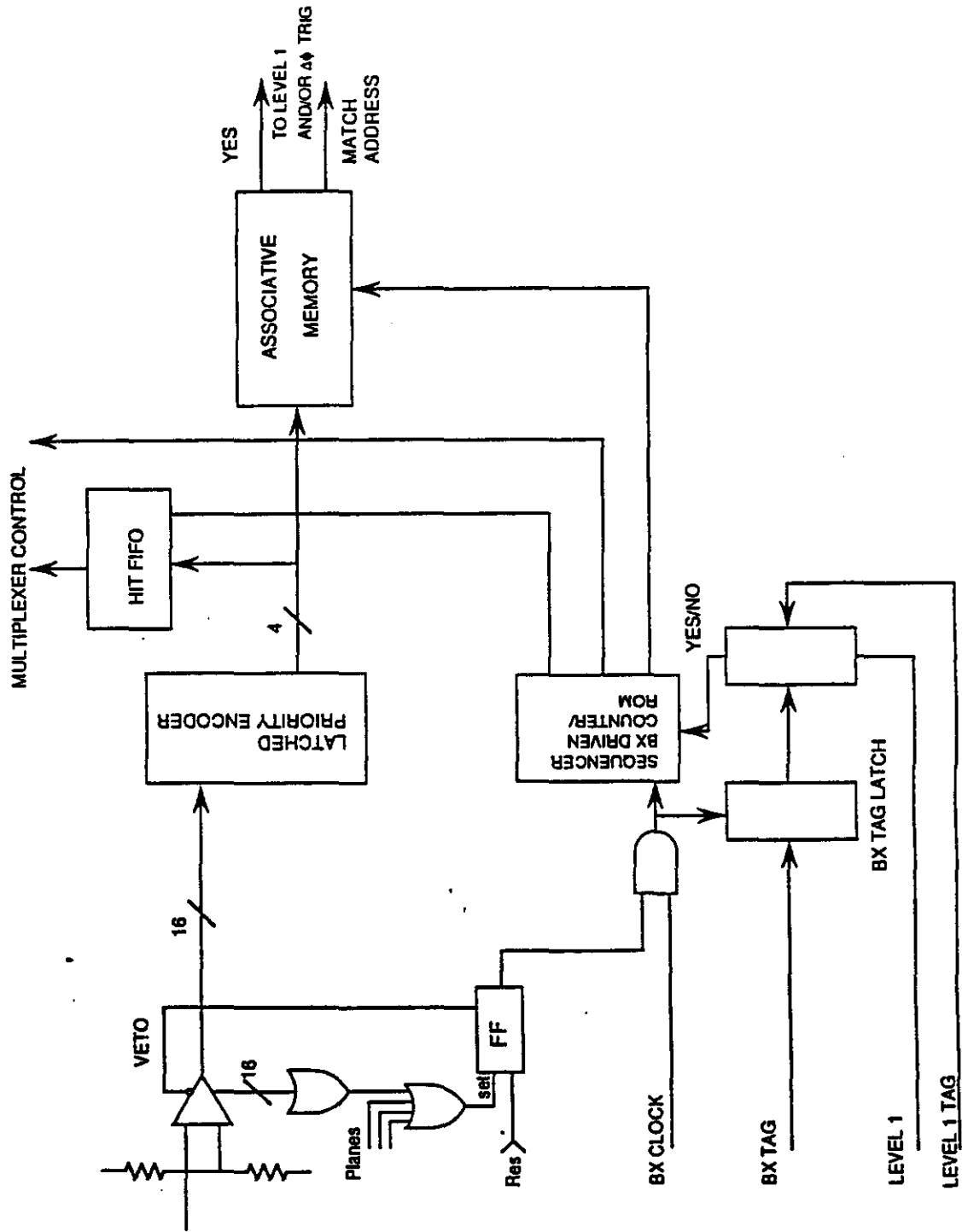


Fig. 5.1







Schematic of Typical Trigger Electronics Logic

Fig. 5.2.2

MUON SYSTEM

(6) Hadron Punchthrough

(persons responsible: Roger McNeil - LSU, Mohammad Mohammadi - SUNY-SB)

Extensive Monte Carlo studies have been performed which indicate that for a calorimeter thickness of greater than 12λ in the barrel region the charged particle rate in the first super-layer of the muon system is dominated by prompt leptons from the primary vertex, and hadron decay in the central tracker and calorimeter. The hadron punch-through is smaller by a factor of 2.

In the endcap region the particle rate increases quite rapidly as the polar angle decreases. Owing to the energy spectrum of the punch-throughs and the prompt muons, and the geometry of the calorimeter and inner tracker, we find that the charged particle rate is decreased with some efficiency up to 14λ , but thereafter with diminishing returns. Hence in the forward direction a calorimeter of 14λ will keep the occupancy low and the trigger operational.

References:

- [1] Hadronic Calorimeter resolution vs. λ .
- [2] GEM Baseline 1, GEM TN92-76, April 23, 1992.
- [3] See for example transparencies talk given by R. McNeil at the GEM Collaborator meeting July 17, 1991.
- [4] R. McNeil, "How Thick should the GEM Barrel Calorimeter Be," GEM TN92-68 March 10, 1992.
- [5] RD5 Collaboration, Status Report, CERN/DRDC/91-53 1992.
- [6] M. Mohammadi, to be submitted as a GEM Note.
- [7] GEM Letter of Intent, SSCL-SR-1184, GEM TN-92-49, Nov. 30, 1992.
- [8] "Study of Hadron Punchthrough and Muon Rates at the SSC", Y. Chang and B. Zhou, GEM-TN-92-101

See the figs. following.

Source: F. Nimblett/F. Taylor
Update: 7/7/92

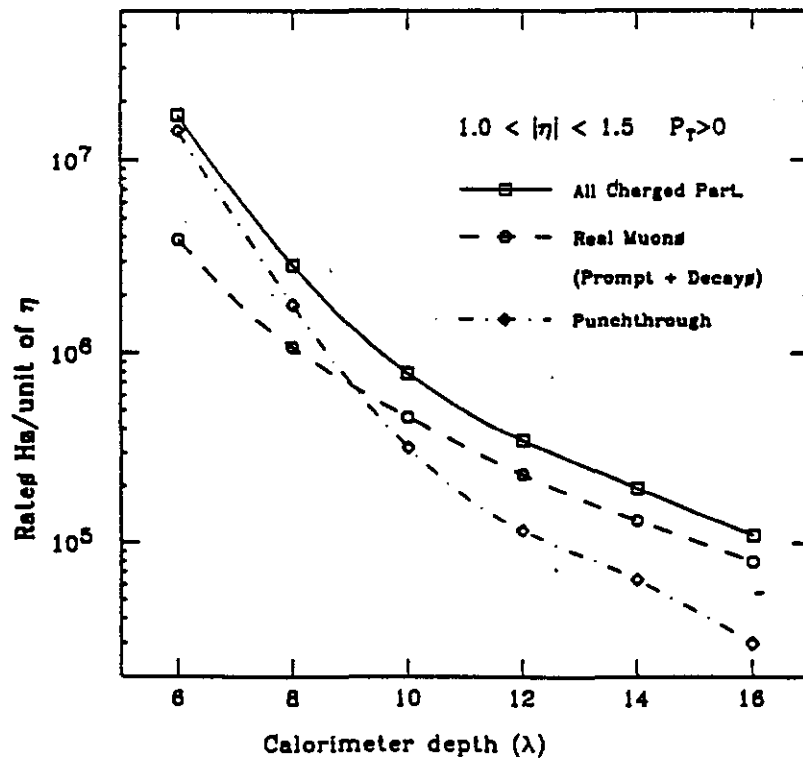
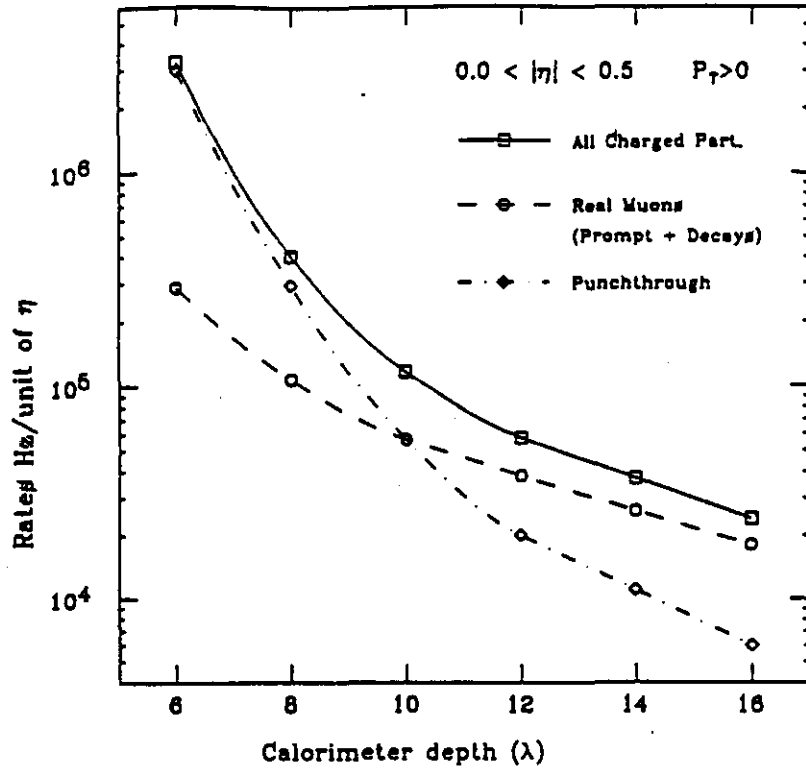


Figure 1. The rate of all Charged particles rates at $10^{33} \text{ cm}^{-2}/\text{s}$ SSC luminosity exiting the barrel calorimeter for a) $|\eta| < 0.5$ and b) $1.0 < |\eta| < 1.5$ rapidity intervals. The solid curve is the total rate, the dashed curve is the rate from prompt muons and π/K decays in the inner tracking region, and the dot-dashed curve is the rate from hadron punchthrough.

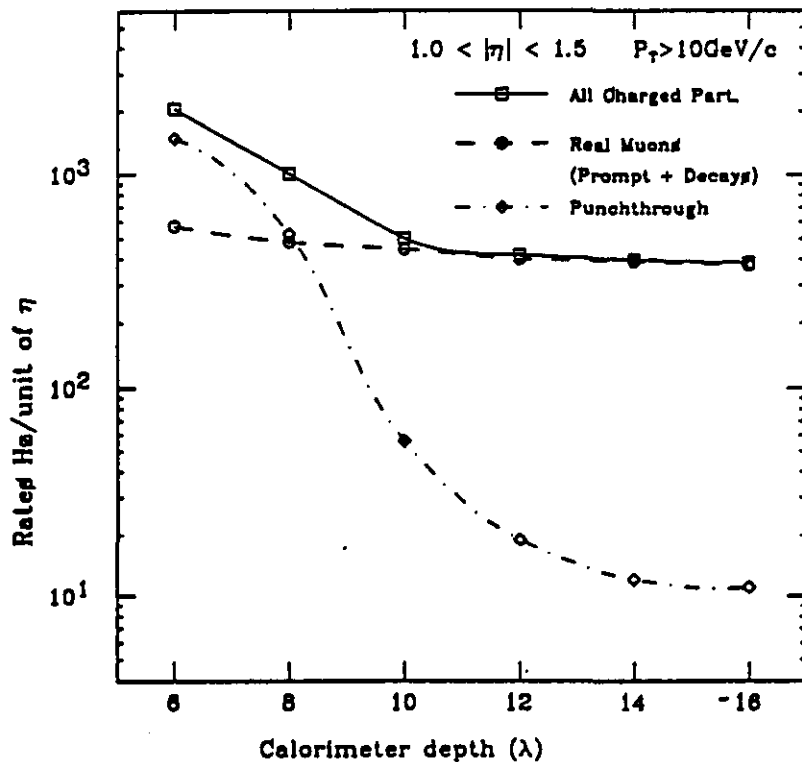
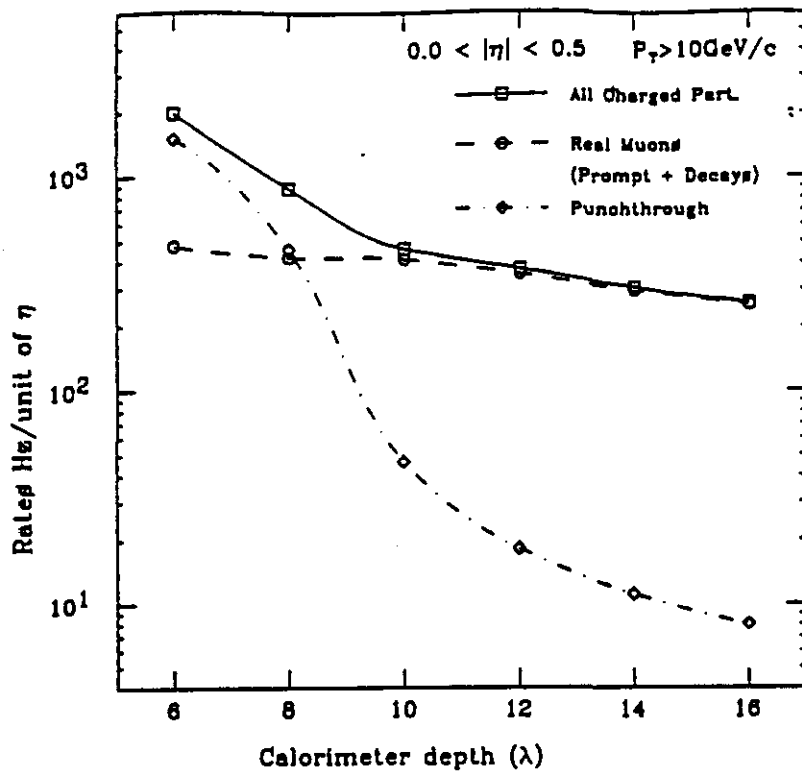


Figure 2. The rate of Charged particles with transverse momentum above $10 \text{ GeV}/c$ at $10^{33} \text{ cm}^{-2}/s$ SSC Luminosity exiting the barrel calorimeter for a) $|\eta| < 0.5$ and b) $1.0 < |\eta| < 1.5$ rapidity intervals. The solid curve is the total rate, the dashed curve is the rate from prompt muons and π/K decays in the inner tracking region, and the dot-dashed curve is the rate from hadron punchthrough.

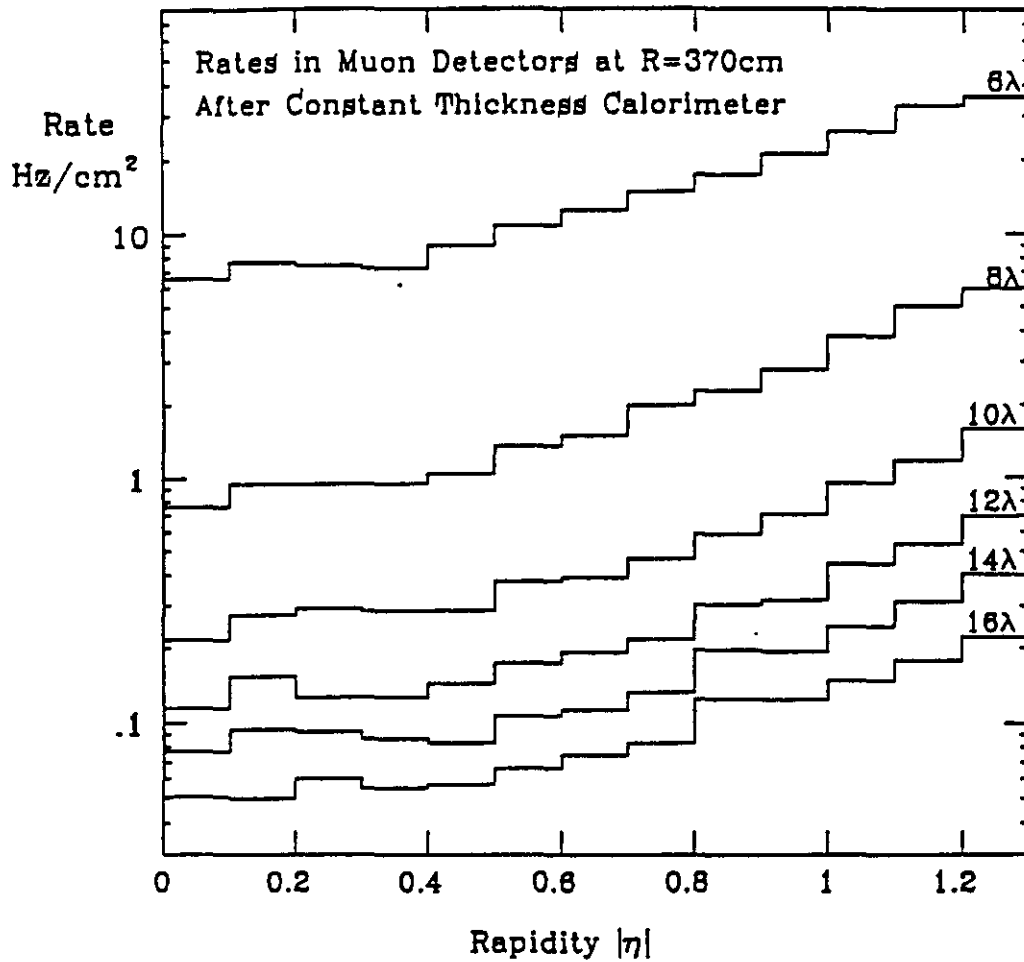


Figure 3. The hit occupancy in the first layer of the GEM barrel muon system at R=370cm at $10^{33} \text{ cm}^{-2}/\text{s}$ SSC luminosity as a function of rapidity for various constant calorimeter thicknesses.

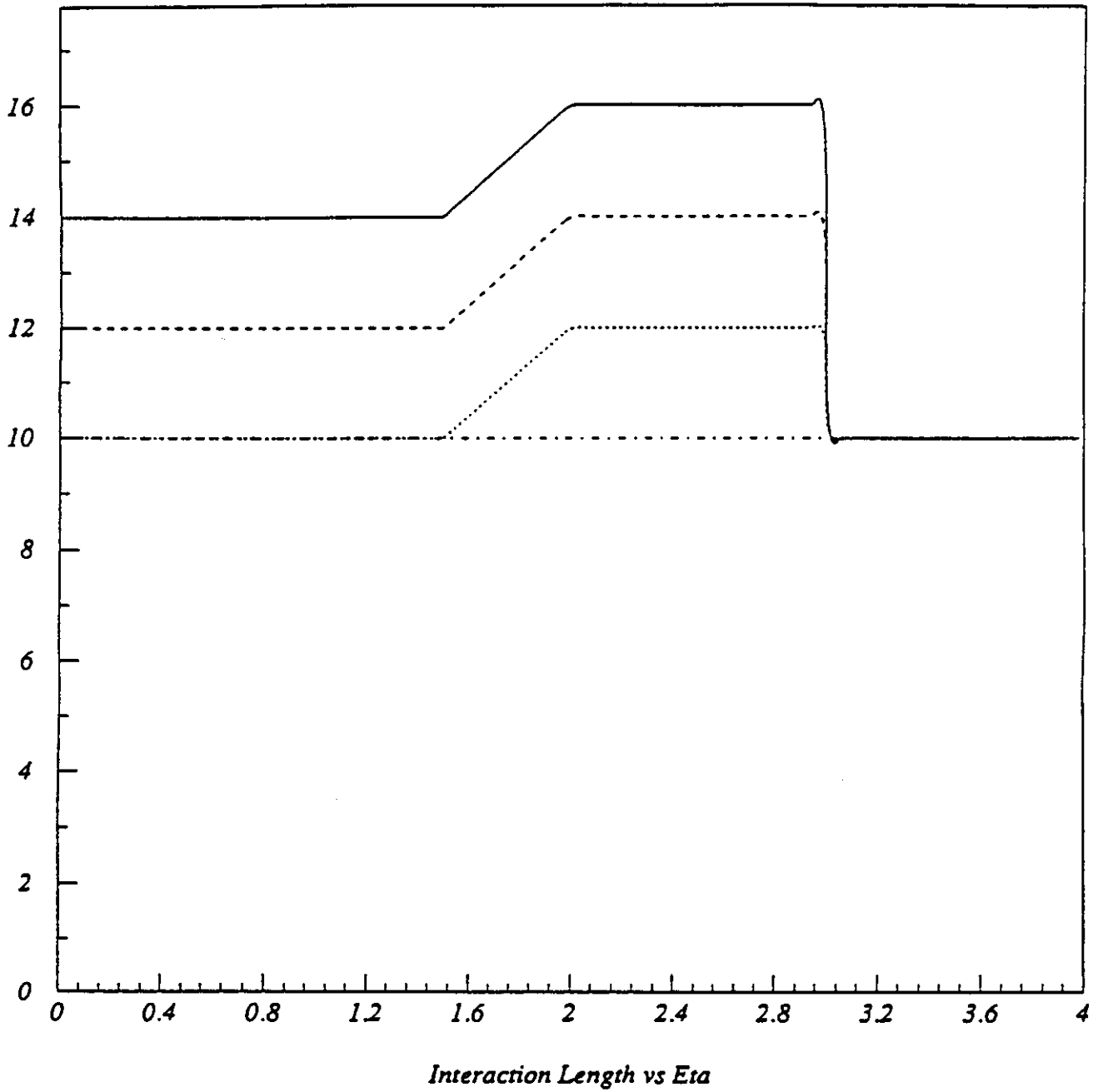


Fig. 4 - Interaction length versus rapidity representing the calorimeter depth model used in the Hit-level Monte Carlo.

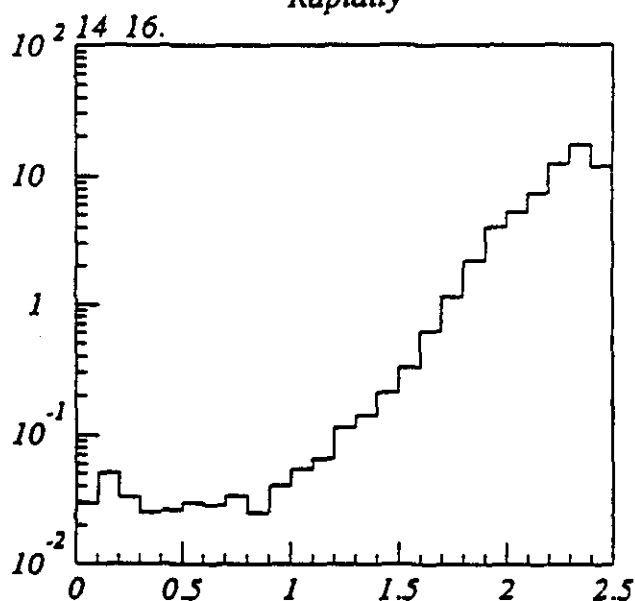
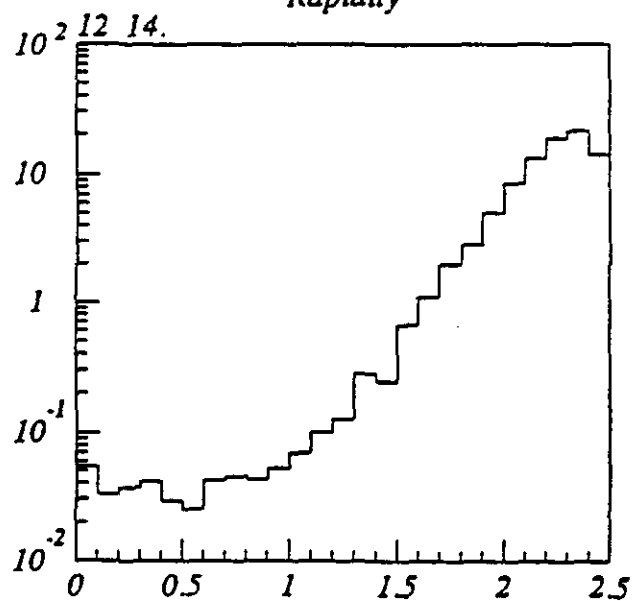
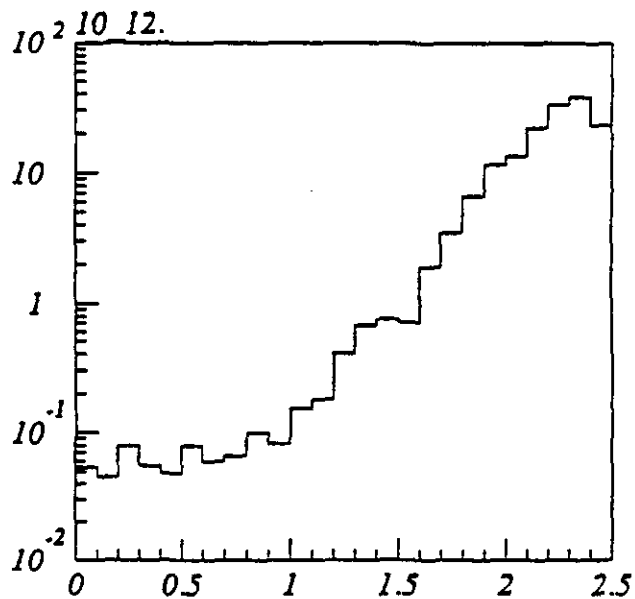
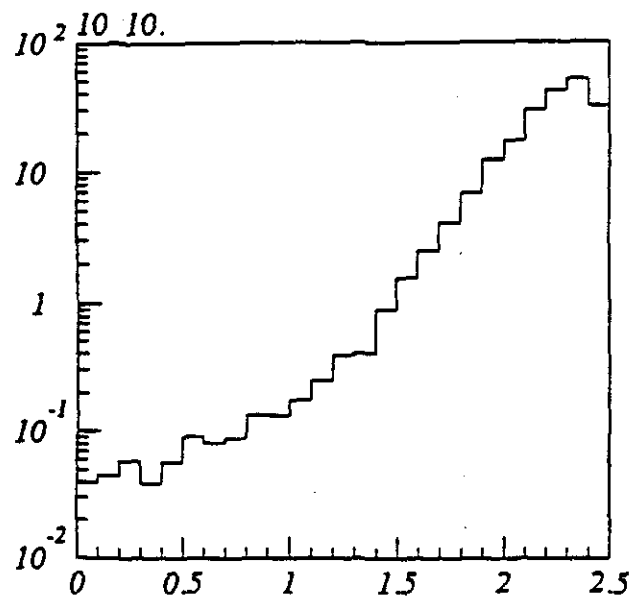
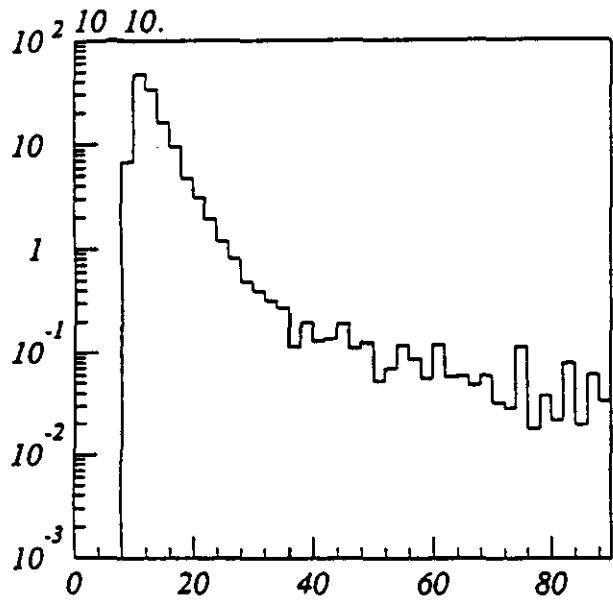
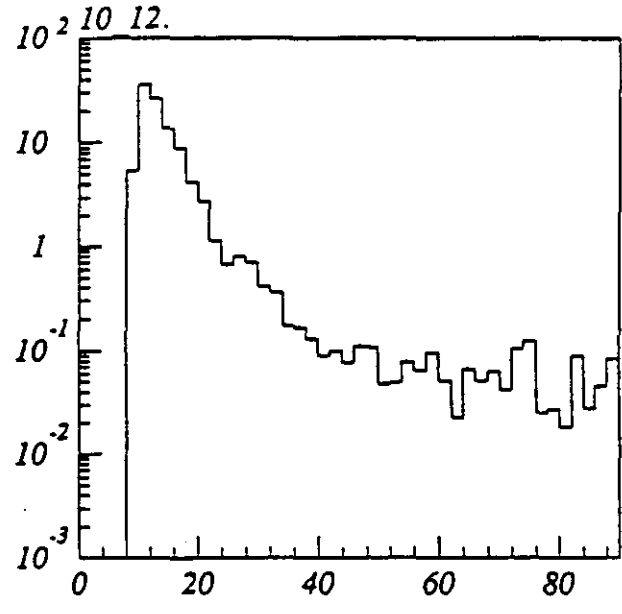


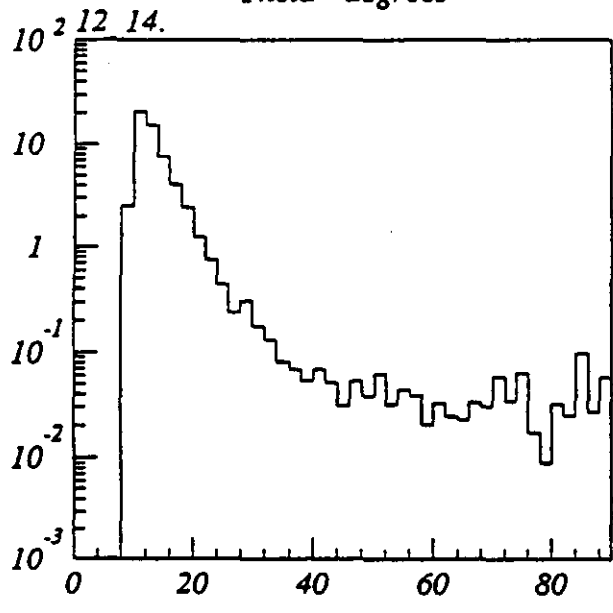
Fig. 5 - Charged particle flux (Hz/cm^2) versus rapidity for four calorimeter depths 10-10, 10-12, 12-14, and 14-16 lambda in the barrel-endcap. ($L=10^{-33} \text{ cm}^{-2} \text{ s}^{-1}$)



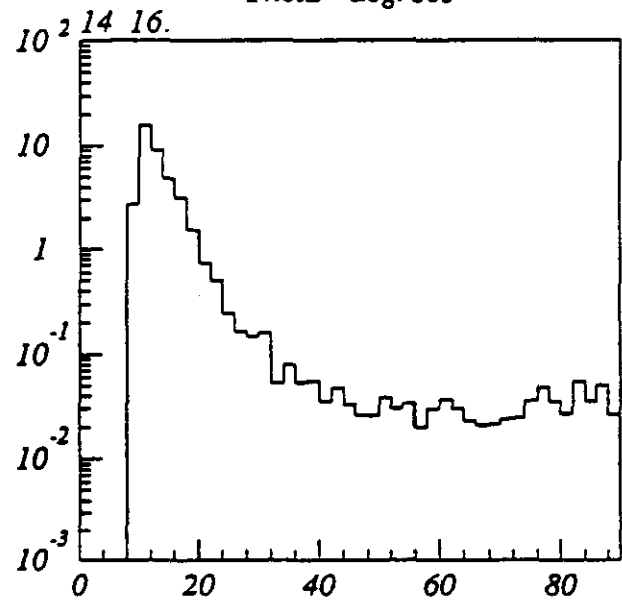
Theta - degrees



Theta - degrees

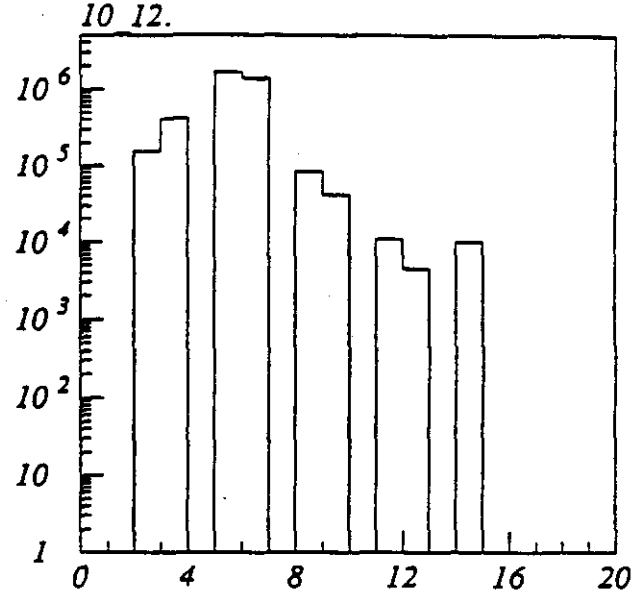
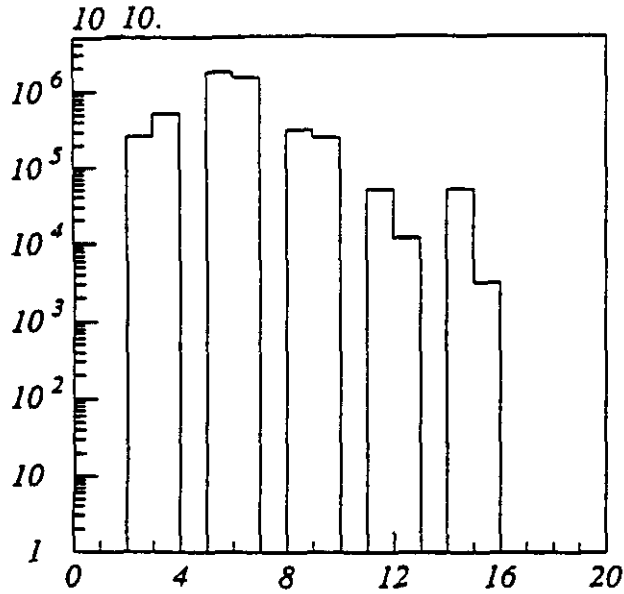


Theta - degrees



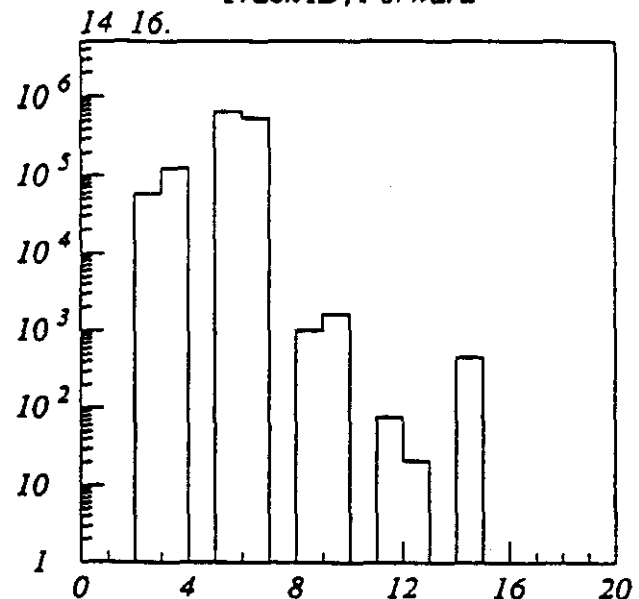
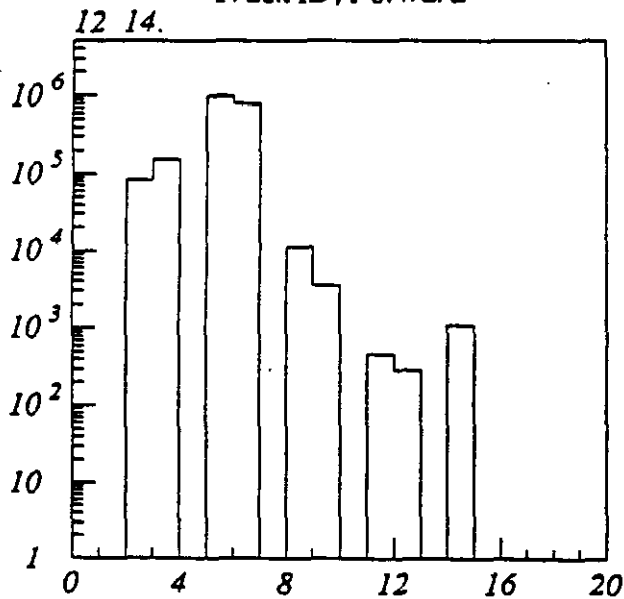
Theta - degrees

Fig. 8 - Charged particle flux (Hz/cm²) versus polar angle theta (degrees) for four calorimeter depths. (L=10⁻³³ cm⁻² s⁻¹)



Track ID, Forward

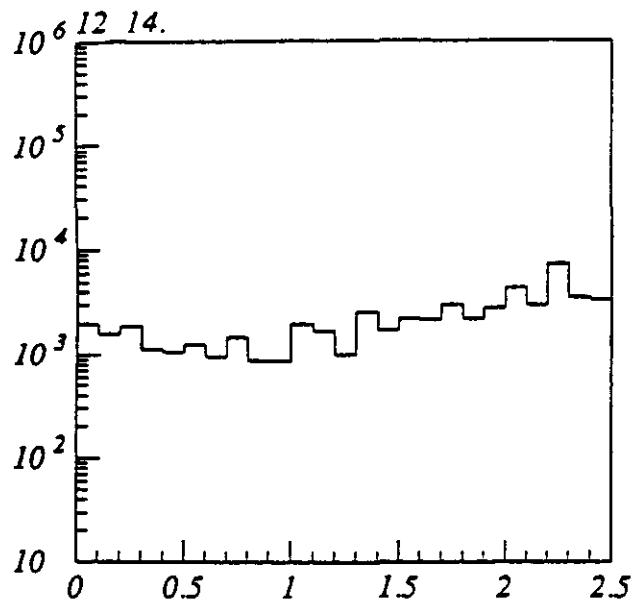
Track ID, Forward



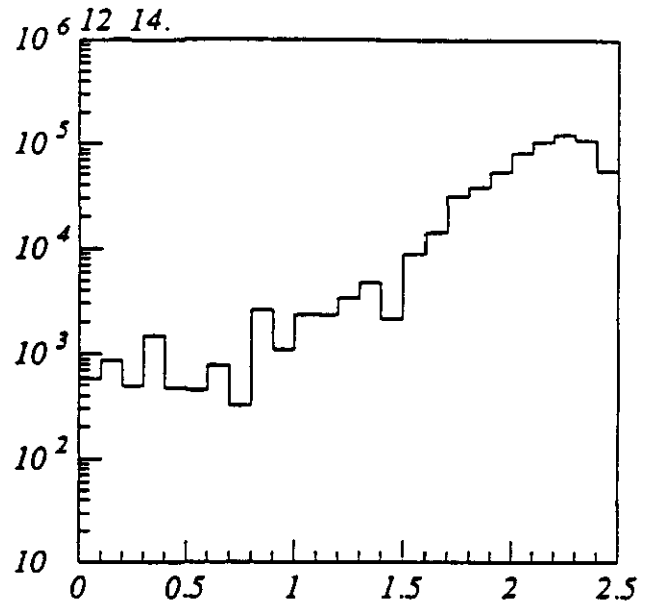
Track ID, Forward

Track ID, Forward

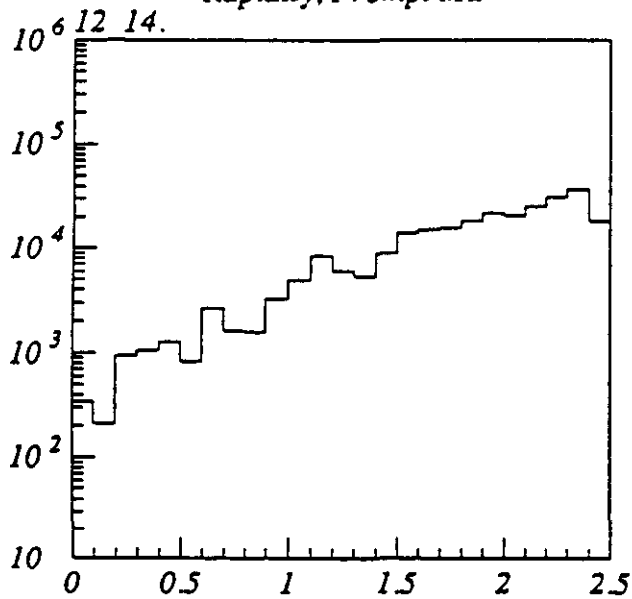
Fig. 7 - Charged particle rate (Hz) in the forward endcap versus track ID for four calorimeter depths. The ID's are: 2 or 3 electrons, 5 or 6 muons, 8 or 9 pions, 11 or 12 kaons, and 15 or 16 protons. ($L=10^{33} \text{ cm}^{-2} \text{ s}^{-1}$)



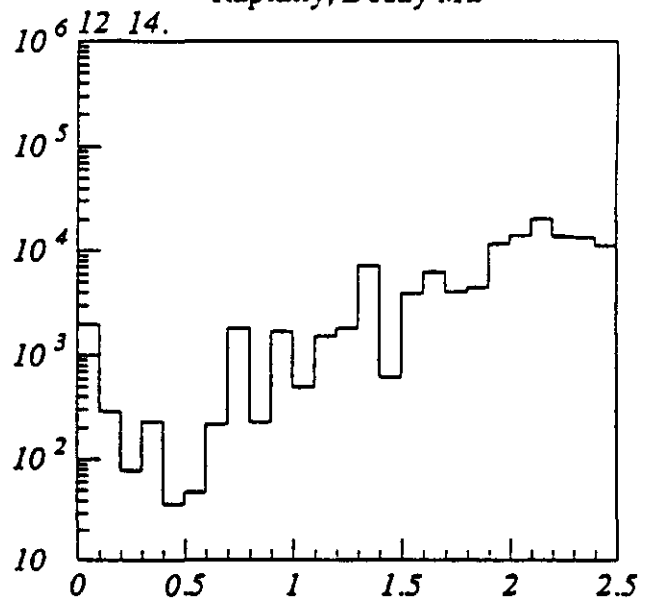
Rapidity, Prompt Mu



Rapidity, Decay Mu



Rapidity, Pchthr



Rapidity, Mu Shower

Fig. 8 - Charged particle rate (Hz) versus rapidity for prompt muons, decay muons, punchthrough particles and muon induced showers for a calorimeter depth of 12-14 lambda in the barrel-endcap. ($L=10^{33} \text{ cm}^{-2} \text{ s}^{-1}$)

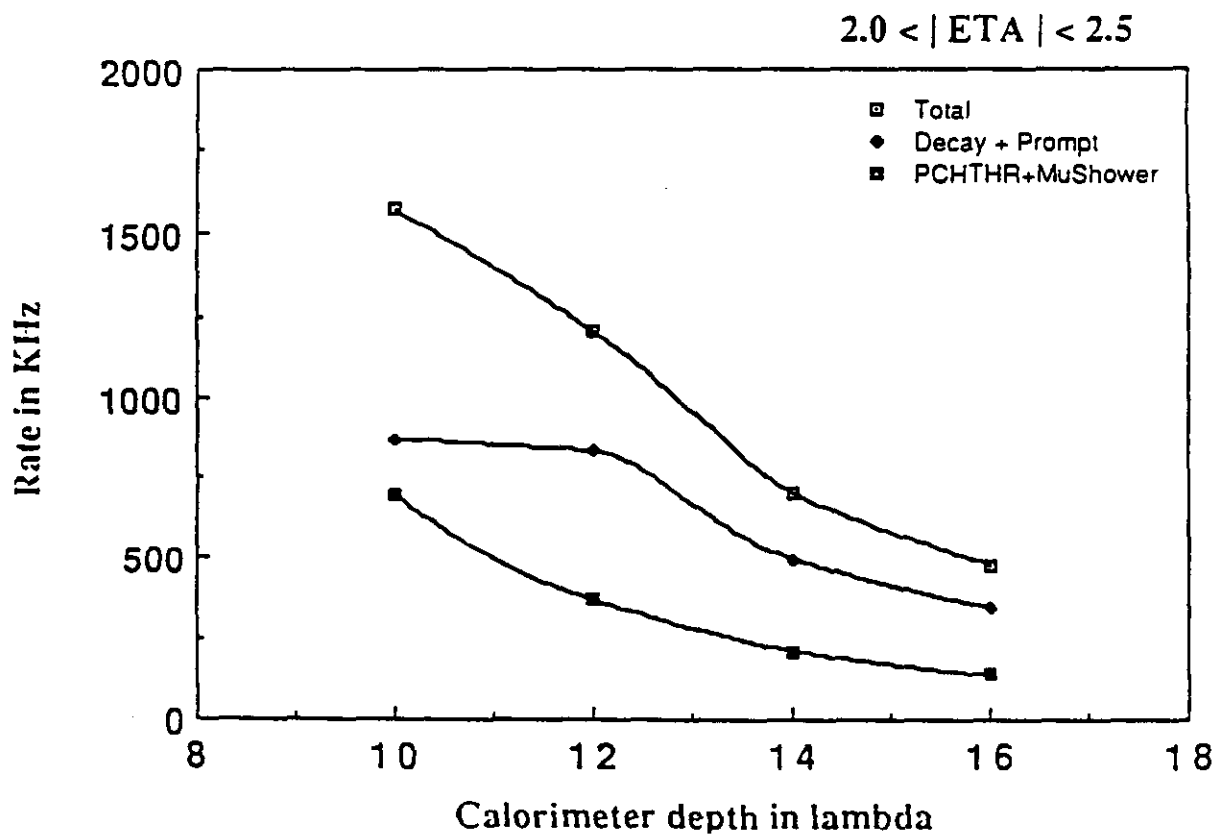
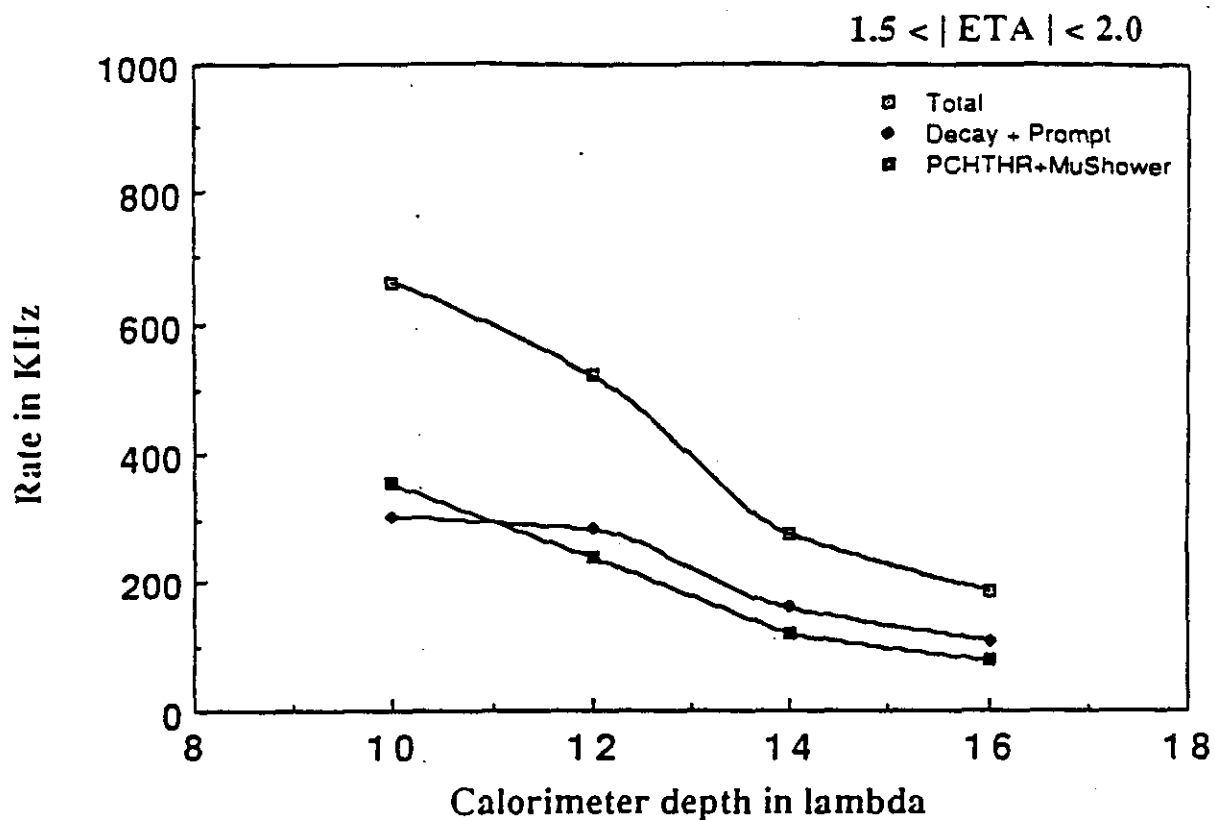


Fig. 9 - Charged particle rate (kHz) versus calorimeter depth (λ) for two rapidity intervals $1.5 < |\eta| < 2.0$ and $2.0 < |\eta| < 2.5$. ($L=10^{33} \text{ cm}^{-2} \text{ s}^{-1}$)

MUON SYSTEM

(7) System Upgrades

(person responsible: Larry Rosenson - MIT)

The muon momentum resolution can be improved by the addition of external chamber planes located outside the solenoid magnet. Additional improvement is gained by constraining the primary vertex.

Reference:

[1] "Considerations on the Addition of Detector Planes Outside the GEM Magnet and on the Implementation of a Vertex Constraint", L. Rosenson, GEM TN-92-97.

Fig. 7-1 Preliminary deployment of external chambers. For the calculations it was assumed that the magnet coil and cryostat present $10 X_0$, to a muon passing through the coils and incident on an external barrel superlayer composed of two planes of detectors.

Fig. 7-2. The overall improvement in the resolution is shown when both external chambers and primary vertex are used to determine the momentum.

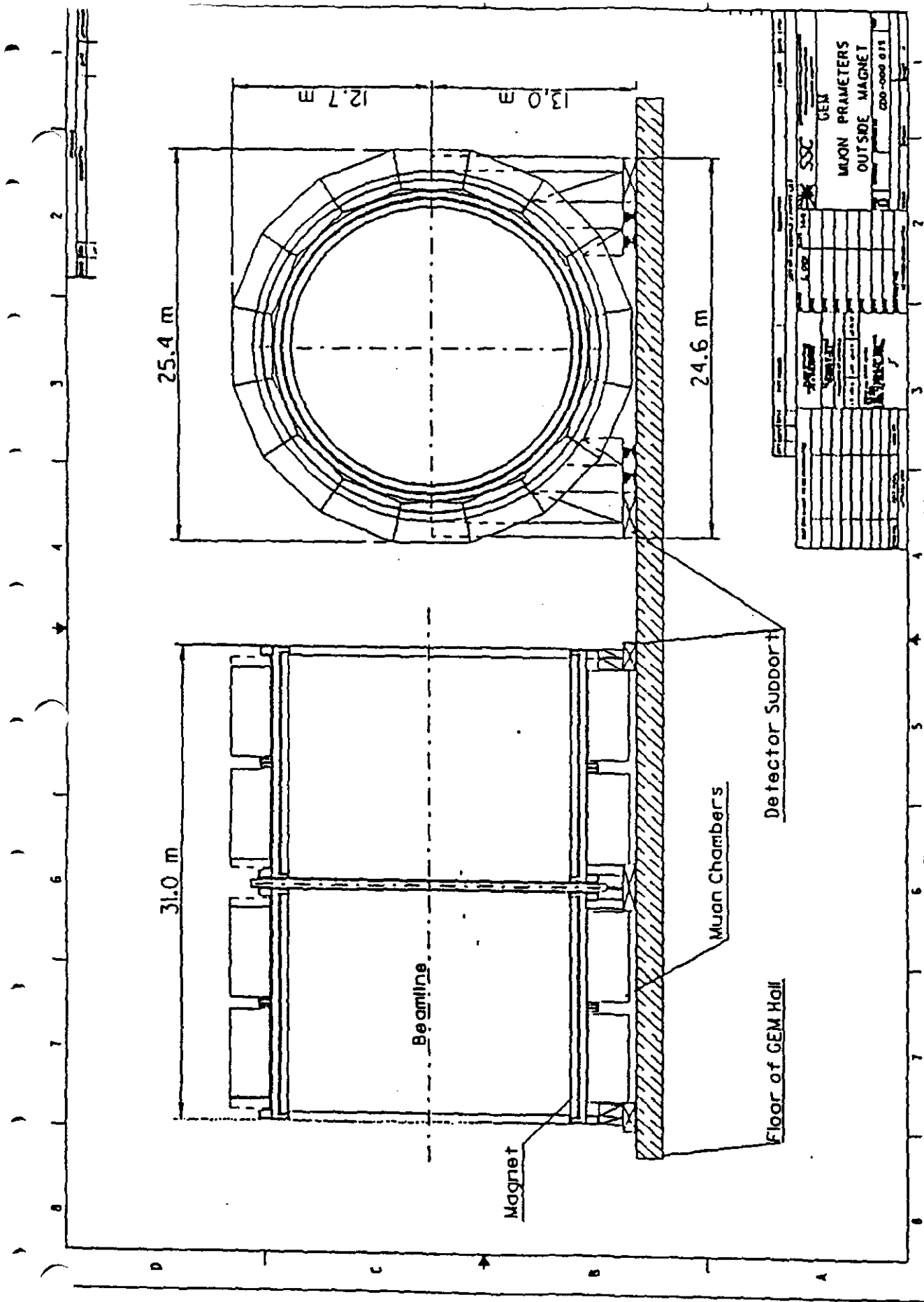


Fig. 7.1

IMPROVEMENT OF P_T RESOLUTION WITH THE ADDITION OF
 AN EXTERNAL SUPERLAYER L_E AND L_B DOWNSTREAM
 OF THE ENDCAP AND BARREL RESPECTIVELY

+ A 200 μm . VERTEX CONSTRAINT 488_7on8.txt

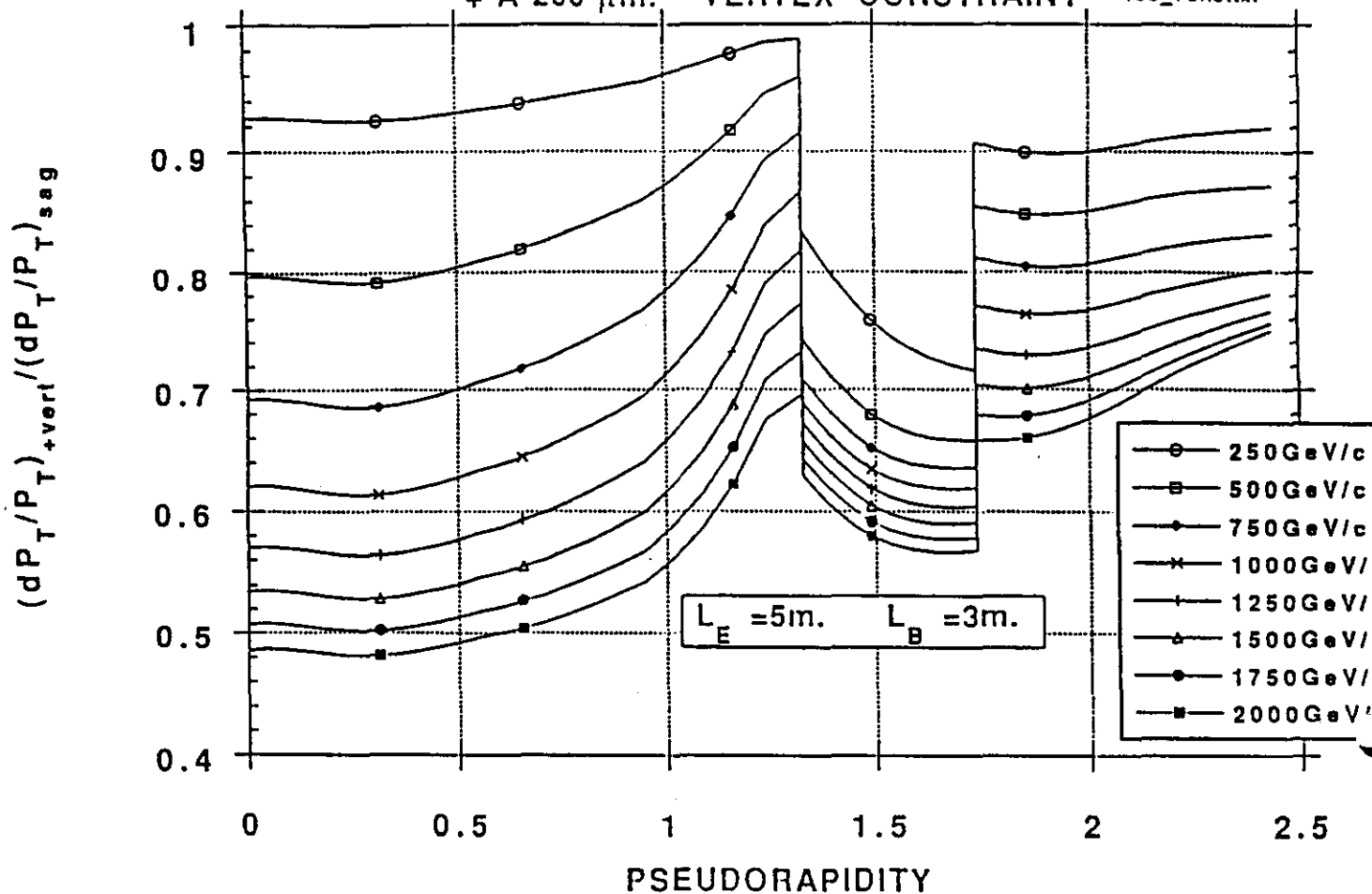
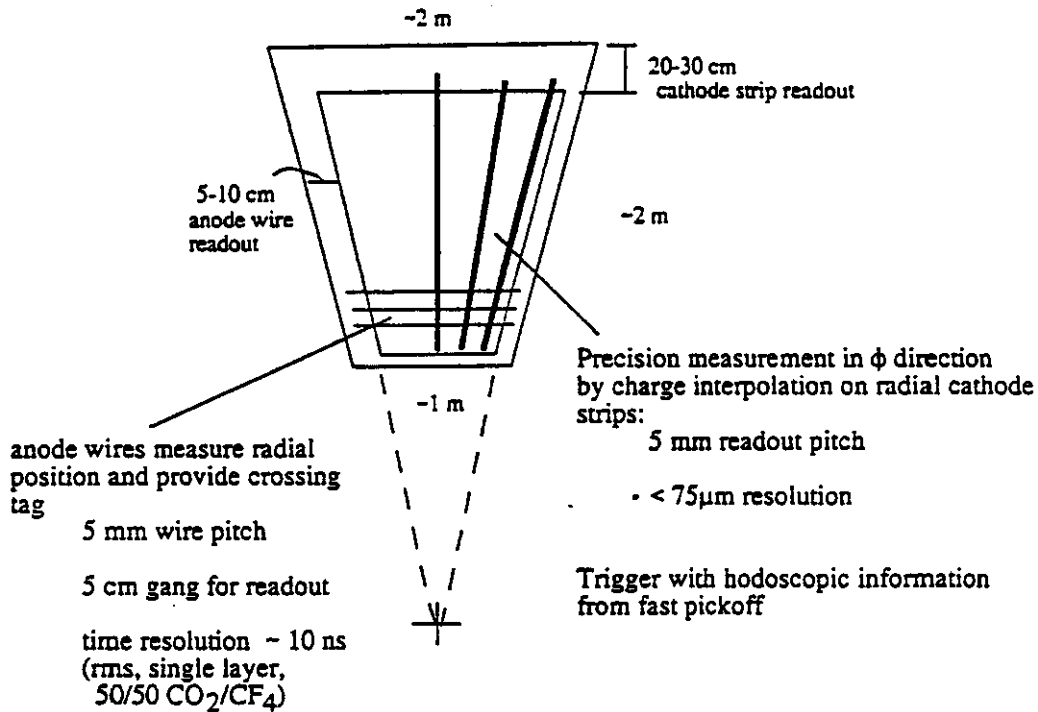


Fig. 7.2

(8) Chamber Technologies:

Cathode Strip Chambers for GEM Endcaps

- Large area, narrow gap (5 mm) multiwire proportional chambers
- Four-layer modules; light, rigid package
- Alignment features integrated with precision cathodes



Chamber size limited by

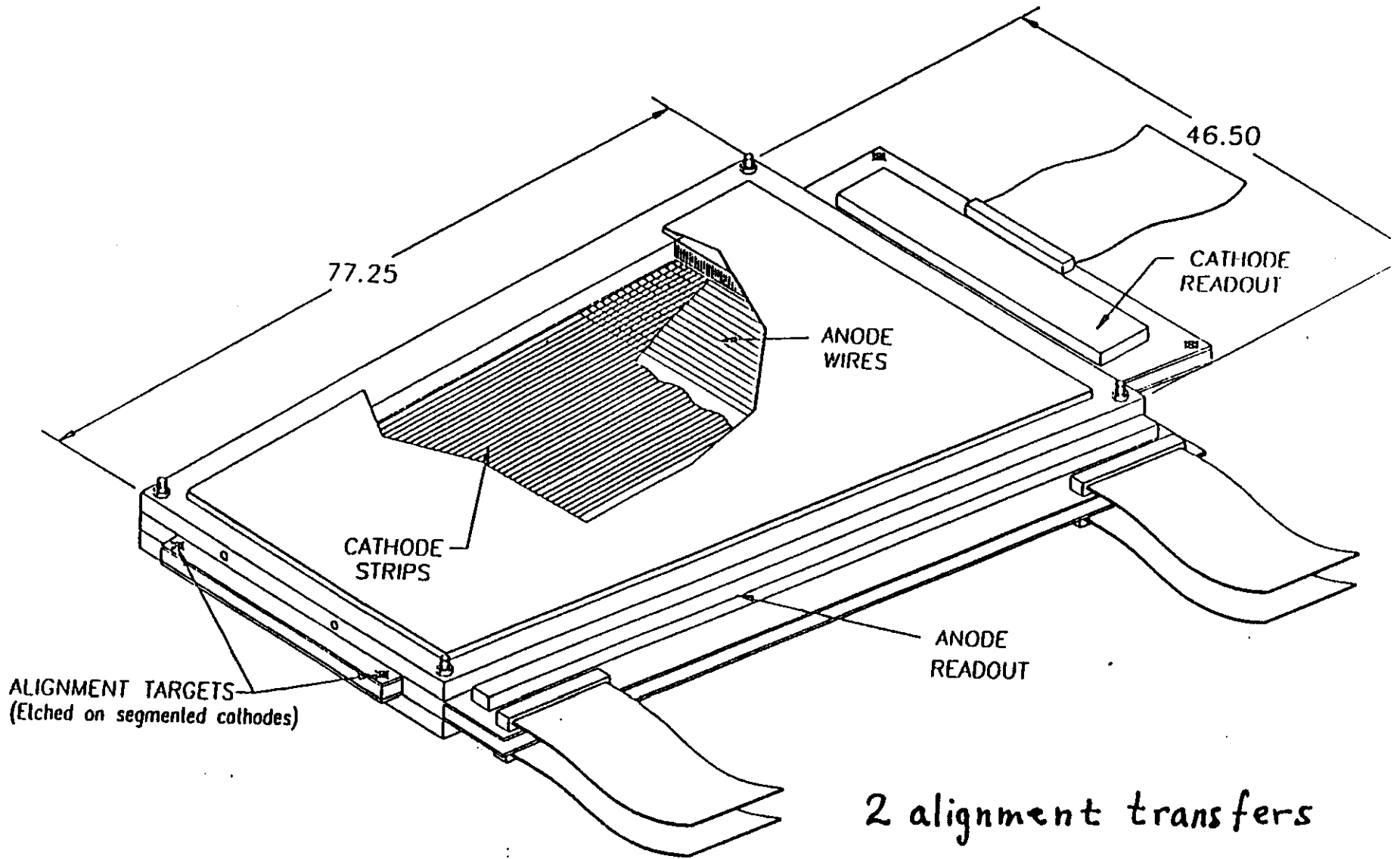
- rate
- noise contribution from strip capacitance
- capacity of circuit board houses

charged particle occupancy $\leq 3\% @ 10^{34}$

Need to overlap chambers to limit acceptance losses

Number of channels:

- bend plane (5 mm strips) 242 k
- nonbend plane (5 cm strips) 29 k

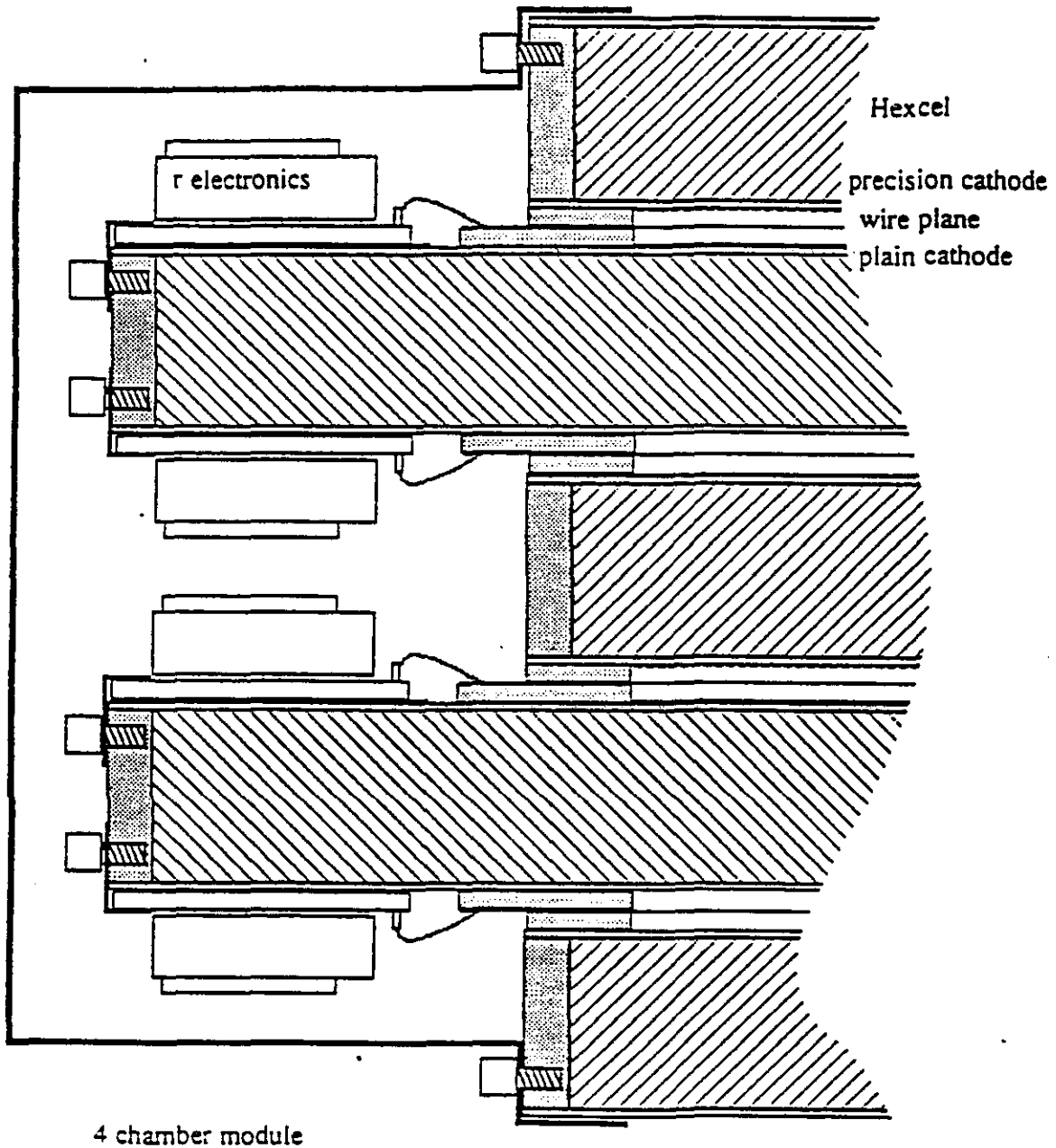


PROTOTYPE CATHODE STRIP CHAMBER

CATHODE STRIP CHAMBERS
MODULE

scale : full

4 - GAP CONCEPT



MUON SYSTEM

Summary of RPC Properties:

Function in GEM Muon System:

Barrel:

- Level 1 muon trigger
- Z-coordinate
- Tracking roads for later analysis

Construction:

- dual 2 mm gap
- 1.3 cm strips - bend plane
- 4 to 9 cm strips - nonbend plane

Properties:

plate bulk resistivity	10^{11} W cm (typical)
electric field	40 kV/cm
pulse charge	100 pC
pulse risetime	< 3 ns
pulse duration	< 50 ns FWHH
discharge area	0.1 cm ²
recovery time	10 ms
pulse jitter	< 1.4 ns (measured)

Gas:

Argon	2%
Freon	2%
CO ₂	86%

Rate limitation	50 to 100 Hz/cm ²
Efficiency	> 96 % over 1x2m ²
Random counting rate	5 to 10 x cosmic rate

References:

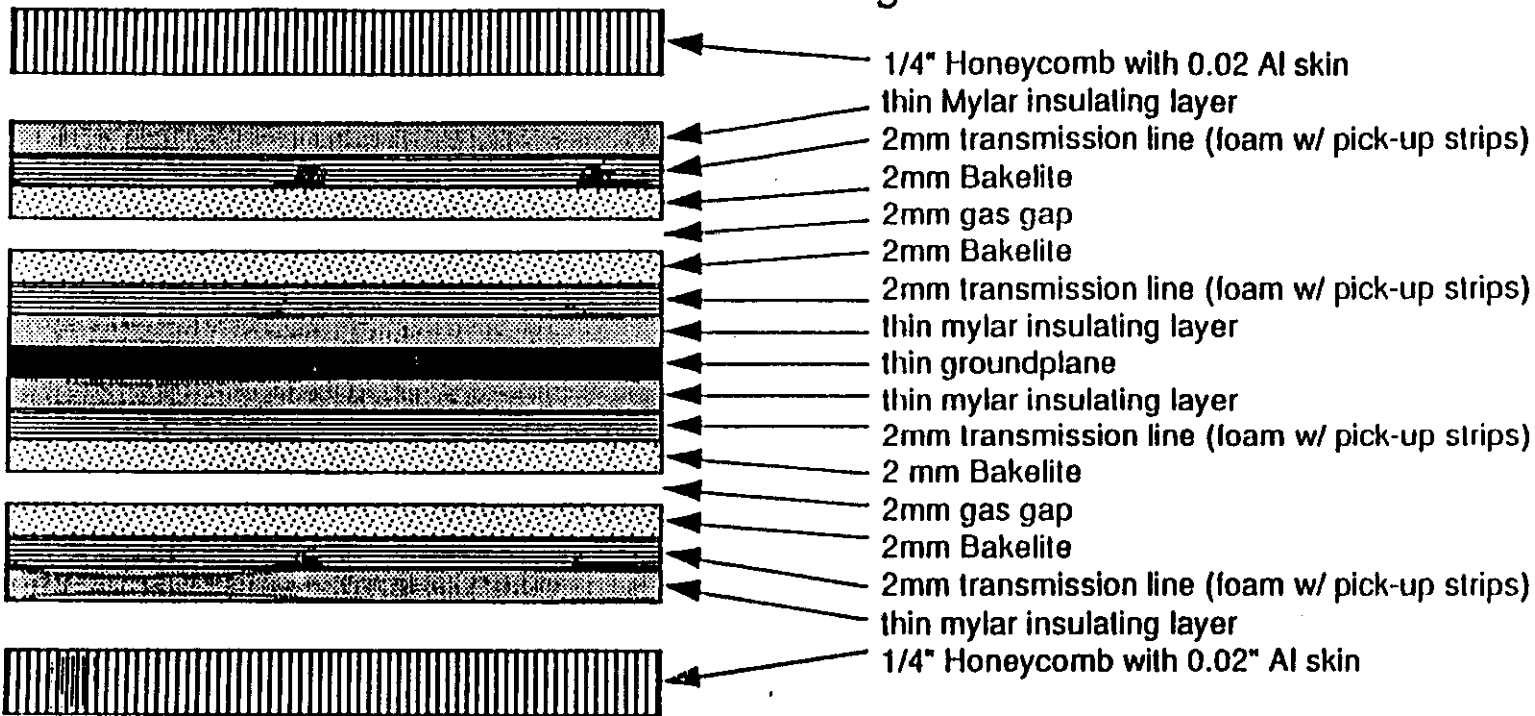
[3.1] "Descoped SSC R&D Proposal for the GEM Muon Beam Tagging Trigger and Z-Coordinate Measuring System using Resistive Plate Counters", C. Wuest, I. Pless, et al.

[3.2] "Progress in Resistive Plate Chambers", R. Cardarelli, et al. NIM A263,20, (1988).

[3.3] "Study of Muon Triggers and Momentum Reconstruction in a Strong Magnetic Field for a Muon Detector at LHC", M. Della Negra, et al. CERN/DRDC/90-36 (August 1990).

Source: F. Nimblett/F. Taylor
Update: 7/7/92

Outer Bakelite RPC cross section and weight calculation: total thickness = 5 cm



Densities: Bakelite and all materials except Honeycomb and foam = 1.5 g/cm³
 Honeycomb = 0.435 g/cm² (7.9 lb/ou. ft., 1/4" thick with 0.02" aluminum skins)
 Foam = 0.2 g/cm³

Areal Mass of two layer RPC = $2 \times (0.435 \text{ g/cm}^2) + 0.8 \text{ cm} \times (1.5 \text{ g/cm}^3) + 0.8 \text{ cm} \times (0.2 \text{ g/cm}^3)$
 $= 2.23 \text{ g/cm}^2 = 3.17 \times 10^{-2} \text{ psi}$

For four 380 cm x 329.6 cm outer sector chambers:

$4 \times (380 \text{ cm} \times 329.6 \text{ cm}) \times 1 \text{ in}^2 / (2.54 \text{ cm})^2 \times 3.17 \times 10^{-2} \text{ psi} = 2462 \text{ lb}$

Aluminum U-channel framework: U-channel @ 3.81 cm H x 5 cm W with 0.159 cm thick ribs, 2.14 cm² cross section

$4 \times ((380 \text{ cm} \times 2) + (329.6 \text{ cm} \times 2)) = 5677 \text{ cm perimeter}$

$5677 \text{ cm} \times 2.14 \text{ cm}^2 \times 2.7 \text{ g/cm}^3 \times 2.205 \text{ lb/1000 g} = 72.3 \text{ lb}$

MUON SYSTEM

Summary of LSDT Properties:

Function in the GEM Muon System:

Barrel:

precision sagitta measurement
Levels 2 and 3 trigger

Construction:

open cathode (top separate)
 $2.5 \times 2.5 \text{ cm}^2$ cells - 100 mm wire
< 1% X_0 Al per layer
Z-coordinate strips
precision wire stringing
wire supported every 2 m (typ)

Spatial resolution

100 mm RMS

Pulses

100 mV into 50 W

10 ns risetime

Drift time

< 300 ns (typ)

Drift velocity

50 mm/ns (typ)

Gas

A(few %):IB(<10%):CO₂

A(few %):IB(<10%):CO₂:CF₄

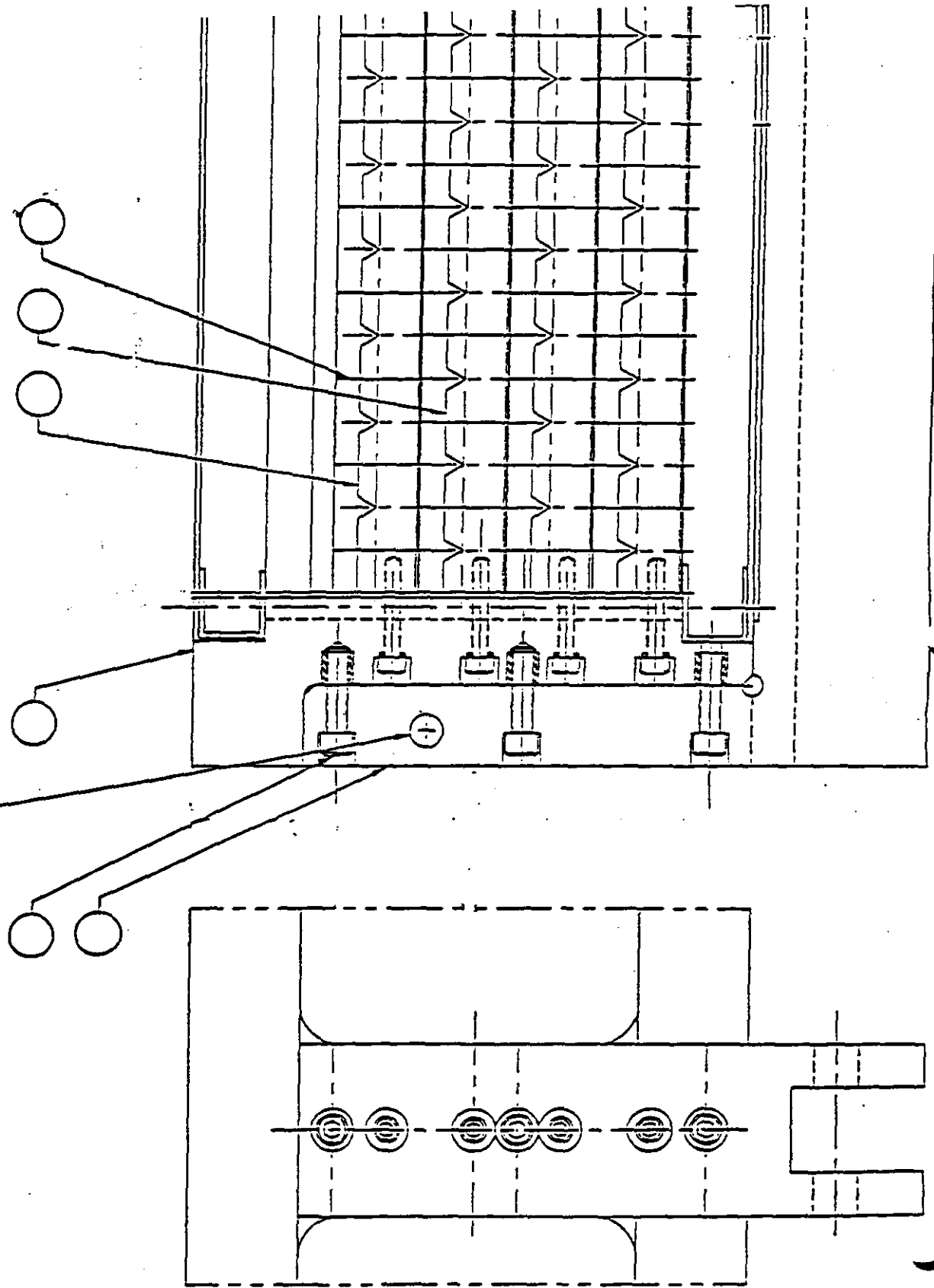
Reference:

[3.4] "Description of an LSDT Muon System for the GEM Detector", L.S. Osborne, et al. Chapter in the GEM TDR.

Source:

Update: 7/7/92

HOLE FOR ALIGNMENT
(TO BE DETERMINED)



LSDT WIRE ALIGNMENT DETAIL

MUON SYSTEM

Summary of PDT Properties:

Function in GEM System

Barrel:

Precision sagitta measurement

Levels 2 and 3 trigger

Construction

25mm wire operated in prop-mode

3.8 cm diameter Al tube 300 mm wall

Precision endplate to constrain tubes

No internal wire support

Gas

A(90%):CO₂(9%):CH₄(1%) @ 2 to 3 ATM

A(50%):Ethane(50%) @ 1 to 2 ATM

Single layer resolution

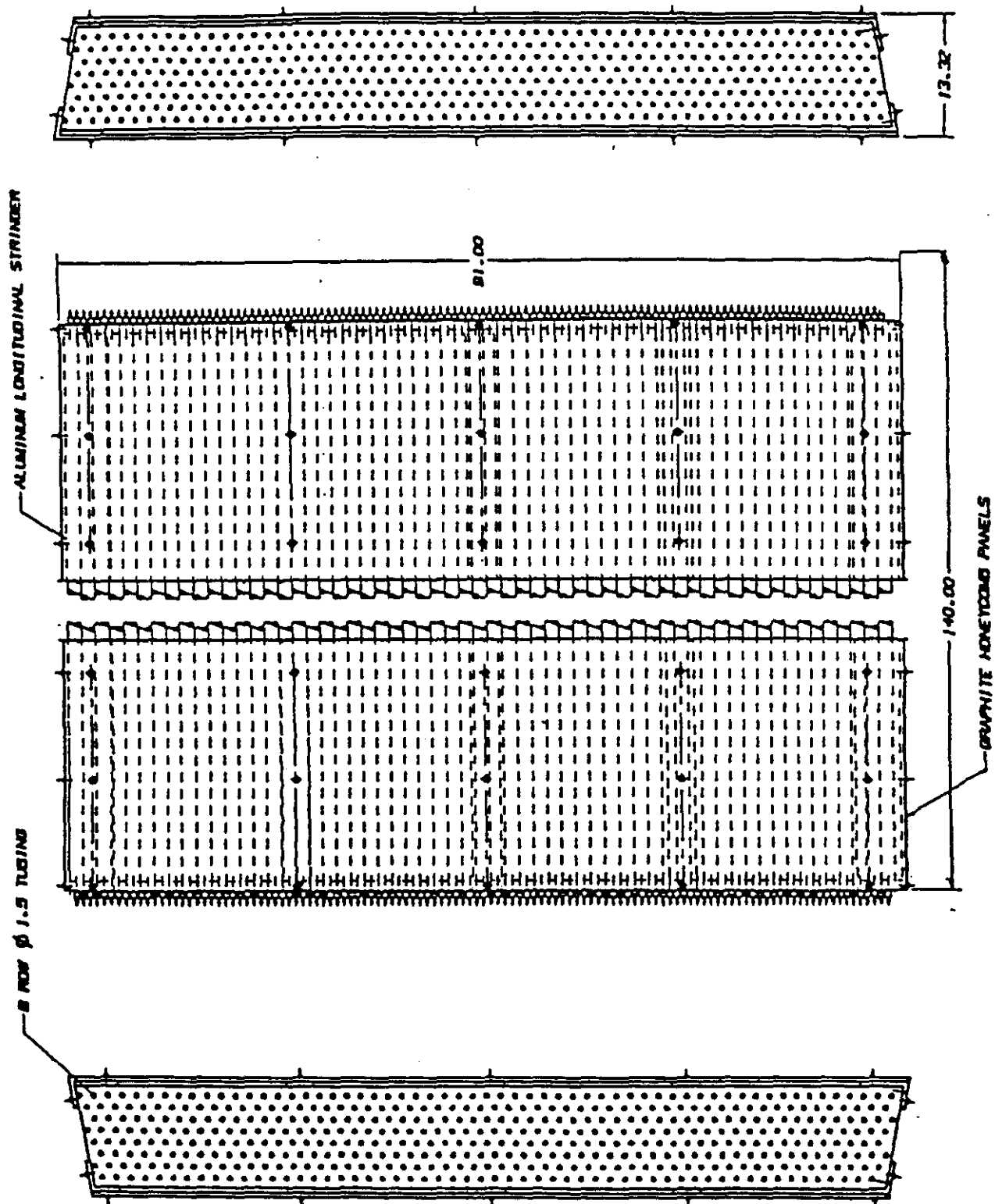
< 100 mm depending on pressure (typ)

Reference:

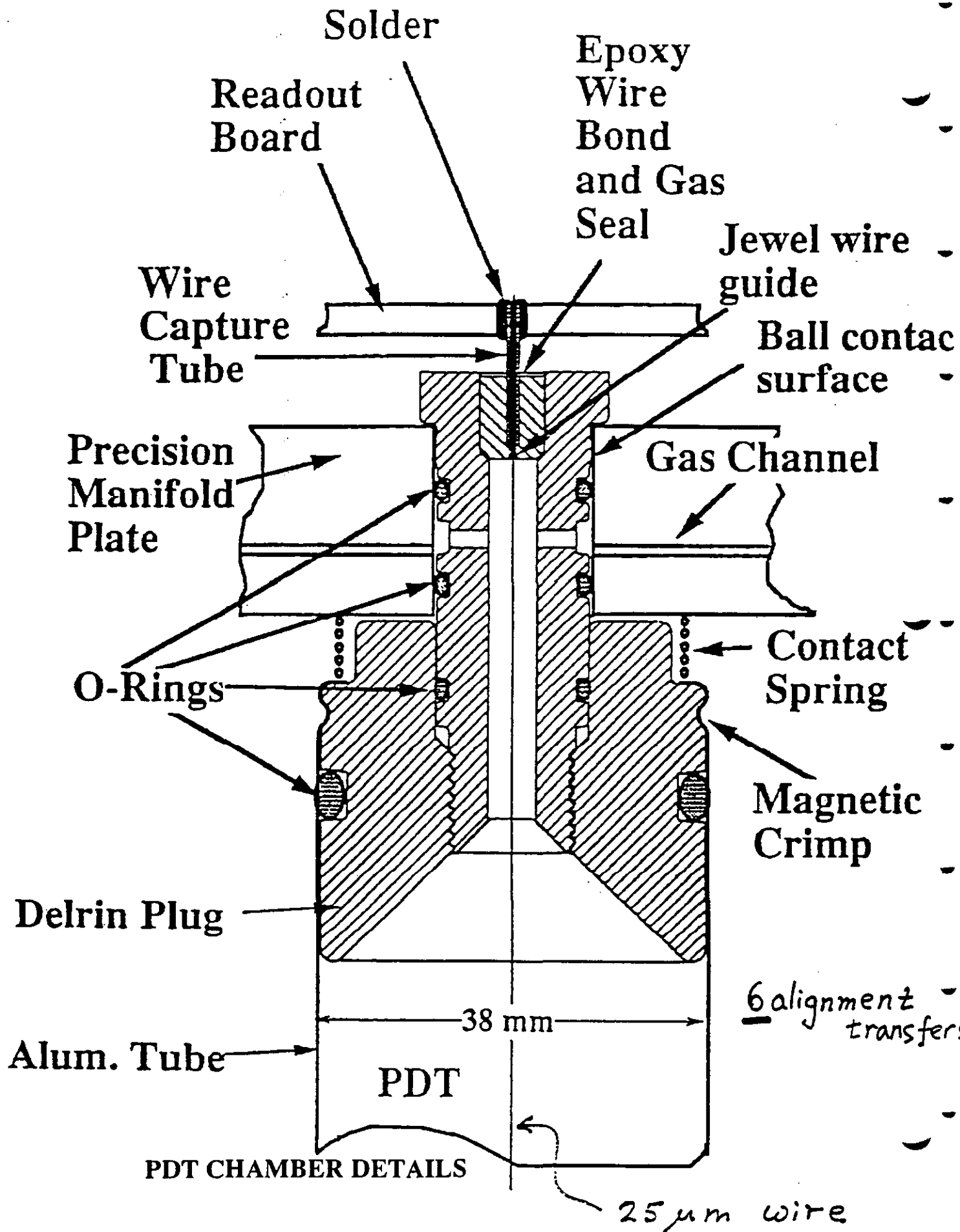
(1) C. Bromberg

Source: F. Nimblett/F. Taylor

Update: 7/7/92



8 LAYER PDT CHAMBER



ALIGNMENT SYSTEM

TABLE OF CONTENTS

OVERVIEW

Introduction
Requirements
Tracker/Calorimeter/Central Support Assembly
Muon/Magnet Assembly

BEAMLINER DEFINITION

Beamline Alignment
Beamline Slope
Consistency of the Installation Beamline

FIGURES:

Basic Straightness Monitor
Straightness Monitor Electronics
Straightness Monitor Paths in Muon Chamber Barrel
Alignment Along Muon Chamber Layer
Alignment Paths in the Muon Endcaps
Strategies for Measuring Global Muon System Alignment
Stretched Wire Alignment Technique
Muon Sector Alignment Scheme
Muon Barrel Module Measurement Accuracy
Muon Endcap Module Measurement Accuracy

TABLES:

Preliminary Global Alignment Requirements
Preliminary Placement Tolerance Matrix
Preliminary Stability Tolerance Matrix
Preliminary Drift Tolerance Matrix
Preliminary Real Time Measurement Tolerance Matrix
Muon System Measurement Accuracy Requirements

ALIGNMENT SYSTEM

ALIGNMENT

OVERVIEW

Introduction

The global alignment of the GEM detector will require meticulous management of many aspects of the design, assembly and installation of each of the major subsystems. Not only must each subsystem satisfy its own precision requirements but it must also recognize and accommodate the requirements of neighboring systems. GEM, therefore, requires an integrated approach to the global alignment issue to assure total compliance of all synergistic requirements.

To date, a preliminary global alignment data base has been assembled which identifies all of the requirements between all systems. These requirements are being integrated into the assembly procedures and system designs.

Requirements

Successful alignment implementation will require that a minimum of three basic concepts be addressed: placement; stability; and precision real time measurement. First, each of the subsystems must be placed in the experiment hall and relative to each other to within defined tolerances. This requirement must take into consideration the accuracy with which the external fiducials have been placed with respect to the internal alignment sensitive components and the uncertainty of the location of the beamline within the experiment hall. In addition long term drift, caused by hall foundation settling and material creep, must be managed and compensated by periodic position adjustments. Once the systems have been placed and are operational the structural design of the subsystems must assure that any environmental perturbation does not alter the placement of any subsystem beyond acceptable tolerances.

Stability refers to short term position variations, typically vibration and thermal motion, that cannot be compensated for because of their high rate of variability.

During a run, real time measurements will be made to obtain the accurate position information of the tracker and muon systems. This information will be used to identify the precise location of the interaction point and enhance particle trajectory and muon momentum calculations.

Source: R Sawicki
Update: 7/1/92

ALIGNMENT

The following table summarizes, at the very highest level, preliminary global alignment requirements in these three categories for each of the main subsystems. Values listed are relative to the actual position of the beamline during a run and are provided in cylindrical coordinates. R is the position tolerance in the radial direction, the phi position tolerance is in the circumferential direction. Muon tolerances refer to the positioning of each muon sector relative to the beam. Local muon tolerances related to straight line requirements between superlayers is not addressed by this table.

Preliminary Global Alignment Requirements
Position Relative to Beamline

	Placement - mm		Stability - mm		Real Time Measurement - mm	
	R	Phi	R	Phi	R	Phi
Central Tracker	5	5	.100	.100	.050	.050
Calorimeter	4	4	.050	.050	-	-
Central Detector Support	10	10	.040	.040	-	-
Muon - Barrel	10	5	.05	.010	4.0	0.7 .20(goal)
Muon - Endcap	4	5	.05	.010	8.0	1.0 .20(goal)
Magnet	10	10	.020	.010	-	-
Forward Field Shaper	10	10	.020	.010	-	-

The placement tolerances are generally within the placement capabilities of conventional industrial installation techniques and can be verified with standard precision surveying equipment. However, these figures represent tolerances with respect to the actual position of the beamline and that position is uncertain at the time of the alignment of the detector. Current estimates of this uncertainty is ± 3 mm when the beam is first turned on. Thereafter the beam may continue to drift up to an additional 1 millimeter. Thus, the actual positioning requirement is reduced by these two factors.

Source: R Sawicki
Update: 7/1/92

ALIGNMENT

Tracker/calorimeter/central support assembly

The first subsystem requiring alignment in the experiment hall will be the central detector support. Initially this structure will be positioned without great accuracy since it is the location of the subsystem which are mounted on it, not the structure itself, that requires accurate placement. The barrel calorimeter will then be placed onto the central detector support.

Once the barrel calorimeter is in position the central tracker can be placed on its kinematic mount inside the calorimeter. The relative position of these two subsystems will be carefully adjusted because after the endcap and forward calorimeters are installed the tracker will be almost completely hidden.

Using fiducials located on the calorimeter the membrane's position adjustment capability will be exercised to locate the calorimeter accurately. The central tracker will, because of its precise relative placement tolerance with respect to the calorimeter, also be accurately located. Concepts are being considered to locate fiducials on the tracker near the beam pipe to provide a more direct measurement of the tracker position relative to the experiment hall. The 5 mm placement tolerance is driven by the concern of radiation damage to the silicon wafers. Deviations greater than this amount will have unacceptable lifetime impact on the tracker components.

Tracker stability tolerance is relieved by the fact that the vertex location will be determined by the tracker at the beam crossing rate. However, stability is still required to maintain track linking capability with the calorimeter and muon systems. The 100 micron tolerance is achievable with careful system design and implementation, but will rely upon the integrated performance of both of the subsystems which support it - the calorimeter and membrane.

Muon/magnet assembly

The muon system can be globally located with respect to the experiment hall after it has been installed in the magnet and the magnet positioned next to the membrane. External fiducials accurately located with respect to the muon sensing wires will be positioned relative to the expected position of the beamline with precision electronic surveying equipment as indicated by the hall monuments. Adjustments will be made with the positioning mechanisms located at the sector mounting point to the magnet. Individual chamber mounts

Source: R Sawicki
Update: 7/1/92

ALIGNMENT

will only be used to correct the relative placement between chambers in a common tower within a sector. The 6 mm placement tolerance (barrel) is driven by the alignment of the trigger roads. Misalignment greater than this would cause trigger losses of about 10%.

Stability of the muon detectors is highly dependent on the structural characteristics of the magnet. Vibration, magnetic forces and thermal motion induced during cool-down will all contribute to muon detector position changes. On-going analyses are addressing the magnitude of these displacements. Results will be used to initiate appropriate design features to insure compliance with all muon alignment tolerances. The global stability requirement of 15 micron (phi direction) stems from the local requirement of superlayer-to-superlayer measurement accuracy of 25 microns. If measurements with this resolution are to be made then the indicated stability must be achieved during an experiment run.

Real time systems which can measure the location of the muon system relative to the beamline are being considered. Position knowledge to within 5 mm (phi direction barrel region) is sufficient to maintain adequate mass and momentum resolution. However, it is possible to substantially improve muon momentum resolution below the 5% baseline by using knowledge of the vertex position relative to the muon superlayers in the momentum calculations. Analysis already performed indicates that measurement accuracy of better than 200 microns is required to achieve this improvement. It is a goal of the GEM detector to strive towards making this measurement within the constraints of the programmatic and technical requirements.

The simplest and most direct method to measure the vertex location appears to be to use background muon tracks. Analysis is commencing to determine the feasibility of this approach. In a parallel effort, concepts are being considered to measure vertex location using external measurement devices. This is a difficult measurement because of the distances involved, the complexity of the muon support system and the inaccessibility of the chambers to any external measurement system. A successful system would have to measure the location of a muon sector relative to some external fiducial, probably located on the forward field shaper, and these locations then translated to a beam position monitor located just outside of the GEM magnet. Concepts involving lasers and stretched wire straight line monitors in coordination with low thermal expansion coefficient reference rods are being considered.

Source: R Sawicki
Update: 7/1/92

Preliminary Placement Tolerance Matrix

	1	2	3a	3b	4	5	6	7	8
	Tracker	Calorimeter	Muon chamber		Magnet	Flux shaper	Membrane	Beamline	Hall
			Barrel	Endcap					
1 Tracker	0.050 0.050 1.000	0.250 0.250 0.500	10.000 10.000 10.000	10.000 10.000 10.000	10.000 10.000 10.000	10.000 10.000 10.000	1.031 1.031 1.118	3.326 3.326 30.037	1.436 1.436 1.000
2 Calorimeter		1.000 1.000 1.000	10.000 10.000 10.000	10.000 10.000 10.000	10.000 10.000 10.000	10.000 10.000 10.000	1.000 1.000 1.000	3.317 3.317 30.033	1.000 1.000 1.000
3 Muon chamber (barrel)			0.063 0.025 1.000	10.000 10.000 10.000	3.000 3.000 10.000	10.000 10.000 10.000	10.000 10.000 10.000	3.317 3.317 30.033	1.000 1.000 1.000
4 Muon chamber (endcap)				1.000 0.025 0.063	10.000 10.000 10.000	3.000 3.000 10.000	10.000 10.000 10.000	3.317 3.317 30.033	1.000 1.000 1.000
5 Magnet					10.000 10.000 10.000	10.000 10.000 10.000	10.000 10.000 10.000	10.488 10.488 31.638	10.000 10.000 10.000
6 Flux shaper						- - -	10.000 10.000 10.000	10.488 10.488 31.638	10.000 10.000 10.000
7 Membrane							- - -	4.458 4.458 30.166	3.000 3.000 3.000
8 Beamline								- - -	3.000 3.000 30.000
9 Hall									1.000 1.000 1.000

9 Intracalor.	10a	10b
	Intramion	
	Barrel	Endcap
1.000	0.700	1.000
1.000	0.700	0.700
2.000	1.000	0.700

All units - millimeters
 Diagonal elements represent fiducialization requirements
 ○ - relative to beampipe (not beamline)

Format: X (radial) placement
 Y (circumferential) placement
 Z (axial placement)

Constraint equations (shaded boxes):

$$\begin{aligned}
 (1,6) &> ((1,2)^2 + (2,6)^2)^{0.5} & (3a,7) &> ((3a,8)^2 + (8,8)^2 + (7,8)^2)^{0.5} \\
 (1,8) &> ((1,2)^2 + (2,8)^2 + (8,8)^2)^{0.5} & (3b,7) &> ((3b,8)^2 + (8,8)^2 + (7,8)^2)^{0.5} \\
 (1,7) &> ((1,2)^2 + (2,8)^2 + (8,8)^2 + (7,8)^2)^{0.5} & (4,7) &> ((4,8)^2 + (8,8)^2 + (7,8)^2)^{0.5} \\
 (2,7) &> ((2,8)^2 + (8,8)^2 + (7,8)^2)^{0.5} & (5,7) &> ((5,8)^2 + (8,8)^2 + (7,8)^2)^{0.5} \\
 & & (6,7) &> ((6,8)^2 + (8,8)^2 + (7,8)^2)^{0.5}
 \end{aligned}$$

Preliminary Stability Tolerance Matrix

	1	2	3a	3b	4	5	6	7	8
	Tracker	Calorimeter	Muon chamber		Magnet	Flux shaper	Membrane	Beamline	Hall
			Barrel	Endcap					
1 Tracker	0.025 0.025 0.100	0.050 0.050 0.100	0.050 0.050 0.100	0.100 0.050 0.050	0.100 0.100 0.100	0.100 0.100 0.100	0.051 0.051 0.141	0.052 0.052 0.142	0.052 0.052 0.142
2 Calorimeter		0.250 0.250 0.100	0.100 0.100 0.100	0.100 0.100 0.100	0.100 0.100 0.100	0.100 0.100 0.100	0.010 0.010 0.100	0.015 0.015 0.101	0.015 0.015 0.101
3a Muon chamber (barrel)			0.010 0.005 0.025	0.100 0.100 0.100	0.010 0.005 0.100	0.100 0.100 0.100	0.100 0.100 0.100	0.023 0.012 0.224	0.023 0.012 0.224
3b Muon chamber (endcap)				0.025 0.005 0.010	0.100 0.005 0.010	0.100 0.010 0.010	0.100 0.100 0.100	0.102 0.015 0.200	0.102 0.012 0.200
4 Magnet					0.100 0.100 0.100	0.100 0.100 0.100	0.100 0.100 0.100	0.021 0.011 0.200	0.020 0.010 0.200
5 Flux shaper						- - -	0.100 0.100 0.100	0.021 0.011 0.200	0.020 0.010 0.200
6 Membrane							- - -	0.011 0.011 0.011	0.010 0.010 0.010
7 Beamline								- - -	0.001 0.001 0.001
8 Hall									0.005 0.005 0.005

9	10a	10b
Intracalor.	IntramMuon (barrel)	IntramMuon (endcap)
0.100	0.030	0.100
0.100	0.020	0.020
0.100	0.100	0.060

Constraint equations (shaded boxes):

All units = millimeters
Diagonal elements represent fiducialization requirements

Format: X (radial) stability
Y (circumferential) stability
Z (axial) stability

$$\begin{aligned}
 (1,6) &> ((1,2)^2 + (2,6)^2)^{0.5} & (3a,7) &> ((3a,4)^2 + (4,8)^2 + (8,8)^2 + (7,8)^2)^{0.5} \\
 (1,8) &> ((1,2)^2 + (2,6)^2 + (6,8)^2 + (8,8)^2)^{0.5} & (3a,8) &> ((3a,4)^2 + (4,8)^2 + (8,8)^2)^{0.5} \\
 (1,7) &> ((1,2)^2 + (2,6)^2 + (6,8)^2 + (8,8)^2 + (7,8)^2)^{0.5} & (3b,7) &> ((3b,5)^2 + (5,8)^2 + (8,8)^2 + (7,8)^2)^{0.5} \\
 (2,8) &> ((2,6)^2 + (6,8)^2 + (8,8)^2)^{0.5} & (3b,8) &> ((3b,5)^2 + (5,8)^2 + (8,8)^2)^{0.5} \\
 (2,7) &> ((2,6)^2 + (6,8)^2 + (8,8)^2 + (7,8)^2)^{0.5} & (4,7) &> ((4,8)^2 + (8,8)^2 + (7,8)^2)^{0.5} \\
 & & (5,7) &> ((5,8)^2 + (8,8)^2 + (7,8)^2)^{0.5} \\
 & & (6,7) &> ((6,8)^2 + (8,8)^2 + (7,8)^2)^{0.5}
 \end{aligned}$$

Preliminary Drift Tolerance Matrix

	1	2	3	4	5	6	7	8
	Tracker	Calorimeter	Muon chamber	Magnet	Flux shaper	Membrane	Beamline	Hall
1 Tracker	0.005 0.005	0.250 0.250	5.000 5.000	5.000 5.000	5.000 5.000	1.031 1.031	2.016 2.016	1.750 1.750
2 Calorimeter		1.000 1.000	5.000 5.000	5.000 5.000	5.000 5.000	1.000 1.000	2.000 2.000	1.732 1.732
3 Muon chamber			0.005 0.005	1.000 1.000	5.000 5.000	5.000 5.000	2.000 2.000	1.732 1.732
4 Magnet				5.000 5.000	1.000 1.000	5.000 5.000	1.732 1.732	1.000 1.000
5 Flux shaper					- -	5.000 5.000	1.732 1.732	1.000 1.000
6 Membrane						- - -	1.732 1.732	1.000 1.000
7 Beamline							- - -	1.000 1.000
8 Hall								1.000 1.000

9	10
Intracalor.	Intramun
0.500 0.500	0.500 0.500

Constraint equations (shaded boxes) :

$$\begin{aligned}
 (1,6) &> ((1,2)^2 + (2,6)^2)^{0.5} & (3,7) &> ((3,4)^2 + (4,8)^2 + (8,8)^2 + (7,8)^2)^{0.5} \\
 (1,8) &> ((1,2)^2 + (2,6)^2 + (6,8)^2 + (8,8)^2)^{0.5} & (3,8) &> ((3,4)^2 + (4,8)^2 + (8,8)^2)^{0.5} \\
 (1,7) &> ((1,2)^2 + (2,6)^2 + (6,8)^2 + (8,8)^2 + (7,8)^2)^{0.5} & (4,7) &> ((4,8)^2 + (8,8)^2 + (7,8)^2)^{0.5} \\
 (2,8) &> ((2,6)^2 + (6,8)^2 + (8,8)^2)^{0.5} & (5,7) &> ((5,8)^2 + (8,8)^2 + (7,8)^2)^{0.5} \\
 (2,7) &> ((2,6)^2 + (6,8)^2 + (8,8)^2 + (7,8)^2)^{0.5} & (6,7) &> ((6,8)^2 + (8,8)^2 + (7,8)^2)^{0.5}
 \end{aligned}$$

All units = millimeters
 Diagonal elements represent fiducialization requirements

Format: turn-on
 longterm

Preliminary Real Time Measurement Tolerance Matrix

	1 Tracker	2 Calorimeter	3a Muon chamber	3b Muon chamber	4 Magnet	5 Flux shaper	6 Membrane	7 Beamline	8 Hall
1 Tracker	none none none	0.250 0.250 0.500	none none none	none none none	none none none	none none none	none none none	0.050 0.010 none	none none none
2 Calorimeter		none none none	none none none	none none none	none none none	none none none	none none none	none none none	none none none
3a Muon chamber (barrel)			none none none	none none none	none none none	0.100 none	none none none	4.000 0.700 50.000	none none none
3b Muon chamber (endcap)				none none none	none none none	none none none	none none none	6.000 1.000 2.000	none none none
4 Magnet					none none none	none none none	none none none	none none none	none none none
5 Flux shaper						none none none	none none none	none none none	none none none
6 Membrane							none none none	none none none	none none none
7 Beamline								none none none	0.050 0.050 none
8 Hall									1.000 1.000 1.000

9 Intracalor.	10a Intrusion		10b Endcap
	Barrel	Endcap	
none	0.030		1.000
none	0.020		0.020
none	1.000		0.060

Constraint equations (shaded boxes):

All units = millimeters
 O goal is .200 mm

Format: X (radial measurement)
 Y (circumferential measurement)
 Z (axial measurement)

BEAM LINE DEFINITION

Beamline Alignment

The geometry of the beam line of the machine is determined by the lattice design, and is established in its correct spatial position by means of the site surface geodetic network. This network of points is measured to the highest precision, and its employment for the positioning of both the machine and the experiments assures the homogeneity between the two. Despite this there will be an inevitable mismatch between the axis of installation of the detector, and of the machine. It is currently estimated that this mismatch will not exceed $\pm 3\text{mm}$. The axes of the detector and of the collider will be essentially parallel (a one millimeter deviation over the length of the hall is estimated to be possible). (See ADOD_AGG_91_034)

This non-coincidence of the installation axis will be quantified, just before machine commissioning, to $\pm 0.5\text{mm}$, when the two arcs of the machine are aligned and smoothed together through the Experimental Hall.

Beamline Slope

The beamline drops $\sim 1.7\text{mm}$ per meter from North to South at IR-5. The plane of the beamline drops $\sim 1.0\text{mm}$ per meter from West to East across the hall. The hall floor will be level and not parallel to the beamline. (See ADOD_AGG_91_038)

Consistency of the Installation Beamline

In order to maintain the consistency of the installation beamline, horizontal and vertical benchmarks will be provided in and around the vicinity of the experimental hall, together with a network of stable survey support brackets. Periodic re-measurement of these survey points will be an essential part of this process, and lines of sight between them must be maintained. (See GEFUR)

Muon Alignment System

(person responsible: Joe Paradiso - Draper Labs)

In summary, the precision required by the muon alignment systems are given below:

Muon Barrel:

Bending Coordinate (ϕ): 25 μm
 Radial Coordinate (r): 120 μm
 Beamline Coordinate (z): 1 mm

Muon Endcaps:

Bending Coordinate (ϕ): 25 μm
 Radial Coordinate (r): 1 mm
 Beamline Coordinate (z): 120 μm

Global Alignment:

Bending Coordinates (r): 200 μm
 Other Coordinates (ϕ, z): 1 mm

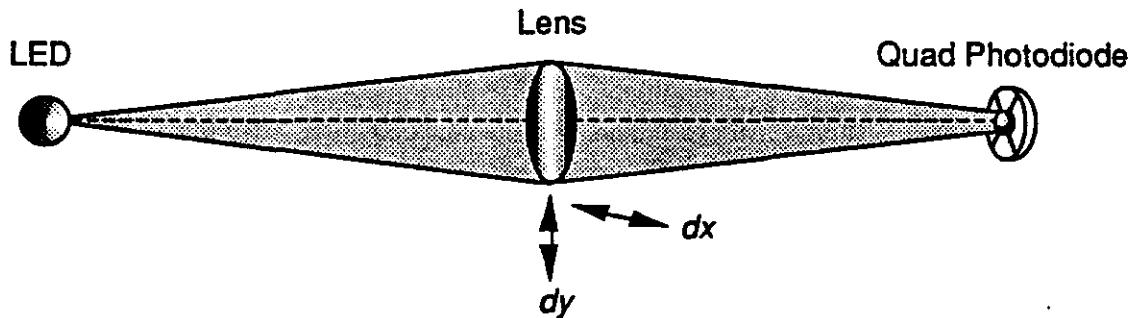


Figure 4.1: The Basic Straightness Monitor

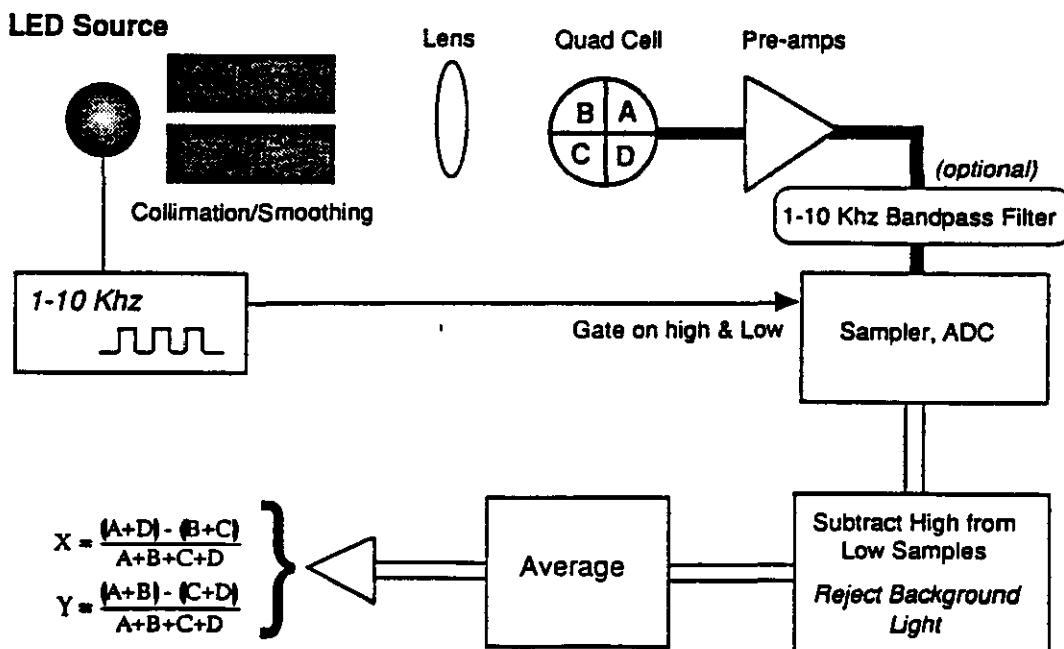
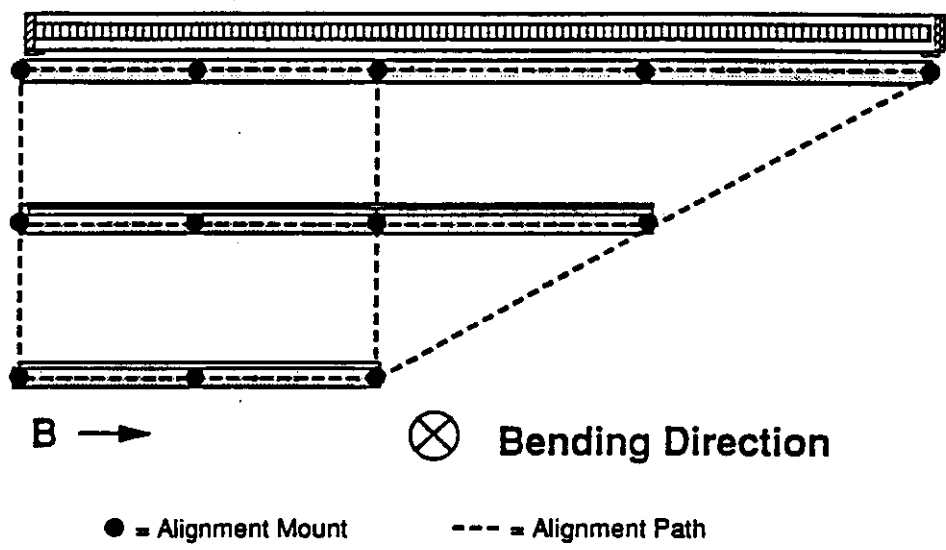
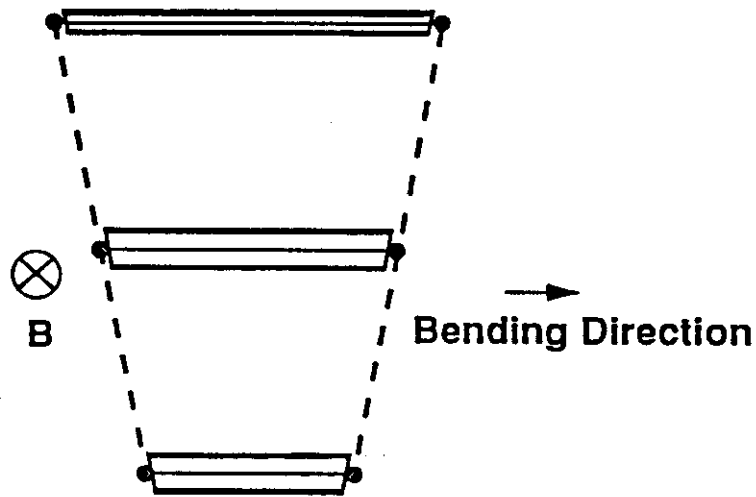


Figure 4.2: Straightness Monitor Electronics



a) $r\theta$ View



b) $r\phi$ View

Figure 4.3: Straightness Monitor Paths in Muon Chamber Barrel

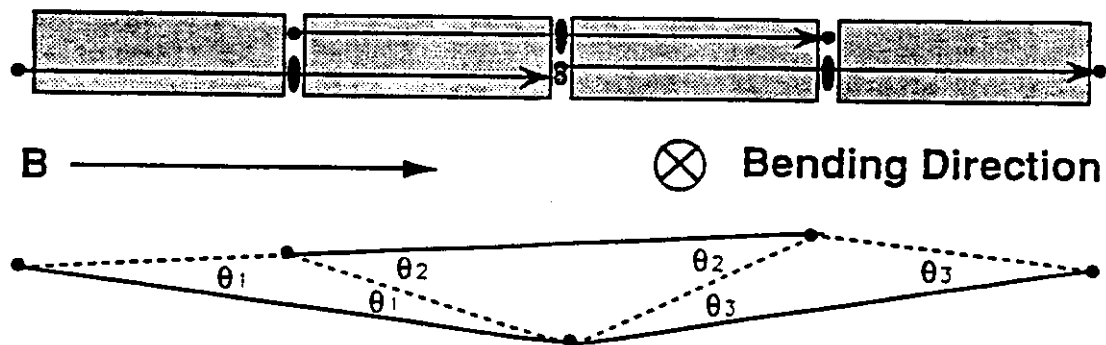
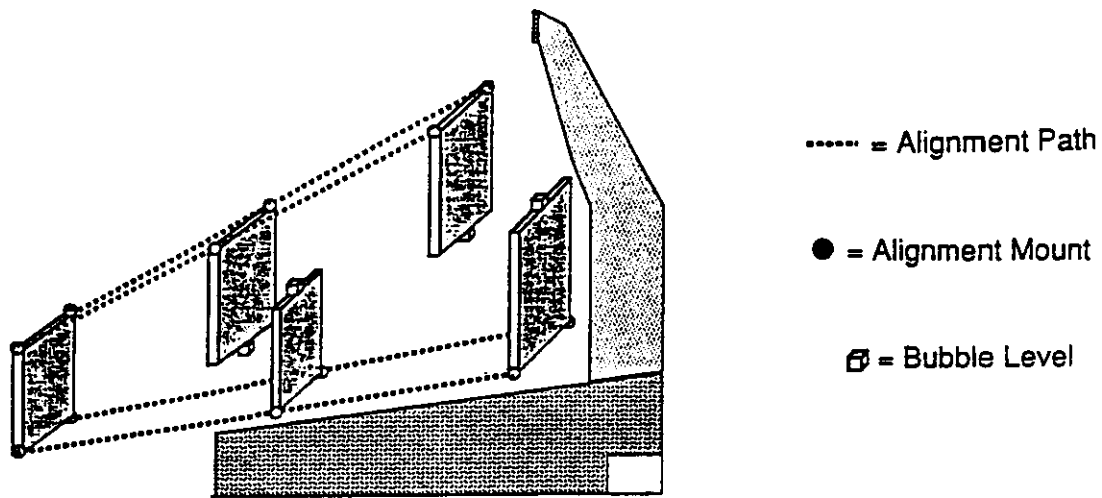


Figure 4.4: Alignment Along a Chamber Layer



Bending Direction ⊗

Figure 4.5: Alignment Paths in the Muon Endcaps

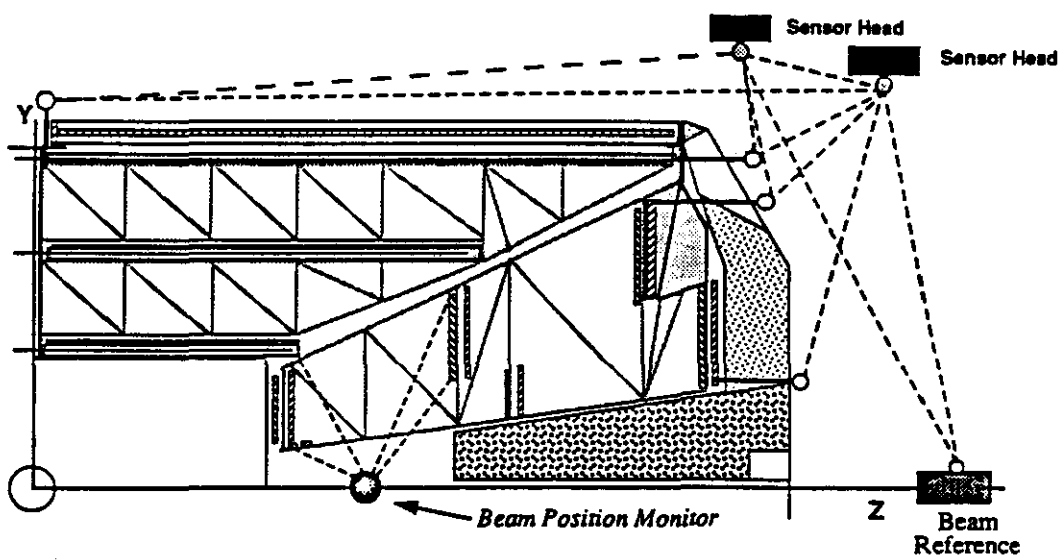


Figure 4.6: Strategies for Measuring Global Muon System Alignment

ALIGNMENT

Muon System Measurement Accuracy

Barrel Layers	x-offset bending coord	y-offset radial coord.	z-offset beamline coord.	parallel of readout in different layers
Inner and outer middle	50 μm 25 μm ($\delta S_{align} \leq 25 \mu\text{m}$)	125 μm 60 μm ($\delta S_{align} \leq 25 \mu\text{m}$)	4 mm 4 mm ($\Delta\phi/\phi \leq 1\%$)	± 0.003 mrad
Endcaps				
Inner and outer middle	50 μm 25 μm ($\delta S_{align} \leq 25 \mu\text{m}$)	1.0 mm 1.0 mm	250 μm 120 μm	± 0.005 mrad

Source: V Zhukov, R Sawicki
Update: 7/2/92

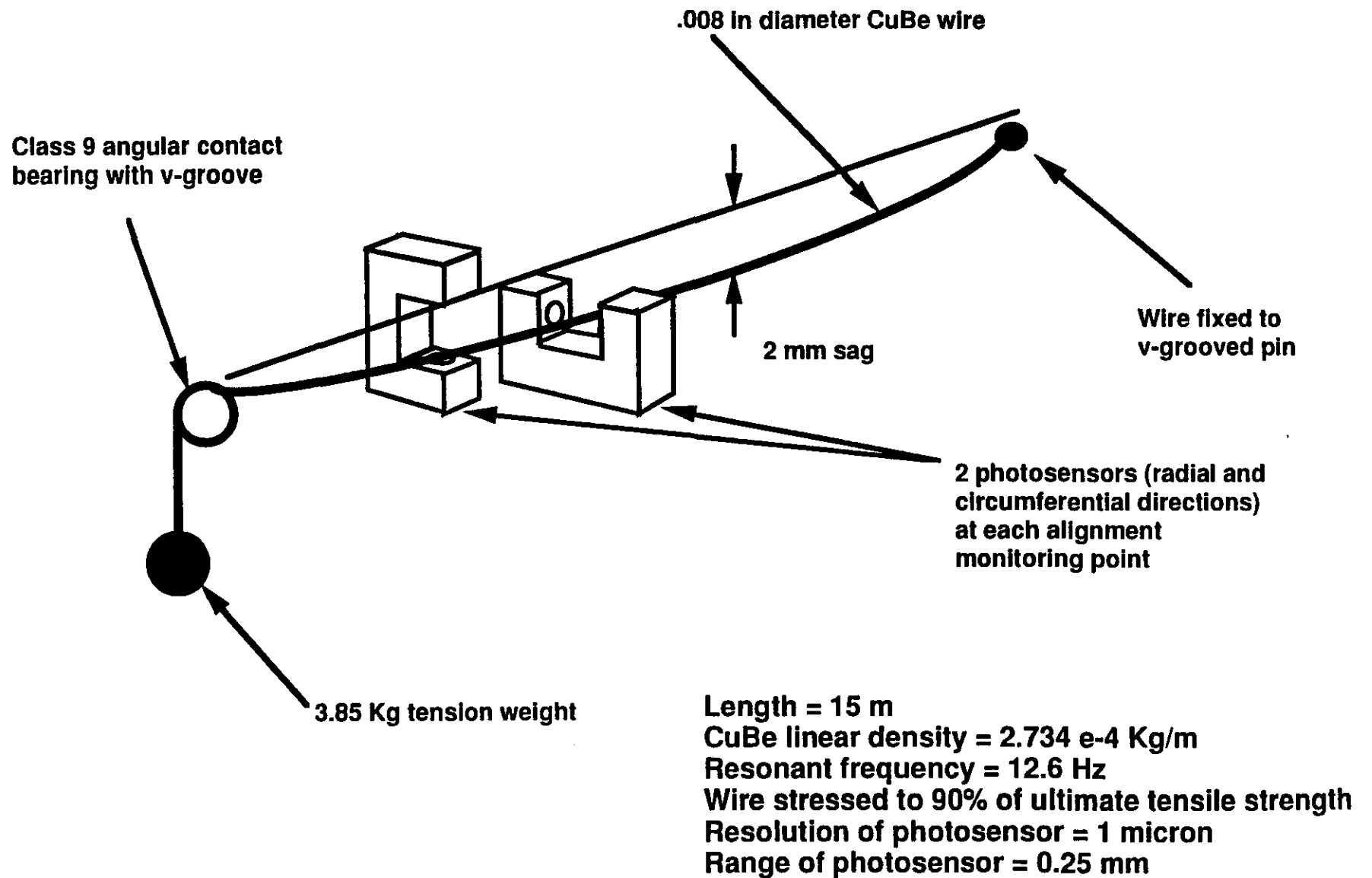
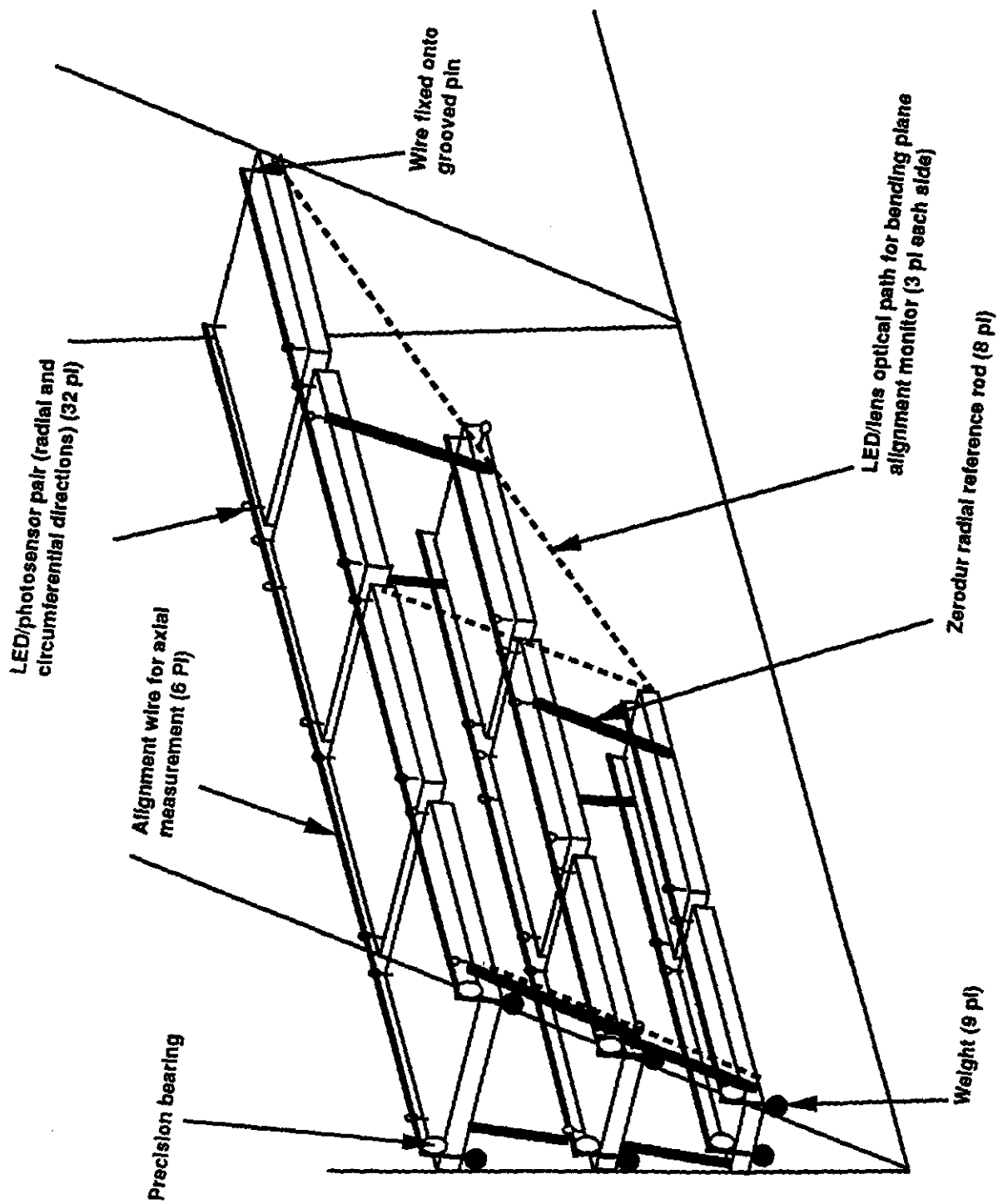
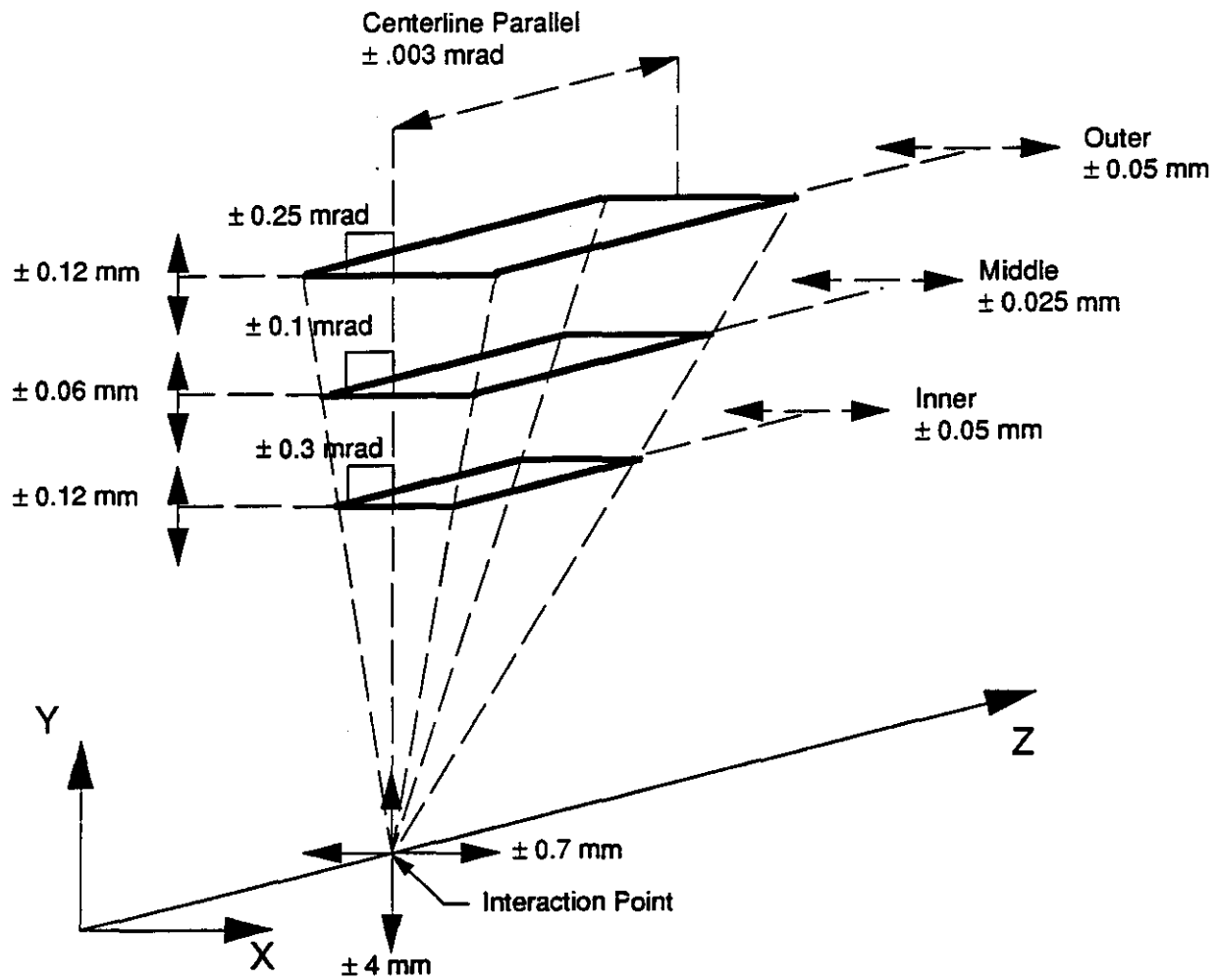


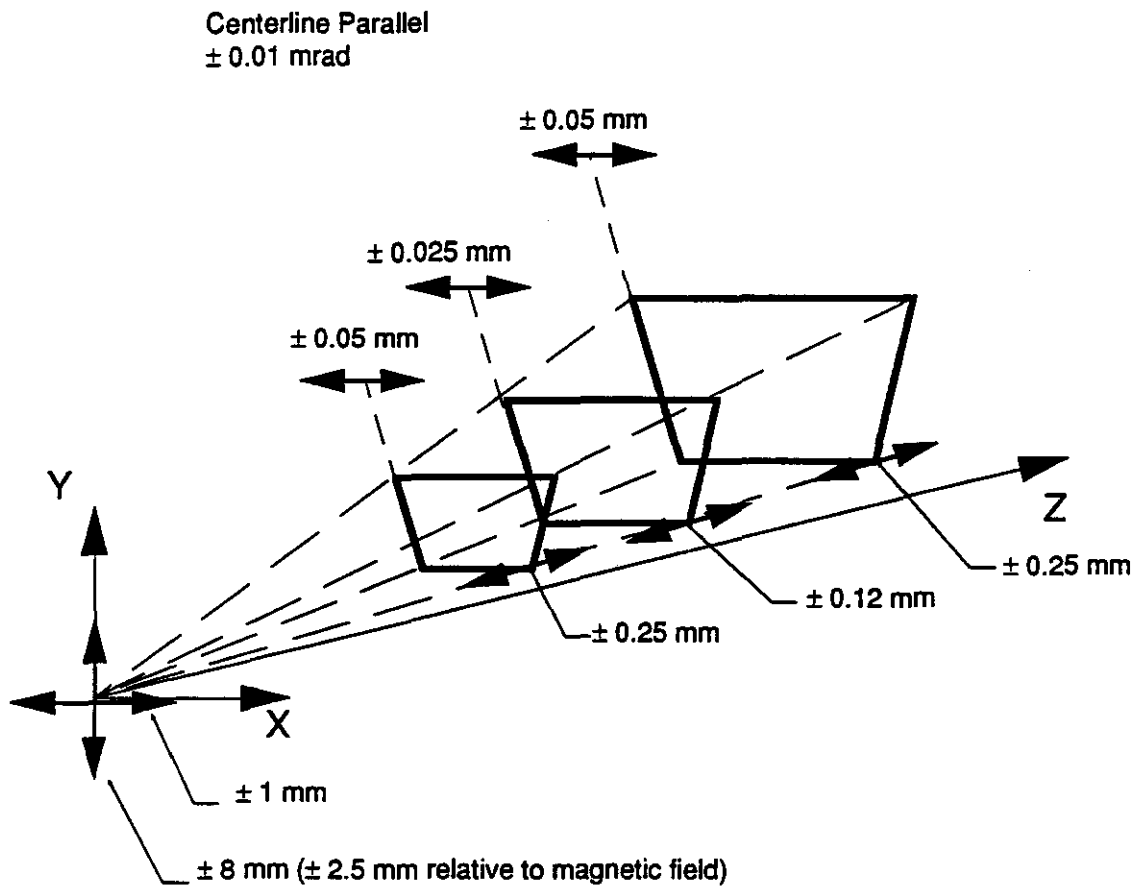
Figure x. Stretched Wire Alignment Technique (SWAT) - for multipoint alignment monitoring requirements



Muon sector alignment scheme



Muon Barrel Module Measurement Accuracy



Muon Endcap Module Measurement Accuracy

ELECTRONICS

TABLE OF CONTENTS

OVERVIEW

Architecture
Electronics Placement

FIGURES:

Electronics System Layout
GEM DAQ Architecture

TABLES:

Trigger Rate Table
Channel Information Table

ELECTRONICS

ELECTRONICS

OVERVIEW

Architecture

- Standard three-level architecture adopted by most SSC/LHC experiments.
- **Level 1**
 - Synchronous: the Level 1 trigger decision is delivered to the front end elements, a fixed number of bunch crossings (~ 120 crossings $\approx 2 \mu\text{s}$) after the event. The trigger elements must tag the bunch crossing.
 - Pipelined: a trigger decision is delivered *every* bunch crossing---i.e. every 16.7 ns.
 - Front end data are stored in digital or analog pipelines for the $2 \mu\text{s}$ delay.
- **Level 2**
 - Asynchronous: the time elapsed between Level 1 and the corresponding Level 2 varies from event to event.
 - Monotonic: the time order of Level 2 decisions is the same as the time order of Level 1 accepts.
 - Front end data from Level-1-accept events are stored in derandomizing buffers (either analog or digital). This permits dead-time-less operation, provided the average time between Level 1 accepts is less than or equal to the average Level 2 trigger decision time.
 - The Level 2 latency time is under study, but is expected to be in the range $10 \mu\text{s}$ to $100 \mu\text{s}$.
- **Level 3**

CPU ranch; $\sim 10^3$ CPU's of $\sim 10^2$ VUP's (VAX 11/780 equivalents) each.

Source:
Updated:

ELECTRONICS

- Design goals call for a factor-of-ten margin between the input rate capacity of a given readout stage and the output rate of the preceding trigger level at $\mathcal{L} = 10^{33} \text{ cm}^{-2} \text{ s}^{-1}$. Thus a Level 1 accept rate of 10 kHz requires a Level 2 input capacity of 100 kHz.

Electronics Placement

- Locate electronics in most readily accessible place consistent with uncompromised performance and acceptable cable plants. Significant portions of the Level 1 trigger, the Level 2 trigger, and the data acquisition (DAQ) electronics are located in the electronics room (ER), which is accessible with the beam on.
- Front-end Electronics
 - Silicon Vertex Tracker: preamps, discriminators, and delay pipelines are mounted on the detector elements. Hit data from detector are transmitted by optical fiber after Level 1. This electronics must be rad hard.
 - IPC Central Tracker: preamps, switched-capacitor analog (SCA) pipeline delays, analog multiplexers, and ADC's are mounted on IPC. Digitized data from detector are transmitted by optical fiber after Level 1. This electronics must be rad hard.
 - Calorimeter: preamps are mounted in the LAr and coupled by copper transmission lines to front-end boards mounted in crates on the membrane. The front end crates house shaping amps, SCA pipeline delays, ADC's, and elements of the Level 1 and Level 2 triggers. Only the preamps need be rad hard.
 - Drift-Wire Muon Electronics: preamplifiers and discriminators are mounted on-chamber and connected to TDC crates mounted on the magnet via twisted pair transmission lines.
 - Cathode-strip Electronics: Low-noise preamps, shaping circuits, storage capacitors, multiplexers, and ADC's are chamber mounted. Digitized data are transmitted off detector over optical links.

Source:
Updated:

ELECTRONICS

- Level 1: After the first level of analog summing or logical OR'ing, which is done in close physical proximity to the front ends, the signals are transmitted to the ER by optical fiber for further processing.
- Level 2 & DAO: After first level of data collection at the front ends, digital data are transmitted to the ER for further processing.
- Level 3 CPU Ranch: Reduced data from the ER are transmitted by optical fiber to the operations center at the surface, where the Level 3 CPU ranch is located.

Source:
Updated:

GEM Trigger/DAQ Design Goals				
Level	Rate In	Rate Out	Latency	Comments
1	60 MHz	10 kHz	2 μ s	Synchronous, Pipelined
2	100 kHz	300 Hz	100 μ s	Asynchronous, Monotonic
3	3 kHz	10 Hz	-	CPU Ranch

Table 13.1 TRIGGER RATE TABLE
Page 13-4

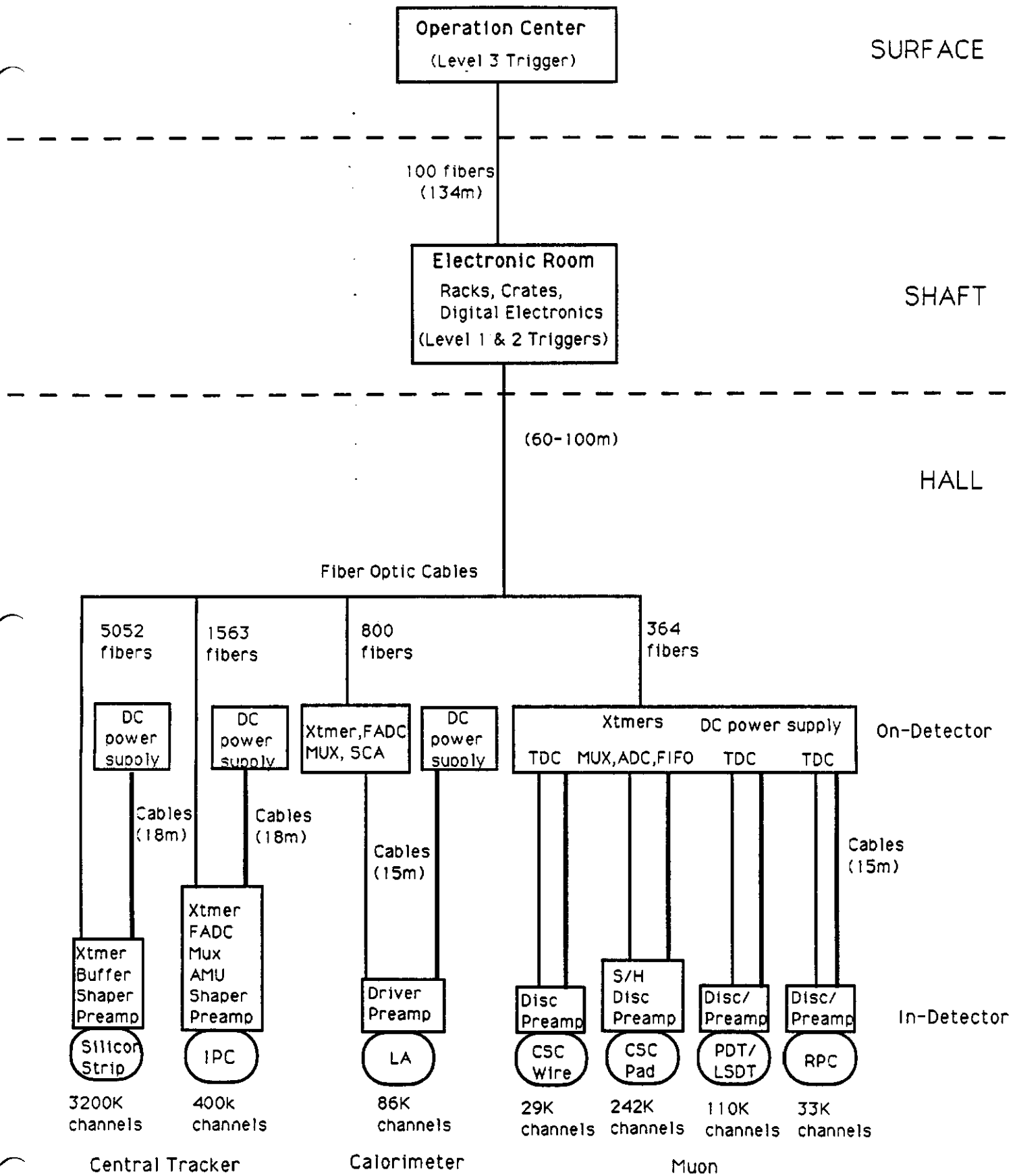
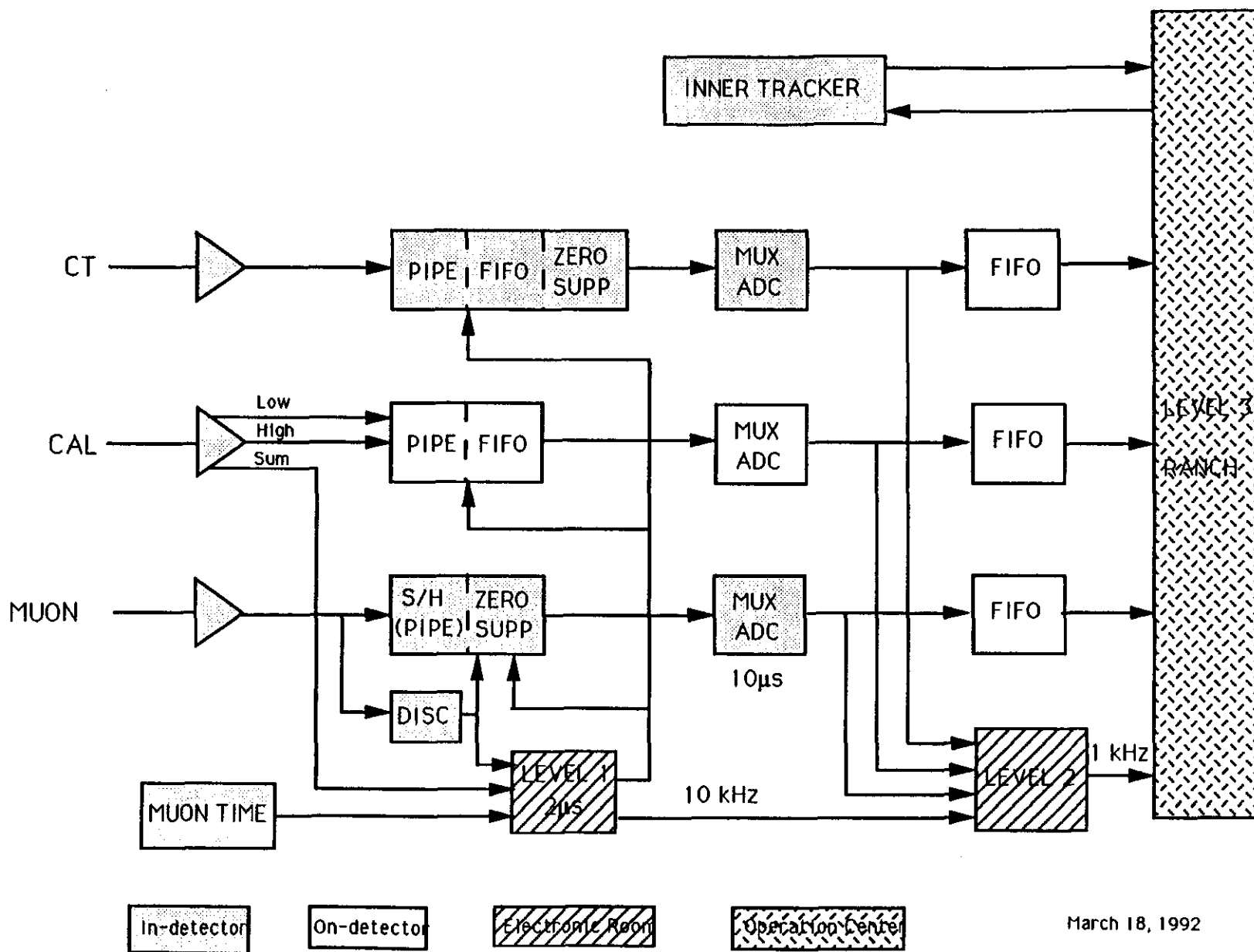


Figure 13-1. Electronics System Layout
Page 13-5

CHANNEL INFORMATION TABLE
(June 17, 1992)

Source: Norman Lau Update: June 17, 1992	Central Tracker		Calori- meter	Muon			
	Silicon Strip	IPC	Liquid Argon	RPC	PDT/LSDT	CSC Wire	CSC PAD
No. of Channels	3200K	400K	86K	33K	110K	29K	242K
Power dissipation/channel (In-detector)	3mW	10mW	100mW	100mW	100mW	100mW	100mW
Power dissipation/channel (On-detector)	0	0	5W	1W	1W		
Resolution	1-bit	7-bit	8-bit	1ns	1ns	1ns	7-bit
Dynamic range	1-bit	9-bit	16-bit	4us	4us(TDC)	4us	9-bit
Occupancy/channel (%)	.06-.22	1.8	5	<1	<1	<1	<1
Number of sample	1	3	5	1	1	1	1
Number of bytes/hit	2	2	2	4	4	2	4
Channel/link	640	256	32	2500	2500	2500	1000
Link bandwidth - 0 suppression (Kbyte/s)	23	48	40	5.3	5.3	5.3	10
Link type (wire/optic)	fiber	fiber	yes	yes	yes	yes	yes
Radiation (rads/yr at 1E33)	0.44M	31-1.1K	OD <1K ID high	<1K	<1K	<1K	<1K
Low-voltage power supply	1.5V,3.3V	yes	yes	yes	yes	yes	yes
High-voltage power supply	100V	2-3KV	2-3KV	yes	yes	yes	yes
Cost (y=mx+b)	\$2.85/ch	\$16+2.3M	\$141+3.1M	\$52+0.4M	\$37+1.2M	\$34+1.4M	\$19+1.9M
Persons contact	G. Mills S.K. Hahn (LASL)	J. Musser (Ind. U)	J. Parsons (Columbia)	M. Atiya (BNL)		V. Polychronahos P. O'Connor (BNL)	

Fig. 13.2 GEM DAQ ARCHITECTURE
Page 13-7



COMPUTING

TABLE OF CONTENTS

OVERVIEW

FIGURES:

GEM Computing System Schematic
Integrated On-line/Off-line Computing Facility
CPU Utilization with Level 3
GEM Slow Control Hardware

TABLES:

Trigger rates, Event Sizes and Rate to Storage
Computing and Data Rate Requirements
Network or Dedicated Data Link Requirements

COMPUTING

COMPUTING

OVERVIEW

The following functions are included under computing: slow control (detector operations), on-line computing (Level 3), off-line computing (PASS1, analysis, simulation), storage, databases and communications. Overall planning is focussed at the SSCL. Figure 14-1 shows the general hardware architecture; the following sections give a brief description of the features of this figure. Main features are:

- 1) Integrated on-line/off-line computing facility
- 2) PASS1 completed in 'real time'
- 3) Integrated storage system

This section deals mostly with requirements such as computing power, data link capacity, and space needs at the IR, but also touches on other aspects.

Open systems

GEM will use an open systems approach. In practice this means, among other things, using operating systems which are variants of Unix, or compatible with Unix at the system level. We plan to fully exploit the capabilities of Unix systems as they evolve while being open to new developments. There is a transitional period during which the installed base of VAX/VMS systems will be catered to.

Integration of functions

There are two aspects to integration: software and hardware.

The overall goal for GEM software is to integrate the computing system so that so that the same environment is used for all tasks from slow control through analysis. This will reduce software development effort and allow the creation of common tools and user interfaces.

A major determinant of costs is the overall required CPU power and the data link capacity. For example, GEM projects requirements for 200,000 SSCUPs for on-line and 600,000 for off-line. These estimates are very tentative, and it is wise to plan for large departures. Rather than partition on-line (Level 3) and off-line into separate systems, GEM is studying the possibility of integrating these functions, allowing great flexibility and full use of what will be a limiting resource. If these studies continue to support the basic idea, this will impact on budget

Source: K McFarlane
Update:

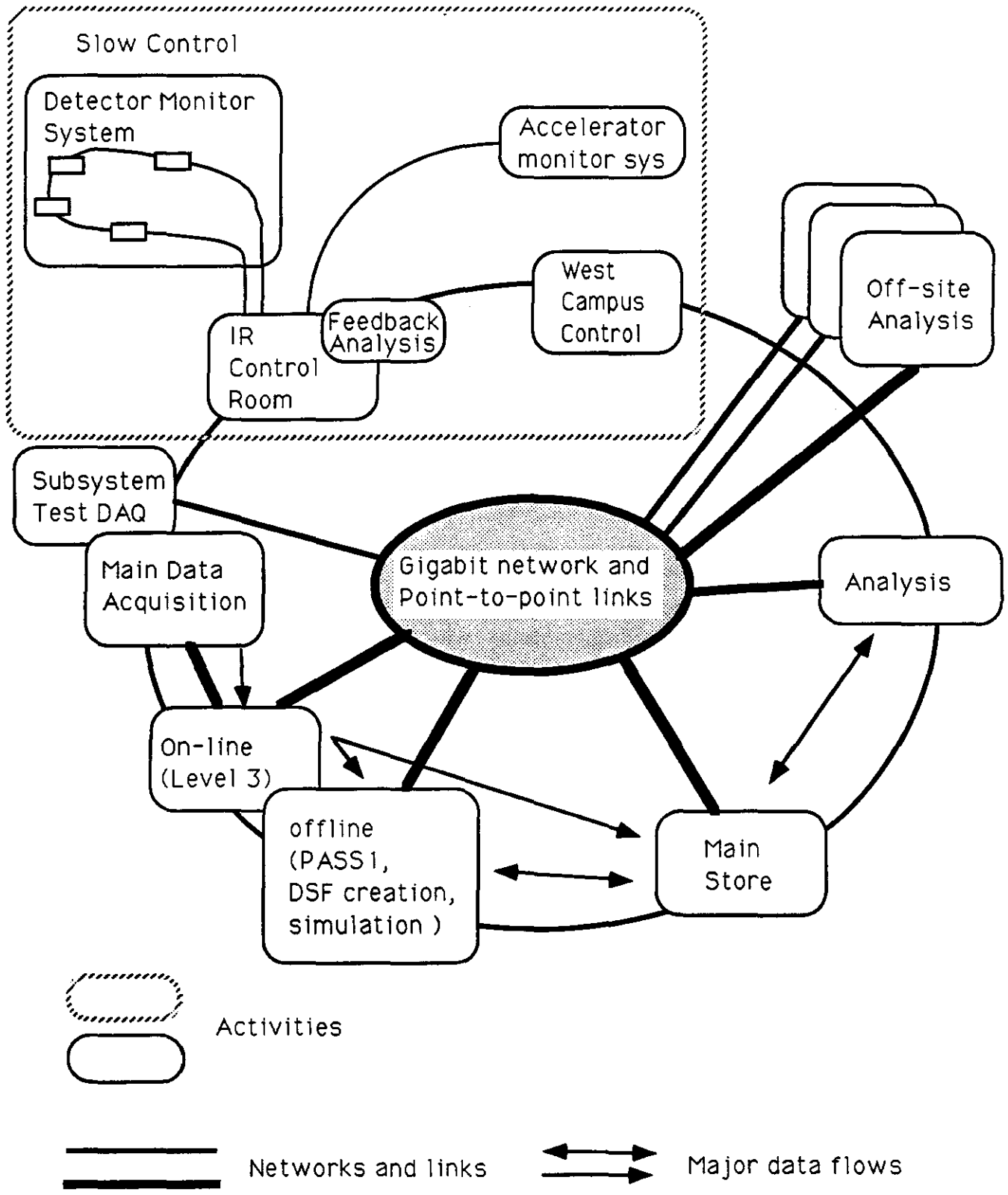


Figure 1 - Gem Computing System schematic

COMPUTING

and facilities. Figure 14-2 shows the outline of one model being evaluated for this integrated facility, while figure 14-3 shows results from a simple model of its performance in terms of CPU utilization as a function of Level 3 input rate and PASS1bis input rate (this model has 1600 CPU's in 400 boxes, and assumes a single data link capacity of 100 MB/s). Note the high utilization of the CPU's and the ability to catch up PASS1bis when the detector is off.

Relation to Industry

We are highly dependent on industry to provide basic hardware and software. We should use commercial or public-domain solutions rather than develop HEP solutions with their attendant maintenance responsibilities and limitations. We are beginning this process in establishing an environment for the development of GEM software.

There will be areas where we (GEM or SSCL) can work with industry to bring techniques to fruition through joint projects, techniques which might otherwise be delayed for lack of motivation. An example may be gigabit rate input directly to workstations. Also, we can help transfer developments like the 'ranches' to industry at the same time as advancing that art. An example is the GEM computing architecture study on combining the on-line (Level 3) and off-line systems, in consultation with industry.

Coordination with SSCL

A group at the SSCL will support and coordinate GEM computing. In addition, the Physics Research Division Computing Support group will support GEM.

Coordination with SDC

There is much in common between the requirements of GEM and those of SDC. Therefore we plan to work with SDC on the development of software and hardware. However, some of our requirements do differ, and some of our approaches may also differ. It is useful to have complementary approaches in computing as well as for detectors.



Data Acquisition
(Pre Level 3)

On-line and Off-line

Mass Storage

Page 14-4

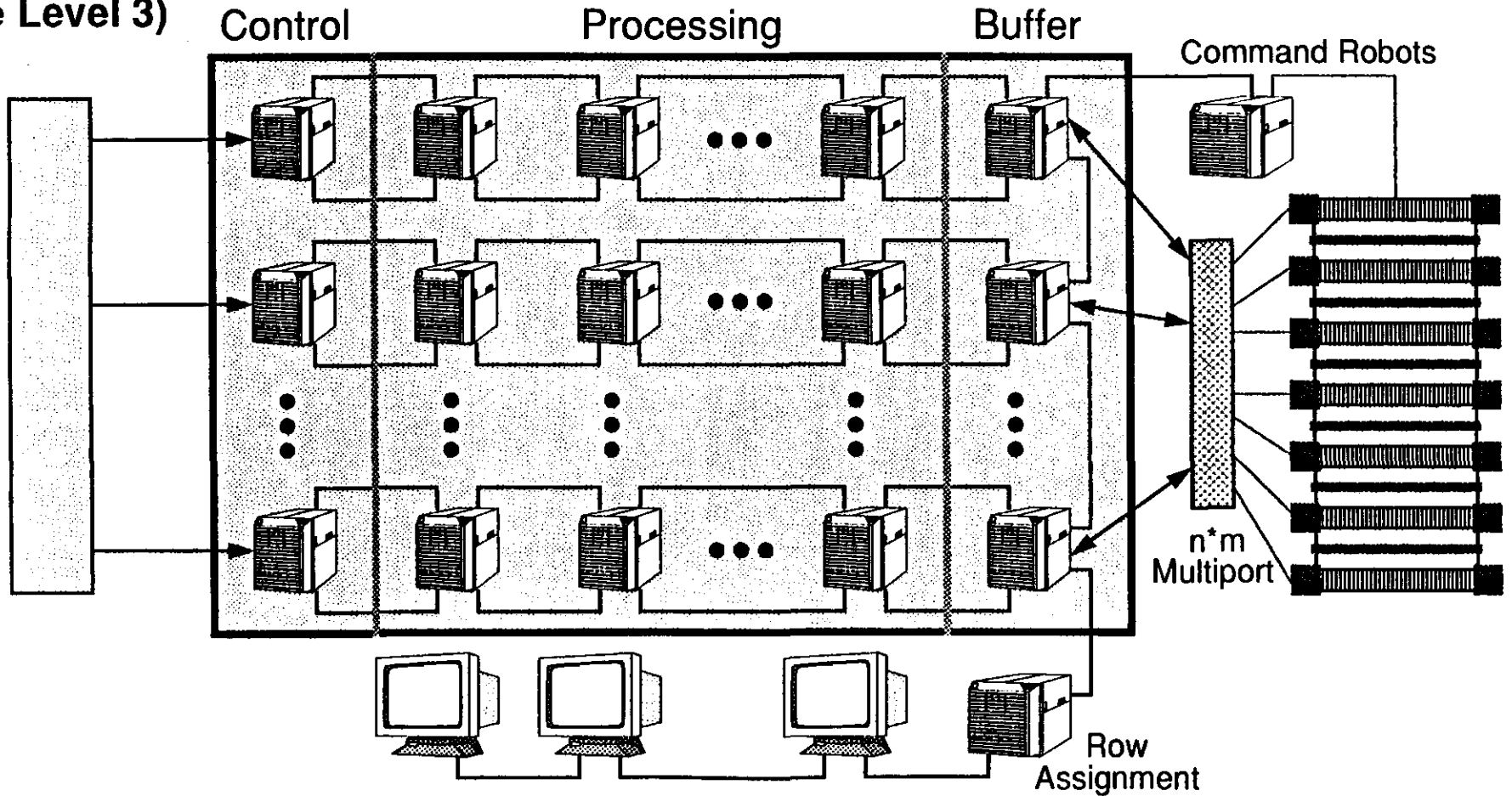
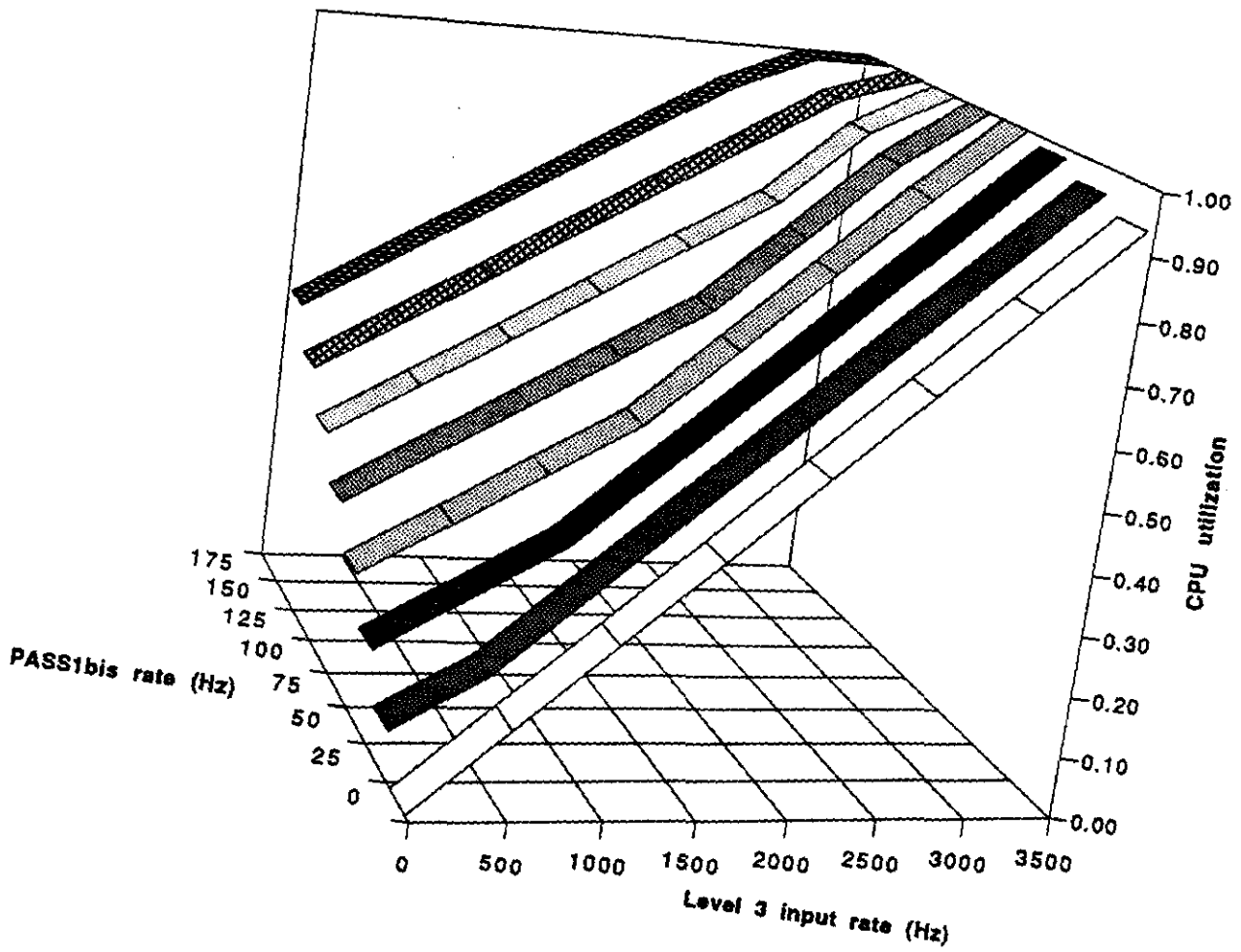


Figure 3 -- CPU utilization with Level 3, PASS1 at 1/30 and PASS1bis



COMPUTING

Requirements Summary

Note that we have adopted the convention of Section 13, that the input capacity of a trigger level should be 10 times the desired output rate from the previous level. This permits variations in the rejection ratio of a given level. However, we desire to have the full capacity available at detector turn on, to allow the use of loose triggers. The expected rates are shown in Table 14-1. It is assumed that the input to PASS1bis is the output of PASS1, not Level 3.

Table 14-1 -- Trigger rates, event sizes and rate to storage

Stage	Input rate	Rejection factor	Output rate	Event size	Rate to store
Level 1	60 MHz	600 - 6,000	10-100 kHz	0.35 - 1 MB	NA
Level 2	10-100 kHz	30 - 300	0.3 - 3 kHz	0.35 - 1 MB	NA
Level 3	0.3 - 3 kHz	30	10 - 100 Hz	0.4 - 1.05 MB	4 - 105 MB/s
PASS1	10 - 100 Hz	1 - 2	5 - 100 Hz	1.4 - 2 MB	7 - 200 MB/s
PASS1bis	0 - 200 Hz	1	0 - 200 Hz	1.4 - 2 MB	0 - 400 MB/s

Source: K McFarlane
Update:

COMPUTING

The compute time for Level 3 is taken as 67 SSCUP-seconds, while that for PASS1 is 2,100 SSCUP-seconds/MB; these numbers are based loosely on CDF experience. These lead to the requirements of table 14-2.

Table 14-2 -- Computing and Data Rate Requirements

System	Input Rate Goal	Input Design requirement	Output rate goal
On-line (Level 3)	300 Hz @ 1 MB from Level 2	3 kHz @ 1 MB from Lvl 2 200kSSCUPS @ 67 SSCUP-s/event	10 Hz
Storage	10 Hz @ 1 MB from Level 3 10 Hz @ 2 MB from PASS1 10 Hz @ 2 MB from PASS1bis 10 Hz @ 2 MB from simulation 10 MB/s from analysis	600 MB/s: 100 MB/s from Level 3, 400 MB/s from Off-line, 100 MB/s from analysis, simulation	400 MB/s
Off-line	10 Hz @ 1 MB from Level 3 10 Hz @ 1 MB for PASS1bis from storage simulation, analysis, DSF creation @ 200,000 SSCUPs	100 Hz @ 1 MB from Lvl 3 for PASS1 @ 2100 SSCUP-s/event 100 Hz @ 1 MB for PASS1bis simulations Total: 600,000 SSCUPs	

Source: K McFarlane
Update:

COMPUTING

Slow Control

The slow control system will monitor and control detector operations, including verifying readiness of the on-line/off-line and storage facilities; a schematic is shown in figure 14-4. The functions of the system are:

- a) Safe operation of the detector and related systems, that is also easy and fast
- b) Assurance of data quality through monitoring of all relevant parameters
- c) Recording of all relevant data
- d) Setup and monitoring of Level 3, PASS1 and storage
- e) Remote capability, e.g for satellite control room at West Campus

It will include data-acquisition equipment (temperature gauges, voltage monitors..) and control equipment (magnet current, detector high voltages, detector ON/OFF) coupled to workstations and possibly high-reliability computers. There will be links to other parts of the computer system (on-line - Level 3, storage, off-line, analysis) to ensure readiness of these systems (possible controlling them) and obtain feedback.

The physicists/staff will use eight to ten workstations in a control room with many additional displays, and a space of at least 25 by 40 feet. Control and monitoring tasks will not be bound to any particular workstation (with the possible exception of safety-related tasks). There will be a set of displays which have a standard layout. Besides this control room there will be auxiliary control points where technical staff will monitor and control subsystems such as refrigerators, etc. The space for these must be specified by the systems concerned. For the control room only, an estimate of 1,500 sq.ft. net is reasonable. Support space (kitchen, emergency shower) must be added. The control room must be at the IR during construction and setup, though some functions can be duplicated in an auxiliary control room at the West Campus as shown in figure 14-1..

Source: K McFarlane
Update:

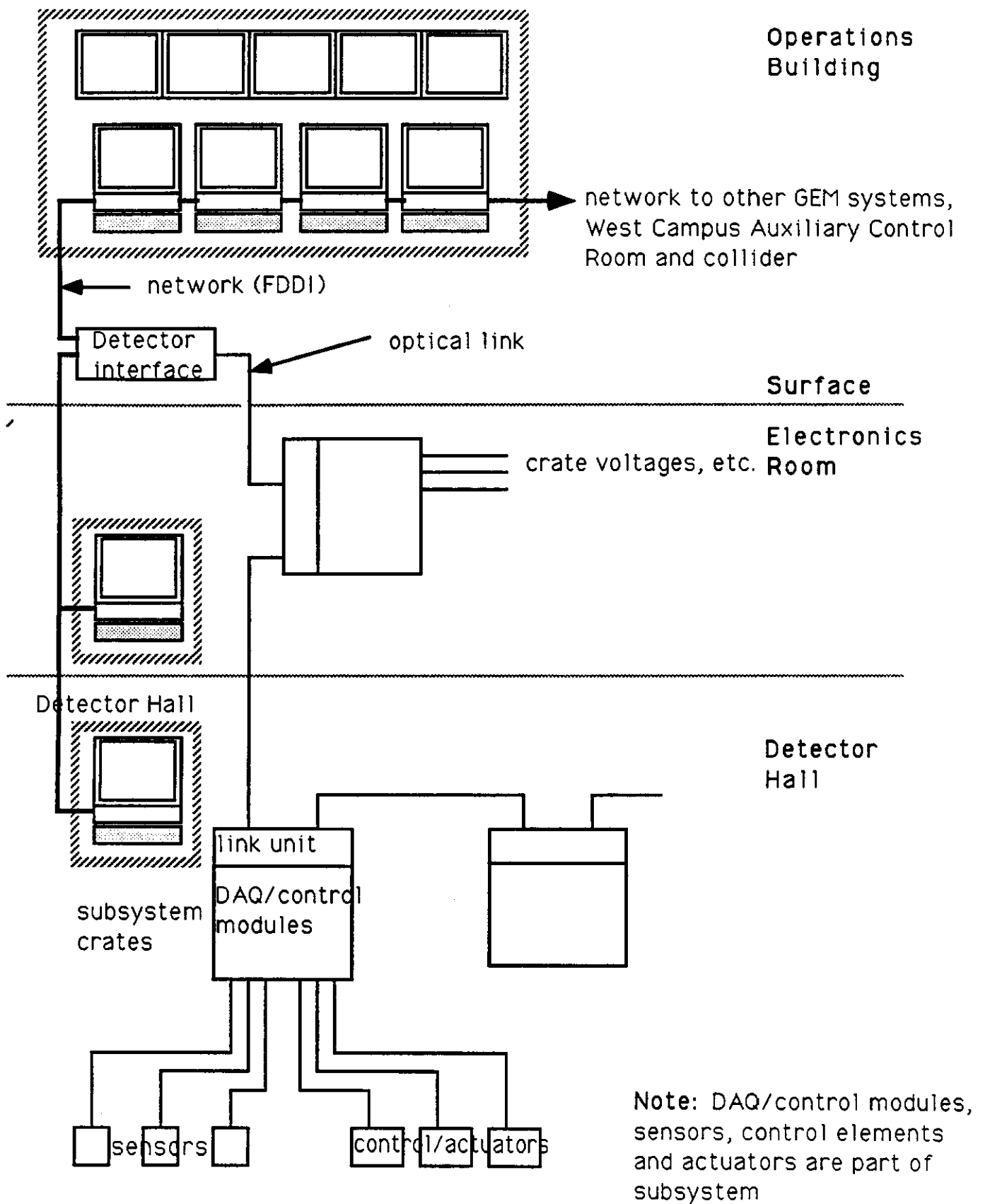


Figure 4 -- GEM Slow Control Hardware

Copy of baseline_slow_fig

COMPUTING

The slow-control data-acquisition equipment will be located near the appropriate systems, and data will be sent to the surface on redundant fiber-optic links; control messages will use the same links. There will be less than 100 such links, which will use a standard communications protocol. Sensors and control equipment are the responsibility of the subsystems.

On-line

This takes data from the Level 2 trigger and reduces it to a flow which can be permanently recorded. The input requirement is to handle up to 3,000 events per second, with events of 1 MB, for an input rate of 3 GB/s, or 24 Gb/s (see Table 14-1). The system is to reduce the output rate to 100 Hz of 1 MB events. Since algorithms are not yet developed, a dependable estimate of the needed computing power is not available. Our baseline estimate is 200,000 SSCUPs (a unit of computing power defined by an SSC benchmark suite, roughly equal to a VAX 11/780, or 1.5 MIPS). The networking and support requirements remain the same, so we can estimate a space of 60 by 60 feet, or about 3,500 sq.ft. Again, this should be at the IR.

As noted above, our preferred option is to combine the on- and off-line processing in one facility.

Subdetector DAO system

The individual subsystems (tracker, calorimeter, muon system) will need the ability to monitor data acquisition independently of the primary DAQ system. This will require an independent data path, likely one or more gigabit networks or links.

Off-line

This serves our off-line needs, and a capacity of 600,000 SSCUPs is needed, based on a mix of activities: 100 Hz for PASS1, the same for a second PASS1 after recalibration (each at 2100 SSCUP-s /MB, from CDF) and a load equal to PASS1 from analysis, simulation, etc. This mix will be detector operation dependent. We estimate 5,500 sq.ft. including some support space.

Source: K McFarlane
Update:

COMPUTING

Main Store

This is a single logical store, where all our data will be stored: raw data, processed data, calibrations, Data Summary files (DSFs), etc. Our baseline model for this is to store 5 years of data, resulting in a possible requirement for 15 Petabytes (PB) of storage. This system would be hierarchical, consisting of bulk store ('tape') with slow access (one second - one minute), rapid access store ('disk') with access times of milliseconds, and fast access ('mass memory') with access times of microseconds.

Database

A database will be needed for a variety of purposes: calibration data, monitor information, catalogs of data files at a minimum.

Analysis

Analysis will consist of the creation of Data Summary Files (DSFs), ntuple files, special reconstruction and fitting tasks, event selection and visualization. The CPU power needed will be small compared with the off-line system. An important demand will be for fast file access. This aspect is illustrated by the possibility of examining a sample of 10^7 Z⁰'s from one year's running (1 pb sample). If a DSF of these events consists of 1 kB per event, then we have 10 GB of data. To transmit this to a single workstation in 100 seconds requires 0.8 Gb/s. If we assume that there are 30 physicists analyzing data, each looking at 1 pb samples with varying amounts of data per sample (average 10 kB), and spending one hour on each sample, we have a total data rate of 1 GB/s, or 8 Gb/s. Clearly, development is needed both for networks and for workstation interfaces, where current data rates are more in the 10 MB/s range.

Space is needed for up to 40 non-SSCL people working at workstations. At least 10 of these should be at the IR, using at least 1,200 sq.ft. there, and a total of 4,800 sq.ft. overall (this assumes that 10 workstations can be fit in a space of 1,200 sq.ft.)

Simulation

We expect to use up to 200,000 SSCUPs for simulation

Source: K McFarlane
Update:

COMPUTING

Communications

Machine

We also need space and facilities for networking -- some is included with each subsystem above, but about 500 sq.ft. ought to be allocated at the IR for general networking. Our computing strategy depends heavily on reliable and wide-band networking, in most cases using dedicated lines, possibly with special protocols. With that, we may have some flexibility in location of the parts of our system; however it is clear that the most likely system to be reliable from this point of view would be one entirely at the IR. Table 14-3 lists some requirements. We expect that gigabit links will be standard items. Note that the use of dedicated link is not meant to preclude use of a network. However, high performance from 'commodity' components may be best achieved by point-to-point dedicated links with light-weight protocols.

Table 14-3 -- Network or dedicated data link requirements

Connection	Rate, Gigabits/second
Slow control to all systems	0.1 Gb/s (network)
DAQ to Level 3	24 Gb/s (multiple streams, links)
Level 3 to Storage (detector on)	0.8 Gb/s (link)
Level 3 to Storage (detector off)	1.6 Gb/s (link)
Storage to Level 3 (detector off)	0.8 Gb/s (link)
Level 3 to PASS1 (detector on)	0.8 Gb/s (link)
Storage to Off-line (PASS1bis+analysis inp)	1.6 Gb/s (link)
Storage and off-line to analysis	0.8 Gb/s (network)
Analysis to storage and off-line	0.8 Gb/s (network)

Source: K McFarlane

Update:

COMPUTING

Human

Teleconferencing space at the IR and at the West Campus. The space needed is about 1,000 sq.ft.

Options

Among options that are being considered are not storing the Level 3 output, but only the PASS1 output. This would reduce storage requirements.

Work Underway

Work underway includes development of a fast simulation package, a full GEANT simulation, architecture studies of an integrated system and gaining of experience with database techniques with the TTR project.

Definitions

Here we clarify some terms as used in GEM:

L1, L2: These are the trigger systems that reduce the trigger rate to a level at which it can both be computed in general-purpose computer and needs to be, since the task is to correlate information from the entire detector. L1 is generally synchronous, while L2 can be asynchronous.

L3: The trigger system, based on general-purpose computing, that accepts the L2 output rate and filters events to a rate at which the data can be permanently stored.

PASS1: An initial reconstruction pass over events, which applies calibrations and does a further filtering. Events passing the PASS1 filters are written to storage with the data generated in PASS1.

PASS1bis: A re-application of the PASS1 stage, with final calibration constants. (Also called PASS2 in some places.)

Slow Control: The system which monitors and/or controls the various parts of the detector. It includes run control and, in our model, control of the on-line, off-line and storage systems.

Subdetector test systems: It will be necessary to permit parallel DAQ from subdetector systems for test and monitoring, independent of the

Source: K McFarlane
Update:

COMPUTING

main data flow. This data flow will be routed around the normal trigger system and into the online-offline system.

On-line: Level 3 and its support systems

Off-line: the software and hardware that supports PASS1, analysis, simulation, making of DSF's (Data Summary Files), etc.

SSCUP: SSC Unit of Processing power for typical HEP code, approximately 0.9 VAX-11/780, and about 1.2-1.8 MIPS.

Source: K McFarlane
Update:

TEST BEAMS

TABLE OF CONTENTS

OVERVIEW

FIGURES:

Floor Plan at Grade

Elevation Section of Calibration Hall Facing Ring Center

Plan View - GEM Detector Test Beam Calibration Layout

TEST BEAMS

TEST BEAMS

Overview

SSCL test beams will initially be 200 GeV beams from the MEB with the possibility of future expansion to include 2 TeV beams from the HEB. However, the HEB will not be operational until 1998. There is currently no funding in the lab baseline for this expansion. Therefore all test beams activity at the SSCL directed at preparing for the first run will be restricted to a maximum energy of 200 GeV.

The start-up date for these beams is January, 1996. At that time, the MEB will still be undergoing commissioning so we cannot necessarily anticipate smooth operation, nor can we anticipate more than 16 hours/day operation--probably less--at least for some period of time. During the hot months, the cooling pond capacity may restrict this even further.

A total of three beams are being designed. One of these will be dedicated to GEM, which implies that extremely careful scheduling will be required to meet the simultaneous needs of the tracking, calorimetry, and muon subsystems. Beam energies from 1 to 200 GeV will be available. Electron, hadron, and muon beams will be available, with varying purities. The beams will come from a secondary target at an angle of 5 mr to prevent accidental dumping of the full primary beam into the calibration hall. Particle identification will be tagged by Cerenkov's or other devices in the secondary beam line. Beam momentum will be determined by a spectrometer to a precision of up to $\pm 0.05\%$, although the exact precision awaits final design. The momentum bite delivered will be up to 6%. Up to 10^7 hadrons per spill of up to 1 second duration per 8 second cycle can be delivered. Hadron purities of up to $10^4:1$ (hadrons:electrons) are planned, at least at high energies.

The distance from the secondary target to the calibration hall will be about 450 meters. Low energy pion beams would decay to an unacceptable level before reaching the devices under test. Therefore low energy tertiary beams will be obtained with a secondary target placed much closer to the calibration hall.

The layout of the calibration hall is shown in Fig. 1. The beams will be incident into the calibration pits from the north. They will be separated by 46 feet. Provision will be made for six-foot shielding walls between pits. Whether these walls are present or not will be determined later.

Source: G Yost
Update: 6/22/92

TEST BEAMS

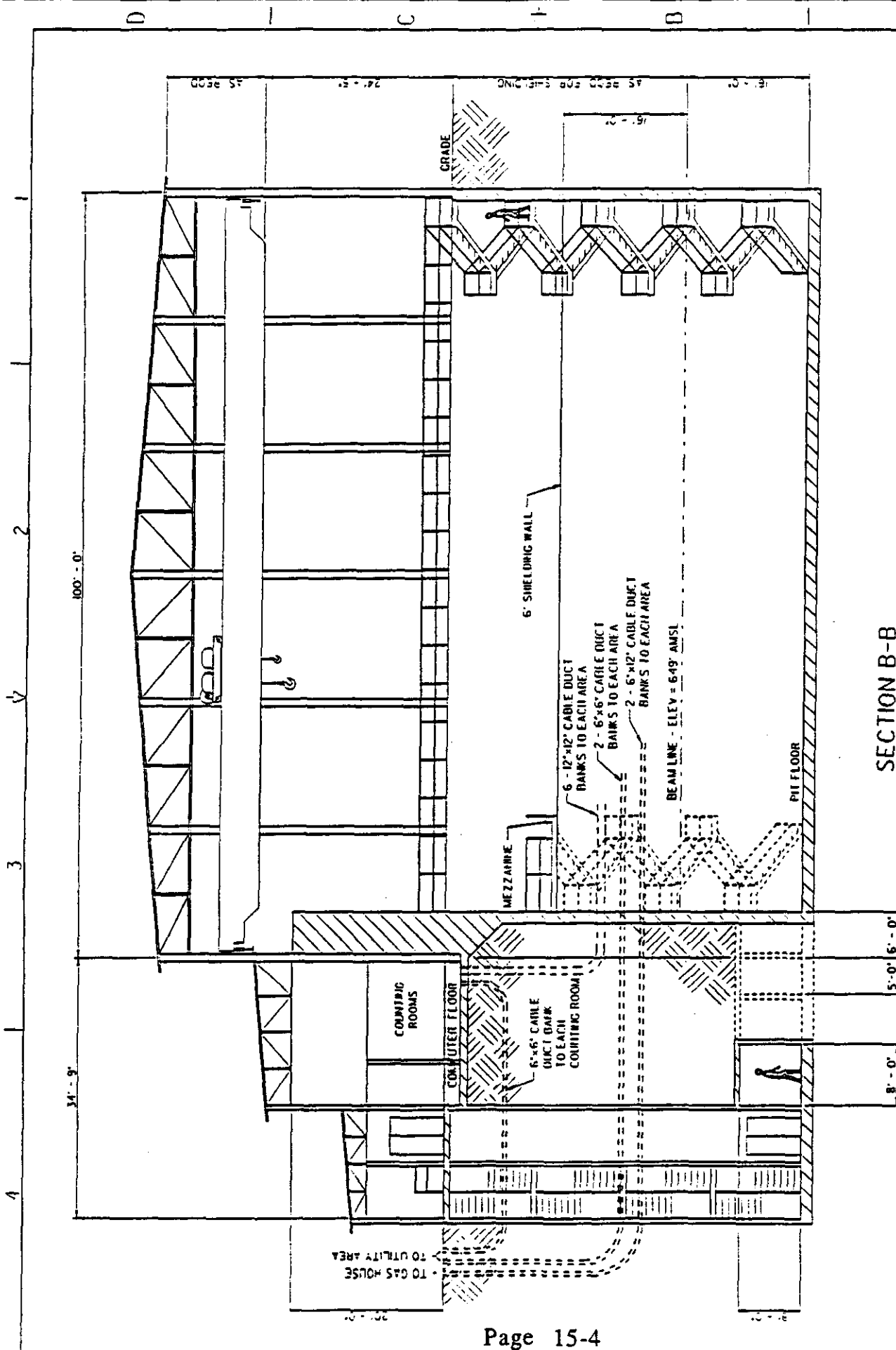
The east pit will be dedicated to SDC, the central pit to small experiments or other usage, and the west pit to GEM. Staging areas and various utility and lab rooms will be provided as shown. A few permanent offices are provided; all other office space will either be in trailers or in permanent West Campus buildings not too far away.

Utilities, power, control, and other electronics for the devices under test will be positioned either in the counting house, on the mezzanine above the pits, in the pits themselves, or external to the building. In particular, a gas building behind the counting house will connect to the pits via underground conduits. Cryogenics supply dewars will be located next to the gas building. Crane coverage of up to 50 tons capacity will extend from the pit area to the staging/assembly area.

Figure 2 shows the B-B section of the calibration hall, showing the cranes, the mezzanine, the pit staircases, and the utilities conduits. The left-most staircase will open into shielded and interlocked tunnels behind the pits, which connect directly to the rear of each pit. This staircase will be adjacent to an elevator for transporting equipment, such as electronics, and people into the pits.

The GEM pit area layout is shown in figure 3. The tracker, a LAr or LKr calorimeter cryostat, and muon chambers are shown in the beam line. Other calorimeter choices will place fewer demands upon the available space, and are therefore not shown. Only the final GEM calorimeter design will be accommodated, due to space and scheduling limitations. All these devices will be on transporters which will rotate and translate them appropriately to scan their components. These transporters will also move them into and out of the beam line. In normal operation, one expects that only one or two of these components will be in the beam line at the same time. The others may be replaced by beam pipes, as necessary.

Source: G Yost
Update: 6/22/92



THIS IS A CAD GENERATED DRAWING. DO NOT MAKE MANUAL REVISIONS OR ALTERATIONS.

NO.	DATE	REVISION
1	10/01/94	ISSUED FOR PERMIT
2	10/01/94	ISSUED FOR PERMIT
3	10/01/94	ISSUED FOR PERMIT
4	10/01/94	ISSUED FOR PERMIT
5	10/01/94	ISSUED FOR PERMIT

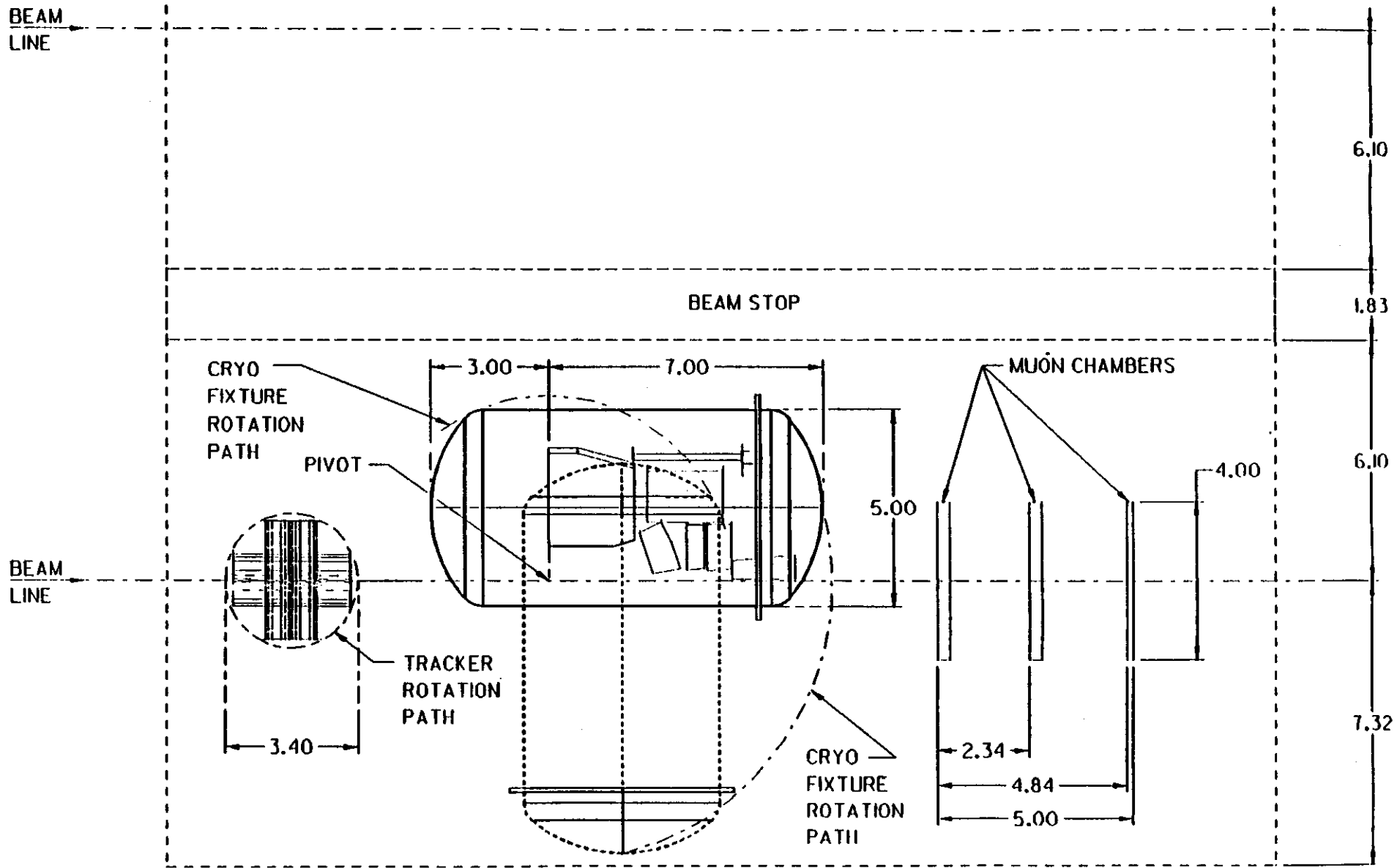
SDC EXPERIMENTAL FACILITIES
 CALIBRATION HALL
 SECTION B-B



PHYSICS RESEARCH DIVISION

NO.	DATE	REVISION
1	10/01/94	ISSUED FOR PERMIT
2	10/01/94	ISSUED FOR PERMIT
3	10/01/94	ISSUED FOR PERMIT
4	10/01/94	ISSUED FOR PERMIT
5	10/01/94	ISSUED FOR PERMIT

NO.	DATE	REVISION
1	10/01/94	ISSUED FOR PERMIT
2	10/01/94	ISSUED FOR PERMIT
3	10/01/94	ISSUED FOR PERMIT
4	10/01/94	ISSUED FOR PERMIT
5	10/01/94	ISSUED FOR PERMIT



PLAN VIEW
GEM DETECTOR TEST BEAM CALIBRATION LAY OUT

RADIATION ENVIRONMENT

TABLE OF CONTENTS

OVERVIEW

Neutron Fluence: Potential Radiation Damage and Background Effects
Material/Component Studies
Activation Studies

FIGURES:

LAHET/MCNP Geometry Simulation for Calorimeters
LAHET/MCNP Geometry Simulation for Drift Chamber and Magnet
Energy Spectra of Neutrons through the Silicon Vertex Detector
Energy Spectra of Neutrons through the First Endcap Muon Chamber
Endcap and FCAL geometry simulations from TN-92-91
FCAL Activity Density
FCAL Dose Equivalence

TABLES:

Material Specifications for Detector Components
Central Tracker Neutron Fluence
Neutron Fluence Through the First Muon Endcap Chamber
Endcap Neutron Fluence at Various Z Values

RADIATION ENVIRONMENT

RADIATION ENVIRONMENT

OVERVIEW

The Los Alamos High Energy Transport (LAHET) simulation package and other codes are now being used to model various aspects of the GEM radiation environment. Several detector geometry alternatives are under investigation, with results periodically issued in the form of GEM Notes (TN-92-91). One design under current study is the Baseline 1 detector geometry shown in figures 16-1 and 16-2, and table 16-1. Results from this design and a summary of the implication of past studies are reviewed in this report. To date emphasis has focused on neutron calculations, and similar results for photons are forthcoming. All results given here are for a luminosity of 10^{33} .

Neutron Fluence: Potential Radiation Damage and Background Effects

The flux of neutrons at sensitive sites such as the silicon vertex detector and the drift chambers is an active area of investigation. Table 16-2 shows the calculated neutron fluence through the silicon vertex barrel. Studies indicate deterioration of silicon detectors at fluences of around 10^{12} , and the numbers calculated for this area indicate a need for a moderator such as borated polyethylene. Table 16-2 also gives the vertex neutron fluence with a B-poly lining of 5 cm along the barrel and 10 cm in the forward direction. Studies of a previous detector design (TN-92-91) indicate little additional reduction can be gained by further increasing the forward B-poly layer thickness. Figure 16-3 shows the neutron energy spectrum along the tracker cylinder. Such information can provide guidance in choosing appropriate neutron sources for radiation damage tests. Table 16-3 and figure 16-4 give neutron fluence calculations for the first muon chamber at the edge of the endcap calorimeter. Similar spectra provided by this code have been used by the muon system designers to investigate the background these particles will cause.

Material/Component Studies

Studies outlined in table 16-4 illustrate the results of neutron flux studies under varying options of the calorimeter geometry and makeup. The detector shown in figure 16-5 (the study was done for the geometry design of TN-92-91) was examined with both copper and uranium as the absorber material. For the copper case, the effect of removing the FCAL and field shaper was studied. In the endcap, the neutron fluence is larger for the uranium option, but only in the first few hadronic sections. The primary showers have ended by the time

Source: L Waters

Update: 6/24/92

RADIATION ENVIRONMENT

the end of the calorimeter is reached. Here, the flux is dominated by leakage from the FCAL. Removal of the FCAL results in a spray of particles backward from the field shaper. This has the effect of doubling the neutron flux into the first endcap muon chamber, indicating the effectiveness of the FCAL as a shield for more forward regions.

Activation Studies

Studies of detector activation will have implications for background from decay particle spectra, the useful life and subsequent long term storage of elements, and for worker health and safety issues. The most immediate concern is for elements at large h ; the beamline and getter pumps, FCAL, field shaper and quads. Preliminary calculations for the FCAL have been carried out with the CINDER90 code for a previous FCAL design shown in figure 16-5. The decay of the residual nuclei from the LAHET reactions and from the MCNP neutron flux are followed for 30 time bins. The beam is considered to run continuously for 6 months, then shut off and the subsequent activation history tracked for another 6 months. As a function of time, figure 16-6 shows the activity density in curies/cm³ for sections 1 and 16. Integration over the entire FCAL gives a total of 18.7 ci after 6 months of beam. After cooling off for one day a total of 9.7 ci is estimated. Corresponding figures for decay power are 52.7 and 18.3 mWatts. A point kernel shielding method calculation of the dose equivalent rate was made with the major radionuclide sources at the one day cool-down time. Results are shown in figure 16-7.

Source: L Waters
Update: 6/24/92

RADIATION ENVIRONMENT

	EM	HAD	FCAL	B-Poly
density (gm/cm ³)	4.369	6.2165	17.022	1.39
elements (%)				
hydrogen	4.95	8.08	.14	11.6
boron				5.0
carbon	4.44	4.82	.32	61.2
nitrogen		.39	.03	22.2
oxygen	2.62	4.45	.06	
silicon	.64	1.89		
argon	43.13	6.15	2.14	
chromium	3.58	1.91		
iron	11.69	6.26	2.14	
nickel	1.98	1.07	9.65	
copper		64.98	4.08	
tungsten			83.58	
lead	26.97			

Table 16-1: Material specifications for detector components. Numbers are given in atomic percent, except for borated polyethylene, which is given by weight. Elements are further broken down into their naturally occurring isotopes. Cryostats are A15083, the beampipe is beryllium out to ± 227 cm, and the getter pumps and remaining beamline are stainless steel 442. All magnet elements are natural iron.

SETUP	Fluence < 100 keV	Fluence > 100 keV	Total Fluence
no shield	30.2	21.3	51.5
5+10 cm B-poly	1.83	2.98	4.81

Table 16-2: Central tracker neutron fluence. As long as the composition of the nearby electromagnetic calorimeter sections does not change, these numbers are insensitive to changes in the material of the hadronic sections. Another study shows that if the endcap calorimeter are moved inward by 10%, the fluence numbers shown increase by 8-9%. The neutrons have a long time distribution, and form a 'dc' background. Numbers are in units of 10^{12} per SSC year, per cm².

Source: L Waters
Update: 6/24/92

RADIATION ENVIRONMENT

Bin (cm)	Fluence < 100 keV	Fluence > 100 keV	Total Fluence
116-178	12.1	5.1	17.2
178-240	3.35	1.44	4.79
240-302	2.11	.89	3.01

Table 16-3: Neutron fluence through the first endcap muon chamber, for three radial bins. Studies indicate lower energy neutrons come primarily from the calorimeter, while the higher energies are dominated by leakage from more forward elements. If the FCAL is removed, these figures increase by factors of 2-3. There is no B-poly shielding in this study. Numbers are in units of 10^{12} per SSC year, per cm^2 .

Z distance (cm)	²³⁸ U	⁶⁴ Cu	⁶⁴ Cu no FCAL	⁶⁴ Cu no fwd
z=263.3	45.1	47.7	43.51	45.83
	26.5	27.1	24.91	26.22
z=318.6	45.3	33.3	30.28	30.39
	25.3	20.2	18.18	18.59
z=372.6	22.7	11.4	10.85	10.79
	12.2	6.2	5.99	5.87
z=427.6	18.1	9.9	8.45	9.24
	9.7	5.3	4.45	4.97
z=482.6	87.5	85.6	17.11	8.32
	39.4	39.0	9.76	4.15

Table 16-4: Endcap neutron fluence at various Z values between a radius from 5.7 degrees to 180 cm. Numbers are in units of 10^{12} per SSC year, per cm^2 . Two lines are given for each interval; the first represents total neutron fluence, the second is the neutron fluence less than 100 keV. The cases studied represent Uranium as primary absorber, a copper option, the copper option with FCAL removed, and copper with FCAL and forward field shaper and shield removed.

Source: L Waters
Update: 6/24/92

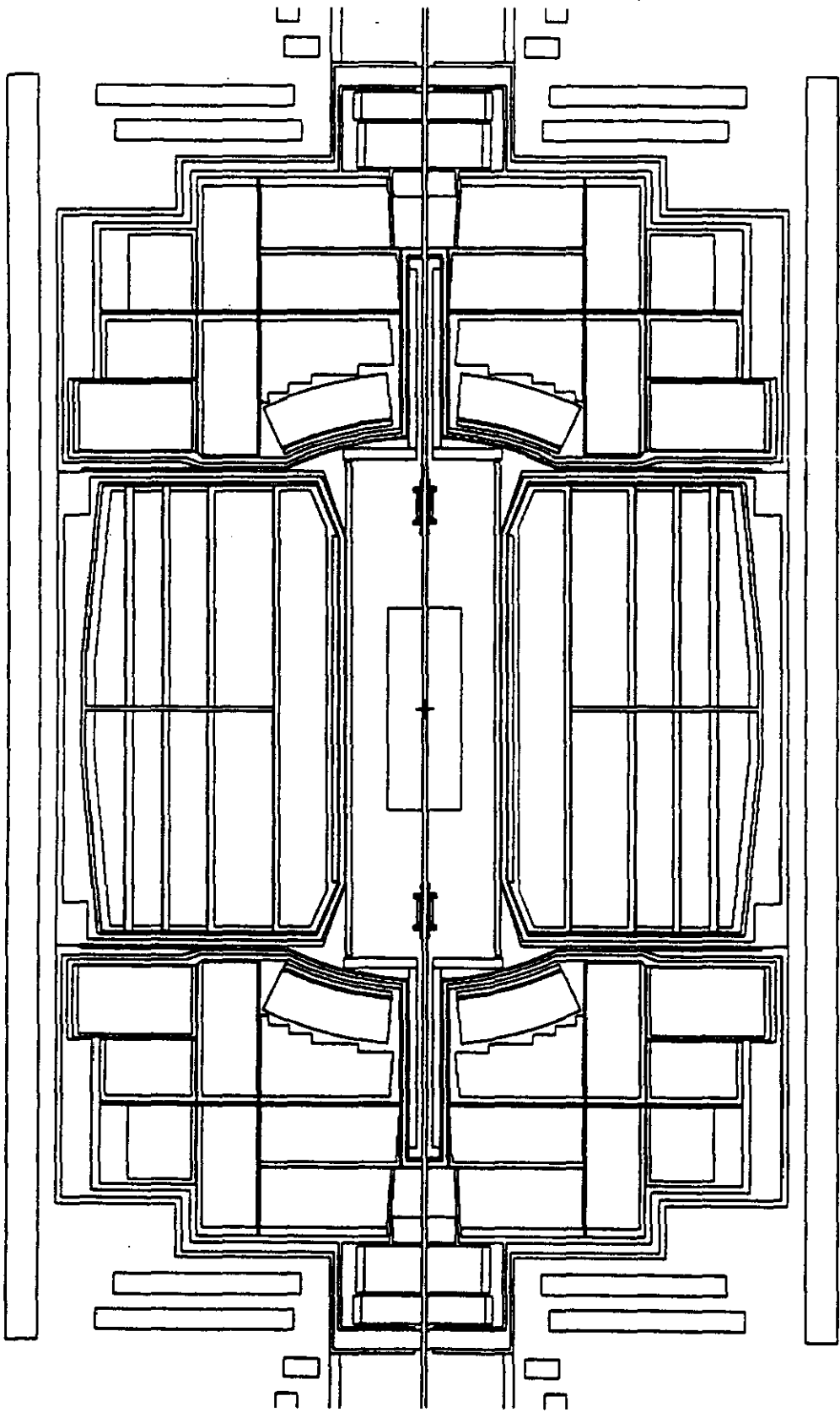


Figure 1 LAHET/MCNP geometry simulation for calorimeters

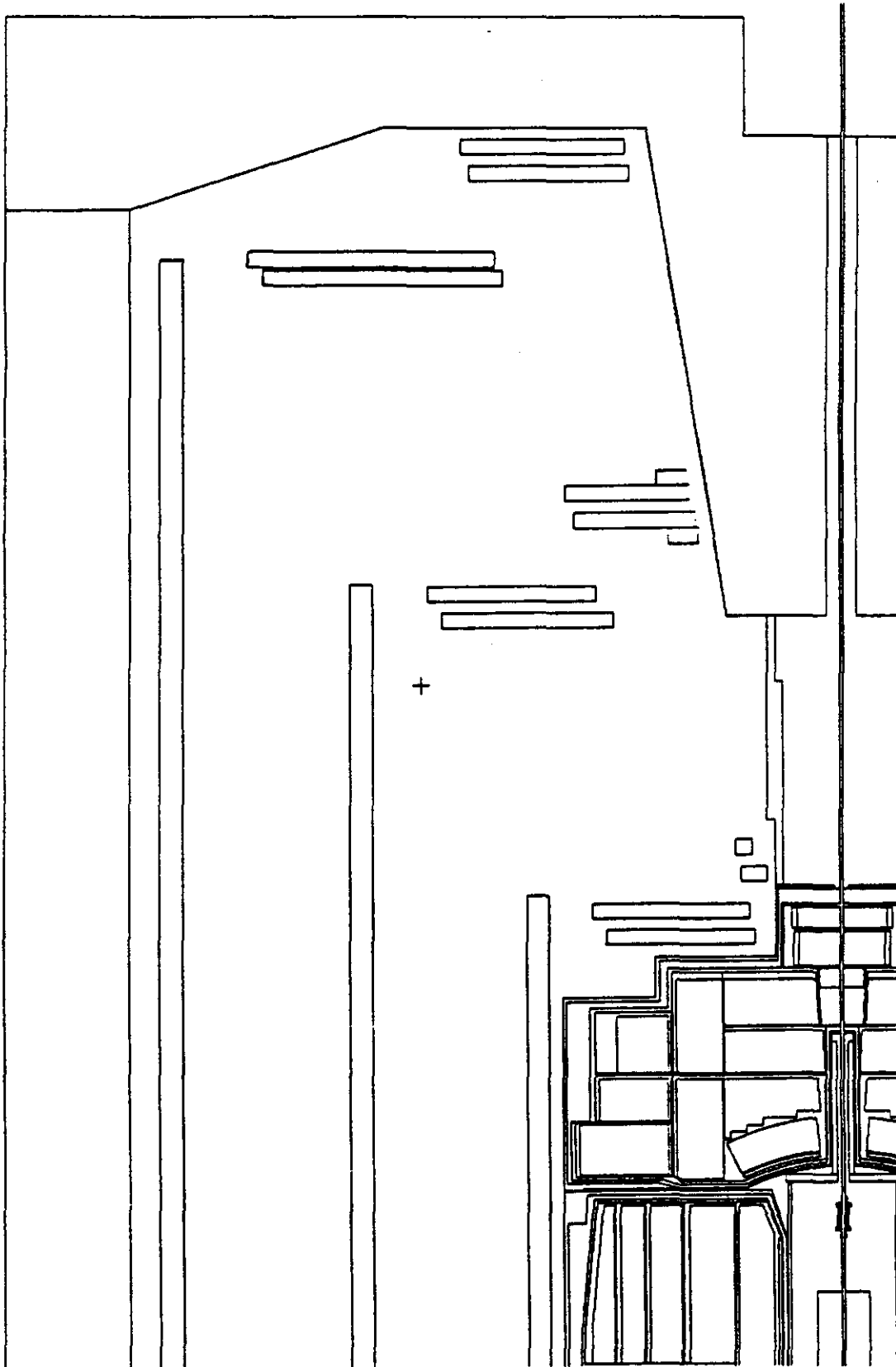


Figure 2 LAHET/MCNP geometry simulation for drift chamber and magnet

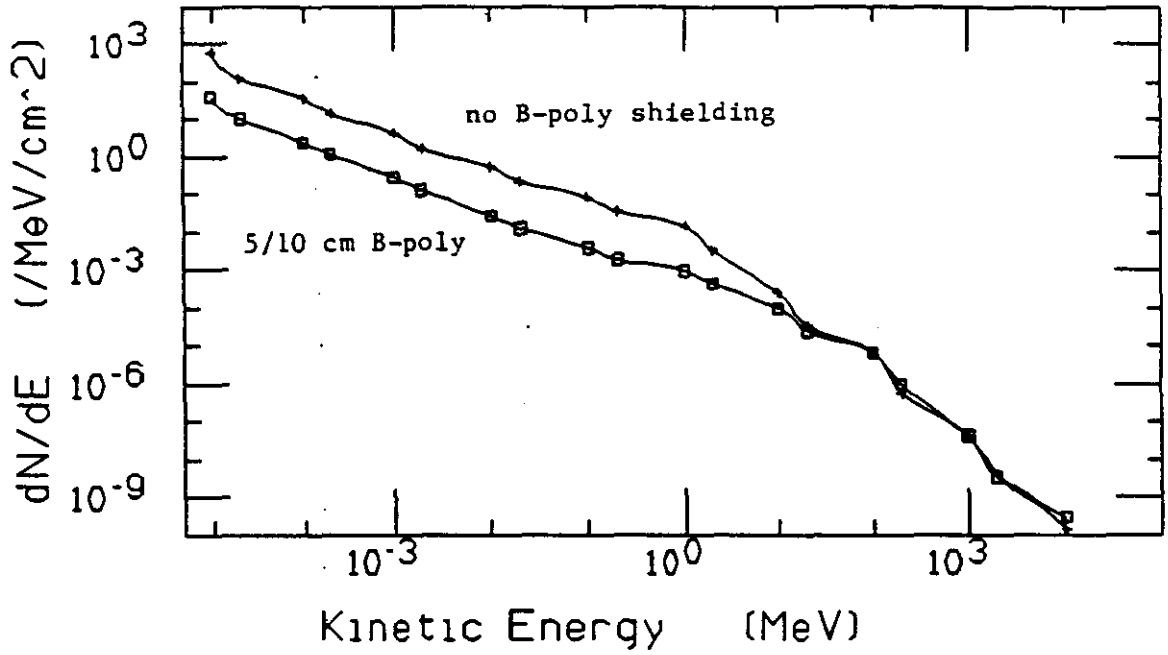


Figure 3 Energy Spectra of neutrons through the silicon vertex detector

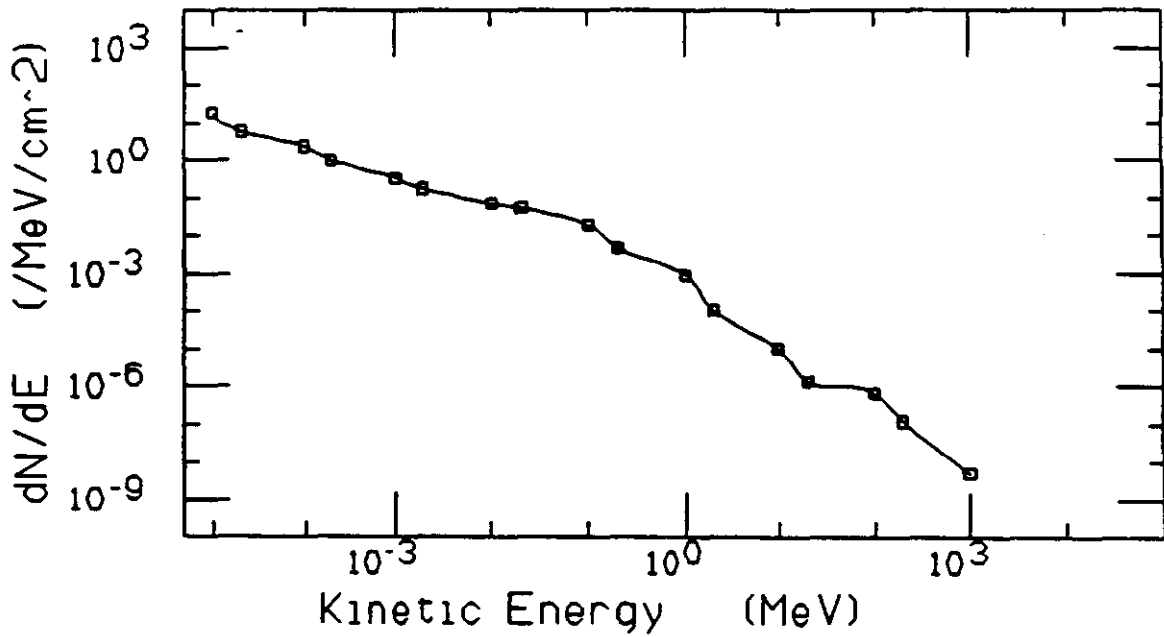


Figure 4 Energy spectra of neutrons through the first Endcap muon chamber

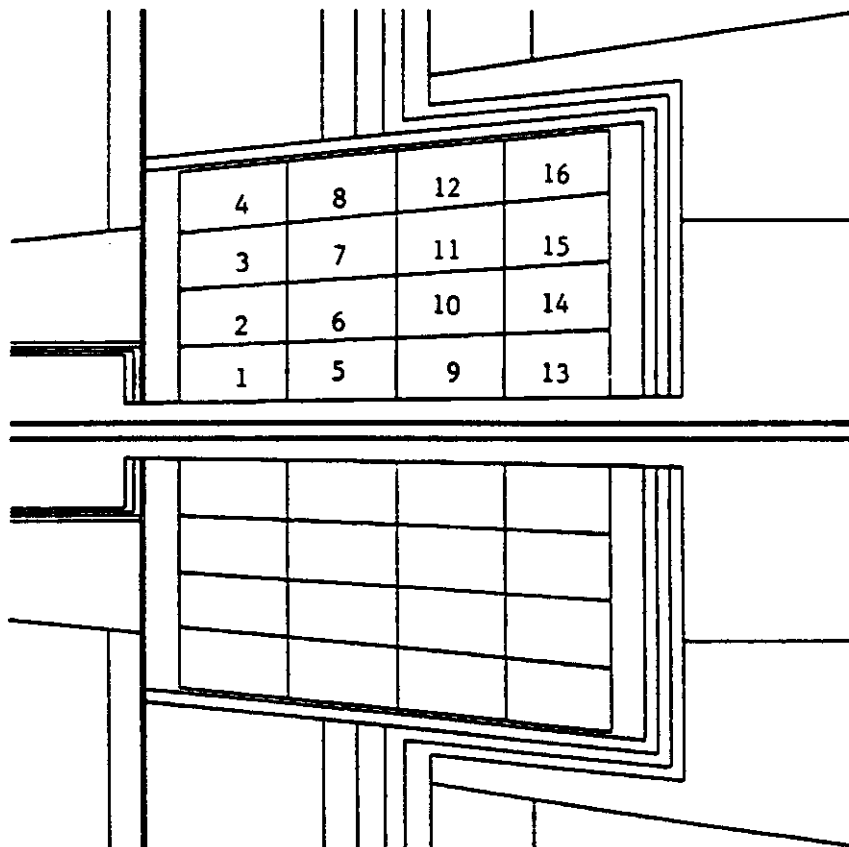
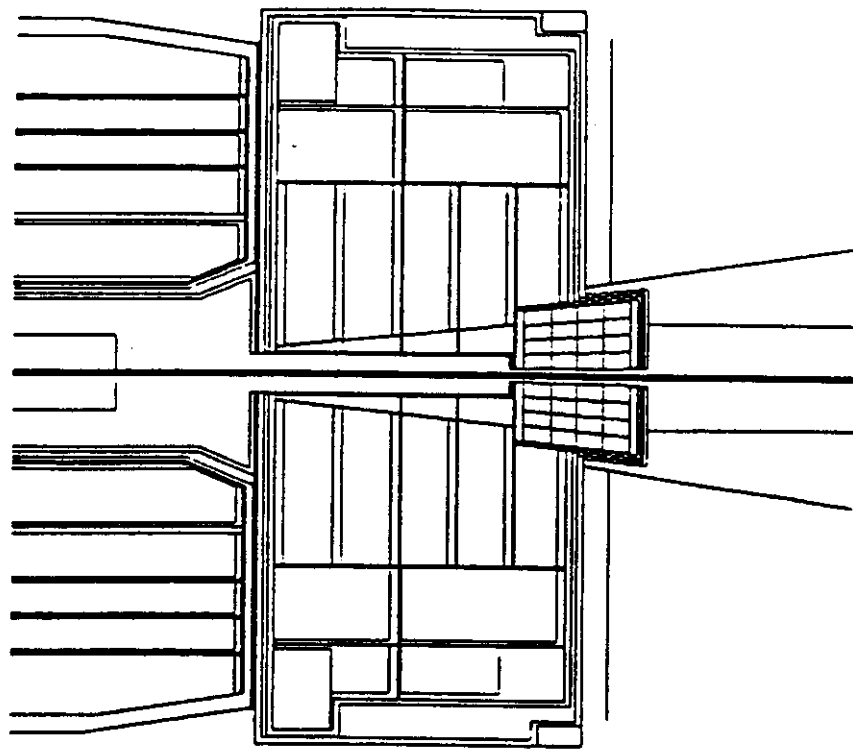


Figure 5 Endcap and FCAL geometry simulations form TN-92-91. This differs from the Baseline 1 configuration. For the activation FCAL calculations, the detector was divided into 16 segments.

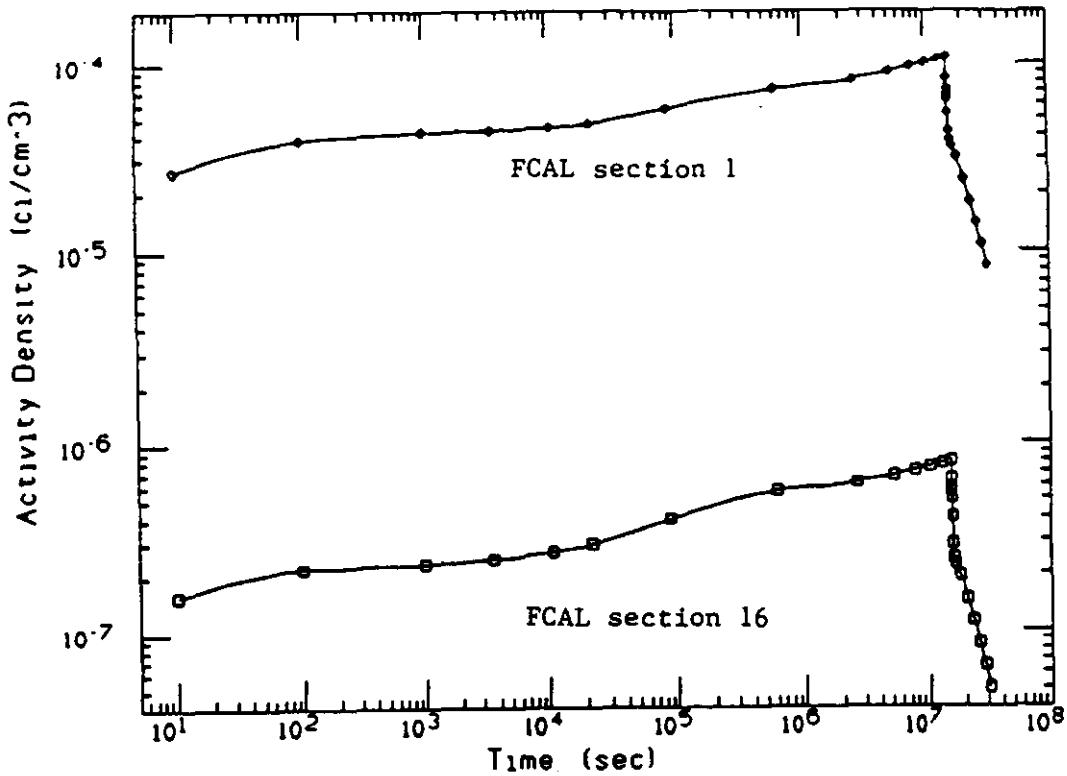


Figure 6 Activity density in the FCAL: preliminary results

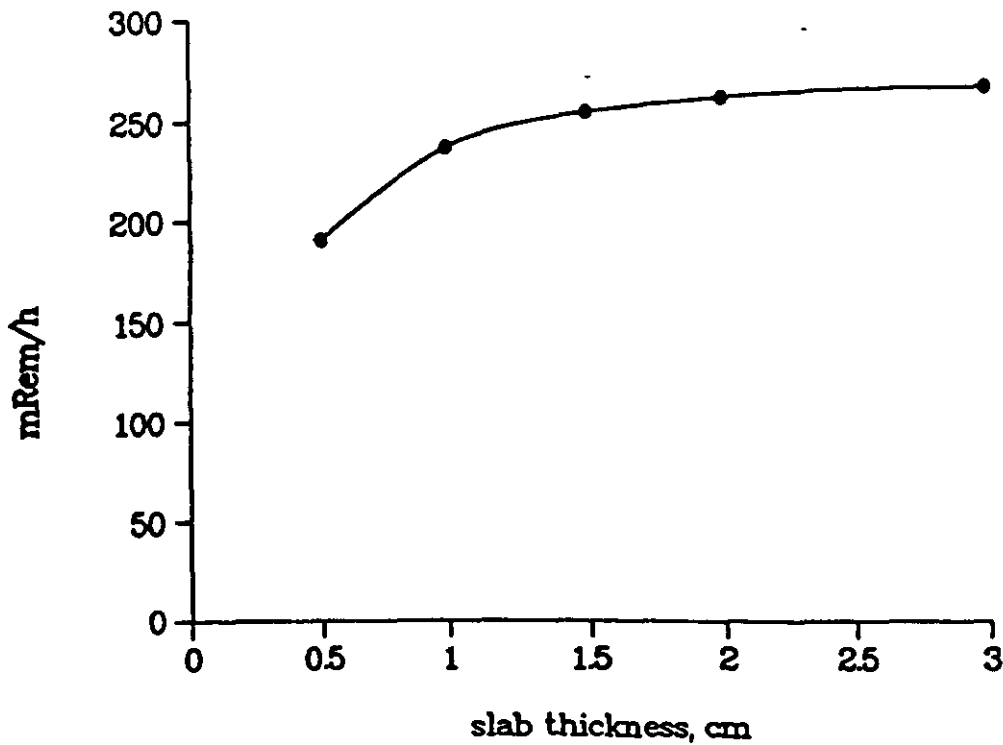


Figure 7 FCAL dose equivalence. The major reaction products were assumed to form an infinite slab of material of varying thickness. The measurement of dose was taken 10 cm away after one day of cooldown. Note the self-shielding properties of the detector.